


# 24th INTERNATIONAL MULTIDISCIPLINARY SCIENTIFIC GEOCONFERENCE - SGEM 2024

**27 – 30 November 2024 – Vienna, Austria**

## CONFERENCE PROCEEDINGS OF SELECTED PAPERS in WATER RESOURCES. FOREST, MARINE AND OCEAN ECOSYSTEMS ISSUE 3.2

**DISCLAIMER**

The **International Multidisciplinary Scientific GeoConference SGEM (Survey, Geology, Ecology, and Management)** serves as a global platform for pioneering research and scientific dialogue across the diverse fields of geosciences. It is dedicated to advancing interdisciplinary solutions for the most pressing environmental challenges of our time — **Global Warming, Climate Change, $CO_2$ Reduction, Biodiversity Conservation, and the Development of Green Technologies**. By fostering a collaborative exchange of knowledge and **aligning its objectives** with the **United Nations Sustainable Development Goals (SDGs), SGEM aims to inspire scientific excellence and drive sustainable practices toward a greener, more resilient future for our planet.**

Authors are responsible for the content and accuracy of the written papers. Opinions expressed are not meant to represent or reflect the position of the SGEM International Scientific Committee members.

No part of this book may be reproduced or transmitted in any form or by any means, electronic or mechanical, for any purpose, without the express written permission of the SGEM International Scientific Committee on Earth and Planetary Sciences.

Copyright © SGEM WORLD SCIENCE (SWS) Scholarly Society 2024
Haidingergasse 1, C / 1113, Vienna 1030, Austria
Published by STEF92 Technology
Total print: 5000

E-mail: **science@sgemviennagreen.org** | URL: **www.sgemviennagreen.org**

**ISBN 978-619-7603-76-7**
**ISSN 1314-2704**
**DOI: 10.5593/sgem2024v/3.2**

## FOREWORD

**The urgent need to reduce carbon emissions, transition to cleaner energy systems, and preserve our planet's ecosystems has never been more critical.** As the impacts of climate change become increasingly evident in our daily lives, green sciences stand at the forefront of this global challenge, offering innovative solutions to mitigate $CO_2$ emissions, combat environmental degradation, and build a sustainable future. This first volume of the **SGEM Vienna Green Conference Proceedings reflects the collective efforts of researchers and experts dedicated to advancing knowledge and practices in these vital areas.**

The section on *Hydrology, Water Resources, and Climate Resilience* underscores the **critical importance of water in maintaining life and supporting sustainable development**. From flood risk assessment using machine learning to innovations in wastewater treatment and groundwater quality monitoring, these studies demonstrate how we can protect and efficiently use this vital resource in the face of climate change and growing global demand.

*Soil Science, Conservation, and Land Restoration* **explores the challenges of land degradation and the solutions needed to restore and sustain healthy soils**. Whether through phytoremediation techniques, geochemical tools, or advanced fertilization methods, the research presented here reinforces the role of soil as a foundation for ecological stability and agricultural sustainability.

**The importance of forests as carbon sinks and biodiversity hotspots** are in the focus in section *Forest Ecosystems and Sustainable Forestry*. From modeling forest landscape permeability to assessing the impacts of sustainable forest tourism, these contributions highlight the indispensable role of forests in reducing $CO_2$ emissions, maintaining ecological balance, and supporting rural economies.

Lastly, section on *Sustainable Oil, Gas, and Energy Transition Exploration* addresses some of the most pressing challenges of our time. From **strategies to reduce greenhouse gas emissions in the energy sector to innovations in sustainable aviation fuels and lithium recovery**, these contributions highlight the intersection of traditional industries and cutting-edge technologies in the fight against climate change. Studies on pollution prevention and climate change mitigation through advanced

exploration methods provide a roadmap for reducing the environmental footprint of energy production.

This volume embodies the spirit of the SGEM Vienna Green Conference, which seeks to bring together **interdisciplinary research, innovative practices, and actionable insights to address the environmental challenges of our time**. By fostering collaboration between scientists, policymakers, and practitioners, this collection serves as a beacon of hope and a source of solutions for creating a more sustainable, equitable, and resilient world.

We extend our deepest gratitude to the authors, reviewers, and organizers who have contributed to this endeavor. **Your commitment to advancing green sciences ensures that SGEM Vienna Green Conference remains a leading platform for inspiring global progress toward environmental sustainability**.

May this volume inspire **further innovation, dialogue, and action as we work together to safeguard our planet for generations to come**.

**Sincerely,**

**Prof. Dr. hab. oec. Baiba Rivza**
Editor-in-Chief of XXIV SGEM GeoConference Proceedings
*Member of the Presidium of the Latvian Academy of Sciences, LATVIA*
*President of the Latvian Academy of Agricultural and Forestry Sciences*
*Vice-chair of the Latvian Council of Higher education*
*President of Latvian universities professors' association*
*Expert from the European Academy of Sciences Academic Advisory Board (EASAC)*

**Prof. DSc. Oleksandr Trofymchuk**
Editor-in-Chief of XXIV SGEM GeoConference Proceedings
*National Academy of Sciences of Ukraine, UKRAINE*

# CONFERENCE PROCEEDINGS CONTENTS

## HYDROLOGY, WATER RESOURCES, AND CLIMATE RESILIENCE

**1. ANALYSIS OF FACTORS AND CLUSTERS IN THE FISHERIES INDUSTRY IN THE EUROPEAN UNION,** Mg.oec. Agnese Eizenberga .....3

**2. APPLICATION OF DRONE TECHNOLOGY FOR FLOOD RISK MONITORING AND MODELING,** Mg. sc. Ing. Toms Lidumnieks, Prof. Dr. sc. ing. Armands Celms, Mg. geogr. Ivars Bergmani .....11

**3. ARSENIC REMOVAL FROM GROUNDWATER BY COAGULATION PROCESS: PERFORMANCE AND LIMITATIONS INFLUENCED BY THE GROUNDWATER SOURCES CHEMISTRY USED FOR DRINKING WATER PURPOSE IN THE WEST REGION OF ROMANIA,** Dr. Pacala Adina.....19

**4. DETERMINING FLOOD SHELTER LOCATIONS: A MULTI-CRITERIA SPATIAL ANALYSIS USING GIS TOOLS,** PhD Dino Dobrinic, Ivan Bertecic, Prof. Dr. Damir Medak.....27

**5. ESTIMATION OF APPROXIMATION ERRORS IN REPRESENTING REAL PARTICLE DIMENSIONS WITH EQUIVALENT DIAMETERS IN SEDIMENTATION ANALYSIS,** Dr. Eng. Tymoteusz Turlej .....35

**6. EVAPOTRANSPIRATION AS A METHOD OF WASTEWATER DISPOSAL,** Ing. Pavel Škarpa.....43

**7. FLOOD PROTECTION IN A MUNICIPALITY WITH THE IMPLMENTATION OFANATURE-BASED SOLUTION,** doc. Ing. Brumarová Lenka, Ing. Brumar Jakub, Ing. Gamonová Patricie .....51

**8. INFLUENCE OF WATER TEMPERATURE ON DROPLET SIZE DISTRIBUTION OF HIGH-PRESSURE WATER MIST NOZZLES,** Ing. Marek Miskay, Ing. Miriam Kadlubcova, Assoc. Prof. Karla Barcova.....57

**9. LIDAR DATA ACQUISITION AND MEASUREMENT ACCURACY IN QC TOOLS USING MOBILE MAPPING SYSTEM TECHNOLOGY,** Assoc. Prof. Dr. Adrian Șmuleac, Prof. Dr. Laura Șmuleac, Prof. Dr. Cosmin Alin Popescu, Assoc. Prof. Dr. Mihai Herbei, Lecturer Dr. Raul Pașcalau .....67

**10. MICROBIAL CONTAMINATION ASSESSMENT OF FIREFIGHTING WATER FOR WATER SUPPLY PURPOSES AND THE POSSIBILITY OF DISINFECTION,** Ing. Patrik Sirotiak, Doc. Ing. Šárka Kročová Ph.D. .....77

**11. POSSIBILITIES FOR DAY-STEP FLOOD FORECASTING IN SMALLER CATCHMENTS USING MACHINE LEARNING METHODS,** Dr. Tomas Kozel, Ruzena Pavelkova .....85

**12. POSSIBILITIES OF USING WATER RESOURCES FROM THE SHALLOW AQUIFER TO SUPPLY WATER TO LOCAL IRRIGATION SYSTEMS,** Assist. Prof. Phd. Eng. Ioana Alina Cretan .....93

**13. PUBLICATION OF DATA FROM THE LATVIAN REGIONAL HYDROGEOLOGICAL MODEL LAMO4,** Assist. Prof. Dr. Math. Irina Eglite, Researcher Master of Comp. Sc. Kaspars Krauklis .....99

**14. STATISTICAL ANALYSIS OF HYDROCHEMICAL PARAMETERS OF THE RACHA-LECHKHUMI AND KVEMO SVANETI REGIONS NATURAL WATERS,** M. Tabatadze, L. Shavliashvili, G. Kuchava, E. Shubladze, E. Elizbarashvili .....107

**15. THE INFLUENCE OF AGRICULTURAL ACTIVITIES ON THE QUALITY OF UNDERGROUND WATER IN THE CENTRAL AREA OF THE BANAT PLAIN UNDER THE CONDITIONS OF ADAPTATION TO CLIMATE CHANGE,** Prof. Dr. Laura Smuleac, Prof. Dr. Florin Imbrea, Assoc. Prof. Dr. Adrian Smuleac, Lecturer Dr. Raul Pascalau, Lecturer Dr. Radu Bertici .....115

**16. THE REMOVAL OF PHOSPHORUS FROM CONSTRUCTED WETLANDS,** Ing. Tereza Tůmová .....123

**17. THE STUDY OF THE INFLUENCE OF THE FORWARD SPEEDS OF A PATROL VESSEL ON THE BANKS OF THE CANALS IN THE DANUBE DELTA,** Assoc. Prof. Gabriel Popescu, PhD Costel Ungureanu, PhD Eugen Gavan .....131

**18. USING RISK MAPPING TO DETERMINE A MODERATE NATURE-BASED SOLUTION,** Ing. Brumar Jakub, Assoc. Prof Ing. Brumarova Lenka, Ph.D., Ing. Nela Kužílková .....139

**19. VOLUMETRIC QUANTIFICATION OF SOIL LOSS IN A PART OF THE MUNICIPALITY OF OTNICE IN THE CZECH REPUBLIC,** Lukáš Buršík, Prof. Dr. Miroslav Dumbrovský, Dr. Veronika Sobotková .....147

**20. WATER RESOURCE EFFICIENCY AND QUALITY MONITORING: A CASE STUDY OF SUCEAVA COUNTY'S DRINKING WATER SYSTEM,** Assoc. Prof. DSc. Anca Mihaela Gatlan, Assoc. Prof. DSc. Amelia Buculei, Prof. DSc. Mircea-Adrian Oroian, Assoc. Prof. DSc. Sorina Ropciuc, PhD Vasile-Florin Ursachi .....155

## MARINE, OCEAN, AND COASTAL ECOSYSTEMS. BLUE CARBON

**21. EVALUATION OF THE SURFACE WATER QUALITY PARAMETERS OF THE SF. GHEORGHE BRANCH - DANUBE DELTA, ROMANIA,** Dr. Irina Catianis, Dr. Ana Bianca Pavel, Dr. Florin Duțu, MSc. Cătălina Gavrilă, Ovidiu Borzan .....167

**22. INTEGRATED ANALYSIS OF SEAWATER INTRUSION DYNAMICS IN THE NORTHERN BLACK SEA COAST OF BULGARIA,** Assoc. Prof. Dr. Olga Nitcheva, Dr. Albena Vatralova, Research Assist. Donka Shopova, Assoc. Prof. Dr. Polya Dobreva .....175

## SOIL SCIENCE, CONSERVATION, AND LAND RESTORATION

**23. ASSESSMENT OF THE IMPACT OF COMPLEX FOLIAR FERTILIZERS ON CORN (ZEA MAYS L.) PRODUCTIVITY,** PhD Laura Crista, Prof. Dr. Florin Crista, Prof. Dr. Isidora Radulov , Assoc. Prof. Dr. Alina Lato, Assoc. Prof. Dr. Adina Berbecea .....187

**24. COMPARISON OF SOIL LOSS DUE TO WATER EROSION BEFORE AND AFTER A CHANGE IN AGRONOMIC PRACTICES,** Ing. Dávid Dežerický, PhD., Mgr. Ing. Marta Lenartowicz, Ing. Sára Daxnerová, Prof. Ing. Zlatica Muchová, PhD. .....195

**25. ASSESSMENT OF THE EFFECTS OF COMPLEX FOLIAR FERTILIZATION ON THE YIELD AND QUALITY OF SUNFLOWER SEEDS (HELIANTHUS ANNUUS L.),** Prof. Dr. Florin Crista, Prof. Dr. Florin Imbrea , Prof. Dr. Isidora Radulov , Dr. Laura Crista, Lecturer Alina Lato .....203

**26. GEOCHEMICAL TOOLS IN ENVIRONMENTAL STUDIES,** PhD Ramona Huzum, Doina Smaranda Sirbu-Radasanu, Delia-Georgeta DUMITRAS .....213

**27. GEOINFORMATION TERRAIN ANALYSIS FOR OPTIMIZING MILITARY EQUIPMENT ROUTES,** Prof. Oleksandr Trofymchuk, PhD Vyacheslav Vishnyakov, PhD Natalia Sheviakina, PhD Viktoriia Klymenko, PhD Snizhana Zahorodnia .....221

**28. PHYTOREMEDIATION OF ARSENIC CONTAMINATED SOILS OF THE AMBROLAURI MUNICIPALITY,** L. Shavliashvili, G. Kuchava, E. Shubladze, M. Tabatadze, S. Iram, E.Elizbarashvili .....229

## FOREST ECOSYSTEMS AND SUSTAINABLE FORESTRY

**29. THE EFFECT OF RIENTS FOLIAR FERTILIZATION WITH UREA UPON THE CONTENT OF MACRONUTIN CAMBIC CHERNOZEM,** Assoc. Prof. Dr. Alina Lato, Prof. Dr. Florin Crista, Assoc. Prof. Dr. Iaroslav Lato, Assoc. Prof. Dr. Alina Neacsu, Dr. Laura Crista .....247

**30. ASSESSING THE ROLE OF WINDBREAKS IN REDUCING WIND EROSION: REMOTE SENSING PERSPECTIVE,** Assoc. Prof. Dr. Lenka Lackóová, Dr. Mária Tárníková .....255

**31. DIVERSITY OF HYPERICUM L SPECIES IN ADJARA, GEORGIA,** PhD Ress Mariam Romanadze, Assoc. Prof. Dr. Inga Diasamidze, Dr. Gia Bolkvadze, Professor Davit Baratashvili, Associate Professor Eteri Jakeli. .....263

**32. DYNAMICS ASSESSMENT OF CHANGES IN FOREST COVER AREA ON THE UKRAINE TERRITORY IN THE 21TH CENTURY BASED ON SATELLITE DATA,** PhD. Alexander Apostolov, PhD. Lesya Yelistratova, Dmytro Todchuk, Igor Onopchuk .....269

**33. EFFECTIVE PROTECTION AGAINST PINE WEEVIL (*HYLOBIUS ABIETIS*) DAMAGES IN CONIFEROUS PLANTATIONS,** Uldis Grīnfelds, Liene Zēberga, Kristaps Ozoliņš, Raitis Rieksts – Riekstiņš, Linda Robalte .....277

**34. GROUND VEGETATION BIOMASS AND CARBON POOL IN HEMIBOREAL OLD-GROWTH CONIFEROUS STANDS ON ORGANIC SOILS,** Mg.silv. Valters Samariks, Mg.silv. Ieva Jaunslaviete, Mg.silv. Andis Adamovičs, Mg.silv. Sabīne Dubašinska, Dr.silv. Āris Jansons .....285

**35. MODELING LANDSCAPE PERMEABILITY USING FOREST PATCHES AND ENVIRONMENTAL VARIABLES,** Nicu Alexandru Gîlea, Ileana Patru-Stupariu, Mioara Clius .....295

**36. SIZE AND VITALITY CHARACTERISTICS OF STELLARIA HOLOSTEA L. PLANTS AND POPULATIONS IN DESNIANSKO-STAROHUTSKYI NATIONAL NATURE PARK,** Prof. Dr. Viktoriia Skliar, PhD Nataliia Yaroshenko, PhD Maryna Sherstiuk, Assoc. Prof. Yurii Skliar .....307

**37. SPECIES DIVERSITY OF HARMFUL BARK BEETLES IN SPRUCE FORESTS OF ADJARA REGION (GEORGIA),** PhD Ress Nino Manvelidze, Prof. Dr. Medea Burjanadze, Assoc. Prof. Dr. Lali Jgenti, Assoc. Prof. Dr. Natela Varshanidze .....315

**38. STRUCTURAL CONNECTIVITY ANALYSIS IN THE CARPATHIAN ECOREGION: PRELIMINARY STEPS FOR DEVELOPING LANDSCAPE NETWORKS,** Radu Tudor, Ileana Patru-Stupariu, Ancuța Fedorca, Mirea Marian .....321

**39. TAXONOMIC STRUCTURE OF THE NEMATODE COMMUNITIES IN AGROECOSYSTEMS OF SHUAKHEVI (AJARA, GEORGIA),** Prof. Dr. Eka Tskitishvili, Assoc. Prof. Dr. Lali Jgenti, Prof. Dr. Nino Lomidze, Tengiz Vadachkoria .....331

**40. VEGETATION OF SMALL-LEAVED LIME TILIA CORDATA MILL. FOREST STANDS IN LATVIA,** Prof. Inga Straupe, PhD Patriks Kikusts, PhD Diana Jansone, Prof. Dr. Aris Jansons .....339

## SUSTAINABLE OIL, GAS, AND ENERGY TRANSITION EXPLORATION

**41. BEST AVAILABLE TECHNIQUES IN OIL AND GAS EXPLORATION: OPPORTUNITIES FOR POLLUTION PREVENTION AND CLIMATE CHANGE MITIGATION,** Dr. Sci. Dmitry Skobelev, PhD Maria Dobrokhotova, PhD Natalia Popadko, Mrs. Yuliya Ukhina, PhD Rauf Ismayilov .....349

**42. NATIONAL GREENHOUSE GAS EMISSION FACTORS AT OIL AND GAS CONDENSATE PRODUCTION AND TREATMENT FACILITIES IN RUSSIAN FEDERATION,** PhD. Nakhutin Alexander, Popov Nikita, Berdin Vladimir, Mironov Andrey, Uledova Anastasia, Kozlova Daria, Karimova Kamila, Simonyan Elen .....357

**43. PHASE BOUNDARY EQUILIBRIUM CONDITIONS FOR CH4, C2H6 AND C3H8 IN MARINE QUARTZ-BASED POROUS SAND: THERMODYNAMIC EVOLUTION OF THE SYSTEM AND DEVIATION FROM THE IDEAL TREND,** Dr. Alberto Maria Gambelli, Dr. Jessica Di Mario, Full Prof. Enrico Gigliotti.....367

**44. PRODUCTION OF sI AND sII HYDRATES WITH BINARY MIXTURES CONTAINING $CH_4$ AND LOWER CONCENTRATIONS OF $C_2H_6$/$C_3H_8$: POSSIBLE CONSEQENCES ON REPLACEMENT IN MARINE NATURAL DEPOSITS,** Dr. Alberto Maria Gambelli, Dr. Jessica Di Mario, Prof. Dr. Giovanni Gigliotti .....375

**45. SMALL UAV SYSTEMS CAPABLE OF CARRYING OUT ECONNAISSANCE MISSIONS TO DETECT LEAKS IN OIL AND GAS PIPELINES, AIMING TO LIMIT ACCIDENTAL ENVIRONMENTAL POLLUTION,** Senior lecturer Eng. Ștefan-Mircea Mustață – PhD., Third degree researcher Eng. Cristian Vidan – PhD., Eng. Ionuț-Mihai Nacu– PhD Ress .....383

**46. ADVANCES IN DROP-IN SUSTAINABLE AVIATION FUELS (SAF): PATHWAYS, CHALLENGES, AND FUTURE DIRECTIONS,** Dr. Odi Alrebei.....391

**47. STRATEGIC SOCIO-ENVIRONMENTAL ASSESSMENT: KEY PPROACHES AND PROSPECTS IN THE PETROLEUM EXPLORATION SECTOR,** Assoc. Prof. Dr. Irina Tikhonova.....397

**48. TECHNO-ECONOMIC ASPECTS OF LITHIUM RECOVERY FROM OILFIELD BRINES USING 3D PRINTED SORBENTS,** Przemysław Ziemba, Ewa Knapik .....405

# SECTION

# HYDROLOGY, WATER RESOURCES,

# AND CLIMATE RESILIENCE

# ANALYSIS OF FACTORS AND CLUSTERS IN THE FISHERIES INDUSTRY IN THE EUROPEAN UNION

**Mg.oec. Agnese Eizenberga**

Latvia University of Life Sciences and Technologies, **Latvia**

## ABSTRACT

The global fisheries industry is growing rapidly and providing an increase in food security for the world's population. Therefore, decision-making plays a key role in national development, which influences national policies across Europe. Effective management can differentiate countries from each other and change the intense growth of economic, technological and social competition. The aim of this study is to identify clusters in the fisheries sector in the European Union. To achieve this objective, a factor and cluster analysis was designed with the use of IBM SPSS software. The analyses were carried out for the 26 European Union Member States on the basis of 18 factors identified by the author, based on fishery parameters (production, fishing vessel data, employment), various social, economic and financial factors, including demographic data, household expenditure, DESI, etc., which provide a profile of each of the selected EU Member States. Data were provided from the EU databases for the same period of time. The author has developed an analysis of the factors and clusters of the fisheries sector in the European Union Member States and has concluded that there are differences in the fisheries sector in the different EU countries, depending on territorial specifics, environmental and sustainability problems. But, in order to address these problems more successfully, a solution is proposed for the promotion of fisheries business development, which would create jobs and reduce unemployment in the country, as well as boost the increase in fish haul as a food resource. This could promote more successful work of Member States involved in the development of fisheries policy and improve the Common Fisheries Policy.

**Keywords:** Fisheries, Environmental, Sustainability, Fisheries policy, EU, Cluster analysis, Factor analysis

## INTRODUCTION

The global fisheries sector is developing rapidly and providing ever more food for the population of the world, therefore, development decision-making on a national level plays a key role in influencing national policies across Europe. Effective management can differentiate countries from each other and change the intense growth of economic, technological and social competition [9]. In the Member States of the European Union, the development of fisheries is influenced by the Common Fisheries Policy, which aims to achieve environmentally sustainable fisheries and aquaculture activities [5], and to provide benefits to economic, social and employment sectors, as well as at promoting food availability [1].

The situation of fisheries in the EU can vary significantly depending on several factors, including fish stock status, fishing practices, and regulatory measures [7]. The European Union has been working to ensure sustainable fishing practices [4] through the Common

https://doi.org/10.5593/sgem2024v/3.2/s11.01

Fisheries Policy (CFP) regulations. Key points about the fisheries situation in the EU include:

1. *Sustainability:* The EU aims to manage fish stocks sustainably, with many fisheries undergoing assessments to determine their health and sustainability.
2. *Stock Status:* Many fish stocks in EU waters have been overfished, but there have been improvements in some areas due to strict quotas and conservation measures.
3. *Regulation:* The CFP includes measures to promote sustainable fishing, including catch limits, technical measures, and efforts to reduce by catch.
4. *Economic Impact*: Fisheries are vital for many coastal communities in the EU, providing jobs and supporting local economies.
5. *Environmental Concerns:* Overfishing, habitat destruction, and climate change are ongoing challenges for EU fisheries.

The environmental impacts of the fisheries sector are significant and multifaceted. Key aspects to consider is overfishing and bycatch, habitat destruction, water pollution, climate change, aquaculture (raises environmental concerns, including water quality issues, habitat destruction, and the spread of disease), regulatory measures and ecosystem-based management [8]. Addressing these environmental issues is crucial for the sustainability of the fisheries sector and the health of marine ecosystems [3]. Efforts to promote sustainable practices can help mitigate negative impacts and ensure that fisheries can thrive for future generations.

The notion of sustainable development is sometimes regarded as an unattainable, even illogical notion because development inevitably depletes and degrades the environment. However, when human dimensions of fishery management include cultural, social, and economic values; individual and social behaviour; demographics; legal and organizational frameworks of management; communication, education, and citizen participation, and decision-making processes, then sustainable fisheries may be possible [2].

When analysing the overall fisheries situation in the European Union, it is essential to conduct an in-depth analysis of fisheries in order to identify these countries, where the promotion of the development of fisheries is particularly important. The demand for this is determined by technological, economic and social conditions, which are differentiated across the Member States of the European Union [6]. Factor analysis and cluster analysis were used to identify potential problem areas in the European Union Member States from the perspective of fisheries management. Factor analysis is an analytical technique that has been extensively used by various social scientists [10]. Factor analysis is data reduction method in which many variables are chosen initially, and they are explained by a few “factors” or “components” [11]. Conversely, cluster analysis can be a valuable tool in fisheries management and research. It can help in stock assessment and sustainability of different fish stocks and analysing environmental [12] data.

## MATERIALS AND METHODS

To achieve the objective of the research, factor and cluster analysis was performed with the use of IBM SPSS software. Factor and cluster analysis was carried out for the 26 European Union Member States on the basis of 18 factors identified by the author,

based on fishery parameters (production, fishing vessel data, employment), various social, economic and financial factors, including demographic data, household expenditure, DESI, etc., which provide a profile of each of the selected EU Member States. Data were sourced from Statista, Eurostat, OECD and World Bank databases. Data for 2023 were collected. Analysis, synthesis, the logical construction method, the induction and deduction methods were employed to execute the research tasks. Scientific literature review was used as well.

## RESULTS

Application of factor analysis - 18 variables for 26 European Union Member States were produced. Such extensive matrix of information is inefficient and cannot be described for analysis, therefore, it is important to establish correlations between the initial characteristics and to obtain a smaller number of factors to be studied, which can be used to assess the fisheries situation in the European Union. The use of factor analysis is justified by the Kaiser-Meyer-Olkin (0.529) and Bartlett test ($\alpha<0.05$) values (see Figure 1).

KMO and Bartlett's Test

| | | |
|---|---|---|
| Kaiser-Meyer-Olkin Measure of Sampling Adequacy. | | 0.529 |
| Bartlett's Test of Sphericity | Approx. Chi-Square | 561.675 |
| | df | 136 |
| | Sig. | 0.000 |

Source: SPSS Output

Figure 1 KMO and Bartlett's Test results

The KMO test statistic indicates whether the bias correlation between the variables is strong enough, and the Bartlett sphericity test is used to determine variables, and if the data are independent of each other, then it will not be possible to condense the original variables. Therefore, when using factor analysis to analyse each weight index, it is necessary to use methods such as Bartlett's spherical test and KMO test to test the original data. Before applying factor analysis, first the value of KMO which measures whether distribution of values is adequate for conducting factor analysis is considered. Kaiser designates level. A measure >0.8 is meritorious, in this case 0.802, this is meritorious. Barlett Test of Sphericity is a measure of multivariate set of normality of distributions. It also checks whether the condition matrix is an identity matrix or not. (Factor analysis is meaningless without Identity matrix). A significant value <0.05 indicates this data do not produce an identity matrix and thus multivariate normal and acceptable for factor analysis. In this case, Barlett Test value is 0.00<0.05, so set of distributions multivariate normal and acceptable for factor analysis.

Factor analysis yielded four complex factors that explain 77.7% of the total set of variables. This is considered a very good indicator, given the fact that 22.3% of the total variance of the data of the 18 original variables was lost. To enable higher probability of defining which variables make up each of the two complex factors, a rotated factor

https://doi.org/10.5593/sgem2024v/3.2/s11.01

matrix was calculated with the use of a variance-maximising (varimax) rotation method (see Figure 2).

| Component Transformation Matrix | | | | |
|---|---|---|---|---|
| **Component** | 1 | 2 | 3 | 4 |
| **Fisheries factor** | 0.817 | -0.558 | -0.105 | -0.101 |
| **Economy factor** | 0.566 | 0.729 | 0.313 | 0.225 |
| **Social factor** | -0.111 | -0.387 | 0.841 | 0.362 |
| **Financial factor** | -0.005 | -0.089 | -0.429 | 0.899 |
| Extraction Method: Principal Component Analysis. Rotation Method: Varimax with Kaiser Normalization. | | | | |

Source: SPSS Output

Figure 2 Component Transformation Matrix results

In the further study, it is important to identify those European Union Member States, where the promotion of the development of fisheries is essential, based on the four complex factors that have been identified. This was done with the use of a clustering method.

To determine the statistical significance of complex factors, an analysis of variance (ANOVA) was performed, the results of which show that the factors used in the clustering are statistically significant (significance does not exceed 0.05). Meanwhile, the identification of the number of clusters was based on Elbow rule. According to that, the optimal number of clusters was found to be 7. The analysis was repeated with the use of K-means clustering.

When evaluating the European Union Member States according to the factor values obtained from the factor analysis, they can be divided into seven groups or clusters - the first cluster includes 3 countries, the second cluster consists of 1 country, the third cluster includes 5 countries, the fourth cluster includes 2 countries, the fifth cluster contains 1 country, the sixth cluster includes 7 countries, and the seventh cluster includes 8 countries. Standard deviations and means were calculated for each cluster (see Figure 3).

| Final Cluster Centers | | | | | | | |
|---|---|---|---|---|---|---|---|
| | Cluster | | | | | | |
| | 1 (Bulgaria, Croatia, Romania) | 2 (Spain) | 3 (Poland, Greece, France, Italy, Portugal) | 4 (Malta, Netherlands) | 5 (Luxembourg) | 6 (Estonia, Latvia, Denmark, Ireland, Austria, Finland, Sweden) | 7 (Czech Republic, Lithuania, Hungary, Slovevia, Slovakia, Cyprus, Belgium, Germany) |
| Fisheries factor | -0.33557 | 4.02766 | 0.85830 | -0.29583 | 0.06514 | -0.42912 | -0.47276 |
| Economy factor | -0.36569 | 0.15479 | -0.40318 | 0.37555 | 4.61284 | -0.32768 | -0.01400 |
| Social factor | -1.92102 | 0.39474 | -0.32531 | 0.53663 | -0.09051 | 1.01294 | -0.13481 |
| Financial factor | -0.26189 | 0.49012 | -0.56227 | 2.72299 | -0.75807 | -0.51276 | 0.25104 |

Source: SPSS Output

Figure 3 Final Cluster Centre results

## DISCUSSION

Four complex factors influence the development of the Member States of the European Union. The first is defined as the "fisheries factor group", as it includes indicators that are primarily representative of fisheries and thus primarily determine their relevance. The second complex factor is related to economic activity and is therefore defined as a "group of economic factors". The third is defined as the "social factors group", as it includes indicators that are mainly characteristic of social factors. Meanwhile the fourth complex factor is related to financial activity and is therefore defined as a "group of economic factors". Factor analysis confirms the differences that determine the differentiation in fisheries management.

By using the principle of mutual comparison of the groups, it was found that each cluster can be assessed in accordance with the characteristics of the situation in the cluster. The first group of factors - the fisheries factor group - is the most important, as it is the primary determinant of the relevance of fisheries. Based on this principle, the clusters are grouped and defined as follows:

Cluster 1: depressive cluster in terms of fisheries. This cluster includes Bulgaria, Croatia and Romania. Fisheries in these countries are less developed than in the Western European maritime powers, therefore, it is singled out as a separate cluster. The fish species available in these countries are limited and sustainability problems exist, for instance, overfishing and pollution. The countries of this cluster share a common desire to expand and develop sustainable fishery and aquaculture methods to reduce the impact of overfishing and pollution, while ensuring the livelihood of coastal communities. European Union funds and initiatives are helping to upgrade the sectors of fisheries and aquaculture to improve sustainability and efficiency in these countries.

Cluster 2: active cluster in terms of fisheries. The sole representative of this cluster is Spain. The cluster is characterised by traditional fishery and fish processing, which are the main types of occupation in Spain. Spain is one of the largest fishing nations in Europe, with fisheries covering both the Atlantic and the Mediterranean, and accounting for a significant share of total fishing haul of Europe. But it should be emphasised that economic and social activity is neither explicitly high nor low. To address economic and social challenges, it would be important to promote the development of traditional entrepreneurship.

Cluster 3: positive cluster in terms of fisheries. This cluster includes Poland, Greece, France, Italy and Portugal - countries with a rich history of fishing and a tradition of exploiting marine resources. In Poland, for instance, fish processing is a very important part of fisheries sector, contributing to the efficient use of fish resources, as well as providing jobs for the population. Fisheries sector is also important for Greece - aquaculture has become one of the most important pillars of the Greek fisheries sector. The countries of this cluster are taking action to improve the sustainability of their fisheries sector through quotas, seasonal bans and support to aquaculture. Like elsewhere in the European Union, the sector here is tightly regulated to preserve resources for future generations. Aquaculture is an important resource in all these countries, offering a sustainable alternative in the context of the growing demand for fish and seafood. Given the current financial and economic problems in the cluster, the issue of fisheries entrepreneurship development with public participation is becoming urgent, as promotion of economic integration is important.

https://doi.org/10.5593/sgem2024v/3.2/s11.01

Cluster 4: neutral cluster in terms of fisheries. This cluster consists of Malta and the Netherlands. This cluster is characterised by a high financial background and a low fishery background. This means that the fisheries activity is insufficient to provide jobs for the population, but the financial factor bears evidence of a financially stable situation in the country. The cluster shares a common approach to promoting sustainability through implementing fisheries regulations, sustainable practices and the development of aquaculture. Malta specialises mainly in Mediterranean tuna and fish farming, while the Netherlands is active in North Sea fishing and shellfish farming. Both countries are parties to the European Union regulatory framework, which helps to ensure the long-term protection of resources.

Cluster 5: insignificant cluster in terms of fisheries. The cluster consists of only one country - Luxembourg. This cluster is represented by a landlocked country with no direct access to the sea and, consequently, no traditional marine fisheries. The fisheries sector in this cluster is very small and consists mainly of freshwater aquaculture and angling in inland waters such as rivers and lakes. This cluster can therefore be considered insignificant in terms of fisheries, but the economic factor in this cluster is higher than in any other cluster.

Cluster 6: the cluster that requires improvement in fisheries sector. The cluster consists of Estonia, Latvia, Denmark, Ireland, Austria, Finland and Sweden, which differ among themselves in scale, main fishing resources and fishing methods. These countries have a variety of coastal and inland water resources, which account for the differences in the approaches to fisheries and aquaculture. These countries observe sustainability principles to preserve fish resources for the future, and most of them have introduced quotas, seasonal bans and aquaculture practices. The Nordic countries and the coastal countries of the Baltic Sea focus on the fishing in the Baltic Sea and the North Sea, while Austria, as a landlocked country, only deals in freshwater aquaculture. Aquaculture is an important alternative to natural fishing in all of these countries and helps to reduce the pressures on wild fish populations. It is therefore important to promote the entrepreneurial fishing activity in the countries of this cluster with the objective of developing their fisheries sector.

Cluster 7: negative cluster in terms of fisheries. This cluster consists of the Czech Republic, Lithuania, Hungary, Slovenia, Slovakia, Cyprus, Germany and Belgium. The fisheries sectors in this cluster are diverse, because the countries of this cluster cover the Baltic coast, inland waters and Mediterranean regions. In these countries, the fisheries sector is based on local resources, freshwater fishing and aquaculture, with different degrees of contribution to the local economy and market. Within this cluster, fisheries differ in terms of scale and resource availability: The Baltic and North Sea countries (Lithuania, Belgium, Germany) focus on coastal and marine fishing, while the landlocked countries (the Czech Republic, Hungary, Slovakia) rely on freshwater aquaculture. Cyprus and Slovenia, with access to the Mediterranean and the Adriatic, are involved in small-scale fishing but are also developing marine aquaculture. Overall, sustainability and EU regulations are relevant in all countries and aquaculture is becoming an important part of the fisheries sector.

## CONCLUSION

The results of factor analysis and clustering bear evidence that fisheries in some Member States of the European Union are underdeveloped. The development of the fisheries sector in these countries would require efficient and innovative solutions. Fisheries entrepreneurship is one way of harvesting fish resources and boosting business activity. Considering the fact that fisheries issues are relevant to several clusters of European Union Member States, the approach to addressing these issues requires additional research to develop scenarios of fisheries development that can be adapted for implementation in all EU Member States. The most important strengths for the development of fisheries in the European Union are the high untapped potential of labour resources and the capacity of the population to set up businesses in the fisheries sector. These are key prerequisites for successful promotion of fisheries business. Equivalent strengths include an interest in sustainable, environmentally friendly approaches to fisheries business. The most important factor that interferes with the development of the fisheries business is the lack of workforce employed in fisheries sector. The equal importance of these factors is based on the fact that not only national stimulation of fisheries is of importance, but also the ability of individuals to take the initiative. Lack of information and knowledge about fisheries is also an important factor that prevents the expansion of fisheries business. The most important opportunity from the development of the fisheries business is the reduction of unemployment in the country, as well as the contribution of fish as a food resource. This will contribute to increasing people's purchasing power for fish and to the balanced and integrated development of the national fisheries sector.

## ACKNOWLEDGEMENTS

This study was prepared by the Latvia University of Life Sciences and Technologies research project "Sustainable solutions for Development of the aquaculture sector in Latvia", research grant No. DG6, contract No 3.2-10/202.

## REFERENCES

[1] Gray T., Fisheries science and sustainability in international policy: a study of failure in the European Union's Common Fisheries Policy, Marine Policy, United Kingdom, vol. 29/issue 3, pp 189-197, 2005.

[2] Huertos M.N., Developing and Appropriating Water, Ecology and Management of Inland Waters, United Kingdom, vol. 3, pp 283-313, 2020.

[3] Berkes F., Implementing ecosystem-based management: evolution or revolution?, Fish and Fisheries, United Kingdom, vol. 13/ issue 4, pp. 465-476, 2012.

[4] Khalilian S., Froese R., Proelss A., Designed for failure: A critique of the Common Fisheries Policy of the European Union, Marine Policy, United Kingdom, vol. 34/issue 6, pp 1178-1182, 2010.

[5] Hadjimichael M., A call for a blue degrowth: Unravelling the European Union's fisheries and maritime policies, Marine Policy, United Kingdom, vol. 94, pp 158-164, 2018.

[6] Eikeset A.M., Mazzarella A.B., Davíðsdóttir B., Klinger D.H., Levin S.A., Rovenskaya E., Stenseth N.C., What is blue growth? The semantics of "Sustainable

Development" of marine environments, Marine Policy, United Kingdom, vol. 87, pp 177-179, 2018.

[7] Carvalho N., Casey J., Guillen J., Rodgers P., Characterising investments in EU fisheries and defining their desirability, Fisheries Research, Netherlands, vol. 221,105396, 2020.

[8] Safina C., Duckworth A., Guillen J., Rodgers P., Fish Conservation, Encyclopedia of Biodiversity (Second Edition), Reference Module in Life Sciences, United States, pp 443-455, 2013.

[9] Matthess M., Kunkel S., Structural change and digitalization in developing countries: Conceptually linking the two transformations, Technology in Society, United Kingdom, vol. 63, 101428, 2020.

[10] Babu S.C., Gajanan S.N., Impact of market access on food security—application of factor analysis, Food Security, Poverty and Nutrition Policy Analysis (Third Edition), United Kingdom, pp 169-218, 2022.

[11] Weiss A., Adams M.J.., Personality, Temperament, and Behavioral Syndromes, Encyclopedia of Behavioral Neuroscience, pp 47-53, 2010.

[12] Frawley T.H., Muhling B., Welch H., Seto K.L., Chang S.K., Clustering of disaggregated fisheries data reveals functional longline fleets across the Pacific, One Earth, United States, vol. 5/ issue 9, pp. 1002-1018, 2022.

# APPLICATION OF DRONE TECHNOLOGY FOR FLOOD RISK MONITORING AND MODELING

**Mg. sc. Ing. Toms Lidumnieks**[1,2]
**Prof. Dr. sc. ing. Armands Celms**[1]
**Mg. geogr. Ivars Bergmanis**[1,2]
[1] Latvia University of Life Sciences and Technologies, **Latvia**
[2] Latvian Geospatial Information Agency, **Latvia**

## ABSTRACT

The increasing frequency and intensity of flood events necessitate innovative approaches for effective monitoring and modeling to mitigate risks. This article explores the application of drone technology in flood risk management, highlighting its advantages over traditional methods. Drones equipped with high-resolution cameras and advanced sensors can rapidly collect spatial data, enabling detailed topographic assessments and hydrological modeling. Their ability to access hard-to-reach areas allows for real-time monitoring of flood-prone regions and infrastructure, improving response times during emergency situations. Case studies illustrate the successful use of drones in flood risk assessment, mapping, and data validation, demonstrating their potential to enhance decision-making for urban planning and disaster preparedness. Drone applications in flood management encompass a range of functionalities that enhance monitoring, modeling and response strategies.

Drones helps and use for Data collection and mapping; Real time monitoring; Risk assessment; Damage assessment - this rapid assessment supports emergency response efforts and aids in recovery planning; Enviromental monitoring; Drones could integrate with other technologies - Geographical information systems (GIS) and data analytics tools to enhance flood modeling and prediction capabilities. The integration of aerial imagery and remote sensing data into flood models underscores the transformative role of drone technology in building resilient communities against flooding. This article emphasizes the need for further research and collaboration across disciplines to optimize drone applications in flood risk management.

The aim of the research is Examine modern drone technologies and their application in flood risk monitoring; The adoption of drone technology in flood management provides a cost - effective, efficient, and innovative approach that significantly enchances preparednes and resilience against flooding events. To fulfill the research aim, certain objectives must be completed: 1. Evaluate currently available drone sensors and their use in data collection for flood modeling; 2. Assess the processes involved in modern flood risk monitoring and modeling; 3. To analyse the area of Latvia that are currently most exposed to flood risk and to assess what are the key conditions that contribute to them; 4. Evaluate the integration of drone technologies and their data into a modern flood monitoring and modeling system.

**Keywords:** Application of Drones, Unmanned Aerial Vehicles Drone Technologies, Flood Risk Management, Drone Monitoring, Flood risk monitoring, Water level modeling.

https://doi.org/10.5593/sgem2024v/3.2/s11.02

## INTRODUCTION

In recent years, the increasing frequency and intensity of flooding events due to climate change and urbanization have significantly heightened the need for effective flood risk monitoring and management strategies. Traditional methods of flood assessment, including ground surveys and satellite imagery, often fall short in providing the timely and detailed data necessary for accurate risk modeling. In this context, drone technology has emerged as a transformative tool that enhances our ability to monitor, model, and mitigate flooding risks [4].

Drones, or unmanned aerial vehicles (UAVs), are equipped with high-resolution cameras, LiDAR sensors, and thermal imaging capabilities that allow for rapid data collection over large areas. This technology enables real-time analysis of flood-prone regions, facilitating the early detection of changes in land use, water levels, and vegetation that contribute to flood risks. Drones can also capture detailed topographical information, which is crucial for hydrological modeling and predicting flood behavior.

The integration of drone technology into flood risk management offers numerous advantages, including cost-effectiveness, accessibility to hard-to-reach areas, and the ability to conduct frequent monitoring without the risk to personnel. Additionally, the data obtained from drones can be used to enhance predictive models, improving the accuracy of flood forecasts and supporting decision-makers in implementing timely interventions.

The application of drone technology for flood risk monitoring and modeling represents a significant advancement in our ability to understand and manage flood risks effectively. By harnessing this innovative technology, communities can build resilience against flooding, ultimately safeguarding lives, property, and the environment. As the field evolves, continued research and development will further enhance the capabilities and applications of drones in flood risk management.

## MATERIALS AND METHODS

The probability and assessment of flood risks is considered in Latvia and in general depending on the terrain and land surface characteristics. The most significant cities in Latvia in 2024, where floods were observed, are Jelgava, Jurmala, Riga, Jekabpils. This study examines the possible possibilities of flooding - precipitation, disorganized drainage system, city location, terrain, etc. Possible solutions and methods for obtaining data, monitoring the situation about the area where the flood risk has occurred can be assessed in real time, which is very useful for emergency services - rescue services, which would be able to deal with predicted actions and save endangered places, houses, property. Extreme rainfall has occurred in central Latvia. The amount of water in many river basins increased – such as Lielupe, Gauja, Daugava. It is important to observe long – term water fluctuations in rivers, climate indicators, and weather forecasts [6].

Sensors types – LIDAR (light, laser); Thermographicl camera sensor (Temperature, Heat); ECHO sounder sensors for depths (Sound waves); AI (Artificial intelligent) algorithms – can serve as an efficient tool to assist monitoring, mapping and detection. Sensors are planted to obtain data that can then be processed and used for modeling; Sensors map and monitor the situation on the ground (in real time); Data collection after flood prevention helps to see the consequences of floods [1].

LIDAR is a remote sensing data technology, works on physical quantity – light. This process get Digital Earth or Surface models, than is possible to create elevation 3D models and maps [9].

An ECHO sounder is device to measure the depth of water. The results of depth measurements using an echo sounder or bathymetric survey can be presented in several forms [11].

Thermographical sensors (camera) – physical quatity – heat, temperature; Water is detected with a thermal imager due to temperature differences caused by evaporation, capacitance or conduction, and these processes can be affected by weather conditions or humidity [10].

Data acquisition and forecasting require the collection of high-resolution photos and point clouds, which can then be processed with photogrammetry computer programs Pix4D, QGIS, ARCGIS - Geographic Information System analysis tools are very useful [5].

The use of drones in assessing the situation is fast, but the effects and approach of floods can be assessed quite successfully by looking at satellite images. In the city, protective barriers, dams, and structures are being implemented to ensure preventive civil protection –Flood forecasting is done with cameras; Rainfall/ humidity sensors; Monitoring of water level observation points; Rip rap seawall; Glass wall barriers [7].

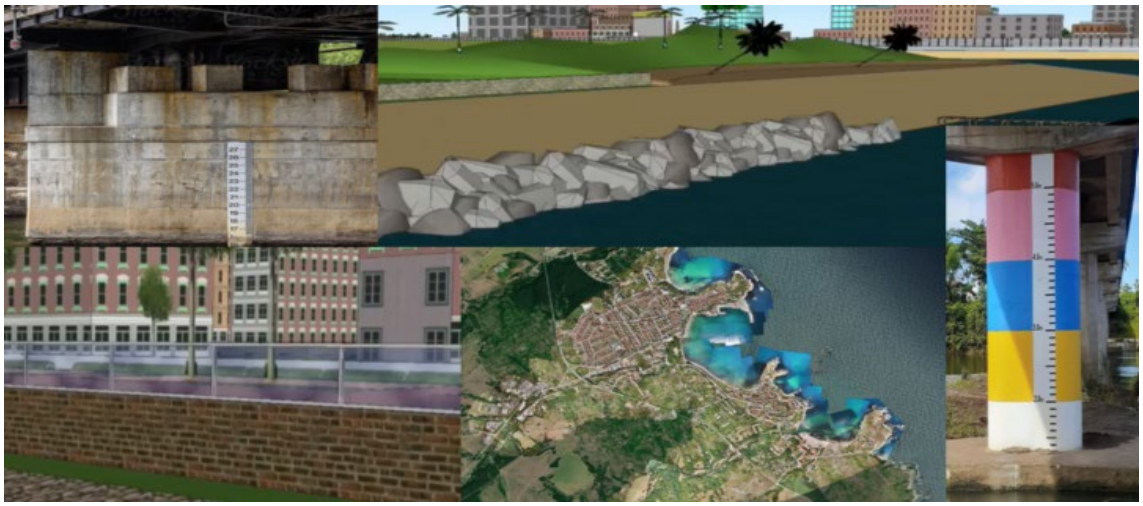


Figure 1.*Protective structures in the city against increasing floods*

## RESULTS

Drones have the potential to be valuable tools in flood risk management. Drones can provide fast and accurate information on flood extent, damage and rescue operations. However, it is important to develop strategic guidelines and protocols to ensure the effective and responsible use of drones [15].

The obtained data can be used to analyze and validate the hydrological model, terrain, and predict the movement of water volume [8].

The territory of Latvia is relatively low above sea level. 57% of Latvia's territory is located below 100 metres below sea level [14].

https://doi.org/10.5593/sgem2024v/3.2/s11.02

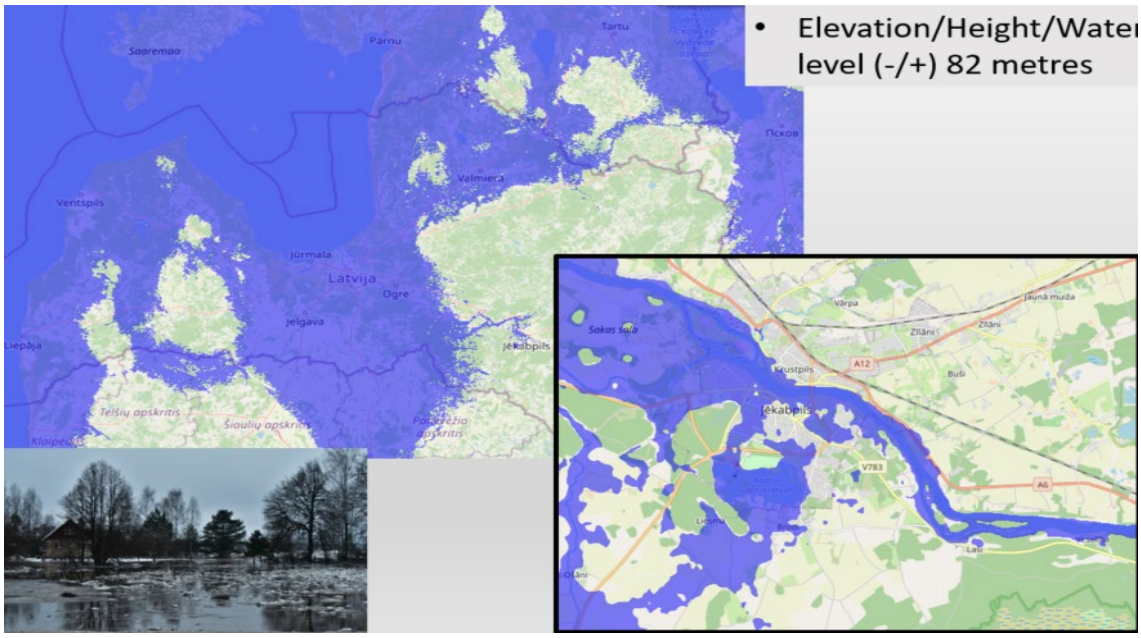



Figure 2. *Flood forecast for the territory of Latvia with a water level +/- 82 metres [13]*

Climate change in nature requires thoughtful human action in all areas of life. Risks that used to occur every 100 years are already occurring much more frequently. In the future, the disaster management industry will see several emerging trends that will have a profound impact on the adoption and market demand for UAV technology. Future technologies includes machine learning – Artifical Inteligence, Drones can detect the emergency so fast and in real time [2].




Figure 3. *Flood forecast for the territory of Latvia with a water level +/- 20 metres [13]*

## DISCUSSION

Flood risk zones are formed depending on various geospatial parameters; Important are slope, soil, geological structure, texture, relief, topography surface, vegetation. Important are the drainage system and its maintenance, ditch network.

Flooded areas block roads, flood inhabited resident buildings, and overflow yards. This type of emergency situation forces civilians to evacuates in many places. Evacuation plans must be developed, and temporary situations must be addressed in the field of civil defense.



Figure 4. *Flood modelling and monitoring is important in crisis and risk management*

## CONCLUSION

The impact of a flood on the environment, whenever it occurs, is usually very difficult to quantify, as is the extent of damage and the number of casualties. Traditional methods for conducting these surveys are typically time – consuming and costly, resulting in a longer time to save an individual than anticipated. Furthermore, the collection of water flow parameters via buoyancy, installation, and data acquisition is complicated and costly, and its area of coverage is typically too limited to the real – world scale. As a result, there is a need for a simpler, more time- saving, and more cost – effective alternative means of acquiring data for rapid and effective flood warning and management. Drones have had a broader interest in many application in recent years, due to their mobility and economic advantages. In relation to flood assessment, drones are held highly on: Easily deployable; Mapping; Quality aerial imagery; Precision; Minimizes obvious danger and health risks [1,3].

Geophysical sensors are widely used in many different types of industries – agriculture, environmental and earth engineering, geology, engineering geodesy, surveying, military, sustainable maintenance of renewable energy, relief, topography modelling.

The most important points to consider when assessing risk and emergency situations are: 1. The use of drones in the economy and various civilian sectors is increasingly widespread. In the military, agriculture, environmental maintenance, and ensuring sustainable processes; 2. Different types of solutions in the applications of drone

https://doi.org/10.5593/sgem2024v/3.2/s11.02

technology allow for further research into each of them; 3. By modelling the shape of the terrain, fluctuations in water level on the surface can be predicted; 4. The principles of drone operation work according to the most basic laws and relationships of physics (light, sound, radio waves).

## REFERENCES

[1] Salmoral, G., Rivas Casado, M., Muthusamy, M., Butler, D., Menon, P. P., & Leinster, P. (2020). Guidelines for the Use of Unmanned Aerial Systems in Flood Emergency Response. Water, 12(2), 521. https://doi.org/10.3390/w12020521;

[2] Zhonghan Chen, (2024). Application of UAV remote sensing in natural disaster monitoring and early warning: an example of flood and mudslide and earthquake disasters. Highlights in Science, Engineering and Technology, Volume 85, 10p;

[3] H. R. Spero, I. Vazquez-Lopez, K. Miller, R. Joshaghani, S. Cutchin & J. Enterkine (2022) Drones, virtual reality, and modeling: communicating catastrophic dam failure, International Journal of Digital Earth, 15:1, 585-605, DOI: 10.1080/17538947.2022.2041116;

[4] Iqbal, U.; Riaz, M.Z.B.; Zhao, J.; Barthelemy, J.; Perez, P. Drones for Flood Monitoring, Mapping and Detection: A Bibliometric Review. *Drones* 2023, *7*, 32. https://doi.org/10.3390/ drones7010032;

[5] Mohamed Saber, Tayeb Boulmaiz, Mawloud Guermoui, Karim I. Abdrabo, Sameh A. Kantoush, Tetsuya Sumi, Hamouda Boutaghane, Tomoharu Hori, Doan Van Binh, Binh Quang Nguyen, Thao T. P. Bui, Ngoc Duong Vo, Emad Habib & Emad Mabrouk (2023) Enhancing flood risk assessment through integration of ensemble learning approaches and physical-based hydrological modeling, Geomatics, Natural Hazards and Risk, 14:1, 2203798, DOI: 10.1080/19475705.2023.2203798;

[6] Seyed Vahid Razavi-Termeh, Abolghasem Sadeghi-Niaraki, Saman Razavi & Soo-Mi Choi (2024) Enhancing flood-prone area mapping: fine-tuning the K-nearest neighbors (KNN) algorithm for spatial modelling, International Journal of Digital Earth, 17:1, 2311325, DOI: 10.1080/17538947.2024.2311325;

[7] Woo H-J, Seo D-M, Kim M-S and Lee H-K (2024) Development of methodology for calculating flooded area and flood volume in small urban areas based on unmanned aerial vehicle images. Front. Built Environ. 10:1482330. doi: 10.3389/fbuil.2024.1482330;

[8] Backes, D., Schumann, G., Teferle, F. N., and Boehm, J, (2019). TOWARDS A HIGH-RESOLUTION DRONE-BASED 3D MAPPING DATASET TO OPTIMISE FLOOD HAZARD MODELLING, Int. Arch. Photogramm. Remote Sens. Spatial Inf. Sci., XLII-2/W13, 181–187, https://doi.org/10.5194/isprs-archives-XLII-2-W13-181-2019;

[9] Emilia Karamuz, Renata J. Romanowicz, Joanna Doroszkiewicz. (2019), The use of unmanned aerial vehicles in flood hazard assessment, Chartered Institution of Water and Environmental Management, Journal of Flood Risk Management Wiley, 12pp, DOI: 10.1111/jfr3.12622;

[10] Trepekli, K., Balstrøm, T., Friborg, T. et al. UAV-borne, LiDAR-based elevation modelling: a method for improving local-scale urban flood risk assessment. Nat Hazards 113, 423–451 (2022). https://doi.org/10.1007/s11069-022-05308-9;

[11] Clasing, R.; Muñoz, E.; Arumí, J.L.; Parra, V. Remote Sensing with UAVs for Flood Modeling: A Validation with Actual Flood Records. *Water* 2023, *15*, 3813. https:// doi.org/10.3390/w15213813;

[12] Rizk, H., Nishimur, Y., Yamaguchi, H., & Higashino, T. (2022). Drone-Based Water Level Detection in Flood Disasters. International Journal of Environmental Research and Public Health, 19(1), 237. https://doi.org/10.3390/ijerph19010237;

[13] Flood Map Modelling calculator; Available online: https://www.floodmap.net/?gi=459283;

[14] Farhan Aziz, Xiuquan Wang, Muhammad Qasim Mahmood, Muhammad Awais, Bill Trenouth, Coastal urban flood risk management: Challenges and opportunities − A systematic review, Journal of Hydrology, Volume 645, Part B, 2024, 132271, ISSN 0022-1694, https://doi.org/10.1016/j.jhydrol.2024.132271;

[15] Flood risk on the rise in Latvia this week; Available online: https://eng.lsm.lv/article/society/environment/29.07.2024-flood-risk-on-the-rise-in-latvia-this-week.a563122/;

# ARSENIC REMOVAL FROM GROUNDWATER BY COAGULATION PROCESS: PERFORMANCE AND LIMITATIONS INFLUENCED BY THE GROUNDWATER SOURCES CHEMISTRY USED FOR DRINKING WATER PURPOSE IN THE WEST REGION OF ROMANIA

**Dr. Pacala Adina**
National Research and Development Institute for Industrial Ecology – ECOIND, Timisoara Subsidiary, **Romania**

## ABSTRACT

Arsenic (As) contaminated groundwater is a critical issue of concern, in view of its toxicity through drinking water and health impacts on the human body. In this regard, the World Health Organization (WHO, 1993) has recommended 10 μg/L for dissolved As concentration in water as standard value for drinking purposes. Special attention should be paid to the monitoring the quality of the groundwater, the chemistry and composition of arsenic-contaminated water are the major factors, determining the applied technologies for removal of arsenic. The coagulation-flocculation process is well known as physico-chemical technique for As removal, which provides high removal efficiency, even at high concentrations of As(V). This method have many advantages: high stability, low cost, simple operation and fast sedimentation. This paper examines the current scenario of arsenic contamination of groundwater in the West Region of Romania, and evaluate the As removal performances and limitation of different coagulants used, their operating conditions, properties, and efficiencies. The coagulation experiments were conducted through the Jar test, which simulates three steps including coagulation, flocculation, and settling. The coagulants tested comparatively were ferric and aluminum-based coagulants, respectively ferric chloride, ferric sulfate, aluminum sulfate and polyaluminum chloride. Better coagulating performance of the ferric salts compared with the aluminum salts has been confirmed due to their higher density of adsorption.

**Keywords:** arsenic removal, coagulation, groundwater treatment, drinking water.

## INTRODUCTION

Water is essential for the sustainability of human life, which contributes to economic development and healthy world ecosystems. Groundwater is widely employed as a water resource for domestic, agricultural, and industrial purposes. The continuous growth of the worldwide population, industrialization, agriculture production and climate change determined a degradation on groundwater quality [1], [7].

The presence of different heavy metals such as arsenic in groundwater in amounts higher than the WHO limit in groundwaters can be attributed to environmental processes and anthropogenic activities. Arsenic contamination in groundwater is a critical issue worldwide due to the impact of arsenic (As) on human health. The sources of exposure are drinking water, crops irrigated with contaminated water and food prepared with polluted water [1], [9].

The presence of As in natural water depends on the local geology, hydrology and geochemical characteristics of the aquifer materials. It is generally associated with the

https://doi.org/10.5593/sgem2024v/3.2/s11.03

geochemical environments such as basin fill deposits of alluvial-lacustrine origin, volcanic deposits, mining wastes, landfills. Higher As contamination has been found particularly in locations of hydrothermal mineralization and geothermal area [1], [7].

The concentration and the structure of arsenic depend on multiple aspects, such as the existence of oxygen in the water, the degree of biological activity, the type of water source, and the closeness of the water supply to arsenic-bearing geological formations [2].

Arsenic can occur in the environment in four oxidation states, which are arsenite (As(III)), arsenate (As(V)), arsenic (As(0)), and arsine (As(III)). The most prevalent forms, which are commonly found in water, are the inorganic form as oxyanions of trivalent arsenite and arsenate. Organic arsenic forms may be produced by biological activity, but rarely are quantitatively important [2], [5], [9]. The arsenite is less efficiently removed than arsenate from aqueous solutions by almost all of the arsenic removal technologies and for a better removal is necessary the preoxidation of As(III) to As(V) using some oxidizing chemical agents (chlorine, sodium hypochlorite, potassium permanganate, ozone) [4], [5].

Providing drinking water with safe arsenic levels in the West Region of Romania is a current challenge, due to arsenic's presence in some specific groundwater sources.

Low-cost, easy to use, efficient, and sustainable solutions are needed to supply arsenic safewater to the rural and peri-urban population in the affected areas [4], [6], [11], [12].

Various technologies are available for the removal of arsenic from contaminated groundwater using physicochemical methods including oxidation, chemical precipitation or coagulation-flocculation, electro-coagulations, adsorption, lime softening, ion exchange, and membrane separation processes like reverse osmosis, nanofiltration and electrodialysis [2], [5], [8], [9].

Coagulation is a simple method for As removal process from contaminated groundwater and most used coagulants are aluminum salts such as aluminum sulfate [$Al_2(SO_4)_3.18H_2O$] and ferric salts such as ferric chloride [$FeCl_3$] or ferric sulfate [$Fe_2(SO_4)_3.7H_2O$]. Ferric salts have been found to be more effective than alum removing As on a weight basis and effective over a wider pH range [3], [5], [9]. Optimized operating coagulants doses needed are dependent on the matrix quality of the groundwater source. [3], [7].

Groundwater monitoring is nowadays mandatory in all member state level in European Union [12], [13] and our previous studies was focused to act in accordance with the legal provisions of this directive adopted [14]. After an adequate conventional monitoring in groundwater, in the Western Region of Romania, in the catchment areas for abstraction points, or in groundwater sources, of some relevant parameters, substances or pollutants, we concluded that the groundwater sources from the West Region of Romania that require water treatment, are generally characterized by high concentrations of iron and manganese, also arsenic being present in fairly high concentrations and in certain situations exceedances may occur for ammonium [6], [10].

Based on these results, the present study investigates comparatively the treatment of a groundwater source (GW) selected from the West Region of Romania used for drinking purpose, contaminated with arsenic (100 $\mu g\ L^{-1}$), by coagulation process, with Jar-test

procedure and aluminium sulfate, polyaluminium chloride, ferric chloride and ferric sulfate as coagulants.

## MATERIALS AND METHODS

*Coagulants and water samples*

For comparison purposes, commercially available PAC (>19% $Al_2O_3$, basicity >80,0%, density >1.20 kg/dm$^3$) was a UNICHEM product (Hungary). Alum stock solution was prepared from liquid aluminium sulphate (approximately 339 g/L $Al_2(SO_4)_3.18H_2O$) obtained from a local Bega water treatment plant. The $FeCl_3$ stock solution (approximately 40%) and the $Fe_2(SO_4)_3$ stock solution (approximately 40%) were prepared by adding commercial $FeCl_3$ product (Chimcomplex S.A. Borzesti, Romania), respectively $Fe_2(SO_4)_3.7H_2O$ (Kemwater Cristal, Romania).

*Experimental and analytical methods*

Coagulation experiments were carried out at room temperature using Jar-test on a six-paddle gang stirrer (Floculator Jar-test, WiteStir JT M6). The 800mL simulated groundwater was added into the 1000mL beaker. A measured amount of coagulant was added by a calibrated pipette (Multipette stream Electronic hand dispenser, Eppendorf, Germany) into the working simulated groundwater under rapid stirring. The groundwater was stirred rapidly at 150 rpm for 2 min after coagulant dosing, followed by slow stirring at 45 rpm for 10 min.

For 20 min after settling, supernatants were collected to measure residual turbidity using a Turbidimeter (HI 88713, HANNA Instruments). Total organic carbon (TOC) and dissolved organic carbon (DOC) was analyzed after filtration through a 0.45 mm membrane and were determined using a TOC Analyzer (Multi N/C 2100 S, Analytik Jena). pH and conductivity were determined on a laboratory pH-meter (Thermo Orion, Cole-Parmer) and conductometer (Starter 3100C, Ohaus). Colour in Hazen units and residual aluminium was measuring using a photometer (Move 100, Merck). The absorbance at 254 nm (due to the Natural Organic Matter/NOM content) was measured with a Spectrofotometer UV-VIS (Specord 205, Analytik Jena), using a 1 cm path length quartz cuvette. The detection technique used for As was Inductively Coupled Plasma Optical Emission Spectrometry (ICP-OES Avio 500, Perkin-Elmer) and the concentration of iron and manganese were determinated with a Spectrofotometer (sAA-280FS, Agilent).

## RESULTS

The comparison of the efficiency of the coagulation-flocculation process by using the 4 types of coagulants (selected according to the data from the specialized literature) was carried out by the Jar-test method, in 2 situations, respectively without and with pre-oxidation with sodium hypochlorite applied as oxidant before coagulation.

Sodium hypochlorite (concentration 14.6%) was added to each sample before the introduction of coagulants, preoxidation which was practically carried out under continuous stirring at a speed of 600 rpm for 2 minutes.

Optimum doses added for each type of coagulant was established experimental (similarly with documented literature data) and are specified on each work set in Tables 1, 2.

https://doi.org/10.5593/sgem2024v/3.2/s11.03

Coagulants were added under rapid stirring simultaneously to all samples using the automatic dosing pipette. Three sets of analysis were performed for each type of coagulant.

**Table 1:** Comparative analysis for quality parameters of raw groundwater (GW) treated with coagulants SA, PAC, $FeCl_3$, $Fe_2(SO_4)_3$.

| ***Parameter, unit*** | **GW** | **SA** | **PAC** | **$FeCl_3$** | **$Fe_2(SO_4)_3$** |
|---|---|---|---|---|---|
| ***Dose, mg/L*** | - | 20 | 20 | 17,5 | 17,5 |
| *Turbidity, NTU* | 5,5 | 0,88 | 0,50 | 0,41 | 0,96 |
| *pH* | 8,1 | 7,24 | 7,66 | 7,46 | 5,59 |
| *Temperature, °C* | 22 | 22 | 22 | 22 | 22 |
| *Color, grd. Hz* | 114 | 53 | 68 | 63 | 88 |
| *Conductivity, µs/cm* | 927 | 918 | 934 | 948 | 958 |
| *MTS, mg/L* | 2,52 | 20,4 | 20,5 | 3,31 | 42,4 |
| *$UV_{254nm}$, $cm^{-1}$* | 0,252 | 0,146 | 0,138 | 0,094 | 0,162 |
| *Aluminium dissolved, µg/L* | - | 33 | <20 | - | - |
| *Iron dissolved, mg/L* | 1,04 | 0,32 | 0,268 | 0,249 | 0,445 |
| *Manganese dissolved, mg/L* | 0,15 | 0,15 | 0,15 | 0,148 | 0,15 |
| *Amonium, mg/L* | 2,28 | 2,20 | 2,15 | 1.87 | 2,00 |
| *Arsen, µg/L* | 98 | 2,5 | 2,6 | 8,3 | 17,0 |

**Table 2**: Comparative analysis for quality parameters of raw groundwater (GW) after preoxidation with 0.2 mg/L NaOCl and treated with coagulants SA, PAC, $FeCl_3$, $Fe_2(SO_4)_3$.

| *Parameter, unit* | GW | SA | PAC | $FeCl_3$ | $Fe_2(SO_4)_3$ |
|---|---|---|---|---|---|
| ***Dose, mg/L*** | - | 20 | 20 | 17,5 | 17,5 |
| *Turbidity, NTU* | 5,5 | 0,73 | 0,41 | 0,33 | 0,77 |
| *pH* | 8,1 | 7,18 | 7,40 | 7,38 | 4,99 |
| *Temperature, °C* | 22 | 22 | 22 | 22 | 22 |
| *Color, grd. Hz* | 114 | 41 | 66 | 35 | 84 |
| *Conductivity, µs/cm* | 927 | 866 | 883 | 978 | 983 |
| *MTS, mg/L* | 2,52 | 20,3 | 16,8 | 1,47 | 36,7 |
| $UV_{254nm}$, $cm^{-1}$ | 0,252 | 0,046 | 0,038 | 0,064 | 0,026 |
| *Aluminium dissolved, µg/L* | - | <20 | <20 | - | - |
| *Iron dissolved, mg/L* | 1,04 | <0,10 | 0,228 | 0,244 | 0,44 |
| *Manganese dissolved, mg/L* | 0,15 | 0,13 | 0,14 | 0,118 | 0,14 |
| *Amonium, mg/L* | 2,28 | 1,95 | 1,72 | 1,39 | 1,80 |
| *Arsen, µg/L* | 98 | <2 | <2 | <2 | 10,5 |

## DISCUSSION

The chemistry and composition of arsenic-contaminated water are the major factors determining the removal of arsenic. For the selected raw groundwater source (GW), the speciation analyzes of arsenic (arsenites/arsenates) were done by the HPLC-ICP-MS method (Inductively Coupled Plasma Mass Spectrometry, Agilent Technologies).

The arsenic speciation was determined as follows: 53 ± 2 µg/L As(III); 40 ± 3 µg/L As(V). For anoxic groundwater, oxidation is an important step since arsenite is the prevalent form of arsenic at near neutral pH. Most of the available removal technologies are more efficient for arsenate given that arsenite is predominantly non-charged at pH below 9.2 [4]. The treatment technologies are believed to be more effective by using a two-step approach consisting of an initial oxidation involves the conversion of soluble arsenite to arsenate. This alone does not remove arsenic from the solution, thus, a removal technique, such as adsorption, coagulation, or ion exchange, must follow [5]. Chemicals, such as chlorine, ozone, and permanganate, can rapidly oxidize As(III) to As(V). However, despite this enhanced oxidation, interfering substances present in water need to be considered in selecting the proper oxidant as these substances can greatly affect and dictate the kinetics of As(III) oxidation [5].

https://doi.org/10.5593/sgem2024v/3.2/s11.03

Thus, to efficiently remove arsenic from a solution by oxidation, oxidants should be selected carefully. In Romania chlorine, hypochlorite and permanganate are the most commonly used oxidants. The application of preoxidation with sodium hypochlorite presented in this experimental study (doses of 0.2 mg/L NaOCl) also significantly improved the degree of reduction of iron, manganese and ammonium ions (table 2).

Coagulation and flocculation are among the most employed and documented techniques for arsenic removal from water [9]. The scientific references shows list of the coagulants used in arsenic removal, together with their operating conditions, properties, and efficiencies. In coagulation, positively charged coagulants (e.g., aluminum sulphate ($Al_2(SO_4)_3$, ferric chloride ($FeCl_3$)) reduce the negative charge of colloids, thereby making the particles colloide and get larger. During these processes, dissolved arsenic is transformed by the coagulants into an insoluble solid, which is precipitated later [9]. Alternatively, soluble arsenic species can be incorporated into a metal hydroxide phase and be co-precipitated. However, the solids can be after subsequently removed by sedimentation and/or filtration.

Arsenic removal efficiency of different coagulants varies as a function of pH. Below pH 7.6, $Al_2(SO_4)_3$, and $FeCl_3$ are equally effective in removing arsenic from water [3]. Between the two inorganic arsenic species, most researchers suggested that arsenate is more efficiently removed compared to arsenite and that $FeCl_3$ is a better coagulant than $Al_2(SO_4)_3$ at pH higher than 7.6 [3], [5], [9].

Due to the high pH of the selected raw groundwater (pH = 8,1), being known that the removal of arsenic is carried out with maximum efficiency in the range of pH = 6 – 9, it was no necessary to carry out the pH correction and $FeCl_3$ confirmed the best performance to arsenic removal.

However, despite their reported inferior performance compared to ferric chloride, aluminum-based coagulants were still able to reduce arsenic concentrations to below the maximum concentration level (MCL) of 10 μg/L given that the initial concentration is 280 μg/L [9].

The experimental results obtained treating the raw groundwater from the West Region of Romania with a total arsenic content of 98 μg/L by preoxidation with hypochlorite followed by coagulation with aluminum or iron salts validate the theoretical aspects documented from the scientific literature.

Preoxidation with hypochlorite followed by coagulation with aluminum or iron salts are valid techniques for arsenic removal, easily applicable, which involves low operating costs and could by a very good option for small water treatment plants for drinking purpose.

## CONCLUSION

Concluding, the experimental study results have showed that all the coagulants tested are found to be effective in reducing As from groundwater with initial As concentration of 98 μg $L^{-1}$.

- Differences were observed between the performances of arsenic removal for the four coagulants compared, ferric chloride proven to be the most effective coagulant.

- However, the degrees of reduction to match the quality of the coagulated and then decanted water within the norms required by the drinking water standards were not achieved, not even for the iron chloride as a coagulant applied to treat the groundwater chemistry matrix selected, with similarity to part of the underground aquifer in the West region of Romania.

Continue research are needed in finding the best available and cost-effective treatment process to remove As and its co-contaminants, for As-free safe and healthy drinking water.

## ACKNOWLEDGEMENTS

This work was carried out through the "Nucleu" Program within the National Research Development and Innovation Plan 2022-2027 with the support of Romanian Ministry of Research, Innovation and Digitalization, contract no. 3N/2022, Project code PN 23 22 03 03.

## REFERENCES

[1] Alarcón-Herrera M.T., Gutiérrez M., Geogenic arsenic in groundwater: Challenges, gaps, and future directions, Current Opinion in Environmental Science & Health, vol. 27, pp 100349, 2022;

[2] Babu D. S., Vijay K., Nidheesh P.V., Kumar M. S., Performance of continuous aerated iron electrocoagulation process for arsenite removal from simulated groundwater and management of arsenic-iron sludge, Sustainable Energy Technologies and Assessments, vol. 47, pp 101476, 2021;

[3] Baskan M.B., Pala A., A statistical experiment design approach for arsenic removal by coagulation process using aluminum sulfate, Desalination, vol. 254 (1-3), pp 42-48, 2010;

[4] Kumar R., Patel M., Singh P., Bundschuh J., Pittman Jr. C. U., Trakal L., Mohan D., Emerging technologies for arsenic removal from drinking water in rural and peri-urban areas: Methods, experience from, and options for Latin America, Science of the Total Environment, vol. 694, pp 133427, 2019;

[5] Nicomel N. R., Leus K., Folens K., Van Der Voort P., Laing G. D., Review-Technologies for Arsenic Removal from Water: Current Status and Future Perspectives, International Journal of Environmental Research and Public Health, vol.13, pp. 62, 2016;

[6] Pacala A., Neidoni D.G., Negrea S.C., Diaconu L.A., Tenea A.G., Dinu C., Stefanescu M., General aspects of the coagulation process for the removal of arsenic from simulated groundwater, Proceedings of 30th International Symposium on Analytical and Environmental Problems, Hungary, ISBN 978-963-688-009-5, pp 146-149, 2024;

[7] Raheja H., Goel A., Pal M., An evaluation of groundwater quality and its suitability for drinking and irrigation uses under the GIS framework, Water Practice & Technology, vol. 00, /issue 0, 1, doi: 10.2166/wpt.2022.134, 2022;

[8] Shafiquzzaman Md., Hasan Md. M., Haider H., Bari Quazi H., Ghoul Y.E., Nakajima J., Evaluating configuration of dual unit ceramic filter for arsenic removal

from highly contaminated groundwater, Journal of Environmental Management, vol. 319, pp 115664, 2022;

[9] Singh R., Singh S., Parihar P., Singh V.P., Prasad S.M., Arsenic contamination, consequences and remediation techniques: A review, Ecotoxicology and Environmental Safety, vol. 112, pp 247–270, 2015;

[10] Order 621/07.07.2014 regarding the approval of the threshold values for groundwater in Romania, Official Monitor 535/18.07.2014, Romania, 2014;

[11] Ordinance 7/18.01.2023 regarding the quality of water intended for human consumption, Official Monitor 63/25.01.2023, Romania, 2023;

[12] Directive 2006/118/EC of the European Parliament and of the Council of 12.12.2006 on the protection of groundwater against pollution and deterioration, 2014;

[13] Guidelines for drinking-water quality: fourth edition Incorporating the first and second addenda. Chemical fact sheets: Arsenic, World Health Organization, 2022;

[14] Directive (EU) 2020/2184 of the European Parliament and of the Council of 16 December 2020 on the quality of water intended for human consumption, Bruxelles: Official Journal of European Union, OJ L 435, 23.12.2020, pp 1-62, 2020.

# DETERMINING FLOOD SHELTER LOCATIONS: A MULTI-CRITERIA SPATIAL ANALYSIS USING GIS TOOLS

**PhD Dino Dobrinic** [1]
**Ivan Bertecic** [2]
**Prof. Dr. Damir Medak**[2]
[1] University of Zagreb, Faculty of Geodesy, **Croatia**
[2] University of Zagreb, **Croatia**

## ABSTRACT

Globally, natural hazards (e.g., forest fires, floods, earthquakes) are expected to become more frequent and severe due to climate change, unplanned urbanization, and population growth in areas prone to extreme events. Therefore, this paper aims to identify the most suitable locations for flood shelters using multi-criteria spatial analysis using GIS tools. GIS tools facilitate the effective preparation, processing, and visualization of spatial data. By using GIS, it is possible to integrate various data sources, simulate potential flooding scenarios, and analyze spatial relationships between different factors that affect the safety and effectiveness of shelters.

Multi-criteria spatial analysis integrates multiple criteria into the decision-making process, ensuring a comprehensive approach to evaluating the safety and suitability of potential sites. Criteria considered in this analysis include elevation, terrain slope, slope orientation, land use, proximity to water bodies, and distance to built-up areas. The use of GIS tools for multi-criteria spatial analysis ensures that all relevant information is taken into account when selecting optimal locations for shelters. This approach enables the development of evacuation models that can contribute to local planning and decision-making, to improve the resilience of communities to flooding and reduce the risk of losses from these natural disasters.

The methodology developed for the selection of optimal locations for shelters will provide guidelines for flood protection planning. Additionally, the methodology could be applied in other cities and regions facing similar challenges, thus promoting the wider use of GIS technologies in disaster risk management.

**Keywords:** multi-criteria analysis, flood hazard, spatial analysis, shelter locations, GIS.

## INTRODUCTION

Flooding (inundation) is the occurrence of an unusually large amount of water in a certain area due to natural forces, such as heavy rainfall or other causes such as dam failures, war destruction, etc. Globally, natural hazards (e.g., forest fires, floods, earthquakes) are expected to become more frequent and severe due to climate change, unplanned urbanization, and population growth in areas prone to extreme events [1]. Croatia is exposed to an increased risk of flooding due to several factors. These include extensive hilly and mountainous regions where heavy rainfall occurs, wide valleys with watercourses in the lowlands and large cities with valuable assets in potentially vulnerable areas. Additionally, the country has inadequately constructed and maintained protection systems. It is estimated that about 6.2% of Croatia's land area has a high

probability of flooding, about 8.1% has a medium probability of flooding and 17.1% has a low probability of flooding [2].

Kekez et al. [3] assessed the flood risk in Kupa River area in Croatia, which has been hit by severe flooding several times in the past decade. Given the lack of empirical data and insurance claims, the analysis focuses on building and inventory damage, emphasizing the uncertainty in the flood damage functions and their impact on the annual damage distribution, especially for low probability and high damage events. For efficient flood management, the planning of evacuation plans (e.g., shelters, evacuation routes) is a necessity to reduce vulnerability to natural disasters in rural communities. Therefore, Chelariu et al. [1] analyzed the suitability of areas for the location of evacuation shelters and evaluated their accessibility in case of flooding in small mountainous catchments. The model developed in this study takes into account the possibility of evacuating the local population and the accessibility of the nearest evacuation points. This analysis was performed using Multi-Criteria Analysis (MCA) and can help improve flood management measures and reduce potential damage by optimizing evacuation processes. MCA is a widely used method in natural hazard mapping and has gained increasing attention as a novel approach. Many studies have used GIS-based MCA to assess extreme events by analyzing the factors that influence or determine their occurrence [4,5]. Vojtek et al. [6] focused on the identification of areas with different levels of flood potential in the Nitra River basin in Slovakia. By using the MCA method and the Analytical Hierarchy Process in combination with geographic information systems (GIS), the authors assessed the flood potential in the river basin, which has not been done before with this methodology. The research results showed significant differences in the classification of areas with high and very high flood potential, depending on the technique used.

The main objective of this work is to identify the most suitable locations for flood shelters using multi-criteria spatial analysis using GIS tools. The use of GIS tools for multi-criteria spatial analysis ensures that all relevant information is taken into account when selecting the optimal locations for shelters. This approach enables the development of evacuation models that can contribute to local planning and decision-making to improve the resilience of communities to flooding and reduce the risk of losses from these natural disasters.

## MATERIALS AND METHODS

In this study, the city of Karlovac was used to determine the locations for flood protection structures. Karlovac is a town in the central part of Croatia. It is located in a lowland plain at an altitude of 112 meters. The town lies at the transition between the Pannonian Plain and the Dinaric Alps. Karlovac is known for its unique hydrogeographical position, as it lies on four rivers: Korana, Kupa, Mrežnica, and Dobra.

In this paper, raster and vector spatial data, were used together with software tools to perform an MCA to determine flood shelter locations. The raster data included a digital terrain model (DTM) with a resolution of 5 m and CORINE Land Cover 2018[7], while the vector layer of roads was acquired from OpenStreetMap (OSM). The DTM was used in this study to analyze topographic features relevant to the assessment of the suitability of the terrain for the construction of shelters. It served as the basis for the analysis of height, slope, and slope orientation. CORINE Land Cover is a cartographic

product that provides an overview of land cover and land use across Europe [7]. The CORINE project (Coordination of Information on the Environment) was initiated by the European Union to standardize and coordinate environmental information. In this study, this data was used to analyze existing land use, distance to water bodies, and proximit to built-up areas, and to identify potential areas suitable for flood shelter construction. OpenStreetMap (OSM) is an open database that containing geographical information that can be freely edited and used by users. In this paper, the vector street layer obtained from OSM was used to calculate isochrones—lines of equal travel time— to analyze the time it takes people from different parts of the city to reach shelters at an average walking speed. To analyze the distances to the selected shelters, i.e. to calculate the isochrones, the Network Analysis tool, which is part of the ArcGIS Pro software, was used. The entire workflow of this research is shown in Figure 1.

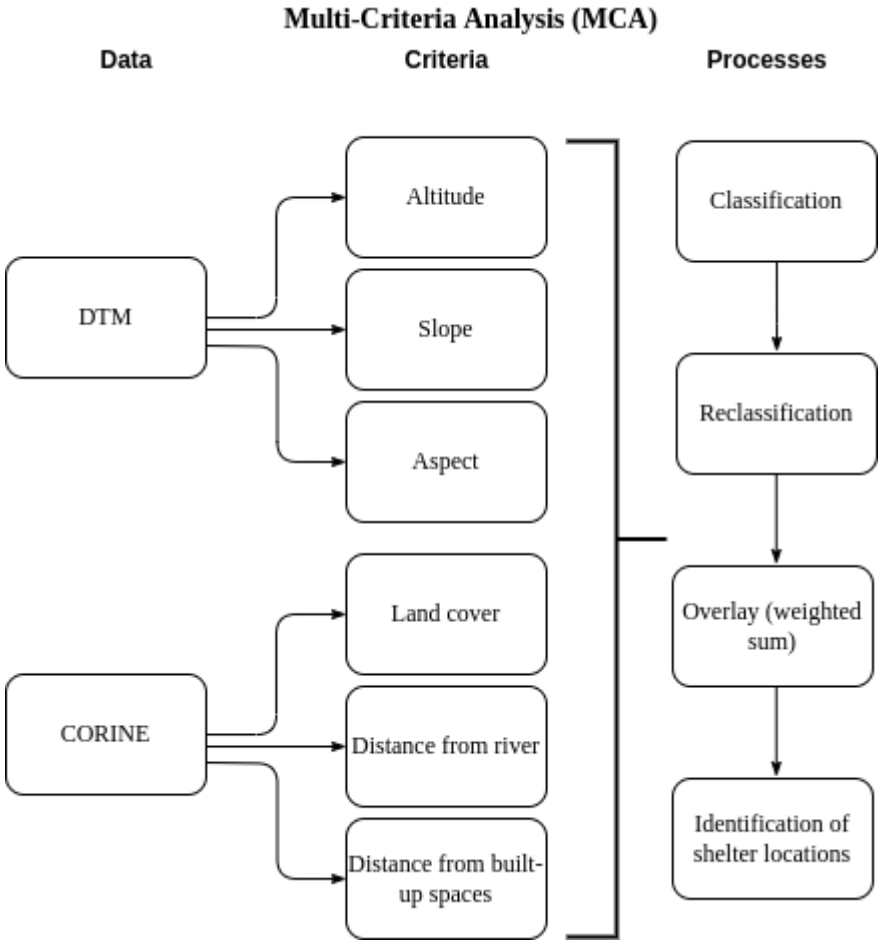



Figure 1. Workflow illustrating the research process for determining flood shelter locations.

## RESULTS

For the first part of the MCA, a detailed analysis of the digital terrain model (DTM) was carried out. Elevation is used in flood modeling to predict the overflow of water bodies from their banks and to identify areas at risk. Since the city of Karlovac is a lowland

area with low elevation differences, the cells were divided into 6 classes, with each class covering an elevation range of 20 meters. After creating this classification, a reclassification was made, assigning each class a score from 1 to 5 (Table 1), with a lower score indicating a lower suitability for selecting that site for a flood protection, and a higher score indicating a higher suitability. Table 1 shows the weighting assessment for each criterion considered in this research. The values for elevation and slope scores were derived from the DTM, while the distances to built-up areas and water bodies were derived from the CORINE land cover maps.

Table 1. Criteria for flood shelter location selection.

| Criterion | Range | Score | Criterion | Range | Score |
|---|---|---|---|---|---|
| Elevation[m] | < 120 | 1 | Slope [°] | < 4 | 5 |
| | 120 – 140 | 2 | | 4 – 8 | 4 |
| | 140 – 160 | 3 | | 8 – 12 | 3 |
| | 160 – 180 | 4 | | 12 – 16 | 2 |
| | 180 – 200 | 5 | | more than 16° | 1 |
| | > 200 | 3 | | | |
| Distance Built-up area [m] | < 200 | 5 | Distance Watercourse [m] | < 200 | 1 |
| | 200 – 300 | 4 | | 200 – 300 | 2 |
| | 300 – 400 | 3 | | 300 – 400 | 3 |
| | 400 – 500 | 2 | | 400 – 500 | 4 |
| | > 500 | 1 | | > 500 | 5 |

Also, scores for the aspect values, which range from 0 to 360, were assigned according to the [1], whereby the scores were weighted according to the duration of sunshine during the day. In addition, land use plays an important role in the multi-criteria spatial analysis when selecting ideal locations for flood shelters, as it significantly influences the accessibility, safety, and effectiveness of evacuation points. Different types of land offer different characteristics that can either facilitate or restrict the use of certain areas as shelters. For example, arable land is considered as the most favourable area due to its openness and low slope, while forests and watercourses were the least favourable areas, as forested areas are often densely vegetated, making access and shelter placement difficult. Watercourses, including rivers, streams, and other types of water bodies, are also unsuitable locations for shelters. Watercourses pose a direct risk of flooding, and areas near them are often the first to be affected when water levels rise. Placing shelters near watercourses would put evacuees at additional risk, which is contrary to the main objective of evacuation – to ensure people's safety. After reclassification based on to the scores from Table 1, the final raster layer ranged from 6 to 30. Shelter locations were selected to be evenly distributed across the city (Figure 2), with cell values greater than 24, and with an area large enough to accommodate a larger number of people. Priority was also given to well-known locations such as cemeteries, hospitals, and similar places.

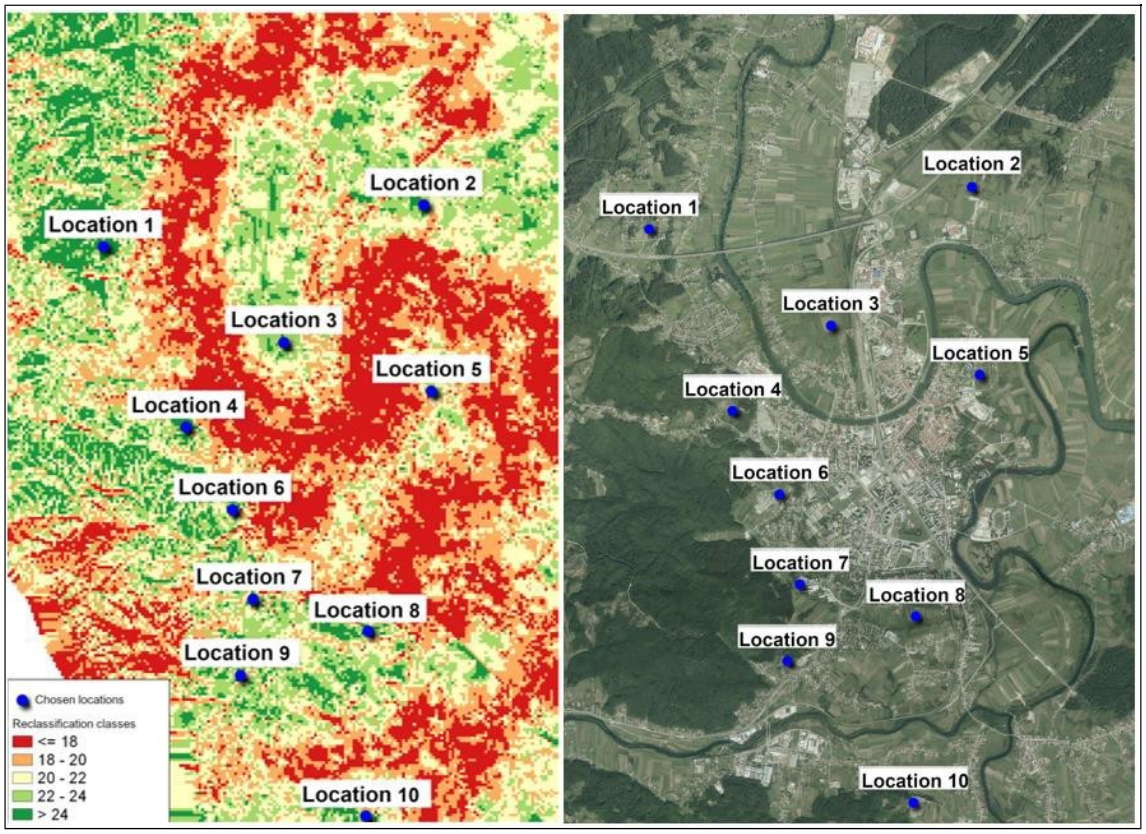



Figure 2. Location of shelters that were identified as the most suitable areas for evacuation.

After identifying the most suitable areas for evacuation, the sites were compared with those described in the Overflow project (Vulnerability assessment of embankments and bridges exposed to flooding hazards) [8]. The results of the project serve as a basis for the development of a risk assessment tool that allows the quantification of the direct and indirect consequences of problems related to critical infrastructure. Most of the shelter locations are consistent with those from the Overflow project. The only difference is for some sites located in properties owned by the City of Karlovac, while we did not take into account the ownership of the most suitable areas for shelters. Despite its many advantages, the multi-criteria spatial analysis also has its disadvantages. One of the main disadvantages is the varying accuracy and resolution of the data used for the analysis. The combined data often comes from different sources and is not always collected at the same time, which can lead to discrepancies in its accuracy and timeliness. For example, a high-resolution DTM may provide very accurate information on topography, but the data on land use or road infrastructure may be outdated or less precise.

In addition, Network Analyst was used to calculate isochrones (Figure 3), i.e., to build the network and perform analysis to assess the spatial accessibility (up to 10, from 10 to 20, and from 20 to 30 minutes) of the shelters. A similar approach was presented in the studies of Sortino Barrionuevo et al. [9] and Park et al. [10]. These works presented cartograms as empirical results that provide helpful insights for more efficient evacuation plans.

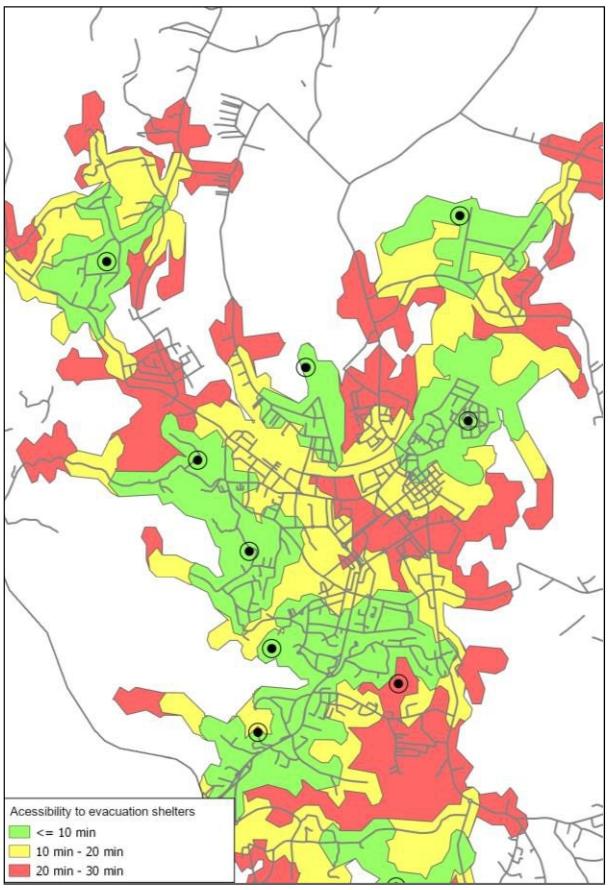



Figure 3. Isochrones showing 10, 20, and 30-minute walking distances around flood shelters.

## CONCLUSION

The aim of this work was to identify optimal locations for flood protection facilities in Karlovac using a multi-criteria spatial analysis with GIS tools. Given the increased flood risk in the city, it was important to apply a method that allows for comprehensive consideration of various spatial factors to ensure that the selected locations are safe and easily accessible to residents. By applying multi-criteria analysis in combination with GIS tools, the integration of different types of data was made possible, resulting in a detailed analysis that served as a basis for the selection of potential shelter locations.

The analysis was based on six key criteria: elevation, slope, aspect, land use, distance to watercourses, and distance to built-up areas. After data processing, classification, and reclassification, the analysis provided results on the suitability of specific sites for flood shelters. Based on this analysis, ten optimal locations for shelters were identified that meet the established criteria and offer the best possibilities for the safe evacuation of citizens in the event of a flooding.

Once the locations were selected, a time-distance analysis was conducted to evaluate the walking distance to the shelters based on an average walking speed of 6 km/h. The results showed that almost the entire city is covered by a network of shelters that can be reached within a 30-minute walk, leading to the conclusion that the research objective was successfully achieved. For future research, it is suggested to include additional criteria and data in the multi-criteria analysis, such as demographic data and more detailed information on infrastructure and land use.

## REFERENCES

[1] Chelariu, O.E., Iațu, C., Minea, I., A GIS-Based Model for Flood Shelter Locations and Pedestrian Evacuation Scenarios in a Rural Mountain Catchment in Romania. Water, vol. 14, 2022, doi:10.3390/w14193074.

[2] Barbalić, D., Barbalić, S., Biondić, D., Vukmanić, L., Prethodna Procjena Rizika Od Poplava 2018. Hrvatske vode, pp 1-165, 2019.

[3] Kekez, T., Andricevic, R., Knezic, S., Flood Risk Modeling under Uncertainties: The Case Study of Croatia. Water, vol. 14, 2022, doi:10.3390/w14101585.

[4] Osman, S.A., Das, J., GIS-Based Flood Risk Assessment Using Multi-Criteria Decision Analysis of Shebelle River Basin in Southern Somalia. SN Applied Sciences, vol. 5, pp 134, 2023, doi:10.1007/s42452-023-05360-5.

[5] Skilodimou, H.D., Bathrellos, G.D., Chousianitis, K., Youssef, A.M., Pradhan, B., Multi-Hazard Assessment Modeling via Multi-Criteria Analysis and GIS: A Case Study. Environmental Earth Sciences, vol. 78, pp 1–21, 2019, doi:10.1007/s12665-018- 8003-4.

[6] Vojtek, M., Vojteková, J., Pham, Q.B., GIS-Based Spatial and Multi-Criteria Assessment of Riverine Flood Potential: A Case Study of the Nitra River Basin, Slovakia. ISPRS International Journal of Geo-Information, vol. 10, pp 578, 2021, doi:10.3390/ijgi10090578.

[7] Dobrinić, D., Gašparović, M., Medak, D., Sentinel-1 and 2 Time-Series for Vegetation Mapping Using Random Forest Classification: A Case Study of Northern Croatia. Remote Sensing, vol. 13, pp 1–20, 2021, doi:10.3390/rs13122321.

[8] Bačić, M., Kovačević, M.S., Jurić Kaćunić, D., Librić, L., Car, M., Gavin, K., Stipanović, I., Reale, C., Classification of a Flood Protection Infrastructure Based on Its Vulnerability to Various Loads. Proceedings of the 7th International Conference on Road and Rail Infrastructures (CETRA 2022), pp 611–618, 2022, doi:10.5592/CO/cetra.2022.1471.

[9] Sortino Barrionuevo, J.F., Castro Noblejas, H., Mérida Rodríguez, M.F., Mapping Tools for Flood Risk Rescue and Assistance Management. Land, vol. 13, 2024, doi:10.3390/land13010068.

[10] Park, S., Lee, G., Kim, J.O., Flood Evacuation Mapping Using a Time-Distance Cartogram. ISPRS International Journal of Geo-Information, vol. 9, pp 207, 2020, doi:10.3390/ijgi9040207.

# ESTIMATION OF APPROXIMATION ERRORS IN REPRESENTING REAL PARTICLE DIMENSIONS WITH EQUIVALENT DIAMETERS IN SEDIMENTATION ANALYSIS

**Dr. Eng. Tymoteusz Turlej**

AGH University of Krakow, **Poland**

## ABSTRACT

Accurate representation of particle dimensions is essential for reliable sedimentation analysis and assessment of settling dynamics. The use of equivalent diameters—such as Stokes, Feret, and volume-based diameters—introduces approximation errors when replacing real particle dimensions, especially for irregularly shaped particles. This study quantifies these errors by capturing high-resolution 2D images of particles within a bentonite, commonly found in bentonite suspensions characteristic of those occurring in riverine environments, and measuring real particle dimensions. Several equivalent diameters are then calculated to evaluate their effectiveness in approximating true particle sizes. The methodology involves a systematic comparison between real particle dimensions and each equivalent diameter, focusing on error margins associated with each approximation method. Results demonstrate variations in accuracy across different equivalent diameters, providing insights into which parameters best minimize error in sedimentation applications. These findings contribute to more precise sedimentation analyses and support optimized predictions of particle behavior in practical applications.

**Keywords:** particle size, equivalent diameter, morphology, image processing

## INTRODUCTION

There are many technological processes in industry that require effective separation of multiphase systems. Examples of such processes include wastewater treatment, water treatment, recovery of raw materials from sludge, or dust separation in industrial processes, which must be carried out in accordance with the principles of sustainable development [1]. One of the key processes used in these areas is sedimentation of suspensions, which involves separating solid phase particles from liquids under the influence of gravity. When designing sedimentation devices, such as settling tanks, it is extremely important to estimate the efficiency and performance of the device [2]. In practice this often involves the need for classical modeling, using either laboratory studies or numerical modeling, of the suspension separation process, in which one of the basic parameters is determining the boundary grain size for the solid phase dispersed in the liquid phase [3], [4]. The boundary grain is the smallest particle that can be effectively sedimented in a given settling tank. This parameter is of key importance because there is a direct relationship between the size of the boundary grain ($d_g$) and its settling velocity ($v_g$) [5]. Accurate estimation of these values allows for optimal design of the device and increase of its efficiency [6], [7].

https://doi.org/10.5593/sgem2024v/3.2/s11.05 

There are many methods for determining the size (diameter) of solid phase particles in suspensions. Methods such as laser diffractometry, sedimentation balance or optical microscopy can be used [8], [9]. However, in practice these particles rarely have a perfectly spherical shape, which requires the use of parameters such as equivalent diameter [10], [11]. The equivalent diameter allows approximation of the actual dimensions of irregular particles using representative values. Examples of equivalent diameters include [12]:

- Volume-based diameter ($d_V$) –the diameter of a sphere with a volume equal to that of the particle, it represents the particle's three-dimensional volume, ideal for characterizing solid particles in various applications.
- Area-equivalent diameter ($d_A$): The diameter of a sphere with the same projected area as the particle's projection, often determined through digital image analysis.
- Hydrodynamic diameter ($d_H$)– the diameter of a sphere with the same settling velocity in a liquid as the particle.
- Feret diameter ($d_F$) – the maximum distance between two parallel tangents on opposite sides of the particle's projected image. This measurement is commonly used for elongated or irregularly shaped particles and provides an insight into the particle's longest dimension.
- Martin diameter ($d_M$) – defined as the chord length of the particle's projected outline that divides the projection area into two equal parts.
- Sauter diameter ($d_{32}$) – the diameter of a sphere with the same volume-to-surface area ratio as the particle.
- Circular Equivalent diameter (CE diameter) – the diameter of a circle with the same area as the particle's projection on a plane.
- Circumscribed diameter - t he diameter of the smallest circle that can fully enclose the particle.
- Inscribed diameter - the diameter of the largest circle that can fit entirely within the particle.

Depending on the adopted criterion for determining the equivalent diameter, these values may differ, which affects the modeling results and the effectiveness of predictions regarding sedimentation processes [13]. This article emphasizes the need to be aware of the error in approximating the actual grain diameter resulting from the use of a specific equivalent diameter, and analyzes its impact on the accuracy of estimating key parameters of the sedimentation process.

## MATERIALS AND METHODS

In the conducted studies bentonite particles were used as the research material, which are characterized by a compact structure and low solubility in water. The studies did not consider any other physicochemical parameters of the particles apart from their shape and size.

The Morphology 4 automated particle size and shape analyzer was used to analyze the shape and size of the particles. The studies were conducted using a dry powder dispersion attachment. 3 $mm^3$ of the research material, previously homogenized, was introduced into the dispersion attachment, and then the sample was evenly distributed

on the measuring glass. Microscopic imaging was performed at 10x magnification, and the examined area covered a field of 20x20 mm.

The full results of the study included obtaining over 100,000 images of individual particles. For the purposes of detailed analyses, the 100 largest recorded particles were selected, shown on Figure 1. These images were used as input material for later image analyses, which allowed for the assessment of the shape and size parameters of the particles.

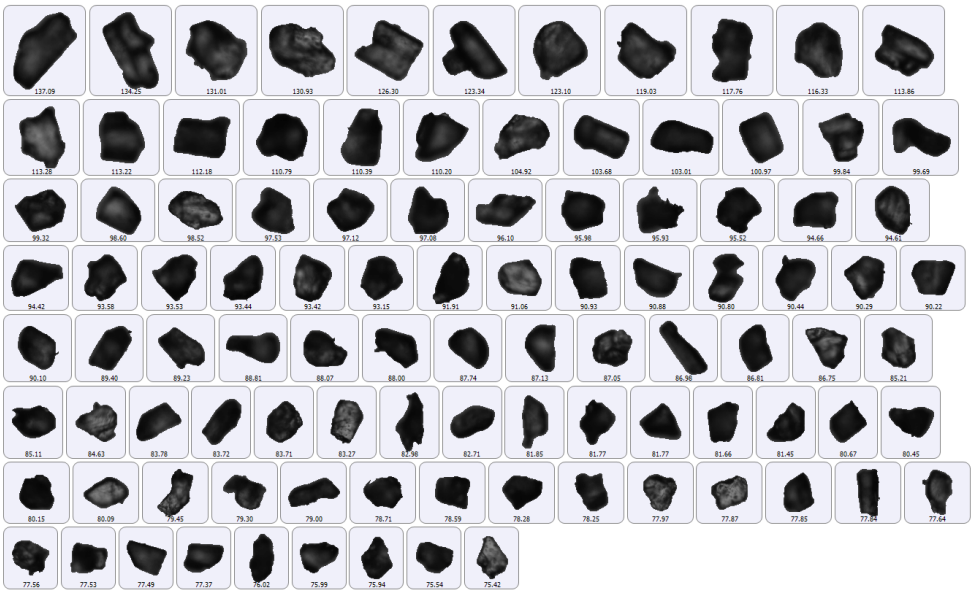


Fig. 1. Images of 100 analyzed particles

## RESULTS

Using MATLAB software, the parameters of the equivalent diameters were determined: equivalent diameter (CE Diameter), area-equivalent diameter ($d_{A,}$), Sauter diameter ($d_{32}$) and inscribed diameter. The analyses also included determining the absolute errors for each of the calculated diameters in relation to the reference CE values.

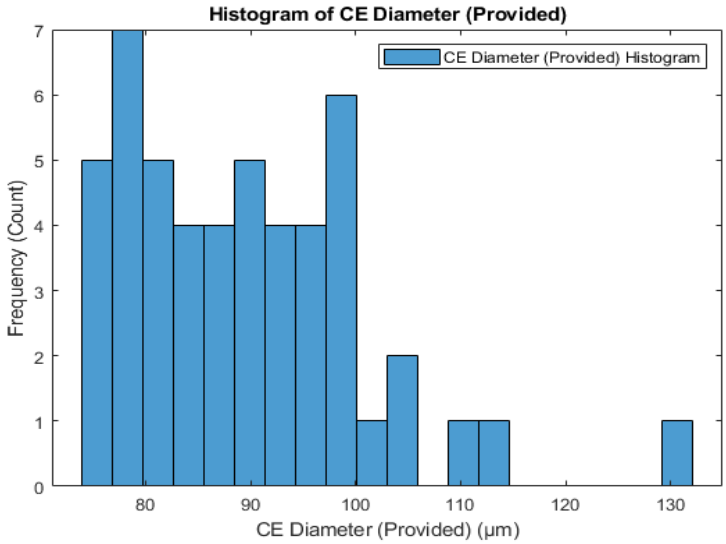



Fig. 2. Histogram of CE Diameter

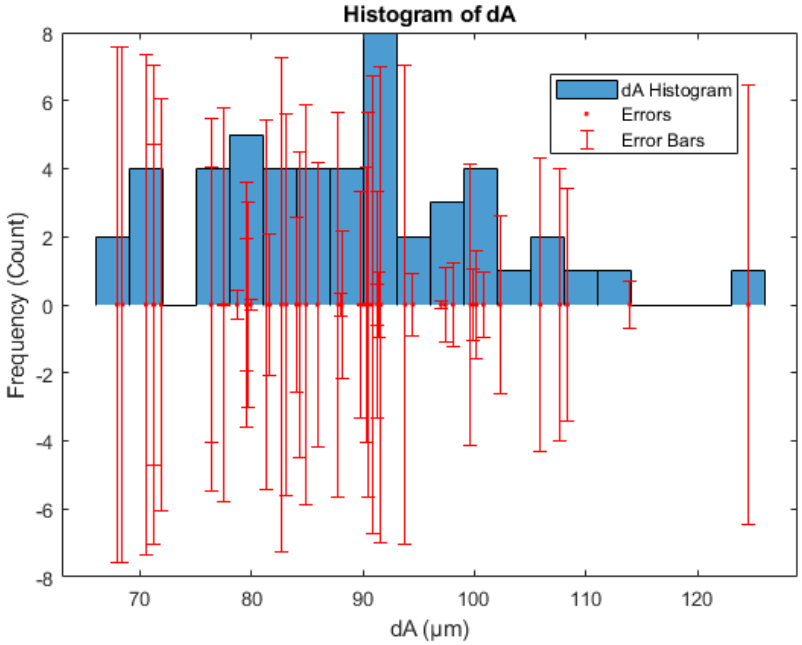



Fig. 3. Histogram of area-equivalent diameter ($d_A$)

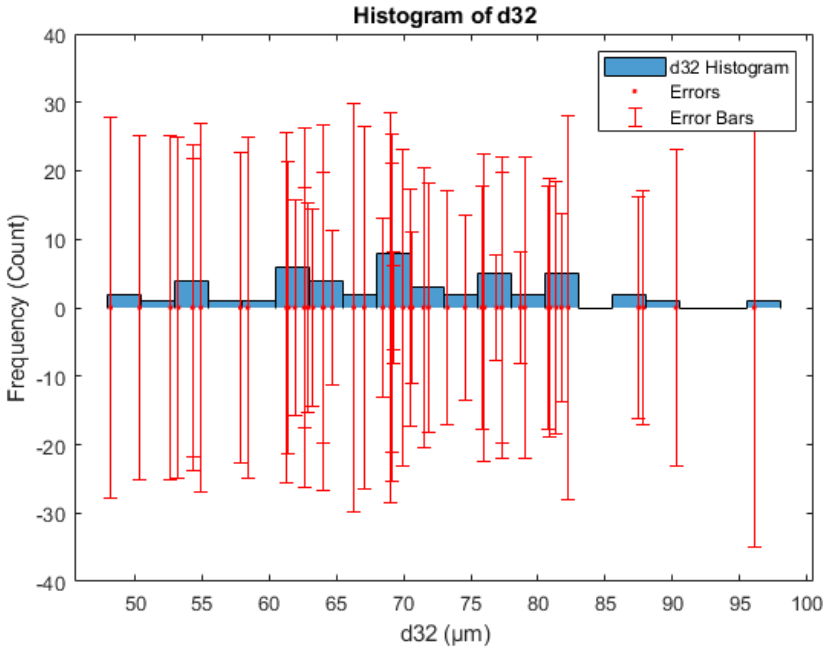



Fig. 4. Histogram of Sauter diameter ($d_{32}$)

The histograms illustrating the distribution of equivalent diameter values are shown in Figures 2–5. Histograms were determined for the equivalent diameter CE (Fig 2), area-equivalent diameter $d_A$ (Fig. 3), Sauter diameter $d_{32}$ (Fig. 4) and inscribed diameter (Fig. 5). These analyses allowed for the assessment of the compliance of various parameters of the equivalent diameters with the reference CE values.

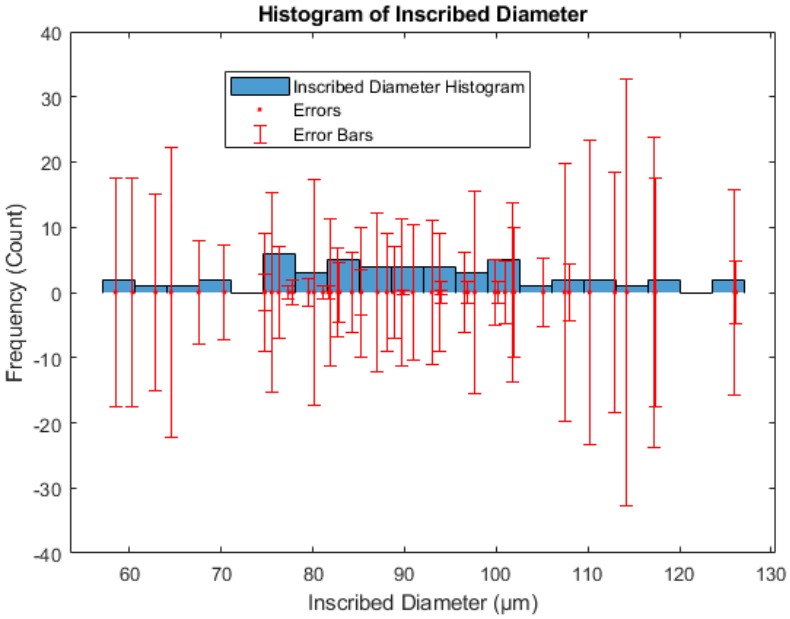



Fig. 5. Histogram of Inscribed Diameter

Tab.1. Average percentage errors for different equivalent diameters

| DiameterType | MeanError |
|---|---|
| $d_A$ | 4.20% |
| $d_{32}$ | 22.48% |
| Inscribed diameter | 10.98% |

The absolute percentage error values were determined for each of the analyzed diameters. The results of the error analysis, including the average percentage error values, are presented in Table 1. The table provides a summary of the average errors for individual equivalent diameters, allowing a straightforward comparison of their accuracy.

## DISCUSSION

From the obtained results presented in Figures from 2 to 5, it is possible to notice clear differences in the distribution of the analyzed particle diameters. The histogram for the equivalent diameter (CE Diameter) shows that the values provided for the samples are characterized by a relatively narrow range, which suggests the homogeneity of the tested particles. The histogram for the surface diameter (dA) shows a strong similarity to CE, confirming that $d_A$ is a well-suited measure describing the particle size in relation to the reference values.

In the case of the Sauter diameter ($d_{32}$), the distribution shows a shift of values towards the lower ranges compared to CE and $d_A$, which is due to the nature of this measure, which takes into account the volume to surface ratio. The histogram for the Inscribed Diameter shows that these values are significantly smaller compared to CE and the

other measures, which is in line with its definition as the largest circle within the particle. These results confirm that the inscribed diameter is a measure that is particularly sensitive to asymmetries and irregularities in the shape of the particles.

The determined error values, presented in Table 1, reveal that the surface-based diameter (dA) has the lowest mean percentage error of 4.20% with respect to the CE Diameter. This confirms its reliability and suitability as a measure of particle size. In contrast, the Sauter diameter (d32) exhibits a significantly higher mean percentage error of 22.48%, which can be attributed to its sensitivity to surface irregularities and particle shape. The inscribed diameter has a mean percentage error of 10.98%, the highest among the evaluated measures. This is understandable, as the inscribed diameter is constrained by the smallest dimensions of the particle, making it particularly sensitive to asymmetry and irregularity in particle shape.

Despite these variations, all the analyzed equivalent diameters demonstrate reasonable consistency in describing particle sizes. The determined percentage errors remain within acceptable limits for practical applications, further supporting the validity of the conducted analysis. These findings highlight the importance of selecting an appropriate diameter measure based on the specific requirements of the application, such as sensitivity to particle shape or precision in size estimation.

## CONCLUSION

In the design of sedimentation devices, such as settling tanks, the correct selection of the equivalent diameter is crucial, as it is one of the basic parameters used in the design of the device geometry and in determining its operating parameters. An improperly selected equivalent diameter can lead to insufficient efficiency of the settling tank, which is manifested by a low degree of thickening of suspensions (sediment) or unclarified liquid overflow (in the case when the product is to be a purified liquid). For this reason, it is crucial to use a properly selected equivalent diameter parameter that precisely reflects the properties of particles subjected to sedimentation.

The efficiency of the settling tank has a significant impact on the energy efficiency of the entire device and the possibility of reducing operating costs and the waste stream. In the case of an optimally designed settling tank, which ensures high efficiency of phase separation, it is possible to reduce energy consumption, which in the long term translates into lower operating costs. Better efficiency allows for a reduction in the amount of waste generated in the process, which reduces the burden on the disposal and environmental protection systems. In situations where it is necessary to use flocculants or coagulants, a properly designed settling tank allows for the optimization of their dosage, which on the one hand reduces the costs of purchasing these chemicals, and on the other reduces the load of pollutants released into the environment. As a result, improving the efficiency of the settling tank affects not only the reduction of operating costs, but also reduces the negative impact on ecosystems, contributing to the implementation of the principles of sustainable development.

Based on the presented results, it can be seen that the choice of the equivalent diameter measure has a significant impact on the obtained values of this parameter. The error in determining the equivalent diameter can reach up to several percent. Such deviations can directly affect the calculation of the suspension settling velocity, and thus the operating conditions of the settling tank. In the context of sedimentation, such

differences can lead to inefficient operation of the device, which can result in improper phase separation in the process.

It is also worth noting that the error in the approximation of the equivalent diameter may be related to other parameters that describe the shape and size of particles. These parameters include, among others, the elongation, compact structure of the particle, and its sphericity. These features affect the discrepancies between different measures of equivalent diameters and their use in process modeling. For this reason, further research should focus on verifying the influence of the shape and other properties of particles on the determined values of equivalent diameters.

A more detailed understanding of the influence of these factors can contribute to improving the models used in the design and optimization of sedimentation devices. Precise determination of equivalent diameters, taking into account the complexity of particle shapes, can lead to more efficient designs of settling tanks, ensuring better phase separation and higher efficiency of the sedimentation process.

## ACKNOWLEDGEMENTS

This research was funded by the Dean's Grant from the Faculty of Mechanical Engineering and Robotics, AGH University of Science and Technology, titled "Development of a mathematical model of the sedimentation process using the particle shape parameter based on data from the sedimentation chamber and video analysis," no. 16.16.130.942

## REFERENCES

[1] Silva, J.A., Wastewater Treatment and Reuse for Sustainable Water Resources Management: A Systematic Literature Review. Sustainability, 15, 10940, 2023, https://doi.org/10.3390/su151410940

[2] Goula A., Kostoglou M., Margaritis Zouboulis, A., A CFD methodology for the design of sedimentation tanks in potable water treatment: Case study: The influence of a feed flow control baffle, Chemical Engineering Journal, 140, 110-121, 2008, https://doi.org/10.1016/j.cej.2007.09.022

[3] Kołodziejczyk K., Construction of a numerical model of suspension in a numerical simulation of sedimentation, E3S Web of Conferences, 46, 00011, 2018, https://doi.org/10.1051/e3sconf/20184600011

[4] Banaś M., Computer simulations of the sedimentation process model which considers internal interactions among solid phase particles, Chemical and Process Engineering, 25, 665-671, 2004

[5] Basson D.K., Berres S., Bürger R., On models of polydisperse sedimentation with particle-size-specific hindered-settling factors, Applied Mathematical Modelling, 33, 4, 1815-1835, 2009, https://doi.org/10.1016/j.apm.2008.03.021

[6] Ferguson R.I., Church M., A Simple Universal Equation for Grain Settling Velocity, Journal of Sedimentary Research, 74, 6, 933-937, 2004, http://dx.doi.org/10.1306/051204740933

[7] Yang J., Tang L., She Y., Sun J.,Laboratory measurements of the fall velocity of fine sediment in an estuarine environment, International Journal of Sediment Research, 35, 2, 217-226 2020, https://doi.org/10.1016/j.ijsrc.2019.08.003

[8] Bieganowski A., Ryżak M., Sochan A., Barna G., Hernádi H., Beczek M., Polakowski C., Makó A., Laser Diffractometry in the Measurements of Soil and Sediment Particle Size Distribution, Advances in Agronomy, 151, 215-279, 2018, https://doi.org/10.1016/bs.agron.2018.04.003

[9] Sedláčková, K.; Ševelová, L.; Igaz, D.; Aydın, E., Determination of Particle Size Distribution: Comparison of Standard Hydrometer Method and Laser Diffraction Analysis for Use in Forestry, Forests, 15, 327, 2024, https://doi.org/10.3390/f15020327

[10] Hayakawa Y., Takashi Oguchi T., Evaluation of gravel sphericity and roundness based on surface-area measurement with a laser scanner, Computers & Geosciences, 31, 6, 735-741, 2005, https://doi.org/10.1016/j.cageo.2005.01.004

[11] Liu B., Zhang X., Wang L., Hong H., Fluidization of non-spherical particles: Sphericity, Zingg factor and other fluidization parameters, Particuology, 6, 2, 125-129, 2008, https://doi.org/10.1016/j.cpart.2007.07.005

[12] Banaś, M.; Hilger, B. Proposal for New Method for Calculating Sedimentation Process Efficiency in Water Treatment Plants, Materials, 17, 3285, 2024, https://doi.org/10.3390/ma1713328

[13] Francalanci S., Paris E., Solari L., On the prediction of settling velocity for plastic particles of different shapes, Environmental Pollution, 290, 2021, https://doi.org/10.1016/j.envpol.2021.118068

# EVAPOTRANSPIRATION AS A METHOD OF WASTEWATER DISPOSAL

**Ing. Pavel Škarpa**
Brno University of Technology, **Czech Republic**

## ABSTRACT

The paper describes the disposal of wastewater by evapotranspiration (ET). In cases where buildings can't be connected to the sewerage or to domestic treatment plant, a cesspool must be built. Economic burden of transporting and requirements of wastewater recycling have lead to invention of a system, that ensures the quality of wastewater needed for recycling, while maximizing ET through evapotranspiration bed (ET-bed).

For actual evapotranspiration (AET) analysis, a laboratory model of ET-bed with water tank was constructed. The water tank is fit with water and atmosphere pressure sensors, and a water pump. Water is transported to the surface of ET-bed, while beds drainage is connected to the water tank. The output data on the level drop in the tank, combined with a nearby meteorological station, are allowing the AET to be analysed.

When measuring the AET, values higher then 7 mm/m2/day were measured. In the summer period, totals of around 5 mm/m2/day were regularly achieved. Regression of AET with potential evapotranspiration (PET) yielded R2 = 0.83 for the Oudin method, R2 = 0.75 for the Thornthwaite method, or R2 = 0.76 for the Hargreaves - Allen method.

The disposal of wastewater by ET with recycling represents an economically less demanding solution compared to cesspools. The research itself is set to establish a method of designing the system, with regards of functionality in the long term with the simplest possible operation.

**Keywords:**

Evapotranspiration, wastewater disposal, constructed wetlands, evapotranspiration bed

## INTRODUCTION

The legislation of Czech republic have set a certain hierarchy for the different methods of wastewater disposal [1; 2]. The most preferred of all is to connect buildings to centralized wastewater treatment plant through sewerage network. When this is not technically possible, the building must be built with domestic wastewater treatment plant. The effluent from the plant should preferably be flowing into water stream, river, etc. When there is no recipient close to the treatment plant, effluent can be absorbed into the bedrock [3]. The legislation allows for the use of cesspool in rare conditions. For example, when the building is located in protected natural area, where effluent can pollute highly sensitive recipients or underground waters. The collected wastewater must then be transported to nearby treatment plant and cannot be discharged on site.

According to the same legislation, it is important to note that alternative wastewater disposal technologies are not prohibited. This allowed the invention of new effluent free technology [4]. The structure of the new way of disposal is highly inspired by constructed wetlands wastewater treatment plants, and cesspools. It is based on the use of septic tank, ET-bed, and a storage tank. The ET-bed is structurally analogous to vertical filter. The

only difference is, that it is built mostly without the need of excavations, and the walls of ET-bed are directly in contact with filter layers. These walls can be designed in a way, that ensures maximal evapotranspiration possible. Together with possibility of using wastewater from the storage tank for recycling, the technology presents an attractive alternative to cesspools.

This paper contains a summary of the development of the design methodology for ET-bed so far. The primary goal of the research is to select the appropriate method for establishing potential evapotranspiration of the ET-bed, that would allow designers to establish the area of the ET-bed needed, in order to achieve reasonable volumes of evapotranspired water with regard to financial cost of construction.

## MATERIALS AND METHODS

An outdoor laboratory model of this technology has been constructed on the land of Faculty of Civil Engineering, Brno University of Technology [4]. The model consists of water tank with volume of 1 000 litres. A water pump and pressure sensors are installed inside the tank. To eliminate measurement errors due to atmospheric pressure fluctuations, a second sensor measures atmospheric pressure near the tank at the same time. This allows the use of barrologic compensation. At the end, only the fluctuations of the water pressure created by drop in water level due to evapotranspiration and increase of the level due to precipitation are measured. The water gain by precipitation is separated from measurements with the data from meteorological station located approximately 200 metres from the laboratory model.

The second part of the model is a small ET-bed, with squared area of 5 $m^2$. And a height of 0,8 m. The layers are very similar to real designs of vertical filters, and the walls are constructed by sacks filled with sand. Both the walls and the surface layer are planted with grass. Water is pumped in the surface of the ET-bed from the water tank, and it is evenly distributed on the walls and surface of layers by drip irrigation. Water that is not evapotranspired is then flowing from drainage layer, which is hydraulically isolated by EPDM foil, back into the water tank by gravity.

The data gathered by pressure sensors were compared with precipitation measured by the meteorological station mentioned before. For the determination of evapotranspiration, increases of water volume in water tank by precipitation had to be removed from the data. Unfortunately, the time difference between precipitations realization and the inflow of rainwater into the water tank could not be precisely determined. As a result the days with precipitation events have been removed from the data.

Daily actual evapotranspiration of 1 $m^2$ surface area was used to calibrate methods for calculating potential evapotranspiration. The methods in question were:

- Hargreaves method [5]
- Thornthwaite method [6]
- Oudin method [6; 7]

The methods were selected with regards to their simplicity in terms of input data. This is because the main aim of the research is to establish a designing method for such technology, and in the Czech Republic, only temperature, precipitation, geographical location and altitude data are commonly available.

Before calculations started, calibration of equations was done. For this purpose, 8 reference intervals were picked. All intervals were 14 days long and were chosen to take into account the spring, summer and autumn seasons.

Calibration was performed in MS Excel using the solver function. A summary of actual evapotranspiration and potential evapotranspiration across all reference intervals was identical. After calibration, potential evapotranspiration for each day of measurement was calculated based on data measured in meteorological station mentioned before.

Subsequently, a two-stage regression of the data was performed using linear, exponential and power regression models. In the first stage, all data were used as input. The resulting regression equation, along with both added and subtracted standard deviation, was used to filter the data. The regression was then performed again on the data that were inside of interval created as described previously. In the two stages, only the same type of regression model (linear, exponential, power) was used. Regression was done with inputs in daily and average weekly forms.

## RESULTS

Known surface area of the water level in water tank together with measured level drop allowed the calculation of actual evapotranspiration on each measurement day. After that, the measured volume of evapotranspired water was divided by the area of ET-bed. In order to visualize the data, the average daily evapotranspiration for 1 $m^2$ ET-bed was calculated.

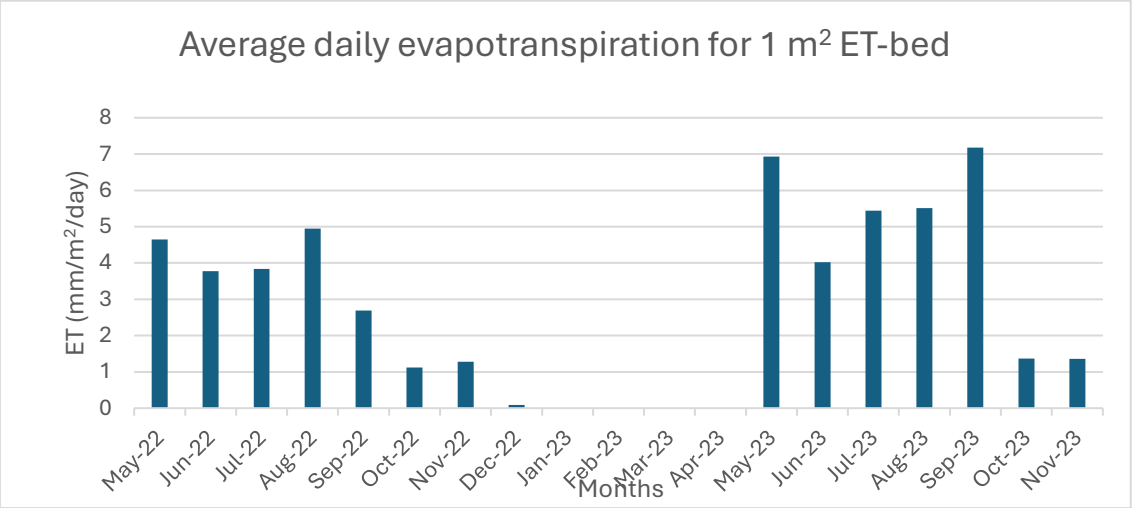



**Figure 1 - Average daily evapotranspiration for 1m2 ET-bed**

The measurement showed that, if the service of the ET-bed is done properly, 5 mm/day of evapotranspiration can be regularly achieved with maximums well over 7 mm/day (as the graph shows only average data by month).

https://doi.org/10.5593/sgem2024v/3.2/s11.06

**Hargreaves method regression**

The regression had better results in the form of weekly averages. Therefore, first stage calculated with 51 inputs. The standard deviation, which was used with regression equation for data filtration, was σ = 2,23 mm/m$^2$/day. The best results in terms of coefficient of determination was achieved using the power model, in which 14% of the data did not pass filtering.

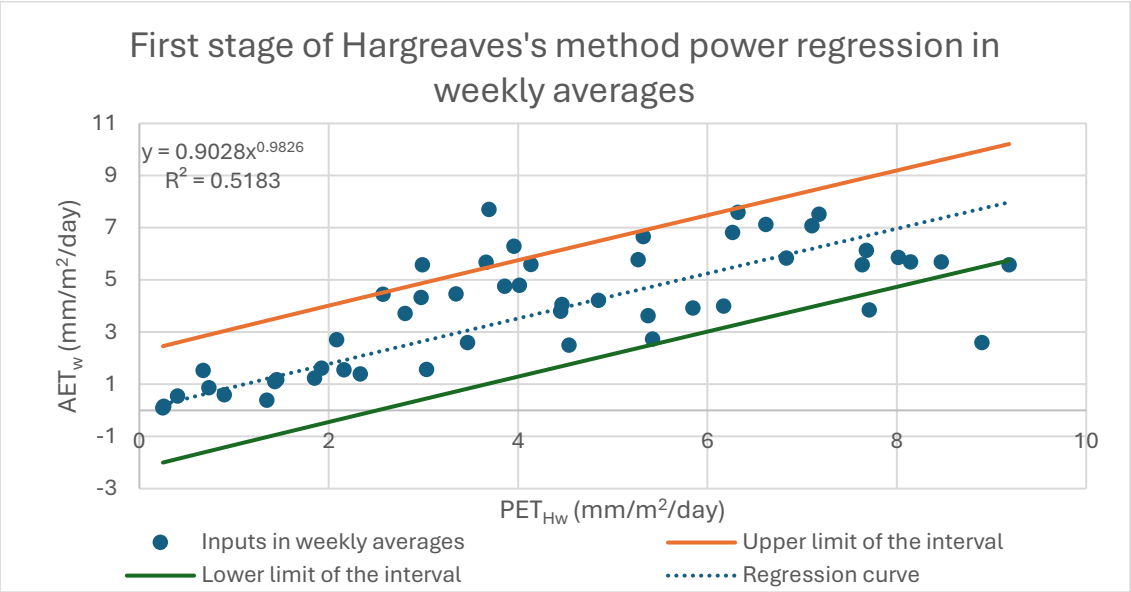



**Figure 2 - First stage of Hargreaves's method power regression in weekly averages**

The result of the first stage regression was equation $AET_w = 0{,}9828 \times PET_{Hw}^{0{,}9826}$. The coefficient of determination was estimated to $R^2 = 0{,}5183$. $AET_w$ represents actual weekly evapotranspiration, $PET_{Hw}$ stands for weekly potential evapotranspiration determined by the Hargreaves method.

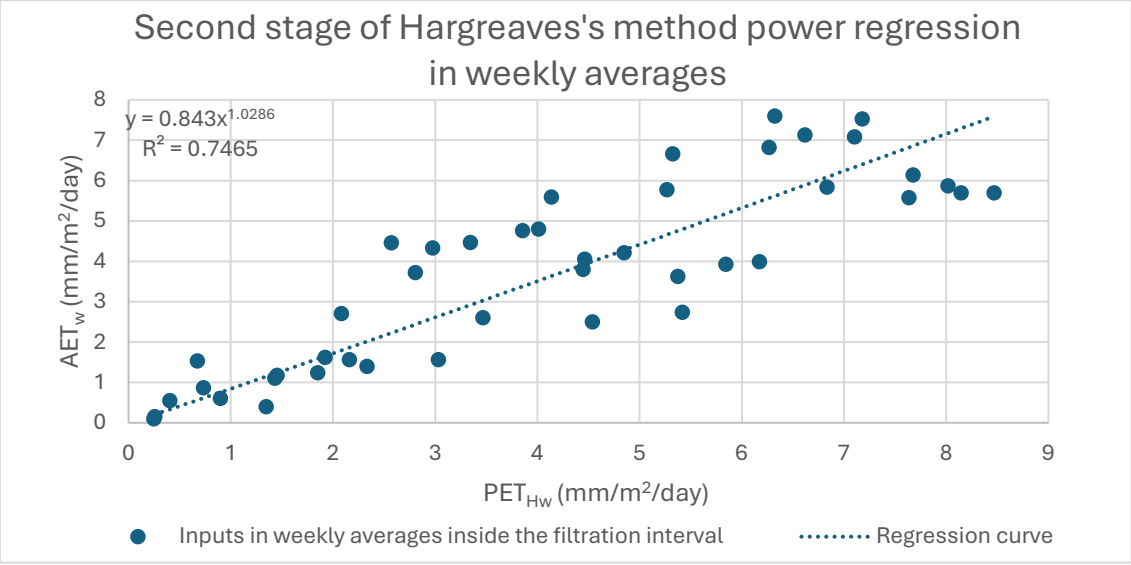



**Figure 3 - Second stage of Hargreaves's method power regression in weekly averages**

The regression equation of second stage regression was set as $AET_w = 0,843 \times PET_{Hw}^{1,0286}$. The coefficient of determination was estimated to $R^2 = 0,7465$.

**Thornthwaite method regression**

A two-stage regression was again done using both daily and average weekly inputs. The best results in terms of the coefficient of determination were achieved by two-stage linear regression with weekly averages. The first stage of regression began with the same data, as mentioned before. Using the same approach in terms of filtration, out of 51 inputs, 40 were used for the second stage. The standard deviation was $\sigma = 2,22$ mm/m$^2$/day. The result of the first stage regression was the equation $AET_w = 0,3946 \times PET_{Tw} + 2,0334$. The coefficient of determination was estimated as $R^2 = 0,3415$. $PET_{Tw}$ stands for weekly potential evapotranspiration determined by the Thornthwaite method.

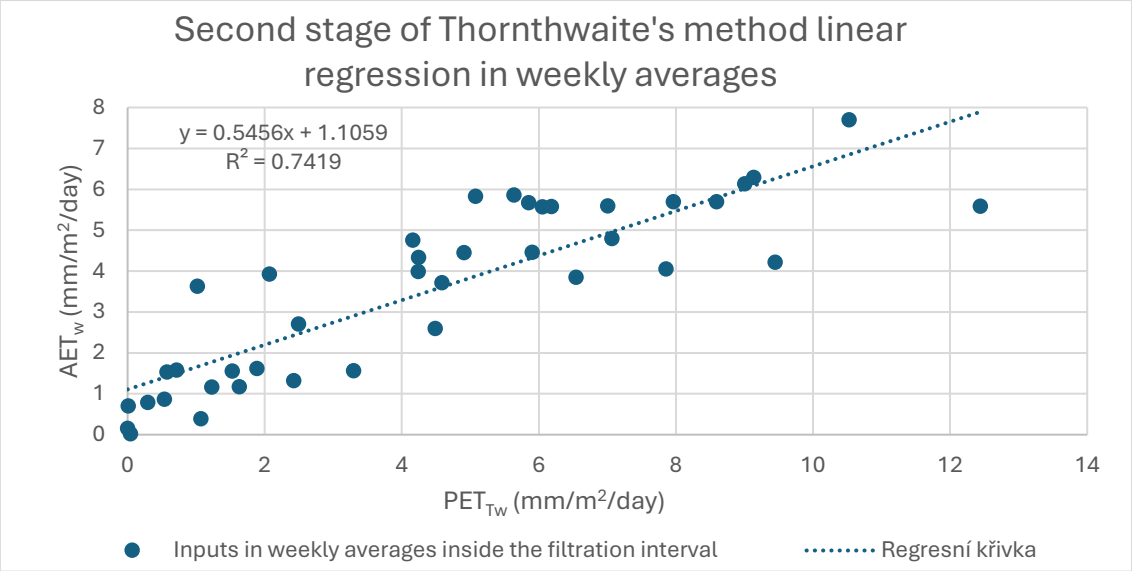



**Figure 4 - Second stage of Thornthwaite's method linear regression in weekly averages**

The second stage of regression resulted with equation $AET_w = 0,3946 \times PET_{Tw} + 2,0334$. The coefficient of determination was estimated as $R^2 = 0,7419$.

**Oudin method regression**

A two stages regression was once again done in both daily and average weekly inputs. For this method, best results in terms of coefficient of determination were achieved were achieved with a two-stage power regression on the weekly averages. The first stage of regression started with the same data, as in both cases described before. Following the same filtering approach, 39 out of 51 inputs were used for second stage regression. The standard deviation was $\sigma = 2,23$ mm/m$^2$/day. The result of the first stage regression was equation $AET_w = 1,0149 \times PET_{Ow}^{1,3756}$. $PET_{Ow}$ stands for weekly potential evapotranspiration determined by the Oudin method. The coefficient of determination was $R^2 = 0,4571$.

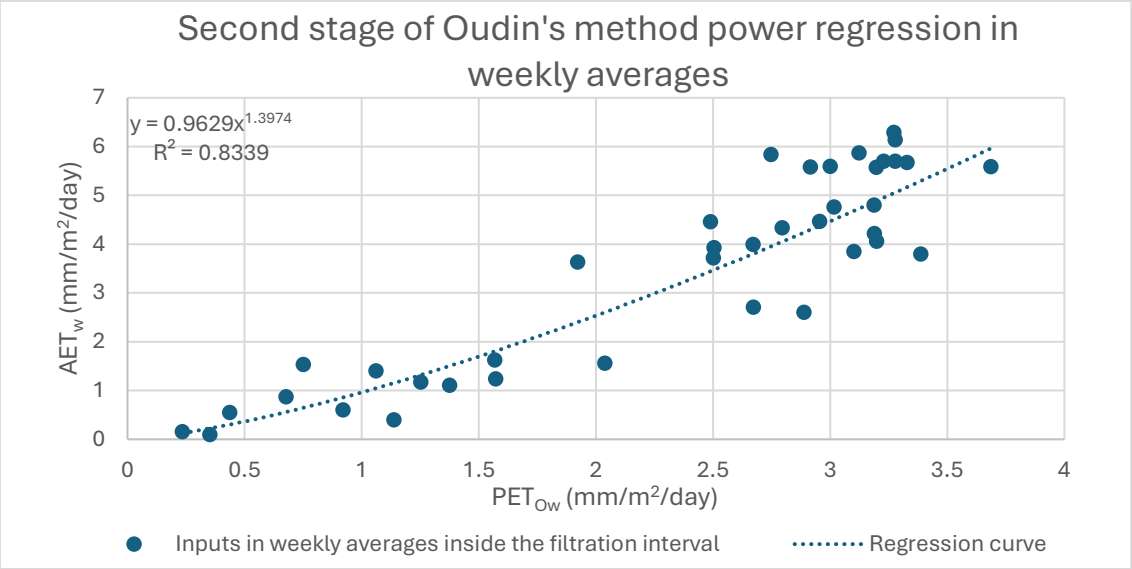



**Figure 5 - Second stage of Oudin's method power regression in weekly averages**

The second stage of regression have set equation $AET_w = 0{,}9629 \times PET_{Ow}^{1{,}3974}$. The coefficient of determination was estimated to $R^2 = 0{,}8339$, which is significantly higher compared to the regression models presented earlier.

## DISCUSSION

Figure 1 shows the measured evapotranspiration from the model. The visibly higher evapotranspiration measured in the second year of measurement could be caused by several factors. In the first year, the grass on the surface of the ET-bed was relatively sparse compared to the second year. Another potential factor could have been different approach to service of the bed. In the first year, the grass was not cut, whereas in the second year, it was cut three times. Evapotranspiration could then be increased by plant growth, during which water is stored in new plant tissue. Moreover, evapotranspiration is tightly coupled to photosynthesis, which occurs on a larger scale in growing plants than in plants that are at the end of their development.

The design methodology itself cannot yet be determined on the results shown in this paper. It may look like the Oudin method could be the biggest favourite in this regard, but there are various uncertainties. First, the measurement used in calculations was only two years long. A longer measurement period as well as more models could lead to more precise results. As of the number of models, several devices using effluent-free wastewater disposal technology based on ET-bed have already been constructed and are equipped with sensors. Therefore, it is believed that there will be far more data to calculate for any future research.

## CONCLUSION

The technology of effluent free wastewater disposal with an ET-bed is a new alternative to cesspools. In comparison, the ET-bed technology seems to be costly to build due to more objects used (such as ET-bed or septic tank). However, the recycling of wastewater combined with the reduced need for transporting it to a treatment plant offers a potential return on the original cost. The actual evapotranspiration of the EP-bed is yet to be

established, but initial measurements have shown that averages of about 7 mm/m$^2$/day are possible in during summer days. Potential evapotranspiration has been calculated using multiple methods. The paper shows the Hargreaves, Thornthwaite, and Oudin methods. To establish their accuracy, various regression calculations were done. The Hargreaves method had the highest value of $R^2$ = 0,7465 in a two-stage power regression in weekly averages. The Thornthwaite method reached its highest value of $R^2$ = 0,7419 in a two-stage linear regression in weekly averages. The Oudin regression had the best values of $R^2$ = 0,8339 in a two-stage power regression in weekly averages. Therefore, the Oudin method showed itself to be the most effective for estimating ET-bed evapotranspiration so far. However, the equation estimated in this regression is not accurate enough for this purpose. It is also worth noting, that coefficient of determination is not the only parameter, that should be considered in regression models. Therefore, more research will be needed in this regards.

## REFERENCES

[1] HANÁK, Jakub. Odborné vyjádření. 2024, roč. 2024, s. 3.

[2] VOJÁČEK, Michal. Vyjádření: Prodejna pro dům a zahradu, ulice Mladoboleslavská, Praha - likvidace odpadních vod pomocí odpařovacího záhonu hydroizolovaného od okolního terénu. 2024, roč. 2024, s. 4.

[3] Zákon č. 254/2001 Sb.: Zákon o vodách a o změně některých zákonů (vodní zákon). Online. In: 2001. 2001, 98/2001. Available at: https://www.zakonyprolidi.cz/cs/2001-254. [accessed 2024-10-27].

[4] ŠKARPA, Pavel. Technologie bezodtokových čistíren pro malé producenty odpadních vod. Bakalářská práce, vedoucí doc. Ing. Michal Kriška, Ph.D. Brno: Vysoké učení technické v Brně, Fakulta stavební, Ústv vodního hospodářství krajiny, 2022.

[5] FOOLADMAND, H. R.; ZANDILAK, H. and RAVANAN, M. H. Comparison of different types of Hargreaves equation for estimating monthly evapotranspiration in the south of Iran. Online. Archives of Agronomy and Soil Science,. 2008, roč. 2008, č. 54 (3), s. 321 - 330. Available at: https://doi.org/https://doi.org/10.1080/03650340701793603. [accessed 2024-10-26].

[6] BEDNÁŘ, Martin and MARTON, Daniel. Porovnání metod výpočtu potenciální evapotranspirace. In: Juniorstav 2022: 24. Odborná konference doktorského studia. Brno: Vysoké učení technické v Brně, Fakulta stavební, 2022, p. 393 - 398. ISBN 978-80-86433-76-9.

[7] PÁTEK, Karel. Metody stanovení evapotranspirace v mokřadech a spotřeba podzemní vody evapotranspirací mokřadů v povodí Liběchovky a Pšovky. Bakalářská práce. Praha: Univerzita Karlova, Přírodovědecká fakulta, 2022.

# FLOOD PROTECTION IN A MUNICIPALITY WITH THE IMPLMENTATION OFANATURE-BASED SOLUTION

**doc. Ing. Brumarová Lenka**
**Ing. Brumar Jakub**
**Ing. Gamonová Patricie**
VŠB – Technical University of Ostrava, Faculty of Safety Engineering,
Lumírova 630/13, 700 30, Ostrava-jih – Výškovice, **Czech Republic**

## ABSTRACT

Nature-based solutions harness the power of nature. Nature-based solution represent an innovative approach that can combine ecological and engineering elements with site security. Nature-based solusion encompass a wide range of measures to protect, restore or sustain landscapes such as watersheds and urban areas. Nature-based solution can be implemented on the basis of a risk analysis of the territory to ensure the safety of the territory, e.g. a municipality. An example of this is the construction of dry polders leading to flood protection in a municipality. These measures may not only lead to flood protection but may also hide other uses such as nature trails and others. This paper presents the construction of dry polders in a selected municipality highlighting their other uses for the residents and the safety of the municipality from flood hazards. The paper describes the implementation of nature-based solution (dry polders) as key to sustainable adaptation to climate change and increasing the resilience of the village to flooding.

**Keywords:** nature-based solution, floods, dry polder

## INTRODUCTION

In recent years, the future of our planet has become a growing concern. With increasing technological change, there are global challenges to overcome. In particular, climate change threatens not only the environment but also the quality of life. The introduction of a nature-based solution (hereafter NbS) can enable us to better address these challenges. [1] NbS makes use of the natural ecosystem and, if well designed, allows for an improved approach to environmental protection and restoration, as well as improving the quality of life of the inhabitants. [2] NbS can be divided into three categories: watershed or landscape scale practices, neighbourhood or site scale practices and coastal practices [3] NbS not only combat climate change but also seek to reduce flood risk. [4] One flood control measure and application of NbS is the introduction of dry polders. [5]

This paper highlights the practical benefits in a case study conducted on dry polders as a type of nature-based solution, with the core of the work focusing on the construction of dry polders in the municipality of Bolatice.

https://doi.org/10.5593/sgem2024v/3.2/s11.07

## MATERIALS AND METHODS

This paper focuses on a case study in the field of NbS particularly on dry polders applied in the municipality of Bolatice. This study can be divided into three stages. The first stage deals with the description of NbS, the second stage focuses on the description of floods and their mitigation, for example by implementing dry polders, and the third stage describes the implementation of dry polders in the municipality of Bolatice.

### Nature based solution

It was not until the 1970s that the idea of environmental services began to take hold. In the 1990s it was recognised that there was a need to focus on improving approaches to ecosystem protection, restoration and sustainable management. At the end of the 21st century, the term "nature-based solution" emerged, which means that people need not only be passive recipients of nature, but could also protect and restore the natural ecosystem. Nature-based solution (hereafter NbS) can be defined, for example, as the use of natural ecosystem and services that can solve societal problems, especially for example climate change or natural disasters, and at the same time can support biodiversity.[6]

NbS is applied in various areas, in particular restoring wetlands and rivers to maintain or increase fish populations, reducing flood risk, protecting forests to support food and energy security, restoring drylands to enhance water security, or developing green infrastructure in urban environments. [6]

### Types of nature-based solution

As there is no clear definition of NbS. Nor is its division given. According to the US Department of Homeland Security, NbS can be divided into three categories [3]:

- Watershed or landscape-scale practices
- Neighborhood or site-scale practices
- Coastal practices

Examples include waterfront parks, which can reduce flooding and generally abate flood impacts; other systems that can minimize flood impacts include bike paths, coral and oyster reefs, coastal wetlands, tree trenches, tree canopy, green roofs, and rain gardens and stormwater parks. Other NbS proposals may include mangrove restoration, which is a forest that can function in a saltwater environment and can sequester carbon and absorb carbon dioxide from the atmosphere. Then Bioswales is a measure that can reduce flooding in parking lots.[3]

In the Czech Republic (hereafter CR) there is no division, but it is possible to introduce flood protection measures within the NbS, which in the CR can be divided into point, linear and area. [7]

For example, dry polders, wetlands and retention ponds are classified as point, a retention dike, ditch or soakaway is classified as linear and grassland, afforestation, strip crop rotation and contour cultivation are classified as area. [7]

### Floods

Floods are one of the most serious natural disasters and their impact brings social and environmental challenges. Studies suggest that by 2050, the 100-year flood will occur

twice as often as today over 40% of the world's land surface. Not only do floods disrupt hydrological processes and ecosystems, but also the quality of life is reduced. [8]

Even though floods are a natural phenomenon in nature, they are one of the threats that the CR is dealing with. However, floods cannot be influenced and are mainly determined by meteorological phenomena, but it is possible to be prepared for floods and to mitigate their consequences. The CR started to focus more on flood protection measures only in 1997, when the country was hit by large-scale floods. On the basis of these events, documents dealing with floods, such as the Flood Prevention Strategy for the territory of the CR or the Plan of the Main River Basins of the CR, were created.[9]

If applied correctly, NbS can not only minimise the occurrence of floods but also bring other benefits, for example, implementing NbS in floodplains will not only mitigate flood impacts but also prevent erosion, improve soil health and restore biodiversity.[10]

**Dry polders**

Dry polders can also be considered as NbS. A dry polder is referred to as a dry detention basin that provides flood protection. Over time, the reservoir does not retain water and may normally serve as a meadow or field, for example, but when excessive rainfall occurs and water threatens to spill over the banks of adjacent watercourses, the reservoir can prevent flooding. The main purpose of these reservoirs is to retain water during high rainfall events and to regulate runoff.[11]

Dry polders can also be implemented on the territory of a municipality as part of the CR flood protection measures. For this reason, a case study was carried out, which deals with the implementation of dry polders in the municipality of Bolatice, which is located in the Moravian-Silesian Region. Based on the fact that there are uplands around the village of Bolatice and almost most of the rainwater flows through the village, flooding has often occurred. In 1967, the municipality decided to carry out the first flood protection measures and implement a dry polder. In the current situation, a total of nine dry polders have been built. This flood protection measure is unique in the CR. For this reason, the municipality has decided to link this NbS-based solution with activities for the local population and has created a nature trail [12]

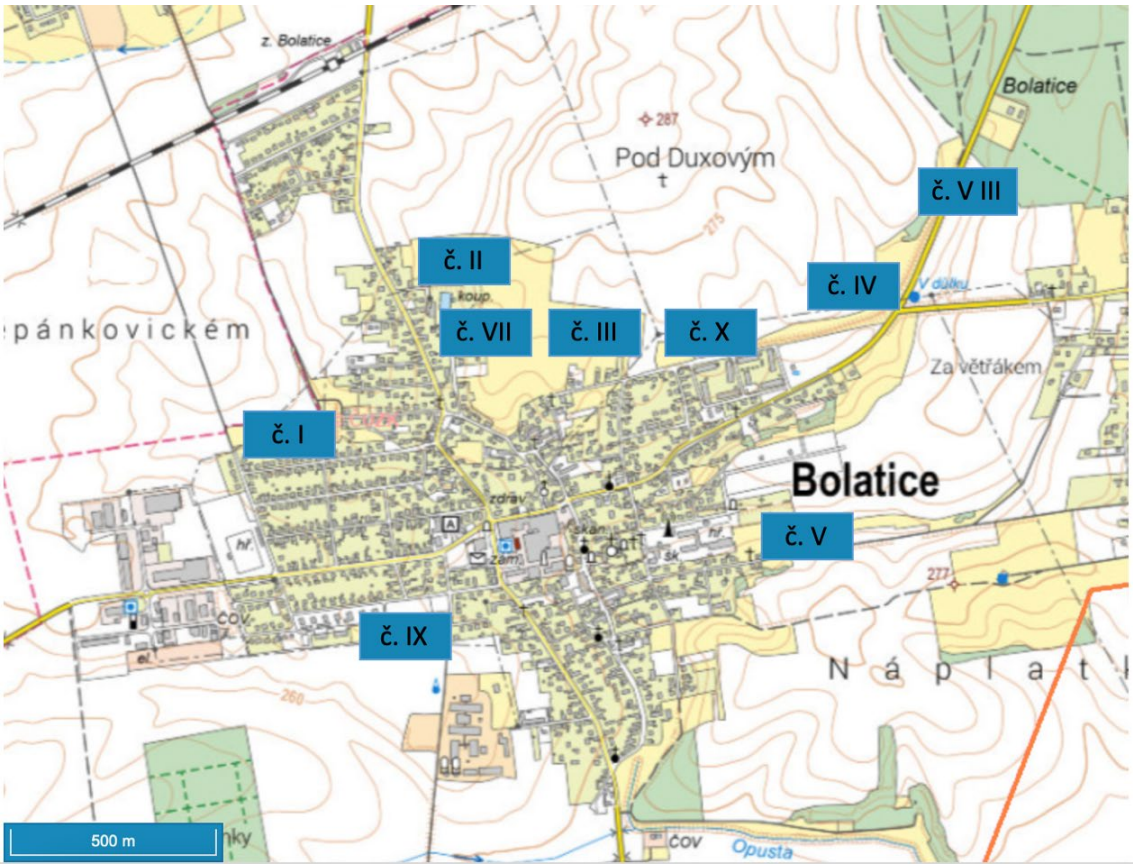
The dry polders in Bolatice consist of four parts. **The dam body** the dam body is usually artificially created, only rarely natural embankments are used. The dyke consists of two slopes: a guide slope towards the retention area and an air slope out of the polder. The highest part of the dyke is called the crown of the dyke. **Outlet facility** The lowest part of the dam incorporates pipes for the discharge of water from the reservoir, known as the bottom or pipe outlet. The pipe outlet includes a closure element, a discharge pipe and a device to dampen the kinetic energy of the outflowing water. On the downstream side, less often on the air side of the dam, a closure is designed to control the outflow. From the **retention area**, which is used to capture the flood wave. Water is only temporarily captured in this area. And the safety spillway, which means that if the flood wave is too large and the polder cannot hold the entire volume of water, the water will overflow the **safety spillway**. This safety feature should be part of every levee and should be designed to minimize damage during floods.[11]

https://doi.org/10.5593/sgem2024v/3.2/s11.07

## RESULTS

### Implementation of dry polders in the municipality of Bolatice

Nine dry polders have been implemented in the municipality of Bolatice. As shown in figure n. 1 the dry polders were applied in the undeveloped part and located rather on the outskirts of the village. These dry polders are also used as a nature trail.




*Figures n. 1 Deployment of dry cops in the municipality of Bolatice. Proccessing according to [12]*

The trail is about 9 km long. Two types of dry polders were created in the implementation of dry polders in the village of Bolatice. The first type was implemented on dry polders I, II, IV, V, VII and IX. The second type was implemented on dry polders III, VIII and X. Dry polder No. VI is missing as it does not meet the definition of a dry polder, but is only a mound.

*Table n. 1 List of dry polders*

| Name of polder | Year of contruction | Year of reconstruction | Length (m) |
|---|---|---|---|
| Dry polder č. I | 1967 | 2010 | 108,7 |
| Dry polder č. II | 1968 | 2010 | 105 |
| Dry polder č. III | 1997 | | 72 |
| Dry polder č. IV | 1972 | 2001 | 752 |
| Dry polder č. V | 1978 | 1998 | 112 |
| Dry polder č. VII | 1999 | | 83 |
| Dry polder č. VIII | 2001 | | 65 |
| Dry polder č. IX | 2010 | | 218 |
| Dry polder č. X | 2010 | | 98,4 |

## DISCUSSION

It can be concluded that the construction of dry polders in the Municipality of Bolatice has mitigated the impacts of floods in recent years, especially during the last event of 13 September 2024, when dry polders played a key role in flood management. Sewerage is subsequently used to drain the dry polders after a flood, which can be considered a minor deficiency.

## CONCLUSION

Based on NbS, floods can be managed or minimized. Key benefits for flood management include, for example, wetland and river ecosystem restoration, stream renaturation, reforestation and forest protection, and green infrastructure in cities. For flood management there is also the possibility of introducing dry polders, which include water flow regulation, soil and landscape protection, biodiversity and also used for recreational purposes such as nature trails. The paper is prepared as a case study that focused on one type of NbS namely dry polders, specifically the implementation in the municipality of Bolatice. The paper shows that the construction of dry polders can not only minimize the effects of floods, but can also improve the quality of life in the area of education. In addition, this initiative can motivate government authorities to become actively involved. It can be concluded that the implementation of NbS is not a simple process. It is necessary to understand the environment where dry polders need to be applied in order to balance the ecological system and sustainable development.

## REFERENCES

[1] Seedon, N., Smith, A., Smith, P., Key, I., Chausson, A., Girardin, C., House, J., Srivastava, S., Turner, B. Getting the message right on nature-based solutions to climate change, Global Change Biology, England, vol. 27, 2021, pp 1518-1546. https://doi.org/10.1111/gcb.15513

[2] Kabisch, N., Frantzeskaki, N., Pauleit, S., Naumann, S., Davis, M., Artmann, M., … & Bonn, A. Nature-based solutions to climate change mitigation and adaptation in urban

areas: perspectives on indicators, knowledge gaps, barriers, and opportunities for action, Ecology and Society, Germany, vol 21, 2016. https://doi.org/10.5751/es-08373-210239

[3] Building community resilience with nature-based solutions, U.S. Department of Homeland Security, 2021.

[4] Griffiths, J., Borne, E. K., Semadeni-Davies, A., Tanner, C. CH. Selection, Planning, and Modeling of Nature-Based Solutions for Flood Mitigation. National Institute of Water and Atmospheric Research, New Zealand. 2024. https://doi.org/10.3390/w16192802

[5] Brasil, J., Macedo, M., Oliveira, T., Oliveira, T., Gomes, M., Lago, C., … & Mendiondo, E. Nature-based solutions and real-time control: challenges and opportunities, The 5th International Electronic Conference on Water Sciences session New sensors, New Methods and Technologies, New Approaches, USA, 2020. https://doi.org/10.3390/ecws-5-08060

[6] Cohen-Shacham, E., Walters, G., Janzen, C., Maginnis, S. Nature-based Solutions to adress global societal challenges. Gland, Switzerland: IUCN. 2016. https://doi.org/10.2305/IUCN.CH.2016.13.en

[7] Macháč, j., Vackova, A., Slavíková, L., et. al. Classification and evaluation of nature-based flood control measures on selected public environmental assets, Saxon-Czech flood risk management II (STRIMA II), Czech Republic, 2018.

[8] Zhou, K., Kong, F., Yin, H., Destouni, G., Meadows, E. M., Andersson, E., Chen, L., Chen, B., Li, Z., Su. J. Urban flood risk management needs nature-based solutions: a coupled social-ecological systém perspective. Urban Sustain 4, 25, 2024. https://doi.org/10.1038/s42949-024-00162-z

[9] Concept of solving the problém offloodprotectionin the Czech Republic with the use of technical and nature-based solutions, Ministry of Agriculture, Czech Republic, 2010.

[10] Vojinovic, Z. Nature-based Solutions for Flood Mitigation and Coastal Resilience. Analysis of EU-funded projects. European Commission. Luxembourg: Publications Office of the European Union. 2020 ISBN 978-92-76-18197-2.

[11] Říha, J., Sedláček, M., Smrž, P., Veselý, R., Žatecký, S. Design and implementation of dry polder from the point of view of technical safety supervision. Ministry of the environment, Czech republic, 2014. ISBN: 978-80-7212-600-2

[12] Adamec, V., Hrdina, P. System Village Bolatice Flood Protection, Spektrum, Czech Repiublic. 2011, pp15-18. ISSN: 1211-6920.

# INFLUENCE OF WATER TEMPERATURE ON DROPLET SIZE DISTRIBUTION OF HIGH-PRESSURE WATER MIST NOZZLES

**Ing. Marek Miskay**
**Ing. Miriam Kadlubcova**
**Assoc. Prof. Karla Barcova**
VSB - Technical University of Ostrava, Faculty of Safety Engineering. **Czech Republic**

## ABSTRACT

Temperature affects the number of water properties. Density, specific heat capacity, surface tension and more change with temperature. The size of the water droplets has strong impact on the shielding of radiant heat or the ability to extinguish and suppress fires. Determining the droplet size distribution of water mist is used in wide range of industries, in fire protections, spray technology, pharmaceuticals or automotive industry. The work deals with the measurement of the droplet size distribution of eight selected nozzles at different temperatures using the laser diffraction method. The selected nozzles are designed for use in fire protection to extinguish and suppress fires. Measurements were taken at the distance of 12.5 cm from the nozzle in the centre of the mist stream. The water source temperatures chosen for the measurements were 25, 40, 55 and 80 degrees Celsius. The purpose of the work was to determine the effect of temperature on the change in Sauter mean diameter and particle size distribution at a working pressure of 70 bar. For the six measured nozzles, a decrease in Sauter mean diameter with increasing temperature was observed. For the two measured nozzles the result was the opposite. The particle size distribution of the four measured nozzles varied significantly at different temperatures.

**Keywords:** High-pressure water mist, Water temperature, Sauter mean diameter, Droplet size distribution, Laser diffraction

## INTRODUCTION

Water is an extraordinary substance with wide variety of properties that change with temperature. The most frequently mentioned temperature-dependent property is density. Water has its highest density at a temperature approaching 277 K. [1] Density is not the only property of water that changes with temperature. Temperature-dependent properties include the speed of sound propagation or specific heat capacity. The value of viscosity, thermal conductivity or surface tension decreases with increasing temperature. On the other hand. The electrical conductivity and saturation vapour pressure increase with increasing temperature. [2]

With the change in properties comes a change in the mechanisms of water. Based on studies [3] and [4], it has been proven that the cooling effect increases with increasing water temperature. The study [5] dealt with the effect of temperature change on fire extinguishing. The study found that water temperature has the effect on the ability to extinguish fire. In the case of diesel, the best temperature was 20 °C. In the case of n-heptane, the result was the opposite, and the best extinguishing time was achieved at 80 °C.

The water mist stream is not a monodisperse system where all droplets are the same size. The number of instruments is used to qualitatively determine the particle size distribution. Among the most used is the Sauter mean diameter, which is an important instrument for the analysis and control of systems where the particle size distribution plays a significant role. Sauter mean diameter is given as the average value of the droplet size, which considers the surface area and volume of the droplets. It offers more accurate and useful information about the particle size distribution compared to the conventional arithmetic mean. Especially in systems where is a wide distribution of particle sizes. The Sauter mean diameter (also referred to as the $d_{32}$ diameter) is defined as the diameter of a sphere having the same volume to surface ratio as the average particle. [6][7] Mathematically, the Sauter mean diameter is expressed by the relation 1:

$$d_{32} = \frac{d_V^3}{d_S^2} \qquad (1)$$

where $d_V$ is volume diameter and $d_S$ is surface diameter. In addition to Sauter mean diameter, we can also find Volume average diameter or Mass average diameter in publications. [5]

The size of water mist droplets is influenced by the nozzle design but can also be affected by other nozzle parameters. Studies [8][9] confirm a significant effect of working pressure on the size of produced droplets. As the working pressure increases, the produced droplets decrease. Study [10] confirms effect of spray angle and flow rate on droplet size. In the case of both spray angle and flow rate, Sater mean diameter increases as the values of these two parameters increase. The use of different additives also affects the droplet size. Different 5% solutions were used in the study [11] and their effect on Sauter mean diameter has been investigated. For all additives there was an increase in Sauter mean diameter compared to the value for pure water. The highest value was achieved by using monopotassium phosphate. The solution with additive of potassium acetate was the closest to pure water.

The size of water mist droplets has an impact across a wide range of industries. In spray technologies, droplet sizes need to be optimised to ensure coverage efficiency and minimise evaporation. [1] The automotive industry works with droplet size distribution to influence efficiency and purity in the combustion process. [12] In pharmaceutics, it is used to optimize drugs in the form of sprays. [13] Significant use and influence is in fire protection. Droplet size has a significant impact on efficiency of extinguishing and fire suppression. [14] Droplet size has also impact on the efficiency in shielding the radiant heat. [15]

## MATERIAL AND METHODS

The following sections contain a description of the measuring apparatus, misting system and experimental methodology.

*Measuring apparatus*

Measuring apparatus consists of a high-pressure unit, multifunctional pump, heating container, filter, distribution piping, pressure sensor with datalogger, thermocouples with datalogger, nozzle ring, nozzle and laser diffraction system with attached laptop (see diagram on Fig. 1):

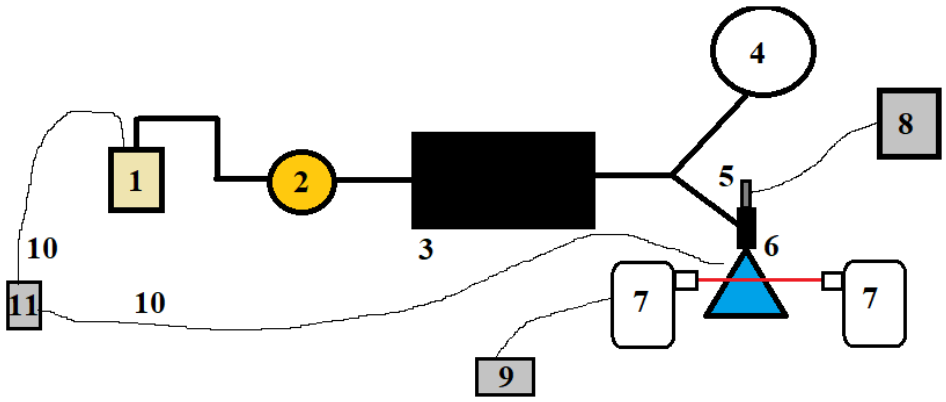



Figure 1 – Diagram of measuring apparatus

*1 – heating container with pump for pumping water to the high-pressure unit, 2 – Water filter, 3 – High-pressure unit, 4 – Stainless-steel ring with nozzles, 5 – Pressure sensor, 6 – Nozzle, 7 – Laser diffraction system, 8,11 – Datalogger, 9 – Laptop, 10 - Thermocouples*

*Misting system*

A container with a total volume of 27 litres was used to heat the water. The container was equipped with a 1 800 W heater and a thermostat that could be used to regulate the temperature. A pump had to be placed in the container, as the high-pressure unit was unable to draw water into its tank on its own. A small multi-purpose pump was used to transfer water from the heating container to the tank of high-pressure unit. The pump was selected based on its dimensions 7 x 7 x 13,2 cm (height x width x depth), because in needed to fit into a container. At the same time, the pump has an inlet on the side, which makes it possible to soak up almost the entire volume of the container and the outlet is located on the top of the pump. Due to the need to remove impurities before entering the high-pressure unit, a plastic water filter with a pulp insert was used. The filter is capable of capturing impurities up to 5 µm in size from the water. The high-pressure unit uses a single-phase electric motor operating at 300-1450 rpm. It provides a working pressure of 70 bar with a variable flow rate between 1 and 5 $l.min^{-1}$. The individual parts are connected by a pressure temperature resistant nylon hose with diameter of 10 mm, an internal diameter of 5 mm and a wall thickness of 2,5 mm. An integral part of the system is a stainless-steel ring with nozzles, whose function is to ensure the required flow in the nozzle. The working pressure was always sensed by a pressure sensor connected to the datalogger. Three metal-clad thermoelectric temperature sensors MTC11-E1-10000-200-23 were used to determine the temperature. A total of 8 hollow cone nozzles were used for the measurements. Four LN type nozzles with orifices in diameter 300, 400, 500 and 600 µm. Four SK (SKA16, SKA17, SKA19, SKA20) type nozzles were then used. Type and individual nozzle designations are based on the manufacturer. The number next to the SK type nozzle name indicates the nozzle insert size.

*Experimental Methodology*

The objective of the measurements was to determine the Sauter mean diameter and droplet size distribution for 8 selected nozzles at 4 different temperatures. All the nozzles produced a hollow cone mist stream. The spray angle was 80 ° for all nozzles. The

working pressure was set at 70 bar. However, the measured pressure was 68,7 ± 0,3 bar. The measurement of Sauter mean diameter was carried out at four selected temperatures – 25, 40, 55 and 80 °C. The initial temperature was 25 °C, which was the temperature of the coldest water available from the tap.

Temperature measurements were taken at three points. One thermocouple was always immersed in the heating container and measured the temperature continuously. The second and third thermocouples were used to measure the temperature in the mist stream. The first was placed at the nozzle and the second at 12,5 cm from the nozzle. Both thermocouples were used only at the moment of completion of the measurements with the laser diffraction system. If they were placed in their positions during the measurement, they would have a significant effect on the produced mist stream. The measured temperature values are divided into four series of measurements according to the temperature in the container and are given in Table 1:

Table 1 – Temperature values at individual points

| | Temperature in container [°C] | Temperature at the nozzle [°C] | Temperature 12,5 cm from the nozzle [°C] |
|---|---|---|---|
| 1st measurements | 25,0 ± 0,1 | 25,1 ± 0,1 | 23,2 ± 0,1 |
| 2nd measurements | 40,0 ± 0,2 | 30,6 ± 0,2 | 25,4 ± 0,1 |
| 3rd measurements | 55,0 ± 0,2 | 37,0 ± 0,2 | 27,2 ± 0,1 |
| 4th measurements | 80,0 ± 0,5 | 45,1 ± 0,2 | 30,1 ± 0,2 |

## RESULTS AND DISCUSSION

The Sauter mean diameter was measured at 12,5 cm from the nozzle. At the distances closer to the nozzle, there was a risk that the droplets would not yet be spherical. If the distance were longer, the smallest droplets could be blown out of the measured area and thus affect the measured values of Sauter mean diameter.

Table 2 shows the measured values of Sauter mean diameters for all measurements. At 80 °C, the pump in the heating container overheated and the measurement could not be continued. It was not possible to transfer the heated water manually to the tank of the high-pressure unit, as the whole apparatus could be clogged with impurities. For this reason, the Sauter mean diameter was measured at 80 °C only for the first four nozzles. Conventional pumps and common parts of apparatus are not designed to operate at temperatures close to the boiling point. Values of Sauter mean diameter were determined using the geometric mean of the measured values on all axes.

Table 2 – Values of Sauter mean diameter at different temperatures

| Water source temperature / Nozzle designation | 25 °C | 40 °C | 55 °C | 80 °C |
|---|---|---|---|---|
| LN 300 | 34,35 μm | 30,11 μm | 29,65 μm | 27,08 μm |
| LN 500 | 35,27 μm | 34,88 μm | 33,93 μm | 32,90 μm |
| SKA17 | 27,67 μm | 27,61 μm | 29,18 μm | 30,67 μm |
| SKA19 | 25,06 μm | 25,49 μm | 25,74 μm | 27,46 μm |
| LN 400 | 32,37 μm | 31,94 μm | 31,26 μm | - |
| LN 600 | 33,51 μm | 32,61 μm | 31,84 μm | - |
| SKA16 | 29,72 μm | 29,49 μm | 28,78 μm | - |
| SKA20 | 31,89 μm | 31,60 μm | 31,13 μm | - |

For nozzles measured at only three temperatures, a slight decrease in Sauter mean diameter with increasing water temperature can be observed. With increasing temperature there was a decrease in the order of tens of μm. The least significant decrease was for nozzle SKA20, namely 0,76 μm when the temperature increased from 25 to 55 °C. In the case of this nozzle, the reduction in Sauter mean diameter was only 2,6 %. The drop was most notable for the LN 600 nozzle. The diameter value decreased by 1,67 μm.

For the LN 300 and LN 500 nozzles, the drop was much more notable. In the case of the LN 500 nozzle, there was a reduction of 2,37 μm. In the case of nozzle LN 300 by 7,27 μm (when the temperature increases from 25 to 80 °C). The opposite results were achieved with nozzles SKA17 and SKA19. For these nozzles, there was an increase in Sauter mean diameter with increasing temperature.

In terms of droplet size distribution, there were three cases. In the first case, there was almost no change in particle size distribution with increasing temperature. The curves at each temperature are almost identical. These are nozzles that showed a slight decrease in Sauter mean diameter with increasing temperature and were measured only at three temperatures. The LN 600 nozzle was selected to illustrate the first case of the droplet size distribution, as shown in Figure 2:

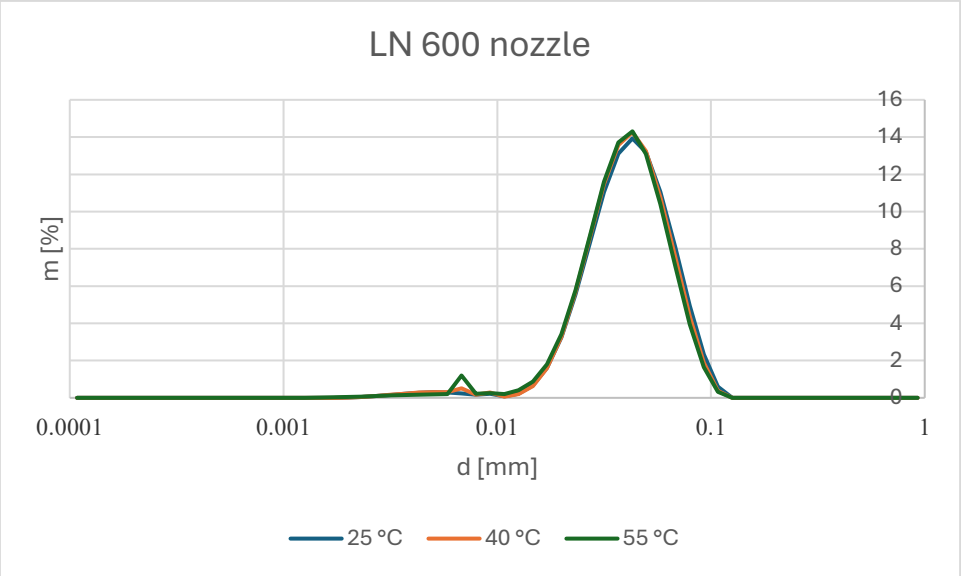



Figure 2 – Droplet size distribution of LN 600 nozzle

For the LN 300 and LN 500 nozzles, the curves could already be recognizable from each other. The most notable peak was at the lowest temperature, 25 °C. In both cases, these are the nozzles with the most significant decrease in Sauter mean diameter with increasing temperature. The LN 300 was selected to illustrate the second case of the droplet size distribution, as shown in Figure 3:

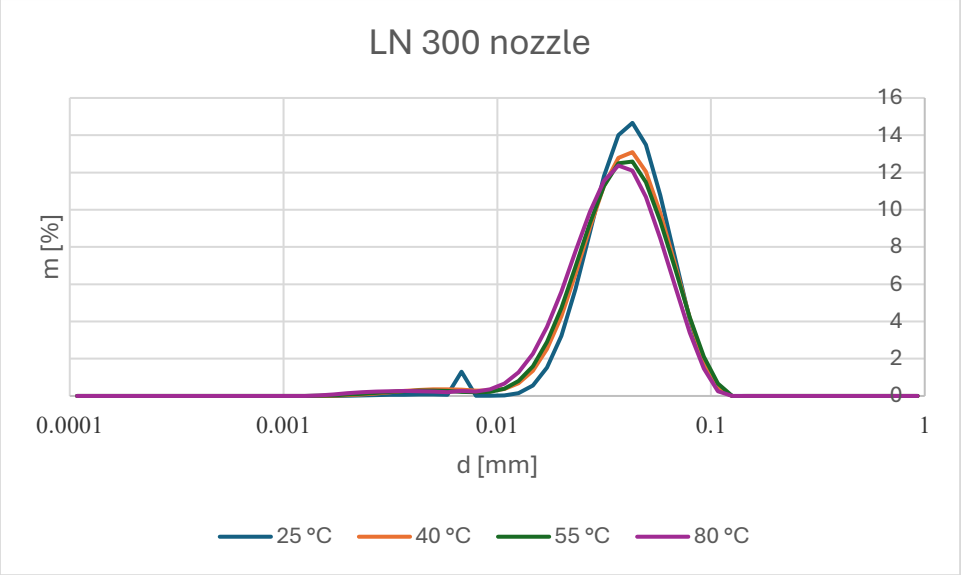



Figure 3 – Droplet size distribution of LN 300 nozzle

In the case of the SKA17 and SKA19 nozzles, the curves could be also recognizable from each other. Unlike the previous two nozzles, in this case the peak was most notable at the highest temperature, namely 80 °C. In terms of Sauter mean diameter, these are the only two nozzles in which was an increase in its value with increasing temperature. The SKA17 nozzle was selected to illustrate the third case of droplet size distribution, as shown in Figure 4:

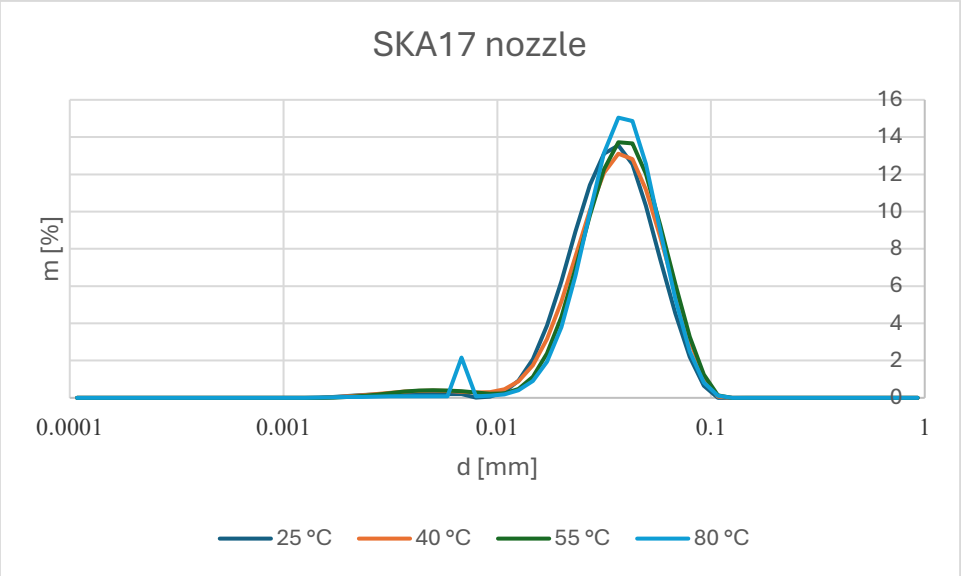



Figure 4 – Droplet size distribution of SKA17 nozzle

## CONCLUSION

This paper investigates the effect of changing water temperature on the change in droplet size distribution and values of Sauter mean diameters of water mist generated by high-pressure mist nozzles with hollow cone shape. To determine the Sauter mean diameter, a laser diffraction system was selected. The value of Sauter mean diameter was measured at 12,5 cm from the nozzle and a working pressure of 70 bar. In total, 8 nozzles were selected. Four of LN type, four of SK type. Inlet temperatures were selected as 25, 40, 55 and 80 °C. Temperatures were measured using thermocouples. One was placed always in a heating container. The other two were placed in the mist stream at the nozzle and at 12,5 cm from the nozzle after the measurements were completed. They were placed after the measurements were completed in order not to affect the measured characteristics of the mist stream.

From the results on the thermocouples, it can be concluded that with increasing distance from the nozzle the temperature of the water mist decreases due to cooling. At the same time, the temperature at the nozzle drops significantly compared to the water in the heating container. Half of the nozzles were measured at all four temperatures. Subsequently, a pump located in the vessel failed and therefore only three temperatures were measured for the other half of the nozzles.

For all four nozzles measured at only three temperatures, slight decreases in the value of the Sauter mean diameter with increasing temperature can be observed. Individual changes are on the order of tenths of µm. For the LN 300 and LN 500 nozzles, there was a more pronounced decrease in Sauter mean diameter with increasing temperature. The opposite results were achieved with two nozzles, SKA17 and SKA19. There was an increase in Sauter mean diameter with increasing temperature. Based on the measurements, it can be concluded that temperature influences Sauter mean diameter of water mist stream. However, it cannot be generally stated that in all cases there is decrease in value with increasing temperature.

In terms of the particle size distribution chart, there were three cases. For all nozzles measured at only three temperatures, the particle size distribution at all temperatures was almost identical. For the LN 300 and LN 500 nozzles, the peak was most notable at the lowest temperature, 25 °C. On the other hand, nozzles SKA17 and SKA19 showed the most notable peak at the highest temperature, namely 80 °C.

Water mist droplet size plays an important role in many industries. Droplet size has influence on extinguishing and fire suppression. Affects how the water mist can shield the radiant heat or trap particles from the air. It is also used via fire protection. The droplet size distribution of water mist is also used in the pharmaceutical, chemical or energy industries.

## ACKNOWLEDGEMENTS

Work on the experiments was possible thanks to the project no. SP2024/020, entitled: „Applicability of water mist on fire classes from ČSN EN 2“, which was approved and implemented under the Specific research of the Ministry of Education of the Czech Republic.

## REFERENCES

[1] Dorr J., Hewitt J., A comparison of initial spray characteristics produced by agricultural nozzles, Crop Protection, vol. 53, pp. 109-117, 2013. DOI: 10.1016/j.cropro.2013.06.017.

[2] Okafor N., Nature, Properties, and Distribution of Water, Environmental Microbiology of Aquatic and Waste Systems, pp. 3-13, 2011. DOI: 10.1007/978-94-007-1460-1_1.

[3] Raudensky M., Hnizdil M., Influence of water temperature on the cooling intensity of mist nozzles in continuous casting, Materials and Technology, vol. 46/issue 3, pp. 311-315, 2012. ISSN 158-2949.

[4] Farnham C., Nakao, M., Effect of water temperature on evaporation of mist sprayed from nozzle, Journal of Heat Island Institute International, vol. 10, pp. 35-44, 2015.

[5] Liu T., Yin X., Influence of Water Mist Temperature Approach on Fire Extinguishing Effect of Different Pool Fires, Processes, vol. 10/issue 8, 2022. DOI: 10.3390/pr10081549.

[6] Kowalczuk B., Drzymala J., Physical meaning of the Sauter mean diameter of spherical particulate matter, Particulate Science and Technology, vol. 34/issue 6, pp.645-647, 2016. DOI: 10.1080/02726351.2015.1099582.

[7] Mishra N., Koegl M., 3D mapping of droplet Sauter mean diameter in sprays, Applied Optics, vol. 58/issue 14, 2019. DOI: 10.1364/AO.58.003775.

[8] Liu Y., Fu Z., Study on the effect of mist flux on water mist fire extinguishing, Fire Safety Journal, vol. 130, 2022. DOI: 10.1016/j.firesaf.2022.103601.

[9] Jun Q., Chow W.K., Experimental data on water mist suppression, Procedia Engineering, vol. 62, pp. 868-877, 2013. DOI: 10.1016/j.proeng.2013.08.137

[10] Liu Y.S., Jiang Z., Experimental research on the water mist fire suppression performance in an enclosed space by changing characteristics of nozzles, Experimental Thermal and Fluid Science, vol. 52, pp. 174-181, 2014. DOI: 10.1016/j.expthermflusci.2013.09.008

[11] Tian-wei Z., Zhi-yue H., Cooling characteristics of cooking oil using water mist during fire extinguishment, Applied Thermal Engineering, vol. 107, pp. 863-869, 2016. DOI: 10.1016/j.applthermaleng.2016.07.043.

[12] Dong P., Nishida K., Characterization of multi-hole nozzle sprays and internal flow for different nozzle hole lengths in direct-injection diesel engines. Proceedings of the Institution of Mechanical Engineers, Part D: Journal of Automobile Engineering, vol. 231, pp. 500-515, 2017. DOI: 10.1177/0954407016653890.

[13] Lelong N., Junqua-moullet A., Comparison of Laser Diffraction Measurements by Mastersizer X and Spraytec to Characterize Droplet Size Distribution of Medical Liquid Aerosols, Journal of Aerosol Medicine and Pulmonary Drug Delivery vol. 27/issue 2, pp. 94-102, 2014. DOI: 10.1089/jamp.2012.1030.

[14] Lal S., Gupta M., Suppression of pool fire in large enclosure with water mist, Internation Journal of Spray and Combustion Dynamics, vol. 5/issue 3, pp. 181-199, 2013. DOI: 10.1260/1756-8277.5.3.181.

[15] Buchlin J.M., Thermal shielding by water spray curtain, Journal of Loss Prevention in the Process Industries, vol. 18/issue 4-6, pp. 423-432, 2005. DOI: 10.1016/j.jlp.2005.06.039.

# LIDAR DATA ACQUISITION AND MEASUREMENT ACCURACY IN QC TOOLS USING MOBILE MAPPING SYSTEM TECHNOLOGY

**Assoc. Prof. Dr. Adrian Șmuleac**
**Prof. Dr. Laura Șmuleac**
**Prof. Dr. Cosmin Alin Popescu**
**Assoc. Prof. Dr. Mihai Herbei**
**Lecturer Dr. Raul Pașcalau**
University of Life Science "King Mihai I" from Romania, Timisoara**, Romania**

## ABSTRACT

The work aims to acquire LiDAR data and checking the scan quality in QC Tools for Sânmihaiu Român hydro technical arrangement located on the Bega Canal, Timiş County, Romania, using mobile scanning technology MMS - Mobile Mapping System, using portable backpack equipment from Swiss manufacturer Leica, the Pegasus Backpack model. The Method of LiDAR Data Collection is a Fused Slam one, where, a Master Station has been located for the purchase of RiNEX data, using some GNSS receiver, the Leica GS 08. The raw data processing was done with the Pegasus Manager program, where the visualization of quality graphs was performed in QC Tools and the data processing was carried out with the Cyclone program, the modelling version (Model), using the SmartPick Point and Virtual Surveyor functions. The scanning accuracy was between 2 and 3 cm. SLAM simultaneous location and mapping technology with IMU (Inertial Measurement Unit) technology of high precision, ensures precise positioning when we have GNSS interruptions. From a technological point of view, MMS is a multi-sensor system consisting mainly of three components: mapping sensors (3D imaging systems), navigation/positioning sensors (IMU/GNSS) and a control unit, which synchronizes and integrates the acquisition of geomatic information, the trajectory of which is calculated.

**Keywords:** LiDAR, MMS, GNSS, IMU, SLAM

## INTRODUCTION

Bega River [1], the second largest river in the area under review, has an area of 2362 km2,2a length of 170 km to the Romanian border and a hydro graphic network density of 0.38 km/km2 [2]. In the 18th century, this river was channelled on the lower course, at 114 km, between the localities of Timişoara (Romania) and Titel (Rep. Serbia), being the first waterway in Romania and, by its completion, Timişoara became the first Romanian city with a navigable canal and a functioning port. The Bega Navigable Canal, which was arranged almost 250 years ago, is from a hydro technical point of view a construction with special technical facilities and, above all, with historical significance, which highlight the progress of conception and execution in the field. The Timișoara waterway, Romania – Klek, Serbia has a total length of 114.50 km, of which 44.5 km on Romanian territory and 70 km on Serbian territory.

The hydro technical node at Sânmihaiul Român is located upstream of the village with same name, about 950 m from the Sânmihaiu bridge over the Bega canal, next to km 28+200 of the left bank pier, measured from the border with Serbia. The construction –

https://doi.org/10.5593/sgem2024v/3.2/s11.09

according to the authentic plate placed on the construction of the house of the mechanisms for the operation of the stasis – was carried out between 1912 and 1915.

Sânmihaiu Román's hydro technical node rehabilitation and safety project was brought to the attention of the beneficiary, Banat Water Basin Administration [2], many years ago, when the improper operation of the hydro mechanical equipment and the structural depreciation of the construction led to the stopping of navigation. The lack of financial availability has prevented constructive rehabilitation for many years.

After 2000, efforts were intensified to access the necessary funds for the rehabilitation and provision of the Sânmihaiu hydro technical trough. According to the press release from 05.06.2014 the National Administration "Romanian Waters", through the Banat Water Basin Administration [3], implements the project "Restore consolidation Bega canal in Timisoara municipality, Timiş County" [4].

The main purpose of this work is to obtain LiDAR (Point Cloud) points clouds and to create a 3D database that will be used to produce 3D heritage documentation. Scans were carried out before the start of the renovation of the Sânmihaiu Román Hydro technical Node using a terrestrial "TLS (Terrestrial Laser Scanner) equipment" scanning equipment, ScanStation Leica C10 [5], as well as with the help of mobile MMS (Mobile Mapping System) technology, the Leica Pegasus Backpack model for data comparison, and during the renovation of the hydro technical node two additional scans were carried out using the Leica Pegasus Backpack.

The research theme is of great importance and topicality for the field of hydrotechnics by applying modern techniques for the creation of a database on heritage conservation and with the possibility of valuing the data obtained whenever necessary.

## MATERIALS AND METHODS

The acquisition of LiDAR data for this work using mobile scanning technology (MMS) was carried out with Leica Pegasus Backpack [6,7] equipment made by the Swiss company Leica. From an analytical point of view, the integration of GNSS and INS data is a very complex task and solved through Kalman filter-based procedures, taking into account a "status vector" and using status equations (motion modelling) and measurement equations (from sensors).

The Kalman filter or Kalman filtration, known as the linear quadratic meter estimation (LQE), is an algorithm which uses a series of measurements observed over time, containing statistical noise and other inaccuracies, and produces estimations of unknown variables that tend to be more accurate than those based on only a single measurement, by estimating a common probability distribution on variables for each time interval.

By integrating the camera with GNSS and INS, it is now possible the automation of the process, in real time or post-processing, to "transfer" to the image a precise location, determined by GNSS. Previous photos are used in online map systems, such as Google Earth. GNSS technology is, also integrated with LiDAR (light detection and measurement) technology, an optical remote objects detection technology, which at LiDAR frequencies is less than one millionth of a meter [8,9].

The Leica Pegasus Backpack is a portable system which combines two Velodyne VLP-16 linear scanners [10,11] (one vertical and one horizontal), plus five data texture cameras, a GNSS/INS system integrated with Novatel SPAN [12] technology (NovAtel's SPAN technology tightly couples our OEM precision GNSS receivers with robust Inertial Measurement Units (IMUs) to provide reliable, continuously available, position, velocity and attitude-even through short periods of time when satellite signals are blocked or unavailable), batteries and control unit (Leica Pegasus Backpack, 2017).

Leica Pegasus Backpack is a reality-capture sensor platform with an extremely ergonomic design which combines five cameras that offer a fully calibrated 360-degree view and two LiDAR sensors (VLP-16) with a chassis of ultra-light weight carbon fibre. It allows to obtain LiDAR points, both indoors (PURE SLAM method) and outdoors (FUSED SLAM method), at a level of precision that is authoritative and professional.

In the case of research carried out, because at the time of the scan there were more than 5 GPS satellites and an open sky, no compensation was applied using the SLAM algorithm (Simultaneous Location and Mapping). This algorithm is used only on the inside, or if the lack of GNSS signal is weak and for a longer period of time. For measurements starting from outside and containing part of the scan on the inside, having scan time less than 5 minutes, this option of clearing and adjusting the point clouds will not be used. Also, outside, for "good" scans with more than 5 satellites and with a correct measurement trajectory planning, the error will usually include values between 2 and 5 cm as a scanning error.

## RESULTS

*1. Acquisition of LiDAR data using MMS*

For the acquisition of MMS data, it was scanned Sânmihaiu Român Hydro technical Node using for everything the method FUSED SLAM. This method is performed for both outdoor and indoor scans. This method uses a SLAM algorithm which combines GNSS/IMU navigation. The final trajectory and SLAM solution, under GNSS conditions, can be influenced by several factors, such as:

**Planning the mission of acquiring LiDAR data**: preparing street lanes for missions performed outside or the route to be followed, or in case of indoor scanning viewing of the interior and creating space for turns and walks, opening and fixing doors. Planning for the three objectives was done using the Google Earth program for the exterior.

**Equipment initialization**: to obtain data with high accuracy, initialization was done next to the objectives which were scanned, in open sky area, not covered by obstacles (trees, buildings). The initialization consists of two stages:

1. STATIC initialization, for a period of 5 minutes, in which the backpack will stand still and can last up to 15-20 minutes in case that the ALMANAC Data needs to update (Figure 1).

https://doi.org/10.5593/sgem2024v/3.2/s11.09





Figure 1. Static and dynamic initialization

2. DINAMIC initialization, lasting 3-5 minutes, during which the backpack is carried on the back, performing a quadrangle, and at the end adopting the diagonals of the quadrangle until the message INS GOOD appears and the INS_GNSS will have a value below 1, usually the indicated value is 0.1-0.2 [13].

The workflow, using mobile scanning technology for the Leica backpack (Leica Pegasus Backpack) 'Mobile Mapping System' backpack is shown in Figure 2.

*2. Acquisition of GNSS data from Master station and GCP control points for MMS*

Figure 2 and 3 shows how to work with the Leica Pegasus backpack using the RADMIN program and the ZUPT button to stop scanning images and to perform a 'refresh' for the predicted location of the position.

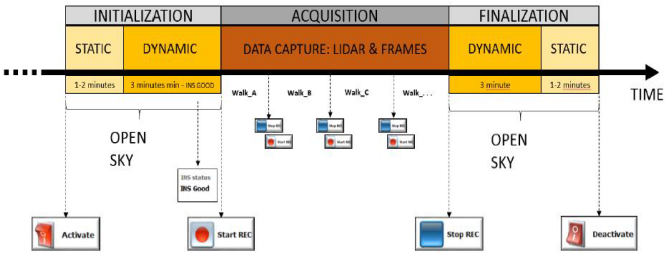



Figure 2. Workflow with Leica Pegasus Backpack (Mobile Mapping System)

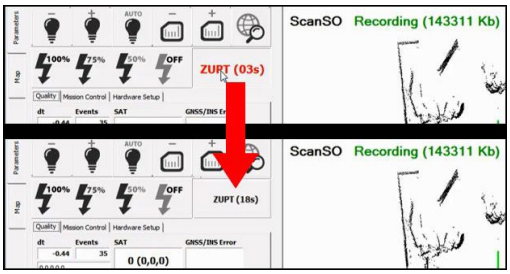



Figure 3. ZUPT button (stop capturing images)

For the acquisition of LiDAR data for the objectives pursued in this paper, the FUSED SLAM method was used, method to which, in addition to the scanning backpack itself, we also need placing a Master station (a GNSS base) for field acquisition and RINEX data, which was set to an interval of 1 second to perform post-processing the measurement trajectory as opposed to static measurements for the storage of the geodesic network that was set to a purchase of RINEX data every 5 seconds.

For the correct collection of RiNEX data, the Master station for all four lenses started 10 minutes before the backpack (Leica Pegasus Backpack) was initialized and was switched off 10 minutes after the LiDAR data collection was completed [14]. For each of these four scans checkpoints were determined directly in the field on the ground, with the GPS equipment from Leica GS 08, points that were used to check and realign the clouds of LiDAR points collected with the Leica Pegasus Backpack equipment.

*3. Post-processing data to improve GNSS and INS quality in Inertial Explorer IE*

To achieve high levels of GNSS + INS accuracy in real time, there must be a link between the data to receive corrections such as RTK or L-Band.

Inertial Explorer easily imports data from NovAtel SPAN GNSS + INS products. It can also import GNSS data from multiple recipient manufacturers and has a generic IMU. The accuracy of the estimated position is shown in Figure 4.

For each point we have two solutions, one forward and one back. The IE program maximizes trajectory accuracy by taking time back and forth, supporting and combining results. This maximizes GNSS+INS performance [15] by providing position, speed and altitude. The trajectory can be extracted and viewed in Google Earth. Inertial Explorer is suitable for mobile cartography, photogrammetry, and hydrographic topography applications. The reality of GNSS+INS in real time is limited by the quality of IMU and the duration of GNSS (interruption period). The performance of these systems can be greatly improved through post-processing. IE significantly reduces the deviation of the solution during the lack of GNSS signal and virtually eliminates the solution convergence time, expressed in real time.

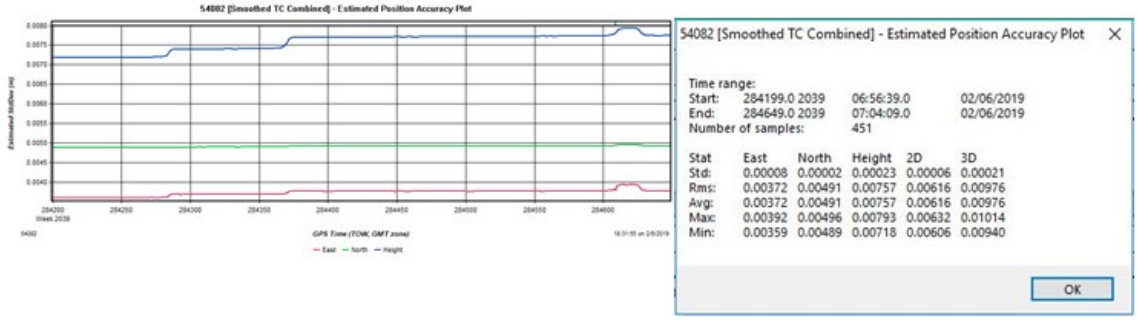



Figure 4. Estimation of accuracy

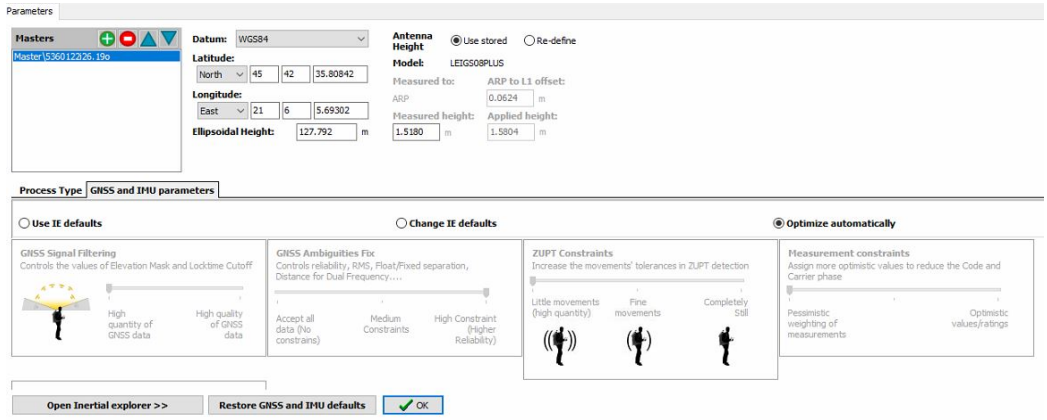



Figure 5. View option in Inertial Explorer (IE)

These precision graphs will be presented below and have been made for the scanned objective: Sanmihaiu Román Lock (Figure 6).

The visualization of the LiDAR scan trajectory processing, the accuracy of the data collection, and the measurement quality (QC Tools – Quality Control Tools) will be visualized in the Inertial Explorer program (Figure 5), using the graphs shown below.

https://doi.org/10.5593/sgem2024v/3.2/s11.09

There is no map or graph showing us the true accuracy of time or location, but just some estimates to which a SLAM data processing algorithm can be applied.

However, for the most accurate scan, we will need to take into account the following:

Number of satellites visible at the time of scanning: ≥ 5 GPS satellites; Value for The Combined Separation graph: <0.10m; Standard deviation: >0.05; PDOP: ≤3;

The number of GPS satellites (NAVSTAR GPS) visible at the time of the scan was between 5-14, and for a period of 14 seconds the number of satellites was 7 and GLONASS 8 satellite (Figure 7).

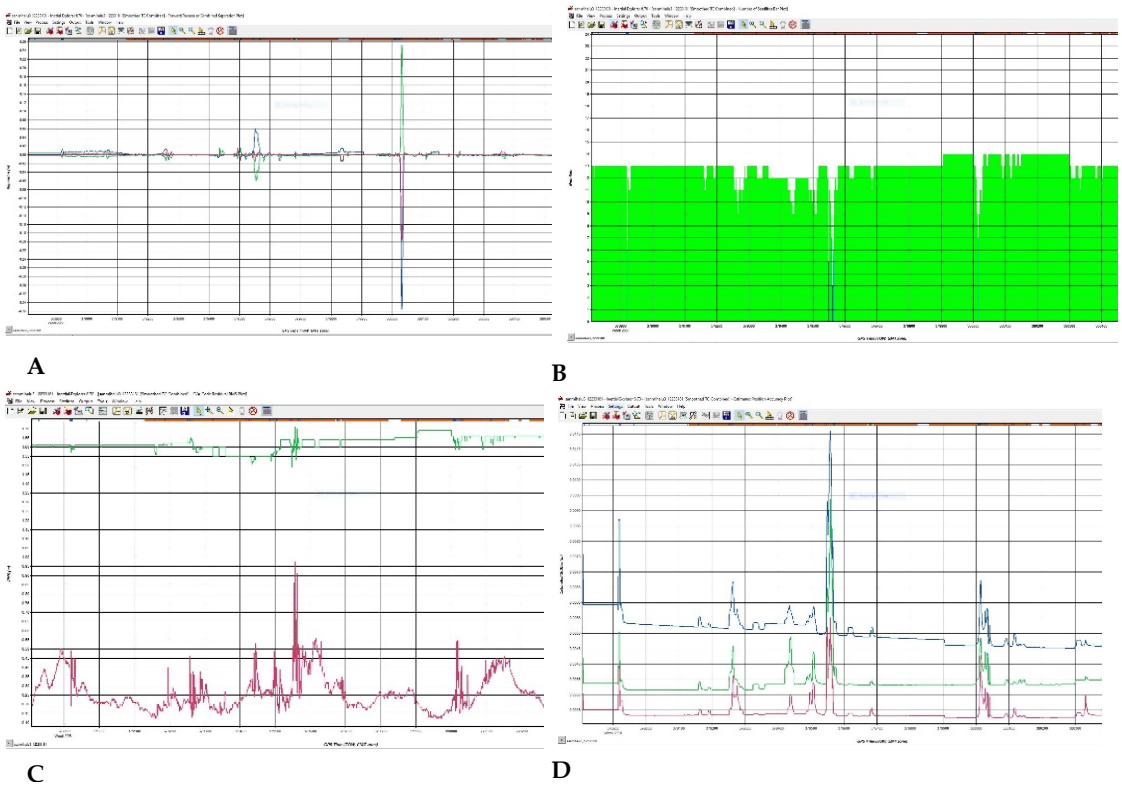



Figure 6. A. View the Correctness of the Scan (Combined Separation); B. Number of visible satellites at the time of scanning; C. RMS values; D. Estimation of data accuracy (X, Y, Z and Time) for the Sânmihaiu Român Hydro technical Node.

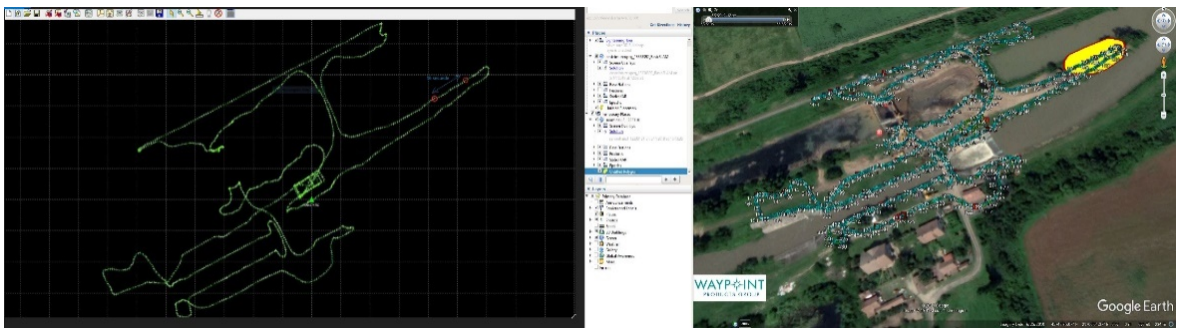



Figure 7. Measuring error for 14 seconds in Google Earth Sânmihaiu Român

## DISCUSSION

The first scanning technology emerged in the 1960s, using lights, cameras and projectors with equipment limitations and long scanning time, where in 1985 scanning appeared that could use white light, lasers and shadows to capture a given surface, where each technology appeared with its own limitations, advantages and costs. Since 1994, it has appeared to be a new land-shaping technology, namely the ALS “Airborne Laser Scanner". Laser scanning systems have been undergoing a major evolution over the past decade. After the initial discovery of air laser scanners (ALS), other types of laser scanning systems, in particular terrestrial laser scanners (TLS) and mobile laser scanners (MMS), emerged.

Mobile scanning technology (MMS) together with terrestrial scanning technology (TLS) and UAV technology, have been designed to help people make better and faster decisions in emergencies (calamities or disasters) thanks to quick access to highly accurate information and data. Route mapping benefits from such clear and detailed images, with the possibility of viewing the number of clouds points, which can warn the authorities, if necessary, of any change in the environment. For the first time, in the event of natural disasters, with the help of MMS technology, 3D data of the devastated area can be retrieved by walking ". Faster response time translates into saved lives and minimization of damages. Real-time data capture is necessary for quick decision-making based on 3D information, thus increasing the chances of survival and the possibility of 1:1 heritage reconstruction.

Examples of this can be found in civil and industrial engineering, road construction and maintenance, urban planning, environmental analysis and precision forestry. LiDAR data have already been widely used over the years to scan objects or to map the environment in 3D. The types of ALS, TLS and MMS systems each have their own applications, advantages and disadvantages.

## CONCLUSION

This equipment is actually a smart backpack or better said, a platform with reality-capture sensors, which has an ergonomic design that combines five cameras that offer a complete 360-degree view and two LiDAR profiles made of carbon fibre. This unique mobile mapping solution is designed to capture reality quickly and at a regular interval. It is fully portable, thus allowing it to be checked as luggage on a flight.

The backpack turns the BIM documentation into reality. It synchronizes images and LiDAR point clouds, ensuring complete documentation of hydro technical nodes, locks and pumping station, buildings for complete management of the 3D model.

The Mobile Mapping System (MMS) is currently a developing technology and is constantly growing. From a technological point of view, MMS is a multi-sensor system consisting mainly of three components: mapping sensors (3D imaging systems), navigation/positioning sensors (IMU/GNSS) and a control unit, which synchronizes and integrates the acquisition of geomatic information, the trajectory of which is calculated and ultimately used for the production of geo-referenced 2D/3D data. The quality of the results is closely related to the quality of the measurements, the scanning itself, as well as the preparation of the equipment for the scanning. RiNEX data were purchased separately for each measurement session, with recorded data at an interval of 1 second.

https://doi.org/10.5593/sgem2024v/3.2/s11.09

All this data presented lead in the end, to a high-precision scan, resulting at the end of data processing and application of the Kalman filter to a cloud point with an accuracy of 1-3 cm, precision that can be verified using the resulting stereographic images, where the positioning accuracy of point clouds can be improved when using ground control points (GCP). These ground control points (GCPs) have both a verification and control role and a role in processing point clouds for time or position offsets, when the result of point clouds requires it and an important role in realigning scans where appropriate.

## ACKNOWLEDGEMENTS

This paper is published from the own research funds of the University of Life Sciences "King Mihai I" from Timisoara, Romania.

## REFERENCES

[1] Șmuleac, Laura, Andrei Toth, Adrian Șmuleac, and Raul Paşcalău. "The impact of anthropic activities on Bega River." Research Journal of Agricultural Science 51, no. 2 (2019). [View Article].

[2] Atlas on Water Cadastre from Romania, Ministry of the Environment, 1992.

[3] Banat River Basin Administration, Timisoara, 2020.

[4] The archives of the Banat River Basin Administration (A.B.A.B.), Timisoara, 2020.

[5] Șmuleac A, Șmuleac L, Man TE, Popescu CA, Imbrea F, Radulov I, Adamov T, Pașcalău R. Use of Modern Technologies for the Conservation of Historical Heritage in Water Management. Water. 2020; 12(10):2895. https://doi.org/10.3390/w12102895

[6] Leica Pegasus Backpack Technical Sheet, **2020**, [View Article].

[7] Masiero, A., Fissore, F., Guarnieri, A., Piragnolo, M., Vettore, A., Comparison of low-cost photogrammetric survey with TLS and Leica Pegasus backpack 3D models. ISPRS Int. Arch. Photogramm. Remote Sens., **2017,** XLII-2/W8, 147–153, [View Article].

[8] Li, D., Shan, J., Gong, J., Geospatial Technology for Earth Observation, Springer: New York, NY, USA, 2009, p. 558, [View Article].

[9] Smuleac A., I. Nemes, Laura Smuleac, Ioana A. Cretan, Nicoleta S. Nemes, Comparisons between classic topographic measures methods and LIDAR method on the corride of 400 Kv power line, Parta-Sag sector, SGEM 2017, ISBN 978-619-7408-03-4, Vol. 17, Issue 23, 439-448 pp, [Article View].

[10] Leica Geosystems, Leica Pegasus: Backpack Datasheet (Mobile Reality Capture), 2016, [View Article].

[11] Velodyne, Velodyne High-Definition LiDAR, 2014, [View Article].

[12] https://novatel.com

[13] Smuleac Laura, Pașcalău Raul, Smuleac Adrian, Imbrea Florin, Lato Alina, The interconnection between preventing water pollution and addressing climate change, International Multidisciplinary Scientific GeoConference: SGEM; Sofia, Vol. 23, Iss. 3.2, (2023). DOI:10.5593/sgem2023V/3.2/sl2.27

[14] Mita, Radu, et al. "Using geographical systems in order to achieve the urban cadastre in the subcetate neighborhood of Arad with the help of modern technologies." (2020): 93-103.

[15] Specht, M.; Specht, C.; Stateczny, A.; Burdziakowski, P.; Dąbrowski, P.; Lewicka, O. Study on the Positioning Accuracy of the GNSS/INS System Supported by the RTK Receiver for Railway Measurements. Energies 2022, 15, 4094. https://doi.org/10.3390/en15114094

https://doi.org/10.5593/sgem2024v/3.2/s11.09

# MICROBIAL CONTAMINATION ASSESSMENT OF FIREFIGHTING WATER FOR WATER SUPPLY PURPOSES AND THE POSSIBILITY OF DISINFECTION

**Ing. Patrik Sirotiak**
**Doc. Ing. Šárka Kročová Ph.D.**
Faculty of Safety Engineering/VSB – Technical university of Ostrava, **Czech Republic**

## ABSTRACT

This paper deals with the results of research on the laboratory analysis of firefighting water in fire trucks and the possibility of its disinfection for subsequent use as an alternative source of safe water supply to the affected areas. The quality of the water in these vehicles after filling the internal tank is relatively unclear. For this purpose, over a period of 5 months (July to November), water samples were taken from firefighting trucks. The samples were then analyzed in an accredited laboratory. Laboratory analyzes focused mainly on indicators of microbial pollution. The microbial analysis included the determination of coliform bacteria, E. coli, Legionella spp., Pseudomonas aeruginosa, and cultivable microorganisms. 42 water samples were taken from firefighting trucks at 31 fire protection units across the Czech Republic. According to the chosen legislation, none of the water samples fulfil the limits of drinking water. This research also focused on measures to ensure safe water in fire truck tanks. The most effective method, based on laboratory analyses, is the use of chemical disinfection, especially chlorine and chlorine compounds. This method of disinfection is inexpensive and effective for all monitored indicators of microbial contamination.

**Keywords:** Water pollution, microbial analysis, water supply, firefighting water

## INTRODUCTION

Water is one of the most important substances in the world. Drinking water is necessary for the existence of humans, animals, and plants. In recent years, we have increasingly encountered two extreme situations related to water and water resources: drought and floods. The water supply can be very problematic, especially in periods of drought, there can be disruptions of the water supply [1]. During floods, there is a high probability of contamination of previously safe water and limited access to drinking water. Some sources predict that these extreme situations will become more frequent [2]. This paper deals with the results of research on laboratory analysis of firefighting water in fire trucks and the possibility of its disinfection for subsequent use as an alternative source of safe water supply to the affected areas.

Firefighting vehicles of the FTT type (fire truck tanks) can be used as an alternative source of water. This water source most often has a capacity of several cubic meters. However, the quality of the water in these vehicles after filling the internal tank is relatively unclear. For this purpose, over a 5 month period (July to November), water samples were taken from the fire trucks. The samples were then analyzed in an accredited laboratory. Laboratory analyzes focused mainly on indicators of microbial pollution, whose occurrence and quantity are regulated by laws on safe water. The numbers of microorganisms and their occurrence in the stored water in fire trucks were analyzed

https://doi.org/10.5593/sgem2024v/3.2/s11.10

primarily because these vehicles are, with exceptions, filled from the hydrant system, which under Czech conditions always contains drinking water. Filling the fire truck with clean water ensures prevention of damage to the pump, pipes or tank. Therefore, clean and safe water is expected in the trucks.

Until now, there has been no research related to the analysis of water in fire trucks in the Czech Republic or abroad. The results of this research can provide important feedback not only for fire brigades but also for emergency authorities. These results can contribute to better water management in critical situations, avoiding water wastage and use as an alternative source of safe water supply to areas affected by water shortages.

## MATERIALS AND METHODS

In the case of the determination of indicators of microbial water pollution, a search of legislative documents was carried out in the Czech Republic and abroad. Czech legislation included laws, decrees and standards regulating the quality of various types of water. The relevant indicators were the parameters and limits for drinking water, swimming water and surface water. From the foreign legislation were used indicators and limits for drinking water. For this purpose were selected the following regulations: the Slovak Ordinance establishing indicators and limit values for drinking water quality, the UK Water Supply and Drinking Water Quality Regulations, the American Safe Drinking Water Act, Directive of the European Parliament and of the Council and WHO limits [3], [4], [5], [6]. From this legislation were selected indicators of water pollution - Escherichia coli, Legionella Spp., Pseudomonas aeruginosa, coliform bacteria and cultivable microorganisms. The selected pollution indicators were discussed with an accredited laboratory.

The water samples were taken from the fire truck tanks using samplers supplied by an accredited laboratory. The water sampling was always performed by a qualified person equipped with sterile gloves. The gloves prevented possible contamination of the hands of the sampling person. This measure prevented affecting laboratory results. The water was always taken from the top of the tank when it was accessible. The water from the tank was taken primarily from the surface. The temperature of the water was measured after the samplers were filled with water. All relevant information was recorded in the protocol, including the actual date and time of sampling, location of sampling, temperature, date the tank was filled with water, source of water used to fill the tank, tank material, age of the fire truck, visual assessment of the tank (algae, corrosion, sediment) and date of tank replacement or cleaning, if relevant. The samplers and sampling protocol were marked with serial numbers and stored in a transport thermobox. If the samples were not immediately transferred to the laboratory, they were stored in the dark and at temperatures between 5 and 7 °C. During transport, the water samples were cooled in thermoboxes. A total of 42 water samples were collected for final analysis. Four samples were discarded because the tank was not filled with drinking water. 18 samples came from units, 20 from volunteer units.

The processing of the results of the laboratory analyzes included mainly a comparison with the selected legislation and evaluation of the quality of the water analyzed on the basis of these parameters. For microbiological indicators, the uncertainty is represented as the 95% confidence interval of the variability of the results according to the Poisson distribution and does not include the sampling uncertainty. For laboratory analysis was used a standard operating procedure based on valid Czech and EU standards. For general

results were applied basic methods of statistical analysis, in particular arithmetic mean calculations of selected values.

The Czech and Slovak legislation also includes the number of cultivable microorganisms at 22 °C and 36 °C. Cultivable microorganisms are an indicator of general water pollution, which may not be specific. For a healthy person, this indicator does not represent a potential problem. Health problems may occur after contamination of water containing these organisms, especially in people with weakened immune systems.

The results of samples that contained cultivable microorganisms more than 3 000 CFU (colony formation units) were adjusted to > 3 000. This value is highly over the legislative limits for safe water and the exact number of CFU over this value is not so relevant. For the same reason, Pseudomonas values greater than 1000 were adjusted to > 1000. In some cases, the laboratory analysis did not determine the exact number above 300, which is also beyond the legislative limits. In these cases, the table includes the designation > 300. In some cases was not possible to determine the date of tank filling due to incomplete information provided by the fire protection units, or by refilling a smaller volume of water several times, it was not possible to determine the ratios of old to new water.

## RESULTS

The following two tables contain the results of laboratory analyzes of water samples from fire truck tanks. Table 1 contains the results for the period July and August, and Table 2 contains the results for the period October and November.

Table 1 - Results of laboratory analyzes of water samples, July and August

| Sample | Month | Coliform bacteria | Cult. org. 22 °C | Cult. org. 36 °C | Pseudomonas aeruginosa | Days |
|---|---|---|---|---|---|---|
| **1.** | July | 1 | 101 | 53 | - | 90 |
| **2.** | | - | > 3 000 | > 300 | 4 | 20 |
| **3.** | | - | > 3 000 | 2 400 | > 1 000 | 9 |
| **4.** | | - | > 3 000 | > 300 | - | 6 |
| **5.** | | 9 | > 3 000 | > 3 000 | > 1 000 | 25 |
| **6.** | | - | > 3 000 | > 300 | - | 2 |
| **7.** | | - | > 3 000 | > 3 000 | - | >365 |
| **8.** | August | 1800 | > 3 000 | > 3 000 | - | 7 |
| **9.** | | - | 122 | 108 | - | 200 |
| **10.** | | - | > 300 | 380 | - | 30 |
| **11.** | | - | 196 | 110 | - | 90 |
| **12.** | | 2 | > 3 000 | > 3 000 | 12 | 10 |
| **13.** | | - | > 300 | 170 | - | 35 |
| **14.** | | - | > 3 000 | 360 | - | 2 |

https://doi.org/10.5593/sgem2024v/3.2/s11.10

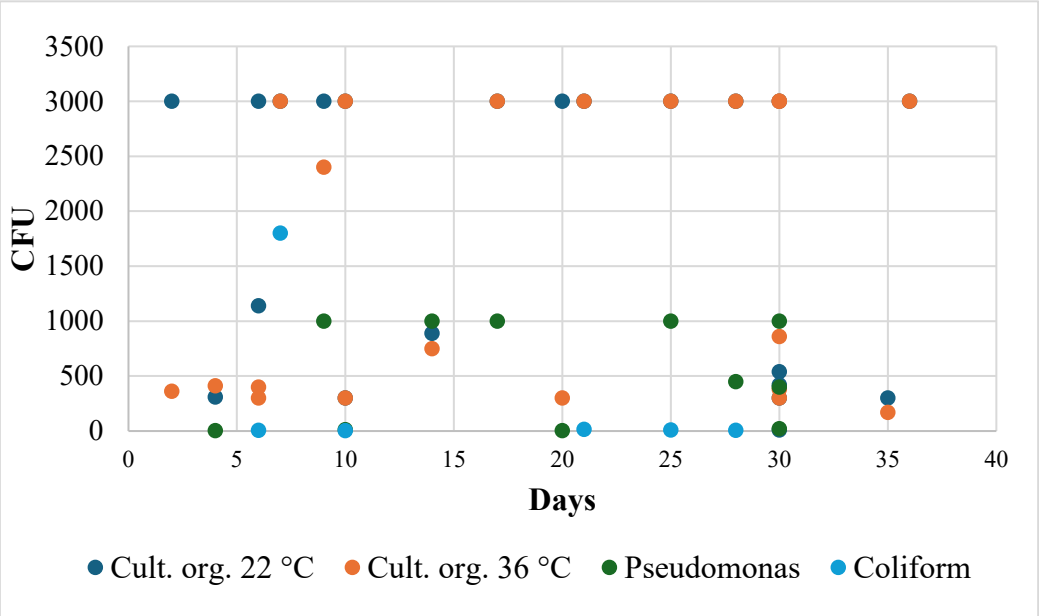
Table 2 - Results of laboratory analyzes of water samples, October and November

| Sample | Month | Coliform bacteria | Cult. org. 22 °C | Cult. org. 36 °C | Pseudomonas aeruginosa | Days |
|---|---|---|---|---|---|---|
| **15.** | October | - | > 300 | > 300 | - | 10 |
| **16.** | | 16 | > 3 000 | > 3 000 | - | 21 |
| **17.** | | 5 | > 3 000 | > 3 000 | 450 | 28 |
| **18.** | | 7 | 1 140 | 400 | - | 6 |
| **19.** | | - | 10 | > 3 000 | - | 30 |
| **20.** | | - | 570 | 490 | - | 90 |
| **21.** | | - | 310 | 410 | 4 | 4 |
| **22.** | | - | 51 | > 3 000 | 31 | / |
| **23.** | | - | > 3 000 | > 300 | > 1 000 | 30 |
| **24.** | | - | > 3 000 | > 3 000 | - | 36 |
| **25.** | November | - | > 3 000 | > 3 000 | > 1 000 | 17 |
| **26.** | | - | 540 | > 3 000 | 21 | 30 |
| **27.** | | - | 510 | 1 110 | > 1 000 | / |
| **28.** | | - | 1 690 | 690 | 220 | 60 |
| **29.** | | - | 890 | 750 | > 1 000 | 14 |
| **30.** | | - | 420 | 860 | 400 | 30 |
| **31.** | | 1 | 910 | > 3 000 | 3 | / |
| **32.** | | - | > 3 000 | 2 960 | 460 | / |
| **33.** | | - | 1 720 | 2 320 | 10 | / |
| **34.** | | - | 1 640 | 850 | 170 | / |
| **35.** | | - | > 3 000 | > 3 000 | 210 | / |
| **36.** | | 3 | > 3 000 | > 3 000 | 260 | / |
| **37.** | | - | 2 640 | 2 880 | 3 | / |
| **38.** | | - | > 3 000 | > 3 000 | 110 | / |

The month represents the period when the sample was taken from the tank, Cult. org. is the designation for cultivable microorganisms, Days represents the number of days from filling the tank with water to sampling. Values for all pollution indicators are reported in CFU. Cultivable microorganisms are measured in CFU/1 ml, other indicators are measured in CFU/100 ml. The zero values in the tables have been replaced by a dash. The slash symbol was used when the monitored data could not be determined. For one sample was not possible to determine the age of the water in the tank; the water had been stored there for a minimum of one year. For this reason, the value of the sample is >365.

Laboratory analyzes did not detect E. coli or Legionella Spp. in any of the samples. For this reason, the values are not shown in the tables.

Since most of the collected water samples were in the range of water age from 2 to 36 days, the results of these samples were processed into a dot plot. Zero values of E. coli and Legionella Spp. are not included in the graph.




Graph 1 - Numbers of CFUs for water samples up to 36 days

The values of Pseudomonas aeruginosa and coliform bacteria are presented in the graph in CFU/100 ml. The cultivable microorganisms are presented in the graph in CFU/1 ml. Visual evaluations were also performed during sampling to detect possible tank corrosion, algae, odor, or sediment. These aspects could have influenced the results of the laboratory analysis of the samples. In 12 cases, tank corrosion was detected, although the tanks were made of stainless steel or iron with anticorrosion protection. Four of the fire truck tanks contained unknown sediment and two of the tanks had an odor in the water.

The project also included determining possible ways to disinfect water or prevent changes in its quality. The following methods were selected as possible methods: periodic movement of the water in the tank, cleaning of the tanks at certain intervals, replacement of a proportion of the water in the tank, periodic replacement, or disinfection. Disinfection was chosen as the best method. The rationale is included in the discussion section.

## DISCUSSION

Graph 1 indicates that the most frequent values of the selected water pollution indicators were in the range of 0 to 1000 points, or more than 3000 points. However, the real dispersion would be much wider as the values of laboratory analyses are limited by certain parameters, as mentioned earlier.

The average number of days that the water in the tank was filled was 33.6 days. The median number of days is 25, the mode is 30. The average temperature of the water in the tank during the sampling was 27.75 °C. A sample with a number of days >365 was not included in these calculations because the exact number of days cannot be determined.

The result of the laboratory analyzes provided useful feedback on the quality of the water in the fire truck tanks. Although all fire trucks were filled with drinking water and tank water was not stored for more than 30 days in most cases, the laboratory results of the

https://doi.org/10.5593/sgem2024v/3.2/s11.10

water samples were nowhere near the quality that drinking water should be. A positive finding was the analysis of E. coli and Lgionella spp. The laboratory analysis did not detect the existence of these microorganisms in any of the samples. Coliform bacteria were detected in 9 water samples, one of which was very strongly contaminated. Pseudomonas aeruginosa was detected in 22 samples. Cultivable microorganisms were detected in all examined samples. More than half of the examined samples had at least one cultivable microorganism value higher than 3 000.

There are strict limits for drinking water that must be strictly observed. Otherwise, there is a risk of contamination of people with contaminated water. However, it is not possible to determine a specific level at which an indicator of water pollution will cause adverse effects or health problems if ingested by humans. These levels are very individual for each person and depend on several factors. For drinking water, all selected regulations consistently require zero levels of E. coli, Pseudomonas aeruginosa and coliform bacteria. For Legionella spp. a level of 1 000 CFU/100 ml is specified in some cases [4], [5]. Based only on these values, 12 water samples from fire trucks could be classified as safe. Cultivable microorganisms, for which the Czech and Slovak Republics report limits, were above these levels in all samples. The limit of Czech legislation for swimming pools would fulfil only one sample out of 38.

The question is where and how the water quality is changing or contaminated. The results of laboratory analyzes show that water samples vary even between volunteer and professional fire protection units. The average values of coliform bacteria were an order of magnitude higher in the volunteer units, this variation is due to the high value of the indicator in one of the monitored volunteer units. The occurrence of coliform bacteria in volunteer units is 3.5 times more frequent than in professional units. The analyzes also revealed a 30 % higher incidence of cultivable organisms at 22 °C in the samples from the voluntary units. The samples of professional units contained on average 26 % more cultivable organisms at 36 °C and 50 % more Pseudomonas aeruginosa. The source of water contamination in volunteer units based on elevated indicators is relatively unclear. The increased Pseudomonas in professional units is probably due to the way the tank is filled. The tank is most often filled with a short filling hose at the fire station. This hose is located at the filling point and very often there is residual water inside after filling. The hose is left undrained in the interior of the station after filling. The favorable climatic conditions and the residual stagnant water in the hose create ideal conditions for the reproduction of this bacterium. During the subsequent filling of the tanks, the bacterium is transported directly into the fire truck tank, where it can reproduce itself. Volunteer units usually replace or dry the hose after filling the tanks. This theory is based on the results of analyses in which in some cases the tank water contained Pseudomonas bacteria even though the tank had been filled only a few days before sampling.

Based on the results, the most effective method can be determined to create safe water in the tanks of firefighting trucks and possibly prevent changes in its quality. Periodic movement of the water in the tank, replacement of a proportion of the water in the tank, and periodic replacement of the water are not relevant methods to maintain water quality. The movement of water in the tank derived from the number of trips of a vehicle does not affect the quality of the water in the tank. Furthermore, incorrect filling of the tank with contaminated hoses and other equipment does not achieve safe water in the tank. The simplest way to create safe water in the tank is to use chemical disinfection [7]. The chemical disinfection method is fast, effective and relatively inexpensive. The most

effective disinfection is chlorine and chlorine-based compounds, which can effectively eliminate all monitored indicators of water pollution. Other methods of disinfection, such as UV radiation, are not as fast or may not be as effective [7], [8], [9], [10]. If necessary, a chlorine-based disinfectant can be applied to the tank and the internal truck pump used to mix the created solution. The time to elimination of the microorganism depends on the used detergent and its concentration.

Cleaning the tank can prevent contamination of the water inside the tank. According to the results of the analyzes and the information from the protocols, there is no correlation between the age of the tank and the quality of the water in it. If any of the tanks have been cleaned or replaced, again this has not affected the water quality results.

If the fire department is called to provide an emergency supply of safe water, a simple application of chlorine disinfectant before leaving the station can ensure that the water in the tank is safe from a microbial perspective. The disinfected water is biologically safe and can be safely used to clean people, animals, materials and equipment. Water can also be used for drinking, but it is necessary to select the right disinfectant and maintain a safe concentration. Otherwise, this water can be hazardous to health and can cause adverse effects on the human and animal bodies. Filling the tank with drinking water is a basic requirement. This ensures compliance with the basic parameters and quality of the water, especially its chemical composition. The final disinfection treatment ensures the biological safety of the water. If then firefighters arrive with a vehicle at the persons affected by the extraordinary incident, they can provide them with a supply of safe water.

As there were no previously published papers or studies dealing with this topic, it was not possible to predict the results. This research disproves the theory that drinking water stored in fire truck tanks still remains of the same quality. Biological changes occur in the water after the tank is filled. Further research is needed to determine the exact process of water contamination. In particular, verification of the theory of contamination of water from filling hoses. There may be several sources of contamination. In addition to the hoses, it could be the vehicle's internal pump, the tank, or residual water in the tank. In addition to sources of contamination, the next step is to verify the disinfection method under real conditions. This research can definitively confirm the theory of quick and easy disinfection using chlorine or chlorine products.

## CONCLUSION

This paper focused on the possibility of using water in fire truck tanks to provide emergency supplies of safe water in extreme situations such as floods or droughts. For this purpose was carried out laboratory analysis of water samples taken from vehicles of selected fire protection units in the Czech Republic. Based on the laboratory analysis, a safe method of disinfection of this water was subsequently determined.

The results of the laboratory analysis of the water samples confirmed the change in water quality compared to the drinking water that the tanks have always contained. In all samples, the microbial quality of the water decreased and microbial contamination occurred. The source of the contamination could not be clearly identified, but it is probably the undrained filling hoses located at the fire stations. The microbial composition and the number of microorganisms also change naturally during the storage period. The laboratory did not detect the presence of E. coli and Legionella spp. in the samples. The occurrence of coliform bacteria was relatively low, except for one sample. Pseudomonas aeruginosa was more frequent and in higher concentrations in the samples.

https://doi.org/10.5593/sgem2024v/3.2/s11.10

Cultured organisms were detected in all taken samples. Based on selected water quality legislation in various countries outside of the Czech and Slovak Republics, 12 of the 38 samples would fulfil the microbial limits. This legislation does not specify requirements for cultivable organisms.

Part of the research included the formulation of a possible disinfection method based on the laboratory results of the water samples. The disinfection of water using chlorine or chlorine products was chosen as the best method. This method is relatively quick, cheap and effective. Thus, fire protection units can apply disinfection before leaving the station and will already have safe water in the tank when they arrive at their destination. The research provided valuable information to determine an effective method to ensure a certain quality of water.

The next step in this research area is to validate the proposed water disinfection measures and determine the potential source of contamination during tank filling. If the results of the research are applied under real conditions, we can effectively help affected people and provide safe water in the places where they need it most.

## REFERENCES

[1] ZEMANOVA, Zuzana; KROCOVA, Sarka and SIROTIAK, Patrik., Risk Management in the Water Industry. In: *The 4th International Conference on Advances in Environmental Engineering*. Basel Switzerland: MDPI, 2023.

[2] FORZIERI, Giovanni; BIANCHI, Alessandra; SILVA, Filipe Batista e; MARIN HERRERA, Mario A.; LEBLOIS, Antoine et al. Escalating impacts of climate extremes on critical infrastructures in Europe. In: *Global Environmental Change*. 2018, p. 97-107. ISSN 09593780.

[3] United Kingdom. The Water Supply Regulations. Statutory Instrument. 647, 2018.

[4] United States. Safe Drinking Water Act. Public Law 93-523, 1974.

[5] European Parliament and Council of the EU. Directive 2020/2184 of 16. 12. 2020 on the quality of water intended for human consumption – The Drinking Water Directive. Official Journal of the European Union, L 435, 23.12.2020, p. 1–62.

[6] Ministry of Health of the Slovak Republic. Ordinance of the Ministry of Health of the Slovak Republic. 91, 2023.

[7] KOIVUNEN, J. and HEINONEN-TANSKI, H. Inactivation of enteric microorganisms with chemical disinfectants, UV irradiation and combined chemical/UV treatments. Water Research. 2005, p. 1519-1526. ISSN 00431354.

[8] CHO, Min; KIM, Jaeeun; KIM, Jee Yeon; YOON, Jeyong and KIM, Jae-Hong. Mechanisms of Escherichia coli inactivation by several disinfectants. *Water Research*. 2010, p. 3410-3418. ISSN 00431354.

[9] OFORI, Isaac; MADDILA, Suresh; LIN, Johnson and JONNALAGADDA, Sreekantha B. Chlorine dioxide inactivation of Pseudomonas aeruginosa and Staphylococcus aureus in water: The kinetics and mechanism. *Journal of Water Process Engineering*. 2018, p. 46-54. ISSN 22147144.

[10] HUANG, Junli; WANG, Li; REN, Nanqi; MA, Fang and JULI. Disinfection effect of chlorine dioxide on bacteria in water. *Water Research*. 1997, p. 607-613. ISSN 00431354.

# POSSIBILITIES FOR DAY-STEP FLOOD FORECASTING IN SMALLER CATCHMENTS USING MACHINE LEARNING METHODS

**Dr. Tomas Kozel**
**Ruzena Pavelkova**
Brno University of Technology, Veveří 331/95, Brno, **Czech Republic**

## ABSTRACT

Today, it is possible to work with a wide range of freely available data, often on a daily basis. These data can be used to create an early warning system for estimating the approximate hazard. It can also be used to develop models of long-term catchment behaviour. Most applications are generally carried out on catchments larger than 200 $km^2$. For this reason, areas between 20 and 350 $km^2$ were selected to test the hypothesis using models based on machine learning methods. How good results can be achieved when using daily data to predict increased flows caused by previous precipitation (summer) or a combination of snowmelt and precipitation (winter). The one day step was chosen for availability data (free data) and for testing area size limit for this step. The results showed that floods caused by a combination of rain and snowmelt were significantly better than those caused by rain alone. Two methods were compared. The neural networks ANN and fuzzy model. For both methods were founded the best architecture in training period. The results of the experiment showed that the limit of applicability of the data is above (around) 130 $km^2$ in the case of pure rainfall. In the case of floods caused by a combination of rain and snow, the daily step can be used even for catchments of about 20 $km^2$ with a one-day time shift.

**Keywords:** Daily data, floods, snow, machine learning methods, small catchments

## INTRODUCTION

Floods occurrence bring with self-many impact on daily life for citizen of hit areas. The floods itself is unappreciable event in long term view in Europe. Forecasting flood for small watershed is much more difficult and rather tricky. The situation in small catchment for flood caused combination of rainfall and snow melting is even more problematic. The best data for a construction of flood predict models are usually hourly data. The hourly data are usually unable for many areas. Therefore, many models are based on daily data (free data). However, working with daily data has some pitfalls in terms of the accuracy of the results.

The flood itself is given by many variable factors. For standard model applications are not usually known all parameters for all time. Therefore used models for flood prediction have to be much simpler. For this reason can be used Machine learning methods ML.

Machine learning methods ML have long been applied to various tasks in applied hydrology [1, 6, 7, 8]. Many methods of ML are described in Rezaeianzadeh, M. [9]. Almost all authors usually use ML methods for basins large than 200 $km^2$ (basin area over 1600 $km^2$) [4, 10], but many small catchments are confronted with flood as well. Rain fall is in small basin often so fast that it can discharge during same day as rainfall, but because the daily data is used sometimes are rainfall data from one event cut off to

https://doi.org/10.5593/sgem2024v/3.2/s11.11

two days. Therefore forecasting relationship between cause and reaction is troublesome from this point of view.

If ML model should be used as spine of flood warning system, some evaluation should be done first. For this purpose was chosen 4 basins. The area of basins is from 20 to 367 km$^2$. Basins will be tested on typical so called "summer flood "(flood from rain) and so called "winter or spring flood" (combination rain + snow melting).

## MATERIALS AND METHODS

For the simulation model itself, NN neural networks [5] and learned fuzzy models [2, 11], which are widely used in the field of hydrology, were chosen. These methods were chosen, because are widely spread in the different hydrology application and the methods are rather simply to use for this purpose.

Within the selected catchments, summer floods (from rain) and winter floods (a combination of snow and rain) occur. For this reason, two models were built for each catchment for both methods (ANN and fuzzy). The available data were divided into summer and winter training matrices. Different inputs were tested within the models. For the actual snow input, snow depth values were converted to water height using the water value. For snowmelt itself, the degree/day method [3] was used and snowmelt was also substituted for NN. Average daily temperature and water level were used as inputs to the model.

## APPLICATION

Four river basins in the Czech Republic within the Svratka river basin and its tributaries were selected for application (Fig. 1). The individual catchments are closed by the final profiles with measurements. The individual sub-basins cover the area of small to (smaller) medium-sized catchments, namely the Borovnice, Kadov, Jimramov and Dalečín profiles. The Dalečín profile was chosen as a comparison catchment because of its size. Further information on the catchment area is given in Table 1.

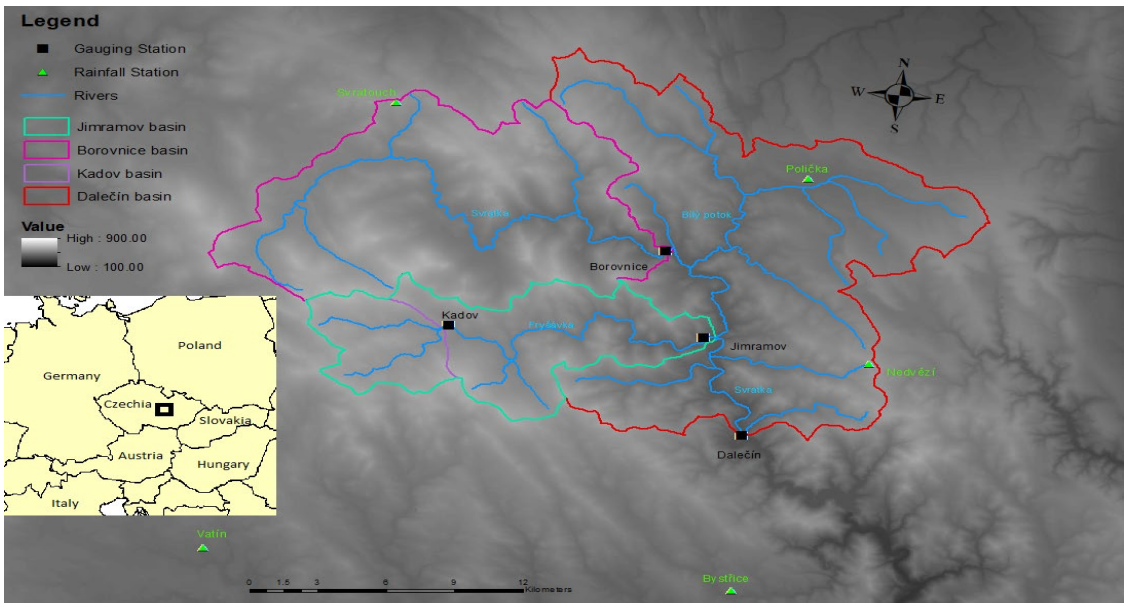



**Fig. 1. Position of tested basins.**

**Table. 1. Basin's info.**

| | Basin area [km$^2$] | River | Percentage afforestation [%] | Qa [m$^3$/s] | Q100 [m$^3$/s] |
|---|---|---|---|---|---|
| Borovnice | 128 | Svratka | 66 | 1.300 | 90 |
| Kadov | 20 | Fryšávka | 59 | 0.274 | 34 |
| Jimramov | 66 | Fryšávka | 51 | 0.709 | 62 |
| Dalečín | 367 | Svratka | 60 | 3.130 | 162 |

The climatic region of the area itself has an average annual temperature of around 5 to 6 °C and an average annual rainfall of around 800 mm/year. The area itself is approximately 60% forested (valid for 2018 according to Czech Hydrometeorological Institute).

*DATA*

The data are daily averages. In the case of meteorological data, these are station data. Therefore, the station data were converted to area using the Horton-Thiesson method [3]. In addition, catchment values were obtained using weighted averages. The meteorological data used were from the stations Bystřice, Svratouch, Vatín, Nedvězí and Polička.

The data were searched for events when the value in the Dalečín gauge profile exceeded 40 m$^3$/s (approximately Q1, when the value of flood hazard level 3 is 52 m$^3$/s). Suitable events were found in the data and are listed in Table 2. The date indicates the date of the flood peak.

**Table. 2. Important events.**

| Summer | | Winter | |
|---|---|---|---|
| Datum | Peak flow [m3/s] | Datum | Peak flow [m3/s] |
| 21.07.2001 | 49.2 | 10.03.2000 | 55.0 |
| 14.08.2002 | 87.4 | 13.02.2002 | 44.8 |
| 08.08.2006 | 72.5 | 18.03.2005 | 82.7 |
| 25.06.2013 | 58.8 | 31.03.2006 | 103.7 |
| 29.06.2020 | 52.4 | 06.03.2009 | 45.5 |
| 14.10.2020 | 67.0 | 29.02.2012 | 44.4 |
| | | 10.01.2015 | 51.6 |

*The length of the episode is given by the day of the peak and three surrounding days on either side (three days before the peak and three days after the peak). The data themselves have been further subdivided into calibration validation. Calibration data are considered* up to and including 2006. The calibration data are progressively extended to include events that have already occurred with respect to the event under consideration.

*MODELS*

Three criteria have been chosen for the actual assessment of model quality. The first is the RMSE and the second is the percentage error of the peak flood wave and the person correlation coefficient. The first criterion takes into account the total error of the

https://doi.org/10.5593/sgem2024v/3.2/s11.11

individual values. For low values of the RMSE criterion, good agreement can be expected even within the volume.

The second criterion considers the ability of the model to predict the average daily peak value, i.e. the predicted maximum value.

$$P_i = \frac{A_i - B_i}{B_i} \times 100, \quad (1)$$

If the relative error is calculated for several episodes (longer periods), the resulting relative error is calculated as the average of the individual errors.

The last criterion is the person correlation coefficient, which takes into account the degree of linear dependence of the test sets. Many model architectures and combinations of model inputs were tested during calibration. The inputs used were Predicted flow $Q_i$ [m$^3$/s];Predicted flow $Q_{i+1}$; Average of flows over a certain period $Q_{pi}$; Flow difference ($Q_{i-1}$-$Q_i$) $\Delta Q$; Temperature $T$ [°C]; Temperature change $\Delta T$; Average of flows over a certain period $Tp$; Predicted rainfall (24h) $Hr$; Average rainfall over a certain period $PRI$; Snow depth $SH$; Water equivalent of snow depth $WSH$; Water value of snow $\Upsilon$ [-].

In terms of calibration, the model architectures mentioned in the following text performed best in the case of summer flooding for the FuzS fuzzy model and for the NSS neural networks:

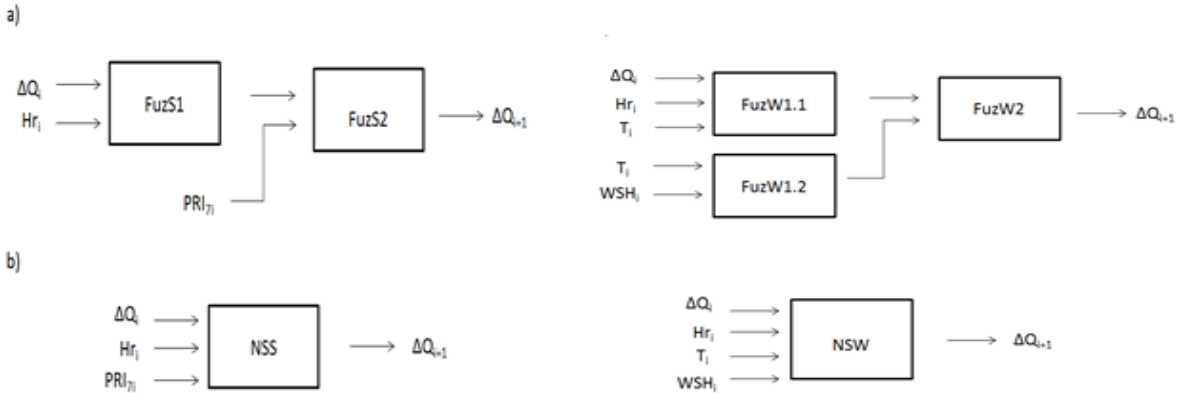



**Fig. 2. Summer's models architekture (left) Winter's models architekture (right) .**

## RESULTS

In the summer flood calibration, the NNL model performed best when the model was run with flow variation rather than directly with flow values. Other inputs were daily rainfall and previous average saturation (length of 7 days).

In the case of the winter flood model calibration for the NNW model, better results were obtained using flow changes rather than values alone. Other inputs were mean daily temperature, precipitation, snowpack height and snowmelt. Within each catchment, both the number of layers and the individual number of hidden neurons varied. The values of the settings were for NNW models two layers ANN for Borovnice (21;21), Kadov (28;28), three layers for Jimramov (44;44;44) and one layer model for Dalečín (43). For winter model ANN were used one layers models (Borovnice- 4;Kadov -4, Jimramov – 41 and Dalečín- 23 hidden neurons).

Different combinations of inputs and the number of hidden layers and hidden neurons in them were tested in the search for a suitable architecture. When calibrating the fuzzy models, the best results were obtained using incremental addition of inputs. In this procedure, the construction of the rule matrix within the partial fuzzy models is significantly easier than using a single fuzzy set with many inputs. In general, the best results were obtained for the 7-membership function (Gaussian curve).

**Table. 3 Models results for calibration period.**

| | Summer (NNL) | | | | Winter(NNW) | | | |
|---|---|---|---|---|---|---|---|---|
| | Borovnice | Jimramov | Kadov | Dalečín | Borovnice | Jimramov | Kadov | Dalečín |
| RMSE | 2.67 | 0.814 | 0.66 | 5.2 | 1.645 | 0.721 | 0.415 | 8.1 |
| Relative error [%] | 13.7 | 19.77 | 14.49 | 17.5 | 8.35 | 15.15 | 12.04 | 20 |
| Correlation coefficient | 0.832 | 0.924 | 0.821 | 0.840 | 0.955 | 0.947 | 0.938 | 0.916 |
| | Summer (FuzL) | | | | Winter(FuzW) | | | |
| | Borovnice | Jimramov | Kadov | Dalečín | Borovnice | Jimramov | Kadov | Dalečín |
| RMSE | 2.88 | 0.77 | 0.36 | 5.03 | 3.02 | 0.64 | 0.82 | 8.69 |
| Relative error [%] | 11.2 | 17.52 | 21.5 | 12.1 | 16.50 | 16.10 | 22.4 | 23.5 |
| Correlation coefficient | 0.71 | 0.75 | 0.62 | 0.77 | 0.68 | 0.61 | 0.59 | 0.73 |

In the NNW model calibration, the snowmelt inputs using the degree-day method and using only snowmelt inputs to the model gave very similar results. When comparing the results of the NN-based and fuzzy models, the fuzzy model results generally achieve lower RMSE values. For the other two criteria, the NN-based models achieve better results.

In a second step, the trained models were validated against the already trained models. The results are shown in Table 4.

**Table. 4 Models results for validation period.**

| | Summer (NNL) | | | | Winter(NNW) | | | |
|---|---|---|---|---|---|---|---|---|
| | Borovnice | Jimramov | Kadov | Dalečín | Borovnice | Jimramov | Kadov | Dalečín |
| RMSE [$m^3/s$] | 3.35 | 1.09 | 1.16 | 5.45 | 1.21 | 1.04 | 0.388 | 5.43 |
| Relative error [%] | 19.1 | 32.2 | 56.4 | 18.9 | 8.35 | 15.15 | 18.04 | 18.6 |
| Correlation coefficient | 0.44 | 0.32 | 0.15 | 0.71 | 0.90 | 0.82 | 0.80 | 0.81 |
| | Summer (FuzL) | | | | Winter(FuzW) | | | |
| | Borovnice | Jimramov | Kadov | Dalečín | Borovnice | Jimramov | Kadov | Dalečín |
| RMSE [$m^3/s$] | 3.78 | 1.08 | 0.62 | 5.36 | 3.05 | 1.61 | 0.61 | 6.61 |
| Relative error [%] | 35.3 | 38.2 | 37.1 | 20.7 | 17.76 | 18.8 | 25.2 | 16.21 |
| Correlation coefficient | 0.52 | 0.54 | 0.40 | 0.83 | 0.68 | 0.62 | 0.59 | 0.77 |

According to Table 4, daily data makes it challenging to capture the dynamic behaviour of summer precipitation within a daily timeframe for catchments below 70 $km^2$.

https://doi.org/10.5593/sgem2024v/3.2/s11.11

Catchments ranging from 60-130 km$^2$, resulted in slightly better outcomes. The results suggest that the model error rises rapidly as the catchment size decreases. For the Kadov basin, the FuzL model achieved a relatively low RMSE culmination error. However, the results are highly skewed, making it challenging to use them for prediction. The trend observed in winter floods is similar but less significant.

The correlation coefficient from the smallest catchment Kadov, where its value is less than 0.3, is not useful. Overall, the coefficients for the NNL and FuzL models were relatively weak, with the exception of the Dalečín station. The correlation coefficients for the NNW and FuzW models were lower than those for the calibration period, but still of good quality. The NNW model showed no significant deviation during validation when using either the degree/day method to obtain runoff or when using only the degree/day method inputs.

## DISCUSSION

When longer episodes were used, there was a relatively high degree of noise in the behavior of the models in predicting the flood and a significant underestimation of peak flows. The models tended to generalize their outcomes promptly and did not differentiate sufficiently between individual floods. Therefore, it is imperative to analyses elevated flows separately from the rest of the data.

Given the length of the data, the incidence of significant episodes was comparatively low and the number of episodes was typical for the dataset, therefore the training matrix was relatively small. However, with a larger training matrix, improvements in model results are anticipated due to the expanded range and variation of appropriate learning patterns. The matrix can be extended with appropriately selected fabricated episodes. However, incorporating winter episodes presents a complex situation. A high number of input variables can result in increased flow.

## CONCLUSION

The primary limitation lies in the accuracy of the input rainfall information. Good results were achieved in the case of winter floods when there was a time lag of 1 to 2 days between the causal precipitation and the flood (today forecast will be applicate on tomorrow). Two days lag was observed in Borovnice and Dalečín basin. On average, there was a deviation of 10-18% from the peak for NNW model and 16 – 25% for FuzW model. Winter floods also have a significantly delayed and smoother runoff compared to that of summer floods. Additionally, the models yielded a comparatively lower margin of error for total runoff, resulting in their potential for precise flood pattern estimations. Classical procedures typically necessitate substantial amounts of data and therefore struggle to accurately simulate winter floods.

From the perspective of applying fuzzy models and neural network models, it seems to be more advantageous to use fuzzy models for summer floods and neural networks for winter floods.

Consequently, a moderately efficient model can be created using daily data. Notwithstanding, it is essential to bear in mind that recording daily data is a rather rudimentary approach for catchments up to 100 km$^2$. When modelling daily flow, it is not particularly useful to test the results against summer floods, as achieving low error values is challenging. Therefore, it may be appropriate to reduce the significance of

errors or exclude them altogether from the model evaluation. Conversely, for more complex processes such as winter floods, models base on ML methods can efficiently attain high quality outcomes. For this reason, reflecting relatively high-quality outcomes in the context of winter floods is feasible by delaying the causal rainfall for two or more days.

## ACKNOWLEDGEMENTS

Acknowledgements: The article was supported by grant FAST-S-24.

## REFERENCES

[1] Apaydin, H., Sattari, M.T., Falsafian, K., Prasad, R., 2021 Artificial intelligence modelling integrated with Singular Spectral analysis and Seasonal-Trend decomposition using Loess approaches for streamflow predictions. J. Hydrol, 600, 126506.

[2] Bezdec, J.C., 1981. Pattern Recognition with Fuzzy Objective Function Algorithms. Plenum Press, New York,

[3] Bras, R.L., 19990. Hydrology: An Introduction to Hydrologic Science. Addison Wesley, New York, NY. ISBN: 978-0201059229.

[4] Dawson CW, Wilby R (1998) An artificial neural network approach to rainfall-runoff modeling. Hydrol Sci J 43(1):47–66

[5] Hopfield, J. J., 1982. Neural networks and physical systems with emergent collective computational abilities". Proceedings of the National Academy of Sciences. 79 (8): 2554–2558.

[6] Jiang G.,Wang W., 2017. Error estimation based on variance analysis of k-fold cross-validation, Pattern Recognition, Volume 69, Pages 94-106, ISSN 0031-3203, https://doi.org/10.1016/j.patcog.2017.03.025.

[7] Leskovar, K., Težak, D., Mesec, J., Biondić, R., 2021. Influence of Meteorological Parameters on Explosive Charge and Stemming Length Predictions in Clay Soil during Blasting Using Artificial Neural Networks. Appl. Sci. 2021, 11, 7317.

[8] Kozel, T., Stary, M., 2022. Adaptive Stochastic Management of the Storage Function for a Large, Open Reservoir Using Learned Fuzzy Models. Journal of Hydrology and Hydromechanics 70, no. 2 213–21. https://doi.org/10.2478/johh-2022-0010.

[9] Rezaeianzadeh, M., Tabari, H., Yazdi, A.A., Isik, S., Kalin, L. Flood flow forecasting using ANN, ANFIS and regression models. Neural Comput. Appl. 2014, 25, 25–37. https://doi.org/10.1007/s00521-013-1443-6

[10] Seo Y, Kim S, Kisi O, Singh VP (2014) Daily water level forecasting using wavelet decomposition and artificial intelligence techniques. J Hydrol 520:224–243

[11] Tagaki, H., Sugeno, M., 1985. Fuzzy identification of systems and its applications to modelling and control. IEEE Transactions on Systems, Man and Cybernetics, SMC-15, 1, 116–132.

# POSSIBILITIES OF USING WATER RESOURCES FROM THE SHALLOW AQUIFER TO SUPPLY WATER TO LOCAL IRRIGATION SYSTEMS

**Assist. Prof. Phd. Eng. Ioana Alina Cretan**

Hydrotechnical Engineering Department, "Politehnica" University Timisoara, **Romania**

## ABSTRACT

The paper aims to identify the availability of water sources for water supply of local irrigation systems. Where the location of the land involved in the works is located at a large distance from the surface water sources, the only viable option is the use of water from the shallow water table. The identification, delimitation and characterization of underground water bodies is done in accordance with the specific methodology developed within the National Institute of Hydrology And Water Management, based on hydrogeological studies supporting the implementation in Romania of the provisions of the Water Framework Directive 2000/60/EC and the guidelines developed within the Common Strategy for the Implementation of the Water Framework Directive. Benefiting from the advantages offered by the programs of the Establishment of Irrigation Systems funded by the Ministry of Agriculture, farmers and their associative forms used these underground water bodies as the source of water supply for the newly established local irrigation systems.

**Keywords:** local irrigation systems, water resources, land reclamation, shallow aquifer layer.

## INTRODUCTION

The paper analyses the suitability of underground water bodies in the western part of the country (Romania) to supply newly created local irrigation systems. Several areas are being studied and a series of technical solutions based on the results of these investigations of the site's hydrogeology will be presented.

## MATERIALS AND METHODS

The first investment that was analysed is in the Bega hydrographic basin, on the Slatina surface water course, cadastral code V-1.21.4.2, underground water body code ROBA01 - Lovrin-Vinga. The groundwater body is confined in porous-permeable deposits quaternary age alluvium. Thin covering layer, in some places non-existent; due to a very low effective infiltration. The Piper, Schoeller and Stiff diagrams (Figures 1 and 2) performed on the waters of the National Hydrogeological Network observation boreholes show that they have a very large variation in chemistry, ranging from magnesium calcium bicarbonate to magnesium chlorocalcium or bicarbonate sodium The body has a cross-border character [1].

https://doi.org/10.5593/sgem2024v/3.2/s11.12

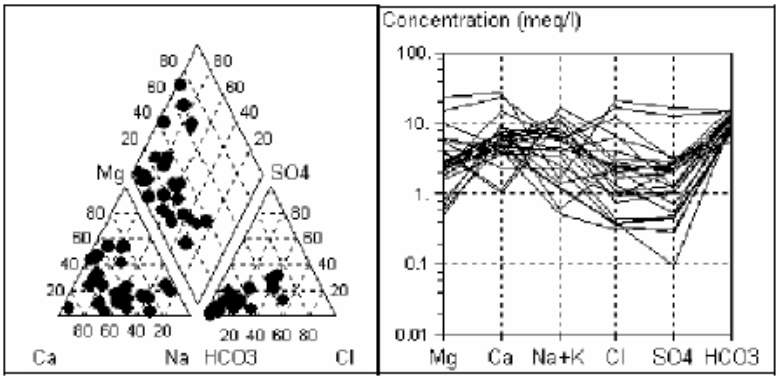



Figure 1 Piper, Schoeller diagrams based on the chemical analyzes of the National Hydrogeological Monitoring Network for the underground water body code ROBA01 - Lovrin-Vinga

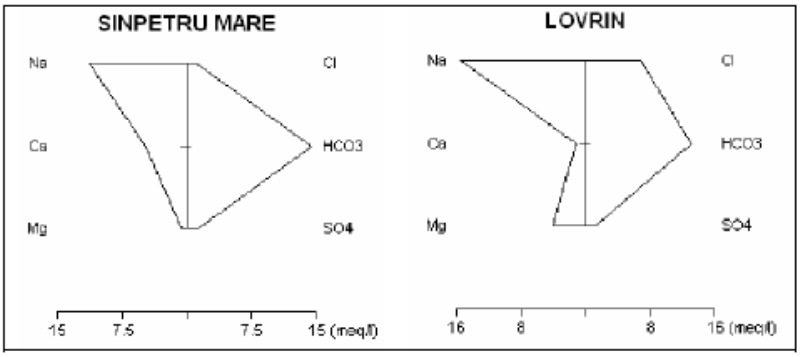



Figure 2 The Stiff diagram based on the chemical analyzes of the boreholes in the towns of Sânpetru Mare and Lovrin

The aquifer structure is represented by the phreatic layer (shallow depth) and the deep aquifer complex. In the area studied, the underground water is confined, in the phreatic horizon, in the Holocene alluvial deposits, and the deep water is confined in the Pleistocene - Pannonian formations.

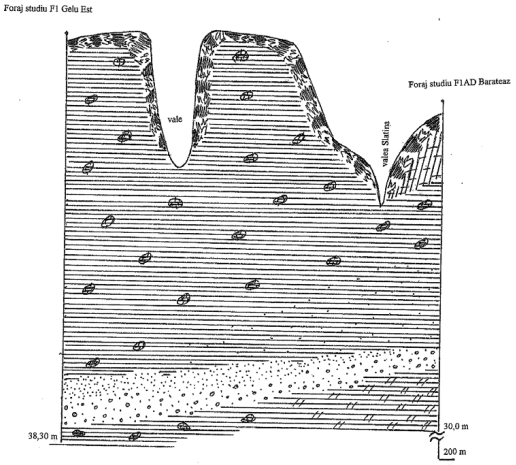



Figure 3 Hydrogeological section through phreatic in the location studied for the underground water body code ROBA01 - Lovrin-Vinga

The second investment analysed is located in the Timis hydrographic basin, on the Timis surface water course, cadastral code V-2, underground water body code ROBA03

- Timisoara. This groundwater body is accumulated in porous-permeable, alluvial deposits of Quaternary age. Silty-sandy-clay and loess cover layer and an effective infiltration of 15-30 mm water column.
The Piper, Schoeller and Stiff diagrams (Figures 4 and 5) executed on the samples of a number of 59 observation boreholes of the National Hydrogeological Network show that they have a very large variation in chemistry. The chemistry of the waters varies from magnesium calcium bicarbonate to magnesium chlorocalcium, chlorosodium or sodium bicarbonate [1].

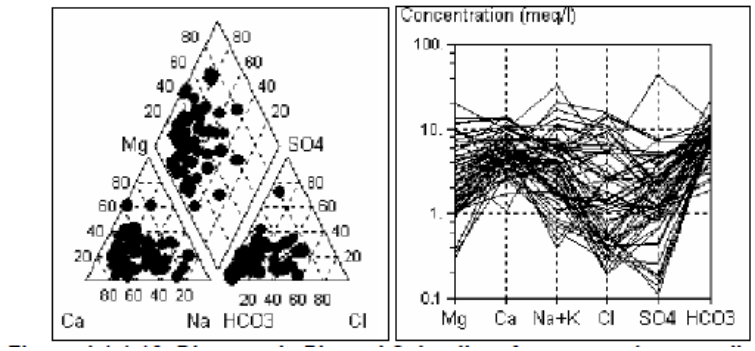



Figure 4 Piper, Schoeller diagrams based on the chemical analyzes of the National Hydrogeological Monitoring Network for the water body code ROBA03 - Timisoara

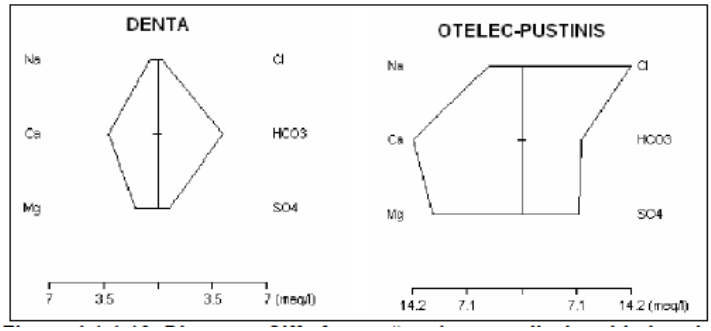



Figure 5 The Stiff diagram based on the chemical analyzes of the boreholes in the towns of Denta and Otelec-Pustiniș

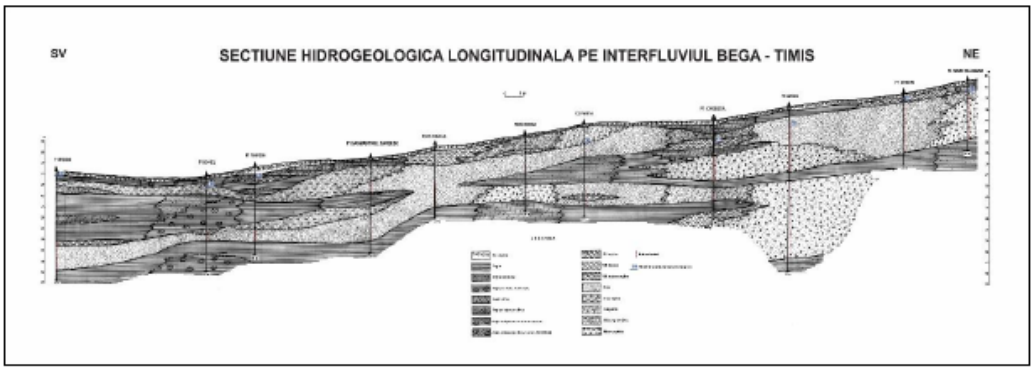



Figure 6 Longitudinal SW-NE hydrogeological section through boreholes belonging to National Hydrogeological Network for the through the Timiș-Bega interfluve

https://doi.org/10.5593/sgem2024v/3.2/s11.12

## RESULTS

From the analysis of the hydrogeological situation detailed in the previous chapters, to ensure the water requirement for irrigation in the *first investment* the total flow required $Q_{TOTAL}$ = 4 l/s from the centralized own source, the optimal solution is recommended to the beneficiary and the general investment designer by proposing to execute 2 boreholes with the following characteristics: F1 and F2 : Q =2 l/s; H = 45 m, Dn = 225 mm. Wells F1 and F2 will be located with the coordinates described in the table below.

Table 1 Indicative coordinates of water supply drilling for irrigation for the underground water body code ROBA01 - Lovrin-Vinga

| Drilling | X | Y |
|---|---|---|
| F 1 | 507810 | 197701 |
| F 2 | 507262 | 197512 |

For the *second investment* analyzed, in the site area, due to the sedimentation conditions, the water table, in the study area, is unevenly developed. In the area of the valleys it appears at shallow depths, at 10-20 m, having a mediocre aquifer potential, and in some areas of interfluves it appears at depths greater than 30-40 m or is absent. In order to supply water to the irrigation system, it is proposed to construct two boreholes F1 and F2 that will capture the water table. The boreholes will be located in the direction of groundwater flow in the CF 406492 plot. Wells F1 and F2 will be located in are with the coordinates described in the table below.

Table 2 Indicative coordinates of water supply drilling for irrigation for the underground water body code ROBA03- Timisoara

| Drilling | X | Y |
|---|---|---|
| F 1 | 444465 | 205881 |
| F 2 | 444426 | 206112 |

## DISCUSSION

Taking into account the reduced potential of the aquifers in meeting the plant's water needs represented by the watering norm and the watering scheme in all situations where the water supply of the proposed investments is made from the groundwater, the use of basins was chosen to store irrigation water, thus so as to ensure a total volume of water required. This storing basins will be supplied by the water from the phreatic layer through drilling, through the entire year in order to ensure the required volume for the crops.

In order to achieve increased productivity on agricultural land by ensuring the water requirement, it is proposed to build local irrigation systems made up of electric pumping units that capture the water from the proposed storage basins, pressure distribution pipes made of PEHD (high density polyethylene), valve chambers and sprinkler irrigation installations in the fixed central pivot type [2].

## CONCLUSION

The use of water from the shallow water table to feed local irrigation facilities is only possible under the conditions of the creation of storage basins in which to pump the

amount of water required during the application of the watering rule during a calendar year. The efficient alternative, both from a technical and economic point of view, is surface water, but unfortunately its availability remains limited in relation to the surfaces interested in the works.

The hydrotechnical scheme of the irrigation network is composed of a pressurization station equipped with electric pumps. The discharge pipes of these pumps enter a collector from which the water distribution pipes to the irrigation facilities start. This manifold is equipped with relief valves and vent valves. Separation valves will be installed on this collector both on the discharge and distribution pipes, and a meter is installed to monitor the water consumed. The pumps are located on a floating pontoon anchored to the shore, suction is carried out with a river screen type floating siphon. The discharge pipes are flexible hose type equipped with a float. The distribution pipe network is dimensioned according to the flow and pressure required at the inlet of the irrigation machine. On these pipelines, massive anchorages are provided at the changes of direction, aeration-deaeration devices at the highest points of the pipelines where necessary and with hydrants to connect the irrigation installations. The most commonly proposed irrigation installations are of the fixed pivot type with end cannon of different watering radius.

An important indicator that must be achieved through the submitted projects is the purchase of Weather Stations with at least 4 measured indicators that will allow the practice of precision agriculture with the aim of monitoring the indicators of humidity, temperature, soil salinity for the application of an efficient and effective irrigation activity at the plant level.

The implementation of the financing projects will also lead to the modernization and restructuring of the holding by improving productivity, respectively creating the premises for obtaining a physical production of grain that approaches the genetic potential by ensuring a vital element for the plants, namely water. The existence of water at the level of the plant when they need it in the critical phases of development will have the effect of obtaining quantities of agricultural products far superior to those that do not benefit from this facility.

The monitoring of the underground water in the area of the agricultural lands to be irrigated will be done through shallow boreholes that will capture the first aquifer layer of the phreatic horizon.

The field of agricultural activity is characterized by a high technical and technological progress that leads to a rapid wear and tear of both the technologies and the machinery and equipment involved in the irrigation process.

The existence of continuous innovation in the agricultural sector requires continuous improvement with the aim of making the activity more efficient, optimizing the activity carried out, reducing production costs, increasing productivity, labor productivity, etc. All this will have a significant impact on the future activity of farmers.

## ACKNOWLEDGEMENTS

The studies used in this article were conducted in order to achieve European financing through the Ministry of Agriculture using the Measure DR-26 - Establishment of irrigation systems.

https://doi.org/10.5593/sgem2024v/3.2/s11.12

## REFERENCES

[1] The updated Management Plan of the Banat Hydrographic Area (2016-2021); (https://rowater.ro/institution-activity/departments/integrated-european-water-resources-management/management-plans/national-management-plans)

[2] APPLICANT'S GUIDE for access DR-26 - Establishment of irrigation systems online submission Version 01 – 2023 (https://bit.ly/DR-26 (RO version)).

# PUBLICATION OF DATA FROM THE LATVIAN REGIONAL HYDROGEOLOGICAL MODEL LAMO4

**Assist. Prof. Dr. Math. Irina Eglite**
**Researcher Master of Comp. Sc. Kaspars Krauklis**
Riga Technical University, **Latvia**

## ABSTRACT

Geographic information systems (GIS) are based on the approach of displaying data from individual layers, where a manageable number of geospatial objects are displayed within a single layer. The entire content of a hydrogeological model (HM) can only be partially included within this framework. HM input data and modeling results as layer surface maps are a way to easily, clearly, and simply publish the model content and simulation experiment results. However, this approach is not sufficient for regional HMs. Regional HM data may be of interest not only to specialists in hydrogeology and state environmental monitoring services, but also to any citizen of the country who owns real estate or land; anyone who cares about the environment and ecology. The three-dimensional nature of HM data and its high density make it difficult for users who are interested not in the overall model maps but in the HM data for a selected location to access when information is published in layers. No GIS can automatically provide such summaries, and their a priori structure is not designed for this task. The Groundwater Vistas modeling environment also does not provide such local summaries. The following describes the extraction of hydrogeological data for each individual location in the territory of Latvia, its mathematical processing, and the publication of the summarized data in the WEB environment.

**Keywords:** LAMO4, hydrogeological data, regional model, WEB

## INTRODUCTION

LAMO4 is a regional hydrogeological model [1], [2] encompassing the entire territory of Latvia. It simulates 3D average annual groundwater flow values with a model grid resolution of 250 meters, resulting in a total of 61.56 million nodes. The model covers zones of potable or industrial groundwater extraction across Latvia, encompassing 27 layers from the surface topography down to the Pernava Horizon (D2pr). LAMO4 is a MODFLOW model run within the Groundwater Vistas 8 environment [3]. Model characteristics: 14 aquifers interconnected by 13 aquitards; Geological layer structure defined by surface (z-maps) and filtration properties (k-maps) - these maps are created using data from Latvian Environment, Geology and Meteorology Centre, geological layer surfaces and boundaries; Digital elevation model, data on 469 major rivers, and 127 lakes - obtained from the Latvian Geospatial Information Agency.

LAMO4 Calculations: groundwater levels in 3D grid nodes (φ-maps); groundwater flow rates (q-maps) and velocities (v-maps); groundwater inflows to rivers and lakes; groundwater flow balances.

The aim of the research is to find a practical solution for collecting and publishing hydrogeological model data, using LAMO4 as an example.

https://doi.org/10.5593/sgem2024v/3.2/s11.13

## GIS DATA COMPILATION

The hydrological model (HM) is capable of providing significantly more localized information at individual HM nodes. This requires additional data acquisition and processing. In the case of the LAMO model, the following additional data is available for every location in Latvia: layer depths and thicknesses; water depth, transmissivity, and quality; flow direction and gradient; and water flow gradation - recharge, transit, or discharge (RTD) [4].

For each HM LAMO node, the following data are available or can be obtained through mathematical processing: surface elevation, thickness, and depth; water level and discharge; magnitude and angle of the water flow gradient; layer filtration coefficient and vertical infiltration in the aquitard; RTD; water quality gradation – drinking water, problematic drinking water and mineral water; protection of the first aquifer from water-soluble pollution. The compiled data form a table with up to 420 cells, and the total number of tables is $1.15\times10^6$, thus covering the terrestrial part of Latvia with data every 250 meters in an HM node cell.

Water level contours, infiltration values, layer surface, and filtration coefficient maps are easily accessible to the user and can be obtained using surface export tools from the modeling environment. In addition to the mentioned parameters, additional mathematical processing is required for vertical infiltration. The vertical flow $V_z$ in the model is given in units [m/day], and therefore the transition to infiltration $Q_z$ [mm/year] occurs according to formula (1).

$$Q_z = 365000 \times V_z \tag{1}$$

The calculation of surface depth, surface thickness, and water level depth is trivial given known surface elevations and water level elevations. For the calculation of water transmissivity km in the *i*-th aquifer, formula (2) is used, which includes thickness and filtration coefficient *k*.

$$km_i = m_i \times k_i \tag{2}$$

For the calculation of the magnitude mod of the water flow gradient, formula (3) is used, which includes *Vx* – model flow in the x direction, *Vy* – model flow in the *y* direction, and *k* – the layer filtration coefficient.

$$mod_i = \frac{\sqrt{V_{xi}^2 + V_{yi}^2}}{k_i} \tag{3}$$

For the water flow direction angle α, formula (4) is used:

$$\alpha = arctg\left(\frac{V_{xi}}{V_{yi}}\right) \tag{4}$$

For the calculation of the flow angle, it is necessary to additionally consider situations where $Vx<0$, $Vy<0$ or $Vx=0$.

To determine the feeding, transit, and discharge zones, the *r* function (5) is used [4]. The function result is divided into three ranges, where ($r>1$) corresponds to feeding, ($1>r>-1$) corresponds to transit, and ($r<-1$) corresponds to discharge.

$$r = 250 \times \frac{V_{zi} - V_{zi+1}}{\sqrt{V_{xi}^2 + V_{yi}^2}} \quad (5)$$

which is the ratio of the difference in vertical flow to the resulting magnitude of the horizontal flow. The number 250 is an empirical constant.

Information about water quality gradation - drinking, problem drinking and mineral water is not part of the current version of the LAMO model. Water quality data were obtained from external sources [5]. This information may be useful when installing a new water extraction well or choosing a residence in a rural area.

Groundwater protection data show how protected the upper horizon of the bedrock is from surface water-soluble pollution. A MODPATH simulation [6] was performed for HM, placing the necessary particles at the midpoint of each HM grid cell, above the aeration zone (HM 2nd layer). The protection gradation – low, medium, and high is sought using the MODPATH simulation, with which it is determined in how long $T$ a tracer from the relief reaches the first bedrock layer. If $T$<1 year – low protection, if 1<$T$<25 years – medium, and if $T$>25 years – high protection. The results are obtained by processing the particle motion trajectory file with specially developed software. An approach that would allow the most accurate determination of how many groundwater layers are protected from pollution has been implemented in the project "Application of Latvian hydrogeological model LAMO4 for prediction and analysis of pollution movement" and it will be described within a separate article.

The HM data described above are mainly processed at the surface operation level, where the resulting surface describes the specific calculated or exported parameter. Each node coordinate corresponds to a significant dataset that includes the parameters described above in various model layers. Among the simplest ways to store such data is to place all the data of a separate HM node in one row of the table, which thus contains a subtable with the summarized information, see Fig. 1.

| A | B | C | D | E | F | G | H | I | |
|---|---|---|---|---|---|---|---|---|---|
| X | Y | Id | virsmas_au | virsmas_au | virsmas_au | virsmas_au | virsmas_au | virsmas_au | virs |
| 662500 | 173000 | 176343 | 152.14 | 152.1 | 152 | 150.3 | 0 | 98.35 | |
| 663250 | 173000 | 176346 | 149.38 | 149.4 | 148.7 | 148.3 | 0 | 99.46 | |
| 658500 | 173250 | 178228 | 135.55 | 0 | 135.5 | 134.5 | 0 | 89.14 | |
| 658750 | 173250 | 178229 | 136.17 | 0 | 136.1 | 135.1 | 0 | 89.9 | |

Fig. 1. Fragment of a combined data table

## WEB PUBLICATION

GIS data publication systems are optimized for the easy visualization of individual base maps, geometric points, lines, and areas, where it is possible to associate a description with properties to a selected object. At the same time, these systems are not designed for the visualization of three-dimensional data from a hydrogeological model, and the visualization of individual nodes of a model plane grid is also difficult due to the large total number of nodes. One of the problems with the availability of hydrogeological model data is the search for technical solutions for publication. Web GIS servers, such

https://doi.org/10.5593/sgem2024v/3.2/s11.13

as ArcGIS Server [7], are widely used for publishing geospatial data. They provide interactive access to various types of data - surfaces, lines, areas, points, as well as attributes of these spatial objects.

Within the framework of the project, approximately 1.15 million data tables were prepared for the entire territory of Latvia. The data in each table correspond to information extracted or additionally calculated from the regional hydrogeological model LAMO for a separate node with a model rectangular plane approximation step of 250 meters, see Fig. 2. The table includes both information directly available from the model - the elevation, thickness, water levels, infiltration, and filtration coefficient of existing layers, as well as additionally calculated values - the magnitude of the water flow gradient, the angle of the water flow direction, the existing basic function of water in the layer: recharge, transit, or discharge. Additionally, layer numbers, layer codes, node coordinates, and an assessment of groundwater protection in the bedrock are provided.

| Layer Nr | Layer code | Surface height [m asl] | Surface depth [m] | Layer thickness [m] | Throughf low [$m^2$/day] | Head level [m vjl] | Head depth [m] | Water quality | Flow gradient module | Flow gradient angle | BTA | Filtration coeff. | Infiltration [mm year] | Vulnerability |
|---|---|---|---|---|---|---|---|---|---|---|---|---|---|---|
| 1 | relh | 153.08 | | | | | | | | | | | | high |
| 2 | aer | 153.1 | 0.02 | 3.4 | | | | | | | | 0.0004 | 256 | |
| 3 | Q2 | 149.7 | 3.38 | 3.7 | 57.05 | 147.55 | 5.53 | drinking | 0.01 | 98 | Transit | 15 | | |
| 4 | gQ2#z | 146 | 7.08 | 38.4 | | | | | | | | 0.0009 | 56 | |
| 5 | Q1# | 107.6 | 45.48 | 12.46 | 87.22 | 141.25 | 11.83 | drinking | 0.0044 | 131 | Recharge | 7 | | |
| 6 | gQ1#z | 95.14 | 57.94 | 95.14 | | | | | | | | 0.0003 | 58 | |
| 13 | D3dg# | 88 | 64 | 20 | 307 | 137 | 16.08 | drinking | 0 | 134 | Recharge | 15.38 | | |
| 14 | D3slp#z | 68 | 84 | 15 | | | | | | | | 0.0007 | 50 | |
| 15 | D3pl | 53 | 99 | 26 | 214 | 134 | 19.08 | drinking | 0 | 128 | Recharge | 8 | | |
| 16 | D3am#z | 27 | 125 | 7 | | | | | | | | 0.0001 | 38 | |
| 17 | D3am | 20 | 132 | 25 | 193 | 126 | 27.08 | drinking | 0 | 122 | Recharge | 7.44 | | |
| 18 | D3gj2z | -5 | 158 | 14 | | | | | | | | 0.00012 | 26 | |
| 19 | D3gj2 | -19 | 172 | 29.44 | 312 | 118 | 35.08 | drinking | 0 | 128 | Recharge | 10.92 | | |
| 20 | D3gj1z | -48.44 | 201.52 | 10.43 | | | | | | | | 0.00006 | 19 | |
| 21 | D3gj1 | -58.87 | 211.95 | 27.18 | 364.75 | 109.05 | 44.03 | drinking | 0.001 | 139 | Transit | 13.42 | | |
| 22 | D3gj1z | -86.05 | 239.13 | 12.29 | | | | | | | | 0.000557 | 11 | |
| 23 | D2brt | -98.34 | 251.42 | 46.16 | 223.32 | 108.38 | 44.7 | drinking | 0.001 | 140 | Recharge | 4.83 | | |
| 24 | D2arz | -144.5 | 297.58 | 15.3 | | | | | | | | 0.000418 | 6 | |
| 25 | D2ar | -159.8 | 312.88 | 41 | 209.92 | 107.74 | 45.34 | drinking | 0.0009 | 141 | Transit | 5.12 | | Coordinates |
| 26 | D2nr#z | -200.8 | 353.88 | 99.2 | | | | | | | | 0.00001 | 2 | 595750 |
| 27 | D2pr | -300 | 453.08 | | | 64.59 | 88.49 | mineral water | | | Transit | | | 305500 |

Fig. 2. Geospatial data table for a single node

The publication of such geospatial data in a web environment is hindered by the following circumstances:

1. The volume and structure of attributes associated with point data. The table shows that it includes 27×15+15=420 table cells, including headings. Although many of these cells are empty, their content cannot be reasonably displayed according to the Shapefile structure principle Property to Value.
2. The high number of points to be displayed can be an obstacle to their efficient interactive selection.
3. The use of a web GIS server is a cost factor for allocating a separate computer for website operation and license acquisition, or purchasing the service as a monthly service.

Web GIS systems provide high-quality functionality for interactive maps. However, in the context of the current problem, where only an interactive interface for accessing tables is needed, the idea of using a Web GIS system was rejected in favor of an individual solution that could be optimized for this specific problem. The solution will be considered according to the Model-View-Controller scheme.

The strategy for storing information in data tables determines the subsequent interaction, data extraction, and processing, which would be part of the Controller. The way each individual table is physically stored is not considered optimal, resulting in increased Internet traffic and slower end-system response. The chosen solution is to store the combined data in a single table, where one record (see Fig. 1) contains all the necessary information to create a table for one node (see Fig. 2).

## WEB USER INTERFACE

The table request is based on the coordinates of a point selected by the user on the map. Thus, at least two possible selection interfaces can be implemented - by directly entering the desired point coordinates and by interactively selecting them on the map. In the first case, two input fields for entering coordinates are embedded in the HTML page, with a subsequent JavaScript function attached to the data table request. To select a point from the map, the map itself and an algorithm are needed, with which the pixel coordinates of the cursor's location are transformed into geographic coordinates. By positioning the image on the webpage from the left and limiting the boundaries of the image itself to the boundaries of the hydrogeological model, the formulas for the coordinate transformation are used:

$$X_{coordinate} = HM_{x_min} + \frac{HM_{x_width}}{Image_{width}} \times Cursor_{x_position} \quad (6)$$

$$Y_{coordinate} = HM_{y_max} + \frac{HM_{y_height}}{Image_{height}} \times Cursor_{y_position} \quad (7)$$

Using formulas (6) and (7), the transition from the variable position of the cursor (X,Y) on the image is ensured, and it is recalculated to geographic coordinates. As you can see, the cursor coordinates in the formulas are the only variables in the formulas.

Given that a full-size map of Latvia cannot be viewed well on a computer screen due to detail limitations, the mouse cursor was supplemented with a magnification area, using the w3schools.com JavaScript sample "Image Magnifier Glass" as a basis. The selected coordinates from the mouse cursor are sent to the coordinate input fields using a JavaScript function, see Fig. 3.

A solution was applied, completely abandoning the display of available points and scaling the entire map. The user is unlikely to select a point on the map with coordinates corresponding to a node in the hydrogeological model.

Mathematical processing of the coordinate data is implemented to determine the nearest node point from the selected point or to notify about a point chosen by mistake outside the national territory.

https://doi.org/10.5593/sgem2024v/3.2/s11.13

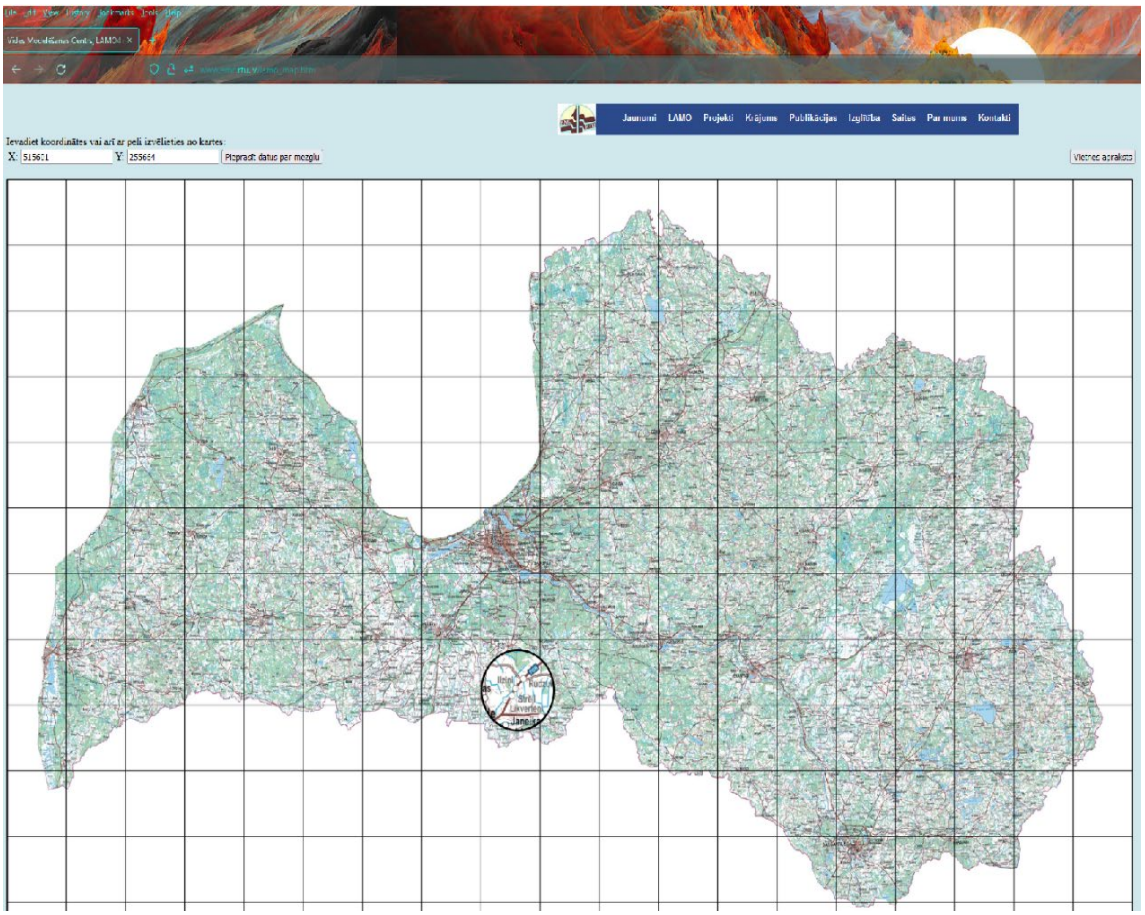



Fig. 3. WEB page interface

## RESULTS: TABLE REQUEST PROCESSING

To retrieve Fig. 2 the visible data, click on Fig. 3 existing maps or by entering the coordinates of the request in the coordinate input boxes of the homepage. It is necessary to realize the request to the DBMS, to receive the data of the selected table and to convert it into a representation of a separate formatted table. The solution used includes the application of AJAX technology. It is required to disable public disclosure of access data to the DBMS, until thereby protecting table data from unauthorized modification or deletion. The graphic of the algorithm can be seen in Fig. 4. The developed system is available online [8]. The HTML, JavaScript, PHP files that make up the system are downloadable, except server PHP, which includes database access, SQL query execution and returning the content of the row of the selected table in JSON data format, see Fig. 5.

## DISCUSSION

The solution described in the study for publishing HM data in the WEB environment has low maintenance costs and has been publicly available since 2022. The main drawback of the system is that it works without integration with WEB GIS, which would primarily ensure the scalability of the selected map and also the options for choosing HM regional maps. Developing the existing system would require a solution that would include a JavaScript page call after clicking on the WEB GIS map.

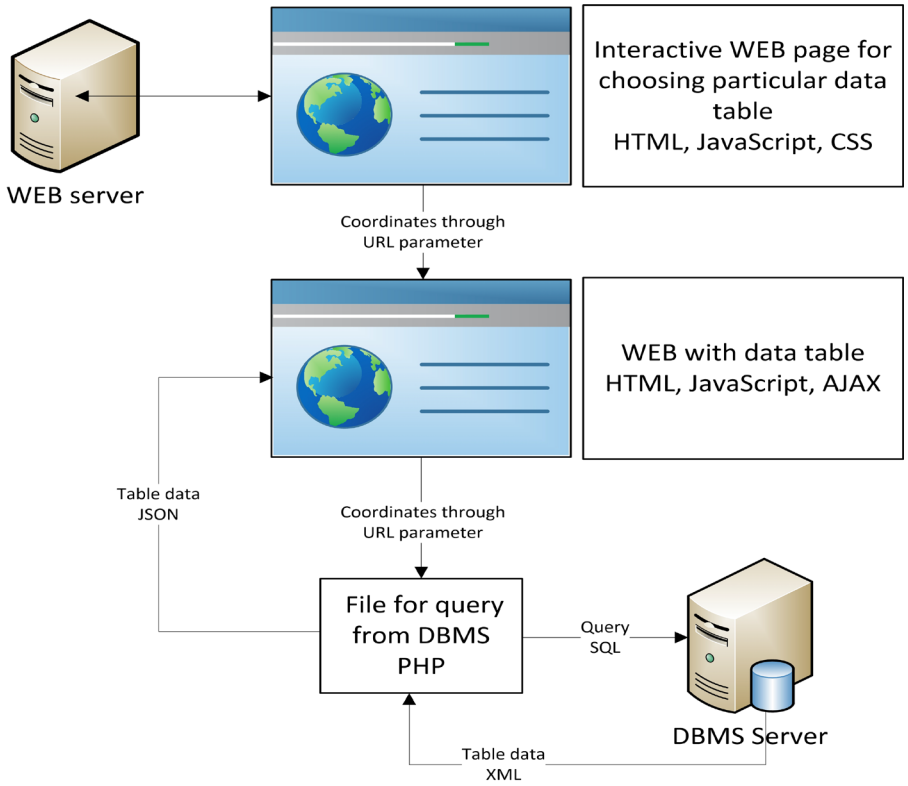



Fig. 4. Website architecture

```php
<?php
header('Content-Type: text/html; charset=utf-8');
$servername = "***********";
$username = "***********";
$password = "***********";
$dbname= **********;
try {
      $conn = new PDO(
        "mysql:host=$servername;dbname=$dbname",
        $username, $password,array(PDO::MYSQL_ATTR_INIT_COMMAND => "SET
NAMES utf8"));

      $conn->setAttribute(PDO::ATTR_ERRMODE,
                  PDO::ERRMODE_EXCEPTION);
} catch(PDOException $e) {
      echo "Connection failed: "
        . $e->getMessage();
}
$q = $_REQUEST["q"];
$x=strval(intdiv($q,1000000));
$y=strval($q-$x*1000000);
$stmt = $conn->prepare("SELECT * FROM Lamo where x=:x AND y=:y");
$stmt->execute(['x' => $x, 'y' => $y]);
$row = $stmt->fetch();
$data=array();
$data[]=$row;
echo json_encode($data, JSON_INVALID_UTF8_IGNORE);
?>
```

Fig. 5. Server PHP

https://doi.org/10.5593/sgem2024v/3.2/s11.13

## CONCLUSIONS

This article discusses the publication of data from a regional hydrogeological model of Latvia, providing data for each individual model node across the entire model. It is an attempt to make hydrogeological data more accessible to both industry specialists and the general public by offering a collection of data for a selected location on the map. The algorithms for obtaining and mathematically processing hydrogeological data are described, and the architecture of the developed interactive web page is shown. The proposed solution can be relevant for the interactive publication of data from any regional hydrogeological model.

Hydrogeological data of a regional nature are basically collected in the form of regional maps. Compilation of data in HM at a vertical section of each individual node provides the user with complete hydrogeological information relevant to a selected location, which is a useful supplement to regional-scale map representations.

## ACKNOWLEDGEMENTS

The study was implemented under project No. 1-08/166/2020 within the framework of "Improving the Latvian hydrogeological model LAMO4 and publishing its results" with funding from the Latvian Environmental Protection Fund.

## REFERENCES

[1] Spalviņs, A. The Geological Model of Latvia Developed by Riga Technical University (2010-2015). Scientific Journal of Riga Technical University, Boundary Field Problems and Computer Simulation, RTU Press, Riga, 2016, vol. 55, e-ISSN 2255-9132, pp. 5-11.

[2] The use of the Latvian hydrogeological model LAMO4 in solving environmental problems. In: Dynamics of Latvian ecosystems under the influence of climate. Riga: LU Academic Press, 2018. ISBN 978-9934-18-381-2, pp. 81-87.

[3] Groundwater Modeling Software, ESI Software, 2022, Online, Available: https://www.groundwatermodels.com/ESI_Software.php.

[4] Spalvins A., Krauklis K., Lace I., The new method for finding borders of groundwater recharge, transit and discharge areas, SGEM 2018, Bulgaria, Conference proceedings Hydrogeology and water resources, vol. 18, Issue 3.1, ISBN 978-619-7408-42-3, pp. 751-758.

[5] Levins I., Levina N., Gavena I., "Groundwater resources of Latvia", State Geological Service, Riga, 1998, 24 p.

[6] Pollock, David W., User Guide for MODPATH Version 6 - A Particle-Tracking Model for MODFLOW, Virginia: USGS, 2012.

[7] What is ArcGIS Server?, Online, Available: https://enterprise.arcgis.com/en/server/latest/get-started/windows/what-is-arcgis-for-server-.htm.

[8] Environment Modelling centre, LAMO4 node data, Online, Available: http://www.emc.rtu.lv/lamo_map.htm.

# STATISTICAL ANALYSIS OF HYDROCHEMICAL PARAMETERS OF THE RACHA-LECHKHUMI AND KVEMO SVANETI REGIONS NATURAL WATERS

**M. Tabatadze**
**L. Shavliashvili**
**G. Kuchava**
**E. Shubladze**
**E. Elizbarashvili**
Institute of Hydrometeorology of the Georgian Technical University, **Georgia**

## ABSTRACT

Water resource protection is significant for Georgia since the intensity of anthropogenic impact on the Georgian ecosystem has been substantially increased over the recent period, at the same time, several diseases with high risk for population life have been considerably increased, as well.

The work provides the physical-chemical and hydrochemical characteristics of rivers, artesian and spring waters available at the territories adjacent to the arsenic processing enterprises in the region for 2021-2024. pH, electric conductivity, biogenic substances, principal ions, mineralisation, total arsenic form, and microbiological parameters have been determined in the water samples taken.

Statistical characteristics were calculated, including the average value, absolute maximum and minimum, and standard deviation - for some indicators of hydrochemical analysis of natural waters. In some cases, an exceedance of some polluting ingredients of natural waters over maximum allowable concentrations has been observed. River waters have a low arsenic hazard index (HQsw<1) and are not at risk. In some artesian and drinking waters, the arsenic hazard index (HQdw>1) is at risk. The correlation coefficient between the concentrations of cations and anions in the rivers was calculated using the Pearson formula. Positive and negative correlations are established. Created linear regression equations for pairs of statistically significant correlation coefficients and calculated coefficients of determination for use in practical calculations.

**Keywords**: water resources, pollution, arsenic, statistical analysis, correlation coefficient.

## INTRODUCTION

Ecochemical and biological monitoring of natural waters is the only opportunity thanks to which it is possible to check the current ecological state of these environmental facilities. Pollution poses a deadly threat to the environment, and it results in the reduction (loss) of biodiversity. This term implies the diversity of life forms (plants, animals and microorganisms) available on the Earth. The heaviest blow falls on rivers and lakes. Protection of water resources is especially important for Georgia since the intensity of anthropogenic impact on the Georgian ecosystem has been substantially increased over the recent period, at the same time, the number of diseases with high risk for population life has been considerably increased, as well.

In this regard, it is worth mentioning the arsenic pollution in Georgia. For several decades, arsenic ore extraction and processing were carried out in the Racha-Lechkhumi and Kvemo Svaneti regions of Georgia, and arsenic-containing compounds were produced in the local Tsana and Uravi villages. To this day, in the villages of Uravi and Tsana, in the territory of the former factory, large batches of toxic waste (more than 130 thousand tons of waste containing 4-9% white arsenic) left over from the production of arsenic from the Soviet period are stored [1]. Currently, both deposits are conserved, and no arsenic is produced. Over the years, the basic mechanism of arsenic waste expansion has been associated with the washing-out and transfer of toxic waste by atmospheric precipitations and waters of overflowing rivers, which poses a high risk of ecological disaster in rivers, artesian waters and soils [2-8].

Arsenic is a natural component of the Earth's crust and is spread in any ecosystem. It is presented in nature in organic and inorganic forms, and the latter is very toxic [9]. Even though arsenic can get into the organism through skin and breathing passages, it mainly penetrates the body with food and drinking water. Organic types of arsenic are most frequently presented in marine products, while in land products, there are inorganic forms of 3-5-valent arsenic. Based on this, arsenic mainly hits a food chain from contaminated soil and water [2,5,8].

In addition, Lukhumi and Tskhenistskali rivers are the tributaries of the Rioni River, which is a main source of drinking water for Kutaisi and is used for irrigation as well. At the same time, this region is one of the most important tourism regions, which, to a considerable extent, determines the size of the catastrophe.

## MATERIALS AND METHODS

The work provides us with the physical-chemical and hydrochemical characteristics of rivers, artesian and spring waters available at the territory adjacent to the arsenic processing enterprises of the Racha-Lechkhumi and Kvemo Svaneti region in 2019-2024. To accomplish the tasks at hand, sampling points for taking river, artesian, and source waters from the background and polluted places of the region have been selected.

The following physical-chemical and hydrochemical parameters: namely, pH, electric conductivity, biogenic substances – $NH_4^+$, $NO_2^-$, $NO_3^-$, $PO_4^{3-}$, principal ions, mineralisation, total arsenic form [10], total coliforms, E-coli and faecal streptococci have been determined in the water samples taken [11].

The risk assessment stage foresees a comparison of the level of measured arsenic concentrations with environmental quality standards in specific mediums (surface waters, drinking water). This comparison envisages risk assessment according to the following formula (1):

$$HQ = MC / EQS_{SW,DW} \quad (1),$$

where, $HQ$ – hazard index;

$MC$ – measured concentration;

$EQS_{SW,DW}$ – environmental quality standards for surface and drinking waters [12].

In the case when HQ >1.0, arsenic is considered a potential risk for water medium and, as a consequence, for population health.

The following EQS limit values will be used:

- surface waters: 0.05 mg/l (maximum allowable concentrations according to Decree №425 on Approval of Technical Regulations for Georgian surface waters protection from pollution);
- drinking waters: 0.01 mg/l (maximum allowable concentrations according to Resolution №58 on Approval of Technical Regulations for Georgian surface waters protection from pollution).

Analyses have been conducted using modern methods and equipment, which meet the requirements and comply with European standards, in particular: 1. Spectrophotometric method - SPECORD 205; ISO 7150-1: 2010; 2. Ion-chromatographic method IC-1000; ISO 10304-1:2007; 3. Plasma-emission spectrometer – ICP-OES; Epa method 200.8; 4. Field portable apparatus - Hanna Combo pH/EC/TDS/PPM Tester HI98129; 5. IDEXX-apparatus - ISO 9308-3; 6. pH meter - Milwaukee-Mi 150.

Methods and approaches of mathematical statistics and probability theory have been used for measurement analysis. Primary processing of observation data envisaged calculation of their statistical performance, including mean value, absolute maximum and minimum, which characterise a range of parameter variation and standard deviation computing [13].

A correlation analysis method has been used, using which a linkage between two different parameters has been established.

The correlation coefficient between $x$ and $y$ parameters is calculated according to Pearson formula (2):

$$r = \frac{\sum_{i=1}^{n}(x_i-\bar{X})(y_i-\bar{Y})}{(n-1)s_x s_y} \quad (2),$$

where $x_{ave}$ and $y_{ave}$ are average values of these parameters, respectively, $S_x$ and $S_y$ – their mean square deviations (standard deviations), $n-$ observation series length, i.e. number of observations. Standard deviations are calculated by formulas (3) and (4):

$$S_x = [\Sigma(x_i - x_{ave})^2 / n]^{1/2} \quad (3), \qquad S_y = [\Sigma(y_i - y_{ave})^2 / n]^{1/2} \quad (4),$$

For the determination of correlation coefficient reliability, the following value is calculated by formula (5):

$$H = r(n-1)^{1/2} \quad (5),$$

where $r-$ correlation coefficient,

$n-$observation series length.

The calculated $\boldsymbol{H}$ value is compared with its critical value taken from a special table. Should it appear that the calculated $\boldsymbol{H}$ value exceeds its critical value (taken from a table), it is considered that the correlation coefficient is considerable at $the\ \boldsymbol{P}$ probability level, and the linkage between the considered values is reliable.

Links between parameters are described by regression equation, while a variable dependence on the predictor is evaluated using a determination coefficient, which is a squared correlation coefficient [13].

## RESULTS AND DISCUSSION

Some of the above-mentioned components determined in the river, artesian, and spring water samples selected in the Racha-Lechkhumi and Kvemo Svaneti region have been selected, and their statistical processing has been conducted.

Important components are biogenic elements, which reflect surface water pollution degree and are the indicators of anthropogenic load. The control of water content of their separated forms ($NH_4^+$, $NO_2^-$, $NO_3^-$, $PO_4^{3-}$), which characterise the intensification of such processes as faecal contamination caused by the discharge of communal and agricultural wastewaters, is of special importance.

Maximum content of ammonia ions – 0.491 mg/l, which equals to 1.3 Maximum permissible concentration (MPC), was registered only once in the Tskhenistkali River below Lentekhi, and its average content is less than MPC. Values of nitrites and nitrates in none of the cases exceed MPC.

As for principal anions, regional rivers feature a high content of hydro-carbonates, an average value of sulfates and a low content of chlorides. As is seen from the obtained results, the rivers to be studied are of hydro-carbonate type. Regarding cations, potassium and sodium sum, calcium and magnesium concentrations are within the norm.

The total dissolved salts (mineralisation) of rivers varies within a range of 150.24–303.28 mg/l. According to mineralisation, surface waters belong to the category of low and average mineralisation waters [14].

As is seen from the obtained results, arsenic content in rivers is low (0,0033–0,0078 mg/l), and its maximum values are considerably less than MPC. As far as all measured concentrations of total arsenic form in the surface waters were less than the MPC value, the hazard quotient ($HQ_{sw} < 1$) is also low, so the waters are not at risk.

Among artesian and drinking waters, sour water is distinguished according to high hardness since its average hardness is at the upper limit of MPC, while at other environmental facilities, it is within the norm.

As for mineral forms of nitrogen, only in one case there has been registered ammonia ions concentration higher than MPC – 0.44 mg/l (1,1 MPC). Sour waters are distinguished by the exceedance of nitrites, and their content equals 5.8 mg/l (29.0 MPC) on average, i.e. far exceeds MPC, while nitrate content is within the norm.

Among anions, relatively high concentrations of hydro-carbonates (882.67 mg/l) and chlorides (194.53 mg/l) are observed in water. Regarding cations, the sum of potassium and sodium (195.07 is maximal in the same water, while calcium and magnesium contents are within the norm. Total dissolved salts (water mineralisation) vary within a range of 90-1500 mg/l and are the largest in sour water, belonging to the category of highly mineralised waters, while other waters are of low mineralisation [14,15].

Arsenic content in artesian and drinking waters exceeds MPC in a mountain spring water flowing in Tsana direction (1.26 MPC), in the same water coming from mountains to Tsana (in the middle) (1.16 MPC) and in this spring water coming from mountain to Tsana (in the end) (1.71 MPC). In other cases, arsenic concentration is within the norm.

Proceeding from this fact, the concentration of total arsenic form in artesian and drinking waters varies from 0.0047 to 0.0171 mg/l, which is why the hazard quotient ($HQ_{dw}$>1) exceeds allowable levels and poses a risk.

Microbiological analyses have been conducted in drinkable water only. As is seen from the results of carried-out analyses, spring water at the Uravi 2 territory and in the Tsana direction contains E-coli, total Coliforms and faecal streptococci that is not permitted by the Georgian legislation, while pollution of sour waters according to microbiological indicators has not been registered.

Table. 1 represents correlation relationships between concentrations of cations ($Na^+$+$K^+$, $Ca^{2+}$, $Mg^{2+}$) and anions ($HCO_3^-$, $Cl^-$, $SO_4^{2-}$) for upper points of Tskhenistskali (Tsana) and Lukhuni (Uravi) rivers, according to 2019-2024 observation data.

Table 1. Correlation matrix between cation and anion concentrations of rivers under investigation

| | **River** | **$SO_4^{2-}$** | **$HCO_3^-$** | **$Cl^-$** |
|---|---|---|---|---|
| $Ca^{2+}$ | Tskhenistskali<br>Lukhuni | 0.13<br>0.84 | 0.99<br>0.53 | 0.07<br>-0.55 |
| $Mg^{2+}$ | Tskhenistskali<br>Lukhuni | 0.19<br>0.03 | 0.87<br>0.82 | 0.11<br>0.40 |
| $Na^+$+$K^+$ | Tskhenistskali<br>Lukhuni | 0.88<br>0.89 | 0.25<br>-0.72 | 0.12<br>0.25 |

(Significant correlation coefficients are marked in bold in the Table).

As seen from Table 1, the correlation relationship between ion concentrations (according to the Pearson scale) is very weak (< 0.3) in 8 cases, average (0.30–0.70) in 2 cases and strong (0.70–0.90) in 6 cases. Among the latter cases, it approaches a functional relationship (approx. 1,0) in one case only. Assessment of statistical significance showed that 6 strong correlation coefficients are statistically significant, among them, a correlation coefficient of one pair ($Ca^{2+}$ – $HCO_3^-$) is significant at the level of 0.99 significance, while five others are significant at the level of 0.95 significance. In cases of such linkages, it is reasonable to write down the equation of linear regression between respective substance concentrations to use it in practical calculations. Such equations for pairs of statistically significant coefficients are given in Table 2.

Table 2. Linear regression equations for pairs of statistically significant correlation coefficients

| **X mg/l** | **Y mg/l** | **River** | **Regression equation** | **Determination coefficient R2** |
|---|---|---|---|---|
| $Ca^{2+}$ | $SO_4^{2-}$ | Lukhuni | Y=-1.084x+47.36 | 0.71 |
| $Ca^{2+}$ | $HCO_3^-$ | Tskhenistskali | Y=2.869x+45.87 | 0.98 |
| $Mg^{2+}$ | $HCO_3^-$ | Tskhenistskali | Y=-20.41x+334.4 | 0.78 |
| $Mg^{2+}$ | $HCO_3^-$ | Lukhuni | Y=4.6x+77.86 | 0.69 |
| $Na^+$+$K^+$ | $SO_4^{2-}$ | Tskhenistskali | Y=1.096x+7.275 | 0.76 |
| $Na^+$+$K^+$ | $SO_4^{2-}$ | Lukhuni | Y=1.388x+4.586 | 0.78 |

The determination coefficient shows what contribution is made by one of the system's components in the formation of the second one. In particular, according to the determination coefficient, the role of the $x$ component, in the formation of the $y$ component, equals 69-98% for different pairs. The remaining 2-31% of the contribution in the formation of the $y$ component is made by other factors. Overall, the obtained equations have practical importance and may be used in practical calculations for solution of respective problems.

As it was mentioned above, the rivers of this region are of hydro-carbonate type, i.e., the number of $HCO_3^-$ ions in river waters is high and is associated with a high percentage of calcium ions, while with a relatively lower percentage – of magnesium ions. Sodium and potassium ions are in high correlation with sulfate ions, which is confirmed by high indicators of determination coefficients.

Thus, a positive correlation has been revealed between $Ca^{2+}$ and $HCO_3^-$ and $SO_4^{2-}$ between $Mg^{2+}$ and $HCO_3^-$; between $Na^+$+$K^+$ and $SO_4^{2-}$; while a negative correlation – between $Ca^{2+}$ and $CL^-$; and between $Na^+$+$K^+$ and $HCO_3^-$.

In general, cations and anions are present in water as ions, though salts are formed as well, which depends on water pH. In the acid area (when pH < 7), hydro-carbonate and chloride salts are not deposited, while in the alkaline area (pH > 7), like in our rivers under investigation, takes place deposition of formed salts – carbonates and sulfates: $CaCO_3$, $MgCO_3$, $CaSO_4$ etc.

## CONCLUSIONS

Based on the conducted research, the following conclusions have been made:

- Methods and approaches of mathematical statistics and probability theory have been used for the analysis of surface, underground and drinking waters. Initial processing of observation data, in particular, calculation of statistical characteristics, such as mean value, absolute maximum and minimum, describing parameter variation range and standard deviation computation, has been made. Regarding natural water-polluting ingredients, in some cases, there is an observed exceedance of some components over the respective MPC;
- River waters have an arsenic hazard index (HQsw<1) and are not at risk;
- In some artesian and drinking waters, the arsenic hazard index (HQdw>1) is at risk;
- The correlation coefficient between the concentrations of cations and anions in the rivers was calculated using the Pearson formula. Positive and negative correlations are established. As it was mentioned above, the rivers of this region are of hydro-carbonate type, i.e., the number of hydrocarbonate ions in river waters is high and is associated with a high percentage of calcium ions while with a relatively lower percentage – of magnesium ions. Sodium and potassium ions are in high correlation with sulfate ions, which is confirmed by high indicators of determination coefficients. A positive correlation has been revealed between $Ca^{2+}$ and $HCO_3^-$ and $SO_4^{2-}$ between $Mg^{2+}$ and $HCO_3^-$; between $Na^+$+$K^+$ and $SO_4^{2-}$; while a negative correlation – between $Ca^{2+}$ and $CL^-$; and between $Na^+$+$K^+$ and $HCO_3^-$.
- Equations of linear regression have been composed for pairs of statistically significant correlation coefficients, and determination coefficients have been calculated for their use in practical calculations.

**ACKNOWLEDGEMENTS**

This study is supported by the Shota Rustaveli National Science Foundation of Georgia with grant No FR-21-427

**REFERENCES**

[1] Aleksidze G., Loliasvilivi R., 2016 - The main aspects of environmental pollution in Georgia - materials of the international scientific conference "Modern technologies for the production of ecologically clean products for the sustainable development of agriculture", Tbilisi, pp 33-45.

[2] Avkopashvili G., Avkopashvili M., Gongadze A., Gakhokidze R., 2017 - Eco-Monitoring of Georgia's Contaminated Soil and Water with Heavy Metals - Carpathian Journal of Earth and Environmental Sciences - vol. 12, No. 2, pp 595-604.

[3] Avkopashvili M., Gongadze A., Matchavariani L., Avkopashvili G., Avkopashvili I., 2019 - Soil, Water and Air Pollution by Manganese Industry in the Imereti Region, Georgia - 19th International Multidisciplinary Scientific Geo Conference SGEM 2019, p. 417-424.

[4] Bakradze Elina, Yuri Vodyanitski, TengizUrushadze, Zaur Chankseliani, Marine Arabidze, 2018. About rationing of the heavy metals in soils of Georgia - Annals of Agrarian Science https://www.sciencedirect.com/science/article/pii/S151218871830016

[5] Fitz, W. J. and W.W. Wenzel., 2002. - Arsenic transformation in the soil rhizosphere-plant system, fundamental and potential application of phytoremediation - *Biotechnology,* 99: 259-78.

[6] Iram S., Ahmad, I. and Akhtar, S. 2012. Distribution of Heavy Metals in Peri-Urban Agricultural Areas Soils. The Journal of the Chemical Society of Pakistan. 34(4) 861-869.

[7] Iram S., Zaman, A., Iqbal, Z. and Shabbir. R. 2013. Heavy metal tolerance of fungus isolated from the soil contaminated with sewage and industrial wastewater. Polish Journal of Environmental Studies.22 (3):691-697.

[8] Li-Xian Yao, Guo-Liang Li, Zhi Dang, Zhao-Huan He, Chang-Min Zhou, Bao-Mei Yang, 2009 - Arsenic uptake by two vegetables grown in two soils amended with As-bearing animal manures - J Hazard Mater, 2009 May 30;164(2-3):904-10. DOI: 10.1016.

[9] Arsenic and Arsenic compounds IARC Monographs – 100 C, (IARC, 1980, 1987, 2004). http://monographs.iarc.fr/ENG/Monographs/vol100C/mono100C-6.pdf

[10] Fomin G.S., Fomin A.G. – Water. Quality control and environmental safety according to international standards. Directory. Moscow, 2001.

[11] Guide to methods of hydrobiological analysis of surface waters and bottom sediments. – Gidrometeoizdat, Leningrad, 240 articles, 1983. Guidance for methods of hydrobiological analysis of surface waters and bottom sediments, 1983.

[12] Risk Analysis Methodology of the arsenic impact on the water resources and its application in pilot basin water - Water Researcher Institute of Slovak Republic, 2019.

[13] Rumshisky Z. - Mathematical processing of experimental results. - Science, M, 1971, 192 p.

[14] Supatashvili G. - Environmental Chemistry (Ecochemistry) - Tbilisi, University Publishing House, 187, 2009.

[15] Supatashvili G. - Environmental Chemistry (Ecochemistry) - Tbilisi, University Publishing House, 187, 2009.Supatashvili G. – hydrochemistry of Georgia - Tbilisi University Publishing House, Tbilisi, 399 pp.2003.

# THE INFLUENCE OF AGRICULTURAL ACTIVITIES ON THE QUALITY OF UNDERGROUND WATER IN THE CENTRAL AREA OF THE BANAT PLAIN UNDER THE CONDITIONS OF ADAPTATION TO CLIMATE CHANGE

**Prof. Dr. Laura Smuleac**
**Prof. Dr. Florin Imbrea**
**Assoc. Prof. Dr. Adrian Smuleac**
**Lecturer Dr. Raul Pascalau**
**Lecturer Dr. Radu Bertici**
University of Life Sciences "King Mihai I" from Timișoara, **Romania**

## ABSTRACT

In the context of global climate change, groundwater is not only a vital source for human survival, but also a strategic resource for the sustainable development of local and global economies. The protection and effective management of these resources must be top priorities for everyone involved in environmental planning and management. The purpose of this work is to monitor the quality of groundwater from two water drillings located in the south of Timisoara and four water drillings in the west of the locality. The samples were taken in the year 2023 and were subjected to several analyzes (pH, nitrites, nitrates, phosphates, chlorides, sulfates, bicarbonates, calcium, magnesium, total hardness, sodium, potassium, dissolved iron and dissolved manganese, temperature) in order to obtain a detailed assessment of the water quality. The influence of agricultural activities was noted by a higher concentration of nitrates in the south of Timisoara, and in the western area the concentrations of nitrites are higher, which may indicate a more pronounced biological or industrial pollution. The proposed solutions focus on an integrated and sustainable approach to agriculture and the economy in general, to ensure that these water resources will remain available and clean for future generations.

**Keywords:** groundwater, climate change, water pollution, agricultural activities, nutrients

## INTRODUCTION

A clean and healthy environment is a fundamental pillar for human well-being and health, requiring efficient and sustainable management of water and air resources. [1], [2]. The essentials of human existence – water, air, food, heat, and light – play crucial roles in ensuring a healthy life on Earth [3]. In this equation, groundwater, as the largest freshwater reserve in the world (with more than 97% of all freshwater resources, excluding glaciers and ice caps), holds great importance [4].

Groundwater is not only essential for human consumption needs, but also for industrial and agricultural activities, providing stability in water quality and natural protection against pollution [5,6,7]. However, they are vulnerable to various sources of pollution, such as intensive agriculture and industries, and the consequences of pollution can persist in the long term, affecting the environment and aquatic ecosystems [8-10].

https://doi.org/10.5593/sgem2024v/3.2/s11.16

To ensure sustainable and efficient management of these resources, it is crucial to pay particular attention to pollution prevention and constant monitoring of groundwater quality [11]. A deep understanding of the impact of human activities on these resources is essential for maintaining the natural balance and protecting life as a whole [12, 13].

Experience over the past few decades has shown that remediating contamination is often difficult and costly, and the effects of pollution can persist over long periods of time, affecting not only the present but also future generations [14]. It is therefore crucial to step up efforts to prevent pollution in order to avoid negative impacts on groundwater resources and associated ecosystems [15-16]. The protection and effective management of these resources must be top priorities for everyone involved in environmental planning and management. Only through an integrated and sustainable approach can we ensure that these resources will remain available and clean for future generations.

## MATERIALS AND METHODS

In this study, the quality of groundwater in the localities of Parța and Sânmihaiul Român, located near the municipality of Timișoara, was investigated. These localities are located in Timiș County, in the Banat region of Romania. The water sources used for human consumption come from local boreholes. The research carried out played a crucial role in assessing the purity of water, given its importance for local communities and beyond.

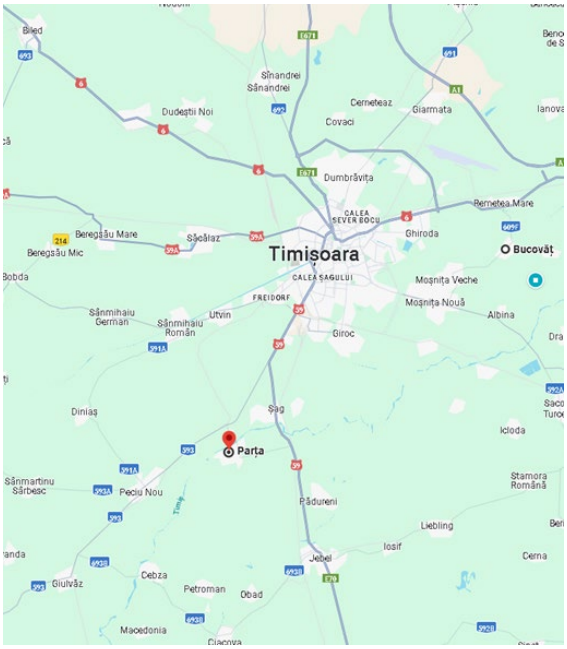



Fig. 1. Location of Parța




Fig. 2. Location of Sânmihaiul Roman

In general, the soils of Parța are classified as brown soils, with a texture ranging from medium to light. These soils are mainly made up of a mixture of clay, sand and humus. They are well-drained and have the ability to retain water to a moderate extent, making them suitable for various agricultural crops such as wheat, corn, sunflower, rapeseed, and vegetables. The hydrographic network in Parța, Timiș County, is integrated into the wider system of the Western Plain of Romania, characterized by the presence of a significant number of rivers and streams. The most important watercourse in the area is the Timiș River, which crosses the region from north to south and plays a central role in draining the land and providing water resources for the local community and agriculture.

**Sânmihaiu Român** (figure 2) is the capital of the commune of the same name, which also includes the villages of Sânmihaiu German and Utvin. The boundaries of the commune are defined by the administrative borders of Timiș County and border with other communes and localities. The Bega River, which passes near the locality, is an important reference point for geographical delimitation. The relief of Sânmihaiu Român is predominantly plain, characteristic of the Timiș Plain, part of the Banat Plain, located in western Romania. This area is known for its flat and slightly undulating terrain, which facilitates both intensive agriculture and the development of rural infrastructure. The soils of Sânmihaiu Român are predominantly chernozem, a category of soils characterized by their high fertility and rich humus content.

Sânmihaiul Român is located in a lowland region in western Romania, characterized by a less complex hydrographic network compared to mountainous areas or with a higher density of rivers and lakes. The main element of the hydrographic network near the locality is the Bega River, one of the most important watercourses in Banat.

There are two such boreholes in the Parța area, from which samples are periodically extracted to see if the quality of the groundwater has undergone any changes. There are 4 boreholes in the Sânmihaiu Român locality, from where ABA Banat monitors the quality of groundwater, taking samples every few months.

The samples were taken in June 2023 and were subjected to several analyzes (pH, conductivity, and concentrations of $NH_4$, $NO_2$, $NO_3$, $PO_4$, chlorides, sulfates, bicarbonates, calcium, magnesium, total hardness, sodium, potassium, dissolved iron ($Fe^{2+}$ and $Fe^{3+}$) and dissolved manganese ($Mn^{2+}$ and $Mn^{7+}$), temperature) in order to obtain a detailed assessment of water quality.

The results were interpreted and compared with the main parameters of the physico-chemical quality indicators, in accordance with Law no. 311 of 28/06/2004, which amends and completes Law 458 of 2002, regarding the quality of drinking water and is completed by Emergency Ordinance no. 22/2017.

## RESULTS

The comparative analysis of the water samples collected from the boreholes in **Parța** reveals significant variations in water quality. The water temperature rose slightly from 12.5°C to 13°C, while the air temperature rose from 20°C to 26°C, indicating seasonal climate changes. The pH value decreased from 8.1 to 7.8, going from a slightly alkaline to an almost neutral environment, which could reflect the influence of environmental factors or contaminants. The conductivity of the water decreased from 1012 µS/cm to 868

https://doi.org/10.5593/sgem2024v/3.2/s11.16

μS/cm, suggesting a decrease in the concentration of dissolved ions, possibly due to a natural dilution or change in the source of contamination.

The ammonia concentration increased significantly from 0.085 mg/l to 0.262 mg/l, indicating recent contamination of biological or industrial origin. The level of nitrites decreased from 0.143 mg/l to 0.06 mg/l, signalling a possible improvement in nitrification processes or a reduction in nitrogen pollution sources. Similarly, a major reduction in nitrate concentration, from 8 mg/l to 0.1 mg/l, suggests a decrease in agricultural pollution or a change in the water source influenced. On the other hand, the increase in phosphate concentration from 0.123 mg/l to 2.15 mg/l is worrying, indicating possible recent contamination with detergents or other sources of phosphorus.

Chloride and sulphate concentrations have decreased slightly, which may indicate a reduction in industrial or agricultural pollution. The decrease in bicarbonate from 604 mg/l to 531 mg/l shows a change in the alkalinity of the water, which can influence the pH balance. As for metal compounds, the calcium concentration has increased significantly from 67.35 mg/l to 92.18 mg/l, which can affect the hardness of the water and indicate a natural source or contamination with calcareous materials. Magnesium decreased from 79.7 mg/l to 53.46 mg/l, reflecting a change in the mineral balance of water. Sodium and potassium concentrations showed changes, with sodium decreasing from 47.8 mg/l to 36.9 mg/l and potassium being measurable at 1.3 mg/l in F2, which could be associated with water sources or local contamination.

In the water samples from both boreholes, the dissolved iron was below the limit of quantification, which is a positive aspect. However, manganese increased from 0.221 mg/l to 0.596 mg/l. The changes observed in the chemical composition of the water in the Parța F1 and Parța F2 boreholes underline the importance of continuous monitoring and careful management of potential sources of contamination to ensure optimal water quality.

During June 2023, water samples taken from the **Sânmihaiu Român** F1, F2, F3 and F4 boreholes were analyzed to assess the water quality in different locations. Water temperatures ranged slightly between 12.5°C and 13.5°C, and air temperatures ranged from 20.5°C to 26.5°C, reflecting normal seasonal and geographical variations.

The pH value fluctuated between 7.0 and 7.8, with the lowest values in F4 and the highest in F1. The conductivity of water showed significant differences, with values ranging from 1341 μS/cm in F1 to 541 μS/cm in F4, suggesting variations in water mineralization.

In terms of organic compounds, we observed remarkable variations in the concentrations of ammonia, nitrites and nitrates between drillings. F3 had the highest concentration of ammonia (2.1 mg/l), while F4 had the lowest levels of nitrates (1.66 mg/l), signalling a water quality influenced by anthropogenic activities and local conditions.

Dissolved minerals and ions also showed significant differences. For example, F1 had the highest concentrations of chlorides and sodium, indicating a stronger saline influence or specific geology, while F4 showed the lowest values, suggestive of less mineralized water.

In conclusion, the comparative analysis showed that each borehole in Sânmihaiu Român has distinct characteristics in terms of water quality. Continuous monitoring is crucial to understand and manage the potential impact of human activities and natural changes on local water resources.

Following the comparative analysis of the water quality from the boreholes located in Parța and Sânmihaiul Român localities, important differences and similarities were observed, reflecting the local geological and anthropogenic variables.

The pH of the water in Parța has values between 7.0 and 8.1, indicating a slight alkalinity, while in Sânmihaiu Român it varies between 7.0 and 7.8, suggestive of a lower acidity. These differences can influence nutrient availability and the overall health of the aquatic ecosystem in each area (Figure 3).

The conductivity of water (Figure 4), which indicates the level of dissolved substances, is higher in Parța, fluctuating between 541 µS/cm and 1341 µS/cm, compared to the narrower range of 541 µS/cm to 770 µS/cm in Sânmihaiu Român. This difference may reflect variations in soil mineralization and the influences of human activities such as agriculture or industry.

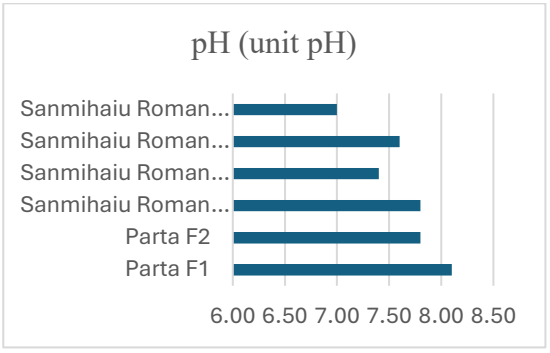



Fig. 3 Evolution of pH

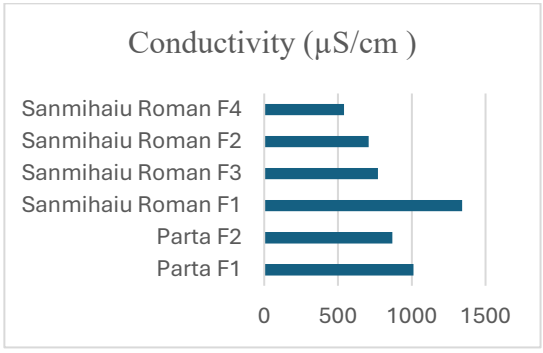



Fig. 4 Water conductivity

Ammonia (Figure 5) had notably higher concentrations in Sânmihaiul Român, reaching 21 mg/l in one borehole, compared to about 0.262 mg/l in Parța. Nitrites and nitrates also showed variations, with nitrites reaching 0.42 mg/l in Sânmihaiul Român and 0.14 mg/l in Parța. The nitrate concentration was higher in Parța (8 mg/l), while in Sânmihaiul Român it varied between 0.62 mg/l and 2.33 mg/l.

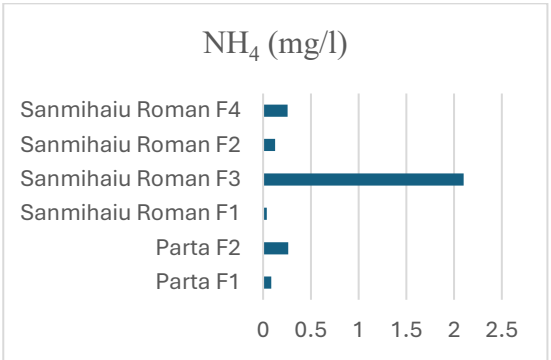



Fig. 5 Evolution of ammonia

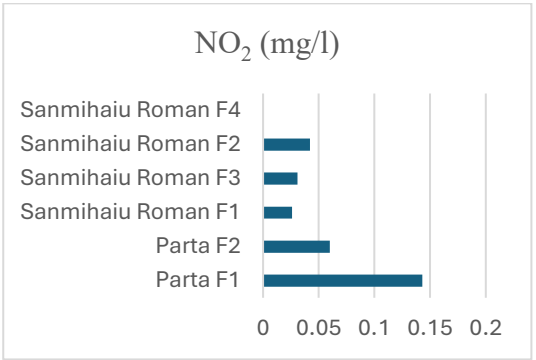



Fig. 6 Content of $NO_2$

https://doi.org/10.5593/sgem2024v/3.2/s11.16

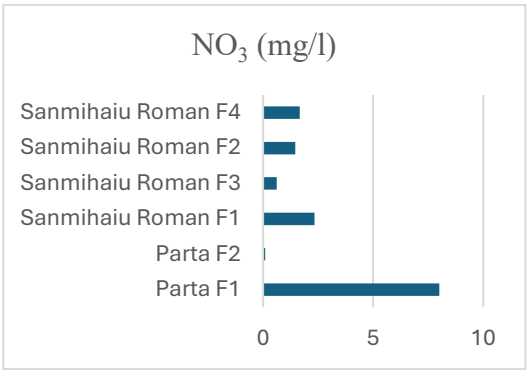



Fig. 7 Content of $NO_3$

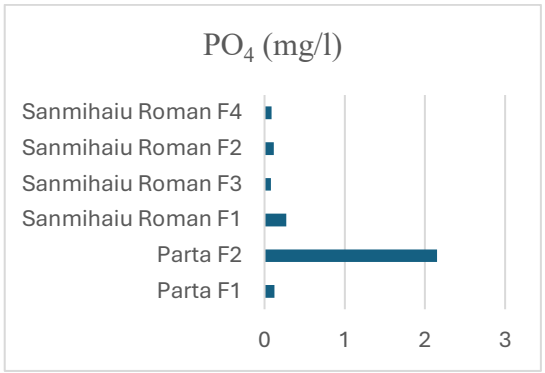



Fig. 8 Content of $PO_4$

The concentrations of chlorides, sulphates and bicarbonates varied significantly between the two localities. In Parța, chlorides had values between 7.09 mg/l and 9.22 mg/l, while in Sânmihaiul Român they ranged between 9.22 mg/l and 87.9 mg/l. Sulfates were higher in Sânmihaiul Român, reaching 181 mg/l, compared to 64.4 mg/l in Parța. Bicarbonates were higher in Parța, with values of up to 604 mg/l, compared to 561.2 mg/l in Sânmihaiul Român.

Dissolved iron concentrations (Figure 9) were below the limit of quantification in both localities, which is a positive aspect. However, manganese (Figure 10) showed higher values in the Sânmihaiul Român, reaching 2.11 mg/l in a borehole, compared to 0.59 mg/l in Parța.

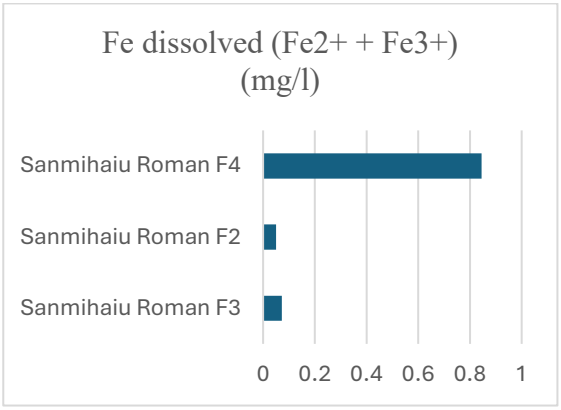



Fig. 9 Dissolved Fe content

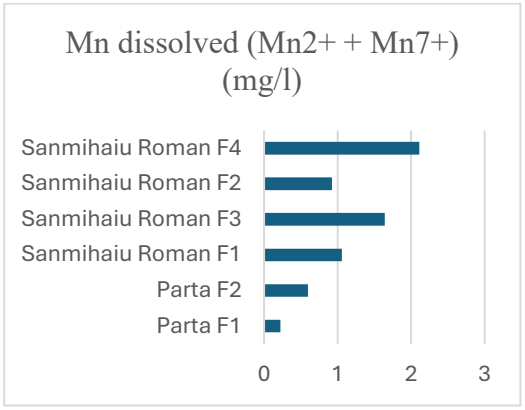



Fig. 10 Manganese content in water

## DISCUSSION

The comparative analysis of water quality in Parța and Sânmihaiu Român highlights the complexity and variability of the aquatic environment in each area. Further monitoring and assessment is crucial to understand the impact of climate change and human activities on water resources and to support their sustainable management in the future.

## CONCLUSION

The purpose of the research was to analyse the water quality from the boreholes located on the territory of two localities in Timiș County, Parța and Sânmihaiul Român.

Following the analyses carried out, the following conclusions resulted:

- The amount of ammonia is much lower in Parta, which indicates low biological or industrial pollution.
- In Parta, the higher concentration of nitrates (8 mg/l) suggests a more pronounced agricultural influence, which is common in fertiliser-intensive areas. However, the level of nitrites is low, indicating that the water is not subject to major biological pollution.
- In the Sânmihaiul Român, nitrite concentrations are higher (0.42 mg/l), which may indicate a more pronounced biological or industrial pollution. However, the nitrate level is lower (0.62 mg/l - 2.33 mg/l), which indicates less agricultural pollution.
- Sulphate levels are lower in Parta, which contributes to higher quality water. Sulphates in high concentrations can affect the taste of water and have laxative effects.

Overall, although both localities have water of relatively good quality, the water in Parța is more suitable for consumption due to lower concentrations of ammonia and manganese, as well as lower levels of sulphates.

## AKNOWLEDGEMENT

This paper is published from the own research funds of the University of Life Sciences "King Mihai I" from Timisoara, Romania. Support was also received by the project Horizon Europe (HORIZON) 101071300 - Sustainable Horizons -European Universities designing the horizons of sustainability (SHEs).

## REFERENCES

[1] Cherchi, C., Badruzzaman, M., Oppenheimer, J., Bros, C. M., & Jacangelo, J. G., Energy and water quality management systems for water utility's operations: A review. Journal of environmental management, 153, 108-120, 2015

[2] Helmer, R., & Hespanhol, I., Water pollution control: a guide to the use of water quality management principles. CRC Press, 1997.

[3] Huang G.H, J. Xia, Barriers to sustainable water-quality management, Journal of Environmental Management, Volume 61, Issue 1, Pages 1-23, ISSN 0301-4797, 2001, https://doi.org/10.1006/jema.2000.0394.

[4] Smuleac Laura, Pașcalău Raul, Smuleac Adrian, Imbrea Florin, Lato Alina, The interconnection between preventing water pollution and addressing climate change, International Multidisciplinary Scientific GeoConference : SGEM; Sofia, Vol. 23, Iss. 3.2, (2023). DOI:10.5593/sgem2023V/3.2/sl2.27

[5] Vidon, P., Allan, C., Burns, D., Duval, T. P., Gurwick, N., Inamdar, S., & Sebestyen, S, Hot spots and hot moments in riparian zones: potential for improved water quality management 1. JAWRA Journal of the American Water Resources Association, 46(2), 278-298, 2010

[6] Parmar, K. S., & Bhardwaj, R., Water quality management using statistical analysis and time-series prediction model. Applied Water Science, 4(4), 425-434, 2014

[7] Dasgupta N., Ranjan S., & Ramalingam C., Applications of nanotechnology in agriculture and water quality management. Environmental Chemistry Letters, 15, 591-605, 2017

[8] Pascalău Raul, Smuleac Laura, Stanciu Sorin, Imbrea, Florin, Smuleac Adrian, Leveraging modern languages and translations for sustainable environmental practices, International Multidisciplinary Scientific GeoConference: SGEM; Sofia, Vol. 23, Iss. 4.2, (2023). DOI:10.5593/sgem2023V/4.2/sl9.36

[9] Ongley, E. D., Water quality management: design, financing and sustainability considerations-II. In Invited presentation at the World Bank's Water Week Conference: Towards a strategy for managing water quality management, 2000

[10] Garcia M. R., Protecting Ecosystems: A Key to Combating Climate Change and Water Pollution. Nature Conservation Society, pp 45-67, 2017

[11] Turner J. M., Water Pollution Control Technologies for a Changing Climate. Environmental Engineering Books, pp 56-72, 2020

[12] Șmuleac A, Șmuleac L, Pașcalau R., Popescu G., Horablaga, A., Using ground control points (GCP) and UAV Poind Cloud processinf in water management, International Multidisciplinary Scientific GeoConference Surveying Geology and Mining Ecology Management, SGEM, 2022, 22(3.2), pp. 231–238.

[13] Adams J. M., International Collaboration on Water Pollution and Climate Change: Achievements and Challenges. International Policy Press, pp 23-34, 2020.

[14] Șmuleac A, Șmuleac L, Man TE, Popescu CA, Imbrea F, Radulov I, Adamov T, Pașcalău R. Use of Modern Technologies for the Conservation of Historical Heritage in Water Management. Water. 2020; 12(10):2895. https://doi.org/10.3390/w12102895

[15] Adamov T, Iancu T, Peț E, Popescu G, Șmuleac L, Feher A, Ciolac R. Rural Tourism in Marginimea Sibiului Area—A Possibility of Capitalizing on Local Resources. Sustainability. 2023; 15(1):241. https://doi.org/10.3390/su1501024

[16] Jurcoane, M. R., Șmuleac, L., & Tulbure, C., Impact of climate changes on the flow regime in the Mureș Hydrographic Basin, Săvîrşin Sector. Research Journal of Agricultural Science, 55(4), 2023

# THE REMOVAL OF PHOSPHORUS FROM CONSTRUCTED WETLANDS

**Ing. Tereza Tůmová**
University of Technology Brno**, Czech Republic**

## ABSTRACT

This article discusses phosphorus precipitation in constructed wetlands, which are effective at removing pollutants from wastewater, except for phosphorus. The PAX-18 coagulant was used to enhance phosphorus removal.

Precipitation equipment was installed in three wetlands, each with different technological arrangements. In two of the wetlands, a gradual dosing of coagulant was implemented, while in the third, a single dose of 200 litres was applied. Dosing was based on the average phosphorus influx, with samples taken at various intervals and analysed in the laboratory using cuvette tests.

In the first constructed wetland, the average concentration of total phosphorus in the precipitation section was 1.8 mg × $L^{-1}$ lower than in the section without precipitation, representing a 28% increase in efficiency. In the second wetland, the total phosphorus concentration was 1.0 mg × $L^{-1}$ lower than during periods without precipitation. In the third constructed wetland, the concentration of total phosphorus decreased by 0.2 mg × $L^{-1}$ due to phosphorus precipitation, while the average concentration of total phosphorus discharged from the wetland was 0.05 mg × $L^{-1}$, resulting in an overall efficiency of up to 98%.

As phosphorus is a biogenic element, its concentration in the aquatic environment, exacerbated by climate change, causes major problems, such as eutrophication. Therefore, it is crucial to begin effectively removing phosphorus from wastewater.

**Keywords:** constructed wetland, phosphorous removal, concentration of total phosphorus

## INTRODUCTION

Phosphorus is a biogenic element that naturally occurs within the Earth's lithosphere. In water, it commonly appears as part of dissolved or suspended compounds and enters aquatic environments from natural or anthropogenic sources [1]. Natural sources include the weathering of rocks and minerals, which introduces phosphorus through soil erosion or the decomposition of organic matter. Another source is the atmosphere, where phosphorus can be transported as dust and settle in water through precipitation [2].

Anthropogenic sources primarily originate from agriculture, where phosphorus, an essential nutrient for plant growth, is added to soil via fertilisers. Domestic and industrial wastewater is another major source, introducing phosphorus through detergents, human waste, and food residues. Poorly treated wastewater releases significant phosphorus into the environment, as do industrial processes and energy production [2].

While phosphorus occurs naturally, human activities can significantly elevate its levels in water. Excess phosphorus can lead to eutrophication, causing ecological problems like

https://doi.org/10.5593/sgem2024v/3.2/s11.17

oxygen depletion, harmful algal blooms, and fish die-offs [3]. Elevated phosphorus in drinking water can also pose health risks, such as an increased risk of cardiovascular diseases.

Phosphorus in aquatic environments primarily occurs as dissolved orthophosphate ions ($PO_4^{3-}$). Phosphates can also be present in the form of organic phosphorus compounds, such as nucleotides and phospholipids, which are vital components of living cells, as well as in the form of condensed polyphosphates [4]. In the context of wastewater treatment plant effluent analysis, the total phosphorus (TP) is measured, which represents the sum of soluble phosphorus (Psol) and insoluble phosphorus (Pins) [5].

Phosphorus removal in these systems occurs through adsorption to filter media, absorption by plants, and microbial degradation. Adsorption to the substrate accounts for 36.2% to 87.5% of total removal, though effectiveness decreases as systems age, while plant and microbial uptake ranges from 1.3% to 26.4% [6]. Since conventional substrates (e.g., gravel, stone) have limited sorption capacity, newer materials like magnesium, steel slag, and iron sponge are being explored [7].

Dense vegetation enhances removal efficiency and resilience to hydraulic loads [8], but replacing substrates with higher-capacity materials is costly and time-consuming, as is vegetation establishment. Therefore, this research focuses on using the aluminium-based coagulant PAX-18.

PAX-18 is a clarifying agent that facilitates the formation of large, separable flocs even at low temperatures. Its use is being explored to improve phosphorus removal efficiency, particularly where conventional methods fall short of legislative standards [9].

## MATERIALS AND METHODS

The research was conducted at three constructed wetlands: Hlína, Dražovice, and Chlumětín. Each of these treatment plants was equipped with a dosing system for the coagulant PAX-18. The coagulant was dosed from a storage tank using a dosing pump, which was powered either by a battery connected to a solar panel or by the mains electrical grid. The dosing of the PAX-18 coagulant was optimised through a testing phase, during which the pump discharge was set at an interval ranging from 1 to 100% of the dosage.

At various time intervals, samples were collected from each of the constructed wetlands and subsequently analysed in the laboratory of the Faculty of Civil Engineering, Brno University of Technology. The analysis was performed using LCK 348 cuvette tests from Hach, employing the phosphomolybdenum blue method.

### Hlína

The constructed wetland in Hlína was built in 2022 for 320 population equivalent (PE). The plant employs an extensive treatment system that includes mechanical pre-treatment using fine screens and three anaerobic separators, followed by a first-stage vertical filter (VF) in whose drainage layer a water level is created to allow denitrification. Additionally, there is a second vertical filter with vegetation, as well as a measurement profile for sampling treated wastewater.

The phosphorus precipitation process at the constructed wetland in Hlína, which was installed in the inlet structure, can be divided into four phases. The first phase commenced

with the launch of the precipitation equipment on 30 March 2023, across all three inflows simultaneously. The pump was set to a 2% flow, corresponding to a coagulant dosage of 1.2 L per day of PAX-18. This 2% setting was maintained for two months, concluding on 29 May 2023.

The second phase began with the pump's output increased to 8%, which corresponded to a dosage of 4.8 L per day of PAX-18. This quadrupling of the pump's output from the initial phase was implemented on May 30 and continued until 10 August 2023.

On 11 August 2023, the pump's output was maintained, but the coagulant was directed solely into the stream C of the constructed wetland. By 19 September 2023, no PAX-18 coagulant was flowing into the streams A and B; only the stream C received a daily dosage of 4.8 L of PAX-18.

The fourth phase began with a change in the pump's output to 8.04% on 20 September 2023, corresponding to a daily PAX-18 dosage of 5.08 L into the stream C.

**Dražovice**

The constructed wetland in Dražovice was put into operation in 2000 to treat wastewater for 850 PE. The Dražovice constructed wetland consists of mechanical pre-treatment, a primary treatment stage that includes both horizontal and vertical filtration fields, and a biological stabilization tank for tertiary treatment.

On 17 April 2023, the phosphorus precipitation process was initiated, with the pump set to a 2% capacity, corresponding to a daily dosage of approximately 1.2 L of PAX-18. The discharge of PAX-18 was implemented immediately after the inflow to the constructed wetland in the inlet structure, prior to the grit chamber.

On 23 May 2023, the pump output was increased to 8%, with the corresponding PAX-18 dosage being approximately 5 L per day. On 29 May 2023, the pump was turned off, and it was reactivated on 15 August 2023, again operating at 8% of its capacity.

**Chlumětín**

The Chlumětín constructed wetland was built in 2020 for 250 PE. The constructed wetland consists of coarse pre-treatment, anaerobic separators, and vertical filters and is part of a system that also includes two clarification tanks, one stabilization tank, and a network of three wetlands.

The actual precipitation process, installed at the influent of the constructed wetland, commenced on 14 April 2023, when the pump was set to 2% of its capacity, corresponding to a dosage of 1.2 L × $day^{-1}$ of PAX-18. Subsequently, in early May 2023, over 200 L of PAX-18 were dosed into the effluent all at once, and the effects of the precipitate in the constructed wetland system were further investigated.

https://doi.org/10.5593/sgem2024v/3.2/s11.17

## RESULTS

### Hlína

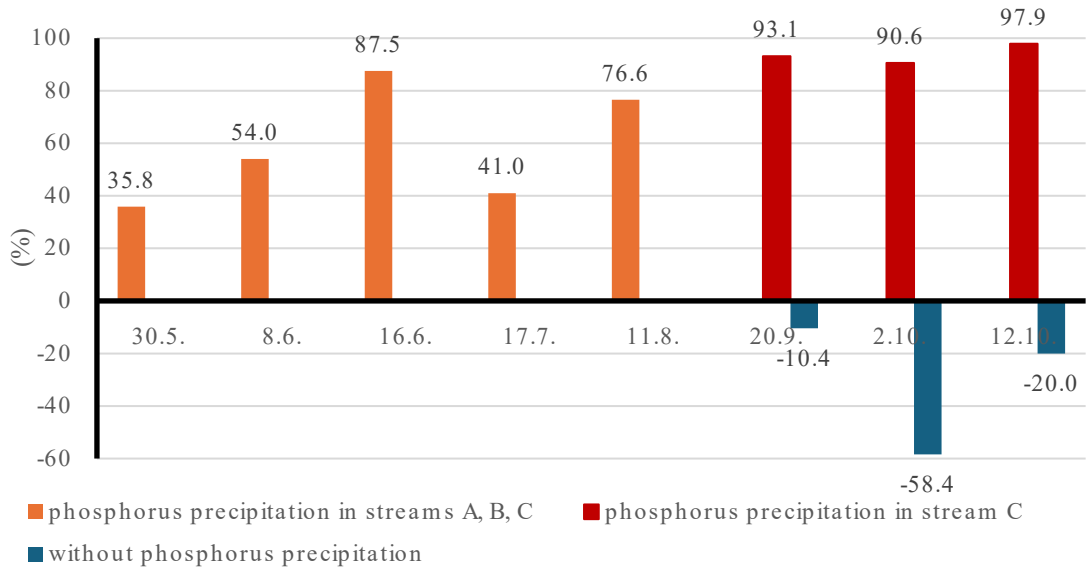



**Figure 1 Efficiency of total phosphorus removal from the separator**

Due to the technological configuration of the Hlína constructed wetland, the effect of the PAX-18 coagulant is most visible in the separator, where the coagulant interacts with the wastewater. The graph above indicates that during the first (orange) stage, all streams of the constructed wetland achieved an average phosphorus removal efficiency of 59%. When the pump power was increased by 6%, the phosphorus removal efficiency rose to nearly 94% (red). Conversely, negative efficiencies were observed in the streams without phosphorus precipitation, resulting in an increase of almost 30% in total phosphorus concentration (blue).

**Table 1 Calculation of the amount of PAX-18 dosed per 1 g of influent total phosphorus.**

| | **Inflow** ($m^3 \times day^{-1}$) | **Amount of TP in the inflow** ($mg \times L^{-1}$) | **Amount of PAX-18** ($L \times day^{-1}$) | **TP** ($g \times day^{-1}$) | **Amount of PAX-18 per gram of TP** ($L \times g^{-1}$) | **Amount of PAX-18 per gram of TP** (%) |
|---|---|---|---|---|---|---|
| **Phase 1** | *13.55* | *5.90* | *1.20* | *80.48* | *0.02* | *51.31* |
| **Phase 2** | *12.31* | *5.40* | *4.80* | *57.85* | *0.12* | *64.42* |
| **Phase 3** | *15.36* | *4.06* | *14.40* | *62.37* | *0.26* | *78.62* |
| **Phase 4** | *17.34* | *7.97* | *15.12* | *142.49* | *0.13* | *80.94* |

The comparison of all stages concluded that phosphorus removal efficiency increases with an increasing dose of PAX-18. However, after reaching the optimum dose of approximately 0.13 $L \times g^{-1}$ of TP, further doses did not yield any significant increase in efficiency.

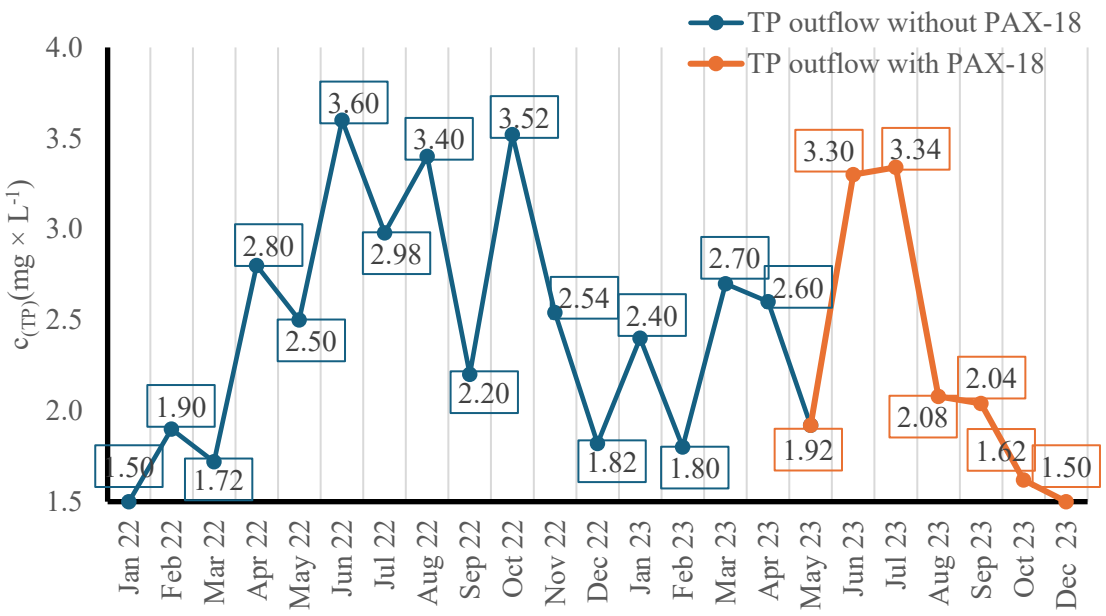



**Figure 2 Outflow concentrations of total phosphorus from the Dražovice WWTP**

The graph indicates that the precipitation of phosphorus by PAX-18 was more visible at the end of the measurement period (September-November). During this time, the efficiency value reached nearly 48%, with an average inflow concentration of approximately 3.1 mg × $L^{-1}$ and an outflow concentration of 2.1 mg × $L^{-1}$ for total phosphorus. When comparing the total period during which phosphorus precipitation was initiated with the same period in 2022, we observe a decrease of 0.6 mg × $L^{-1}$ in the average concentration of total phosphorus at the outflow.

## Chlumětín

**Table 2 Concentration of total phosphorus (mg × $L^{-1}$).**

| | Inflow CW | Outflow CW | Wetland outflow |
|---|---|---|---|
| **Average** | *2.58* | *0.86* | *0.23* |
| **Maximum** | *8.40* | *2.48* | *0.64* |

**Table 3 Phosphorus removal efficiency (%)**

| | CW | Wetland | Together |
|---|---|---|---|
| **Average** | *63.26* | *60.72* | *86.12* |
| **Maximum** | *81.58* | *95.83* | *98.95* |

The average influent to the constructed wetland has a low concentration of total phosphorus, measuring 2.6 mg × $L^{-1}$, which is up to five times lower than that of the Hlína constructed wetland. The average phosphorus concentration at the outflow before precipitation was 1.0 mg × $L^{-1}$, decreasing to 0.75 mg × $L^{-1}$ after precipitation. The treated effluent continues to flow into the wetland, where phosphorus is removed with over 60% efficiency. The average total phosphorus concentration at the wetland outflow throughout the year is 0.23 mg × $L^{-1}$, with the efficiency of the wetland varying seasonally. During

https://doi.org/10.5593/sgem2024v/3.2/s11.17

the colder months, the efficiency tends to be lower, while the maximum concentration of total phosphorus in the wetland outflow reached 0.64 mg × $L^{-1}$.

The average removal efficiency of total phosphorus at the constructed wetland is over 63%, while the overall system achieves an efficiency exceeding 86%. At the tertiary wetland outflow, the average total phosphorus concentration is 0.23 mg × $L^{-1}$, with the wetland removing total phosphorus at an efficiency greater than 65%. After the discharge of treated wastewater into the receiving water body, it is further diluted with the water from the Chlumětín Brook. The final concentration of total phosphorus in the watercourse is 0.05 mg × $L^{-1}$.

## DISCUSSION

### Hlína

The precipitation of phosphorus occurs in four stages, with significant differences between streams with and without precipitation evident in the third and fourth stages. On average, the total phosphorus concentration in streams with precipitation is 1.8 mg × $L^{-1}$ lower than in those without. Following the construction of a new sewage system in Hlína, a clear correlation between wastewater volume and total phosphorus levels was observed. Increasing the coagulant dosage improves phosphorus removal efficiency.

Specifically, higher doses of PAX-18 result in lower phosphorus concentrations in the effluent, demonstrating that operational costs correlate with coagulant application. The most notable phosphorus removal efficiency is observed immediately after coagulant application in the anaerobic separator, where mixing causes visible precipitation that settles to the bottom of the tank.

The hypothesis that streams with precipitation have better phosphorus removal than those without was confirmed. It was found that dosing 0.13 L of PAX-18 per gram of incoming phosphorus achieved the highest efficiency of 80.94%. However, increasing the dosage to 0.26 L decreased efficiency to 78.62%, suggesting a theoretical limit to the coagulant's effectiveness.

Additionally, a relationship between effluent total phosphorus concentration from the second filter and sewage charges was identified, indicating that as sewage charges increase, total phosphorus concentration in the effluent decreases.

### Dražovice

In the initial months of operation, no effect of the coagulant was observed. This lack of effect could be attributed to several factors, including the significant amount of phosphorus present in the constructed wetland itself, an insufficient quantity of coagulant being dosed, the amount of rainfall, which can greatly influence the overall results of precipitation, or the technological arrangement of the constructed wetland. Specifically, horizontal filters may exhibit a slower response due to the longer retention time of wastewater on the filter.

During the autumn of 2023, the constructed wetland began to show phosphorus removal efficiency exceeding 40%, indicating the influence of the coagulant PAX-18.

**Chlumětín**

The natural wastewater constructed wetland in the municipality of Chlumětín receives wastewater that is heavily diluted with rainwater. According to the results, it was found that PAX-18 had a negligible effect on the outflow concentration of total phosphorus. Since the results at the influent already show very low pollution concentrations, the final efficiencies appear to be low.

Regarding the entire system, the removal efficiency for total phosphorus is exceedingly satisfactory, around 86%. Even though over 200 liters of coagulant were overdosed, the treatment plant still did not show a deterioration in outflow concentrations after several months, for example, due to the formed precipitate. On the contrary, the reduced effect of the coagulant on phosphorus precipitation continued to be evident. In the municipality of Chlumětín, there is a clear demonstration of excellent cooperation among the various components of the system, resulting in very low pollution concentrations in the outflow.

The final concentration of total phosphorus in the outflow from the system, equal to 0.05 mg × $L^{-1}$, is in accordance with the Czech legislation regarding the acceptable concentration of total phosphorus in water bodies relative to drinking water standards.

## CONCLUSION

This research confirmed that the dosing of the aluminum-based coagulant PAX-18 is an effective method for improving phosphorus removal in natural wastewater constructed wetlands. The results demonstrate that the proper application of this coagulant can significantly reduce phosphorus concentrations in effluent, thereby aiding wastewater treatment plants in meeting increasingly stringent legislative requirements for treated water quality.

A key finding of this research is that the dosing efficiency of PAX-18 is influenced not only by precise dose adjustments based on the phosphorus concentration in the influent but also by the operational conditions of the individual treatment systems. Significant differences in efficacy were identified among the study sites. While treatment sites such as Hlína achieved very high phosphorus precipitation efficiencies, other sites, particularly Chlumětín, exhibited lower efficiencies. These lower efficiencies were partly attributable to specific conditions, such as reduced phosphorus concentrations in the influent due to high dilution from stormwater.

These results suggest that aluminum-based coagulants, such as PAX-18, may be particularly beneficial in situations where the phosphorus concentration in the influent is stable or elevated. Conversely, for constructed wetlands experiencing periodic fluctuations in inflow, particularly due to stormwater, the efficiency of phosphorus coagulation may be limited. Further investigation into additional factors that could enhance performance under these conditions is warranted.

## REFERENCES.

[1] LAGOVÁ, M. and MALÁ, J. Celkový fosfor ve vodě a sedimentech drobných vodních toků. Brno: Juniorstav 2012. odborná konference doktorského studia s mezinárodní účastí - sborník anotací, 2012. ISBN 978-80-214-4393- 8.

[2] CARPENTER, S.; CARACO, N.; CORRELL, D.; HOWARTH, R.; SHARPLEY, A. et al. Nonpoint Pollution of Surface Waters with Phosphorus and Nitrogen. online.

https://doi.org/10.5593/sgem2024v/3.2/s11.17

Ecological Applications. 1998, roč. 8, č. 3. ISSN 10510761. Available at: https://doi.org/10.2307/2641247. [accessed 2023-10-29].

[3] KRÁSA, Josef. Hodnocení ohroženosti vodních nádrží sedimentem a eutrofizací podmíněnou erozí zemědělské půdy: certifikovaná metodika pro praxi. online. Praha: ČVUT v Praze, Fakulta stavební, 2013. ISBN 978-80-01-05428-4. [accessed 2023-03-05].

[4] LELLÁK, Jan. Hydrobiologie. Praha: Karolinum, 1991. ISBN 80-706-6530-0.

[5] PITTER, Pavel. Hydrochemie. 4., aktualiz. vyd. Praha: Vydavatelství VŠCHT Praha, 2009. ISBN 978-80-7080-701-9

[6] NGUYEN, T.A.H.; LE, T.V.; NGO, H.H.; GUO, W.S.; VU, N.D. et al. Hybrid use of coal slag and calcined ferralsol as wetland substrate for improving phosphorus removal from wastewater. online. Chemical Engineering Journal. 2022, roč. 428. ISSN 13858947. Available at: https://doi.org/10.1016/j.cej.2021.132124. [accessed 2023-09-09].

[7] LU, Hongbin; XIAO, Liping; WANG, Tao; LU, Shaoyong; WANG, Huanhua et al. The application of steel slag in a multistage pond constructed wetland to purify low-phosphorus polluted river water. online. Journal of Environmental Management. 2021, roč. 292. ISSN 03014797. Available at: https://doi.org/10.1016/j.jenvman.2021.112578. [accessed 2023-09-08].

[8] KILL, Keit; GRINBERGA, Linda; KOSKIAHO, Jari; MANDER, Ülo; WAHLROOS, Outi et al. Phosphorus removal efficiency by in-stream constructed wetlands treating agricultural runoff: Influence of vegetation and design. online. Ecological Engineering. 2022, roč. 180. ISSN 09258574. Available at: https://doi.org/10.1016/j.ecoleng.2022.106664. [accessed 2023-10-07].

[9] GROCHOWSKA, Jolanta Katarzyna; ŁOPATA, Michał; AUGUSTYNIAK-TUNOWSKA, Renata and TANDYRAK, Renata. Sequential Application of Different Types of Coagulants as an Innovative Method of Phosphorus Inactivation, on the Example of Lake Mielenko, Poland. online. Sustainability. 2023, roč. 15, č. 23. ISSN 2071-1050. Available at: https://doi.org/10.3390/su152316346. [accessed 2024-10-17].

# THE STUDY OF THE INFLUENCE OF THE FORWARD SPEEDS OF A PATROL VESSEL ON THE BANKS OF THE CANALS IN THE DANUBE DELTA

**Assoc. Prof. Dr.eng. Popescu Gabriel** [1]
**Lecturer Dr.eng. Costel Ungureanu** [1]
**Lecturer Dr.eng. Eugen Gavan** [1]
**eng. Florin Moruzov** [2]
[1] "Lower Danube" University of Galati, **Romania**
[2] Administration of the Danube Delta Biosphere Reserve, Tulcea, **Romania**

## ABSTRACT

The basic argument of the present study lies in the request of the agency of the Danube Delta Biosphere regarding the regulation of travel speeds of different types of boats.

One among the cases of analysis was the one that refers to a patrol vessel.

The purpose of this paper aims to follow the creation and study of the displacement of a ship of maritime patrol produced by the Damen company, inside the Danube Delta on 3 channels of different sizes. To carry out this work, the patrol vessel named "Stan Patrol" it was created in the AutoCAD.

The results of this study are expressed in graphs that highlight the percentage the interdependence between the speed of the patrol vessel and the width of the channel, the volume and the mass water fractions produced by the ship and their influence on the 3 channel dimensions software using the shape plan, with all the details from the project. The model 3D was exported to the SolidWork application, for C.F.D. analyses.

The results obtained in this study will allow the Administration of the Danube Delta biosphere to update the speed rules for boats on the canals depending on the water level.

**Keywords:** Danube Delta, channels, speed vessel.

## INTRODUCTION

The basic argument of the present study lies in the request of the agency of the delta biosphere Danube regarding the regulation of travel speeds of different types of boats. One among the cases of analysis was the one that refers to a patrol vessel.

The purpose of this paper aims to follow the creation and study of the displacement of a ship of maritime patrol produced by the Damen company, inside the Danube Delta on three channels of different sizes. To carry out this work, the patrol vessel named "Stan Patrol" it was created in the AutoCAD software using the shape plan, with all the details from the project. The model 3D was exported to the SolidWork application, for C.F.D. analyses. The results of this study are expressed in graphs that highlight the percentage the interdependence between the speed of the patrol vessel and the width of the channel, the volume and the mass water fractions produced by the ship and their influence on the differently channel dimensions.

## MATERIALS AND METHODS

The Danube Delta is a natural ecosystem mostly located in Dobrogea, Romania and partly in Ukraine. It is considered UNESCO World Heritage since 1991 and until present. The delta has over 23 ecosystems, having found several conditions: flowing water, fresh, salt flats, canals, lakes, pastures, beaches, etc. And these conditions also offer resources such as: food, agricultural land, raw materials (reed).

Today in the Delta we find over 4000 species of animals and birds, thus the Danube described as the paradise of birds with the largest colony of Pelicans outside of Africa. Exist over 135 species of fish, one of them being the sturgeon that comes precisely from the Black Sea for lay their eggs. About 20,000 locals live in the delta, and they live in the sea part with fishing, agriculture and tourism.

Delta attracts approximately 35,000 tourists during the summer season. Also in addition to the fact that the delta is used for leisure, agriculture and tourism, it also has a role the border, the delta since ancient times having a strategic position at the crossroads of continents, the proof being the ruins of the cities that existed on this earth. So that this ecosystem is not destroyed and continues to coexist with man, the circulation in this area is regulated both from the point of view of the types of boats and ships as well as their speeds.

In the Danube Delta there are 3 speeds of Navigation:

1. Speed of 40 km/h (21.59 Kn) mostly on Canals and Lakes;

2. Speed of 15 km/h (8.09 Kn);

3. The speed of 5 km/h (2.69 Kn) in the area of Lakes, Canals, Bays.

In free and unrestricted sectors (15 km/h regulated zone), canal navigation speed is determined by mutual agreement with the pilot on board and cannot exceed the limits of in any case speed set below for normal hydrometeorological conditions :

**Table 1** Maximum navigation speeds

| Ship Type | Upstream | Downstream |
|---|---|---|
| Small ships | 8Nd | 9 Nd |
| Tugs or Convoys | 8Nd | 9 Nd |
| Passenger, rescue, extinguishing, fire and military ships | 9Nd | 10 Nd |
| Maritime vessels up to 4,000 twd | 7Nd | 9 Nd |
| Maritime vessels between 4,000 tdw and 12,000 tdw | 6Nd | 8 Nd |
| Maritime vessels between 12,000 tdw and 25,000 tdw | 5Nd | 7 Nd |

Following these classifications, we chose to focus our study on a patrol ship that is part of from the "Patrol Type Ships" category. The study vessel is a Stan Patrol 4207(3).

This vessel is built by the Damen shipyard, the vessel having a length of 42.8m, a beam of 7.1m and a speed that reaches 26.5 knots (3). The traffic speed is 40 km/h in the areas of Canals and Lakes and 5 km/h in the area of Lakes, Canals, Bays. Since the Study Ship is part of the Patrol Vessels category, it will allows instead of 15 km/h (8.09 Nd) to

travel at a speed of 16.66 km/h (9 Nd) in the Upstream and 18.52 km/h (10 Nd) Downstream according to the table above.

**Generation of the 3D model of the study ship.**

To model the ship, the AutoCAD software program was used using the plan of forms available procured from the DAMEN website (3) with all its related details.

The following settings were used to execute the drawing:

Orthomode – On or off (as appropriate); Polar tracking – On or off (as appropriate);

Object Snap Tracking – On; Line weight – On.

Themes/styles used:

• Drafting & Annotation;

• 3D Modeling,




**Figure 1** Patrol Vessel [1]

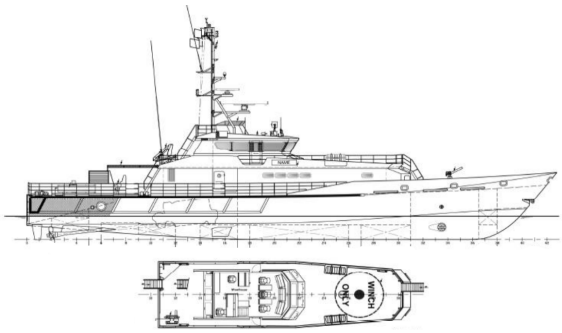


**Figure 2** General Arrangement Plan [1]

The next step was to export the ship in the SolidWork program [6], a software that also has a the C.F.D (Computational Fluid Dynamics) analysis module for carrying out simulations and getting results on the 3 channels for the 4 speeds.

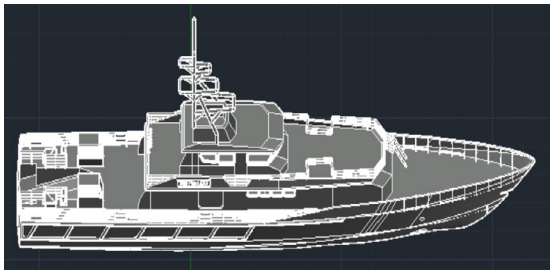


**Figure 3** Autocad 3D Model

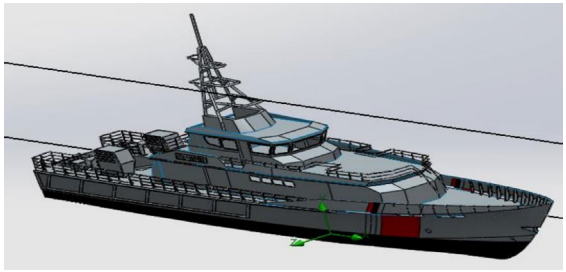


Figure 4 SolidWorks 3D Model

**The nominal definition of the channels on which the study takes place**

In the Danube Delta there are a variety of canals of different sizes, and for the study three channels of three different sizes were chosen to observe how they behave the craft on each of these. These channels are adjacent to each other, interconnected and they have nearby lakes that are protected by law, but also open to tourists and fishermen amateurs. Channels of interest are as follows:

The first channel is "Mila 35" the entrance to this channel is from the Sulina branch, initially having two entrances, but following the submissions, one of the entrances became inaccessible. This channel can connect the Sulina arm and the St. The cell. It has a length approximately 11km, a width of 40m and a depth of 4-5m. For our study we have chose a length of approximately 270m, a width of 30m and a depth of 4m [3].

The second channel is "Canalul (Gârla) Şontea Veche" a navigable canal all the time year, has a length of 43.52 km, rivaling the Titcov canal, considered the longest channel from the Danube Delta. The Şontea Canal is very long and is formed by Gârla Şontea Veche and Gârla Șontea Lată nicknamed the Western Delta.

It is a place frequented by both tourists and professional fishermen, it has a width of approximately 25-35m and a depth of 2.5-3m. For our study we chose an area in the canal where the width is 20m and the length is 20m entered in the program was 270m [4].

The third Channel is called Archipenco, a small channel being cataloged with a degree of navigable difficulty rather high high 4/5, has a length of 9.13 km long, a width of 10m and a depth of 2m. The entrance is made from the Sulina arm, and the canal it can only be traversed when the water is medium or high due to the critical points [5].

## RESULTS

Below are presented the results obtained during the runs in SolidWorks, using the Flow Simulation C.F.D. module, for the three channels. The results obtained for each channel and the speed for which the studies were done are presented by the percentage change of the volume of water, of the mass of water in view and cross-section.

**Mila 35 channel, width 30m.**

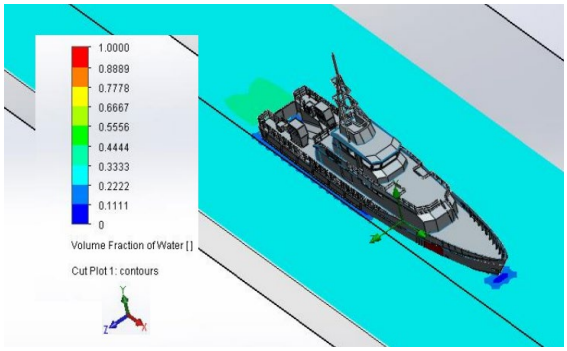



**Figure 5** Volume Fraction of water 5km/h

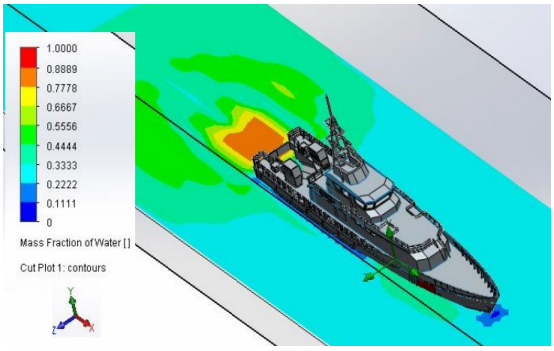



**Figure 6** Mass fraction of water 5km/h

Figure 6 above shows that the mass of water influenced by the ship in the shore area is 33% more greater than the initial mass fraction of water.

For a better visualization of the wave formation behind the ship, the cross section along the direction of travel was chosen. The results expressed by changing the water masses at the four speeds 5, 15, 40 and 49 km/h on the Mila 35 channel.

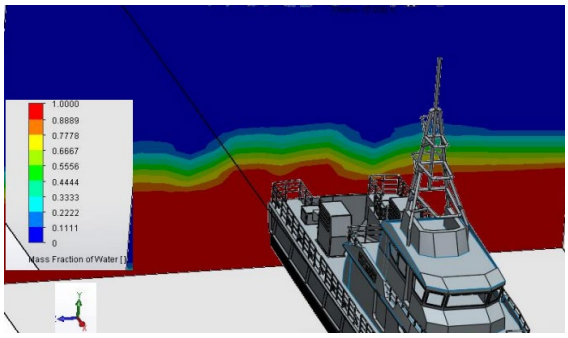



**Figure 7** 5 km/h

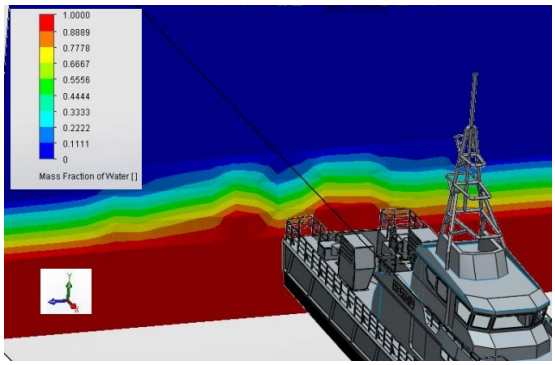



**Figure 8** 15 km/h

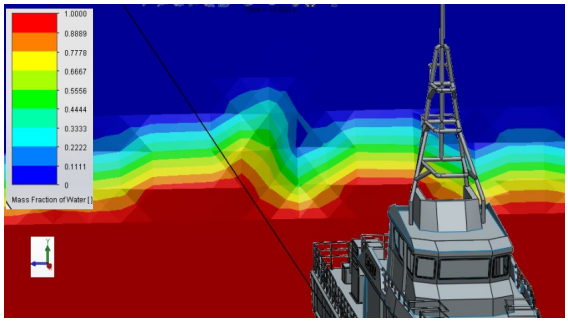



**Figure 9** 40km/h

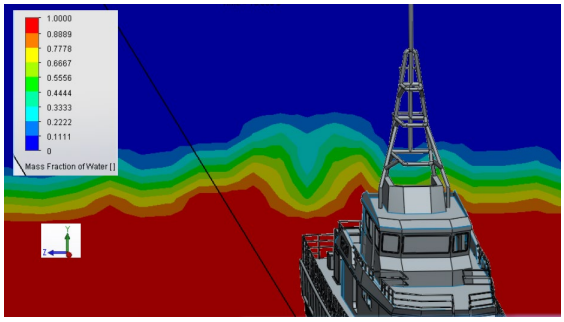



**Figure 10** 49 km/h

**Mass Fraction of Water** Mila 35 channel

In the case of a forward speed of 15 km/h, the mass of the water fraction in the area of the banks changes by 44%.

In the case of a forward speed of 40 km/h, the mass of the water fraction in the area of the banks changes by 66%.

In the case of a forward speed of 49 km/h, the mass of the water fraction in the area of the banks changes by almost 77%.

The results are shown in the figures 7,8,9 and 10.

In the same way, the results were generated for the Sontea (20m wide) and Arhipenco (10m wide) canals at the same ship speeds (5, 15, 40 and 49 km/h). These were centralized by the appearance of the fractions of water masses transversely along the navigation direction graphically in figure 11.

https://doi.org/10.5593/sgem2024v/3.2/s11.18

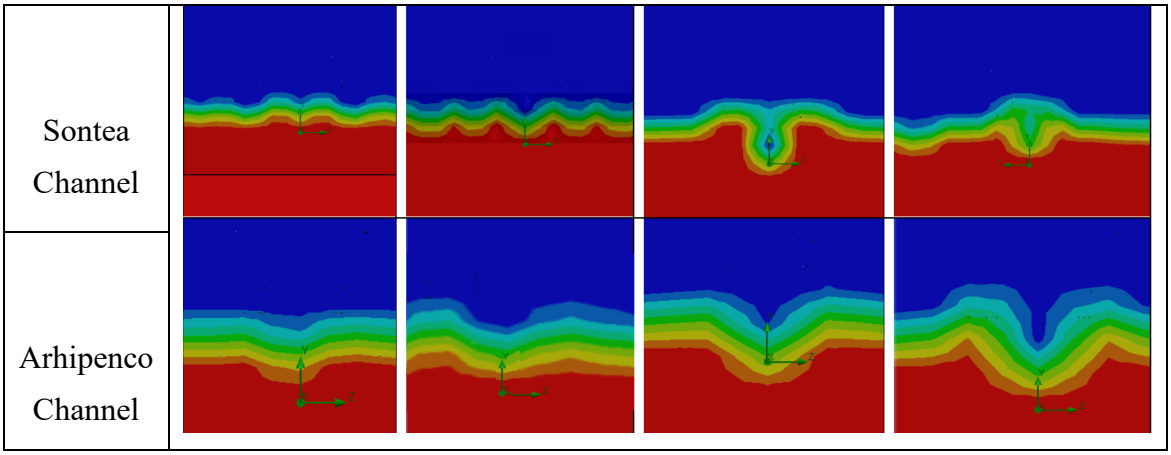



**Figure 11** Mass Fraction of Water profile for 5,15,40 and 49km/h (in horizontal)

Regarding the changes in the masses of the water fractions in the two canals Sontea and Arhipenco for the four speeds, the percentage values are:

- for the Sontea canal at a speed of 5 km/h the mass of water fractions is 0.444, for a speed of 15 km/h the mass of water fractions is 0.555, for a speed of 40 km/h the mass of water fractions is 0.777 and for a speed of of 49 km/h, the mass of the water fractions is 0.888;

- for the Arhipenco canal at a speed of 5 km/h the mass of water fractions is 0.666, for a speed of 15 km/h the mass of water fractions is 0.777, for a speed of 40 km/h the mass of water fractions is 0.888 and for a speed of of 49 km/h, the mass of the water fractions is 0.998.

These values were concentrated in table 2

**Tabel 2**

| Speeds | Channel 30m | Channel 20m | Channel 10m |
|---|---|---|---|
| **5 km/h** | 0.333 | 0.444 | 0.666 |
| **15 km/h** | 0.444 | 0.555 | 0.777 |
| **40 km/h** | 0.666 | 0.777 | 0.888 |
| **49 km/h** | 0.777 | 0.888 | 0.998 |

The graphic transposition of these values led to figure 12.

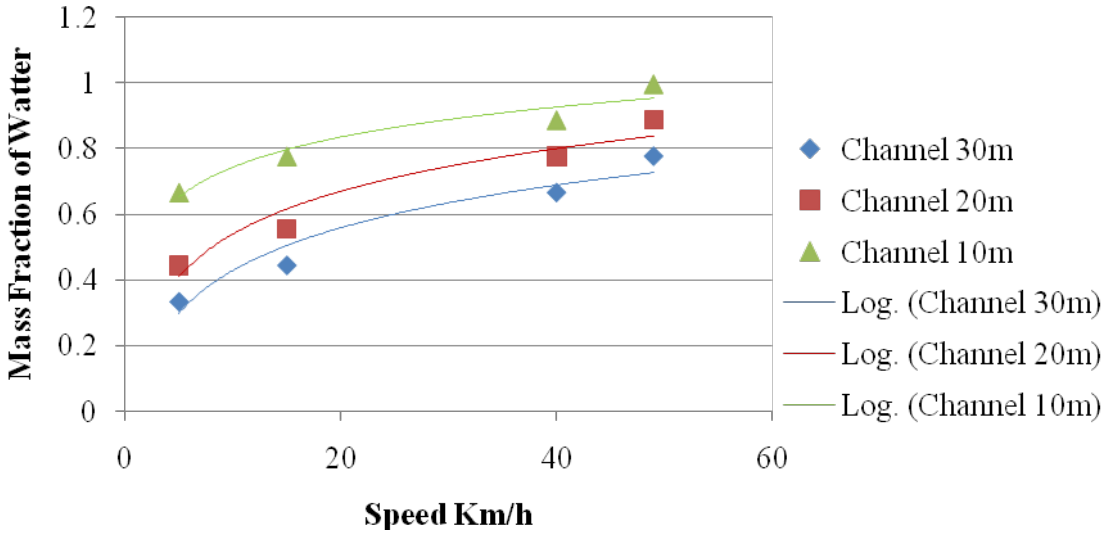



**Figure 12** The graphs of the values of the masses fractions of the water for the three channels in the case of the four ship speeds

## DISCUSSIONS

In essence, the amplitude of the waves produced by a boat are the same at the same speeds. The values listed in table 2 are those estimated in the proximity of the banks of the three canals. The dynamics of the fractions of water masses could be expected to have the same shape of the trend curves in the three cases (see figure 12). The trend curves were estimated by logarithmic functions.

In all three cases, there is a rapid increase in them between speeds of 5 and 15 km/h, the increase being due to the speed ratio of 3 to 1.

Between the speeds of 15 and 40 km/h the evolution of the trend curves is blurred as a result of the ratio of 2.666 of the speeds which continues with a sharp decrease between the speeds of 40 and 49 km/h (ratio 1.225).

The modified values of the fractions of the water masses at the shore are very important in terms of the danger of flooding the areas adjacent to the canals even during the passage of the boat. It is known that the birds and animals of the Danube delta make their nests, shelters near the water shine. These are also the places where large birds, swans, pelicans, egrets, hummingbirds, terns and cormorants nest and lay their eggs.

The period of the year when large birds nest in the dwarf willows on the banks of the canals is March, April, May. [3]

The results obtained in this study must be correlated with two important factors, the time of year for navigation in the Danube Delta as well as the water level in the canals.

The period of the year is important from the perspective of non-aggression on the perpetuation of fauna diversity by flooding the egg-laying areas.

It is noted that the critical period March - May coincides in most years with the period of rising water levels in the Danube Delta (the second factor).

It is easy to imagine that in the situation where the water level is raised on the canals, approaching the height of the banks, any change in the fractions of the water masses (over 0.444) attracts the flooding of the banks.

The higher the modified values of the water fractions, the larger the flooded area on the banks.

In the periods of the year when the water level is low (summer) or in dry years, the same modified values of the fractions of the water masses can influence the flooding of the banks less or not at all. If the water level is one meter lower than the bank, even a water mass fraction value of 0.888 may not have an effect on the ecosystem in the vicinity of the canal.

## CONCLUSION

The Administration of the Danube Delta Biosphere Reserve has a series of published rules regarding speed regimes on canals.

These must also be granted with the periods of the year with different water levels as well as with the types and sizes of boats.

The present study was carried out in the framework of a partnership between the Faculty of Naval Architecture and the Danube Delta Biosphere Administration with the aim of providing them with some results that would allow them to update the rules for observing boat speeds. The major challenge in the continuation of these studies is related to the climate changes with repercussions in the Danube Delta so that, in addition to the natural factors, the human factor is limited or even excluded.

## REFERENCES

[1] Stan Patrol 4207 - Damen

[2]Reguli speciale de navigatie pe sectorul Dunarii cuprins intre rada Sulina si portul Braila (km 175) | R.A. Administrația Fluvială a Dunării de Jos Galați

[3] Canalul Mila 35 - Loc de pescuit in Delta Dunarii - Info-Delta.ro

[4] Delta de Vest – Canalul (Garla) Sontea Veche

[5] Delta de Vest – Canalul Arhipenco

[6] https://www.solidworks.com/product/solidworks-flow-simulation

# USING RISK MAPPING TO DETERMINE A MODERATE NATURE-BASED SOLUTION

**Ing. Brumar Jakub**
**Assoc. Prof Ing. Brumarova Lenka, Ph.D.**
**Ing. Nela Kužílková**
VŠB – Technical University of Ostrava, Faculty of Safety Engineering,
Lumírova 630/13, 700 30, Ostrava– Výškovice, **Czech Republic**

## ABSTRACT

Emergency preparedness plays a key role in the safety of the territory. The emergency or crisis preparedness of the territory has a prospective character. The proposed preparedness measures are implemented in the long term. The measures are implemented on the basis of strategic planning for the development of the territory within the framework of spatial planning. One type of measures can be nature-based solutions, which are linked to nature and frame the natural character of the territory. Alternatively, these measures may have a different function in the territory (e.g. recreational use). For the design of measures in the territory, risk mapping can be used, which visualises the risks in the territory using a colour scale on a map. Risk maps identify areas with different levels of risk and show the interaction of the manifestations of different types of hazards, vulnerabilities and preparedness in the territory. The maps thus provide comprehensive information on the risk burden on the territory and the possibility to set up selected preventive measures to reduce the potential risk. The article describes the mapping of risks in the territory of the Czech Republic, pointing out the possible application of measures in the form of nature-based solutions, taking into account respect for nature and the opinions of local residents.

**Keywords:** risk mapping, nature-based-solution, preparedness

## INTRODUCTION

The Czech Republic is faced with emergencies (natural, anthropogenic, combined). The negative impacts of these events threaten protected interests - human life and health, economy (property), environment and social stability. The basic duty of the state is to ensure the safety and protection of protected interests. Preparedness of the territory for emergencies is one of the basic tasks of all stakeholders in the field of public protection. Emergency preparedness refers to the measures taken to prepare for emergencies and to reduce their impact. Emergency preparedness provides a platform for the design of effective, realistic and coordinated planning. The issue of preparedness is generally perceived on a national and international scale. Internationally, the concept of preparedness is seen as the amount of knowledge, forces and resources of organizations, communities and individuals to anticipate, respond and recover from disasters, as stated by e.g. Sendai [1]. In the Czech Republic, emergency preparedness and crisis preparedness can be perceived. Emergency preparedness and crisis preparedness can be perceived in the Czech Republic. Emergency preparedness (procedural approach) [2] is the ability to recognize the occurrence of emergencies and to implement measures set out in emergency plans (emergency plan of the region, external emergency plan). In

https://doi.org/10.5593/sgem2024v/3.2/s11.20

case the event has a more extensive waste in the territory, the concept of crisis preparedness is introduced. The basis of preparedness activities is to answer the questions of what types of emergencies and crisis situations need to be prepared for, what types of hazards exist in the territory and consequently how big is the risk resulting from them. To ensure the preparedness of the territory for an emergency, a risk assessment of the territory is used. To determine the level of risk in the Czech Republic, the Hazard Analysis for the Czech Republic [3] can be used (note: a unified approach for assessing risks in the Czech Republic) with a link to the mapping of risks in the territory. From the perspective of risk mapping, it is a trend to visualize the quantified risk into a map base using the Geoinformation System. The resulting quantified risks are visualised in colour on a map with the possibility of using a software application. The applications allow the creation of risk maps from available source data and provide the end user with a better understanding of the risk context of the area, and thus subsequent exploration of the risk mapping results from different perspectives. The results from the risk assessment provide the basis for deciding on the most appropriate approach and with the possibility of using a nature-based solution (NbS) to reduce risks on the site.

NbS exploit the characteristics and complex system processes of nature. It is the design of solutions leading to the reduction of the risk of emergency/disasters in order to improve human well-being. Some definitions of NbS show a difference in perception - IUCN [4] emphasizes natural or altered ecosystems, EC [5] allows the possibility of including artificially created systems (e.g. restored wetlands) as a type of NbS. However, it is still a measure leading to risk reduction in a given territory.

## MATERIALS AND METHODS

Flood hazard and risk mapping is used in Europe. This involves the use of flood hazard, vulnerability and risk maps with links to flood protection and disaster management [6]. In Germany, the software tool FloodCalc is used and has been validated in a study for the Mulde River in Saxony [7]. In Slovakia, the simulation method is used for flood hazard maps and flood risk maps of watercourses. In Kenya (e.g. Eldoret Municipality) according to [8], integrated Analytical Hierarchy Processes (AHP) and Geoinformation Systems Analysis techniques are used for flood risk modelling. Côte d'Ivoire (e.g. Abidjan district) also uses AHP as a multi-criteria analysis method, allowing the integration of several elements within the two criteria of hazard and vulnerability [9]. Some of the more common types of hazards using risk mapping include drought risk in Australia [10], avalanche risk in Iceland according to [11], slope instability according to [12] In Germany, a new method for mapping and simulating complex multi-hazard situations was proposed and demonstrated within the RIESGOS project in 2018 [13]. In foreign countries, risk mapping is used for specific risks, i.e. there are no partial tools for comprehensive visualization of risks in a given area. Based on this fact, the possibility of complex (multi hazard/multi risk) risk quantification with visualization on the territory, i.e. risk mapping, appears to be a suitable tool for preparedness in the Czech Republic. In the Czech Republic, a methodology has been developed; [14] within the project VH20182021037 Risk Mapping on the Territory of the Czech Republic; which offers a comprehensive risk assessment on the territory with subsequent interpretation/visualization of the quantified risk into relevant maps using Geoinformation Systems (GIS).

The methodology provides for the implementation of risk mapping based on defined basic characteristics of the territory, description of calculation algorithms using mathematical models in the implementation of risk mapping, recommendation of specific types of hazards in the Czech Republic for inclusion in risk mapping and recommendation of elements of vulnerability of the territory and elements of preparedness with cartographic representation equivalents suitable for inclusion in risk mapping. On the basis of the methodology, a model with geoprocessing tools has been created to enable spatial analyses and calculations according to the model for risk mapping in the Czech Republic based on available spatial data and the use of a web application. The philosophy of the methodology is based on the used Analysis of Threats for the Czech Republic (ATCZ), which assessed and quantified the risks on the territory of the Czech Republic in classical terms of risk, frequency and consequences. The risk mapping therefore refines the risk by adding additional parameters such as vulnerability and preparedness.

The mapping works with a specific territory. The term risk is used as 'territory risk', i.e. risk is related to a specific territory. "Territory risk" can be defined mathematically according to formula (1) [14]:

$$TR = [(F \times C) \times V] / P \quad (1)$$

Where:

TR is the territory risk

F is the frequency

C is the consequence

V is the vulnerability

P is preparedness

F x C is the risk according to ATCZ

In addition, the definition of 'territorial risk' includes preparedness, which is the ability of the territory to reduce the risk. The variables risk (according to the ATCZ), vulnerability and preparedness are certain characteristics of a territory from the perspective of risk mapping.

In the case of determining the degree of vulnerability, the following vulnerability categories are defined: people, transport infrastructure, technical infrastructure, civil equipment, integrated rescue system, industry and environment. Each vulnerability category has its own sub-category, called vulnerability elements, with a total of 20 elements (e.g. the transport infrastructure category has elements of roads, railways, metro, airports, waterways). Following the determination of the level of preparedness, the categories of fire protection, health, internal order and security, and protection of the population are established. Each category of preparedness has a total of 10 preparedness elements (e.g. internal order and safety has elements of the Police of the Czech Republic, Air Service of the Police of the Czech Republic, Municipal Police). Figure 1 shows the steps in the risk mapping methodology.

https://doi.org/10.5593/sgem2024v/3.2/s11.20




Figure 1 Steps in the process risk mapping

The first step in risk mapping is the description of the area, including the identification of hazards, which are then recorded on a hazard map. This stage involves visualising the frequency of the consequences of each hazard. The next step is to determine the vulnerability to each defined hazard. The vulnerability map captures the results of the vulnerability rate determination for each vulnerability element, specifically those elements that have suitable spatial data. The vulnerability elements are modified using refinement coefficients. The cumulative risk map is the resulting map from the hazard map and the vulnerability map. The preparedness map captures the results of the preparedness determination for each vulnerability element, namely elements that have suitable spatial data. The adjusted risk map is therefore the result of the hazard map, the vulnerability map (cumulative risk map) and the preparedness map.

## RESULTS

The results, cumulative risk maps and corrected maps can be used to identify risks that have been assessed as high risk, including location, and where NbS can be applied. Using geo-information system (GIS) input data, the methodology was implemented in the ArcGIS desktop application and then made user-friendly for the web application. Verification of the methodology was carried out on a selected site in the city of Olomouc, Czech Republic, in a practical demonstration of the resulting cumulative risk map, Figure 2, and corrected risk map, Figure 3.

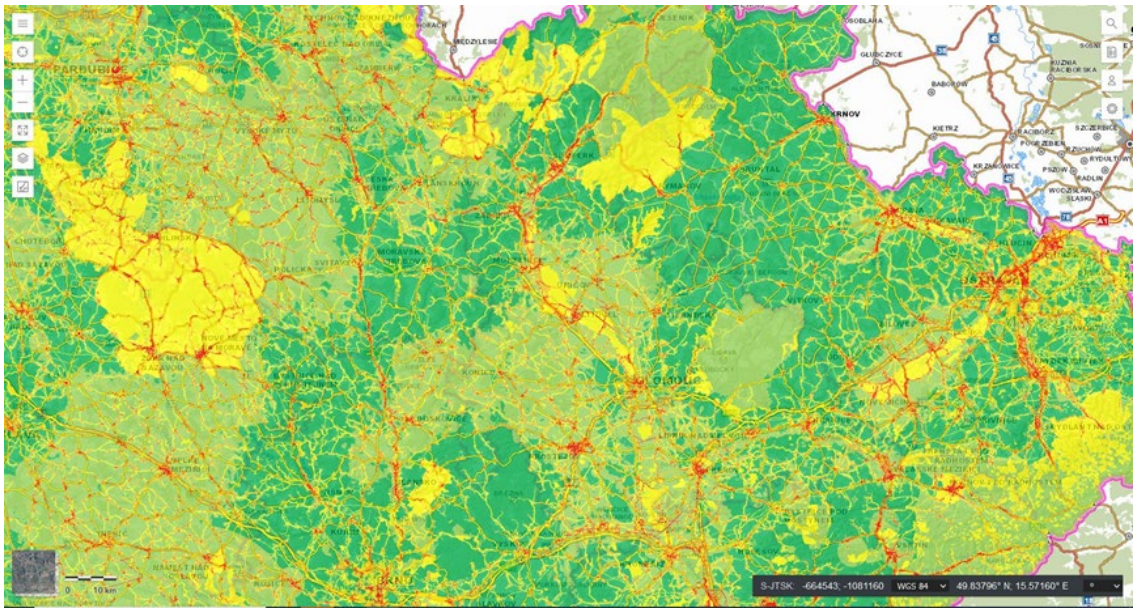


Figure 2 Map of the cumulative risk of the city of Olomouc [2].

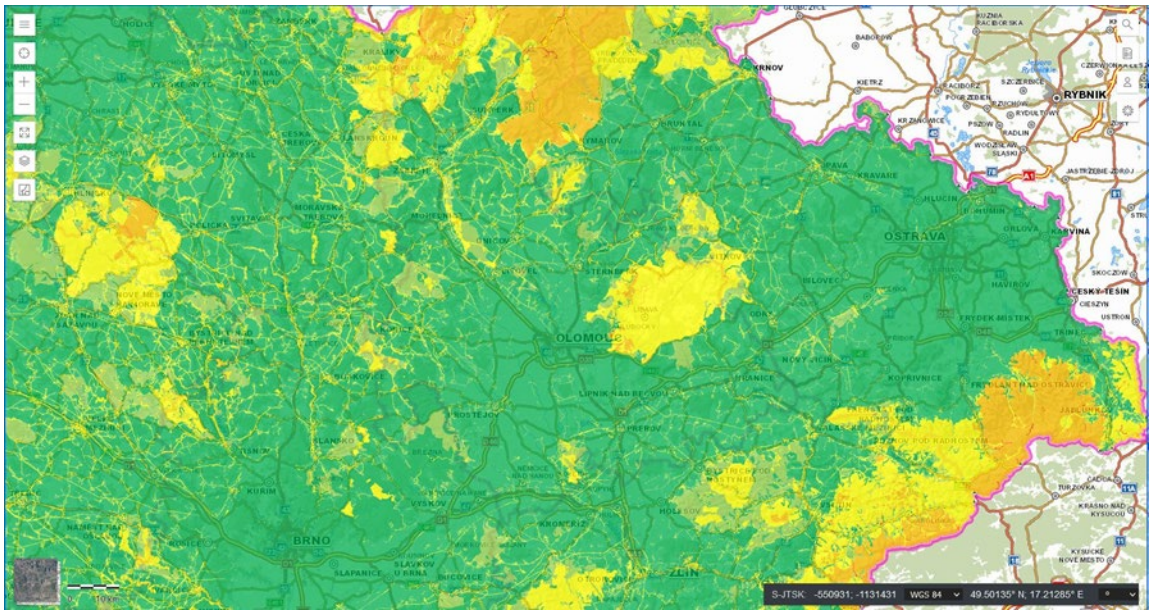



Figure 3 Map of adjusted risk [2].

A comparison of the submitted maps shows that there is a refinement of the risk in the area. Thus, there is a change in the level of risk from high risk to medium risk or even to low risk.

## DISCUSSION

The present article describes the use of risk mapping in the Czech Republic as a tool for determining the level of risk with the use of NbS as an option for risk reduction in the area. It should be emphasized that input data are important for the results of risk mapping. In the Czech Republic, the necessary data are not available, e.g. the Hazard - epidemic Map. Thus, it is not always possible to use risk mapping for the use of NbS. However, it is a possible tool for use in the Czech Republic with the possibility of modification abroad, e.g. the Slovak Republic. Another observation is that it is not always possible (even when identifying with the help of risk mapping) to set NbS measures in every high risk. A more detailed analysis on the possibility to apply NbS is needed. Another question is the appropriateness of using NbS, whether based on the hazard map or cumulative risk map performed or only on the resulting corrected risk map.

## CONCLUSION

International preparedness plays a key role in mitigating the negative impacts of emergencies. The overall objective of preparedness is to reduce the humanitarian, social, economic and environmental impacts on the affected population and to help them recover and get on with their lives.In the Czech environment, preparedness in the territory is one of the basic tasks in the field of population protection and crisis management. Territorial preparedness is perceived as the ability of a territory, or its security system, to recognise the possibility of emergencies, prevent their occurrence, mitigate their consequences, maintain the availability of human, material and other resources and territory for their liquidation and create conditions for the recovery of the territory affected by the consequences of an emergency. The risk mapping methodology

https://doi.org/10.5593/sgem2024v/3.2/s11.20

offers a new procedure for quantifying risk in the territory based on defining the basic characteristics of the territory, including defining categories and elements of vulnerability and preparedness. The article includes the verification of risk mapping on the territory of the Czech Republic city of Olomouc in the form of cumulative and corrected maps. The article offers an extended view of the methodology on risk mapping in the territory with application to foreign countries with applicability of risk reduction in the territory using nature-based-solution. This approach of mapping using NbS can be used to investigate resilience and commensuration for policy decision making in assessing the security system in the Czech Republic. The users of the methodology, desktop and web applications are mainly members of the Fire Rescue Corps of the Czech Republic and crisis management authorities at all levels of local government in the Czech Republic. With appropriate modification of the risk mapping methodology, it is possible to use it abroad.

## ACKNOWLEDGEMENTS

The article was prepared with the support of the project Nature-Based Solutions for Demonstration Climate-Resilient Critical Infrastructure (NATURE-DEMO), project number 101157448

## REFERENCES

[1] Sendai Framework for Disaster Risk Reduction 2015-2030. UNISDR. UNISDR/GE/2015 - ICLUX EN5000 1st edition, 2015, pp 37;

[2]. Brumarová, L., Ensuring the preparedness of the territory [Habilitation thesis]. Ostrava: VSB-Technical university of Ostrava. Faculty of Safety Engineering, 2021, pp 153;

[3] Paulus, F., Krömer, A., Černý, J., Petr, J. Threat Analysis for the Czech Republic: Final Report, 2015, pp 9;

[4] IUCN (International Union for the Conservation of Nature) (2009). No time to lose – make full use of nature-based solutions in the post-2012 climate change regime. Position paper for the Fifteenth session of the Conference of the Parties to the United Nations Framework Convention on Climate Change (COP 15). Gland: IUCN;

[5] European Commission (EC) (2015). Nature-Based Solutions and Re-Naturing Cities. Final Report of the Horizon 2020 Expert Group on Nature-Based Solutions and Re-Naturing Cities. Brussels: European Commission;

[6] Merz, B., Thieken, A., Gocht, M., Flood Risk Mapping At the Local Scale: Concepts and Challenges. In Begum, S., Stive, M.J.F., Hall, J.W. (eds) Flood Risk Management in Europe. Advances in Natural and Technological Hazards Research, vol 25. Springer, Dordrecht, 2009, doi: 10.1007/978-1-4020-4200-3_13;

[7] Meyer, V., Scheuer, S., Haase, D., A multicriteria approach for flood risk mapping exemplified at the Mulde river, Germany. Natural Hazards, 2009, pp 48, 17–39. doi: 10.1007/s11069-008-9244-4;

[8] Ouma, Y.O., Tateishi, R., Urban Flood Vulnerability and Risk Mapping Using Integrated Multi-Parametric AHP and GIS: Methodological Overview and Case Study Assessment. Water, 6, 2014, pp1515-1545. doi: 10.3390/w6061515

[9] Danumah, J.H., Odai, S.N., Saley, B.M. et Al., Flood risk assessment and mapping in Abidjan district using multi-criteria analysis (AHP) model and geoinformation techniques, (cote d'ivoire). Geoenvironmental Disasters. 3(10), 2016, doi: 10.1186/s40677-016-0044-y;

[10] Dayal, K.S., Deo, R.C., Apan, A.A., Spatio-temporal drought risk mapping approach and its application in the drought-prone region of south-east Queensland, Australia. Natural Hazards. 93, 2018, pp. 823–847. doi: 10.1007/s11069-018-3326-8y;

[11] Keylock, C., Mcclung, D., Magnússon, M. Avalanche risk mapping by simulation. Journal of Glaciology. 45(150), 199, pp. 303-314. doi: 10.3189/S0022143000001805;

[12] Hervás, J., Bobrowsky, P., Mapping: Inventories, Susceptibility, Hazard and Risk. In Sassa K., Canuti P. (eds) Landslides – Disaster Risk Reduction. Springer, Berlin, Heidelberg, 2009, pp 321-349. doi: 10.1007/978-3-540-69970-5_1;

[13] Rieger, CH. Risikoanalyse – Risiken erkennen und vergleichen. In Bevölkerungsschutz, č. 1/2007, 2007, pp 5–8, Bundesamt für Bevölkerungsschutz und Katastrophenhilfe (BBK);

[14] Brumarová, L., et A., Risk Mapping Methodology in the Czech Republic. Security research project VH20182021037 – Risk mapping in the territory of the Czech Republic. Ostrava. pp 66.

https://doi.org/10.5593/sgem2024v/3.2/s11.20

# VOLUMETRIC QUANTIFICATION OF SOIL LOSS IN A PART OF THE MUNICIPALITY OF OTNICE IN THE CZECH REPUBLIC

**Lukáš Buršík**
**Prof. Dr. Miroslav Dumbrovský**
**Dr. Veronika Sobotková**
Brno University of Technology, **Czech Republic**

## ABSTRACT

This paper deals with the volumetric quantification of soil loss. A device called erosion bridge was used for the quantification. It was designed and created at the Institute of Landscape Water Management, Faculty of Civil Engineering, Brno University of Technology. The principle of the measurement with the use of this device is that the needles are lowered onto the terrain surface and their profile copies the terrain profile. A camera attached to the erosion bridge is important, which is used to take photographs of the erosion bridge with the profile of the rill. For the quantification, a deep erosion rill was chosen in the municipality of Otnice, which is located in the South Moravian Region of the Czech Republic. According to LPIS (Land Parcel Identification System), the land in the locality is used as a grassland (on an arable land). The soil there is composed of brown soil modal (HNm), in terms of soil depth it is deep soil (soil depth is more than 60 centimetres). The rill was measured at the length of 145 metres, a total of 23 profiles at different distances were measured. The field measurement resulted in above-mentioned photographs. These were afterwards assessed by a software program called Erosion bridge. By evaluating the measured profiles and calculating theoretical ones, it was found that the average depth of the rill was 0.25 metres, and its average width was 0.58 metres. It was discovered that the soil loss in the locality was approximately eight cubic metres. That implies that roughly eleven tonnes of soil were eroded at a bulk density of 1.35 grams per cubic centimetre.

**Keywords:** volumetric quantification, soil loss, erosion bridge

## INTRODUCTION

Since soil is a fundamental component of production from agriculture, it needs our attention, but primarily our protection. The loss of high-quality agricultural land is seen as a severe issue globally. [1] Erosion of agricultural soils in the Czech Republic is a serious threat to their productive and non-productive functions. [2] It devastates and removes the most fertile part of the soil, which is topsoil, reduces the strength of the soil profile and the nutrient and humus content. Moreover, physical, chemical, and biological properties of soils are weakened by erosion. [2, 3] It subsequently pollutes watercourses and water reservoirs with both suspended matter and dissolved and colloidal substances. [3]

A common form of soil degradation in the Czech Republic is rill erosion. Sloping agricultural land is especially at risk from this kind of water erosion. When there is no vegetation covering the soil surface, as may occur when wide-row crops such as maize, beet or potatoes are planted, the threat level rises. The trigger for rill erosion is most

https://doi.org/10.5593/sgem2024v/3.2/s11.21

commonly torrential rain. Concentrated runoff can be the consequence of precipitation that initially runs off the surface, subsequently concentrates in individual rills. [4]

The erodibility of the soil may be the only factor limiting the erosivity of flowing water when it concentrates on hillslopes. Such rills and ephemeral gullies frequently have detrimental effects on crop production and downstream sedimentation, and concentrated flow paths may eventually develop into permanent drainage channels. [5]

Surface runoff and the particles transported by it from inter-rill area, and subsequently concentrated surface runoff of small depth in the erosion rills themselves, contribute to rill erosion. The stability and resistance of the soil, height and direction of runoff, and the vegetation cover of the soil surface all influence the spatial arrangement and shape parameters of rill erosion. [6]

## MATERIALS AND METHODS

*Description of Area of Interest*

For the purposes of this paper, one block of LPIS (Land Parcel Identification System) was chosen, where a deep erosion rill was formed (see Fig 1 and Fig. 2). The block is located in the municipality of Otnice belonging to the South Moravian Region (NUTS 3) of the Czech Republic (see Fig. 3), in the Vyškov District (NUTS 4). It can be found at a distance of approximately 20 km southeast of the city of Brno.



Fig. 1 Erosion rill in the area of interest – view downslope [own source].



Fig. 2 Erosion rill in the area of interest – view upslope [own source].

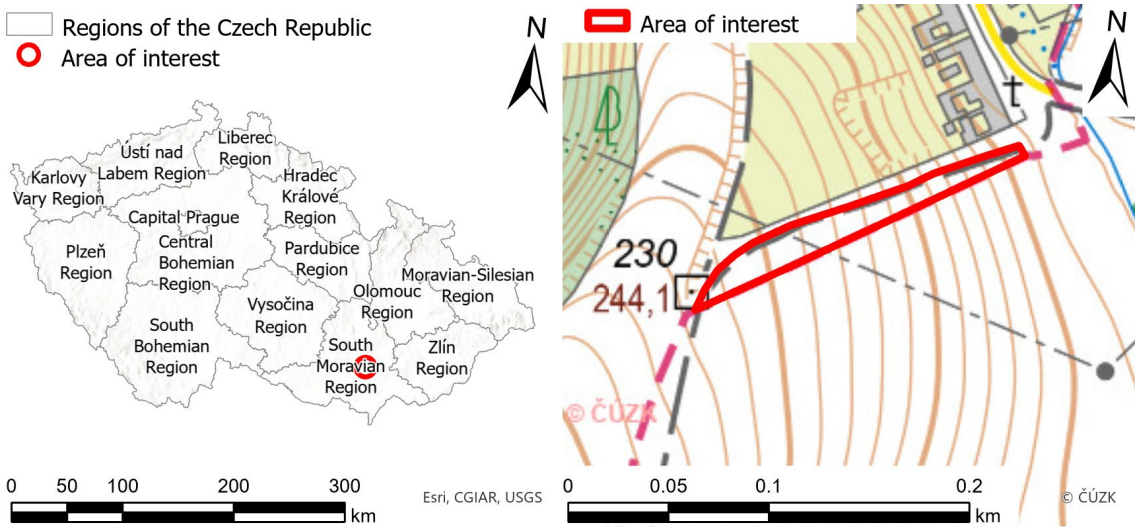



Fig. 3 Location of the area of interest on the map of the Czech Republic (left) and within the municipality of Otnice (right).

The selected block of LPIS is used as a grassland (on an arable land), but it is not perfect due to low vegetation coverage (this is also evident in Fig. 1 and Fig. 2). Its area is about 0.23 hectares and its altitude ranges from 219 to 243 metres above sea level. The locality is made up of brown soil modal (HNm) and only deep soil (with soil depth larger than 60 centimetres) can be found there.

*Volumetric Quantification of Soil Loss*

Volumetric quantification of soil loss on the field is a method of direct measurement of the terrain profile. [4]. For this purpose, so-called erosion bridge can be used (see Fig. 4). It was developed at the Institute of Landscape Water Management, Faculty of Civil Engineering, Brno University of Technology. The basic idea behind the measurement using this device is that the needles are lowered onto the ground and their profile copies the terrain profile. It is crucial to have a camera attached on the erosion bridge so that pictures of it with the rill profile can be taken.

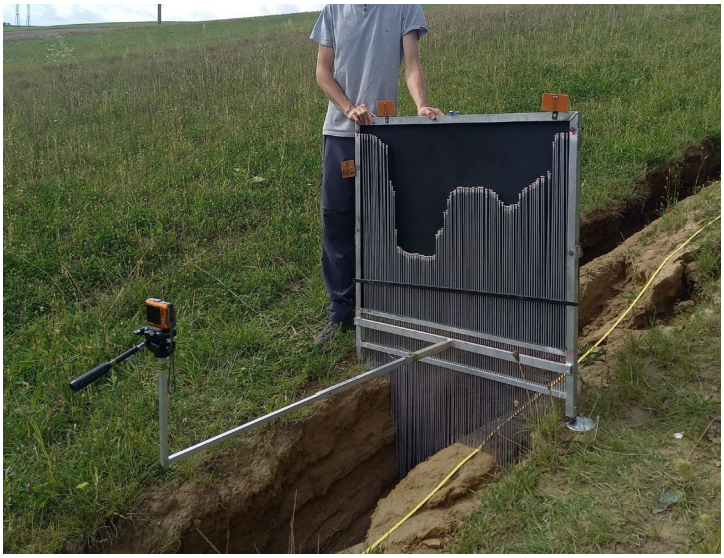


Fig. 4. Measurement using the erosion bridge and its main parts [own source].

https://doi.org/10.5593/sgem2024v/3.2/s11.21

As part of his Bachelor's Thesis [7], Lukáš Dobrovolný, a student at the Faculty of Mechanical Engineering, Brno University of Technology, developed a software program called Erosion bridge using MATLAB. It allows us to evaluate photos and export them to DXF files that can be opened in AutoCAD. The erosion rill in the municipality of Otnice was measured at the length of 145 metres. A total of 23 profiles were measured, initially at 5-metre intervals, then in some places chosen according to the shape and course of the rill (in places where changes occurred). Finally, measurements were taken at 10-metre intervals. This can be also visible in Tab. 1 where Δ [m] indicates the interval in metres.

**RESULTS**

AutoCAD was used to obtain several parameters of the measured profiles. Profiles between those that were measured were subsequently calculated using their average values. For example, the values of the first two profiles were used to get Profile 1–2. Tab. 1 shows the values of parameters of the computed profiles. These are as follows: area (A), wetted perimeter (P), width (B), and maximal depth ($d_{max}$). To calculate the volume, the individual areas were multiplied by the distances. In this way, partial volumes ($V_i$) were obtained. Their sum represents the total volume. It is evident that approximately 8.12 cubic metres of soil was eroded (lost) in the rill.

Tab. 1 Parameters of the computed profiles.

| Profile | Δ [m] | A [$m^2$] | P [m] | B [m] | $d_{max}$ [m] | $V_i$ [$m^3$] |
|---|---|---|---|---|---|---|
| 1–2 | 5.0 | 0.02 | 0.36 | 0.23 | 0.11 | 0.08 |
| 2–3 | 5.0 | 0.10 | 0.94 | 0.45 | 0.33 | 0.49 |
| 3–4 | 2.0 | 0.16 | 1.49 | 0.72 | 0.42 | 0.31 |
| 4–5 | 1.8 | 0.17 | 1.52 | 0.76 | 0.39 | 0.31 |
| 5–6 | 2.2 | 0.18 | 1.60 | 0.82 | 0.47 | 0.40 |
| 6–7 | 5.0 | 0.17 | 1.57 | 0.76 | 0.51 | 0.84 |
| 7–8 | 5.0 | 0.14 | 1.18 | 0.52 | 0.43 | 0.69 |
| 8–9 | 6.0 | 0.13 | 1.09 | 0.36 | 0.45 | 0.77 |
| 9–10 | 6.0 | 0.16 | 1.28 | 0.52 | 0.48 | 0.94 |
| 10–11 | 1.7 | 0.14 | 1.34 | 0.69 | 0.37 | 0.24 |
| 11–12 | 4.3 | 0.14 | 1.43 | 0.61 | 0.39 | 0.60 |
| 12–13 | 1.0 | 0.09 | 1.10 | 0.58 | 0.29 | 0.09 |
| 13–14 | 10.0 | 0.04 | 0.70 | 0.57 | 0.13 | 0.39 |
| 14–15 | 10.0 | 0.02 | 0.54 | 0.46 | 0.09 | 0.24 |
| 15–16 | 10.0 | 0.02 | 0.69 | 0.62 | 0.06 | 0.22 |
| 16–17 | 10.0 | 0.03 | 0.69 | 0.50 | 0.11 | 0.30 |
| 17–18 | 10.0 | 0.02 | 0.54 | 0.37 | 0.10 | 0.20 |
| 18–19 | 10.0 | 0.02 | 0.71 | 0.65 | 0.05 | 0.16 |
| 19–20 | 10.0 | 0.02 | 0.74 | 0.68 | 0.08 | 0.23 |
| 20–21 | 10.0 | 0.02 | 0.80 | 0.72 | 0.08 | 0.20 |
| 21–22 | 10.0 | 0.02 | 0.74 | 0.66 | 0.08 | 0.21 |
| 22–23 | 10.0 | 0.02 | 0.61 | 0.55 | 0.08 | 0.24 |
| | | | | | | **8.12** |

Tab. 2 shows minima, maxima, and averages of the parameters. It is understandable that the minimum of $d_{max}$ is nonsense, hence it is not given.

Tab. 2. Minima, maxima, and averages of the parameters.

| | A [$m^2$] | P [m] | B [m] | $d_{max}$ [m] | $V_i$ [$m^3$] |
|---|---|---|---|---|---|
| MIN | 0.02 | 0.36 | 0.23 | – | 0.08 |
| MAX | 0.18 | 1.60 | 0.82 | 0.51 | 0.94 |
| AVERAGE | 0.08 | 0.98 | 0.58 | 0.25 | 0.37 |

## DISCUSSION

According to the results, the soil loss in the rill was circa 8.12 cubic metres. The bulk density of the soil in the locality is 1.35 grams per cubic centimetre. As a result, approximately 11 tonnes of soil were eroded. The area of locality is about 0.23 hectares, resulting in the soil loss of roughly 35.30 tonnes per hectare.

In reference to related studies or publications, for instance Kubát et al. [8] conducted measurements of erosion rills in paths of concentrated runoff in the Luha and Jičínka catchments. The cross sections were determined at certain distances along their entire length. The result is a calculation of the soil loss from the given path of concentrated runoff. The soil loss for one of these is shown as an illustration of the outcomes. This path was measured at the length of 220 metres. The volume of the rill was computed to be circa 75 cubic metres and total soil loss was determined to be about 75 tonnes. Regarding the comparison with our results, the erosion rill measured by them was much longer and its average width was also larger (about 2.6 metres). Thus, it is understandable that their soil loss was many times greater.

Drongová and Sobotková [9] made measurements of ephemeral gullies in the paths of concentrated runoff in the cadastral area of Šardice (South Moravian Region, Hodonín District). These were formed in a field with a wide-row crop, shortly after it was sown a torrential rainfall event occurred. A total of 13 of these gullies were identified, ranging in length from 100 metres to 870 metres. One of them was almost the same length as the rill we measured (150 metres), but its volume was roughly 25.6 cubic metres. This corresponded to a soil loss of approximately 41 tonnes. Unfortunately, the other parameters of the rills (e.g. width) are not given in this article. Therefore, these results cannot be fully compared with ours.

Dumbrovský et al. [6] carried out volumetric quantification of erosion rills in area of Šardický stream in the cadastral area of Šardice. For this purpose, as previously stated, they designed and developed the erosion bridge. The measurements were taken after each heavy rainfall event, in 2010 three times per growing season on parcels where maize was grown. Two transects were measured along the fall line (in direction of maize sowing). Each transect comprised five square plots of 2 by 2 metres distanced 15 metres from each other. Within each square plot, five transects of 2 metres were measured. This resulted in a calculation of soil loss per 4 square metres and then converted to 1 hectare by calculation. The resulting soil loss was approximately 691 tonnes per hectare for the first measurement, 938 tonnes per hectare for the second, and 977 tonnes per hectare for the third. The results showed that the highest soil loss occurred after the fist rains (up to 71% of the total soil loss), when the wide-row crop (maize) was a low height and thus neither formed any barriers to surface runoff nor mitigated the degrading capacity of the kinetic energy of falling raindrops. However,

https://doi.org/10.5593/sgem2024v/3.2/s11.21

even these results cannot be entirely compared, because the parameters of the rills are not available here either.

## CONCLUSION

The primary objective of this paper was to use the erosion bridge, which was developed at the Institute of Landscape Water Management, Faculty of Civil Engineering, Brno University of Technology, to quantify soil erosion volumetrically. One block of LPIS in the municipality of Otnice, where a deep erosion rill was formed, was selected for the purposes of the paper. It can be found in the South Moravian Region of the Czech Republic, in the Vyškov District, about 20 kilometres southeast of the city of Brno.

The erosion rill was measured at the length of 145 metres. A total of 23 profiles were measured at various distances. Subsequently, the Erosion bridge software program was used to evaluate the photographs of the terrain, and the results were generated as DXF files. Several of parameters of the terrain profiles were acquired in AutoCAD. These are as follows: area, wetted perimeter, width, and maximal depth. In addition, their minima, maxima, and averages were computed. At the end, overall soil loss in the erosion rill was calculated to be approximately 11 tonnes.

The findings and methodology could serve as motivation for additional scientific investigation into soil erosion and volumetric quantification of soil loss due to water erosion on-site.

Erosion risk not only from rill erosion but also from erosion in general can be reduced by implementing soil erosion control measures. These include, among others, grassed anti-erosion strips, contour farming or linear technical features (e.g. broad-base terraces).

## ACKNOWLEDGEMENTS

This paper is a result of a standard research FAST-S-24-8540 “Innovative measurement and modelling in water management for the sustainability of water resources” and was created with the support of state budget by the Technology agency of the Czech Republic and the Ministry of the Environment of the Czech Republic under the Environment for life Programme (Project No. SS06010290).

## REFERENCES

[1] Podhrázská J., Kučera J., Karásek P., Konečná J., Land degradation by erosion and its economic consequences for the region of South Moravia (Czech Republic), Soil and Water Research, Czech Republic, vol. 10, pp 105–113, 2015, DOI https://doi.org/10.17221/143/2014-SWR

[2] Sobotková V., Dumbrovský M., The new volumetric approach for field measurements of rill erosion, Eurasian Journal of Soil Science, Turkey, vol. 4, No. 2, pp 94–99, 2015, ISSN 2147-4249.

[3] Pavlík F., Dumbrovský M., Podhrázská J., Konečná J., The influence of water erosion processes on sediment and nutrient transport from a small agricultural catchment area, Acta Universitatis Agriculturae et Silviculturae Mendelianae Brunensis, Czech Republic, vol. 60, No. 3, pp 155–164, 2011, DOI https://doi.org/10.11118/actaun201260030155

[4] Uhrová J., Bachan R., Štěpánková P., Determination of soil loss from erosion rills by method of digital photogrammetry and method of volumetric quantification, Water Management Technical and Economical Information Journal, Czech Republic, vol. 60, No. 6, pp 34–38, 2018, ISSN 0322-8916, DOI https://doi.org/10.46555/VTEI.2018.09.005

[5] Wells R. R., Momm H. G., Bennett S. J., Gesch K. R., Dabney S. M., Cruse R., Wilson G. V., A Measurement Method for Rill and Ephemeral Gully Erosion Assessments. Soil Science Society of America Journal, United States, vol. 80, pp 203–214, 2016, DOI https://doi.org/10.2136/sssaj2015.09.0320

[6] Dumbrovský M., Sobotková V., Pavlík F., Uhrová J., The volumetric quantification of erosion rills in the catchment area of Šardický stream, Littera Scripta, Czech Republic, vol. 4, No. 1, pp 145–154, 2011, ISSN 1802-503X.

[7] Dobrovolný L. Development of SW for automatic evaluation of photos from measurements using the erosion bridge (Bachelor's Thesis), Brno University of Technology, Czech Republic, 2022.

[8] Kubát J. et al., Evaluation of the floods in June and July 2009 on the territory of the Czech Republic (summary report), Czech Hydrometeorological Institute, Czech Republic, 2009.

[9] Drongová K., Sobotková V., Manifestations of water erosion in paths of concentrated surface runoff, Littera Scripta, Czech Republic, vol. 6, No. 2, pp 151–161, 2013, ISSN 1802-503X.

# WATER RESOURCE EFFICIENCY AND QUALITY MONITORING: A CASE STUDY OF SUCEAVA COUNTY'S DRINKING WATER SYSTEM

**Assoc. Prof. Dr. Anca-Mihaela Gâtlan**
**Assoc. Prof. Dr. Amelia Buculei**
**Prof. Dr. Mircea-Adrian Oroian**
**Assoc. Prof. Dr. Sorina Ropciuc**
**dr.ing. Vasile-Florin Ursachi**
Faculty of Food Engineering/University Ştefan cel Mare of Suceava, **Romania**

## ABSTRACT

Resource efficiency is an important aspect in the efforts to support and evolve economic development, while maintaining all natural systems unaffected. However, resource efficiency cannot guarantee the perpetual use of existing water resources. Water resource efficiency policy must be based on an awareness of the number of resources that can be used, but also the impact of activities on the environment and how it is affected. Developing and increasing the number of consumers. Options for water sources used for drinking water and irrigation will continue to evolve, with a growing dependence on groundwater and alternative sources, including wastewater. This study aims to monitor the quality of water distributed to consumers from Suceava county. The physico-chemical and microbiological analysis of the drinking water in the city was carried out in several strategic points, covering the entire distribution network. Samples were taken both from the catchment wells area and from the storage/storage tanks for drinking water and were analyzed. Physical-chemical parameters (pH, turbidity, conductivity, oxidability, oxidation, etc, free residual chlorine, nitrates, nitrites and ammonium, hardness and in the case of the water station was also performed iron analysis) and microbiological (total number of aerobic mesophilic germs and number of coliform bacteria). The analysis points were chosen according to the way of distribution of water in the city, taking into account its route (7 different points). The day of the week, the time interval, the volume of water consumed, and the number of accidental damages occurred on the distribution network are the factors that influence the values of the analyzed parameters. During the study, there were no exceedances of the maximum concentration allowed by national legislation, for none of the analyzed parameters.

**Keywords:** Groundwater management; Environmental impact; Water distribution network; Water pollution indicators; Sustainable water sources.

## INTRODUCTION

When choosing a water treatment technology, the most important issue is the quality of water intended for the final consumer, with no compromise on quality [1,2]. The World Health Organization (WHO) has issued a framework regulation on drinking water quality standards, from this regulation each country has set its own standards according to living conditions, existing financial resources, respect for the consumer and environmental impact [3]. The second major problem is the raw water source to be treated. Depth waters differ in physico-chemical composition and microbiological load from surface waters [4]. Although they are often superior to characteristics such as

https://doi.org/10.5593/sgem2024v/3.2/s11.22

turbidity, bacteriological content and total organic concentrations, they can have high hardness values, or they may show a charge above the maximum permissible dose of iron, chromium, fluorine, manganese, etc. [5]. Water drinking is the process by which water, surface or deep, is treated physico-chemical and microbiologically to serve human consumption without harming it. The water is carefully monitored throughout the technological flow from the extraction to the consumer tap. At national level, the main law that imposes the quality of drinking water is Law no. 458/2002b [6]. The ways in which drinking water can be obtained differ from one area to another depending on several external factors such as: water type, geographical location, economic conditions, technology used, etc, labor force, dimensions, complexity of processes. Iron is the second most abundant metal in the Earth's crust, of which it accounts for about 5%. In the drinking water supply, iron (II) salts are unstable and are precipitated as insoluble iron(III), which is established as a rust-colored product [7,8]. Anaerobic groundwater may contain iron (II) at concentrations up to several mg/l without discoloration or turbidity. The coloring of water from the taps and plumbing can occur at concentrations above 0.3 mg/l. Iron also promotes unwanted bacterial growth (iron„bacteria") within a water plant and distribution system, which results in the deposition of a thin layer on the transport pipes [9,10,11]. The main objective is to continuously monitor the water quality that will distribute to consumers.

## MATERIALS AND METHODS

At the level of the City of Suceava, the water supply for the subscribers (about 96% of the urban population) is realized through a centralized system, through a branching network of pipes of different construction (steel, asbestos-cement, polyethylene). The water source used for distribution is only the water captured from the Berchisesti area (deep water) in a perimeter located on the left side of the river Moldova upstream. The perimeter includes a number of 75 catchment wells from the aquifer layer of the river Moldova, with a depth of 18-20 meters. The catchment perimeter is divided into two areas, located about 4 km from each other, being built in proportion to the level of consumption in the Suceava area. At the city level, the distribution network has an approximate length of 233.6 Km, plus the private network portions, used only for water transport by consumers. Every day, physico-chemical analyses of the following pH parameters, turbidity, residual chlorine, color, odour, total hardness, iron, oxidability, conductivity, nitrites, nitrates, ammonium are performed. In order to carry out the water study, were taken and analyzed according to SR ISO 5667-5:2017, samples from several points on the Suceava City network. PH determination - indicates the alkaline or basic character of the water at the time of the analysis. The pH value is determined using the electronic multi-meter. The electromotive force corresponding to the sample, a reference electrode and a glass electrode varies linearly with the pH value. (the analysis method is in accordance with SR EN ISO 10523:2012) [12]. The turbidity of the water in the network was analyzed using the electric turbidimeter, the recorded value was 1.8 degrees, while the maximum permissible limit is 5 degrees. Determination of Total Chlorine - SR EN 16693:2016 consists of the reaction with DPD (N,N-diethylphenylene-1,4-diamine) in the presence of potassium iodide, then follows the titration with ammonium and iron sulfate until the color disappears. It was carried out both in the Berchisesti plant and in the Saint Elijah plant. The water pumped from the capture wells is chlorinated with gaseous chlorine from the departure from Berchisesti to Suceava. Determination of electrical conductivity. The realization of the experiment

is done with the electronic multimeter, which has the ability to determine in successive stages for the same sample temperature, pH and electrical conductivity [13]. The determination of Nitrites, Nitrates and Ammonium is made by using the spectrophotometer at different wavelengths by interpolating the result on the calibration curve. Nitrite/nitrite - read absorbance at 650nm in 1cm bowl. Determination of iron is carried out using the Merck kit [14]. The first step is to make a colorimetric scale, in a series of 10 test tubes where the following standard solutions for Iron (100.0 mg/l Fe NIST) are introduced. (Tab.1) For primary analyses the colorimetric scale has been extended, although the AAC is 0.2 mg/l.

**Table nr.1** Making the colorimetric scale

| **Nr.test tube** | **1** | **2** | **3** | **4** | **5** | **6** | **7** | **8** | **9** | **10** |
|---|---|---|---|---|---|---|---|---|---|---|
| Nr. ml. | 0 | 0,05 | 0,10 | 0,15 | 0,20 | 0,25 | 0,30 | 0,35 | 0,40 | 0,45 |
| Concentration | 0 | 0,05 | 0,10 | 0,15 | 0,20 | 0,25 | 0,30 | 0,35 | 0,40 | 0,45 |

6. Determination of the hardness of drinking water consists of complexometric titration of Ca and Mg ions with an aqueous solution of EDTA 0,01m (at pH=10). Complecșii care se formează sunt nedisociabili, solubili și incolori. Use the Ericrom T indicator (mordant black 11) that will lead to the color turning to intense purple or red, and at the end of the reaction the color will turn to blue [14]. The turbidity of the water in the network was analyzed using the electric turbidimeter.

## RESULTS

The scale of the pH value is between the value 1 and 14, in the middle, for the value 7 (7 moles/liter), the ideal neutral point is considered. Hydrogen potential or pH of a solution is the value of the reverse sign decimal logarithm of hydrogen ions. According to the national rules in force, the pH value must be within the range of 6.5-8. Exceeding the minimum value indicates an acidic character, this indicates the possibility of corrosive action on the transmission pipelines and the distribution facility. Water with a pH value greater than 9.5 does not pose a risk to consumer health, but may cause stone deposits on transport facilities. Determination of water color - Water distributed to consumers must be inodorous, insipid and colorless, any small deviation from these characteristics is a quality indicator. If the water has a differentiated taste or smell from normal, it is advisable not to consume it until the identification and remediation of the causes. Following laboratory analysis, the mean turbidity value was 1.8 degrees, the maximum permissible concentration being 5 degrees. Following the study of the free residual value at the 13 work points, the following values were obtained, show in Fig. 2. According to national legislation, the concentration of free chlorine found in drinking water after chlorination should be between 0.1 and 0.5 mg/liter, the results showed values close to the maximum.

https://doi.org/10.5593/sgem2024v/3.2/s11.22

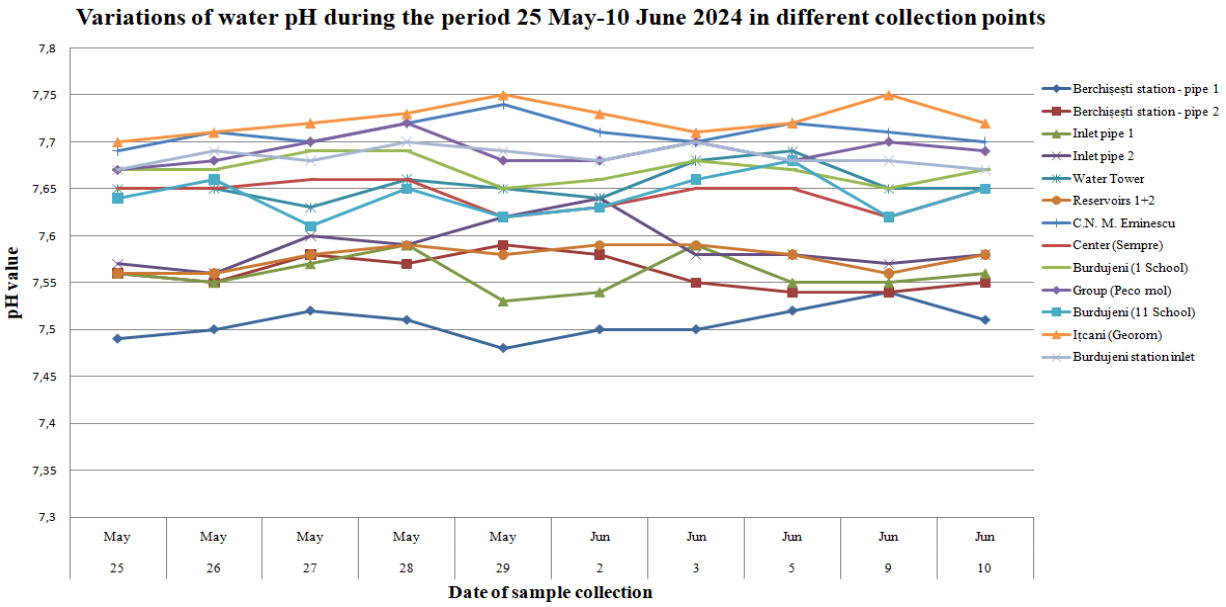



**Fig. 1.** Graphical representation of variations of water pH during the period 25 May-10 June 2024 in the distribution network

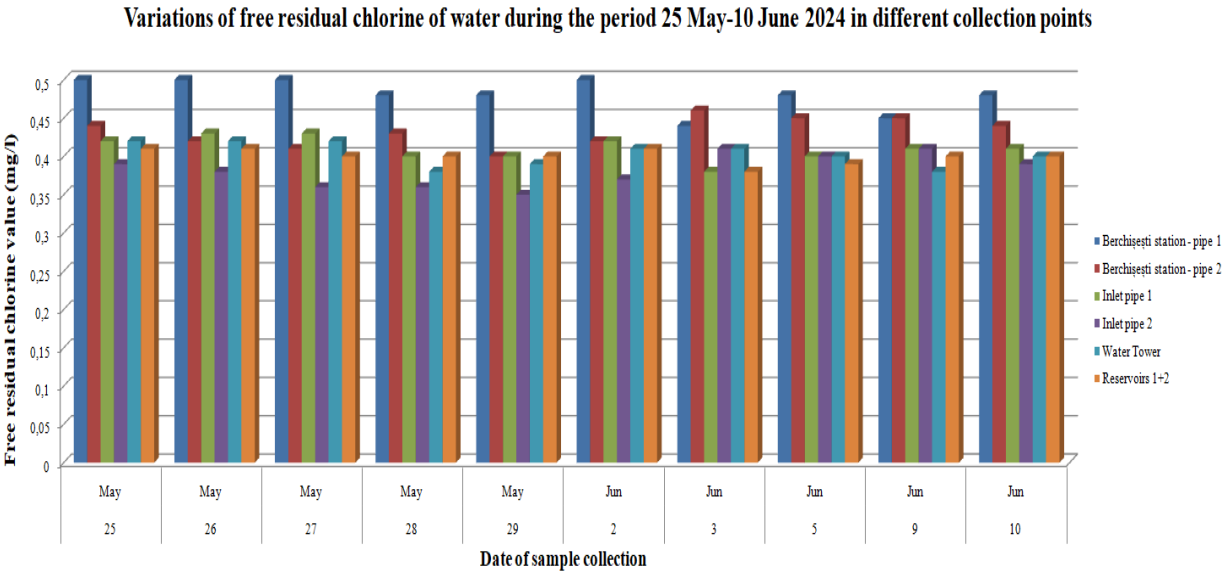



**Fig. 2.** Graphical representation of the variation of residual chlorine during the period 25 May-10 June 2024 in the water distribution network

Following the study of the electrical conductivity value at the 13 working points, the following values were obtained, shown in Fig. 3. The values obtained for conductivity indicate an optimal level of mineral substances without exceeding the maximum permissible amount. Experimentally obtained values are within the range of 465-495 mg/l. A high electrical conductivity value indicates a higher amount of minerals dissolved in water. Depending on the recorded consumption, the amount of chlorine will be determined. Residual chlorine values in the distribution network vary depending on the distance from the tank to the consumer, from the time at which the sample was taken for analysis and the time of stagnation of water in the pipeline until it is used by the consumer.

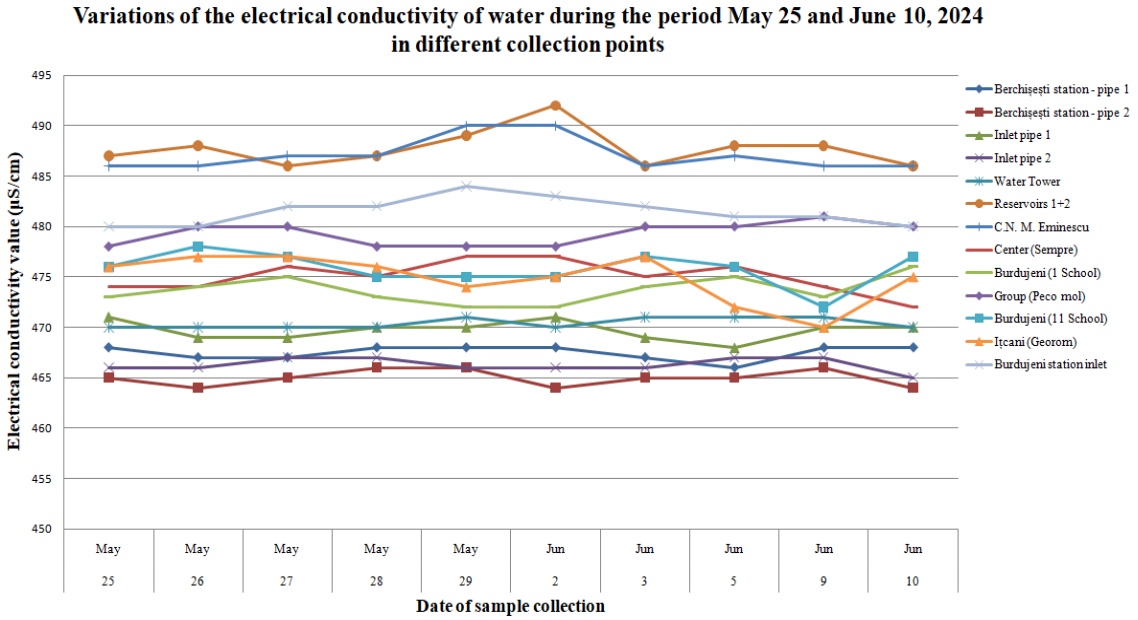



**Fig. 3.** Graphical representation of the variation of electrical conductivity during the period 25 May-10 June 2024 in the water distribution network

**Table 2.** Values of nitrates, nitrites and ammonium

| **Punct de recoltare** | 25 -28 May | 29.05 | 2.06 | 3.06 | 5.06 | 9.06 | 10.06 |
|---|---|---|---|---|---|---|---|
| Berchișești station - pipe 1 | 0 | 0 | 0 | 0 | 0 | 0.01 | 0.01 |
| Berchișești station - pipe 2 | 0 | 0 | 0 | 0 | 0 | 0.01 | 0.01 |
| Inlet pipe 1 | 0 | 0 | 0 | 0 | 0 | 0.01 | 0.01 |
| Inlet pipe 2 | 0 | 0 | 0 | 0 | 0 | 0.01 | 0.01 |
| Water Tower | 0 | 0.01 | 0 | 0 | 0 | 0.01 | 0.01 |
| Reservoirs 1+2 | 0 | 0.01 | 0 | 0 | 0 | 0.01 | 0.01 |
| C.N. M. Eminescu | 0 | 0 | 0 | 0 | 0 | 0.01 | 0.01 |
| Center (Sempre) | 0 | 0 | 0 | 0 | 0 | 0.01 | 0.01 |
| Burdujeni (1 School) | 0 | 0 | 0 | 0 | 0 | 0.01 | 0.01 |
| Group (Peco mol) | 0 | 0 | 0 | 0 | 0 | 0.01 | 0.01 |
| Burdujeni (11 School) | 0 | 0.01 | 0 | 0 | 0 | 0.01 | 0.01 |
| Ițcani (Georom) | 0 | 0 | 0 | 0 | 0.02 | 0.01 | 0.01 |
| Burdujeni station inlet | 0 | 0.1 | 0 | 0 | 0.02 | 0.01 | 0.01 |

Maximum limit allowed: Nitrate 50 mg/l; Nitrite 0,5 mg/l; Ammonium 0,5 mg/l.

**Table 3.** The values obtained for iron determination

| | **Date of sample collection** | |
|---|---|---|
| | **CMA 0,2 mg/l** | |
| **Collection point** | **28 mai** | **5 iun** |
| Berchișești station - pipe 1 | 0 | 0.02 |
| Berchișești station - pipe 2 | 0 | 0.02 |

https://doi.org/10.5593/sgem2024v/3.2/s11.22

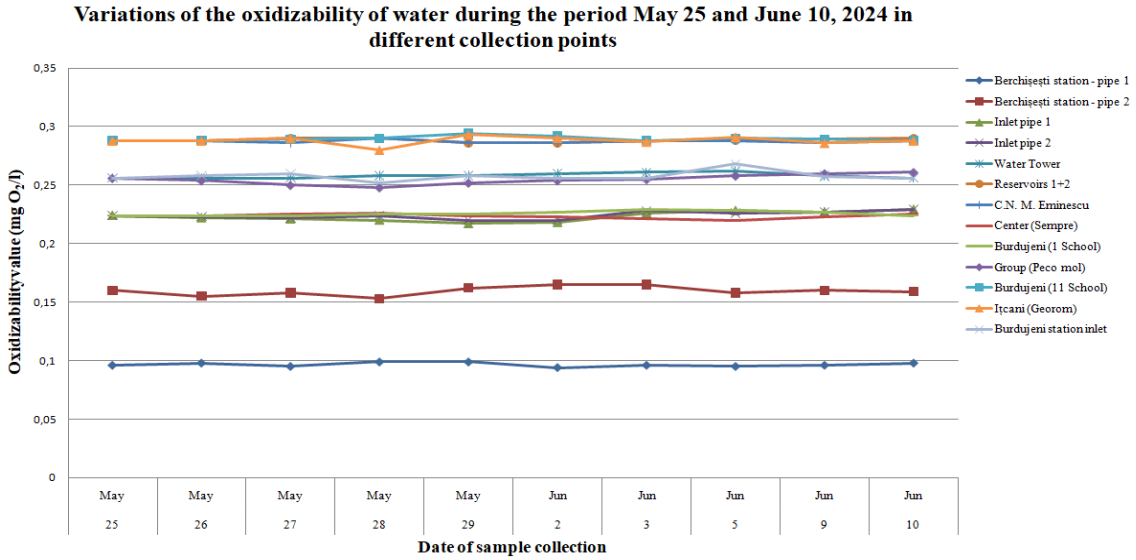



**Fig.4.** Graphical representation of the variation of water oxidizability in the period 25 May-10 June 2024 in the water distribution network

## DISCUSSION

From the two graphs presented, it is noted that the water distributed to consumers in the city of Suceava falls within the limits of 7.5-7.75. The pH differences are due to the water quality in the Berchişeşti area in the catchment wells area being due to the transport time, the time of sampling and the water level in the wells. Depending on the consumption on the distribution network, operators will stop or start pumps so as to achieve a balance between the amount of water entering/exiting from the tanks. The entire system is monitored by the SCADA system, shown in Fig.nr.5. Nitrate and nitrites in drinking water can have negative effects on human health, while ammonium is not of direct importance to human health.

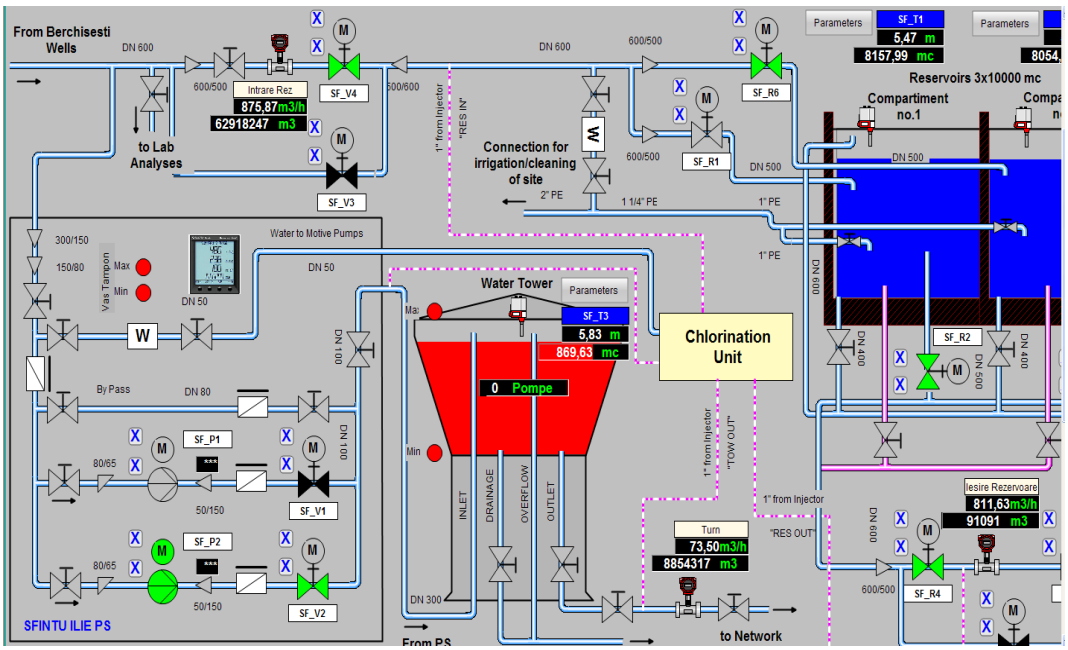



**Fig.5.** Sistemul de monitorizare al apei

The values established by law for the maximum permissible limits of the three parameters are: for nitrates, the CMA value is 50 mg/l, for nitrites the CMA value is 0.5 mg/l, for nitrites, and for ammonium CMA is 0.5 mg/l [15]. Although nitrate concentration may not vary seasonally, a greater number of samples will provide more accurate information about the quality of water reaching the consumer. The analysis carried out at the Berchisesti water plant showed that there is no iron in the deep water. Thanks to the distribution network made of steel, it is possible to find a small amount of iron ions in the water distributed to consumers. The water color did not register deviations from the standards, in all the cases analyzed the water was compliant, presenting total transparency without any suspension or smell. Evidence of color variation in areas where it was intervened to remedy accidental failures was reported on the water network. The situation was urgently remedied by the company's operators by performing network washes at the zonal hydrants, or emptying the indoor facilities at the affected blocks and recharging with clean water. The main source of capture being groundwater, increases the degree of clarity, and makes the water subjected to laboratory analysis not absorb a large amount of the emitted light beam. The small value of the turbidity parameter is a lower possibility of microbiological contamination, since the lack of suspended particles will not be a convenient substrate for the development of pathogens. Laboratory values for all oxidable substances found in drinking water or CCO-Chemical Oxygen consumption after the tests are between 0.095 and 0.290 well below the maximum allowable limit (5,0 mg O2/L) [15]. The values obtained for conductivity fall within the values of 465-495 mg/l and indicate an optimal level of mineral substances without exceeding the maximum permissible amount. According to the differentiation parameters, the water of Suceava can be classified in the water catheter with high rigidity, this being due to the geomorphological characteristics of the soil in the area of the Berchisesti capture wells. Groundwater has the ability to dissolve and retrieve Ca and Mg ions from the soil, which are directly responsible for the quality and characteristics of water.

## CONCLUSION

The performance and quality of the product distributed to domestic and industrial consumers must be monitored on an ongoing basis to ensure that a product conforms to standard 485/2002 is guaranteed. In this study, a chemical physico analysis of the water in the city was carried out at several strategic points, covering the entire distribution network. Samples were taken both from the catchment well area and from the storage/storage tanks of drinking water. The day of the week, the time interval, the volume of water consumed and the number of accidental damage occurred on the distribution network are the factors that influence the values of the analyzed parameters. During the study period, the maximum permissible concentration for none of the analyzed parameters were recorded. Drinking water should be suitable for human consumption and for all common internal purposes. When an indicative value is exceeded, the case must be investigated and corrective action taken as a matter of urgency. If important parametrically exceeded that can endanger the health of the consumer, the supply of drinking water will be interrupted until the situation is remedied. Once the situation has been remedied, operators will perform column washes and hygiene of the pipe where appropriate. In developing national standards for drinking water quality, it will be necessary to take into account various local, geographical, socio-economic and cultural factors. Safe quality for water supplied to

https://doi.org/10.5593/sgem2024v/3.2/s11.22

communities is important, in terms of protection of human health and well-being, for this reason, periodic monitoring is required to comply with the legislation in force.

## REFERENCES

[1] Jiang J., Zhang X., Wen G., Zhu M., Zheng Y., Purification Resistance Index: A new water quality assessment method toward drinking water production, Water Research, Volume 267,122555, ISSN 0043 1354,

https://doi.org/10.1016/j.watres.2024.122555, 2024

[2] Baroudi H., Ouazzani C., Moustaghfir A., Er-Ramly A., Essebbahi I., Youssef El Baroudi, Abdallah Dami, Lhousaine Balouch, Evaluation of drinking water quality and potential health risks on the population in Morocco, Desalination and Water Treatment, Volume 320, 100715, https://doi.org/10.1016/j.dwt.2024.100715., 2024

[3] Eid M., H., Mikita V., Eissa M., Ramadan H., S., Mohamed A., Abukhadra M., El-Sherbeeny A., Kovács A., Szűcs P., An advanced approach for drinking water quality indexing and health risk assessment supported by machine learning modelling in Siwa Oasis, Egypt,Journal of Hydrology: Regional Studies,Volume 56,101967,ISSN 2214-5818,https://doi.org/10.1016/j.ejrh.2024.101967., 2024.

[4] Gutiérrez-Capitán M., Brull-Fontserè, M., Jiménez-Jorquera, C., „Organoleptic Analysis of Drinking Water Using an Electronic Tongue Based on Electrochemical", https://www.ncbi.nlm.nih.gov/pmc/ articles/PMC6471140/), 2019.

[5] Connolly, D., Paull, B. „Rapid determination of nitrate and nitrite in drinking water samples using ion-interaction liquid chromatography", Analytica Chimica Acta, 441(1), 53–62. (https://www.sciencedirect.com/science/ /S0003267001010686), 2001.

[6] „Guidelines for drinking-water quality", 2nd ed. Vol. 2. Health criteria and other supporting information. World Health Organization, Geneva, (https://www.who.int/water_sanitation_health/dwq/chemicals/iron.pdf), 1996.

[7] Shokoohi, M.; Tabesh, M.; Nazif, S.; Dini, M. Water quality based multi-objective optimal design of water distribution systems. Water Resour. Manag., 31, 93–108. 2017

[8] Ling, F.; Whitaker, R.; LeChevallier, M.W.; Liu, W.-T. Drinking water microbiome assembly induced by water stagnation. ISME J. 2018, 1.

[9] Zhang, L.; Liu, S.; Liu, W. Investigation of organic matter migrating from polymeric pipes into drinking water under different flow manners. Environ. Sci. Process. Impacts 16, 280–290. [Google Scholar], 2014

[10] WHO. Copper in Drinking-Water: Background Document for Development of Who Guidelines for Drinking-Water Quality; WHO: Geneva, Switzerland,2004

[11] Prest, E.I.; Hammes, F.; van Loosdrecht, M.; Vrouwenvelder, J.S. Biological stability of drinking water: Controlling factors, methods, and challenges. Front. Microbiol., 7, 45, 2016

[12] Inkinen, J.; Kaunisto, T.; Pursiainen, A.; Miettinen, I.T.; Kusnetsov, J.; Riihinen, K.; Keinänen-Toivola, M.M. Drinking water quality and formation of biofilms in an office building during its first year of operation, a full-scale study. Water Res., 49, 83–91, 2014.

[13] Gholson, Drew M., et al. "Consumer water quality evaluation of private and public drinking water sources." Journal of Water and Health 16.3: 369-379, 2018.

[14] Zlatanović, Lj, Jan Peter van der Hoek, and J. H. G. Vreeburg, "An experimental study on the influence of water stagnation and temperature change on water quality in a full-scale domestic drinking water system" Water research 123: 761-772, 2017.

[15] Gray, John, "Water contamination events in UK drinking-water supply systems" Journal of water and health, 6.S1 (2008): 21-26.

https://doi.org/10.5593/sgem2024v/3.2/s11.22

# SECTION

# MARINE, OCEAN, AND COASTAL ECOSYSTEMS.

# BLUE CARBON

# EVALUATION OF THE SURFACE WATER QUALITY PARAMETERS OF THE SF. GHEORGHE BRANCH - DANUBE DELTA, ROMANIA

**Dr. Irina Catianis**
**Dr. Ana Bianca Pavel**
**Dr. Florin Duțu**
**MSc. Cătălina Gavrilă**
**Ovidiu Borzan**
National Research and Development Institute for Marine Geology and Geoecology, GeoEcoMar, **Romania**

## ABSTRACT

Generally, water quality involves the water's physical-chemical and biological attributes that depend on the natural surrounding environment and anthropogenic impacts. Through the years, the river water quality in the Sf. Gheorghe Branch has been subjected to various hydro-sedimentary impacts, due to the anthropogenic meander cut-off plans initiated for navigational objectives. In this study, the Sf. Gheorghe Branch water quality evaluation was performed using in-situ observations, measurements, and datasets provided by EXO Water-Quality Sondes and Sensors, during May 2024, a period defined by the high-water levels of the Danube River. Thereby, surface water quality parameters. *i.e.,* water temperature (°C), pH (unit.), dissolved oxygen (mg/L), dissolved oxygen saturation (%), chlorophyll "a" (µg/L), electrical conductivity (µS/cm), total dissolved solids (mg/L), salinity (psu), turbidity (NTU) and oxidation-reduction potential (mV) were evaluated immediately in-situ, at each site location. The results were plotted spatially as binary diagrams and corroborated with the national and international water reference standards to estimate the water quality status. The longitudinal distribution (along the upstream-downstream gradient) of the investigated water quality parameters along the entire Sf. Gheorghe River water (km 85 – km 15) has been identified as suitable for biodiversity, natural ecosystem assets, and ecological processes. In the context of high-water levels of the Danube River (May 2024), the obtained results complied with the imposed limits provided for the water quality criteria (Very Good and Good). The importance of this study may be considered as an approach to yield a basis for water quality assessment. Subsequently, these contributions may be used to water management strategies to overcome the insidious challenges to which the ecosystems of the Danube Delta are subjected.

**Keywords:** Danube River, dissolved oxygen**,** environmental, physical-chemical parameters, surface water quality

## INTRODUCTION

Freshwater is the basis for supporting ecology and biodiversity life on Earth, being essential for environmental sustainability, *i.e.,* socio-economic development, beneficial freshwater ecosystems, and human health [1]. In the context of continuous urban expansions and previously intense industrializations, emerging environmental issues could impact the water quality status [2]. River water sources are triggered by natural factors (climate conditions, geological background) and human-related activities

https://doi.org/10.5593/sgem2024v/3.2/s14.23

(agricultural runoff, effluents, sewage, urban wastewaters) manifesting in the river's catchments [3]. As the world's most international river basin, passing through or bordering ten European countries, including four capital cities, the Danube River collects considerable amounts of residential, industrial, and agricultural waste, chemical manufacturing pollutants, and municipal effluent discharges, all of which deteriorate its water quality [4]. Over time, several scientific studies have been dedicated to a comprehensive assessment of the quality of the Danube River to yield relevant information related to sustainable development (economic growth, social development, and environmental protection) of its natural freshwater ecosystems (water, sediment, and biota) [5, 6, 7]. The Danube River is an integral part of an extensive European geo-system, incorporating the Danube River – Danube Delta – Black Sea. The Danube River stretches out into its delta by three main distributaries *i.e.,* Chilia, Sulina, and Sf. Gheorghe. The Sf. Gheorghe distributary (112 km in length; transporting 22% of the upstream Danube's flow) is the oldest branch of the Danube River. Due to a higher channel river sinuosity, the Sf. Gheorghe Branch has undergone a major transformation linked to its size, lessening now to 70 km of navigable water. The artificial meander cut-offs planned to improve navigability induced significant changes related to the water discharge and sediment flux variations among the delta distributaries [8]. Generally, the negative environmental impact of artificial meander cut-offs is marked by a series of morphodynamical processes *i.e.,* reducing channel sinuosity, modifying rates of lateral migration, and affecting floodplain sedimentology, erosion downstream, and reducing sediment deposition in delta regions [9, 10]. Moreover, the meander cut-offs are subject to flow pattern modifications of rivers, water level fluctuations, impairing water quality status (nutrient distribution and oxygen levels) [11, 12], and habitat biodiversity. Therefore, this study aimed to assess the water quality status of the Sf. Gheorghe Branch, appealing to the main physical-chemical parameters of surface water. Subsequently, the resulting contributions may be used to water management strategies to overcome the insidious challenges to which the ecosystems of the Danube Delta are subjected.

## MATERIALS AND METHODS

**Study area.** The areas investigated in this study are located in the fluvio-marine delta plain of the Danube Delta, Romania. The aquatic ecosystems associated with the Danube Delta Biosphere Reserve demand cyclic environmental assessment and protection considering that these environments have been internationally acknowledged, *i.e.,* World Heritage Site, UNESCO Biosphere Reserve and Ramsar Site [13]. Over long-time scales, the cutoff perturbations along the Sf. Gheorghe Branch (1984-1988) may influence the upstream and downstream hydrodynamic change (velocities, discharge, sediment fluxes and water quality) through the active Danube's distributary [14]. To identify some specific water environmental indicators' longitudinal distribution (along the upstream-downstream gradient), sampling was carried out in a particular sector of the Sf. Gheorghe Branch from km 85 to km 15, including: *Mahmudia Meander, Uzlina Lake, Isac Lake, Dunavăț Meander, Dranov Meander, Ivancea Meander etc.* (Fig. 1). The investigated sampling sites are intensely influenced by the active hydrodynamic conditions of the Danube River alluvial input (flow velocity, discharge, water disturbances). Moreover, they could be vulnerable to various upstream Danube pollution sources, including local intensive fluvial transport and shipyard activities along the water course. Certain sampling sites represent the main

redistribution waterways of the Danube fluvial input (water and sediments) through the principal (the Danube branches) and secondary hydrographic network (canals, tributaries, etc.) to the inter-depression areas of the Danube Delta (lakes, swamps, etc.).

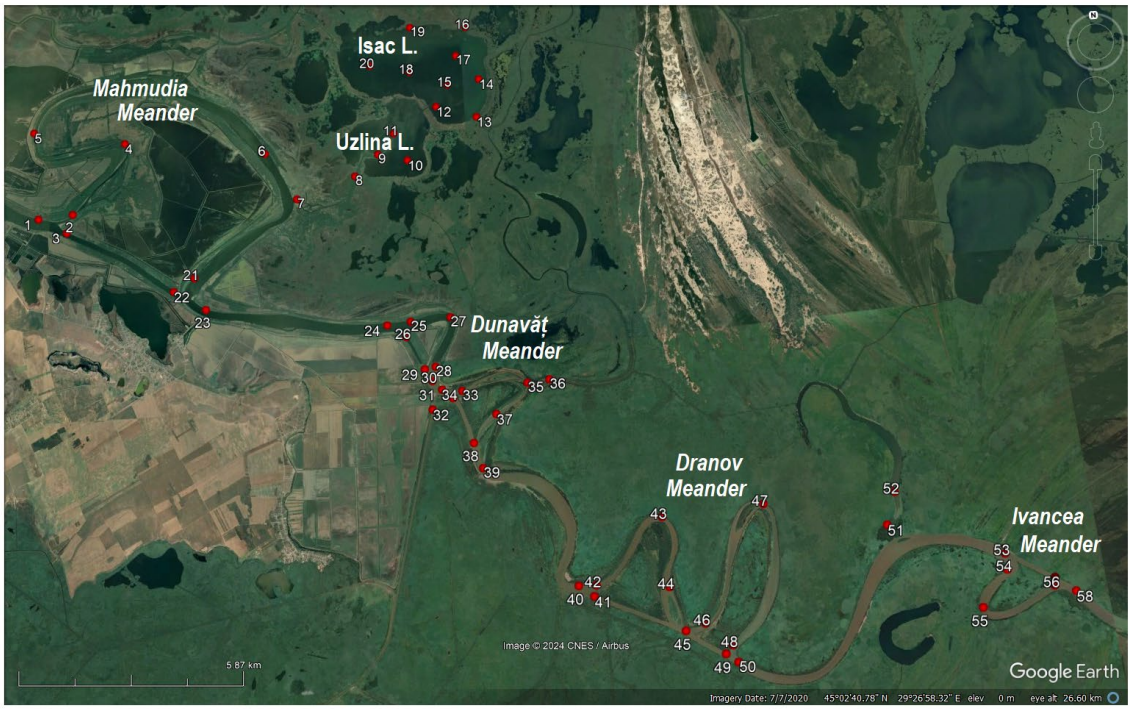



Fig. 1. Map of the Sf. Gheorghe Branch (km 85- km 15) showing the location of the sampling sites (displayed in red marks)

**Data collection.** A total number of 58 water sampling sites were investigated during the wet season (May 2024) a period marked by the high-water level of the Danube River. The overall characterization of the surface water quality in the investigated sections, in terms of the physical-chemical properties, was carried out based on data and information obtained from *in situ* measurements. A series of indicators were analyzed on-site using the EXO 2 (YSI – USA) pre-elevator, a multiparameter instrument that collects data on water quality. The EXO probe collects data using various sensors, each measuring parameters through a variety of physical, optical, electrochemical, and other detection methods. Thus, parameters such as water temperature (°C), pH (units), dissolved oxygen (mg/L), saturated oxygen (%), chlorophyll "a" (µg/L), electrical conductivity (µS/cm), total dissolved solids (mg/L), salinity (psu), turbidity (NTU), and redox potential (mV) have been estimated immediately on-site. The assessment of water quality was primarily based on the current national legislation [15], establishing: Class I (very good status), Class II (good status), Class III (moderate status), Class IV (poor status), Class V (bad status), as well as by other reference standards (both national and international) available in the specialized literature.

## RESULTS AND DISCUSSION

The analysis results of the main physical-chemical parameters are presented below (Table 1). The graphical representation of the evolution of the investigated physical-chemical parameters (compliant or non-compliant) at the previously mentioned locations is shown in the form of binary diagrams (*i.e.,* Fig. 2). In general, the

https://doi.org/10.5593/sgem2024v/3.2/s14.23

measured/analyzed physical-chemical parameters in specific monitoring sections along the Sf. Gheorghe Arm (km 85 – km 15): *Mahmudia Meander, Uzlina Lake, Isac Lake, Dunavăț Meander, Dranov Meander, Ivancea Meander*, etc., show comparable values. Overall, no significant increases or decreases were recorded, except for some isolated cases, which will be presented further.

**Water Temperature (°C).** Water temperature is generally closely related to air temperature trends, which are characteristic of the spring season. The values obtained fell within the natural variability limits of the investigated areas, ranging within a relatively narrow interval (16.31-20.30; mean=18.50). The lowest value was recorded at station *SG-1-24-P36* (*Perivolovca Stream*), while the highest was at station *SG-1-24-P19* (*Isac L.*).

**The pH of the water (pH units)**. The values obtained classify the tested water from most samples investigated within the normal pH range (6.5-8.5 pH units). However, it is noted that the pH reaction of the tested water in *Isac L.*, falls within a range that occasionally trends towards a slightly alkaline pH. The variation range of the values was relatively narrow (8.06-9.42; mean=8.58), with the lowest value found at station *SG-1-24-P36* (*Perivolovca Stream*), and the highest value measured at station *SG-1-24-P16* (*Isac L.*).

**The dissolved oxygen regime (mg/L)** classifies the tested water from the monitored sections into the category of well-oxygenated surface waters (quality class I) (9 mg/L) [15]. The concentrations of dissolved oxygen (measured in all evaluated water samples) were above the value of 5 mg/L. A minimum concentration of 5 mg/L of dissolved oxygen is recommended to support aquatic life. The range of values shows a relatively wide variation (6.82-14.81; mean=10.67), with the lowest value found at station *SG-1-24-P36* (*Perivolovca Stream*) and the highest value measured at station *SG-1-24-P19* (*Isac L.*) (Fig. 2).

**The concentration of chlorophyll "a"** measured in the samples from the investigated control sections varies within a relatively wide range (0.26-8.57; mean= 3.93). The lowest value was found at station *SG-1-24-P20 (Isac L.)*, while the highest value was measured at station *SG-1-24-P46* (*Dranov de Jos Meander-bifurcation-rectified meander*). Based on the results obtained, it was observed that most samples had values below the limit (25 µg/l) corresponding to Class I quality (very good status) [15].

**The level of electrical conductivity** categorizes the tested water from all investigated samples into class I quality (500 µS/cm) [15]. The range of values was relatively narrow (254.11-382.14; mean=331.19), with the lowest value recorded at station *SG-1-24-P16 (Isac L.)* and the highest value measured at station *SG-1-24-P51 (Erenciuc C.)*.

**The concentration of TDS** (total dissolved solids, both organic and inorganic) classifies the tested water as being in good condition (values corresponding to freshwater = 0-1000 mg/L TDS) [16, 17]. The range of values was relatively narrow (182.36-290.38; mean = 246.02), with the lowest value recorded at station *SG-1-24-P16 (Isac L.)* and the highest value measured at station *SG-1-24-P52 (Erenciuc L.).*

Table 1. Results of the physical-chemical parameter measurements of the investigated sites

| No. Crt. | Location Sf. Gheorghe Arm | | Values | Temp. (ºC) | pH (unit.) | $O_2$ (mg/L) | $O_2$ (%) | Chla (µg/L) | EC (µS/cm) | TDS (mg/L) | Sal. (psu) | Turb. (NTU) | ORP (mV) |
|---|---|---|---|---|---|---|---|---|---|---|---|---|---|
| 1 | km 85 – km 60 | Mahmudia Meander (n = 9) | *Min.* | 17.84 | 8.40 | 9.58 | 101.30 | 3.79 | 330.89 | 245.58 | 0.18 | 8.05 | 33.33 |
| | | | *Max.* | 18.68 | 8.58 | 10.70 | 114.65 | 5.16 | 336.09 | 251.35 | 0.19 | 11.55 | 39.63 |
| | | | *Mean* | 18.15 | 8.49 | 10.11 | 107.17 | 4.27 | 332.75 | 248.89 | 0.18 | 10.10 | 37.21 |
| 2 | Inter-distributary area | Uzlina L, Isac L. (n = 14) | *Min.* | 18.79 | 8.46 | 10.32 | 111.07 | 0.26 | 254.11 | 182.36 | 0.13 | 0.18 | 1.74 |
| | | | *Max.* | 20.30 | 9.42 | 14.81 | 163.92 | 2.91 | 336.95 | 248.67 | 0.18 | 33.42 | 27.14 |
| | | | *Mean* | 19.47 | 8.77 | 12.10 | 131.91 | 1.01 | 310.03 | 225.51 | 0.16 | 7.01 | 17.86 |
| 3 | km 60 – km 48 | Dunavăț Meander (n = 16) | *Min.* | 16.31 | 8.06 | 6.82 | 69.66 | 0.45 | 332.59 | 247.80 | 0.19 | 1.73 | 35.24 |
| | | | *Max.* | 18.47 | 8.57 | 10.40 | 111.02 | 5.66 | 354.37 | 276.06 | 0.21 | 16.00 | 49.14 |
| | | | *Mean* | 18.13 | 8.49 | 9.94 | 105.38 | 4.51 | 338.66 | 253.43 | 0.19 | 10.63 | 38.74 |
| 4 | km 42 – km 15 | Dranov Ivancea (n = 19) | *Min.* | 17.35 | 8.18 | 9.26 | 97.18 | 1.86 | 330.55 | 246.83 | 0.18 | 2.28 | 33.38 |
| | | | *Max.* | 18.94 | 8.73 | 12.08 | 129.26 | 8.57 | 382.14 | 290.38 | 0.22 | 57.55 | 100.96 |
| | | | *Mean* | 18.26 | 8.56 | 10.51 | 111.60 | 5.43 | 339.74 | 253.53 | 0.19 | 13.85 | 61.87 |

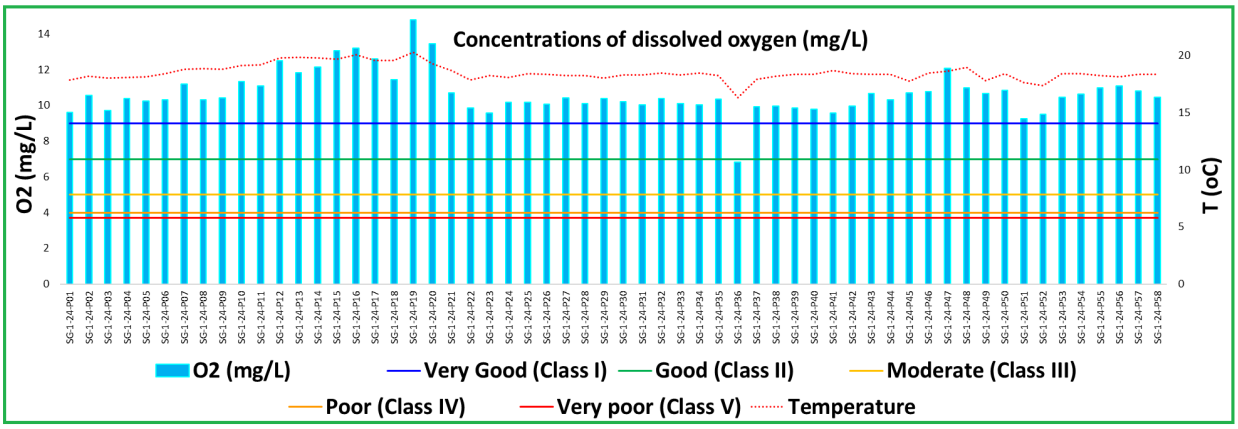



Fig. 2. Spatial variation of DO (mg/L) in the investigated sampling stations

**Salinity Level (‰)** – The water samples investigated showed salinity values ranging from 0.13 to 0.22 ‰ (mean=0.18). These values indicate freshwater surface waters with low salinity (salinity below 0.5‰), characteristic of the transitional fluvial domain [18].

**Turbidity (NTU)**. The turbidity values measured in water samples taken from control sections show a range of variations that fall within the normal range for surface waters (1-1000 NTU) [19]. The range of values was relatively wide (0.18-61.61; mean=11.42), with the lowest value found at station *SG-1-24-P20 (Isac L.)* and the highest measured at station *SG-1-24-P42* (*Dranov de Sus Meander-bifurcation-rectified meander*). However, relatively higher values were observed in several samples, indicating a deterioration in water quality from this perspective. Overall, the increase in turbidity values is attributed to the contributions from the Danube River (water and sediments) loaded with dissolved or suspended organic/inorganic substances, which propagate through the secondary network of ditches and internal channels.

**The oxidation-reduction potential (ORP) (mV)** places the tested water in a good state. The values obtained for the tested water samples fall within the natural water ORP range (with values between -500 and +700 mV) [19, 20]. The variation range was in the positive spectrum (1.74-100.96; mean=41.04), with the lowest value found at station

https://doi.org/10.5593/sgem2024v/3.2/s14.23

*SG-1-24-P19 (Isac L.)* and the highest value measured at station *SG-1-24-P58 (Ivancea Meander-confluence-main branch)*.

A range of physical-chemical parameters (water temperature, pH, dissolved oxygen, chlorophyll "a," electrical conductivity, total dissolved solids, salinity, turbidity, and redox potential) were considered to determine the water quality status in the investigated control sections.

The determination and interpretation of the results obtained were carried out using methods outlined in reference standards. Overall, no significant increases or decreases were recorded, except for some isolated cases primarily attributable to local conditions of the transitional environmental medium (riverine and lacustrine).

The results generally fall within the limits of the first quality classes (Very Good Status, Good Status). Therefore, the investigations did not record evident or significant variations regarding:

• *Water temperature (°C):* Seasonal fluctuations within natural variability limits;

• *Water pH (pH units):* Neutral to slightly alkaline pH, depending on local conditions of the transitional riverine and lacustrine environment (Good Status);

• *Dissolved oxygen regime (mg/L):* Well-oxygenated surface waters (values>5 mg $O_2$/L) (Very Good Status);

• *Chlorophyll "a" concentration (µg/L):* Values corresponding to Quality Class I (25 µg/L) (Very Good Status);

• *Electrical conductivity level (µS/cm):* Values corresponding to Quality Class I (500 µS/cm) (Very Good Status);

• *Turbidity level (NTU):* Values within the normal range for surface waters (1-1000 NTU) (Good Status);

• *TDS concentration (total dissolved organic and inorganic substances) (mg/L):* Values corresponding to freshwater environments (0 – 1000 mg/L TDS) (Good Status);

• Redox potential (ORP) (mV)**:** Obtained values fall within the natural ORP range of waters (-500 to +700 mV) (Good Status).

## CONCLUSIONS

The results presented here indicate that the levels of the physical-chemical parameters measured in this study were not risk-ranged, and the insignificant deviations are owed mainly to natural processes, without becoming a concern for the health of the aquatic ecosystems. However, it is important to focus on re-mobilizing potentially harmful chemical elements from sediments, as their impact can become significant during periods of low water flow in the river, both seasonally and over the years. Therefore, conducting routine analyses of the physical-chemical levels in water, in real-time is beneficial, using *in situ* equipment, such as EXO water quality sondes and sensor datasets.

**ACKNOWLEDGEMENTS**

This scientific paper was performed through the support of the Romanian Ministry of Research, Innovation and Digitalization of the Research Core Program, within the National Plan for Research, Development and Innovation 2022-2027, Projects – PN 23 30 03 04 and PN 23 30 03 02.

**REFERENCES**

[1] Goncharuk W., Goncharuk V.V., Water is everywhere. It holds everything a key to understanding the universe. D. I. Mendeleev's law is the prototype of the universe constitution, J. Water Chem. Technol., 41, pp 341-346, 2019.

[2] Ameen R. F. M., Mourshed M, Urban environmental challenges in developing countries - A stakeholder perspective, Habitat International, 64, pp 1-10, 2017.

[3] Li Z., Xiao J., Evaristo J., Li Z., Spatiotemporal variations in the hydrochemical characteristics and controlling factors of streamflow and groundwater in the Wei River of China, Environ. Pollut. pp 254, 2019.

[4] Habersack H., Hein T., Stanica A., Liska I., Mair R., Jäger E., Hauer C., Bradley C, Challenges of river basin management: Current status of, and prospects for, the River Danube from a river engineering perspective, Sci Total Environ., 543(A), pp 828-845, 2016.

[5] Gasparotti C**.,** Rusu E., Dragomir S., The impact of anthropogenic activities on the water quality in the Danube River Basin, Conference Bulgaria, Ecology, Economics, Education and Legislation, I, pp 987-994, 2013.

[6] Chapman D.V., Bradley C., Gettel G.M., Hatvani I.G., Hein T., Kovács J., Liska I., Oliver D.M., Tanos P., Trásy B., Várbíró G., Developments in water quality monitoring and management in large river catchments using the Danube River as an example, Environmental Science and Policy, Published by Elsevier Ltd., pp 141-154, 2016.

[7] Hein T., Schwarz U., Habersack H., Nichersu I., Preiner S., Willby N., Weigelhofer G., Current status and restoration options for floodplains along the Danube River, Sci Total Environ, 543(A), pp 778-790, 2016.

[8] Panin N., Jipa D., Danube River sediment input and its interaction with the north-western Black Sea, Estuarine, Coastal and Shelf Science, 54 (3), pp 551-562, 2002.

[9] Zinger J. A., Rhoads B. L., Best, J. L., Extreme sediment pulses generated by bend cutoffs along a large meandering river, Nature Geoscience, 4(10), pp 675-678, 2011.

[10] Duţu F., Duţu L., Catianis I., Ispas B-A., Sediment dynamics and hydrodynamical processes in the Danube Delta (Romania): A response to hydrotechnical works, Zeitcshrift fur geomorphologie, 63 (4), pp 365-378, 2022.

[11] Cullum R.F., Knight S.S., Cooper C.M., Smith S., Combined effects of best management practices on water quality in oxbow lakes from agricultural watersheds, Soil and Tillage Research, 90, pp 212-221, 2006.

[12] Bonitatibus T., Cantrell M. A., Duncan W. W., Hamstead B., Krueger E., Wolf M., A Scientific Basis for the Reconnection of Savannah River Artificial Meander Cutoffs through Flow Releases and Physical Reconfiguration, IN: McDowell RJ, CA

Pruitt, RA Bahn (eds.), Proceedings of the 2015 Georgia Water Resources Conference, April 28-29, 2015, University of Georgia, Athens, pp 1-4, 2015.

[13] Ramsar Convention, Convention on Wetlands of International Importance especially as Waterfowl Habitat, Ramsar (Iran), 2 February 1971, UN Treaty Series No. 14583, As amended by the Paris Protocol, 3 December 1982, and Regina Amendments, 28 May 1987, Ramsar Convention on Wetlands, Gland, Switzerland, 1987.

[14] Duțu F., Duțu L., Catianis I., Dramatic reduction of the water and sediment fluxes in a human-modified meandering ecosystem from the Danube Delta, Romania, Scientific Papers. Series E. Land Reclamation, Earth Observation & Surveying, Environmental Engineering, Print ISSN 2285-6064, CD-ROM ISSN 2285-6072, Online ISSN 2393-5138, ISSN-L 2285-6064, XII, 2023, pp 267-274, 2023.

[15] Order of the Ministry of Environmental and Water No 161/2006 for the Approval of the Norm Concerning the Reference Objectives for the Surface Water Quality Classification (Including Quality Standards for Sediments), Official Monitor of Romania, 1, No 511 bis, in force in Romania since 13.06.2006, 2006, [In Romanian].

[16] Lehr J. H., Gass T. E., Pettyjohn W. A., DeMarre J., Domestic Water Treatment, New York, NY: McGraw-Hill Book Company, pp 264, 1980.

[17] De Zuane J., Handbook of Drinking Water Quality (2nd ed.), John Wiley and Sons, ISBN 0-471-28789-X, pp 592, 1997.

[18] Montagna P., Palmer P., Pollack J., Hydrological Changes and Estuarine Dynamics, Springerbriefs in Environmental Science, 8, pp 94, 2013.

[19] Chapman D., Water Quality Assessments. A Guide to Use of Biota, Sediments and Water in Environmental Monitoring - Second Edition, Published on behalf of UNESCO, WHO, UNEP. E /FNSPON. London, Great Britain, University Press, Cambridge, pp 626, 1996.

[20] Sigg L., Redox Potential Measurements in Natural Waters: Significance, Concepts and Problems, IN: Schüring, J., Schulz, H.D., Fischer, W.R., Böttcher, J., Duijnisveld, W.H.M. (eds) Redox., Springer, Berlin, Heidelberg, Germany, pp 1-12, 2000.

# INTEGRATED ANALYSIS OF SEAWATER INTRUSION DYNAMICS IN THE NORTHERN BLACK SEA COAST OF BULGARIA

**Assoc. Prof. Dr. Olga Nitcheva**[1]
**Dr. Albena Vatralova**[2]
**Research Assist. Donka Shopova**[2]
**Assoc. Prof. Dr. Polya Dobreva**[1]
[1] Institute of Mechanics, Bulgarian Academy of Sciences, **Bulgaria**
[2] Climate, Atmosphere and Water Research Institute, Bulgarian Academy of Sciences, **Bulgaria**

## ABSTRACT

Managing water deficits in coastal areas presents significant challenges amid current climate fluctuations. This study examines the hydrological and water management factors contributing to seawater intrusion along the Bulgarian Black Sea coast. Utilizing data from field monitoring and hydrological model simulations, the research highlights the anthropogenic impacts shaped by the structure and dynamics of water supply. Findings reveal that rainfall levels in the Bulgarian Black Sea coastal region are below the national average. Coupled with excessive groundwater extraction for domestic purposes, this has led to seawater intrusion in the central and northern coastal areas. Over the past 50 years, marine intrusion processes in the area have remained inactive, primarily due to reduced economic and demographic activities following political changes in 1989. However, no significant improvements have been observed. Groundwater levels in the recharge zone, approximately 30 km inland, have risen by 1 meter, but no changes have been recorded in the marine intrusion zone. A decline in spring flow rates in coastal zones and continuous contamination of groundwater with chloride and sodium underscore the severity of the issue. The containment and mitigation of marine intrusion in Northeast Bulgaria require the implementation of unconventional methods. The persistence of this issue emphasizes the urgent need to explore alternative water sources and adopt specific water treatment methods.

**Keywords:** water deficit, groundwater abstraction, marine intrusion, Bulgarian Black Sea Coast

## INTRODUCTION

Coping with water deficit in coastal areas is a challenge when groundwater extraction must be relied upon. This can be the overexploitation of groundwater, which occurs when groundwater abstraction exceeds recharge [1]. This leads to a lowering of the groundwater table and creates conditions for seawater to enter the groundwater system. When the problem of excessive water abstraction is not controlled, the process of saltwater intrusion is activated. Then seawater hydraulic gradient is lower, the salinity and contamination occurs in the fresh groundwater aquifer. These changes in the aquifer may be permanent or may take many years to recover [2], [3].

The fresh groundwater coastal aquifers are impacted by seawater intrusion in regions where the surface runoff is limited. This is the case with the northern part of the Bulgarian Black Sea region. From 1984 until now, in the Krapets – Shabla - Tyulenovo section

https://doi.org/10.5593/sgem2024v/3.2/s14.24

(Fig.1), fresh groundwater has been constantly polluted, despite its improved quantitative status and an increase in the water level in the unconfined aquifer. A 1999 study [4] of groundwater chlorine and sodium monitoring data of 1996 found that salinization into the aquifer spreads to 2.5-3.5 km inland. In the national strategy document from 2020 [5], the boundaries of the territory of salinized onshore aquifers due to the progression of the sea intrusion process are outlined, and here the entry of salty sea water into the aquifer is up to 3.5 km of the inland. Therefore, for 25 years there is no improvement.

The purpose of the research is to trace the development of the marine intrusion process on the Bulgarian north-eastern coast and to make a proposal for refreshing the groundwater horizon after a review of the conventional methods, the physical and hydraulic barriers.

## MATERIALS AND METHODS

### 2.1. Scope of the analysis

To achieve the research objective three aspects of the problem were analyzed:

- the variation of the water level in the wells located on the groundwater flow path, from the recharge zone to the drainage zone in the coastal section;
- in parallel with monitoring the change in the concentrations of sodium (Na) chlorides (Cl) and electrical conductivity (σ), in the unconfined aquifer (Neogene) in the active zone of marine intrusion identified by the Ministry of Environment and Water (MOEW);
- as well as the specific features of water resources and water use in the study area with detailed data for the years 2010-2014, and available data for 1970 and 1971.

### 2.2. Study area

The study area is the north-eastern part of the Bulgarian Black Sea region (Fig. 1) where marine intrusion process has been identified in the area of Krapetz – Shabla – Tyulenovo. Due to water extraction with maximum flow rate during the active season, the altitude of the dynamic water levels is below sea level and salt water is drawn from the Black Sea. In order to clarify the hydrogeological conditions and the anthropogenic factor for the progression of marine intrusion processes, the area of the Dobrich region, Sarmatian carbonate complex was examined.

This is a region with an area of 3400 sq km, with a continuous distribution of Miocene marine and brachlish sediments covered by eolian sediments (loess). In the area of Dobrich the altitude is 220 m, the groundwater flow moves to the east. The groundwater level is from 50-60 m to 10-12 m and less in the coastal area. Figure 1 (the cross section I-I) shows the carbonate complex where porous karst aquifer prevails. Due to the high water-absorbing and water-conducting capacity of the carbonate limestone complex, there is no surface runoff. Groundwater is recharged by infiltration of rainfall (about 19% of rainfall being infiltrated). This is the richest area of groundwater in the country, and the area with the least rainfall - about 400 mm per year (380-460 mm). Two carbonate aquifers are formed, which are the main source of water supply. The upper unconfined aquifer is covered by Quaternary loess, the Sarmatian limestones reach 200 m in the coastal area, of which 150 m is an aquifer with average thickness of about 60 m.




Simplified geology sketch is given on the cross-section (Fig. 1). The upper unconfined aquifer, consisting of limestones, sands and loess of Miocene age, is up to 250 m thick. Underlying is Miocene clay. The deep aquifer of Jurassic age has an average thickness of 400 m, which is higher in the eastern direction. Meteoric recharge is in the area of the town of Dobrich and Dabrava village [6], [7], [8], [9].

### 2.3. Assessing seawater intrusion in the ecosystem water-subsurface environment-economic nexus

Integrated analyses of seawater intrusion dynamic were developed by collection of aquifer characteristics, groundwater data (groundwater level and *Cl*-, *Na*- concentrations), water resources, water supply and demographic statistics. Results of the CLM (Community Land Model) hydrological model have been used to calculate and map the runoff and the rain for the Bulgarian territory and for the Bulgarian Black sea basin.

The average values of *Cl, Na* and electrical conductivity ($\sigma$) for the period of 2010-2024 are compared with the hydro chemical criteria for a rapid assessment of the degree of intrusion set by the environmental authorities of the MOEW. These are (i) the quality standards (equal to that for drinking water) set in the Bulgarian Regulation No. 1/2007 on

https://doi.org/10.5593/sgem2024v/3.2/s14.24

the exploration, use and protection of groundwater, and (ii) the threshold values for the observed groundwater body BG2G000000N044 calculated according to a national methodology based on the EC Guidance Document No. 18: Guidance on Groundwater Status and Trend Assessment of 2009. They were used in the second River Basin Management Plan for the Black Sea River Basin District (2016-2021) and are proposed in the latest River Basin Management Plan (2022-2027) (Table 1).

**Table 1.** Quality standards and threshold values of *Cl, Na* and *σ* for BG2G000000N044

| Quality standards | | | Threshold values | | |
|---|---|---|---|---|---|
| **Na, mg/dm3** | **Cl, mg/dm3** | **σ, µS/cm** | **Na, mg/dm3** | **Cl, mg/dm3** | **σ, µS/cm** |
| 200 | 250 | 2000 | 156.6 | 192 | 1682 |

An overview was done of the management strategies to reduce and control the seawater intrusion in freshwater coast aquifers.

## RESULTS AND DISCUSSION

### 3.1. Analysis of water resources, water consumption and demographic development

The results of the research show that in the Bulgarian Black Sea coastal zone the rainfalls in the past decade are below the country average.

The investigation for the water use in the study area was implemented for the whole Black Sea Region for 2010-2020 with reference to the long-term demographic changes for the 1934-2021 period (Fig. 2). The amount of water used for drinking and domestic purposes varies in the period 2010-2020. For the country it is 96-102 liters/per person/day; for the Black Sea basin - 94-99 l/p/d, and for the Black Sea Dobrudzha rivers it varies more widely - 86-102 l/p/d.

Before 1989, the country's irrigation water was annually about 3500 million $m^3$, now it is about 250 million $m^3$ (NSI data). At present the population tends to decrease, however the water used for domestic needs and irrigation does not. This can be explained by an increase in the standard of living.

The drinking water supply system in the Dobrich district of the Northeastern Bulgaria is entirely from ground waters. The town of Dobrich itself is supplied from 43 drilling wells. Reclamation dams have mainly been built along the Black Sea Dobrudzha rivers. The total number of those operating at the moment is 16. Only the „Odrintsi“ Dam Reservoir has a volume of 24 million $m^3$, the others have a volume of less than 1 million $m^3$. The only one large dam does not serve the coastal area.

The city of Varna (being to the south of the studied area) is supplied with water from the "Kamchia" Dam Reservoir and from the "Devnevski Izvori" water supply system, which includes about 50 groundwater sources. There are 70 dams on the territory of Varna region. The "Tsonevo" Dam Reservoir (volume 330 million m3) and the “Ticha” Dam Reservoir (volume 312 million $m^3$) do not serve the coastal area. The rest are micro-dams, of which 14 are almost dry.

For the entire Burgas region (being to the south of the studied area and Varna), the following surface water sources are used for drinking water supply: catchment of the Zelenikovska River, "Kamchia" Dam Reservoir, "Yasna Polyana" Dam Reservoir, "Novo Panicharevo“ Dam Reservoir. There are 289 groundwater sources. There are over 300 dams on the territory of Burgas region. The district is mainly supplied with water from surface water sources.

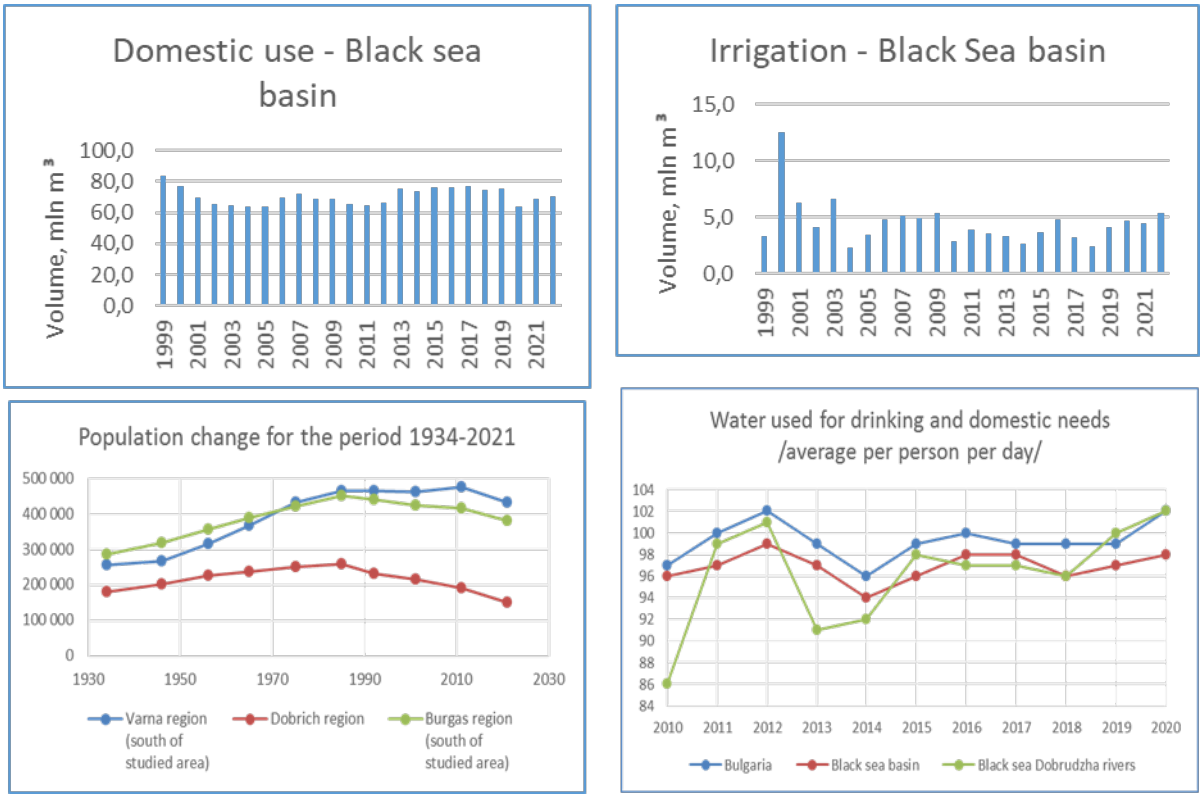



**Fig. 2**. Water use in the Bulgarian Black Sea Region, *Source of data: National Statistical Institute (NSI)*

The data on water use in the Black Sea basin highlights several key trends and challenges. The stable consumption of drinking water, as evidenced by the domestic water use graph, persists despite a declining population. This suggests that socio-economic factors, such as improved living standards and changes in consumption habits, play a more significant role in determining water demand than demographic trends alone. However, the lack of modernization in water supply infrastructure contributes to inefficiencies and losses, which may further sustain high consumption levels. This reinforces the need for careful planning and consideration of social and structural factors in water resource management.

The reliance of the Dobrich district on groundwater poses significant challenges, especially in the context of climate change. Groundwater remains the primary source of water, given the absence of large reservoirs and alternative surface water sources. Historical patterns of over-extraction have led to long-term problems, such as saline intrusion in coastal aquifers, with no significant improvement in groundwater quality observed over the past decades [10]. While there has been a slight increase in groundwater levels in recharge areas further inland, this has not translated into recovery in coastal zones, where seawater intrusion remains a persistent threat. The graph showing irrigation water use underscores a sharp decline since 2000, reflecting significant structural changes in agriculture. This decline points to a shift toward less water-intensive crops and a reduction in overall agricultural water demand. However, questions remain regarding the productivity and economic sustainability of this transition.

The stable but relatively low levels of irrigation water use in recent years also highlight the limitations in developing more efficient irrigation systems and technologies. Reduced natural recharge of groundwater, combined with increasingly frequent drought periods,

https://doi.org/10.5593/sgem2024v/3.2/s14.24

exacerbates the risk of aquifer depletion. The domestic water use trends further emphasize the growing per capita water consumption, which adds pressure on limited resources. This increasing demand, despite a shrinking population, suggests that resource management policies must focus not only on supply-side solutions but also on reducing losses and promoting sustainable consumption patterns.

Addressing these challenges requires a comprehensive approach. Infrastructure investments are essential, particularly in developing alternative water sources, such as offshore freshened groundwater or desalination technologies. Improved water management practices, including stricter controls on groundwater extraction and enhanced monitoring systems, are needed to mitigate the effects of saline intrusion and stabilize the water balance. Policies to promote water-saving technologies in both domestic and agricultural use can also play a significant role. In the absence of infrastructure modernization, maximizing the efficiency of existing systems and ensuring equitable access to resources become critical priorities.

The analysis of water resource trends in the Black Sea basin underscores the region's vulnerability to both environmental and socio-economic risks. The persistence of challenges such as saline intrusion, combined with the limited capacity to adapt existing systems to climate variability, calls for urgent and innovative solutions. Effective water management must integrate demographic, agricultural, and environmental considerations to secure a sustainable future for the region's water resources.

### 3.2. Quantitative analysis of the hydrogeological regime in the Dobrich region

Community Land Model (CLM) simulation of the runoff is illustrated in Fig.3 for 2013 year with 638 mm annual precipitation and the month of June being the most wet month [11]. The calculations show that the mean rain in June for the country is 175 mm and the monthly mean runoff is 45 mm. However, in the Black sea basin the monthly mean runoff happens to be 19 mm with monthly mean rain being 104 mm – far below the country average.

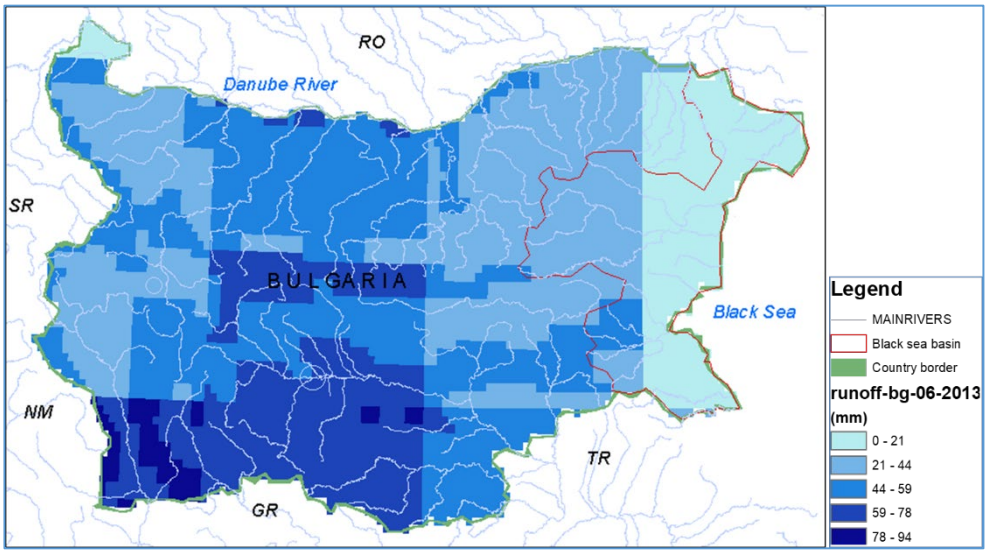



**Fig. 3.** Results from CLM model simulations, calculated runoff for the June 2013

The analysis of variations of the water level in the wells located on the groundwater flow path, from the recharge zone to the drainage zone in the coastal section, shows that the

level of the groundwater in the recharge zone, 50 km from the sea coast, has risen by 2-4 m. The levels in the wells in the zone of marine intrusion do not change during the studied period but a decrease in the flow rate of the springs in the coastal zone is observed.

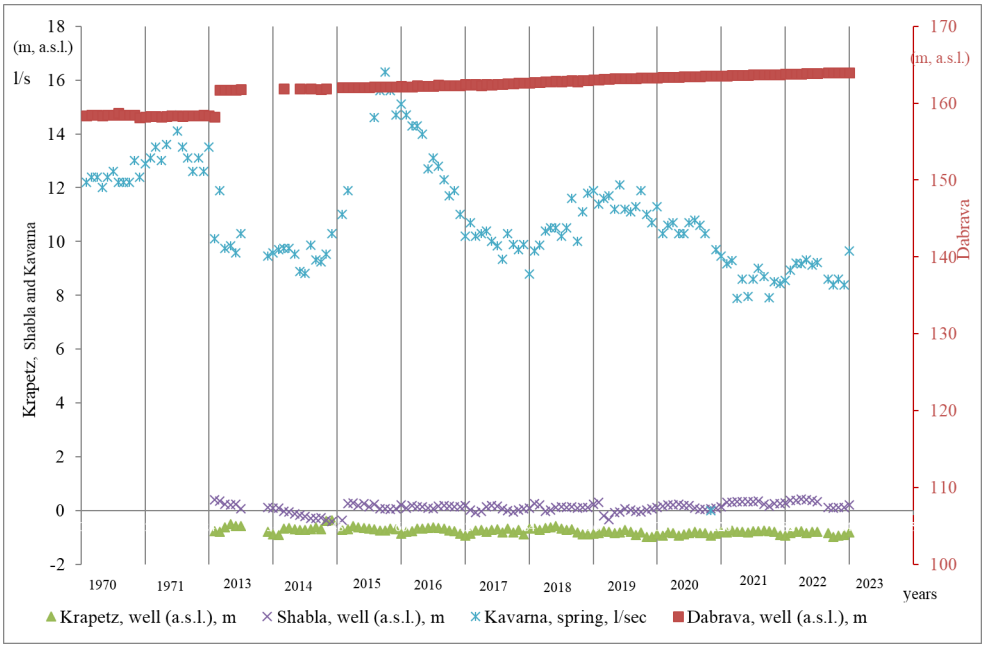



**Fig. 4.** Field data observations for porous waters in the Neogene-Sarmatian Northeast and Middle Dobrudzha (hydrogeological monitoring of the National Institute of Meteorology and Hydrology)

### 3.3. Qualitative analysis of groundwater in relation to marine salinization

Available data from the Bulgarian Ministry of Environment and Water (MOEW) monitoring networks for the chemical status of the groundwater body BG2G000000N044 (karst-pore waters in the Neogene-Sarmatian aquifer in Northeastern Dobrudzha) are used covering the 15-year period 2010-2024. Figure 5 clearly shows marine intrusion in the areas of Krapetz-Shabla-Tyulenovo where persistently elevated chlorides, electrical conductivity and sodium values are observed. This happens particularly in the summer months because of intensive groundwater extraction for drinking and irrigation purposes. The quantitative monitoring of the control agencies proves that when water is extracted with maximum flow during the active season, the dynamic water level falls below the sea level, which leads to the attraction of salt water from the Black Sea. Such trends in groundwater contamination align with the principles outlined in the European Union's framework for groundwater status and trend assessment [12].

Average annual data of 1970 and 1971 for Cl and Na in the area of Krapetz reported by the then Main Directorate of Hydrology and Meteorology (GUHM) are considered also. The comparison shows lower values at present times but they are still above the standards. Hence, the chemical status of the groundwater body continues to be declared "Bad" by the Black Sea Basin Directorate in the year 2023 as in the previous years due to the high values of Na, Cl, As, $NO_3$- and $PO4_3$-. According to the authorities, the detected higher values do not exceed 20% of the exposed area of the groundwater body. That is why there is not specific programme of measures planned for mitigation of the negative effects and achievement of good water status for this area. The only one measure applied so far is limitation of the groundwater abstraction. This is not adequate policy provided the ongoing climate change threats for potential water resources scarcity and droughts.

https://doi.org/10.5593/sgem2024v/3.2/s14.24

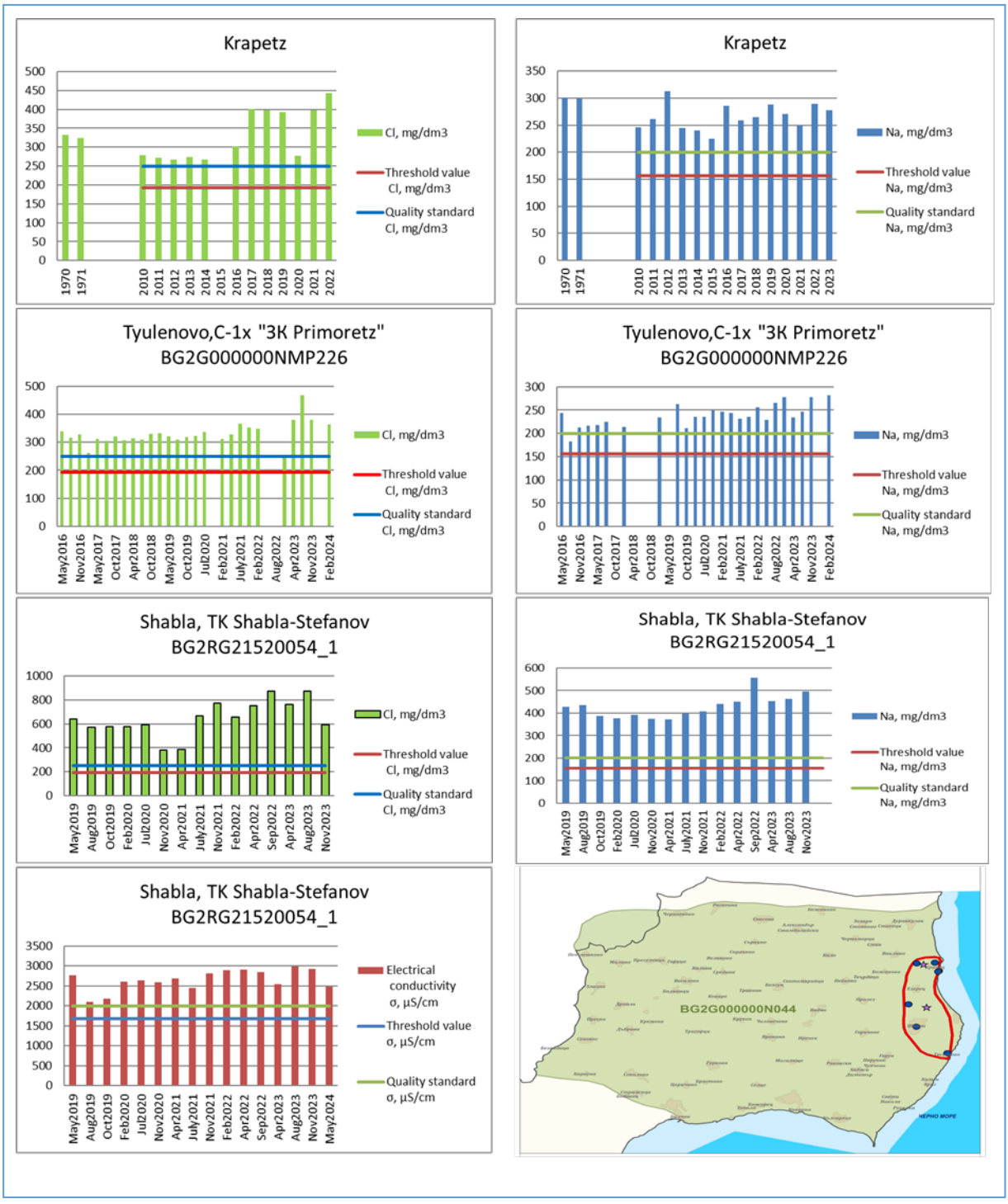



**Fig. 5.** *Cl, Na* and electrical conductivity ($\sigma$) in the groundwater body BG2G000000N044 and the boundaries of the Krapetz, Shabla and Tyulenovo area of potential seawater intrusion as outlined by the MOEW

Alternative water sources could be used for the human activities such as desalinated seawater, reclaimed wastewater and offshore freshened groundwater. Some analyses show [13] that desalination for agricultural needs is economically viable due to the low salinity of the Black Sea water. Many countries around the world are actively working in this direction, realizing that seawater is the alternative to traditional sources particularly

during the summer months when water demand in seaside resorts increases and water supply is often inadequate. Innovative approaches, such as the utilization of offshore freshened groundwater, have been proposed as a sustainable alternative to mitigate seawater intrusion and ensure reliable water supply in coastal regions [14].

## CONCLUSION

Combination of both natural process and anthropogenic activities in the Bulgarian Northwestern Black Sea costal area has led to contamination of the fresh groundwater reserves with salty seawater due to marine intrusion in the Krapetz – Shabla - Tyulenovo area. For the last 50 years, no activation of the marine intrusion process has been observed in the considered area. The persistence of saltwater intrusion, despite a slight recovery in inland recharge zones, underscores the need for a more integrated and proactive approach to water resource management.

The lack of targeted mitigation measures further compounds the risk of long-term degradation of groundwater quality. The cost and the time needed for groundwater remediation requires a multipronged strategy for preservation of the coastal area for its environmental, economic and social sustainability. For achieving this purpose different approach is necessary to be introduced in addition to the only one applied so far with limitation of the groundwater abstraction.

First, enhanced monitoring systems and stricter regulatory controls on groundwater abstraction are essential to mitigate the progression of saline intrusion. Advanced hydrological modeling must be leveraged to refine groundwater management plans and predict future scenarios under varying climate and extraction conditions. Second, investments in infrastructure modernization leakage reduction in water supply systems, will be crucial in addressing inefficiencies. Additionally, public awareness campaigns and policies promoting water-efficient technologies in both domestic and agricultural sectors can significantly reduce consumption. Lastly, innovative research on developing alternative water sources, including the potential use of desalinated seawater, offshore freshened groundwater and reclaimed wastewater to reduce reliance on over-extracted aquifers, offers a promising avenue for meeting future water demands sustainably.

The findings of this study emphasize the urgent need for a holistic approach that integrates demographic, hydrological, and environmental considerations. Ensuring sustainable water resource management in the northeastern Black Sea region is vital not only for preserving groundwater quality but also for supporting socio-economic development and resilience in the face of climate change.

## ACKNOWLEDGEMENTS

This publication is based upon work from COST Action CA21112 “Offshore freshened groundwater: An unconventional water resource in coastal regions? (OFF-SOURCE)”, supported by COST (European Cooperation in Science and Technology), and the National Science Programme "Environmental Protection and Reduction of Risks of Adverse Events and Natural Disasters", approved by the Resolution of the Council of Ministers № 577/17.08.2018 and supported by the Ministry of Education and Science (MES) of Bulgaria (Agreement № Д01-27/06.02.2024).

https://doi.org/10.5593/sgem2024v/3.2/s14.24

## REFERENCES

[1] Hussain M. S., Abd-Elhamid H. F., Javadi A. A., Sherif M. M., Management of Seawater Intrusion in Coastal Aquifers: A Review, Water, Switzerland, vol. 11 (12), pp. 2467, 2019.

[2] Brzozowski C., Protecting Drinking Water from Saltwater Intrusion, Water World, USA, 2017, Online Resource.

[3] Saltwater intrusion EEA, Are the impacts of water abstractions being reduced?, European Environment Agency, Denmark, 2023, Online Resource.

[4] Pulido-Bosch A., López-Chicano M., Calaforra J. M., Calvache M. L., Machkova M., Dimitrov D., Velikov B., Pentchev P., Groundwater problems in the karstic aquifers of the Dobrich region, northeastern Bulgaria, Hydrological Sciences Journal, United Kingdom, vol. 44, issue 6, pp. 913-927, 1999.

[5] Integrated Development Plan of Shabla Municipality 2021–2027, strategic planning and programming documents for regional development regulated by the Regional Development Act (State Gazette, issue 21/13.03.2020).

[6] Antonov H., Danchev D., Ground Waters in Bulgaria, Tehnika Publishing House, Bulgaria, 1980, pp. 360.

[7] Pulido-Bosch A., Machkova M., López-Chicano M., Calvache M. L., Dimitrov D., Calaforra J. M., Velikov B., Penchev P., Hydrogeology of the Upper Aquifer, Dobrich Region, Northeastern Bulgaria, Hydrogeology Journal, Germany, vol. 5, issue 2, pp. 75-85, 1997.

[8] Marinova T., Malcheva K., Bocheva L., Trifonova L., Climate profile of Bulgaria in the period 1988–2016 and brief climatic assessment of 2017, BGMH, Bulgaria, vol. 22, pp. 2-15, 2017.

[9] Pentchev P., Spasov K., Shopova K., The Role of the Ground Waters for the Durankulak Lake Development, Annual of the University of Mining and Geology St. Ivan Rilski, vol. 51, pp. 144-148, 2008.

[10] MOEW, Regulation No. 1 of 10.10.2007 on research, use, and conservation of groundwater, last amended as of December 2016, Bulgaria, Legislative Document.

[11] Nitcheva O., Milev B., Trenkova T., Philipova N., Dobreva P., Kamchia watershed groundwater recharge assessment by the CLM3 model. 13th National Congress on Theoretical and Applied Mechanics, 6 – 10 September 2017, Sofia, Bulgaria. DOI: https://doi.org/10.1051/matecconf/201814503011.

[12] European Commission, Guidance Document No. 18: Guidance on Groundwater Status and Trend Assessment, Belgium, 2009, Official EU Report.

[13] Letskovska, S., Milen Baltov, Kamen Seymenliyski, Radostin Dolchinkov. Black Sea – a renewable source of energy and resources. Annual of the Burgas Free University, Vol. XLII, 2020, 211-238. ISSN: 1311-221X (in Bulgarian)

[14] Micallef A., Person M., Berndt C., Bertoni C., Cohen D., et al., Offshore Freshened Groundwater in Continental Margins, Reviews of Geophysics, USA, vol. 58, issue 4, 2020, DOI: 10.1029/2020RG000706.

# SECTION SOIL SCIENCE, CONSERVATION,

# AND LAND RESTORATION

# ASSESSMENT OF THE IMPACT OF COMPLEX FOLIAR FERTILIZERS ON CORN (ZEA MAYS L.) PRODUCTIVITY

**Dr. Laura Crista**
**Prof. Dr. Florin Crista**
**Prof. Dr. Isidora Radulov**
**Lecturer Alina Lato**
**Lecturer Adina Berbecea**
University of Life Science Timisoara, **Romania**

## ABSTRACT

This study investigates the effects of foliar fertilization (FF) on the yield and quality of corn grains, utilizing Principal Component Analysis (PCA) to optimize foliar treatment applications. The PCA approach enabled the identification of the most effective FF formulation for enhancing grain production and quality. The experiments were conducted in 2022 and 2023 at the university's experimental field, evaluating seven treatment variants, each with distinct chemical compositions labelled from V1 to V7, along with a control group. FF applications were carried out during the 15-16 BBCH and 20-22 BBCH vegetative stages of corn, with application rates ranging from 2 to 6 L/ha, according to the product specifications. Foliar fertilization of corn can directly influence the nutritional composition and quality of grains, affecting key components such as proteins, lipids, carbohydrates, fibers, and minerals. By applying nutrients directly to the leaves, this method can stimulate essential metabolic processes, leading to an improved nutritional profile of the grains. The FF treatments showed significant improvements in both the yield and quality of corn grains, as assessed through quality indicators such as moisture content, protein levels, lipids, carbohydrates, fibers, and minerals.

**Keywords:** foliar fertilization, corn, proteins, lipides, carbohydrates

## INTRODUCTION

Maize (Zea mays L.) is the second-largest cultivated crop worldwide due to its remarkable adaptability. It occupies extensive areas not only in Romania [1] but also across Europe [2] and other regions globally [3]. In 2021, Romania ranked first in Europe in both maize cultivation area (2,493,000 hectares) and production volume (14,445,000 tons) [2]. Maize remains a vital crop for agricultural and industrial purposes, attracting significant economic interest, particularly in countries like Romania, which offers optimal pedoclimatic conditions for its growth [1]. Maize serves as a critical source of nutrition for humans and animals and as an important energy source for biofuel production.

Modern agriculture heavily relies on fertilizers to ensure high-quality yields while minimizing costs. Enhancing the efficiency of nitrogen (N), phosphorus (P), and potassium (K) fertilizers is critical, especially as environmental regulations increasingly demand reduced soil mineral fertilization to protect ecological and chemical balances

[5]. The rising costs of fertilizers, driven by energy consumption, especially from fossil fuels, have renewed interest in foliar fertilizers (FF). These solutions provide lower concentrations of traditional mineral nutrients, enriched with oligoelements and microelements, to enhance nutrient absorption by plants. Additionally, being applied as aqueous solutions, they also deliver water, an essential factor for plant development [6,7].

Foliar fertilizers have gained attention due to their ability to optimize nutrient absorption. Several factors influence their efficiency: (1) the physicochemical properties of the spray solution (e.g., particle size, solubility); (2) environmental conditions (e.g., temperature, humidity); and (3) plant-specific traits (e.g., leaf morphology, nutrient mobility). Despite advancements in understanding root nutrient uptake, the mechanisms of foliar nutrient absorption, involving pathways such as cuticles, stomata, and trichomes, remain less understood [6–9]. Two main pathways for nutrient absorption through leaves are identified: a lipophilic route for non-polar substances like insecticides and herbicides, and a hydrophilic route for polar substances such as mineral nutrients [10,11]. Leaf morphology further influences nutrient movement; herbaceous plants, with linear leaf arrangements and dense venation, show more efficient nutrient transport than broadleaf species, which present more complex pathways [12–14].

While nitrogen, phosphorus, and potassium (NPK) are essential for maize growth, sulfur (S) is the fourth most important macronutrient. Despite being the 13th most abundant element in the soil crust, sulfur plays a critical role in plant mineral nutrition, especially in high-demand crops like maize. It contributes to chlorophyll synthesis, facilitates the production of sulfur-containing amino acids (e.g., cystine, cysteine, methionine), and supports photosynthesis and carbohydrate metabolism. Sulfur deficiency often manifests as chlorosis in younger leaves, distinct from nitrogen deficiency, as symptoms persist even after nitrogen supplementation [15–18].

Boron (B), though required in trace amounts, is vital for maintaining plant cell wall stability and elasticity. It supports the structural integrity of primary cell walls through borate ester cross-linking. In maize, boron deficiency causes developmental issues in reproductive structures, leading to reduced grain yield and quality [19–23].

Micronutrients such as copper (Cu), iron (Fe), manganese (Mn), zinc (Zn), cobalt (Co), and molybdenum (Mo) play essential roles in maize nutrition. These elements support metabolic pathways, including ATP synthesis, lignification, and carbohydrate, lipid, and protein metabolism [24–26]. Zinc deficiency is particularly notable in maize, causing stunted growth, shortened internodes, and chlorosis on leaves, followed by necrosis. Foliar application of zinc enhances plant growth and yield by promoting nutrient absorption and distribution [27]. However, excessive amounts of trace metals, especially Cu and Fe, can induce cellular damage through mechanisms like lipid peroxidation, highlighting the need for careful monitoring of micronutrient levels [28].

This study aimed to evaluate the quantitative and qualitative impacts of complex foliar fertilizers enriched with oligoelements and microelements as a sustainable fertilization approach for maize. By optimizing fertilizer composition and application rates, sustainable agricultural practices can be improved. Using principal component analysis (PCA), we analyzed the effects of seven different foliar fertilizer treatments on parameters such as yield, moisture, ash, macro- and micronutrient content, lipids, crude

protein, fiber, and carbohydrates. This methodology facilitated the identification of optimal formulations and dosages for enhancing maize production and quality [5–7].

## MATERIALS AND METHODS

*Natural Framework of Experimentation: Relief, Climate, and Soil*

The study took place during 2023–2024, and the experimental fields were located near the city of Timișoara, on U.S.V.T. lands. As a form of relief, the area is located in a vast plain, called the Western Plain, one of the most important agricultural regions of Romania. The coordinates of the location are 45°48.298′ N 21°09.350′ E.

Romania generally experiences a continental climate. However, in the Western Plain, this climate is moderately influenced by oceanic and even sub-Mediterranean elements. The average annual temperature is 10.8 °C, with an observable upward trend in recent years. April, typically the month for corn sowing, saw temperatures above the long-term average only in 2020.

*Chemical properties:*

The soil exhibits a slightly acidic reaction in the top 59 cm, shifting to slightly alkaline between 59 and 119 cm, and becoming fully alkaline at greater depths. Humus levels are moderate within the upper 50 cm, with a substantial humus reserve in this layer (273.45 t/ha). Mobile phosphorus content in the plowed layer indicates a moderate supply status, similar to the medium status observed for mobile potassium. Carbonate content reflects mild salinization at depths exceeding 100 cm, and $CaCO_3$ levels are notably high from 59 cm down to 170 cm [33,34].

*Physical and hydro-physical properties:*

The soil texture is medium-fine (LA) throughout the profile from 0–148 cm, transitioning to medium (LL) at deeper levels. Both porosity and water permeability are very low, with a marked degree of compaction. Drainage—internal, external, and overall—is minimal. The soil's morphological thickness, extending down to the parent rock, classifies it as a deep soil, and the physiological thickness, where most root development occurs, is substantial [33,34].

*Sowing and Fertilization, Experimental Scheme*

The corn crop was sown aligning with the optimal sowing period for this region, based on soil moisture and temperature at a depth of 6–8 cm. The P0216 hybrid from Pioneer was selected, a semi-late (FAO 450) hybrid with a high yield potential, strong roots, and a rapid drying rate at maturity. Designed for intensive farming, it is particularly suited to arid and semi-arid plains in Romania's southern and western regions. Recommended plant densities are 60,000–65,000 harvestable plants per hectare for non-irrigated fields and 68,000–75,000 for irrigated fields. The hybrid typically has 16–18 rows per cob and 47–50 seeds per row, with a thousand kernel weight (MMB) ranging from 365 to 400 g.

Fertilization involved a base application of 100 kg/ha of a solid complex fertilizer (18:46:0 N, $P_2O_5$, $K_2O$) and 150 kg/ha of nitrogen in ammonium form. The complex fertilizer was incorporated during seedbed preparation, and ammonium nitrate was added at the 2–3 leaf stage. This initial fertilization was followed by two foliar applications across all V1–V7 treatments, applied at maize-specific growth stages

(BBCH 15–16 for 5–6 leaves and BBCH 20–22 for 10–12 leaves) to meet peak nutrient demands.

Due to the slow early growth of maize, a pre-emergent herbicide application of Adengo SC 465 (225 g/L Isoxaflutole, 90 g/L Thiencarbazone-methyl, and 150 g/L Cyprosulfamide) was performed at 2 L/ha using SCHACHTNER equipment, BOSPHO type (horizontal boom sprayer with 300 cm length, 50 cm height, and 2.6 bar pressure), fitted with six LECHLER nozzles (IDK120-02), calibrated to apply 300 L/ha. Conditions during application included air temperatures of 18.3–21.7 °C, wind speeds of 0.3–0.8 m/s, and relative humidity of 52.3–61.2%. Foliar fertilizer application rates ranged from 2 to 6 L/ha, varying by product composition, and were supported by favorable precipitation in May and June.

The field experiment was organized in subdivided plots, with three replicates per treatment. Eight variants (including control) were tested, with each plot covering 24.5 m² (7 m by 3.5 m) and 1-meter paths between treatments. The fertilization treatments were as follows:

V1: FF 10:10:10 + ME at 6 L/ha
V2: FF 8:8:8 + 8B + ME at 6 L/ha
V3: FF 8:10:0 + 8B + ME at 2 L/ha
V4: FF 15:0:0 + 2S + 1B + ME at 6 L/ha
V5: FF 24:0:0 + 3Zn + ME at 4 L/ha
V6: FF 15:0:0 + 5Zn + ME at 4 L/ha
V7: FF 15:0:0 + 4B + ME at 4 L/ha
Mt: Control (basic soil fertilization only)

Here, "FF" denotes foliar fertilizers, with nitrogen (N), phosphorus ($P_2O_5$), and potassium ($K_2O$) concentrations expressed as weight percentages (w/w), and boron (B) at 0.01% (w/w) and sulfur (S) at 1% (w/w). Micronutrient mix (ME) included Fe (0.057%), Cu (0.006%), Mn (0.026%), Zn (0.008%), and Co (0.002%) chelated with EDTA, plus Mo at 0.004% (w/w).

*Chemical Analysis and Statistical Data Processing Methods*

The analysis of maize grain samples from seven experimental variants (three samples per variant) was conducted at the Soil and Plant Analysis Laboratory of the Office for Pedological and Agrochemical Studies in Timișoara (OSPA-Timișoara), an accredited facility serving both agricultural research and the University of Life Sciences, King Michael I, in Timișoara. The quality assessment of maize kernels (moisture, protein, lipids, fiber, ash) employed ISO-standardized methods:

- Moisture (%): Determined by drying samples at 110°C using a POL-EKO oven (SR EN ISO 712:2010).
- Ash (%): Measured by burning samples at 550°C in an electric furnace (SR ISO 2171:2002).
- Crude Protein (%): Determined using the Kjeldahl method with a VELP DK20 heating digestion and UDK 149 distillation unit.
- Total Fat (%): Extracted using the Soxhlet method (SR ISO 1443:2008).
- Dietary Fiber (%): Analyzed with the FOSS Fibertec system (2010&M6 method).

Mineralization: Conducted through calcination and wet digestion using aqua regia (HNO3, 1:3 ratio), with phosphorus measured colorimetrically using a CINTRA spectrophotometer, and metal nutrients analyzed via flame atomic absorption spectrometry (FAAS) with a VARIAN AA 240 FS spectrometer.

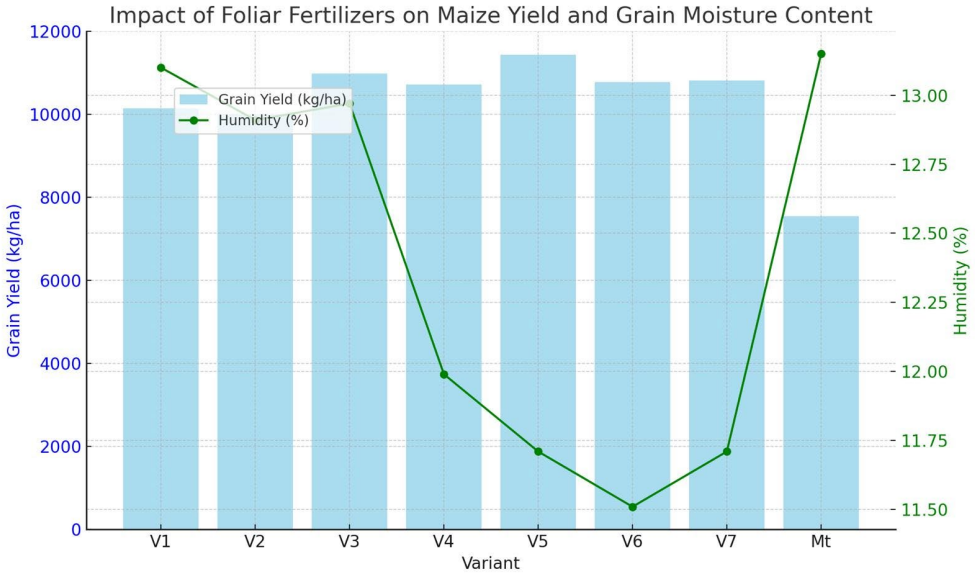
Carbohydrates (%): Calculated by subtracting the sum of other macronutrients from 100.

This comprehensive, standardized analytical approach ensured reliable characterization of maize grain quality and nutrient composition.

## RESULTS AND DISCUSSIONS

*Impact of FF on Production and Humidity of Maize Grain*

The production yields and seed moisture content resulting from the applied foliar treatments are presented in Figure 1.

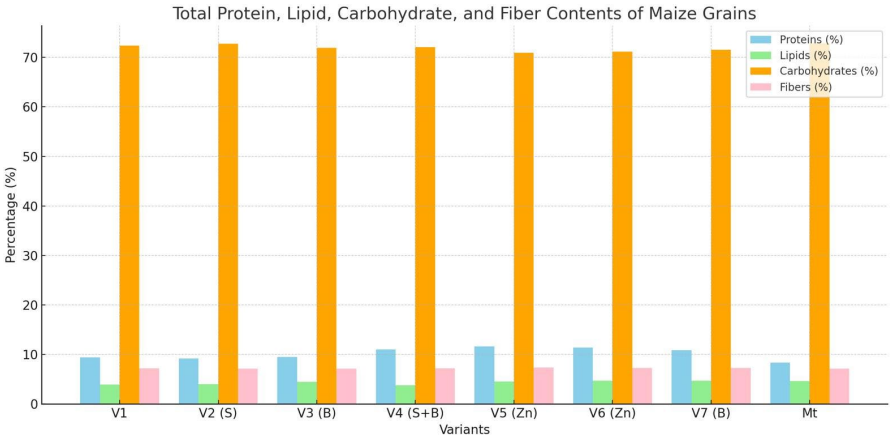



Maize yields showed a significant increase in all foliar-fertilized (FF) variants compared to the control group (Mt). The highest yield was recorded in the V5 variant (11,433 kg/ha), which included zinc (Zn), followed by the V3 variant (10,987 kg/ha), enriched with boron (B) and micronutrients in addition to the base nitrogen and phosphorus fertilizers. Generally, foliar application of nitrogen fertilizers enhances grain production in various crops, including maize.

Maize grains from all FF-treated variants exhibited reduced moisture content compared to the control, with the difference being particularly notable in variants V4–V7. Research on maize, sunflower, and brassica crops has demonstrated that boron and zinc, especially when combined with molybdenum, can significantly improve seed production [55–57].

*The Influence of Foliar Fertilizers on the Protein, Lipid, Carbohydrate, and Fiber Content of Maize Grains*

Raw protein, total lipid, carbohydrate, and fiber contents of maize grains are given in Figure 2:




Mineral fertilization plays a pivotal role in shaping the qualitative parameters of crop production, including protein, lipid, carbohydrate, and fiber content. The following observations were made regarding maize grains under foliar fertilization (FF):

Protein Content: Foliar fertilizers, especially those enriched with nitrogen and zinc (e.g., V5 and V6), significantly increased protein levels compared to the control group (8.29%). Variants V5 (11.62%) and V6 (11.38%) demonstrated the highest protein content, with zinc supplementation contributing substantially to this improvement.

Lipid Content: Nitrogen-dominant foliar fertilizers resulted in a marked reduction in lipid content. For instance, V4 recorded the lowest lipid percentage (3.72%) compared to the control (4.57%). While sulfur and boron aid in protein and lipid synthesis, their combination with nitrogen-rich FF led to statistically significant decreases in lipid levels across all treated variants.

Carbohydrate Content: Variations in carbohydrate content were minor, with values ranging from 70.91% (V5) to 72.82% (control). However, nitrogen-enriched FF consistently reduced carbohydrate levels across treatments, indicating a significant and predictable impact of nitrogen on this parameter.

Fiber Content: All foliar-fertilized variants exhibited higher fiber content compared to the control. Variants V5 (7.30%) and V6 (7.27%) had the highest fiber levels, supported by the role of zinc in enhancing carbonic anhydrase activity, which contributes to polymeric carbohydrate production.

In conclusion, foliar fertilization with nitrogen and micronutrients, particularly zinc, significantly influences maize grain quality. While it enhances protein and fiber content, it reduces lipid and, in some cases, carbohydrate levels. These findings highlight the need for balanced nutrient management to optimize both yield and quality in crop production.

*Effects of foliar fertilization:*

Different experimental variants demonstrated the impact of foliar fertilization with various nutrient combinations on maize grain yield and composition.

Group 1 (V1, V2, V3 - Complex Mineral Fertilization): These variants produced maize grains with moisture and carbohydrate content similar to the control group, indicating limited deviation from baseline characteristics.

Group 2 (V5, V6, V7 - Nitrogen, Zinc, and Boron Fertilization): These treatments achieved the highest production levels and superior nutritional profiles, characterized by elevated protein, fiber, and lipid content.

Group 3 (V4 - Nitrogen with Sulfur and Boron): This variant showed the lowest lipid content but recorded the highest yield and protein levels among all treatments, highlighting the specific impact of sulfur and boron supplementation.

The graphical analysis underscores the distinct effects of various foliar fertilization strategies on both maize grain composition and yield. These insights are instrumental in optimizing fertilization practices to balance productivity and quality. Similar effects of sulfur, boron, and other micronutrients, when combined with classical mineral fertilizers, have been reported in numerous studies, supporting these findings.

## CONCLUSIONS

All tested foliar fertilizers positively influenced maize seed production, with the V5 variant (24:0:0+3Zn+ME, 4 L/ha) achieving the highest grain yield. This variant also enhanced protein and fiber content, reduced grain moisture, and exhibited high macro- (Ca, Mg, K, P) and micro-mineral (Fe, Zn, Cu, Mn) levels. Variants V5, V6, and V7, containing nitrogen as the primary macro-fertilizer along with zinc and boron, formed a distinct group characterized by superior yield and quality parameters, as shown by the PCA-nutrient model. Meanwhile, the V3 variant (8:10:0+8B+ME, 2 L/ha) stood out for its balanced yield and superior grain quality.

The study highlights that the combined use of nitrogen, boron, and zinc as foliar fertilizers was the most effective approach to maximize both maize yield and quality.

## REFERENCES

[1] Fernández, V.; Brown, P.H. From plant surface to plant metabolism: The uncertain fate of foliar-applied nutrients. Front. Plant Sci. 2013, 4, 289. [CrossRef]

[2] Fernández, V.; Sotiropoulos, T.; Brown, P.H. Foliar Fertilization: Scientific Principles and Field Pratices; International Fertilizer Industry Association (IFA): Paris, France, 2013; ISBN 979-10-92366-00-6.

[3] White, P.J.; Brown, P.H. Plant nutrition for sustainable development and global health. Ann. Bot. 2010, 105, 1073–1080. [CrossRef]

[4] Schreiber, L.; Schönherr, J. Water and Solute Permeability of Plant Cuticles. Measurement and Data Analysis; Springer-Verlag: Berlin/Heidelberg, Germany, 2009; pp. 1–29. [CrossRef]

[5] Wang, H.; Cui, S.; Fu, J.; Gong, H.; Liu, S. Sulfur Application Improves the Nutritional Quality of Maize by Regulating the AminoAcid Balance of Grains. Agronomy 2023, 13, 2912. [CrossRef]

[6] Wimmer, M.A.; Abreu, I.; Bell, R.W.; Bienert, M.D.; Brown, P.H.; Dell, B.; Fátima Gotz, L.; Silvestrin, F.; Motta, A.C.V.; Pauletti, V. Response to Application and Tissue

Diagnosis of Boron Deficiency and Toxicity in Maize. Commun. Soil. Sci. Plant Anal. 2021, 52, 2898–2911. [CrossRef]Kumar, S.;

[7] Mohapatra, T. Interaction Between Macro- and Micro-Nutrients in Plants. Front. Plant Sci. 2021, 12, 665. [CrossRef]

[8] Sharma, R.K.; Agrawal, M. Biological Effects of Heavy Metals: An Overview. J. Environ. Biol. 2005, 26 (Suppl. S2), 301–313.

[9] Radulov, I.; Sala, F.; Berbecea, A.; Crista, F. Changes of soil microelements content after intesive mineral fertilization. Res. J. Agric. Sci. 2009, 41, 487–492.

[10] Crista, F.; Radulov, I.; Crista, L.; Berbecea, A.; Lat,o, A. Influence of mineral fertilization on the amino acid content and raw protein of wheat grain. J. Food Agric. Environ. (JFAE) 2012, 10, 47–50.

[11] BBCH. Available online: https://www.bionity.com/en/encyclopedia/BBCH-scale_(maize).html (accessed on 28 March 2024)

[12] Kiandokht Ghanati, K.; Farid Zayeri, F.; Hedayat Hosseinia, H. Potential Health Risk Assessment of Different Heavy Metals in Wheat Products. Iran J Pharm Res. 2019, 18, 2093–2100. [CrossRef]

[13] Boldea, M.; Sala, F.; Radulov, I.; Crista, F. A Mathematical Model on the Dependence between the Agricultural Production and Chemical Fertilizer. In International Conference on Numerical Analysis and Applied Mathematics; American Institute of Physics (AIP):College Park, MY, USA, 2010; pp. 1363–1366. [CrossRef]

[14] Olive, D.J. Principal Component Analysis. In Robust Multivariate Analysis; Springer: Cham, Switzerland, 2017; pp. 189–217.

[15] Gergen, I.; Hărmănescu, M. Application of principal component analysis in the pollution assessment with heavy metals of vegetable food chain in the old mining areas. Chem. Cent. J. 2012, 6, 156. [CrossRef] [PubMed]

[16] The PAST Software. Available online:
https://www.nhm.uio.no/english/research/resources/past/ (accessed on 15 February 20

# COMPARISON OF SOIL LOSS DUE TO WATER EROSION BEFORE AND AFTER A CHANGE IN AGRONOMIC PRACTICES

**Ing. Dávid Dežerický, PhD.**[1]
**Mgr. Ing. Marta Lenartowicz**[2]
**Ing. Sára Daxnerová**[2]
**Prof. Ing. Zlatica Muchová, PhD.**[2]
[1] AgroBioTech Research Centre, Slovak University of Agriculture in Nitra, **Slovakia**
[2] Institute of Landscape Engineering, Slovak University of Agriculture in Nitra, **Slovakia**

## ABSTRACT

Between September 13th and 16th, 2024, heavy rainfall led to widespread flooding across the municipalities in the Senica district, as well as significant soil erosion on intensively farmed arable land. According to data from the Slovak Hydrometeorological Institute (SHMÚ), the Senica district received a total of 230 millimeters of precipitation during this period. In the village of Smolinské, located in the lowlands of Záhorie in western Slovakia, experienced substantial flooding of agricultural areas, leading to considerable surface and gully erosion across many agricultural parcels.

In this study, we present the effects of this rainfall on soil block 5002/1 Šaštín (LPIS designation), with a total area of 34.86 ha.

In the area, we conducted a detailed unmanned aircraft system (UAS) flight from a height of 70 m, producing an orthophotomosaic that depicted the erosion-damaged areas. These areas were vectorized and used to verify the results of the erosion rate calculation. The calculation of water erosion was performed using the Universal Soil Loss Equation methodology. The K and R factors were determined based on tabular data derived from the national soil rating system (BPEJ) and on the data of the rainfall measuring stations. The LS factor was derived from airborne laser scanning data based on DMR5.0 (1 m resolution). The support practice - P and cover management - C factors were determined through field reconnaissance conducted during the flooding event. The estimated soil loss was approximately 2.5 $t.ha^{-1}.yr^{-1}$.

The proposed change to the status was implemented by altering the current land management. We proposed the measure of strip crop rotation, which significantly affects the C and P factors. The erosion loss calculation was again carried out. The two outputs were compared, and the differences were balanced. The results suggest that even a "simple" change in agrotechnical measures can mitigate the effects of extreme events.

**Keywords:** water erosion, USLE, land management change, UAS, contour strip rotation

https://doi.org/10.5593/sgem2024v/3.2/s12.26

## INTRODUCTION

Changes in natural climatic and hydrological cycles are increasingly triggering extreme weather events, such as droughts followed by intense rainfall, which drive surface runoff, soil erosion, and aquatic ecosystem degradation [1, 2]. Poor soil water retention, exacerbated by current land management practices, significantly contributes to these issues [3]. Water erosion is a leading cause of topsoil loss, diminished agricultural productivity, and global surface water pollution [4]. The loss of topsoil presents major environmental, economic, and social challenges, as intense rainfall accelerates erosion processes that reshape land and increase reclamation costs [5]. Erosion also drives eutrophication by depositing nutrient-rich sediment in water bodies, worsening water quality and harming aquatic ecosystems [6]. In Slovakia, soil degradation is severe, with nearly 70.000 hectares of agricultural land lost from 1996 to 2020 due to erosion and mismanagement [7]. Advances in Unmanned Aerial Systems (UAS) now enable precise soil erosion mapping and cost-effective monitoring, supporting conservation efforts [8, 9]. Soil loss, often estimated by the Universal Soil Loss Equation (USLE), depends on factors like rainfall, soil erosion susceptibility, slope, vegetation, and conservation practices [10]. Integrating UAS data with models like USLE supports improved erosion risk assessment and land management. Sustainable practices that improve soil resilience and protect water quality are essential for long-term resource management [3, 4]. This study examines the effectiveness of strip crop rotation as a practical measure to reduce erosion impacts from extreme weather events.

## MATERIALS AND METHODS

### The study area

The area is a land parcel with the registration code 5002/1 parcel A – Šaštín, registered as arable land intended for agricultural production with a total of 34.86ha (Fig. 1). The parcel is located in Smolinské Cadastral area, Senica District, Trnava Municipal, Slovak Republic (geographically located at x: -566260.8061 to -565933.2169; y: -1220068.2838 to -1221336.722. The parcel is situated within the geomorphological unit of the Chvojnická Pahorkatina (hilly land), part of the Záhorská nížina (lowland) with the site's maximum elevation at 233.73 meters above sea level, while its minimum elevation is 208.93 meters above sea level, while the average slope is 7.65 %. Parcel is formed by deep soil (over 60 cm) and 2 types of soil HPJ 57 - psuedoglaye typical on loess and polygenic clays, moderately heavy on the surface (13.72ha / 39.34 %) and HPJ 59 – light arenic regosols on windblown sands (21.15 ha /60.66 %). The site is classified as a warm, very dry, lowland region, with an average air temperature of T=16°C per growing season [IV-IX]. According to the Slovak Hydrometeorological Institute (http://www.shmu.sk/), the long-term average rainfall for the period 1961-2019 for the region is 589 mm.

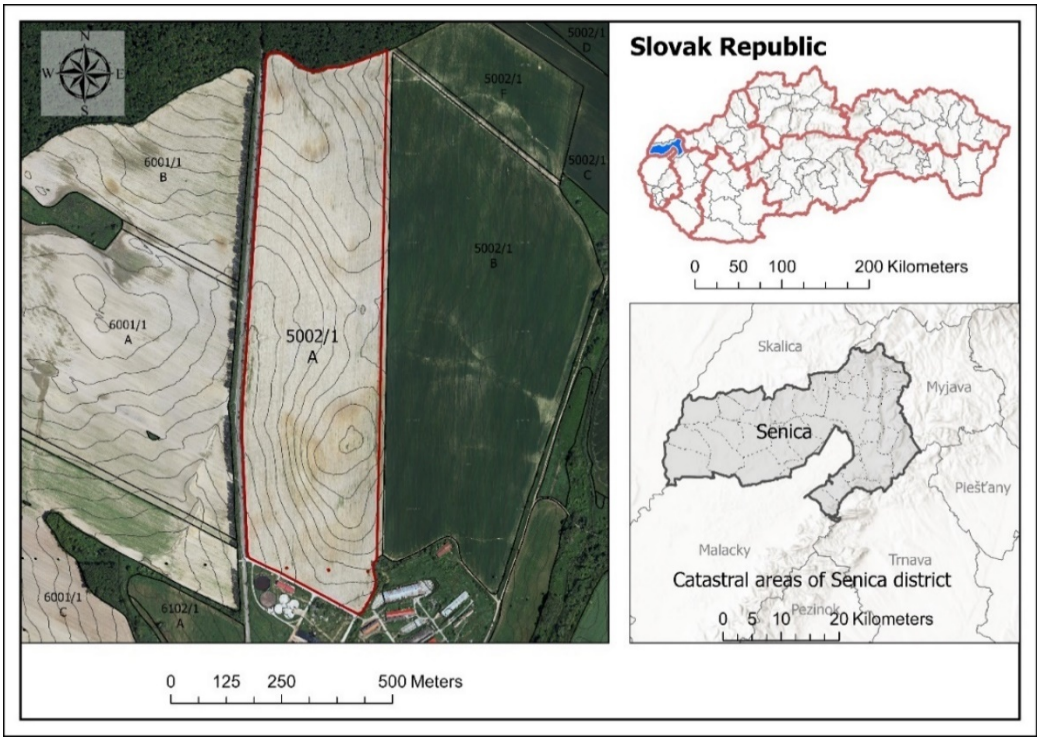



*Fig. 1: Parcel 5002/1A layout*

The reference layer for our water erosion modelling was generated using close-range aerial photogrammetry with a DJI Phantom 4 Pro V2 (https://www.dji.com/). This drone features a 1-inch CMOS sensor with a 20 MP resolution and an 8.8 mm focal length. The flight mission was conducted at an altitude of 70 meters above ground level, with both frontal and side overlap set to 80 % to ensure high image overlap, minimizing blind spots in post-processing. A camera angle of 90° was used to capture nadir images. A total of 405 images were processed using Agisoft Metashape software (https://www.agisoft.com/). During processing, the software calculated the position and orientation of each photo, generating layers such as sparse and dense point clouds essential for creating a high-resolution 3D mesh model. This model served as the basis for constructing the orthomosaic, which we produced with a spatial resolution of 25x25 cm/pixel.

Water erosion was calculated using the Universal Soil Loss Equation (USLE) according to [11] in the following equation:

$$A = R.K.LS.C.P$$

Where: A - is the average annual soil loss ($t \cdot ha^{-1} \cdot yr^{-1}$), R is the rainfall erosivity factor ($MJ \cdot ha^{-1} \cdot cm \cdot h^{-1}$), K is the soil erodibility factor ($t \cdot ha^{-1} \cdot mm \cdot h^{-1}$), LS is the topographic factor (dimensionless), C is the cover management factor (dimensionless), and P is the support practice factor (dimensionless).

R factor was derived based on the nearest ombrographic station in Senica, where the value of R factor is 67.2 $MJ.ha^{-1}.cm.h^{-1}$ according to [12].

The K factor values (constants) for individual soil types are determined based on the primary soil units, as outlined by [13]. These values range between

https://doi.org/10.5593/sgem2024v/3.2/s12.26

0.21-0.30 $t.ha^{-1}.mm.h^{-1}$, reflecting the soil's susceptibility to erosion under specific rainfall conditions.

The topographic factor (LS), representing slope length and steepness, was calculated following the model proposed by [14]. This data layer was generated from a digital elevation model (DEM) raster, specifically DMR 5.0 (https://www.geo-portal.sk/sk/zbgis/lls/). From this DEM, additional layers were derived to quantify the slope gradient percentage and uninterrupted slope length necessary for the LS factor calculation.

The field survey indicated that the block had been recently sown with a winter crop, leaving the soil exposed without vegetative cover for protection. Consequently, a C-factor value of 1 was assigned, reflecting the lack of protective vegetation. Additionally, the P-factor (support practices) was assigned a value of 1, indicating the absence of any erosion-control measures in place.

To propose an effective mitigation measure that respects the highly fragmented land ownership in Slovakia [15], we introduced strip crop rotation as an intervention that could feasibly be implemented without disrupting ownership boundaries. Strip cropping was chosen due to its compatibility with the existing land structure and its potential to reduce soil erosion rates by influencing the C and P factors. The principle of strip crop rotation involves alternating strips of crops with varying erosion protection effects, with more protective crops placed alongside those with lower protection. These strips are typically arranged along or near the contours of the land. The design allows water to flow from the less-protected areas onto the more-protected ones, where it is captured and allowed to infiltrate the soil, reducing erosion [16].

## RESULTS

The USLE modelling for parcel 5002/1 Šaštín, spanning 34.86 ha, estimated an average soil loss of approximately 10 $t.ha^{-1}.yr^{-1}$ to under the current management regime, highlighting the parcel's vulnerability to surface erosion (fig. 2). The soil loss rate is particularly concerning given the soil depth and its classification under Technical norm (STN 75 4501, Protierózna ochrana poľnohospodárskej pôdy/ Protection of agricultural land against erosion). Our analysis classified 14% (approximately 5 hectares) of the parcel as slightly endangered by erosion and 6% (around 2.18 hectares) as severely endangered. This spatial differentiation indicates that erosion control measures could be effectively targeted to mitigate losses in the most vulnerable areas.

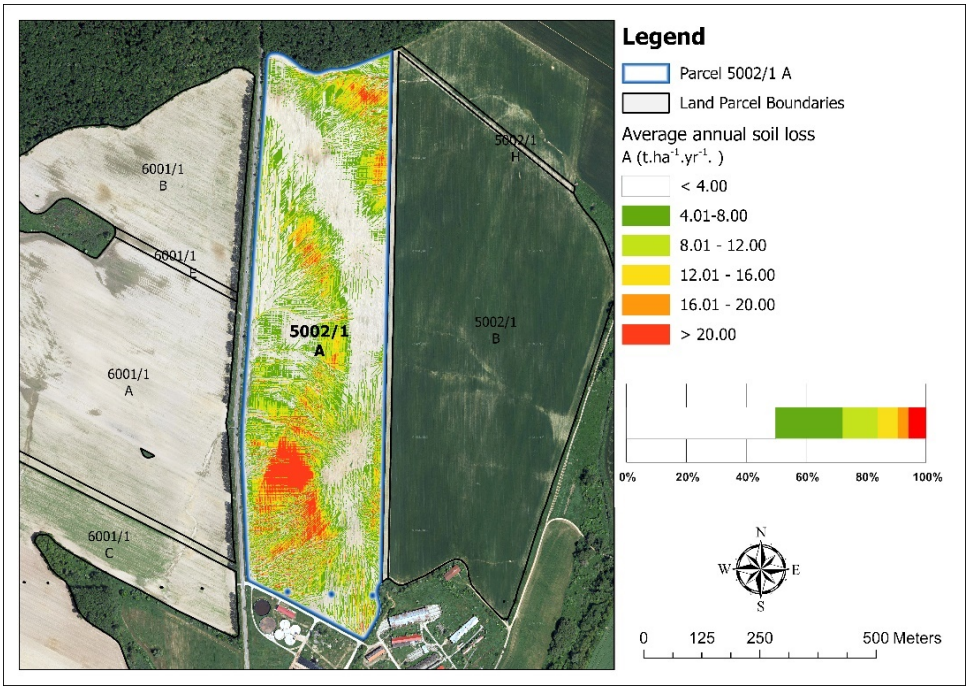



*Fig. 2: Evaluation of water erosion without vegetation cover*

Using UAS-based orthophotographic imagery, two primary subcatchments (Fig. 3) were identified as significant sources of water erosion. These areas direct sheet erosion into well-defined path of concentrated surface runoff, which pose a direct threat to the infrastructure of the III. class route (route no. 1155), as Critical Profile [17]. The erosion further extends onto adjacent parcels 6001/1A and 6001/C, resulting in the accumulation of alluvial material within the watercourse of Lúčny potok. This process contributes to watercourse siltation and may exacerbate nutrient runoff, potentially accelerating eutrophication at the stream's headwaters.

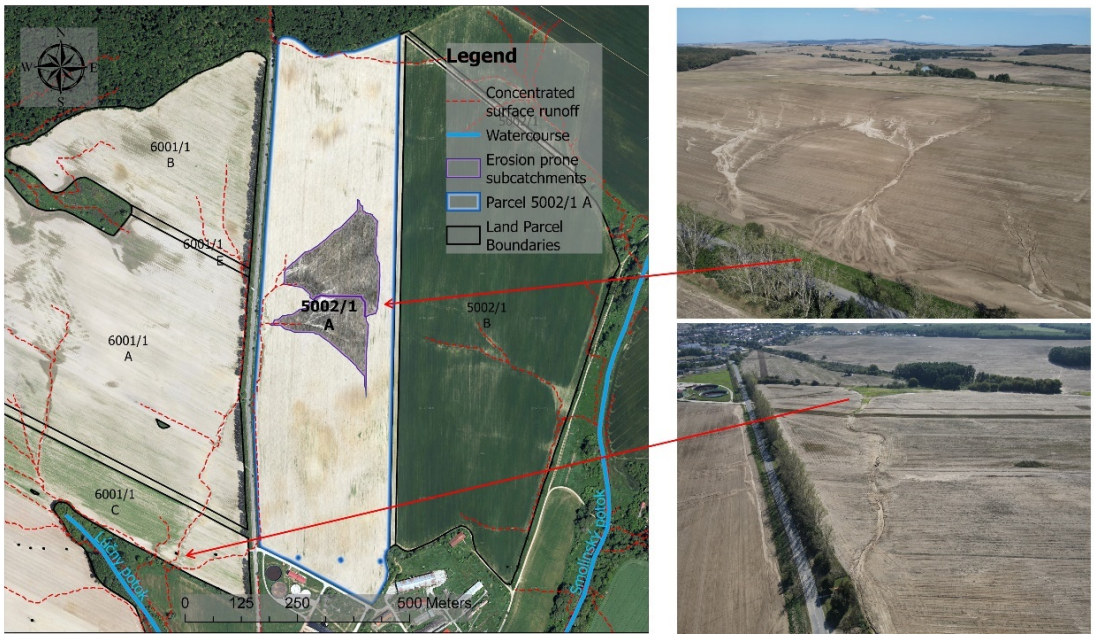



*Fig. 3: UAS-Identified erosion runoff in Parcel 5002/1A and adjacent parcels*

https://doi.org/10.5593/sgem2024v/3.2/s12.26

Implementing a strip crop rotation system with 36 m wide strips, designed to suit agricultural machinery and incorporating contour farming (P factor of 0.65), led to a significant reduction in soil erosion. This system used carefully selected crops maize (*Zea mays*) (C factor of 0.61) and barley (*Hordeum vulgare L.*) (C factor of 0.17) to enhance soil cover and stability, especially during peak rainfall periods. As a result, soil loss on the parcel dropped markedly to an estimated 2.5 $t.ha^{-1}.yr^{-1}$, representing a nearly 75% reduction in erosion rates (fig. 4).

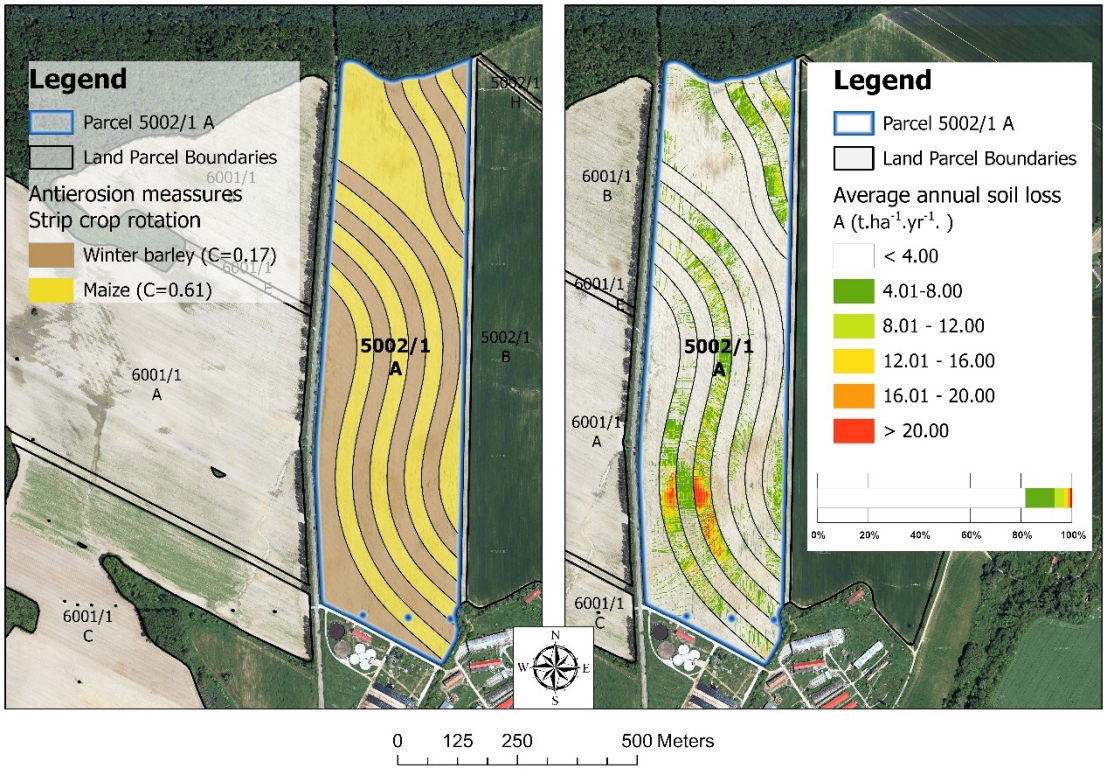



*Fig. 4 Evaluation of water erosion after application of anti-erosion measures*

This approach effectively reduces soil loss to levels well within the permissible erosion limits specified by Technical norm. Following this adjustment, 98.29 % of the area is now classified as either unthreatened or only moderately threatened by erosion, with just 1.71 % categorized as slightly endangered.

## DISCUSSION

The implementation of strip crop rotation with contour farming (P=0.65) effectively reduced soil erosion by nearly 75 %, decreasing soil loss from 10 $t.ha^{-1}.yr^{-1}$ to 2.5 $t.ha^{-1}.yr^{-1}$. This approach, aligning with strip crop rotation guidelines, alternates high and low erosion-resistance crops along contour lines, reducing sheet and gully erosion and limiting sediment and nutrient runoff, which supports both soil and water conservation [16].

These results validate the hypothesis that contour-aligned strip cropping enhances soil retention, especially during extreme rainfall. The recalculated erosion rate now meets Technical norm limits, classifying over 98% of the parcel as low risk. Additionally, this strategy improved water infiltration and reduced runoff, consistent with findings that strip cropping increases resilience on moderate slopes while additional measures may be

needed for steeper terrain. This study confirms strip cropping and contour farming as effective practices for sustainable soil management under challenging weather conditions and ownership fragmentation.

## CONCLUSION

This study examined the effects of extreme rainfall on soil erosion in the Senica district of Slovakia, specifically focusing on the 5002/1 Šaštín parcel. The results revealed significant erosion, with an estimated soil loss of 10 tons per hectare per year under current management practices (minimum soil coverage). The use of UAS and USLE methodology highlighted the vulnerability of the land to water erosion, particularly in steeper areas. By implementing strip crop rotation with contour farming, soil loss was reduced by 75 %, dropping to 2.5 tons per hectare per year. This change significantly improved the erosion risk, with over 98 % of the area now classified as low risk for erosion. These findings demonstrate that simple land management changes, like strip crop rotation, can greatly mitigate the impacts of extreme weather events, reducing erosion and preserving soil quality. Further research could focus on the long-term sustainability of such practices and their effectiveness across varying soil types and climatic conditions, helping to refine and scale erosion control methods for broader agricultural use.

## ACKNOWLEDGEMENTS

This study was supported by the Slovak Research and Development Agency under grand (No. APVV-23-0530), by the Scientific Grant Agency of the Ministry of Education, Research, Development and Youth of the Slovak Republic and the Slovak Academy of Sciences (No. 1/0244/21), Cultural and Educational Grant Agency of The Ministry of Education, Research, Development and Youth of the Slovak Republic (No. 029SPU-4/2022) and the European Union's Horizon 2020 research and innovation programme under grant agreement (No. 101082169).

## REFERENCES

[1] Anders I., Stagl J., Auer I., Pavlik D., Climate Change in Central and Eastern Europe. In: Rannow S., Neubert M. (eds) Managing Protected Areas in Central and Eastern Europe Under Climate Change. Advances in Global Change Research, Springer, Dordrech, New York, London vol. 58, pp 17-30, 2014. DOI:10.1007/978-94-007-7960-0_2

[2] Albrecht J., Hartmann T., Land for flood risk management - Instruments and strategies of land management for polders and dike relocations in Germany, Environmental Science & Policy, vol. 118, pp 36-44, 2021. https://doi.org/10.1016/j.envsci.2020.12.008

[3] McIvor I., Youjun H., Daoping L., Eyles G., Pu Z., Agroforestry: Conservation Trees and Erosion Prevention, Encyclopedia of Agriculture and Food Systems, 2014, pp 208-221. DOI:10.1016/B978-0-444-52512-3.00247-3

[4] Lal R., Soil erosion and the global carbon budget, Environment International, vol. 29, no. 4, 2003, pp. 437-450, ISSN 0160-4120, https://doi.org/10.1016/S0160-4120(02)00192-7.

[5] Kothyari, U. C., Soil erosion and sediment yield modeling, Journal of Hydraulic Engineering, vol. 14, pp 84–103, 2008. DOI: 10.1080/09715010.2008.10514895

[6] Quinton J.N., Catt J.A, Enrichment of heavy metals in sediment resulting from soil erosion on agricultural fields, Environmental Science & Technology, vol. 41, pp 3495-3500, 2007. DOI: 10.1021/es062147h

[7] Gazzola P., Belčáková I., Pauditšová E., Case studies. Landscape impact assessment in planning processes, De Gruyter, Berlin/Boston, vol. 163, pp 139-189, 2019. DOI:10.1515/9783110601558

[8] Meinen B.U., Robinson D.T., Agricultural erosion modelling: Evaluating USLE and WEPP field-scale erosion estimates using UAV time-series data, Environmental Modelling & Software, vol. 137, pp 104962, 2021. https://doi.org/10.1016/j.envsoft.2021.104962

[9] d'Oleire-Oltmanns S., Marzolff I., Peter K.D., Ries J.B., Unmanned Aerial Vehicle (UAV) for Monitoring Soil Erosion in Morocco, Remote Sensing, vol. 4, pp 3390-3416, 2012. https://doi.org/10.3390/rs4113390

[10] Lal R., Soil Erosion by Wind and Water: Problems and Prospects, Soil Erosion Research Methods, pp 1-10, 2017. DOI:10.1201/9780203739358-1

[11] Wischmeier W.H., Smith D., Predicting rainfall erosion losses, *Agricultural Handbook No. 537*, USDA, Washington D.C., 1978.

[12] Onderka M., Pecho J., Update of the erosive rain factor in Slovakia using data from the period 1961–2009, *Contributions to Geophysics and Geodesy*, vol. 49, no. 3, 2019, pp. 355–371. https://doi.org/10.2478/congeo-2019-0018

[13] Ilavská B., Jambor P., Lazúr R., Identification of threats to soil quality from water and wind erosion and proposals for measures, *VÚPOP*, Bratislava, 2005, 60 pp. (in Slovak).

[14] McCool D.K., Foster G.R., Mutchler C.K., Meyer L.D., Revised slope length factor for the Universal Soil Loss Equation, *Transactions of the ASAE*, vol. 32, no. 5, 1989, pp. 1571-1576, doi: 10.13031/2013.31192.

[15] Janus J., Ertunç E., Muchová Z., Tomić H., Impact of selected land fragmentation parameters and spatial rural settlement patterns on the competitiveness of agriculture: Examples of selected European and Asian countries, *Habitat International*, vol. 140, 2023, Art. No. 102911, ISSN 0197-3975. DOI: 10.1016/j.habitatint.2023.102911

[16] Dumbrovský, D., Šarapatka B., Bednář M., Sobotková V., Pražan J., Mrnuštík Konečná M., Vrstevnicové obdělávání a pásové střídání plodin. Certifikovaná metodika, *VUT v Brně*, 2021. https://protieroznipasy.vumop.cz/data/Vrstevnicov%C3%-A9%20obd%C4%9Bl%C3%A1v%C3%A1n%C3%AD%20a%20p%C3%A1sov%C3%A9%20st%C5%99%C3%ADdan%C3%AD%20plodin.pdf

[17] Dežerický D., Šinka K., Pipíšková P., Dumbrovský M., Schaffhauser T., Muchová Z., An approach to classify areas for appropriate rainfall-runoff risk management: A case study in Drevenica basin, Slovakia, *Ecological Engineering*, vol. 196, 2023, Art. No. 107083, ISSN 0925-8574. https://doi.org/10.1016/j.ecoleng.2023.107083

# ASSESSMENT OF THE EFFECTS OF COMPLEX FOLIAR FERTILIZATION ON THE YIELD AND QUALITY OF SUNFLOWER SEEDS (HELIANTHUS ANNUUS L.)

**Prof. Dr. Florin Crista**
**Prof. Dr. Florin Imbrea**
**Prof. Dr. Isidora Radulov**
**Dr. Laura Crista**
**Lecturer Alina Lato**
University of Life Science Timisoara, **Romania**

## ABSTRACT

This study aims to evaluate the effects of foliar fertilization (FF) on the yield and quality of sunflower seeds. Foliar fertilization (FF) applied to sunflower crops can have significant impacts on seed yield and quality, influencing their chemical composition and nutritional values. Unlike soil fertilization, which delivers nutrients through the root system, foliar fertilization supplies nutrients directly to the leaves, ensuring a rapid and efficient absorption of essential elements during critical growth stages. The study was conducted during the 2022 and 2023 agricultural seasons at the university's experimental field, using split plots with three replications and six fertilization variants. The experimental variants included: Control (Mt), V1-FF 10:10:10+ME (microelements), V2-FF 8:10:0+8B (boron)+ME, V3-FF 15:0:0+2S (sulfur)+1B+ME, V4-FF 15:0:0+4B+ME, and V5-FF 8:8:8+ME. FF treatments were applied during specific vegetative stages, with doses ranging from 2 to 6 L/ha depending on the chemical composition of each product. The application of foliar fertilization resulted in a positive increase in both yield and seed quality, as evidenced by quality parameters such as protein content, lipids, carbohydrates, fibers, and minerals. The results were analysed using both classical statistical methods and Principal Component Analysis (PCA) for a deeper understanding of the impact of foliar fertilization on the yield and quality of sunflower seeds.

**Keywords** foliar fertilization, sunflower, chemical composition

## INTRODUCTION

The sunflower (Helianthus annuus) stands as a pivotal oilseed crop globally, valued not only for its versatility in adapting to a range of environmental conditions but also for its significant role in agricultural economies. It occupies substantial cultivation areas across Romania, Europe, and worldwide, contributing both economically and nutritionally. Given recent political and economic fluctuations in Europe, sunflower cultivation has garnered heightened interest across various sectors, including agriculture and industry. Romania, in particular, has maintained a leading position in the European Union for sunflower production since 2015, with a notable yield average of around 2.3 t/ha. Beyond its primary function in producing edible oil for human consumption, sunflower is also an essential source of protein for livestock feed. This study was conducted to assess the impact of foliar fertilizers on sunflower seed yield and quality, both quantitatively and qualitatively, thus strengthening a critical component of the

https://doi.org/10.5593/sgem2024v/3.2/s12.27

sunflower production chain. The research addresses the increasingly vital role of agricultural chemistry, particularly the judicious use of fertilizers, in maximizing yield per hectare and enhancing crop output.

Modern agricultural systems heavily rely on fertilizers to optimize both yield and quality, while also minimizing input costs. However, as the costs associated with fertilizers have surged in recent decades—largely due to energy demands, particularly fossil fuel consumption—alternative fertilization strategies such as foliar fertilization have become essential topics of study. Foliar fertilizers, which are applied directly to plant foliage, are formulated with lower quantities of traditional mineral components, supplemented with trace elements, or micronutrients, which facilitate enhanced absorption and utilization of macronutrients. This application method introduces nutrients in an aqueous solution, additionally supplying plants with water, a key growth factor. Since the 19th century, it has been established that plants can absorb nutrients through leaves, a discovery that popularized foliar fertilization. However, despite extensive research on root nutrient absorption, the precise mechanisms underlying foliar absorption—specifically through plant cuticles, stomata, and trichomes—remain only partially understood, presenting a critical area for further investigation.

The foliar absorption pathways are complex due to the chemical and structural nature of the cuticle. Research has identified two primary pathways within the epidermis for nutrient absorption: a lipophilic pathway for non-ionic, non-polar compounds (e.g., insecticides and herbicides), and a hydrophilic pathway for ionic, polar substances, such as essential minerals. Furthermore, intensive cultivation practices have depleted soil fertility, reducing the availability of essential nutrients and resulting in lower productivity. Thus, sustainable sunflower production necessitates precise and balanced fertilization practices to meet plant nutritional demands, including macronutrients like nitrogen (N), phosphorus (P), potassium (K), and sulfur (S). Notably, nitrogen alone has been shown to increase sunflower yield by 19–40%, underscoring its critical role in crop growth and productivity. Following N, P, and K, sulfur is the fourth most vital macronutrient for plants, crucial for protein synthesis, photosynthesis, and enzyme activity. Research indicates that adequate sulfur application can significantly improve sunflower yields, especially as rising crop outputs increase sulfur removal from soils, necessitating its replenishment to sustain productivity.

Sulfur's involvement in plant metabolism extends beyond basic nutrition; it plays an active role in nitrogen and potassium utilization, thereby enhancing nutrient efficiency and overall plant health. In plants, sulfur contributes to chlorophyll formation, the synthesis of sulfur-containing amino acids (e.g., cysteine, methionine), and serves as a cofactor in various enzyme systems. Sulfur can be absorbed as sulfate ions via the roots or as sulfur dioxide gas through the foliage. In oilseed crops such as sunflower, sulfur is particularly important, with studies recommending applications of 16–25 kg S per hectare for optimal yield and quality. By supporting chlorophyll biosynthesis, sulfur aids in photosynthesis and promotes the conversion of carbohydrates into lipids, a process essential for oil production in sunflower seeds. Notably, symptoms of sulfur deficiency resemble those of nitrogen deficiency, manifesting as chlorosis (leaf yellowing) that appears initially in younger leaves.

Boron is another micronutrient crucial for sunflower growth, and its uptake is influenced by soil pH and nutrient availability. The minimum critical boron

concentration for sunflower growth is 20 mg/kg of soil, though achieving this concentration through direct soil application is often cost-prohibitive, leading farmers to prefer foliar boron supplementation. Foliar application of boron has been shown to enhance sunflower growth, especially under drought conditions, by modulating physiological responses to water stress. For instance, applications at specific growth stages (e.g., BBCH 15–16 and 20–22) have been found to increase seed yield and nitrogen content, underscoring boron's importance in crop resilience and productivity. Boron demand in sunflower varies by growth stage, with younger plants requiring higher concentrations; for example, boron concentrations of 46–63 mg/kg dry matter are needed at four weeks, decreasing to 36 mg/kg at eight weeks. Recent studies, particularly in water-limited regions, have demonstrated that foliar boron applications (0.3% concentration) administered twice during critical growth stages (BBCH 15–16 and BBCH 20–22) can improve nitrogen uptake and enhance yield, without significantly affecting oil content.

In addition to boron and sulfur, trace micronutrients like copper (Cu), iron (Fe), manganese (Mn), and zinc (Zn) are integral to plant physiological processes. Copper functions as a cofactor in photosynthesis and respiratory chains, and also contributes to lignification processes in cell walls. Due to its dual nature as both essential and potentially toxic, copper is typically applied in low concentrations. Iron, essential for chlorophyll biosynthesis and various redox reactions, is integral to chloroplast function, with deficiency leading to reduced protein synthesis and photosynthetic efficiency. Foliar iron application, such as with Fe-aspartate, has been shown to improve photosynthesis and nutrient acquisition. Iron absorption via foliar application varies by plant species due to differences in stomatal and venation patterns. In broadleaf plants like sunflowers, iron is absorbed symplastically from the substomatal chambers into the phloem, a pathway distinct from the direct absorption seen in grass species.

Manganese (Mn) supports photosynthetic activity, particularly in Photosystem II, and contributes to oxidative stress regulation through enzymes like superoxide dismutase (MnSOD). Mn deficiency significantly impairs oxygen evolution in young leaves, leading to chlorosis and diminished photosynthetic efficiency. Studies indicate that higher Mn concentrations in sunflower seeds increase oil content but reduce protein levels, highlighting its influence on seed composition and quality. Zinc (Zn) plays a key role in carbon metabolism, acting as a cofactor in enzymes like carbonic anhydrase and aldolase. For sunflower cultivation, foliar application of macronutrients like boron and sulfur at early growth stages supports critical physiological processes including flowering, fertilization, seed filling, and root and foliage development. To optimize the benefits of foliar fertilization, it is essential to determine the optimal timing, frequency, and dosage based on crop-specific requirements and environmental conditions. In this study, various foliar fertilization treatments were evaluated to determine their effects on sunflower seed yield and quality. Using chemometric techniques like Principal Component Analysis (PCA), researchers assessed interactions between foliar fertilizer applications and seed quality parameters, including moisture, ash, macro- and microelements, lipids, protein, fiber, and carbohydrate content. This approach enabled the identification of the most effective foliar fertilizer combinations for enhancing sunflower seed production, both quantitatively and qualitatively.

https://doi.org/10.5593/sgem2024v/3.2/s12.27

## MATERIALS AND METHODS

*Natural Framework of Experimentation*

The study was conducted during 2022–2023 at the Cioreni experimental fields (coordinates: N 45°48.298′, E 21°09.350′, altitude 79 m, measured using a Garmin GPSMAP 64 st device) of the University of Life Sciences "King Michael I" in Timișoara. The site is situated in Romania's Western Plain, characterized by a temperate-continental climate with slight Mediterranean and Oceanic influences [32]. These climatic conditions make the area highly suitable for cultivating sunflowers. [33].

The study focused on the properties of a cambic low-gleyed chernozem soil, which is characteristic of the local geomorphological and environmental conditions of a low subsidence plain. Granulometric analysis revealed a balanced distribution of soil particles, resulting in a medium-fine texture. The composition of granulometric fractions reflects a stable sedimentation environment, characterized by aquatic, basic, and calm conditions. Fine sand (28–33%) and clay (40–42.0%) dominate the soil structure, while coarse sand (0.3–0.6%) occurs in minimal quantities, indicating sporadic and chaotic deposition events. Dust fractions are present in normal proportions (27–30%). The soil exhibits relatively high density (2.45–2.73 g/cm³), signifying advanced organic matter mineralization and intensified melanization of upper horizons. The apparent density of the processed horizon (Ap) was the highest, measured at 1.50 g/cm³. Total porosity showed small to medium values (43–47%), while aeration porosity was extremely low (12%) in this horizon due to the collapse of non-capillary pores. At greater depths, where human activities such as agricultural machinery use are less pronounced, aeration porosity improved significantly, reflecting typical conditions for soils on loess deposits and those in intermediate stages of pedological evolution.

Chemically, the soil solution is weakly acidic in the upper horizons (pH = 6.16) and weakly alkaline in the lower horizons (pH = 8.4), correlating strongly with carbonate content. Debasification processes in the upper layers have led to the eluviation of carbonates to a depth of 95 cm, removing calcium salts from the upper third of the soil profile. This has resulted in a basic environment in the lower horizons, where calcium ions remain in the soil solution in substantial quantities.

*Soil Organic Matter and Fertilization Practices*

The humus content of the soil ranges between 1.8% and 3.3%, reflecting an adequate supply of organic matter, a characteristic of mollisols. Total nitrogen content is relatively low, oscillating between 0.120% and 0.221%, with its availability strongly correlated with humus levels. The supply of mobile phosphorus is also limited, ranging from 4 to 23 ppm, highlighting the necessity of chemical fertilizers containing phosphorus to meet crop demands. Potassium availability is moderate, ranging from 120 to 138 ppm, further supporting a medium supply of this essential nutrient [36, 37].

*Sowing and Fertilization Practices*

Sunflower sowing was conducted during the optimal period, leveraging previous experimental experience. The Neoma hybrid, provided by Syngenta Company, was used as the crop model, with a sowing density of 58,000 seeds per hectare. Fertilization began with an autumn application of 120 kg/ha of a solid chemical fertilizer (18:46:0; N, $P_2O_5$, $K_2O$), followed by two foliar fertilizations tailored to sunflower-specific nutrient demands during vegetative phases. The fertilization stages corresponded to the

BBCH scale 15–16 (5–6 unfolded leaves) for the first application and BBCH scale 20–22 (10–12 unfolded leaves) for the second, ensuring sufficient nutrient supply during critical growth phases [4, 15].

Given the slow early growth rate of sunflowers, early weed control was prioritized through herbicide applications [38]. Foliar fertilizer doses ranged from 2 to 6 L/ha, depending on the specific chemical composition required. Additional single fertilization was conducted during the autumn using solid fertilizers.

The experimental design was based on subdivided plots, with three replications and six fertilization variants. Each experimental plot measured 24.5 m² (7 m in length, 3.5 m in width), with a harvestable area measuring 1 m in width. Treatments included the following variants:

- V1: FF 10:10:10 + ME, 6 L/ha
- V2: FF 8:10:0 + 8B + ME, 2 L/ha
- V3: FF 15:0:0 + 25B + ME, 6 L/ha
- V4: FF 15:0:0 + 4B + ME, 4 L/ha
- V5: FF 8:8:8 + ME, 6 L/ha
- Mt-Control: No fertilizer applied.

The fertilizers provided various combinations of soluble nutrients, including nitrogen (N), phosphorus ($P_2O_5$), potassium ($K_2O$), and trace elements such as boron (B, 0.01%), sulfur (S, 1%), and micronutrients like iron (Fe), manganese (Mn), zinc (Zn), cobalt (Co), and molybdenum (Mo), all expressed as percentages by weight. Micronutrients were chelated and incorporated with EDTA to enhance nutrient bioavailability.

## RESULTS AND DISCUSSION

Abiotic stress is known to significantly affect plant growth, fertility, and yield, as well as the quality and quantity of oil produced by oilseed crops. The deficiency of essential nutrients during critical growth phases can impair plant development and production. Foliar fertilization has been shown to effectively mitigate nutrient deficiencies, especially during critical periods, thus improving yield and quality in sunflower crops [13, 31, 54].

*Impact on Production*

The experimental data indicate that foliar treatments significantly increased sunflower seed production compared to the control group (Mt). On average, a yield of approximately 370 kg/ha was recorded for the foliar-fertilized variants, particularly those enriched with nitrogen and phosphorus, which are known to enhance seed production. Among all treatments, the V2 and V4 variants yielded the highest production levels, reflecting the critical role of micronutrients such as boron (B), which demonstrated a favorable impact on grain yield, particularly when combined with zinc (Zn) and molybdenum (Mo).

The humidity levels of the seeds in the V2 foliar treatment group were found to be lower compared to other groups, highlighting its efficiency in improving seed quality. The differences in seed production across treatments were statistically significant compared to the control, aligning with results reported for other oilseed crops such as brassica species. This suggests that boron may serve as a limiting factor in oilseed production, particularly when associated with the availability of Zn and Mo [28, 56].

https://doi.org/10.5593/sgem2024v/3.2/s12.27

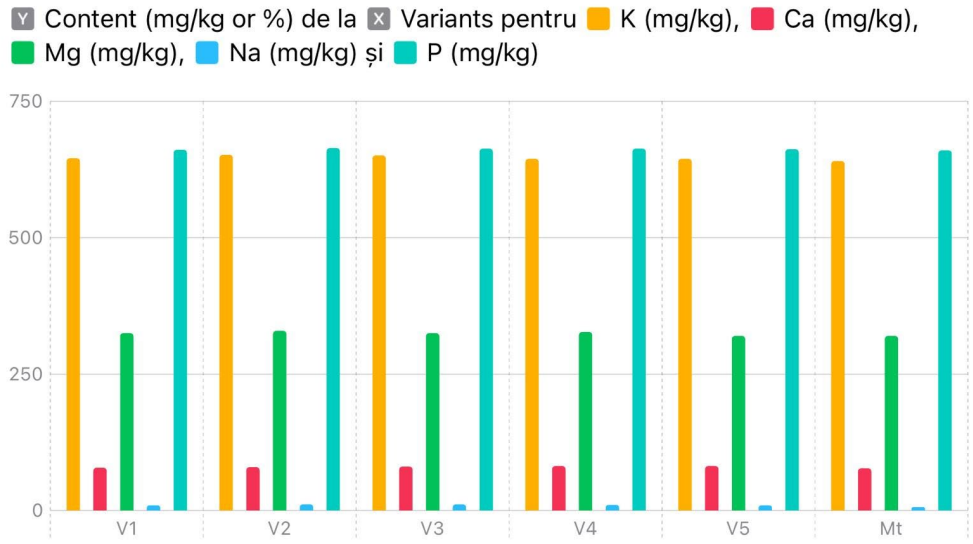



Figure 1 The content of macroelements across the different sunflower seed treatment variants

Magnesium, as a key component of chlorophyll, is critical for photosynthesis and overall plant development. It plays a significant role in enzyme activation, phosphorus absorption, and sugar storage. Magnesium deficiencies manifest in weak stalks, yellowing, and browning of leaves, with some loss of greenness. Despite relatively low increases in magnesium compared to the control, all foliar fertilization variants exhibited consistent magnesium content in seeds, with the V2 (8:10:0+1B+ME) and V4 (15:0:0+4B+ME) variants showing the highest increase (6–9 ppm or 1.9–2.8%).

Calcium contributes to the structural integrity of plant cell walls, aiding in tissue development, root formation, and overall plant vigor. It neutralizes toxic effects of various substances and improves nutrient transport. Calcium deficiencies cause visible symptoms such as yellow and brown spots on leaves, stunted growth, and reduced development. Foliar fertilization increased calcium content in seeds from 2 to 4 ppm (2.6–5.2%), with V4 (15:0:0+4B+ME) and V5 (8:8:8+ME) showing the most significant improvement.

Phosphorus is essential for root and flower development and is critical in energy metabolism and sunflower resistance to environmental stress. A deficiency in phosphorus leads to reduced growth and lower seed production quality. Among the tested variants, V2 (8:10:0+1B+ME), V3 (15:0:0+1B+2S+ME), and V4 (15:0:0+4B+ME) demonstrated the highest phosphorus content in seeds, with increases of 2–4 ppm (0.3–0.6%) over the control.

While ash content was minimally influenced by foliar fertilization, macronutrient levels (calcium, magnesium, and phosphorus) showed significant increases, particularly in the V2 variant. Boron presence was a noticeable factor in improving macronutrient content, suggesting its role in enhancing foliar fertilizer efficacy.

*Impact of Foliar Fertilization on Essential Microelements*

Microelements (Fe, Zn, Cu, Mn) are vital despite their smaller required quantities. Deficiencies in these elements negatively affect physiological and metabolic processes, plant growth, and seed development. Figure 2 highlights that foliar treatments

significantly influenced iron (Fe) and manganese (Mn) levels, particularly in the V2 variant, which showed the highest improvement. Copper (Cu) levels were notably elevated in the V3 variant. However, zinc (Zn) levels were consistently lower in foliar-treated seeds compared to the control, especially in V1, V2, and V4 variants.

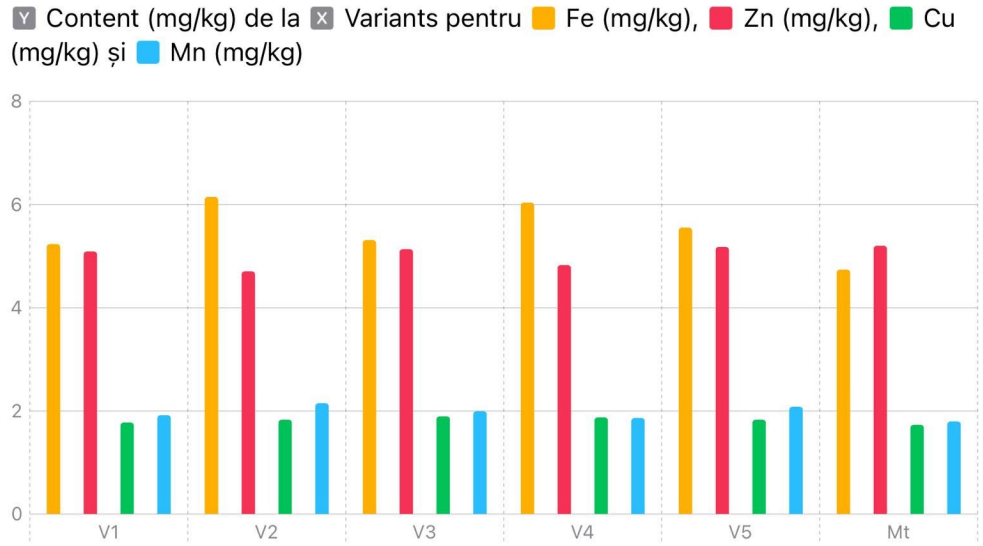



Figure 2 The content of microelements in sunflower seeds under the influence of foliar fertilization

## CONCLUSION

The study demonstrates that all tested foliar fertilization treatments positively influenced sunflower seed yield and quality. Among the variants, the V2 (8:10:0+B+ME; 2 L/ha) treatment was the most effective, yielding the highest increases in key parameters such as seed yield, protein, and lipid content, while also improving mineral concentrations (K, Fe, Mn) and maintaining the lowest seed humidity. These outcomes underline the superior effect of the V2 treatment in enhancing both the quantitative and qualitative attributes of sunflower seeds compared to the control and other treatments.

Using Principal Component Analysis (PCA), the V2 and V4 (15:0:0+4B+ME) treatments were identified as optimal, with V4 showing the highest improvement in fiber content and overall seed quality, while V5 (8:8:8+ME) exhibited the highest levels of saturated fatty acids. The combined application of nitrogen, phosphorus, and boron in these treatments was critical to achieving these improvements. The study concludes that the application of tailored foliar fertilizers plays a pivotal role in improving the nutrient composition and quality of sunflower seeds. This research provides a framework for optimizing fertilization strategies to meet agricultural productivity goals while ensuring food security and sustainable crop production. These findings support a pragmatic approach to designing foliar fertilizers based on the desired crop characteristics, enabling precise nutrient management in modern agriculture

https://doi.org/10.5593/sgem2024v/3.2/s12.27

## REFERENCES

[1] The Food and Agriculture Organization (FAO). Available online: www.fao.org/faostat/en/#compare (accessed on September 2024).

[2] Aboudrare, A.; Debaeke, P.; Bouaziz, A.; Chekli, H. Effects of soil tillage and fallow management on soil water storage and sunflower production in a semi-arid Mediterranean climate. Agric. Water Manag. 2006, 83, 183–196. [CrossRef]

[3] Radulov, I.; Lat,o, A.; Berbecea, A.; Lat,o, I.; Crista, F. Nitrate Pollution of Water in Romanian Serbia Cross-Border Area as a Consequence of Agricultural Practices. In Proceedings of the 16th International Multidisciplinary Scientific GeoConference, SGEM 2016, Vienna, Austria, 2–5 November 2016; Volume III, p. 205.

[4] Schreiber, L.; Schönherr, J. Water and Solute Permeability of Plant Cuticles. Measurement and Data Analysis; Springer: Berlin/Heidelberg, Germany, 2009; pp. 1–29. [CrossRef]

[5] Li, S.T.; Duan, Y.; Guo, T.W.; Zhang, P.L.; He, P.; Majumdar, K. Sunflower response to potassium fertilization and nutrient requirement estimation. J. Integr. Agric. 2018, 17, 2802–2812. [CrossRef]

[6] Zubillaga, M.M.; Aristi, J.P.; Lavado, R.S. Effect of Phosphorus and Nitrogen Fertilization on Sunflower (Helianthus annus L.) Nitrogen Uptake and Yield. J. Agron. Crop Sci. 2002, 188, 267–274. [CrossRef]

[7] Singh, F.; Ghosh, G.; Debbarma, V. Effect of Different Levels of Nitrogen, Sulphur and Foliar Application of Boron in Sunflower (Helianthus annuus L.). Int. J. Curr. Microbiol. App. Sci. 2017, 6, 1336–1342. [CrossRef]

[8] Kumar, K.A.; Reddy, S.; Kaur, G.; Chhabra, V. Effect of Sulphur Fertilization on Growth and Yield of Sunflower Crop-A Review. Indian J. Agric. Allied Sci. 2002, 8, 31–35.

[9] Asad, A. Boron requirements for sunflower and beet. J. Plant Nutr. 2002, 25, 885–889. [CrossRef]

[10] Asad, A.; Blamey, F.P.C.; Edwards, D.G. Effect of foliar boron application on vegetative and reproductive growth of sunflower. Ann. Bot. 2003, 92, 565–570. [CrossRef] [PubMed]

[11] Rashid, A.; Rafique, E. Internal boron requirements of young sunflower plants, proposed diagnostic criteria. Community Soil Sci. Plant Ann. 2005, 36, 2113–2119. [CrossRef]

[12] Milev, G. Effect of foliar fertilization on sunflower (Helianhtus annuus L.). Agric. Sci. Technol. 2015, 7, 324–327.

[13] Available online: https://www.meteoromania.ro/servicii/date-meteorologice/ (accessed on october 2024).

[14] Crista, F. Conservarea Fertilitătii Solului Si Managementul Nutrientilor, 2nd ed.; Eurobit: Timis, oara, Romania, 2017; pp. 66–71,ISBN 978-973-132-377-0.

[15] Crista, F.; Radulov, I.; Crista, L.; Berbecea, A.; Lat,o, A. Influence of mineral fertilization on the amino acid content and raw protein of wheat grain. J. Food Agric. Environ. (JFAE) 2012, 1, 47–50.

[16] Corches, M.T.; Lat,o, A.; Popa, M.; Radulov, I.; Berbecea, A.; Crista, F.; Nit,ă, L.; Lat,o, K.I. Evaluation of Cu, Mn and Zn Content in Ploughed Soil Layer. Sci. Pap. Ser. E Land Reclam. Earth Obs. Surv. Environ. Eng. 2017, 6, 120–123.

[17] Boldea, M.; Sala, F.; Radulov, I.; Crista, F. A Mathematical Model on the Dependence between the Agricultural Production and Chemical Fertilizer. AIP Conf. Proc. 2010, 1281, 1363–1366. [CrossRef]

[18] Olive, D.J. Principal Component Analysis. In Robust Multivariate Analysis; Springer: Cham, Switzerland, 2017; pp. 189–217.

[19] Kaleri, A.A.; Laghari, G.M.; Gandahi, A.W.; Kaleri, A.H.; Nizamani, M.M. Integrated foliar fertilizer effects on growth and yield of sunflower. Pak. J. Agric. Agric. Eng. Vet. Sci. 2019, 35, 25–28.

[20] Crista, F.; Radulov, I.; Borza, I.; Sala, F.; Berbecea, A.; Lat,o, A.; Gaica, I. Mineral fertilization influence upon soil chemical properties. In Proceedings of the 47th Croatian and 7th International Symposium on Agriculture, Opatija, Croatia, 13–17 February 2012; pp. 48–50

[21] Crista, F.; Radulov, I.; Crista, L.; Lat,o, A.; Stroia, C.; Băghină, N.; Gaica, I. Changing quality indicators of maize grain followingmineral fertilizers application. Curr. Opin. Biotechnol. 2013, 24, S69. [CrossRef]

https://doi.org/10.5593/sgem2024v/3.2/s12.27

# GEOCHEMICAL TOOLS IN ENVIRONMENTAL STUDIES

**Dr. Huzum Ramona**[1]

**Dr. Sirbu-Radasanu Doina Smaranda**[2]

**Dr. Dumitraş Delia-Georgeta**[3]

[1]Integrated Center of Environmental Science Studies in the North-Eastern Development Region (CERNESIM), Department of Exact and Natural Sciences, Institute of Interdisciplinary Research,'Alexandru Ioan Cuza' University of Iași, **Romania**
[2]Department of Geology, Faculty of Geography and Geology, "Alexandru Ioan Cuza" University of Iași, **Romania**
[3]Department INI, Geological Institute of Romania, **Romania**

## ABSTRACT

Geochemistry, a young earth science discipline, has evolved with chemical analysis techniques and is now integrated with environmental issues. Industrial development has increased the input of toxic elements into soil, water and air, potentially affecting the food chain. Geochemical tools investigate these sources and assess the risk of contamination. The combination of background enrichment indices and contamination indices provides a robust framework for understanding soil contamination. This dual approach enables researchers and environmental managers to effectively monitor, assess, and manage soil quality, ensuring that contamination is addressed based on a thorough understanding of both natural baselines and anthropogenic impacts. Based on ED-XRF analyses, the current study aims to evaluate eight potentially toxic elements (PTE) from a vineyard plot in the southern part of Iași city: Cr, Co, Ni, Cu, Zn, Cd, Pb, and As. Vineyard soils require long-term agrochemical treatments for fertility and plant disease prevention, accumulating potentially toxic elements. The geoaccumulation index and contamination factor were used to evaluate PTE contamination in vineyard soils, showing variable pollution levels. Generally low risk for PTEs was noted, but with significant contamination from Cu and Pb and very high from Zn and As. Anthropogenic activities, especially agricultural practices and urban traffic, significantly contributed to this contamination. Consequently, the soil accumulates potentially harmful substances that need to be observed, particularly in light of land use change, which is a current issue for the community.

**Keywords:** geochemical index, natural geochemical background, anthropogenic input, potentially toxic elements, vineyard soil

## INTRODUCTION

Looking back, history shows that the term geochemistry was first used in 1838 by the chemistry and physics professor Christian Friedrich Schönbein, referring to the fact that geochemistry would slide the formation of planets and inorganic matter [1]. From the very beginning the development of geochemistry was closely linked to the development of chemical analysis techniques. Thus, F.W. Clarke (1847-1931), V.I. Vernadsky (1863-1945), A. Fersman (1883-1945) and V.M. Goldschmidt (1888-1947), considered the fathers of modern geochemistry, published and described the first laws and processes for

https://doi.org/10.5593/sgem2024v/3.2/s12.28

the distribution of chemical elements in the Earth's crust, meteorites, and the solar system [2].

In 1959, the first and the only Department of Geochemistry in Romania was opened at the “Alexandru Ioan Cuza” University of Iași, thanks to the initiative of Prof. Mircea Savul, who was appointed professor in 1937 and is considered the pioneer of Romanian geochemistry [3].

Geochemistry is a relatively young discipline within the geosciences, developing at the beginning of the 20th century with the development of chemical analysis methods for minor, trace and ultratrace elements. With the development of analytical techniques, subfields such as biogeochemistry, environmental geochemistry, isotope geochemistry and medical geochemistry have also developed. Starting with trace element analysis, first in rocks and then in any type of sample matrix, the geogenic or anthropogenic origin has been highlighted in relation to the natural geochemical background value during the prospecting period. The anthropogenic impact increases and the geogenic background of the soil/sediment changes. The geochemical tools were designed to investigate the PTE sources and the degree or risk of contamination/pollution, usually through comparison with the natural geochemical background or typical threshold level [4,5]. The distinction between the normal and anomalous content of an element is known as the "geochemical background” and was first used in Exploration Geochemistry as a tool for identifying ore deposits. The word was later used to refer to a range of elements of normal abundance with anomalies related to contamination and/or pollution [4,5]. For environmental and monitoring studies, a contaminant occurrence and its source can be recognized or detected based on the geochemical background of a particular area. The calculation of various geochemical indices, which can be divided into the following categories, provides effective and practical methods for soil contamination: (1) Background enrichment indices, which compare the results of PTE with various background levels published in the literature as regional upper limit of background (baseline or threshold) or global (upper continental crustal composition). More recently, more practical monitoring studies have recommended the use of control or reference samples close to the study area or the local background range for comparison; (2) Contamination indices are used to compare contaminants with references from the study area or the legal threshold for soil quality in the national or the European Community [4,5].

The potential toxicity of some elements in soil, water and in the food chain, and thus their impact on human health, has been demonstrated by a number of tools grouped into the following types of geochemical indices: (1) assessment of pollution indices estimated on the basis of the natural background for single or multiple elements; (2) toxicity risk assessment based on the toxicity of each element; (3) health risk assessment. Using these frameworks, geochemistry is essential for regulating and monitoring soil quality, which helps us understand and reduce the impact of pollution on ecosystems and human health.

The objective of the present study is mainly related to the application of geochemical tools in understanding the sources of PTE and the associated risks. Because of the importance of food production and food security, the problem of excessive PTE concentrations, especially in agricultural soils, is a global environmental challenge. A vineyard was chosen for this study to emphasize the importance of application of geochemical index patterns. Vineyard soils are known as soils that are used for a very long period of time and require agrochemical treatments to maintain fertility. In addition,

the plant itself requires a series of treatments to prevent various diseases. These leads to an accumulation of potentially toxic elements in the soil, which must be monitored, especially in the context of land use change, which is a current problem for the community.

## MATERIALS AND METHODS

Iași, called "the city of the 7 hills", represents a favorable place for the cultivation of vines, being located at 47°10' north latitude and 27°35' east longitude, in the north-eastern region of Romania. The altitude of the steep relief rises from northwest to southeast up to 340 m. The climate, with a tendency to dryness, is characteristic of a temperate continental zone. The geological context is associated with the Moldavian Platform, which is the southwestern part of the Eastern European Platform [8]. Quaternary sediments, mostly formed by redeposition of eroded Sarmatian shales or Sarmatian sedimentary formations, are covered by soil [8]. Typical chernozemic soils found in suburban areas are cambisol in the highlands and argic in forested areas and interfluvial peaks [6]. Soil samples were collected from 0 to 40 cm depth, air dried and then sieved to remove particles larger than 1 mm. Four replicate plots of each sampling site were established and randomly distributed within the plot to account for spatial variation in the soil. All soil samples were air dried at approximately 30℃, lightly crushed, and then sieved through a 1 mm stainless steel sieve prior to testing. The fraction smaller than 1 mm was used for all studies. Using the Epsylon 5 spectrometer (PANalytical N.V.), pressed pellets weighing 9 g were prepared at a ratio of 5:1 = soil: synthetic raisins for ED-XRF studies to determine the PTE contents (Co, Cu, Ni, Pb, Zn, As). The soil and raisin mixture were agitated for 15 minutes at 180 rpm using an agate ball mill (Fritsch Planetary Mill Pulverisette 5) for a better homogenization. Subsequently, 9 g of the mixture was transferred to a thin aluminum container (spec cap) and compressed for 30 seconds at a force of 20 t/cm² using a hydraulic press (Fluxana PR-25A Press) to produce a uniform pellet. The use of several geological reference materials (SO-1-4: regosolic clay soil, podzolic B horizon soil, calcareous C horizon soil, and chernozemic A horizon soil; STSD-1-4: stream sediment powder; JLk-1: lake sediments, JSd-1-3: stream sediments) was necessary to standardize the ED-XRF equipment. Pb = 2.9 $mg \cdot kg^{-1}$, Ni=4.65 $mg \cdot kg^{-1}$, Cu = 1.64 $mg \cdot kg^{-1}$, Zn = 2.27 $mg \cdot kg^{-1}$, and As = 1.13 $mg \cdot kg^{-1}$ are the detection limits for each of the elements analyzed. Except for As and Cd, which require 90 seconds for detection, the exposure time was 60 seconds. The average of two measurements is the final concentration of each element.

Descriptive statistics and geochemical indices were calculated according to literature formulas to interpret the data (see the relations 1-5). The geoaccumulation index (Igeo) allows the assessment of PTE contamination in soil based on the concentration of the base element in the soil sample (topsoil) and the geochemical background of the element as a reference level:

$$Igeo = \log_2 \left\lfloor \frac{Cn}{1.5 \cdot GB} \right\rfloor \quad (1)$$

where Cn – concentration of individual element, GB – value of geochemical background and 1.5 – constant, allowing for an analysis of the variability of PTE as a result of natural processes. There are six classes of descriptive Igeo interpretation, as follow: Igeo≤0 as uncontaminated; 0<Igeo<2 as uncontaminated to moderately contaminated; 2<Igeo<3 as

https://doi.org/10.5593/sgem2024v/3.2/s12.28

moderately contaminated; 3<Igeo<4 as moderately to heavily contaminated; 4<Igeo<5 as heavily contaminated and 5<Igeo as extremely contaminated [9].

The *contamination factor* (single element index) and *contamination degree* (multiple element index) were also used in the geochemical evaluation of soil contamination. For single element assessment, the contamination factor (CF), as suggested by[10], is computed using the following formula:

$$\mathrm{CF} = \frac{\mathrm{C_{n\ sample}}}{\mathrm{C_{n\ background}}} \quad (2)$$

where: $C_{n\ sample}$ – PTE concentration in the sample, $C_{n\ background}$ – PTE concentration in the background. Based on the CF values, several contamination classes are described as follows: CF <1: low contamination; 1≤ CF <3: moderate contamination; 3≤ CF <6: significant contamination; CF ≥ 6: very high contamination.

The contamination determined by a single element can be found by taking the average of the enrichment factor or contamination factor. The cumulative effect of PTE on soil composition is sometimes required and can be expressed as the sum of the contamination factors calculated for all PTE divided by the contaminants studied. This relationship is known as reflecting the soil contamination [11] and seven classes were proposed to describe the contamination degree (CD) for the studied area:

$$\mathrm{CD} = \frac{\sum_{i=1}^{i=n} CF^i}{\mathrm{n}} \quad (3)$$

where: n = number of elements analysed, i = element and CF = contamination factor of the element. Suggested classes for describing CD depending on the value obtained are:

CD < 1.5 – no to very low level of contamination; 1.5 ≤ CD < 2 – low level of contamination; 2 ≤ CD < 4 – moderate contamination; 4 ≤ CD < 8 – high degree of contamination; 8 ≤ CD < 16 – very high degree of contamination; 16 ≤ CD < 32 – extremely heavy contamination; CD ≥ 32 – very heavy contamination.

The *potential ecological risk index (PER*) is expressed as the potential ecological risk index, (Ej) and combine the single index of ecological risk factor (Cj) and the toxic response factor of individual PTE (Tn):

$$\mathrm{PER} = \Sigma \mathrm{Ej} = \Sigma\ \mathrm{Tn} \cdot \mathrm{Cj} \quad (4)$$

$$\mathrm{Cj} = \frac{\mathrm{Ci}}{\mathrm{Cn\ background}} \quad (5)$$

where: Cj pollution factor for element i; Ci measured concentration of element in soil sample; Cn background value of element. The biological toxic factor *T*n is defined as 2, 5, 6, 5, 1, 30, 5 and 10 respectively for Cr, Co, Ni, Cu, Zn, Cd, Pb and As. Five classes are used for PER interpretation: low risk for Ej<40; moderate risk for 40<Ej<80; considerable risk for 80<Ej<160; high risk for 160<Ej<320 and very high risk for Ej>320 [12 ].

As a reference for the value of the natural geochemical background of the Iasi region, the studies of [6] and [7] are used.

## RESULTS

The estimation of environmental quality indices is the foundation of quantitative approaches. The concentrations of eight PTE are showed in Table 1.

Table 1: Summary of the individual concentrations of PTE (mg·kg$^{-1}$), background values (blue color) and Romanian legislative limits in force [13] (green color)

| | Cr | Co | Ni | Cu | Zn | Cd | Pb | As |
|---|---|---|---|---|---|---|---|---|
| Mean | 41.4 | 10.35 | 36.6 | 120 | 80.90 | 0.331 | 30.6 | 11.04 |
| Minimum | 38.5 | 9.65 | 31.5 | 57 | 65 | 0.140 | 28.5 | 10.6 |
| Maximum | 46 | 11.05 | 43 | 146 | 91 | 0.625 | 33.5 | 11.75 |
| Total no of samples | 15 | 15 | 15 | 15 | 15 | 15 | 15 | 15 |
| Iancu&Buzgar, 2008 [6] | 34.83 | 8.73 | 34.86 | 30.31 | 72.09 | 0.36 | 20.04 | - |
| Sirbu et al., 2012 [7] | - | - | 27.1 – 54.5 | 20.5 – 98.9 | 47.4 – 188 | - | 8.15 – 41 | 7.58 – 10.95 |
| Normal values | 30 | 15 | 20 | 20 | 100 | 1 | 20 | 5 |
| Alert threshold | 100 | 30 | 75 | 100 | 300 | 3 | 50 | 15 |
| Interventional threshold | 300 | 50 | 150 | 200 | 600 | 5 | 100 | 25 |

The summary data resulting from the estimation of the individual indices are presented in Table 2.

Table 2. Summary data of individual indices

| Geochemical indexes | | Cr | Co | Ni | Cu | Zn | Cd | Pb |
|---|---|---|---|---|---|---|---|---|
| Igeo[1] | average | 0.6 | 9.3 | 1.2 | 5.99 | 30.0 | 1.0 | 6.2 |
| | min | 0.6 | 5.0 | 1.2 | 5.53 | 6.0 | 0.9 | 5.4 |
| | max | 0.7 | 11.1 | 1.3 | 6.33 | 36.5 | 1.0 | 7.4 |
| CF[2] | average | 1.2 | 1.2 | 1.1 | 3.97 | 1.1 | 0.9 | 1.5 |
| | min | 1.1 | 1.1 | 0.9 | 1.88 | 0.9 | 0.4 | 1.4 |
| | max | 1.3 | 1.3 | 1.2 | 4.80 | 1.3 | 1.7 | 1.7 |
| Ej[3] | average | 0.594 | 5.93 | 6.31 | 10.88 | 1.12 | 27.61 | 7.63 |
| | min | 0.553 | 5.53 | 5.42 | 4.80 | 0.90 | 11.67 | 7.11 |
| | max | 0.660 | 6.33 | 7.40 | 23.01 | 1.26 | 52.08 | 8.36 |

1. Geochemical index; 2. Contamination factor; 3. Ecological risk index

https://doi.org/10.5593/sgem2024v/3.2/s12.28

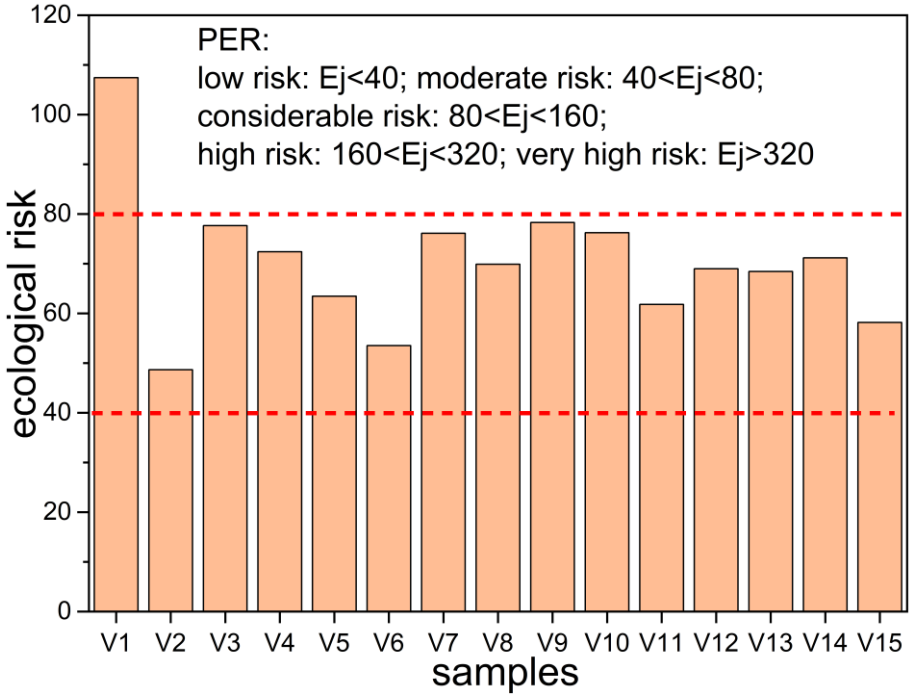



Figure 1. Potential ecological risk

## DISCUSSION

Table 1 demonstrates that the mean values of all elements, with the exception of Cd, exceed the natural background values, indicating an enrichment resulting from the agrochemical treatments applied to the vines. A straightforward comparison of the data with the legal values in force [13] reveals that only Cr, Ni, Cu, Pb and Cu exceed the normal value in soils, with only Cu exceeding the alert threshold. The results are within the same limits as those obtained for the soils of the northern part of Iași [14,15] and for those of the Huși wine-growing area [16], which belong to the same geological unit. The estimation of geochemical indices is seen to be a useful tool for turning unprocessed environmental data into information that non-specialists can understand. Decision-makers can use this transformation to rank and prioritize the polluted locations for more research. The individual indices, namely the geoaccumulation index (Igeo) and the contamination factor (CF), were employed for the purpose of assessing the anthropogenic impact of PTE contamination of vineyard soils. The Igeo values for Cr, Ni, and Cd suggest unpolluted to moderately polluted soils, while the values for Co, Cu, Zn, Pb, and As indicate highly polluted soils. The mean CF values indicate low contamination for Cr, Co, and Cd; moderate contamination for Ni; significant contamination for Cu and Pb; and very high contamination for Zn and As.

The degree of contamination (CD) indicates that 53.34% of the samples are uncontaminated, while 46.66% exhibit low levels of contamination. The average PER indicates a moderate risk for all the PTE under study, while the ecological risk index demonstrates the following order of increase: $E_{Cr} < E_{Zn} < E_{Co} < E_{Pb} < E_{Ni} < E_{As} < E_{Cu} < E_{Cd}$. Figure 1 shows the trend for each of the samples. It can be seen that only one sample shows a significant risk. The remaining samples range from moderate to significant risk.

## CONCLUSION

The PTE contamination in the soils of vineyards in the southern region of Iasi is thoroughly investigated in this study. The study shows that all elements, except Cd, exceed natural background levels, indicating enrichment by agrochemical treatments. The normal soil level is exceeded by Cr, Ni, Pb and Cu, whereas Cu is above threshold alert. The Igeo and CF were used to assess the anthropogenic impact of PTE contamination in vineyard soils. Igeo values indicate unpolluted to moderately polluted soils, while CF values indicate low contamination for Cr, Co and Cd, moderate contamination for Ni, significant contamination for Cu and Pb and very high contamination for Zn and As. The average combined PER index indicates a low risk for all PTE. Anthropogenic activities were the main cause of the distribution and accumulation of PTEs in the soil, as certain agro-technical treatments for vineyards, as well as buildings surrounding the study plot and urban traffic, pose a serious risk to human health and soil and environmental contamination. An assessment of the impact on human health is a concept for further research in the context of the growing tendency to expand residential areas.

## REFERENCES

[1] White W.M., History of Geochemistry. In: Encyclopedia of Earth Sciences Series, Springer, Cham, 2017.

[2] Müller A., Viktor Moritz Goldschmidt (1888–1947) and Vladimir Ivanovich Vernadsky (1863–1945): the father and grandfather of geochemistry? J Geochem Explor, 147, pp. 27–45, 2014.

[3] Petrescu, L., Sirbu-Radasanu, D.S., Geochimia. În Istoria geoştiinţelor în România - Ştiinţele Geologice, Editori: Rădulescu, D., Panin, N., Anastasiu, N., Brustur, T., Ed. Acad. Rom, pp. 17-35. 2018 (in Romanian).

[4] Dung T.T.T., Cappuyns V., Swennen R., Phung N.K., From geochemical background determination to pollution assessment of heavy metals in sediments and soils, Rev Environ Sci Biotechnol, 12, pp. 335–353, 2013.

[5] Kowalska J.B., Mazurek R., Gasiorek M., Zaleski T., Pollution indices as useful tools for the comprehensive evaluation of the degree of soil contamination–A review, Environ Geochem Health, 40, 2395, 2018.

[6] Iancu O.G. & Buzgar N., Eds., The geochemical atlas of heavy metals in the soils of the municipality of Iasi and its surrounding areas. "Al. I. Cuza" University, Editorial Press, 2008.

[7] Sirbu-Radasanu D. S., Buzgar N., Iancu O.G. The ambient and geogenic background of the soil from the surrounding area of the city of Iasi (NE Romania), SGEM 2012 Conference Proceedings, Bulgary, vol. IV, pp. 229-238, 2012.

[8] Ionesi L., Ionesi B., Rosca V., Lungu A., Ionesi V., Middle and Upper Sarmatian on the Moldavian Platform, Ed. Acad. Rom., pp.5 58, 2005 (in Romanian).

[9] Müller G., Index of geoaccumulation in sediments of the Rhine River, Geol J, 2, pp.109–118, 1969.

[10] Hakanson L., An ecological index for aquatic pollution control. A sedimentological approach. Water Research, 14, 8, 975-1001, 1980.

https://doi.org/10.5593/sgem2024v/3.2/s12.28

[11] Abrahim G.M.S, Parker R.J., Assessment of heavy metal enrichment factors and the degree of contamination in marine sediments from Tamaki Estuary, Auckland, New Zealand. Environmental monitoring and Assessment, 136**,** 227-238, 2008.

[12] Sutherland R., Bed sediment-associated trace metals in an urban stream, Oahu, Hawaii, Environmental Geology, 39, pp. 611–627, 2000.

[13] The Romanian Ministry of Waters, Forests and Environmental Protection. Order no.756/1997, Romania, 1997.

[14] Sirbu-Radasanu D.S., Huzum R., Iftode S.P., Iancu G.O., Buzgar N., Geochemical assessment of soil potentially toxic elements from Copou-Iasi vineyard area (NE Romania), Analele Stiintifice de Universitatii AI Cuza din Iasi. Sect. 2, Geologie, 61,1/2, 5, 2015.

[15] Sirbu-Radasanu D.S., Huzum R., Buzgar N., The influence of anthropogenic input upon selected trace elements distribution from suburban area of the city of Iasi (NE Romania),13th SGEM GeoConference on Water Resources. Forest, Marine and Ocean Ecosystems, 709, 2013.

[16] Huzum R., Sirbu-Radasanu D.S., Iftode S.P., Buzgar N., Iancu G.O., Soil surface geochemistry for environment monitoring in vineyard soil of Husi area, Romania,15th International Multidisciplinary Scientific GeoConference SGEM2015, pp. 295-302, 2015.

# GEOINFORMATION TERRAIN ANALYSIS FOR OPTIMIZING MILITARY EQUIPMENT ROUTES

**Prof. Oleksandr Trofymchuk**

**PhD Vyacheslav Vishnyakov**

**PhD Natalia Sheviakina**

**PhD Viktoriia Klymenko**

**PhD Snizhana Zahorodnia**

Institute of Telecommunications and Global Information Space of the National Academy of Sciences of Ukraine, **Ukraine**

## ABSTRACT

To enable effective operational decisions and combat mission execution on the battlefield during war, access to reliable, accurate, and timely data is essential. We propose utilizing Geographic Information Systems (GIS) to analyze extensive datasets, as modern military operations rely on accurate spatial terrain mapping for command, control, communication, and coordination. This study introduces a terrain analysis approach tailored to military vehicle movement, focusing on assessing ground resilience to vehicle traffic and predicting terrain trafficability for optimal route planning.

For this analysis, we calculated effective movement zones between designated points, factoring in landscape, terrain relief, and soil conditions. Movement routes were strategically planned, incorporating both potential obstacles and forecasted trafficability. GIS was employed to generate maps showing equipment reach within specific timeframes and to document optimized routes.

This method provides a predictive assessment of soil trafficability, enabling precise route calculation for military vehicles across various operational settings within designated areas.

**Keywords:** GIS, terrain analysis, military equipment, military operation

## INTRODUCTION

To make operational decisions in military conditions, it is essential to have reliable, accurate, and timely data. The successful execution of combat missions by ground forces and their coordination largely depend on effective spatial terrain mapping. Terrain trafficability assessment is crucial for calculating movement routes for military equipment, impacting planning, organization of combat operations, logistics, reconnaissance, monitoring, and defensive measures.

A Geographic Information System (GIS) enables the processing of large volumes of data, minimizing risks and increasing the chances of successful military operations. The use of digital geospatial data in military operations has become an integral part of military actions worldwide, providing rapid access to information on terrain conditions through digital cartographic and tabular data [1].

The integration of GIS with combat and logistics management systems is a significant factor that enables efficient military operations [2]. GIS also ensures the protection of spatial data from unauthorized access and cyberattacks. With the capabilities of GIS, military institutions can better assess terrain conditions, forecast hydrometeorological conditions, and determine enemy positions [3].

Since combat operations can take place under various conditions, it is important for command to consider the nature of the terrain during operational planning. In adverse weather, the issue of equipment trafficability becomes particularly relevant [4]. This often necessitates forecasting trafficability several days in advance, which can be complicated by the lack of necessary equipment and conditions for field measurements.

The approach proposed by the authors utilizes weather prediction models, environmental monitoring, and ESRI GIS technologies to forecast both general and localized trafficability for various types of military equipment. This enhances the efficiency of military operations, reduces risks, and ensures effective coordination of military equipment movement routes under combat conditions.

## MATERIALS AND METHODS

Geographic Information Systems (GIS) find applications in various fields, including urban planning, agronomy, transportation, education, and navigation. Military operations also require GIS to create comprehensive products for terrain analysis, including obstacle maps, hydrological overlays, slope maps, movement routes, lines of sight, and problem areas that affect the mobility of military equipment. Each GIS includes subsystems for data input, storage, processing, presentation, management, analysis, and the creation of cartographic products [5, 6].

A leader in the GIS field is Esri with its ArcGIS product, which is widely used for military purposes in terrain analysis [7]. An adequate analysis of the terrain is essential for effective combat planning, as it allows for predicting the enemy's intentions and considering factors that influence terrain trafficability: infrastructure (bridges, roads), relief, vegetation, groundwater, and soil type.

Military operations also require consideration of additional aspects, such as the speed of equipment movement over different sections, the time needed to traverse a route, and the availability of alternative paths to avoid congestion [8]. This study calculated soil trafficability based on soil type and moisture content in the upper layer. It also proposed a method for predicting the trafficability of military equipment and calculating optimal routes. The methodology includes a comprehensive classification of data based on satellite imagery, topographic models, field studies, hydrometeorological forecasts, and other auxiliary resources.

Terrain analysis and calculation of movement routes for military equipment was conducted using the following methodology:

1) Determination of key parameters:

- The starting point and destination point are selected.
- The types of equipment that will be moving and the volumes of equipment to be transported are identified.
- The conditions of the terrain are analyzed using GIS to determine the trafficability of the area.

2) Calculation of effective movement:

- The zone of effective movement between points is calculated, considering the landscape, relief, and soil conditions. Satellite data and digital elevation models are utilized.
- Speed and time indicators for the movement of each unit of equipment over different sections are determined.

3) Analysis of routes and constraints:

- Movement routes are calculated, taking into account column width, maximum allowable length of echelons, and mobility corridors (brigades, battalions, companies).
- Potential obstacle locations are analyzed: bridges, tunnels, minefields, and engineering structures that may restrict movement.

4) Forecasting trafficability conditions:

- The trafficability of soils is predicted based on moisture and other terrain parameters, considering the improvement or deterioration of movement conditions for equipment. GIS aids in visualizing these indicators on maps.

5) Visualization and accounting of routes:

- Maps display movement speed and time required to traverse sections, as well as potential congestion and obstacle locations.
- Maps are created indicating the reach zones of equipment within a specified time.

6) Creation of march (route) documentation:

- A route sheet is created with recommendations regarding speed, column width, stops, and measures to enhance the trafficability of equipment in challenging conditions.

The methodology outlined demonstrates an integrated approach to terrain analysis and calculation of movement routes for military equipment using modern GIS technologies and multi-component data, allowing for increased accuracy and effectiveness in military operations. The developed approach enables the prediction of soil trafficability for military equipment, which can be applied to all types of military ground operations in the designated areas.

## RESULTS

This paper discusses the methodology for calculating the conditional ability of the soil to withstand the load from the movement of military equipment depending on the type of soil and its moisture content in the upper meter layer. The modeling was performed using Esri ArcGIS Pro, which provides a comprehensive approach to analyzing the passability of individual sections by combining various weather forecasting and environmental monitoring models within geographic information systems. Esri Military Ground Mobility technology was also used to improve the accuracy of the passability assessment.

Before starting the calculation, key inputs were identified, such as:

- The calculation area (the territory of military equipment movement).
- The boundaries of the range, set in .shp format or directly in the application.
- Roads and routes that can be used by the equipment.

- Water bodies (rivers, lakes, seas) that can be crossed or bypassed by vehicles.
- Terrain that affects the passability.
- Soil types and their moisture content that form the top layer of the surface.

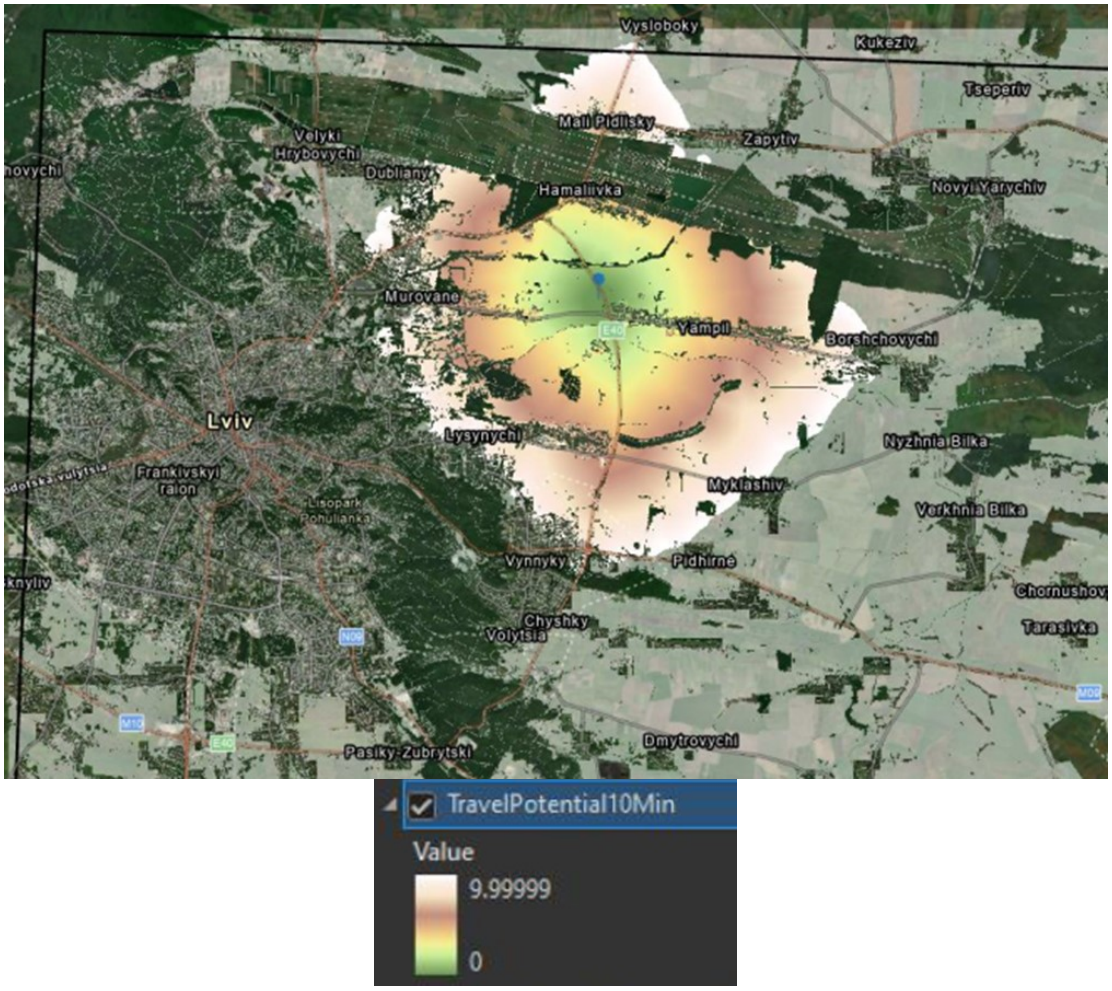



**Fig. 1.** Map of the potential 10-minute reach zone in the selected calculation area.

Soils provide favorable conditions for equipment movement when they have sufficient density and uniformity. However, movement is complicated in soft, marshy, or washed-out conditions. Data for the analysis were initially downloaded from OpenStreetMap and the ArcGIS server. The properties of the terrain regarding the trafficability of military equipment are classified on maps as follows: easily passable, passable, moderately passable, hard to pass, and impassable. As a result, the areas of accessibility for equipment over a specific time interval were determined, for example, from 1 to 10 minutes (Fig. 1). This means that the map displays the zone of possible movement for military equipment in the selected area, taking into account soil moisture and the type of equipment.

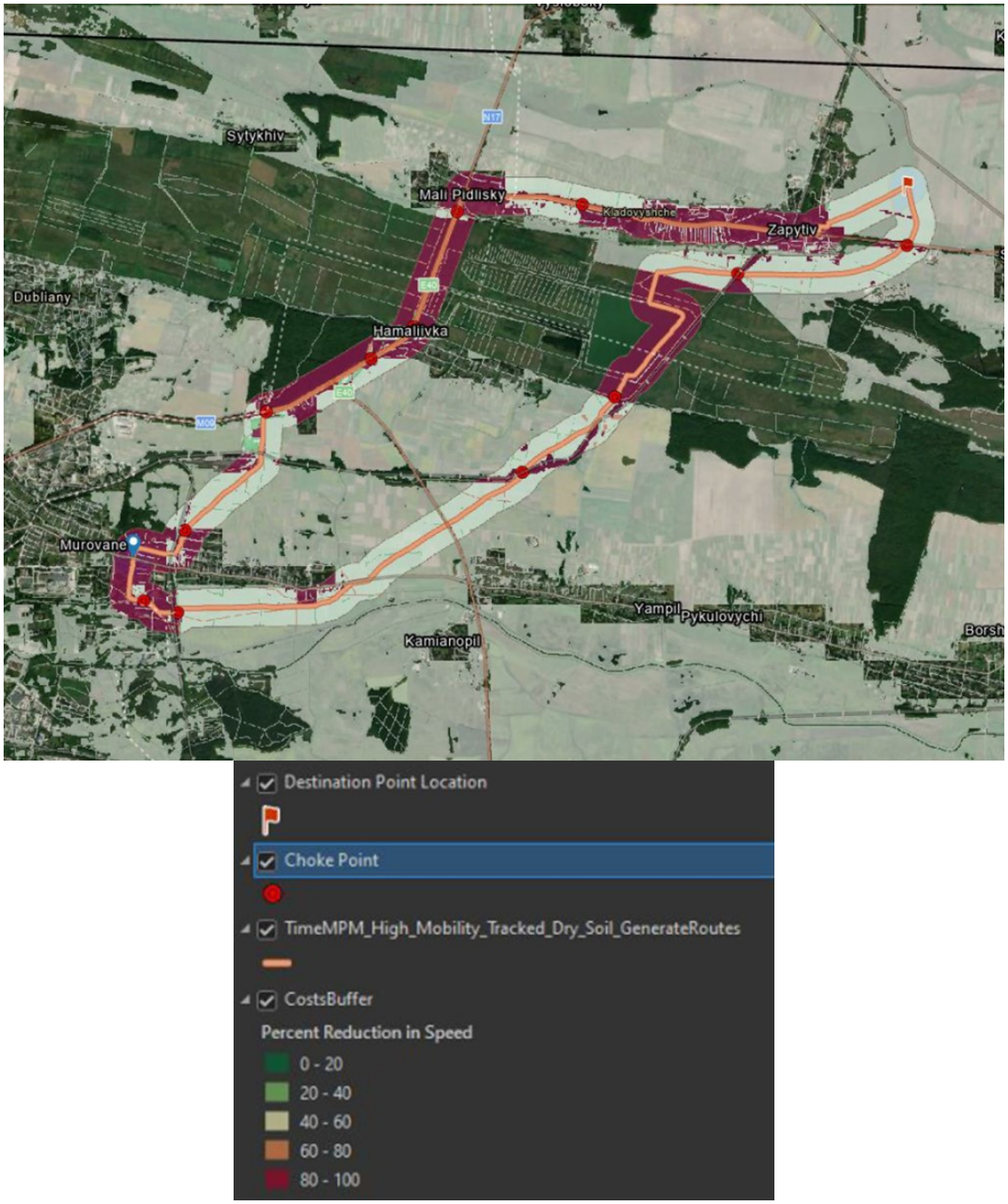



**Fig. 2.** Map of possible traffic jams along the route

Modern GIS technologies allow the use of multi-component data regarding potential congestion points along routes (Fig. 2). Multiple routes can be created with a specified distance or buffer between each route. The routes are calculated considering the maximum length of echelons between mobility corridors and their typical width. The typical maximum distance between mobility corridors is 10 km for a brigade, 6 km for a battalion, and 2 km for a company. The typical width of mobility corridors is 6 km for a division, 3 km for a brigade, 1.5 km for a battalion, and 500 m for a company. The width of the route may vary (becoming narrower or wider). This can be seen as a potential obstacle for which preemptive actions should be taken. Identifying these

locations allows for expediting the route or preventing congestion and delays on the roads.

As a result, a project of maps (the final information product) has been developed that can be provided to military units. A separate map has been created for each type of military equipment. This final information product is used in specific areas to determine the route for military vehicles necessary for executing combat missions. For example, the trafficability zone for military equipment in the area of Avdiivka, Donetsk Oblast, Ukraine, as of April 4, 2024, is presented. This area is a zone of active hostilities and requires detailed professional analysis.

## DISCUSSION

The developed project of maps and methodology provide reliable tools for assessing soil trafficability and calculating movement routes for military equipment. This significantly enhances the planning and execution of combat tasks, improving unit mobility and minimizing the risks of congestion and delays. The application of modern GIS technologies ensures the accuracy of analysis and enables rapid decision-making in real time.

Esri's ArcGIS software offers a wide range of tools for military use, allowing for effective planning and conducting of operations, analyzing terrain and relief data, monitoring situations in real time, and improving situational awareness. Thanks to integration with other systems and extensive customization options, these tools are indispensable for modern military operations.

As a result of the work conducted, the authors identified the following advantages of using GIS:

- Accurate geographic identification of trafficable areas.
- Targeted calculation of trafficability and movement routes for military equipment.
- Consideration of hydrometeorological impacts with the subsequent creation of predictive maps for one to three days ahead.

Alongside the advantages, there are also disadvantages:

- The necessity for high-precision updated cartographic data of the underlying surface.
- High cost of software.
- Large volumes of data for processing.

## CONCLUSION

During military operations, assessing terrain trafficability for military equipment and forecasting conditions for several days ahead is crucial. Accordingly, one of the key tasks in planning operations is to predict the state of trafficability and calculate movement routes for equipment.

As a result of the conducted research, a comprehensive approach to forecasting the overall and local trafficability of various types of military equipment has been developed. This approach is based on the use of weather forecasting models, environmental monitoring, geographic information systems (GIS), and the Esri Cross

Country Mobility technology. The proposed methodology includes calculating the conditional bearing capacity of soils to withstand the movement of equipment, depending on soil type and moisture content in the upper layer.

Forecasting terrain trafficability and calculating movement routes were performed using an integrated algorithm that encompasses data collection, processing and analysis, modeling in GIS, and the creation of cartographic products for use on the battlefield.

The final information product consists of trafficability maps and movement routes for military equipment. As a result, zones of possible movement speeds for equipment in kilometers per hour, the locations of bridges, tunnels, and artificial obstacles such as engineering structures, minefields, and craters have been calculated. Maps of equipment accessibility over a specified time interval and maps of movement speed in kilometers per hour for selected approach areas have been created. Route options from the departure point to the destination have been calculated, considering potential congestion points along the route.

The proposed approach enables forecasting the trafficability state of soils for military equipment, which is vital for conducting ground military operations. Utilizing this methodology enhances the effectiveness of troop deployment, reduces risks, and ensures better coordination of units on the battlefield.

## REFERENCES

[1] Zakiev, Erlan S.; Pankov, Sergey V.; Kalabay, Komesh B. Application of geoinformation systems in the armed forces and other military formations in the republic of Kazakhstan. Vojnotehnicki glasnik/Military Technical Courier 2020, 68 (2), pp. 356- 382. DOI: 10.5937/vojtehg68-25830; DOI:10.5937/vojtehg68-25830;

[2] Sunil Kumar Pundir, Rahul Dev Garg, Development of rule based approach for assessment of offroad trafficability using remote sensing and ancillary data. Quaternary International, Volumes 575–576, 2021, pp. 308-316. DOI:10.1016/j.quaint.2020.07.017;

[3] Rafael Jardima, Marcos dos Santos, Edgard Neto, Fernando Martins Muradas, Bruna Santiago, Miguel Moreira. Design of a framework of military defense system for governance of geoinformation. Procedia Computer Science. Volume 199, 2022, pp. 174-181. DOI:10.1016/j.procs.2022.01.022 ;

[4] Ezra Chipatiso. Application of Geographic Information Systems and Remote Sensing in Military Operations: A Systematic Review. TechRxiv. January 26, 2024. DOI: 10.36227/techrxiv.170630596.64838976/v1;

[5] Oleksandr Trofymchuk, Vyacheslav Vishnyakov, Natalia Sheviakina, Viktoriia Klymenko, Serhii Slastin. Monitoring of fires and assessment of changes in the state of nature-protected territories of Ukraine as a result of military operations. International Multidisciplinary Scientific GeoConference – SGEM, 2022 (2), pp. 369 – 377. DOI:10.5593/sgem2022V/3.2/s14.43;

[6] Tomchenko, O., Khyzhniak, A., Sheviakina, N., Zahorodnia, S., Yelistratova, L., Yakovenko, M. & Stakhiv, I.().Assessment and monitoring of fires caused by the War

in Ukraine on Landscape scale. Journal of Landscape Ecology,16 (2), pp. 76-97, 2023. DOI: 10.2478/jlecol-2023-0011 ;

[7] Cvijanović Bojan, Pavlović Marko, Tomašević Lazar Implementation of geographic information system in military terrain assessment Vojno delo. 2018, vol. 70, br. 1, str. 90-102 DOI: 10.5937/vojdelo1801090C ;

[8] Skorodid S., Pochinok S., Determination of the terrain passability coefficient. Multidisziplinäre Forschung: Perspektiven, Probleme und Muster. 2021, pp.84-85. DOI: 10.36074/logos-09.04.2021.v1.28

# PHYTOREMEDIATION OF ARSENIC CONTAMINATED SOILS OF THE AMBROLAURI MUNICIPALITY

**L. Shavliashvili**[1]

**G. Kuchava**[1]

**E. Shubladze**[1]

**M. Tabatadze**[1]

**S. Iram**[2]

**E.Elizbarashvili**[2]

[1]Institute of Hydrometeorology of Georgian Technical University, Tbilisi, **Georgia**
[2]Department of Environmental Sciences, Fatima Jinnah Women University, Rawalpindi, **Pakistan**

## ABSTRACT

Phytoremediation technology is environmentally friendly and inexpensive to clean soils of harmful toxins.

The study aims to introduce phytoremediation of arsenic in the Racha-Lechkhumi and Kvemo Svaneti regions to restore soil fertility.

For this study, three plants, Amaranthus gangeticus, Chenopodium album and Helianthus annuus, were selected for the accumulation and translocation of Arsenic from the contaminated soil.

The seeds of selected plants were treated with the bioactivator Biorag to increase the plant's green mass. Plants were sown in May and harvested in August and October. Plants were gathered in their raw state they were dried for two weeks, after drying, the plants (their parts – roots, shoots or a whole plant) were processed by decomposer–Milestone – Start D Microwave system and the total form of arsenic was determined on the Inductively coupled plasma atomic emission spectroscopy - ICP-OES.

Several parameters were calculated that affect phytoremediation potential, such as arsenic concentration, bioconcentration factor (BCF), translocation factor (TF) and arsenic content in the total mass of the plant. As a result of the research, it was established that the selected plants can accumulate and remove arsenic from contaminated soil, which is a necessary condition for the successful implementation of phytoremediation.

Phytoremediation efficiency was determined, and it was equal to 58.7% (extracted by the plant), while the amount remained in the soil –41.3%.

The methods and techniques of mathematical statistics and probability theory were used for the analysis of measurements in the paper.

**Keywords:** Pollution, Arsenic, Soil, Phytoremediation, Biorag.

https://doi.org/10.5593/sgem2024v/3.2/s12.29

## INTRODUCTION

Environment pollution is an extremely relevant, global and undesired problem. Population growth increased demand for foods, international development, maximal extraction of minerals and exploitation of the earth's interior, and the relentless attitude of humans toward the environment gave rise to many ecological problems in many countries, including Georgia.

One of the most important sources of technogenic pollution of nature is mining enterprises, which play a negative role in environmental pollution processes and pose a major risk factor for the region's ecosystem and population health. Increased levels of heavy metals in soils and water have a detrimental effect on the ecosystems [1-4].

Soil is a heterogenic system of complex composition, and it unites dense, liquid, gaseous and living soil particles, which are very vulnerable to exogenic substances. The accumulation and fixation of technogenic agents also feature it. In some cases, they transform the environment into even stronger toxins. Normed substances cause changes in soil nature, its chemical and biological properties, microflora degradation and plant development slowdown. Thus, several important components and centuries-old soil balance are disturbed during soil pollution, which significantly worsens its normal functioning and lengthens its time for restoration [2, 4-8].

Arsenic is a natural component of the earth's crust and is widespread in any ecosystem. In nature, it is represented by organic and inorganic forms, among them, the latter is very toxic [9].

Although arsenic may penetrate through the skin, respiratory organs, etc., it still mainly hits the human body with food and drinking water. Organic varieties of arsenic are commonly found in sea products, while in land products, there are mainly inorganic forms of $As_2O_3$ and $As_2O_5$ arsenic. Based on this, arsenic mainly enters the food chain from contaminated soils and waters [10,11].

Racha-Lechkhumi and Kvemo Svaneti region, where arsenic ore extraction, processing and arsenic-containing preparations production was conducted for a dozen years, is a good example of pollution induced by mining enterprises of Georgia. Even today, large batches of the toxic waste remaining as a result of arsenic production, kept as far as from the Soviet period, are stored in the territory of Uravi and Tsana villages [12]. They were not safely disposed and posed a high risk of ecological catastrophe for rivers, ground waters and soils [8,13-16], this hazard endangers the environment, health and life of thousands of humans.

There are different adopted methods of combating the soil pollution problem. One of the most safe and effective methods is phytoremediation. The word "phytoremediation" means the following: "phyto" is a plant, "remedium" is restoration. With the purpose of soil remediation, phytoremediation uses plants which have high hyper-accumulation abilities. During phytoextraction, plants absorb polluting agents from soil and water and keep them in their biomass. The concentration of metals absorbed by hyper-accumulating plants is 100 times higher on average compared to ordinary plant species [13,14,17,18].

As is known from the literary sources, the method of soil cleanup using phytoremediation has the best potential of purification from pollutants due to the following reasons: phytoremediation methods enable the removal of virtually all types of toxicants from the environment; it is applied close to the earth surface; have a feature of irreversibility; don't

pose a risk to human health and environment; and covers large surfaces. At the same time, this method is ecologically safe and not expensive, which is why it is widely used in many developed countries. Phytoremediation may also find widespread use in developing countries thanks to its low cost and ease of use. Although this method is of great promise, it requires plenty of time for complete reclamation of contaminated soil. Several years are necessary when using phytoremediation to reduce arsenic levels in the soil. Therefore, the assortment (list) of corresponding plants is of great importance for specific heavy metals to conduct soil cleanup as fast as possible. Even though different technologies are used for the remediation of soil and water polluted with arsenic, researchers working on phytoremediation issues think this advancing technology is the most prospective and environmentally friendly.

## GENERAL DESCRIPTION OF THE REGION

Racha-Lechkhumi-Kvemo Svaneti region is located in the northern part of western Georgia, on the southern slopes of the Central Caucasus and belongs to the highland zone. The region is located at an altitude of 400 m to 4000 m above sea level in the humid district of the sea climate. In the lowlands, the type of moderately cold and relatively hot summer climate is characteristic, and the highland zone is characterised by a humid, snowy mountain climate. The area of the region is 4600 sq. km, with four municipalities: Ambrolauri, Lentekhi, Oni and Tsageri and with a population of 46.7 thousand people.

The soils of the study are located in the Ambrolauri district of western Georgia, under the humid subtropical climate. Geographical cords are northern latitude 42.520, east latitude 43,150, and 544 m high above sea level. The average annual temperature is 11.2 $^0$C, January is minus 0.3 $^0$C, and July is 21.9 $^0$C. During the year, 1075 mm of precipitation is typical, with a maximum in spring. Snow cover is characteristic from the third decade of December to mid-March. The average annual wind speed does not exceed two m/s) [19].

Based on soil analyses carried out during the first year of studies there were identified vulnerable areas (points) of arsenic pollution in different places of the region, whereby the arsenic pollution map in the GIS system was created [8]. Namely, according to these points, we selected new technology introduction sites in the Ambrolauri Municipality. It should be noted as well that though high arsenic concentrations were registered in soil samples taken in Tsana village, these places are situated much higher from sea level and are featured by cold climate, in addition, they are distinguished by poor infrastructure, which is why we selected for phytoremediation agricultural lands of Abari and Likheti villages of Ambrolauri Municipality.

## MATERIALS AND METHODS

Agricultural lands of Abari and Likheti villages of the Ambrolauri municipality were taken for this research. In the investigated municipality, there are mainly ash-grey and ash-grey acid soils. Grey soils are distinguished by the more or less monotonic grey colouring of the profile and the existence of metamorphic, clayey horizons in the middle part. In West Georgia, these soils are situated within 800(900)-1800(2000) meters altitude about sea level. These soils are characterised by slight acid reactions and a high content of moving iron forms. Soils are moderately humus (6-7% humus at a depth of 0-10 cm) and deeply humus here (in the lowest horizons, the humus content sometimes reaches

https://doi.org/10.5593/sgem2024v/3.2/s12.29

1%). Calcium prevails in exchange cations. According to mechanical composition, they are ranked among average and light loams, less frequently heavy loams. Due to the presence of cambial horizons (layers), grey soils belong to the cambisol group of the world correlation base of soil resources. Grey acid soils stand out by the acid reaction of the whole profile, with a gradual reduction of humus with depth [20].

In 2022-2023, some field works were conducted in the Ambrolauri Municipality, in particular, soil sampling, labelling, storage and transportation according to the standard methods of the International Standard Organization (ISO). A laboratory study was performed using standard methods of ISO and US EPA [21].

## SOIL SAMPLING AND PROCESSING

Soil sampling in the villages under investigation was made from the agricultural land soils using a soil auger and a special spatula (small shover), which was washed before each subsequent sampling to eliminate the error. To take a mixed soil sample, the selected plot of land was divided diagonally into four parts, and soil samples were taken at several locations on the diagonals: 0-10, 10-20, 20-40, and 40-60 cm depth [21]. After the samples were mixed, one common sample was prepared according to depths. With the purpose of ultimate study, the samples taken were transported to the laboratory, where they were dried first, then milled and sieved in the sieve with holes 1mm in size. With the aim of soil sample extraction, 10 ml of nitric acid was added in a 50 ml flask to 2 gr of soil specimens. The total arsenic form was determined in the soil samples.

At the same time, we carried out phytoremediation not in the vegetation vessels, to which increased arsenic concentrations are artificially entered and arsenic amount absorbed by the plant from soil reaches large values, but it was conducted on agricultural lands.

Soil treatment (in particular, ploughing, organic fertiliser's application, loosening and soil preparation for seeding) was conducted in the phytoremediation sites. One sq. m of land was allotted for each plant.

## COLLECTION AND PROCESSING OF PLANT MATERIAL

With the purpose of phytoremediation and phytomigration, different species of cosmopolite plants, which can adapt well to local climate conditions, were selected, in particular Amaranthus gangeticus, Chenopodium album and Helianthus annuus.

Seeds of plants selected for introduction of phytoremediation technology (Amaranthus gangeticus, Chenopodium album, Helianthus annuus) were treated in laboratory conditions using bioactivator Biorag aimed to their stimulation and increase of plant green mass (copyright of Georgian scientist, professor Ramaz Gakhokidze) [22].

It should be noted that plant mass indeed increases when using bioactivator Biorag. Plant volume gain on frequent occasions leads to the accumulation of large quantities of polluting agents in plant cells, which is extremely important for phytoremediation technologies, both from scientific and innovative and environmental and social viewpoints.

For seed material checking purposes, we put seeds in 3-5% table salt solution for 5-6 minutes, then planted only those seeds which were drowned in the solution, then they must be preliminary washed and dried; afterwards, we placed seeds in Biorag solution,

which was diluted in clean water according to information indicated on the label (20 ml of Biorag solution was dissolved in 1 litre of water), in which we placed seed materials for indicated time. Bioactivator solution may be prepared 1-2 days ahead of time of seed material treatment. Seeds removed from the solution were dried for several hours at 25-30°C and planted in 3-5 days [22].

With the purpose of the phytoremediation study, plants were planted in May 2023.

Each plant was settled at a one sq. m area. At that, the distance between Amaranthus gangeticus and Chenopodium album plants was equal to 10 cm, so 25 plants were accommodated at one sq. m. area; while in the case of Helianthus annuus, the distance between plants was 20 cm, and 16 plants were housed in 1 sq. m area.

In August and October, the plants were gathered in raw conditions in Abari and Likheti villages. Plants were cleaned from the soil and washed. Then, the plants' length was measured. Plants' roots, stems, leaves and flowers were separated from each other, placed in the respective packs with labels and transported to the laboratory for drying and further treatment. They were dried at room temperature (25°C). After drying, plants were treated with „Microwave Digestion"decomposer and the total arsenic form was determined.

To determine total arsenic forms in soil and plant analytical samples, the following devices were used:

1. Inductively coupled plasma atomic emission spectroscopy - ICP-OES;

2. Soil decomposer–Milestone – Start D Microwave system;

3. pH meter– Milwaukee-Mi 150.

## MATHEMATICAL PROCESSING OF DATA

For measurement analyses, the methods and techniques of mathematical statistics and probability theory were used. The primary processing of observation data envisaged the calculation of their statistical performance, including mean value, absolute maximum, and minimum, which characterise the parameters' variation range and the computation of standard deviation [23].

There is a widely used method of graphical representation of tabular material based on which the histograms are obtained.

The method of correlation analysis, which establishes the link between two different parameters, is used.

The correlation coefficient between $x$ and $y$ parameters is calculated according to the Pearson formula [23]:

$$r = \frac{\sum_{i=1}^{n}(x_i-\bar{X})(y_i-\bar{Y})}{(n-1)s_x s_y} \qquad (1),$$

Where $x_{ave}$ and $y_{ave}$ are average values of these parameters, respectively, $S_x$ and $S_y$ – their mean square deviations (standard deviations), $n-$ observation series length, i.e. number of observations. Standard deviations are calculated by formulas:

$$S_x = \mathbf{[\Sigma(}x_i - x_{ave}\mathbf{)^2/\ n]^{1/2}}, \text{ and} S_y = \mathbf{[\Sigma(}y_i - y_{ave}\mathbf{)^2/\ n]^{1/2}} \quad \mathbf{(2),}$$

https://doi.org/10.5593/sgem2024v/3.2/s12.29

For the determination of correlation coefficient reliability, the following value is calculated:

$$\boldsymbol{H = r(n-1)^{1/2}} \quad \textbf{(3),}$$

Where $\boldsymbol{r}$ – correlation coefficient and $\boldsymbol{n}$ –observation series length.

The calculated $\boldsymbol{H}$ value is compared with its critical value taken from a special table. Should it appear that the calculated $\boldsymbol{H}$ value exceeds its critical value (taken from a table) then it is considered that the correlation coefficient is considerable at *P* the probability level, and the link between the considered values is reliable.

Links between parameters are described by regression equation, while variable dependence on predictor is evaluated using determination coefficient, which is a squared correlation coefficient.

## CALCULATION OF BIOCONCENTRATION FACTOR, TRANSLOCATION FACTOR AND TOTAL ARSENIC CONTENT

Arsenic concentration and transformation characteristics, namely bioconcentration factor (BCF), translocation factor (TF) and total arsenic content in plants after phytoremediation, were calculated in plants during the research process. Bioconcentration factor is the ratio of arsenic concentration available in the whole plant to soil concentration of this element; translocation factor is determined as a ratio of arsenic concentration available in the upper part of the plant to arsenic concentration in its roots; The total content of arsenic in the plant is calculated by the sum of the concentrations of arsenic accumulated in each part of the plant (root, stem, leaf, flower), mg/kg.

## RESULTS

Soil samples were taken in May before phytoremediation (before plants seeding) from agricultural lands of Abari and Likheti villages using the envelope method according to soil horizons, where the mixed samples were prepared according to these depths. Arsenic concentration in Abari village soils at 0-60 cm depth varies from 27.5 to 36.0 mg/kg, while the average value of arsenic concentration comprises 32.5 mg/kg.

Arsenic concentration in Likheti soils at 0-40 cm depth varies from 16.0 to 22.0 mg/kg, and the average value of arsenic concentration is 19.0 mg/kg.

Arsenic content in both soils at 0-20 cm depth is higher compared to that in the lower layers.

Figure 1 represents the statistical performance of arsenic concentration, including mean, maximum, minimum and standard deviation, before phytoremediation (in May) and after phytoremediation (August, October 2023) in the soils of Abari village. The significance of the differences between the mean and extreme values of arsenic concentration was analysed based on the analysis of the double deviation criterion of SD.

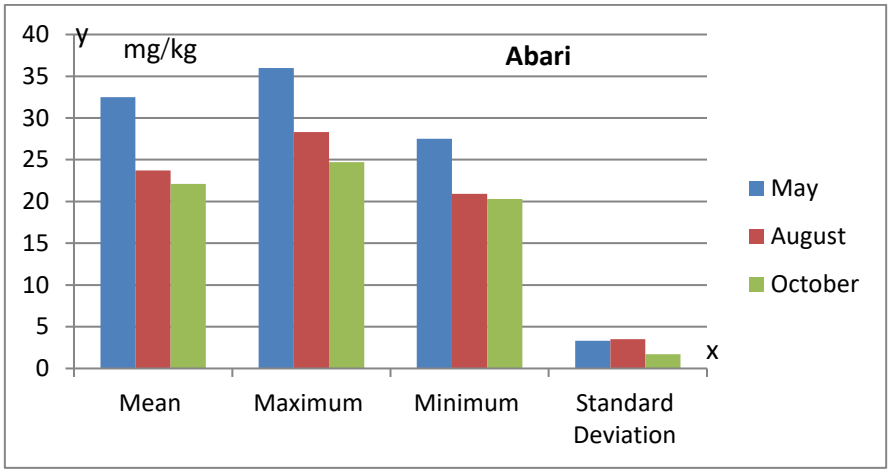



**Figure 1. Statistical performance of arsenic concentration in soils before and after phytoremediation**

According to Figure 1, average and extremum values of arsenic concentration in the period preceding phytoremediation exceed its double standard deviation arsenic concentration after phytoremediation, which points to the statistical reliability of the difference. Average arsenic concentration in the soil of Abari village at 0-60 cm depth before phytoremediation comprised 32.5 mg/kg, while after phytoremediation, these indices were equal to 23.7 mg/kg in August and 22.4 mg/kg in October, respectively. The same picture is kept at different depths in May (1), August (2) and October (3), which is confirmed by histograms given in Fig. 2.

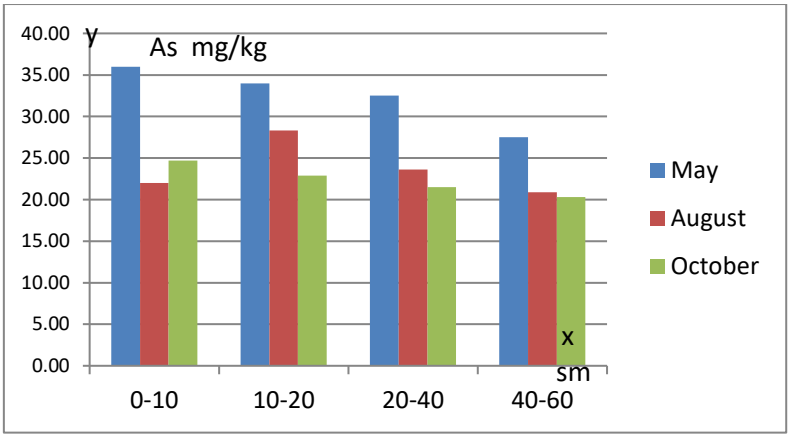
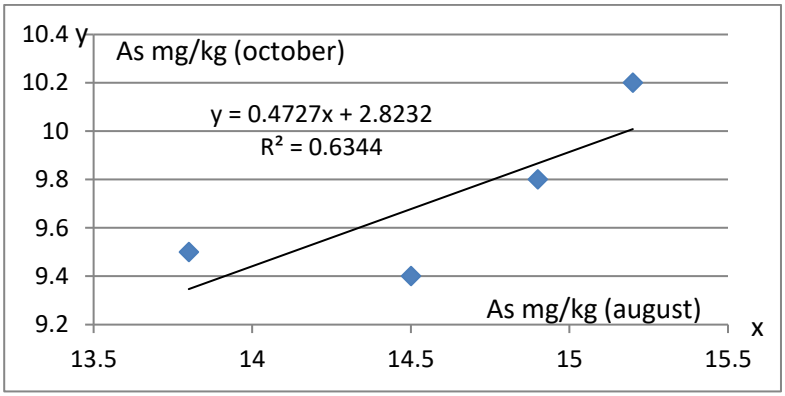


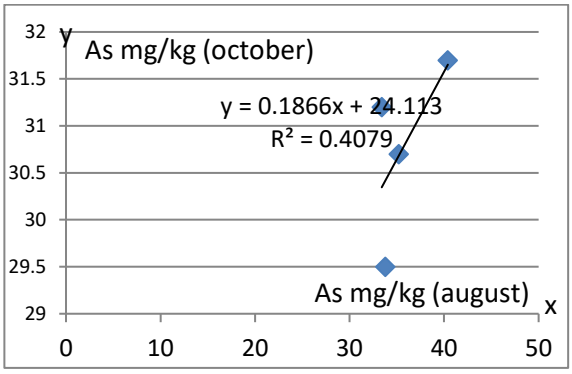

**Figure 2. Arsenic content in soil at different depths Abari village**

As is seen from Fig. 2, arsenic content in May at all depths substantially surpassed the respective data for August and October. Fig. 3 represents the correlation relationship between arsenic content available in the soil of Abarivillage in August and October for different plants, as well as the regression equation and determination coefficient ($R^2$).

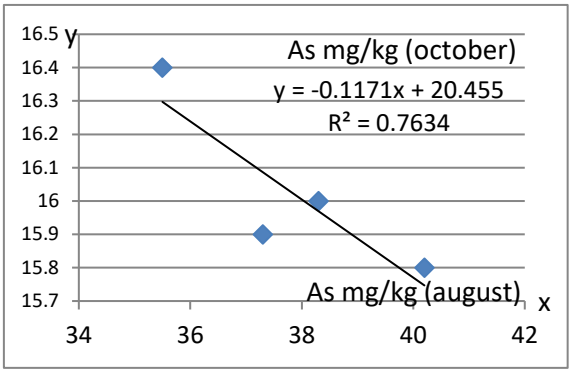
https://doi.org/10.5593/sgem2024v/3.2/s12.29




a)




b)




c)

**Figure 3. Correlation relationship between arsenic content in Abari village soil in August and October, regression equation and determination coefficient ($R^2$): a – Amaranthus gangeticus, b – Helianthus annuus, c – Chenopodium album**

Proceeding from the determination/correlation coefficient, the mutual dependence between arsenic content in the soil in August and October is quite high according to the Laplace classification in the case of Amaranthus gangeticus. As for Helianthus annuus, correlation is kind of reduced, though it remains high according to the Laplace classification. In the case of the Chenopodium album, the correlation is negative and very high. Despite this fact, these links are not statistically significant at the level of 0.95 probability. According to the determination coefficient, a share of initial (August) data in arsenic content formation in October in the case of Amaranthus gangeticus comprises 63%. The rest 37% share in arsenic content formation in the soil is contributed by other factors. As for Helianthus annuus, a share of initial data exceeds 40%, while the rest of the share (up to 60%) is caused by other factors, while in the case of Chenopodium album, the share of initial data (August) in arsenic content formation in October exceeds 76%, and up to 24% of the share falls on other factors.

Among the mentioned plants, when gathering Amaranthus gangeticusin August, the following fact was revealed that from May (i.e. sowing) to August (harvesting), it managed to fully ripen and put forth flowers and seeds in time, respectively, it was able to absorb arsenic from soil to the maximum, that is seen well when calculating concentration and translocation factor. As for Helianthus annuus, this plant, due to bad weather and frequent rains, developed late and had no time to ripen and bear fruits. However, it developed well until October, and in this period, the maximum quantity of arsenic was absorbed by this plant from the soil. Probably namely due to this reason, the share of initial data in the case of Helianthus annuus exceeded 40%, while the rest of the share (up to 60%) falls to other factors. Helianthus annuus immaturity, climatic factors, etc., may be among these factors.

Arsenic concentration was determined in different parts of the plant (Table 1, Fig. 4).

**Table 1. Arsenic content in different parts of plants (root, flower, leaf and stem) Gathered from phytoremediation places (Abari and Likheti), August, October 2023**

| № | Village, plant (plants part) | As, mg/kg | Plant biomass, g | As, mg/kg | Plant biomass, g |
|---|---|---|---|---|---|
| | | August | | October | |
| **1** | Abari- Amaranthus gangeticus (root) | 1.91 | 14.91 | 0.41 | 9.84 |
| **2** | Abari- Amaranthus gangeticus (flower) | 3.59 | | 0.47 | |
| **3** | Abari- Amaranthus gangeticus (leaf) | 0.19 | | 0.50 | |
| **4** | Abari- Amaranthus gangeticus (stem) | 0.27 | | 0.35 | |
| **5** | Abari- Helianthus annuus (root) | 1.30 | 33.41 | 4.65 | 31.22 |
| **6** | Abari- Helianthus annuus (flower) | 0.31 | | 0.15 | |
| **7** | Abari- Helianthus annuus (leaf) | 0.93 | | 1.95 | |
| **8** | Abari- Helianthus annuus (stem) | 0.05 | | 0.41 | |
| **9** | Abari- Chenopodiumalbum (root) | 0.17 | 37.33 | 0.39 | 15.86 |
| **10** | Abari- Chenopodiumalbum (flower) | 0.11 | | 0.09 | |
| **11** | Abari- Chenopodium album(leaf) | 0.10 | | - | |
| **12** | Abari- Chenopodiumalbum(stem) | 0.12 | | 0.47 | |
| **13** | Likheti- Amaranthus gangeticus (root) | 0.68 | 22.64 | | |
| **14** | Likheti - Amaranthus gangeticus (flower) | 0.48 | | | |
| **15** | Likheti - Amaranthus gangeticus (leaf) | 0.43 | | | |
| **16** | Likheti - Amaranthus gangeticus (stem) | 0.25 | | | |

Based on Table 1, the bioconcentration factor (BCF), the translocation factor (TF) and the total content of arsenic in the plant are calculated.

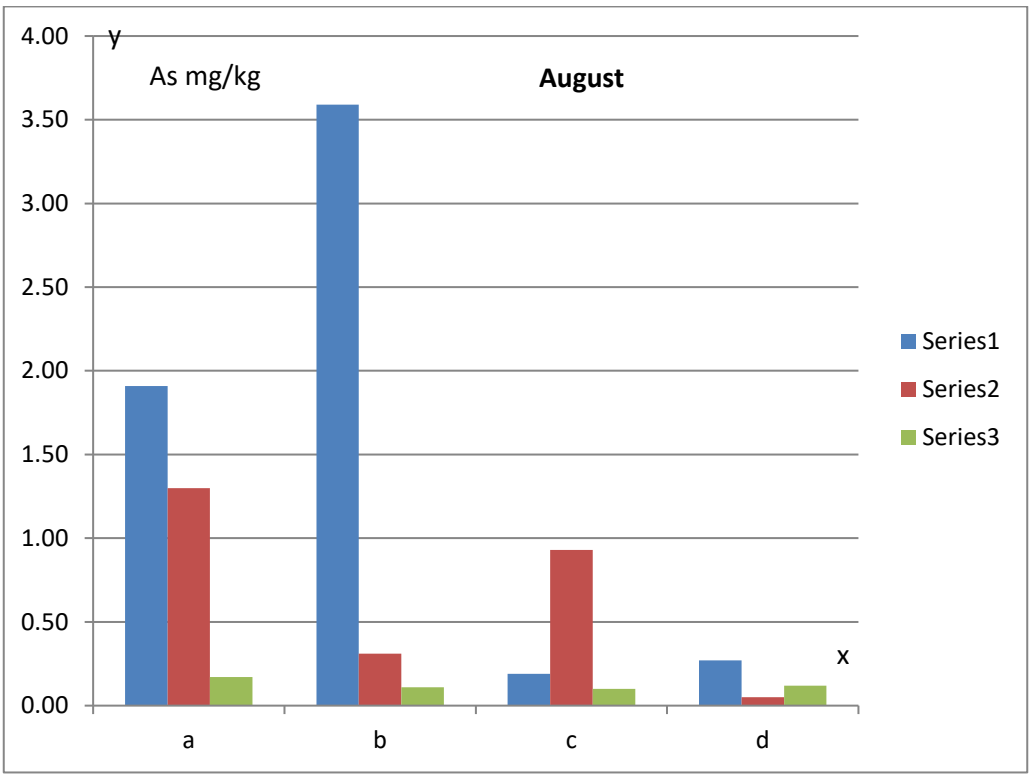
In August, the average content of arsenic in the soil after phytoremediation became 23.7 mg/kg. In August, the amount of arsenic released by a single plant of Amaranthus gangeticus was 5.96 mg/kg, for Helianthus annuus - 2.59 mg/kg and Chenopodium album - 0.50 mg/kg, for all three plants, it was 9.1 mg/kg (28 %), and 72% of arsenic remained in the soil.

In October, the average content of arsenic in the soil became 22.4 mg/kg, which will be calculated similarly as in August: The total content of arsenic for all three plants was 9.84 mg/kg (41.5%), and 58.5% of arsenic remained in the soil.

https://doi.org/10.5593/sgem2024v/3.2/s12.29

In August and October, the total content of arsenic was 18.94 mg/kg. That released plants was 58.3%, and 41.7% remained in the soil.

In Fig. 4, the arsenic content in different parts of plants in Abari village soils in August, in particular, arsenic content in plant roots, flowers, leaves and stems, is given in the form of a histogram.




a)

**Figure 4. Arsenic content in different parts of the plant in Abari village soils, August.**

**At the abscissa axis, there are given: a – root, b – flower, c – leaf, d – stem of plans: Series: 1 - Amaranthus gangeticus, 2 – Helianthus annuus, 3 – Chenopodium album.**
**At the ordinate axis - Arsenic content at these parts of plants**

It follows from the represented histogram (Fig. 4) that arsenic concentration in different parts of the plant depends to a significant degree on the species of the plant itself. In particular, in the case of Amaranthus gangeticus, arsenic content is highest in the flower and exceeds 3.5 mg/kg; its value in roots slightly reduces, and it is minimal in leaves and stems. In the case of Helianthus annuus, arsenic concentration is highest in roots – 1.3 mg/kg and leaves – approximately 1 mg/kg. As for the Chenopodium album, arsenic concentration is almost uniformly distributed in its parts and comprises 0.1-0.17 mg/kg.

In case of any initial metal concentration in soil, plants accumulate the major part in aerial (aboveground) portion than in roots. Very few plants can translocate large quantities of metals from roots to shoots. Good hyper-accumulator plants collect metals in sprouts than in roots, which is why Amaranthus gangeticus is a good arsenic hyper-accumulator (Nazir F. et al., 2016), which is confirmed by our studies, as well. In October, after phytoremediation, a situation undergoes significant changes (Fig. 5).

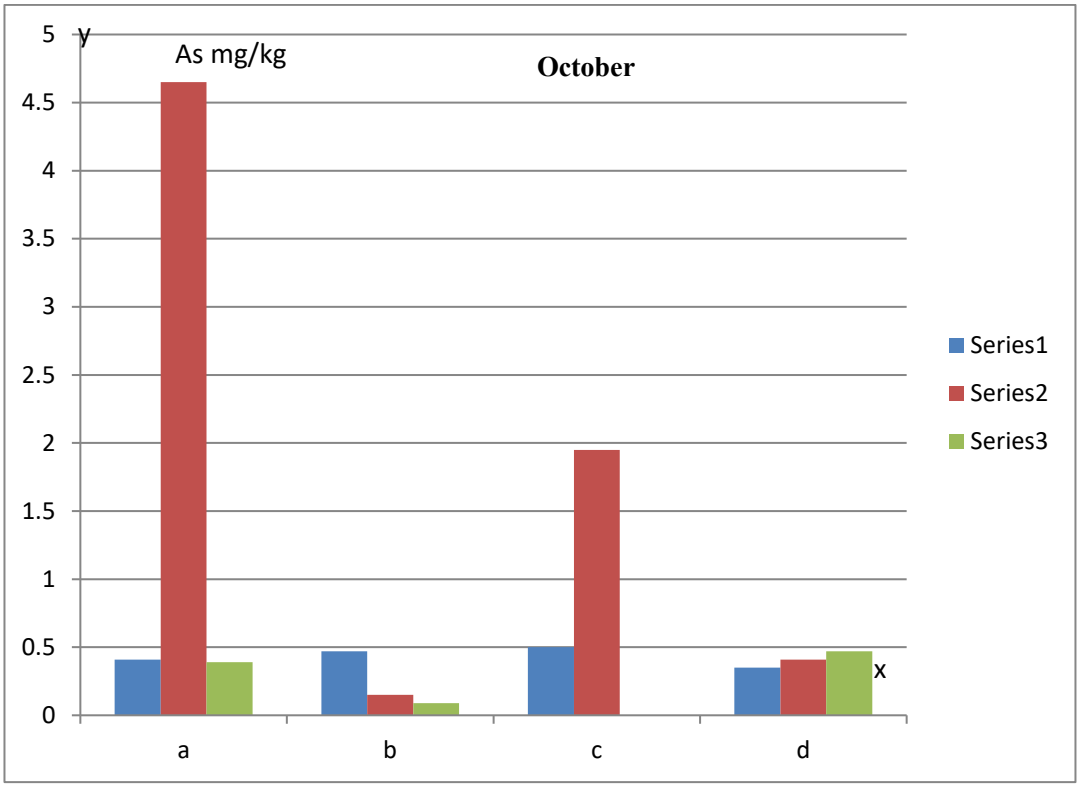



**Figure 5. Arsenic content in different parts of plants in Abari village soils, October. At the abscissa axis, there are given the different parts of the plants: a – root, b – flower, c – leaf, d – stem, of the plants: Series 1 - Amaranthus gangeticus, Series 2 – Helianthus annuus, Series 3 – Chenopodium album. At the ordinate axis - Arsenic content at these parts of plants**.

In October, in the case of Amaranthus gangeticus, arsenic content substantially reduces and insignificantly varies in its separate parts within limits of 0.35-0.5 mg/kg. As for Helianthus annuus, arsenic concentration is highest in roots and leaves, 4.65 and 1.95 mg/kg, respectively. In the case of Chenopodium album, arsenic concentration is almost uniformly distributed in its parts, though it is slightly increased and comprises 0.09–0.47 mg/kg. It should be mentioned the fact that in August, in the case of Helianthus annuus, the accumulation factor calculated for one plant equals 2.7, while in October, this index is 9.4. Thus, Helianthus annuus terminates its growth and development in autumn, in contradistinction from Amaranthus gangeticus, which ceases its growth and development in August, and its accumulation factor is maximal in August and minimal in autumn, the accumulation factor for plant equals 2.7 in August, and 0.7 – in autumn; while for Chenopodium album this factor is even smaller.

https://doi.org/10.5593/sgem2024v/3.2/s12.29

In Fig. 6, there are represented arsenic concentration and translocation characteristics: bioconcentration factor (BCF), translocation factor (TF) and total arsenic content in plants in August and October.

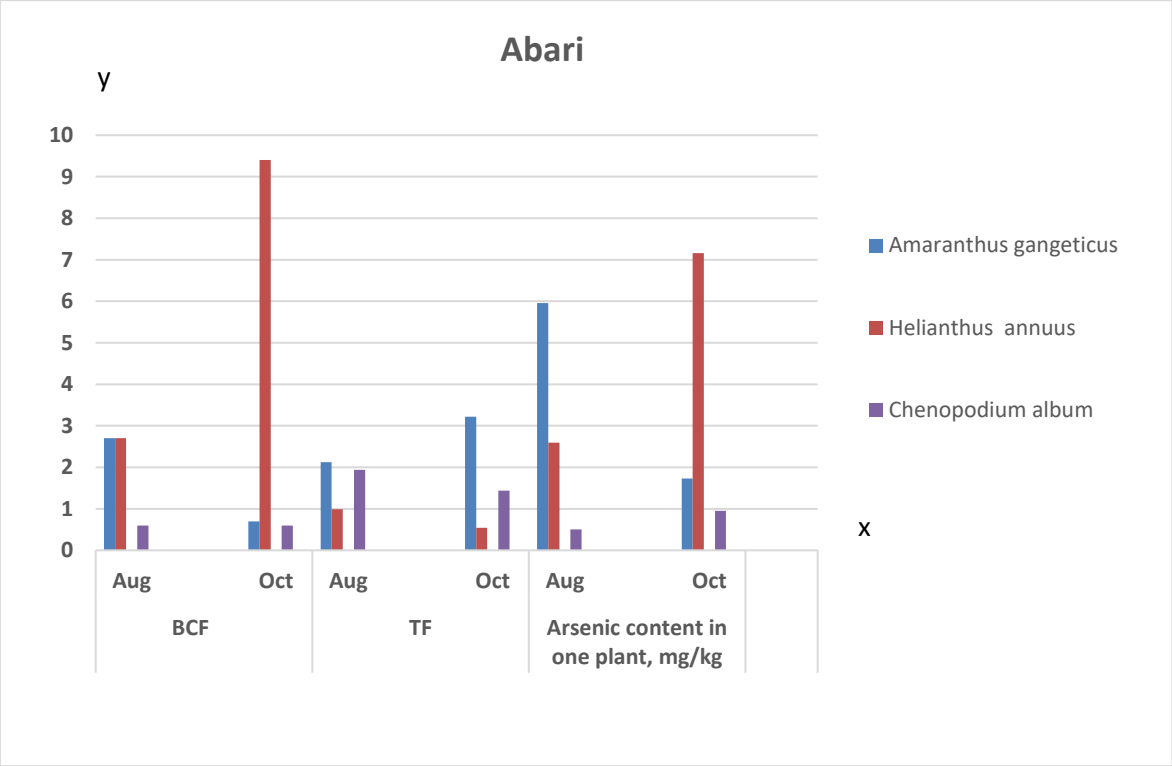



**Figure 6. Bioconcentration factor (BCF), translocation factors (TF) and total arsenic content in plant**

Based on Fig. 6, among considered plants, only Chenopodium album was unable to manifest good element accumulation ability, while Amaranthus gangeticus and Helianthus annuus have good performance.

Translocation factor TF > 1 points at the metal shift from plant roots to its aerial portion [14,24]. In the given study, as is seen from the data, TF value exceeds 1 for different plants and at different places, where TF is more than one almost everywhere. So, in plants under investigation, accumulation factor (BCF) (except for Chenopodium album) and translocation factor (TF) are more than 1 in all cases, and the process runs normally.

Plants taking part in the phytoremediation must be burnt with removal from these agricultural lands.

In 2024, phytoremediation will be repeated in the same places.

## CONCLUSIONS

Uravi village soils are the most polluted with arsenic. The average level of arsenic pollution was identified on agricultural lands. The arsenic content in all cases is higher in upper soil layers than in lower ones. Arsenic concentration, accumulation and translocation factors were determined in plant samples gathered in August and October after phytoremediation, while arsenic content was established in total plant mass. Among the considered plants, in August, Amaranthus gangeticus had the best accumulation ability, followed by Helianthus annuus, and only Chenopodium album did not show a good accumulation ability of arsenic; in October, the Helianthus annuus had the best accumulation ability, then the Amaranthus gangeticus and finally the Chenopodium album.

Translocation factor TF>1, which indicates that the plants have a good translocation ability, in particular, the movement of metal from the root to the aerial parts.

The effectiveness of phytoremediation in the soil of village Abari is the following: 18.94 mg/kg (58.3%) was removed by plants at a depth of 0-60 cm in August and October, and 41.7% remained in the soil;

Statistical characteristics of arsenic concentration in the soil before phytoremediation (May) and after phytoremediation (August, October 2023) were determined. The regression equation and the coefficient of determination were calculated based on the correlation between plants and arsenic in the soil (R2);

Based on the coefficient of determination/correlation, the correlation between the arsenic contents in the soils in August and October in the case of Amaranthus gangeticus, according to the Laplace classification, is very high. In the case of Helianthus annuus, the correlation somewhat decreases, although it remains high according to the Laplace classification. In the case of the Chenopodium album, the correlation is negative and very high. However, these associations are not statistically significant at the 0.95 probability level.

## ACKNOWLEDGEMENTS

This study is supported by the Shota Rustaveli National Science Foundation of Georgia with grant No. FR-21-427

## REFERENCES

[1] Shavliashvili L., Bakradze E., Arabidze M., Kuchava G., 2017- Arsenic pollution study of the rivers and soils in some of the regions of Georgia - International Journal of Current Research Vol.9, Issue, 02, pg.47002-47008, February.

[2] Avkopashvili M., Gongadze A., Matchavariani L., Avkopashvili G., Avkopashvili I., 2019 - Soil, Water and Air Pollution by Manganese Industry in the Imereti Region, Georgia - 19th International Multidisciplinary Scientific Geo Conference SGEM 2019, pg. 417-424.

[3] Felix-Henningsen P., M.A.H.A. Sayed, E. E-Narimanidze-King, D.Steffens,T.Urushadze, 2011 - Bound forms and plant availability of heavy metals in

irrigated, highly polluted kastanozems in the Mashavera valley - SE Georgia, J. Annals of Agrarian Science 9 (1), pg. 111-119.

[4] Bakradze E., Vodyanitski Y., Urushadze T., Chankseliani Z., Arabidze M. 2018- About rationing of the heavy metals in soils of Georgia - Annals of Agrarian Science https://www.sciencedirect.com/science/article/pii/S151218871830016.

[5] Iram S., Ahmad, I. and Akhtar, S. 2012. Distribution of Heavy Metals in Peri-Urban Agricultural Areas Soils. The Journal of the Chemical Society of Pakistan.34(4), pg. 861-869.

[6] Iram S., Zaman, A., Iqbal, Z. and Shabbir. R. 2013. Heavy metal tolerance of fungus isolated from the soil contaminated with sewage and industrial wastewater. Polish Journal of Environmental Studies.22 (3), pg.691-697.

[7] Munawar, S. and Iram. S.2014. Chelating impact assessment of biological and chemical chelates on metal extraction from contaminated soils. Journal of the Chemical Society of Pakistan. 36(3), pg.548-555.

[8] Shavliashvili L., Kuchava G., Shubladze E., Tabatadze M., Buachidze N., 2023- Arsenic contamination in soils of Racha-Lechkhumi and Kvemo Svaneti region of Georgia - International Conference Organized by World Research forum for Engineers and Researchers, Barcelona, Spain, 23-24.09. pg.9-13, ISBN:978-93-90150-28-1, Edn:464.

[9] Arsenic and arsenic compounds IARC monographs – 100C (IARC, 1980, 1987, 2004). http://monographs.iarc.fr/ENG/Monographs/vol100C/mono100C-6.pdf.

[10] Li-Xian Yao, Guo-Liang Li, Zhi Dang, Zhao-Huan He, Chang-Min Zhou, Bao-Mei Yang, 2009 - Arsenic uptake by two vegetables grown in two soils amended with As-bearing animal manures - J Hazard Mater, 2009 May 30;164(2-3):904-10. DOI: 10.1016.

[11] Avkopashvili G., Avkopashvili M., Gongadze A., Gakhokidze R., 2017 - Eco-Monitoring of Georgia's Contaminated Soil and Water with Heavy Metals - Carpathian Journal of Earth and Environmental Sciences - vol. 12, No. 2, pg. 595-604.

[12] Aleksidze G., Loliasvilivi R., 2016 - The main aspects of environmental pollution in Georgia - materials of the international scientific conference "Modern technologies for the production of ecologically clean products for the sustainable development of agriculture", Tbilisi, pg.33-45.

[13] Sagiroglu, A. Sasmaz, Ö. Sen,2006 - Hyperaccumulator Plants of the Keban Mining District and Their Possible Impact on the Environment - Polish J. Environ. Stud. Vol. 15, No. 2 pg. 317-325.

[14] Nazir Ashfaq, Riffat Naseem Malik, Muhammad Ajaib, Nasrullah Khan and Muhammad Faheem Siddiqui,2011 - Hyperaccumulators of heavy metals of industrial areas of Islamabad and Rawalpindi - Pakistan Journal of Botany, 43(4): 1925-1933.

[15] Tabatadze M., Shavliashvili L., Kuchava G., Shubladze E., Buachidze N., 2023- Arsenic contamination of natural waters of Racha-Lechkhumi and Kvemo Svaneti region of Georgia - International Conference Organized by World Research forum for Engineers

and Researchers, Barcelona, Spain, 23-24.09. p.5-8. ISBN:978-93-90150-28-1, Edn:464.

[16] Shavliashvili L., Tabatazdze M., Kuchava G., Shubladze E., Dumbadze G., 2023- Research of arsenic-contaminated areas of Racha-Lechkhumi and Kvemo Svaneti region of Georgia and assessment of environmental impact risks - International Symposium in soil Knowledge and Plant Nutrition. December 8-9, Turkey.

[17] Iram S., Shabbir R., Zafar H. and Javaid.M. 2015. Biosorption and Bioaccumulation of Copper and Lead by Heavy Metal-Resistant Fungal Isolates. Arabian Journal for Science and Engineering. 40 (7):1867-1873.

[18] Shazia Iram., RabiaBasri., Khuram Shahzad Ahmad and Shaan Bibi Jaffri. 2019. Mycologically assisted phytoremediation enhancement crops Zea mays and Helianthus annus in heavy metal contaminated lithospheric zone. Soil and Sediment contamination. 28,4, pg.411-430.

[19] Climate of Georgia: Racha-Lechkhumi, Kvemo Svaneti, Institute of hydrometeorology of the Georgian Technical University, vol.N130, 132pg., 2021.

[20] Urushadze T., 2020- Agro soil science - Publishing House of Free and Agrarian Universities, Tbilisi, pg. 315.

[21] Fomin G.S., Phomin A.G., 2001- Soil, Quality control and environmental safety according to international standards – Moscow, VNII standard, pg.300.

[22] Gakhokidze R., 2008 - Effects of Bioenergoactivators on Productivity of Plants - Chemistry of Advance Compounds and Materials. New York, Nova Science Publ. Inc., pg. 269-275.

[23] Rumshisky Z.-Mathematical processing of experimental results. - Science, M, 1971, 192 pg.

[24] Nasir F.B., Islam S., Munna G. M, S. Ray, R. Awal, 2016 - Effectiveness of Amaranthus gangeticus in Arsenic Extraction from Soil - Journal of Scientific Research 8(1), pg.71-79. www.banglajol.info/index.php/JSR.

https://doi.org/10.5593/sgem2024v/3.2/s12.29

# SECTION FOREST ECOSYSTEMS

# AND SUSTAINABLE FORESTRY

# THE EFFECT OF FOLIAR FERTILIZATION WITH UREA UPON THE CONTENT OF MACRONUTRIENTS IN CAMBIC CHERNOZEM

**Assoc. Prof. Dr. Alina Lato**
**Prof. Dr. Florin Crista**
**Assoc. Prof. Dr. Iaroslav Lato**
**Assoc. Prof. Dr. Alina Neacsu**
**Dr. Laura Crista**
University of Life Sciences "King Mihai I" from Timisoara, **Romania**

## ABSTRACT

Sunflower and maize are two crops of particular importance, especially in the current context of the food crisis, cultivated on large areas worldwide, used both for animal and human nutrition. This study proposed to test the effectiveness of several types of foliar fertilizers with urea, for the two previously mentioned crops, in the pedo-climatic conditions of West of Romania, and the type of soil chosen for experimentation was Cambic Chernozem. The chemical compounds used for fertilizing crops were different urea solutions. As for the pH of urea solutions, they all have a value of 7.5 pH units, which places them in the neutral reaction class. In order to see if these types of fertilizers have an effect on the soil, samples were collected before the crops were sown but also after they were harvested. The indicators determined according to the current methodologies were: soil pH in aqueous solution, and the content of main macronutrients: total nitrogen, phosphorus and potassium. After analyzing the obtained results, a slight decrease in the concentration of these macronutrients in the soil was found, as well as an insignificant decrease in the pH values of the soil.

**Keywords:** sunflower, maize, urea, foliar fertilization, soil.

## INTRODUCTION

The deficiency of nitrogen in the soil is the major limiting factor that affects crop yield [4]. Nitrogen fertilization is the most influential in terms of increasing crop production. Mineral nitrogen, in addition to increasing the content of nitrate in soil, leads to changes in soil pH and other properties. In intensive agricultural production the soil receives large quantities of nitrogen. Nitrogen fertilizers primarily affects the soil pH, resulting in an increase in acidity. Upon oxidation $NH_4^+$ can release $H^+$ ions, a potential source of soil acidity [3].

Soil acidification is a worldwide spread natural phenomenon in regions with medium to high rainfall, and agricultural production systems can accelerate soil acidification processes through perturbation of the natural cycles of N, P and S in soil, through removal of agricultural produce from the land, and through addition of fertilizers and soil amendments that can either acidify soil or make it more alkaline [3]. Changes in soil pH might be advantageous or detrimental depending on the starting pH of the soil and the direction and speed of pH change: decreases of soil pH in alkaline soils might be advantageous for crop production due to benefits in terms of the availability of P and Zn; decreases of soil pH for a highly acidic soil might be detrimental in terms of

https://doi.org/10.5593/sgem2024v/3.2/s12.30

increasing crop susceptibility to toxicity induced by increased solubility of Al and Mn as soil pH decrease; soil pH is one of the main factors affecting solubility of trace elements and their phyto-availability [3].

Urea fertilizers cover 73.4 % of all N fertilizers used worldwide. Liquid urea enables faster hydrolysis to scatter inside the soil profile, which increases the N adsorption by the soil aggregates. These processes reduce the N loss potentiality and ensure immediate N availability to meet the current crop demand [7, 11]. Liquid urea, after entering the plant, is reaching to plant parts where nitrogen is required and release nutrients in a controlled manner, thereby reducing wastage into the environment [4, 6]. Liquid urea is more eco-friendly with efficient uptake, and about 19 % higher nitrogen use efficiency. Moreover, liquid urea is superior in terms of N uptake, N use efficiency, and yield [7, 9]. The application of liquid urea can reduce the substrate concentration in soil, which stabilize the soil pH. A higher application frequency at a lower rate, also lowers the substrate concentration than at a higher rate and lower application frequency. Loamy soils have more potential for higher hydrolysis than strong clayey soils [7]. The liquid urea decreases the substrate concentration by dispersing rapidly inside the soil profile. The higher application frequency at the lower dose of urea reduces its concentration than a single application at the higher dose [7, 10].

Effects of urea fertilizers upon soil pH and nutrients are described by other researchers as follows. Urea might be the possible reason for soil pollution, nutrient imbalance, acidification and salinization [7]. Nitrogen fertilizers are increasing the acidity of soils, so that annual long-term applications of urea led to soil acidification [1, 3]. Permanent fertilization with nitrogen can lead to its leaching, where firstly the processes of nitrification build up nitrate ions, which are weakly associated to soil adsorptive complex [3, 8]. Addition of high amounts of nitrogen can lead to a decreasing content of P, which is probably induced by reduced solubility of P compounds due to increased acidity, but the content of P may increase in some cases, depending on the rate of N application [1, 3]. The content of N is increasing corresponding to the applied fertilizer rate, but increased urea application frequency with lower doses can lower the $NH_4^+$ concentration in soil compared to a single application. These mechanisms reduce the N loss potential and increase the N crop uptake potential of applied N from fertilizers [1, 7]. The content in K increase may not be regular [1]. Liquid urea reduces N loss from the soil-crop system by adsorption into soil aggregates. The liquid urea application reduces the $NH_4^+$ concentration in the soil by dispersing the $NH_4^+$ into the soil profile and decreasing $NH_4^+$ concentration in the soil [7].

## MATERIALS AND METHODS

Research on liquid urea fertilizers was carried out in an experimental field, on a Cambic Chernozem soil, in the plain area of Western Romania [2]. The fertilizers used in the study were the following: U+S- liquid fertilizer with urea and sulphur; U+BIOS- liquid fertilizer with urea and bio-stimulator; U+MICRO – liquid fertilizer with urea and micro-elements; U+AA – liquid fertilizer with urea and ammonium nitrate.

Soil samples were collected from the experimental field before sowing the crop plants and after their harvest, with the idea of following the effects of these types of fertilizers on the soil reaction, as well as on the main plant macronutrients: N, P and K. The soil samples were collected at a depth of 20 cm, with the help of a specific probe, and were

later processed and conditioned for analysis. The pH of the soil was determined in aqueous suspension, in a soil: solution ratio of 1:2.5, by the potentiometric method. The content in total nitrogen in the soil was determined by the Kjeldahl method, and that in phosphorus and potassium by the Egner-Rhiem-Domingo method.

## RESULTS

Two crops were chosen for the study: maize and sunflower, because they are grown on large areas worldwide, being used both for animal and human food [5].

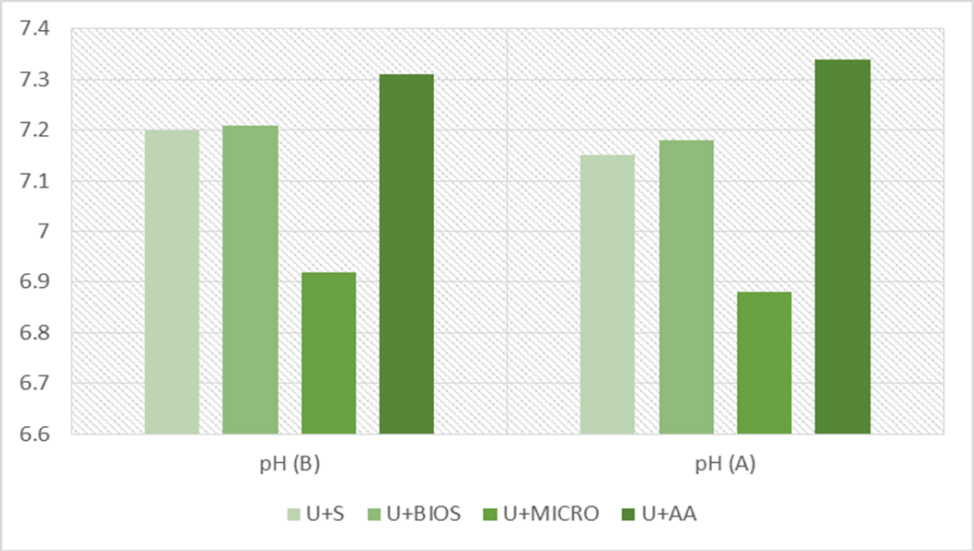



Figure 1. Variation of soil pH under the sun flower crop.
*B- before fertilization; A-after fertilization*

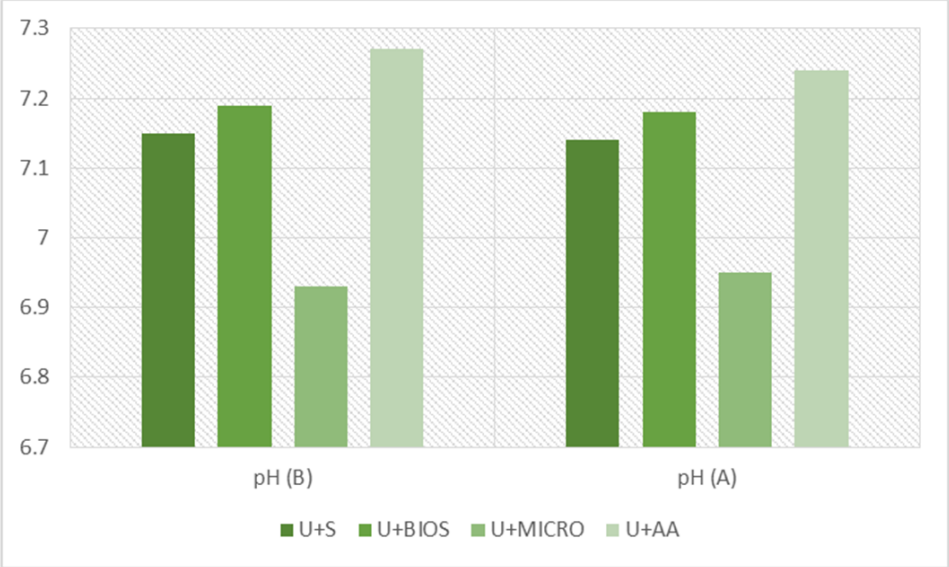



Figure 2. Variation of soil pH under the maize crop.
*B- before fertilization; A-after fertilization*

Figures 1 and 2 present the soil pH values, which are included in the neutral reaction class to slightly alkaline, the values recorded in the case of the sunflower crop being lower than those of the maize crop.

https://doi.org/10.5593/sgem2024v/3.2/s12.30

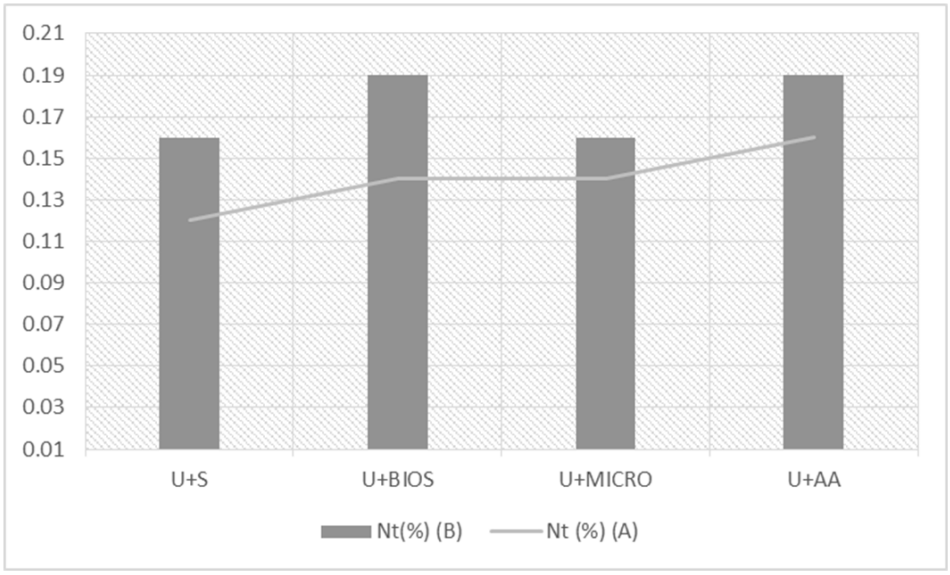



Figure 3. Variation of soil's total nitrogen content (Nt %) under the sun flower crop.
*B- before fertilization; A-after fertilization*

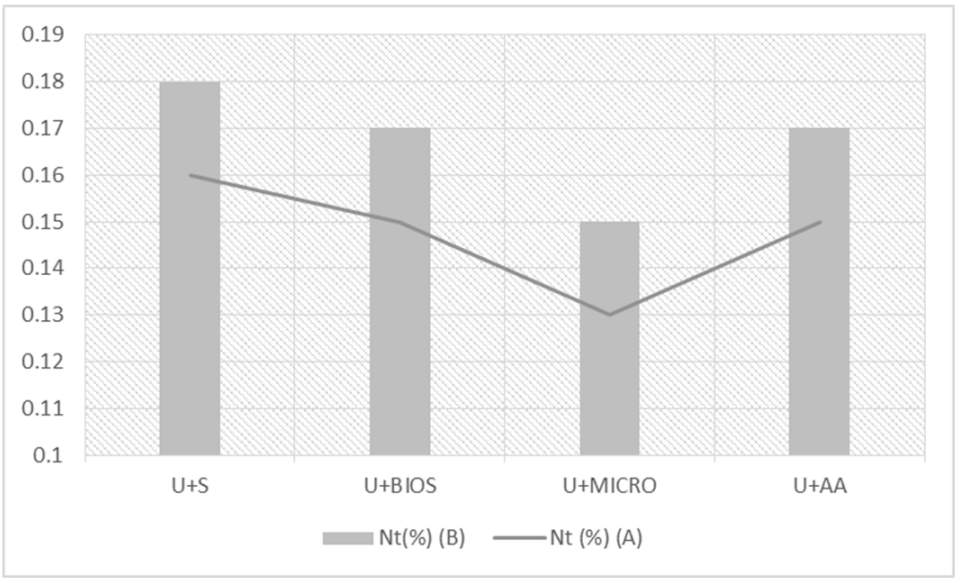



Figure 4. Variation of soil's total nitrogen content (Nt %) under the maize crop.
*B- before fertilization; A-after fertilization*

In graphs 3 and 4, the total nitrogen content of the soils is represented, which is included in the medium to normal supply class for field crops. For the sunflower crop, the values of this nutritional element are higher compared to those recorded for the maize crop.

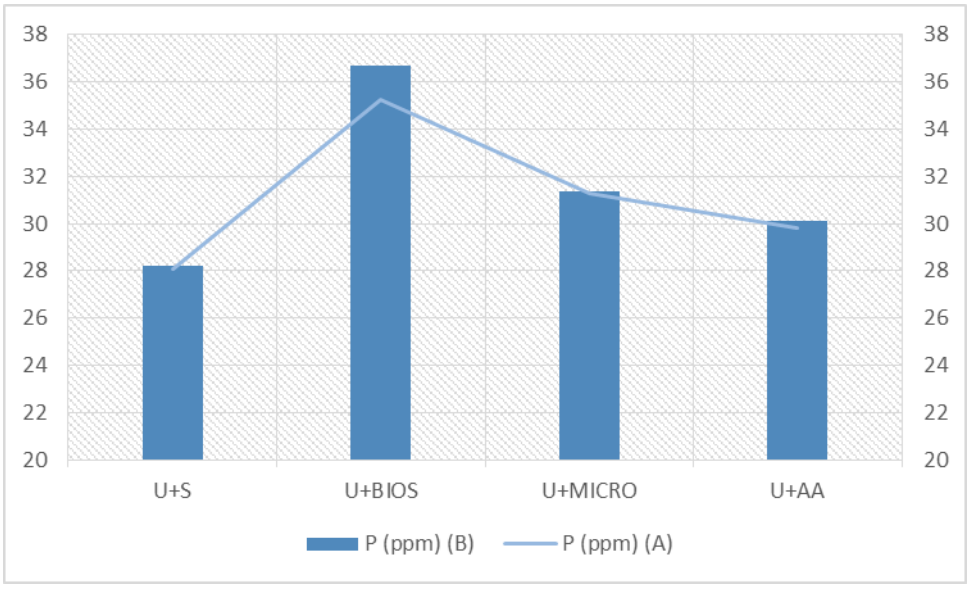



Figure 5. Variation of soil's phosphorus content (P ppm) under the sun flower crop.
*B- before fertilization; A-after fertilization*

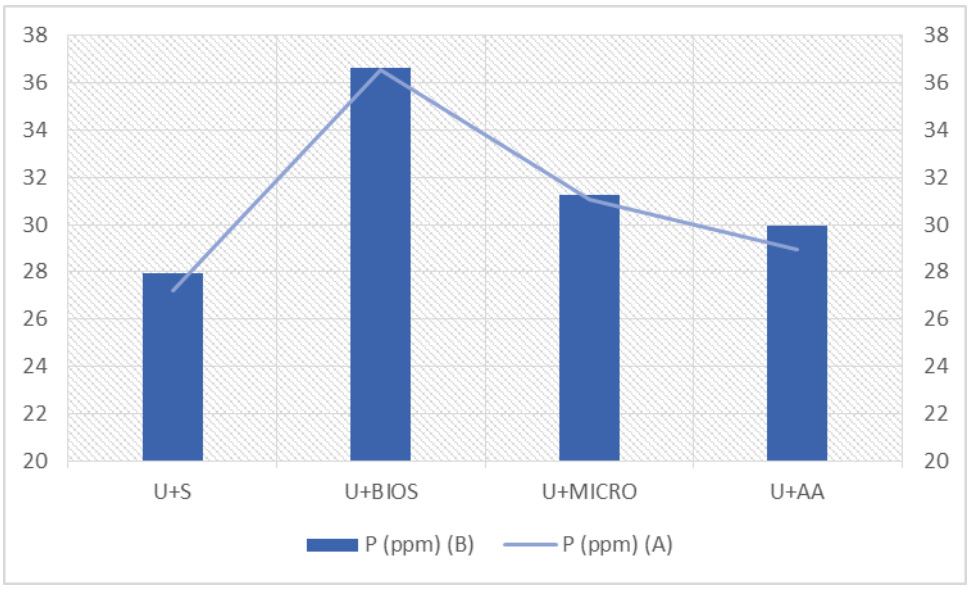



Figure 6. Variation of soil's phosphorus content (P ppm) under the maize crop.
*B- before fertilization; A-after fertilization*

The phosphorus content of the soil is in the medium to normal supply class, highlighting higher values for the sunflower crop.

https://doi.org/10.5593/sgem2024v/3.2/s12.30

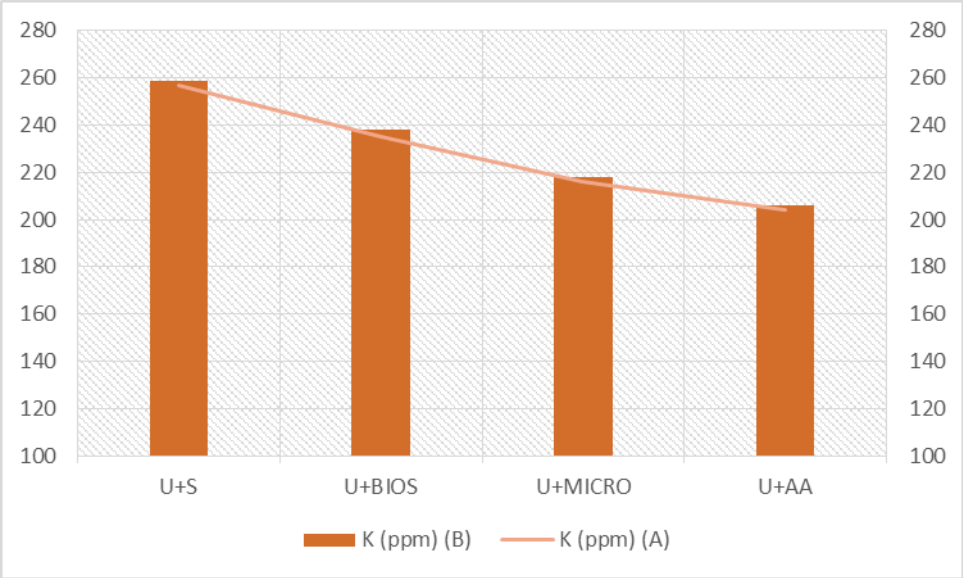



Figure 7. Variation of soil's potassium content (K ppm) under the sun flower crop.
*B- before fertilization; A-after fertilization*

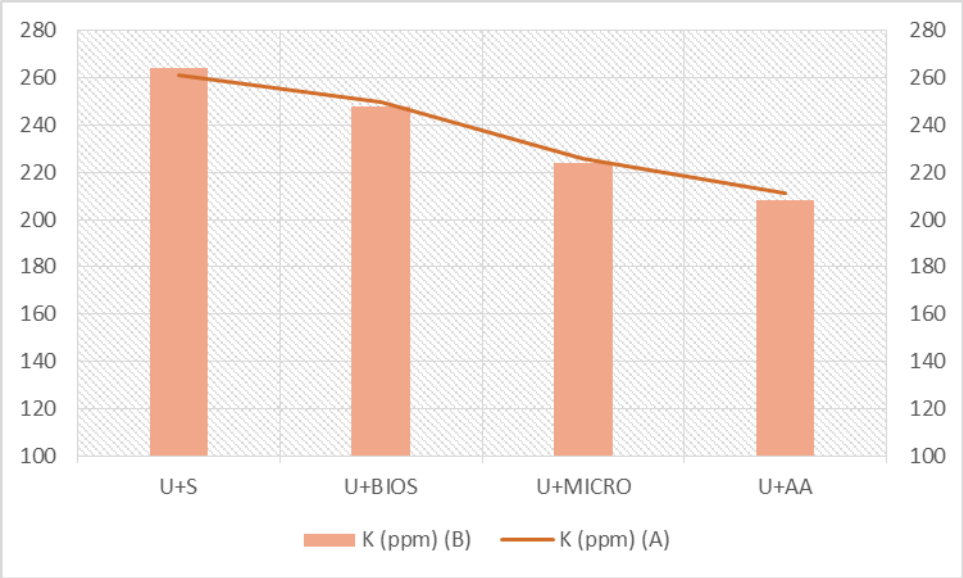



Figure 8. Variation of soil's potassium content (K ppm) under the maize crop.
*B- before fertilization; A-after fertilization*

The potassium supply of the analysed soils is high, in the case of both crops, recording higher values in the case of maize crop.

## DISCUSSION

The pH values decrease within the limits between 6.88 and 7.34 pH units. The minimum value was recorded for the sunflower crop in the variant fertilized with U+MICRO and the maximum for the same crop in the variant fertilized with U+AA. In the case of both crops, a decrease of pH values is observed after fertilization with urea, a fact also specified by other researchers [1, 3, 7].

The total nitrogen content of the soil is between a minimum of 0.12% when fertilized with U+S and a maximum of 0.19%, when fertilized with U+AA, in the case of the sunflower crop. The decrease in the total nitrogen content of the soil is found in all fertilization variants, after harvesting the crops, a fact also noted by [7, 12].

The nutrient element phosphorus, records values of its content in the soil, which vary from 27.21 ppm when fertilizing with U+S for maize, up to 36.71 ppm when fertilizing with U+BIOS for sunflower [1]. After harvesting the crops, there is a slight decrease in its content in the soil, a fact recorded in all the experimental variants, as noted by [3].

The minimum potassium content is 204 ppm and was determined for sunflowers in the variant fertilized with U+AA, while the maximum of 264 ppm was recorded for maize in the variant fertilized with U+S. Also, as in the case of the other nutrients, the potassium also decreases slightly after harvesting the crops, as stated by [1].

## CONCLUSION

Based on our researches, on analyses results and the observations that were made in the experimental field, we can conclude that the liquid urea fertilizers are efficient for spring crops and also they produce a benefit for soil reaction and the content of macronutrients. The most visible effects were recorded for the following fertilizers: urea + ammonium nitrate (U+AA), urea + bio-stimulator (U+BIOS), urea + Sulphur (U+S) and urea + microelements (U+MICRO) is not so efficient, as it can be observed from our experimental data. A slightly decrease of the soil pH was registered after the harvesting, but it is not outside the range of neutral reaction class. The total nitrogen content in the soil does not decrease so that it is outside the range of medium supply with this essential nutrient for crops. The phosphorus content of the soil is negatively influenced by liquid urea fertilization, recording a decrease, but which is not outside the medium supply range. The only nutrient that is maintained with a high supply in the soil is potassium, it not being influenced by liquid urea fertilization.

## ACKNOWLEDGEMENTS

This research was carried out during project No. 8662/2018 in University of Life Sciences "King Mihai I" from Timisoara.

## REFERENCES

[1] Cakmak D., Saljnikov E., Perovic V., Jaramaz D., Mrvic V., Effect of long-term nitrogen fertilization on main soil chemical properties in Cambisol, 19th World Congress of Soil Science, Soil Solutions for a Changing World, 1-6 August 2010, Brisbane, Australia.

[2] David G., Țărău D., Sandor C., Niță L., Soil and climate factors that define land productivity in the lower plain of Banat. International Multidisciplinary Scientific GeoConference: SGEM vol. 18(3.2), pp 465-472, 2018.

[3] Dikir W., Effect of long-term chemical fertilizer application on soil chemical properties: a review, Journal of Biology, Agriculture and Healthcare, vol. 13(5), pp. 11-18, 2023, DOI: 10.7176/JBAH/13-5-02.

[4] Lakshman K., Chandrakala M., Siva P.M., Babu G., Srinivas T., Ramesh N., Korak A., Liquid nano-urea: an emerging nano fertilizer substitute for conventional urea, Chronicle of Bioresource Management, vol. 6(2), pp. 54-59, 2022.

[5] Lato I., Neacsu A., Crista F., Radulov I., Berbecea A., Boldea M., Lato A., Lopez A., The essential role of nitrogen fertilization upon protein and oil content of maize and sunflower yields in Banat Plain, Western Romania, Scientific Papers-Series A-Agronomy, vol. 64(2), pp 57-62, 2021.

[6] Moridi A., Zarei M., Moosavi A.A., Ronaghi A., Effect of liquid organic fertilizers and soil moisture status on some biological and physical properties of soil, polish Journal of Soil Science, vol. LIV(1), pp. 41-58, 2021, DOI: 10.17951/pjss/2021.54.1.41.

[7] Motasim A., Samsuri A., Nabayi A., Akter A., Haque M., Sukor A., Adibah A., Urea application in soil: processes, losses, and alternatives-a review, Discover Agriculture, vol. 2(42), 2024, DOI: 10.1007/s44279-024-00060-z.

[8] Ogunboye O., Adekiya A., Ewulo B., Olayanju A., Effects of split application of urea fertilizer on soil chemical properties, maize performance and profitability in Southwest Nigeria, The Open Agriculture Journal, vol. 14, pp. 36-42, 2020, DOI: 10.2174/1874331502014010036.

[9] Solihin E., Yuniarti A., Damayani M., Rosniawaty S., Application of liquid organic fertilizer and N, P, K to the properties of soil chemicals and growth of rice plant. IOP Conf. Seies: Earth and Environmental Science 393, 2019, DOI: 10.1088/1755-1315/393/1/102026.

[10] Swify S., Mazeika R., Baltrusaitis J., Drapanauskaite D., Barcauskaite K., Review: Modified urea fertilizers and their effects on improving nitrogen use efficiency (NUE), Sustainability, vol. 16, 2024, DOI: 10.3390/su16010188.

[11] Webber H., Zhao G., Wolf J., Britz W., Vries W., Gaiser T., Hoffmann H., Ewert F., Climate change impacts on European crop yields: Do we need to consider nitrogen limitation?, European Journal of Agronomy, pp 123-134, 2015.

[12] Zhang Y., Li D., Zhang K., Xiao F., Li Y., Du Y., Xue Y., Zhang L., Gong P., Song Y., Wu K., The effects of long-term application of stabilized and coated urea on soil chemical properties, microbial community structure, and functional genes in Paddy Fields, Agronomy, vol. 13, 2023, DOI: 10.3390/agronomy13092190.

# ASSESSING THE ROLE OF WINDBREAKS IN REDUCING WIND EROSION: REMOTE SENSING PERSPECTIVE

**Assoc. Prof. Dr. Lenka Lackóová**
**Dr. Mária Tárníková**
Slovak university of Agriculture in Nitra, Faculty of Horticulture and Landscape Engineering, Tr. A. Hlinku 2, 949 01 Nitra, **Slovakia**

## ABSTRACT

Remote sensing (RS) imagery is widely used to assess and detect environmental changes in various areas and the numerous methods resulting from natural and human activities. To understand landscape change, including the role of windbreaks in agricultural regions, RS datasets are essential. Detected by the CORINE Land Cover (CLC) project, agricultural landscapes have undergone changes such as an increase in complex cropping patterns by 164.19% and in pastures by 15.3%, but a decrease in coniferous forest by 10.19% and in land mainly occupied by agriculture with significant areas of natural vegetation by 10.17% between 1990 and 2018. These trends highlight the changing dynamics of land cover, which is critical for assessing the environmental and economic value of windbreaks as soil conservation structures. Monitoring these changes helps to understand the effectiveness of windbreaks in reducing soil degradation. By utilizing data from the remote sensing, this paper analyses land use changes and the spatial distribution of windbreaks, correlating their presence with reductions in soil degradation. By tracking land cover changes over time, RS data provides valuable insights into the effectiveness of windbreaks as measures to combat soil degradation in agricultural landscapes.

**Keywords:** windbreaks, wind erosion, remote sensing, soil conservation, agricultural landscape

## INTRODUCTION

The issue of wind erosion (WE) and subsequent mitigation measures, such as the identification of windbreaks in the landscape and the analysis of their function, has become a frequently discussed topic in soil conservation scientific bodies. WE is a process of wind-forced movement of soil particles [1] and therefore wind erosion is one of the primary processes leading to land degradation [2]. WE of agricultural land can easily occur due to a lack of vegetative cover, poorly aggregated soils, high winds and human activities (e.g. tillage). Windbreaks are an important part of wind erosion control, play a crucial role in a significant environmental challenge in agricultural landscapes. Windbreaks, consisting of trees, provide multiple ecosystem services and benefits. They primarily reduce wind speed, control erosion, protect livestock, and manage snow distribution [3]. The effect of windbreaks is important on WE and particle concentrations on agricultural fields during dust episodes. Research articles and scientists who focus on this topic suggest that windbreaks can improve air quality by reducing dust emissions and lowering the concentration of particulate matter linked to agricultural WE [3]. This study uses RS data to assess the distribution and impact of windbreaks in agricultural regions. CLC uses satellite imagery such as LANDSAT, Sentinel-2, and other high-resolution

https://doi.org/10.5593/sgem2024v/3.2/s13.31

satellites to collect data. The images are then analysed and processed to categorize land cover into various classes. CLC was specified to standardize data collection on land in Europe to support environmental policy development. Since the late 1980s, five iterations of this land cover inventories have been realized (timed around 1990, 2000, 2006, 2012 and 2018) [4]. For understanding landscape change, including the role of windbreaks in agricultural areas, the RS is crucial. By analysing land cover changes and WE patterns, we aim to better understand the role of windbreaks in promoting sustainable land management and protecting soil resources in agricultural landscapes.

## MATERIALS AND METHODS

### Study area

The study area, located in south-west Slovakia, covers a total area of 57.08 km$^2$. It includes five cadastral areas of Čechynce, Veľké Janíkovce, Malý Cetín, Veľký Cetín and Golianovo (Figure 1). This part of Slovakia has a moderate continental climate, with precipitation ranging between 500 and 700 mm annually. The average annual temperature ranges between 9°C and 11°C. In terms of potential natural vegetation, the lowland areas would naturally support mixed oak forests (*Quercus robur, Quercus petraea*), while higher elevations, would be dominated by beech forests (*Fagus sylvatica*) with interspersed hornbeam (*Carpinus betulus*). Study area exhibits a diverse land cover composition, with a significant portion dedicated to agriculture. CLC dataset identifies large areas of arable land and pastures, interspersed with patches of forest and urbanized areas. Windbreaks, particularly along field boundaries, are crucial landscape elements in the agricultural matrix, serving both ecological and functional roles. The ecological stability (ES) of the region varies, with intensively cultivated agricultural areas often exhibiting lower ES due to habitat fragmentation and monoculture practices. However, the presence of windbreaks, and small-scale mosaic landscapes contributes to ecological resilience. The region's soil types are primarily composed of fertile loamy and clayey soils, especially in the lowland agricultural areas.

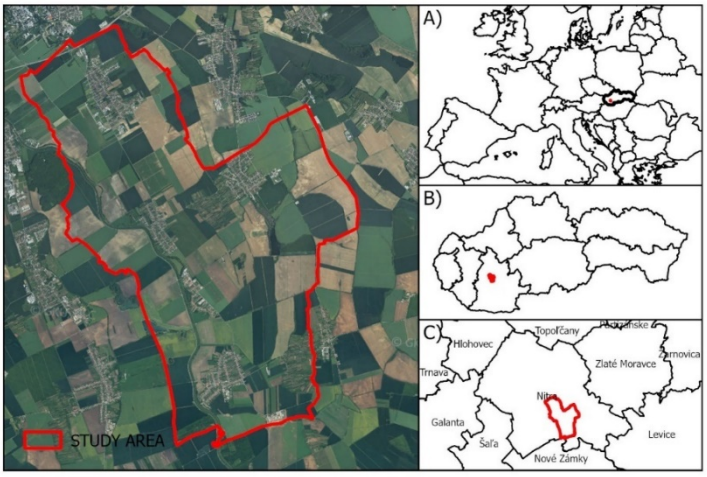



**Figure 1** Study area A) within Europe B) within Slovakia regions C) in the Nitra district

**CLC** provides a pan-European inventory of land cover and use, spanning 44 thematic classes from forests to specific agriculture types like vineyards. Updated every six years, with the latest in 2018, it uses a 25-hectare Minimum Mapping Unit (MMU) for areal

features and 100 meters for linear features, with change layers at a finer 5-hectare MMU. Windbreaks may fall under categories like "Agricultural areas" or "Forest and semi-natural areas," but smaller features, such as individual windbreaks, are generally not mapped due to the 100-meter resolution. The class 'Discontinuous urban fabric' might also include areas with some windbreaks, although they are not mapped individually. However, broader patterns suggesting windbreaks may still be detectable. To capture smaller features, we supplemented CORINE data with high-resolution local datasets from RS techniques, including LANDSAT imagery. This enhanced spatial detail, especially for detecting changes in smaller landscape features. Cloud-free scenes (<10% cloud cover) were selected to ensure consistency across years. The imagery used includes:

**1990**: LANDSAT 5 TM (Thematic Mapper), acquired on 31.08.1990, with a spatial resolution (SR) of 30 m.

**2000**: LANDSAT 5 TM, acquired on 19.08.2000, SR 30 m.

**2006**: LANDSAT 5 TM, acquired on 12.09.2006, SR 30 m.

**2012**: LANDSAT 5 MSS (Multispectral Scanner), acquired on 20.08.2012, SR 60 m.

**2018**: LANDSAT 8, acquired on 12.08.2018, SR 30 m.

**Geographic Information System** (GIS) tools were employed to overlay land cover maps from these years to calculate changes in land cover types and assess the presence and evolution of landscape features, including windbreaks, over time.

**Fractional vegetation cover** (FVC) is a crucial parameter for understanding land-atmosphere interactions and vegetation dynamics. It can be derived from satellite imagery using normalized difference vegetation index (NDVI) data [5], [6]. Global FVC datasets have been created, revealing significant interannual variability in shrublands, savannas, and grasslands [7]. These datasets are valuable for land surface modelling and complement discrete land cover classifications [6]. Since windbreaks and fragmented vegetation are primarily composed of trees and shrubs, NDVI can be used to differentiate vegetation from other land cover types. FVC was calculated using the NDVI according to the following equation:

$$FVC = \frac{NDVI - NDVI_{min}}{NDVI_{max} - NDVI_{min}}$$

Where $NDVI_{max}$ represents the NDVI value of fully vegetated areas, and $NDVI_{min}$ corresponds to bare soil. FVC was classified into five categories based on the following thresholds: 0–0.09 as Bare Soil or Very Low Vegetation Cover, 0.1–0.39 as Low Vegetation Cover, 0.4–0.69 as Moderate Vegetation Cover, 0.7–0.99 as High Vegetation Cover, and 1 as Very High Vegetation Cover. RS data was used to calculate the FVC for each land cover type, and the values were assigned to these categories to assess vegetation density.

## RESULTS

The comparison of CLC changes across the study periods (1990, 2000, 2006, 2012, and 2018) (Figure 2), reveals notable shifts in land cover types. Non-irrigated arable land consistently accounted for the highest percentage of land use, though it slightly declined from 84.44% in 1990 to 77.53% in 2018. Complex cultivation patterns exhibited a significant increase from 4.48% in 1990 to 12.44% in 2006, followed by a slight decline

https://doi.org/10.5593/sgem2024v/3.2/s13.31

to 10.36% in 2012 and 2018. Discontinuous urban fabric steadily increased from 7.33% in 1990 to 8.36% by 2018, reflecting ongoing urbanization in the region. Other land cover types remained relatively stable, with industrial or commercial units fluctuating between 0.3% and 0.4%, and broad-leaved forest maintaining a consistent presence at approximately 0.73%. In contrast, water courses experienced temporary increases. The observed changes in land cover types, particularly the decline in non-irrigated arable land and the increase in discontinuous urban fabric and complex cultivation patterns, may indicate shifts in land use practices that affect the landscape's ability to resist WE. The rise in complex cultivation patterns suggests more fragmented and diverse agricultural systems, which could include the implementation of windbreaks or other erosion control measures. Windbreaks may be more easily detected in such heterogeneous landscapes. RS tools, such as LANDSAT imagery or CORINE data, allow the monitoring of these subtle changes in vegetation structure over time, contributing to the assessment of windbreak effectiveness. The stability of certain land types, like broad-leaved forests, further supports the idea that vegetated areas play a critical role in reducing WE.

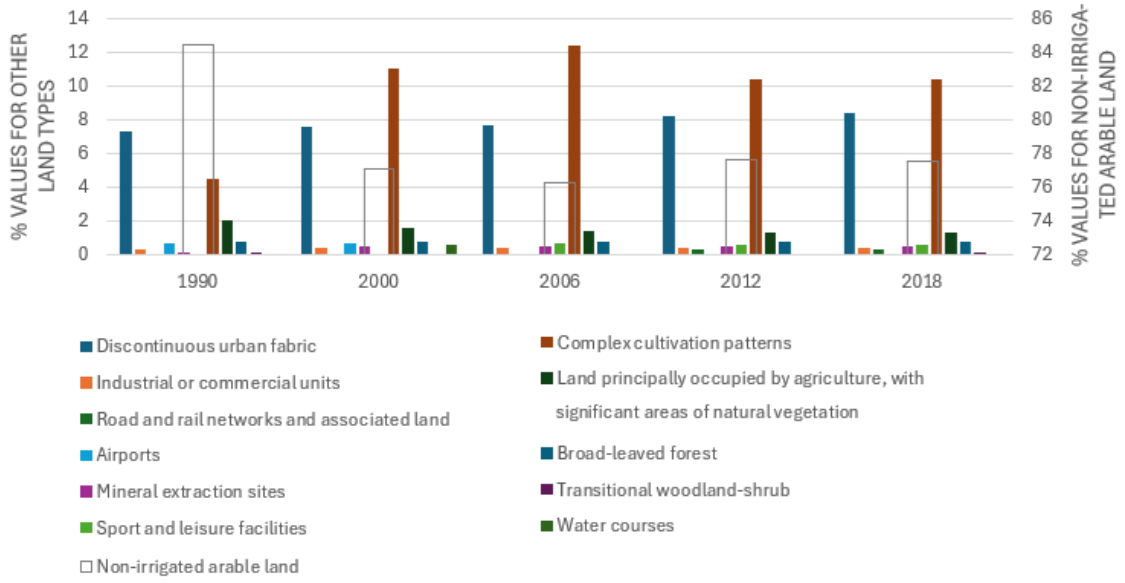



**Figure 2 Comparison of CLC changes in study periods**

The temporal and spatial changes in the FVC across the study area from 1990 to 2018 provide crucial insights into the role of windbreaks in reducing WE from a RS perspective. In 1990 and 2000, large portions of the landscape were covered with sparse or no vegetation, which would have made the area highly vulnerable to WE, particularly in non-irrigated arable land. The lack of moderate or high vegetation indicates that natural wind barriers were likely limited, increasing the susceptibility of the landscape to soil erosion. By 2006, there was a noticeable increase in vegetation density, especially in areas with moderate and high vegetation cover, suggesting improvements in land management. By 2018, although some areas of sparse cover reappear, low vegetation cover. This continued presence of moderate and high vegetation cover serves as a natural barrier, reducing wind speed and providing effective protection against soil erosion. RS data highlights how windbreaks and increased vegetation cover, detected through FVC changes, have contributed to stabilizing the landscape and mitigating wind-driven soil erosion over time.

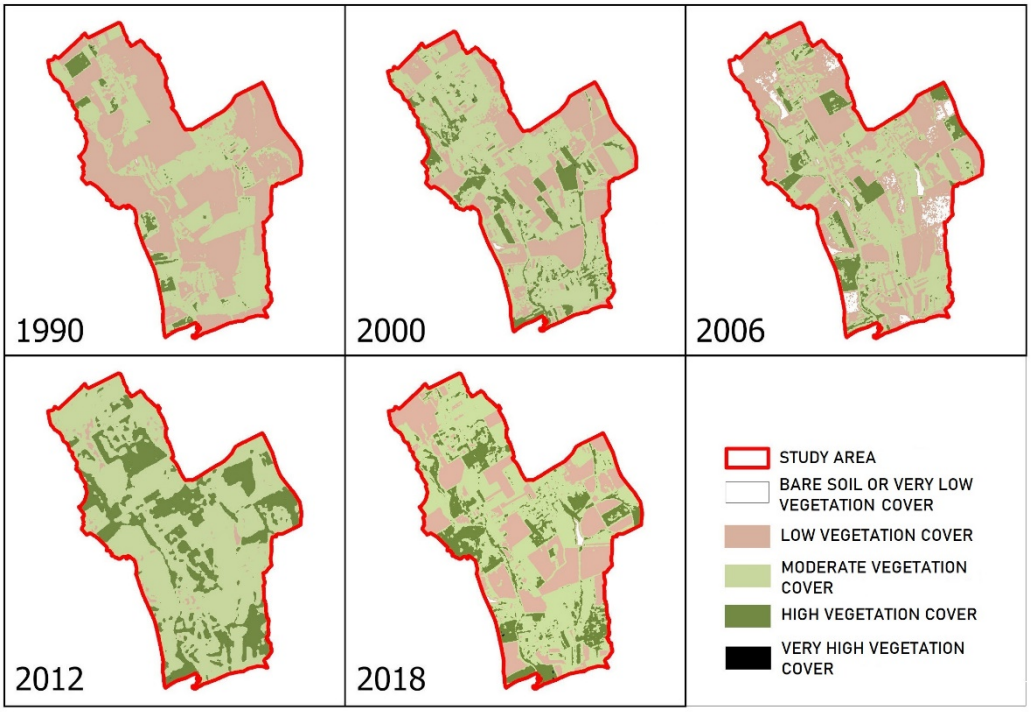



**Figure 3 FVC comparison within the study periods**

The results of comparison FVC (Figure 3) indicate significant temporal shifts in landscape stability and vegetation cover from 1990 to 2018. In 1990, 58.49% of the landscape was characterized by unstable elements, while only 41.51% was considered stable. By 2000, there was a marked increase in stability, with 66.94% of the landscape being stable, but this reverted in 2006 when unstable elements rose again to 50.39%. However, by 2018, the proportion of unstable elements increased to 30.53%, though stability remained relatively high at 69.47% (Table 1). The overall pattern suggests periods of fluctuation, with notable improvements in stability in the later years, which also corresponded to significant vegetation growth and landscape consolidation.

**Table 1 Temporal Dynamics of Landscape Stability and Coefficient of Ecological Stability (CES) from 1990 to 2018**

| YEAR | 1990 | 2000 | 2006 | 2012 | 2018 |
|---|---|---|---|---|---|
| **Unstable elements in the landscape in %** | 58.49 | 33.06 | 50.39 | 1.94 | 30.53 |
| **Stable elements in the landscape in %** | 41.51 | 66.94 | 49.61 | 98.06 | 69.47 |
| **CES** | **0.71** | **2.02** | **0.98** | **50.48** | **2.28** |

The figure 4 illustrates the CES values across five years: 1990, 2000, 2006, 2012, and 2018. The CES measures the balance between stable and unstable landscape elements, with higher values indicating greater ES. In 1990 CES was 0.71, indicating a relatively unstable landscape, with more bare soil or low vegetation cover, making the area susceptible to WE. In 2000 the CES increased to 2.02, reflecting improved ES. This change may be attributed to land use changes that introduced more stable elements like vegetation, possibly including windbreaks that contributed to soil protection. In 2006 CES dropped to 0.98, suggesting a decrease in ES. This could indicate landscape changes

https://doi.org/10.5593/sgem2024v/3.2/s13.31

or disturbances that increased bare soil or less stable elements. There is a significant spike in CES to 50.48 in 2012. This sharp increase is likely an artifact of the lower spatial resolution of the LANDSAT 5 MSS (60 meters) imagery used that year, which may have overestimated stable elements by merging small vegetation features like windbreaks into larger stable areas, skewing the CES value upward. In 2018 CES returned to 2.28, consistent with other years that used 30-meter resolution imagery. This suggests the landscape returned to a more balanced state with stable elements, accurately captured at the finer resolution, including windbreaks and vegetated areas contributing to WE mitigation. The sharp contrast in CES for 2012 highlights the importance of spatial resolution in accurately assessing small-scale features like windbreaks that are essential for reducing WE. The higher resolution imagery used in other years provided a more precise measure of landscape stability.

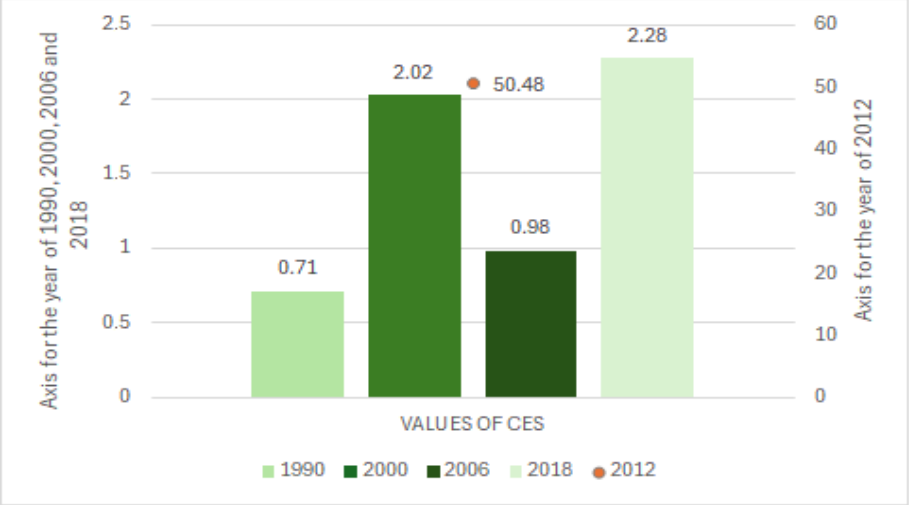



**Figure 4 Values of CES within study period**

## DISCUSSION

In this study, we examined the role of windbreaks and vegetation cover in stabilizing agricultural landscapes and reducing wind-driven soil erosion. Our findings align with [8], who noted that the continuous increase in construction land has led to a decrease in natural vegetation and a rise in landscape fragmentation. Similarly, in our study, urbanization and complex cultivation patterns contributed to landscape instability and decreased ecological resilience. However, the implementation of windbreaks helped mitigate these impacts by providing stable vegetative barriers. While our results emphasize vegetation's role in landscape stability, they also suggest that other factors, such as policy and environmental conditions, may influence ecosystem services, as noted by [9]. The use of LANDSAT imagery in our study also supports [10] assertion that satellite data can effectively monitor long-term changes in forest and land cover. Our analysis demonstrates how LANDSAT's continuous coverage enabled us to track shifts in vegetation density and windbreak presence across nearly three decades, providing valuable insights into temporal changes in the study area. Nevertheless, the limitations of CORINE data for local-scale analysis, as pointed out by [11], are evident in our study. While CORINE was instrumental in providing an overall land cover classification, discrepancies emerged when compared to higher-resolution LANDSAT imagery,

particularly for smaller landscape elements such as windbreaks. Future research should focus on combining higher-resolution RS datasets, like those from drones or newer satellite platforms, to further enhance the precision of landscape stability analysis. This will enable better monitoring of small-scale elements like windbreaks and provide more accurate data for sustainable land management practices.

## CONCLUSION

This study highlights the critical role of windbreaks and vegetation cover in reducing wind-driven soil erosion and enhancing landscape stability in agricultural regions. RS data from 1990 to 2018 revealed notable shifts in land cover and ES, with improvements observed in 2000 and 2018. The CES increased during these years, but a sharp spike in 2012 was likely due to the use of lower-resolution satellite imagery, which overestimated stable landscape features like windbreaks. Overall, increased vegetation cover and windbreaks contributed significantly to stabilizing the landscape. However, the results also demonstrate the importance of using high-resolution imagery for accurate monitoring of small-scale features. Future research should focus on using higher-resolution satellite or drone imagery to refine assessments of landscape stability and evaluate the long-term ecological and economic benefits of windbreaks. These findings support the integration of windbreaks as a valuable soil conservation strategy in agricultural landscapes.

## ACKNOWLEDGEMENTS

This research is the result of the project: VEGA 1/0186/23 Windbreaks in the agricultural landscape - ecological, environmental and economic value of multifunctional structures acting as soil degradation measures.

## REFERENCES

[1] Shao Y., Physics and Modelling of Wind Erosion, Springer Science & Business Media, New York, 2008.

[2] Zhi D., A Review of Wind Erosion Prediction Research. Journal of Desert Research, 1999.

[3] Borrelli P., Robinson D.A., Panagos P., Lugato E., Yang J.E., Alewell C., Wuepper D., Montanarella L., Ballabio C., Land use and climate change impacts on global soil erosion by water (2015-2070), Agriculture, Ecosystems & Environment, Netherlands, vol. 292, pp. 106815, 2020.

[4] Alewell C., Borrelli P., Meusburger K., Panagos P., Using the USLE: Chances, challenges, and limitations of soil erosion modelling, In: Stolte J., Tesfai M., Øygarden L., Kværnø S., Keizer J., Verheijen F., Panagos P., Ballabio C. (Eds.), Soil Erosion in Europe, Netherlands, vol. 26, pp. 137-157, 2015.

[5] Lele N., Joshi P.K., Agarwal S., Fractional Vegetation Cover Analysis for Understanding Vegetation Cover Dynamics in Northeast India, International Journal of Geoinformatics, Thailand, vol. 1, pp. 61-66, 2005.

[6] Zeng X., Dickinson R.E., Walker A., Shaikh M.J., DeFries R.S., Qi J., Derivation and Evaluation of Global 1-km Fractional Vegetation Cover Data for Land Modeling, Journal of Applied Meteorology, United States, vol. 39, pp. 826-839, 2000.

https://doi.org/10.5593/sgem2024v/3.2/s13.31

[7] Zeng X., Rao P., DeFries R.S., Hansen M.C., Interannual Variability and Decadal Trend of Global Fractional Vegetation Cover from 1982 to 2000, Journal of Applied Meteorology, United States, vol. 42, pp. 1525-1530, 2003.

[8] Yang S., Li S., Zhang B., Yu R., Li C., Hu J., Liu S., Cheng E., Lou Z., and Peng D., "Accurate estimation of fractional vegetation cover for winter wheat by integrated unmanned aerial systems and satellite images," Frontiers in Plant Science, vol. 14, p. 1220137, 2023. doi: 10.3389/fpls.2023.1220137.

[9] Li K., Zhang B., "Analysis of the relationship between landscape fragmentation and ecosystem service value in northern Shaanxi, China," Environmental Science and Pollution Research, vol. 30, pp. 94537–94551, 2023. doi: 10.1007/s11356-023-29065-9.

[10] Hussain K., Mehmood K., Anees S. A., Ding Z., Muhammad S., Badshah T., … Khan W. R., "Assessing forest fragmentation due to land use changes from 1992 to 2023: A spatio-temporal analysis using RS data," Heliyon, vol. 10, no. 14, p. e34710, 2024. doi: 10.1016/j.heliyon.2024.e34710.

[11] Falťan V., Petrovič F., Oťaheľ J., Feranec J., Druga M., Hruška M., Nováček J., Solár V., and Mechurová V., "Comparison of CORINE Land Cover Data with National Statistics and the possibility to record this data on a local scale—Case studies from Slovakia," Remote Sensing, vol. 12, no. 15, p. 2484, 2020. doi: 10.3390/rs12152484.

# DIVERSITY OF HYPERICUM L SPECIES IN ADJARA, GEORGIA

**PhD Ress Mariam Romanadze**[1]
**Assoc. Prof. Dr. Inga Diasamidze**[1]
**Dr. Gia Bolkvadze**[2]
**Professor Davit Baratashvili**[1]
**Associate Professor Eteri Jakeli**[1]

[1] Batumi Shota Rustaveli State University, **Georgia**
[2] Phytopathology and Biodiversity Institute, Batumi Shota Rustaveli State University**, Georgia**

## ABSTRACT

Out of the 36 "hot spots" of global biodiversity, Georgia is part of the Caucasus and Iran-Anatolian hot spots. In the Caucasus ecoregion, two refugia have been identified: the Colchic and Hyrcanian. Adjara is part of the Colchis Refugium, it is the richest floristic region in the Caucasus in terms of the number of plant species per unit area. In the flora of Adjara, up to 1837 species of plants are recorded. The genus Hypericum L. stands out for its variety of species, it is represented by 18 species in Georgia, there are 12 species of this genus in Adjara: 1. *H. tetrapterum Fries.,* 2. *H. androsaemum* L., 3. *H. nordmanii* Boiss., 4. *H. bupleuroides* Griseb. 5. *H.caucasicum* (Woronow) Gorschk., 6. *H.grossheimii* Kem.-Nath., 7. *H. linarioides* Bosse., 8. *H.montanum* L., 9. *H. perforatum* L., 10. *H.venustum* Fenzl, 11. *H. xylosteifolium* Spach., 12. *H. mutilum L*. *Hypericum* L. is a well-known medicinal plant. Its species are also popular from an ethnobotanical standpoint, It has been used in folk medicine since ancient times. As a healing agent for open wounds, pain reliever, sedative, etc. One of the most widespread and well-studied species is *Hypericum perforatum*, there are many scientific studies on it, covering both phytochemical composition and biological activity. In the last period, the distribution areas of the species have come under anthropogenic pressure. Habitat degradation threatens species, some of which have narrow local distributions and include: northern Caucasus, Transcaucasia, and Turkey. Our goal was to study the biodiversity of Hypericum species common in Adjara and to evaluate and describe species populations using the releve method, especially species with a narrow local distribution.

**Keywords:** Hypericum, Biodiversity, Adjara flora, Caucasus Ecoregion

## INTRODUCTION

The genus *Hypericum* L (*Hypericaceae*) is distinguished by a great diversity of species. The genus *Hypericum* is distinguished by a great diversity of species. It includes more than 450 species. It is represented by both annual and perennial herbaceous plants, as well as shrubs and trees. This genus is widely distributed worldwide, especially in the temperate zone of the Northern Hemisphere, but can also be found in the high mountainous areas of tropical regions [1]. Turkey is distinguished by the greatest diversity of species, with 82 species, of which 45 are endemic [2]. *Hypericum* species are commonly known by the general name "St. John's wort." This plant is very interesting from an ethnobotanical standpoint, as it has been used as a medicinal plant since ancient times. Even in modern times, Hypericum species are considered medicinal

https://doi.org/10.5593/sgem2024v/3.2/s13.32

plants, among which Hypericum perforatum is the most famous. There are numerous studies on this and other *Hypericum* species regarding their biochemical composition and biological activity. *H. perforatum* is particularly known for naphthodianthrones, such as hypericin, *H. perforatum* is particularly known for naphthodianthrones, such as hyperforin, pseudohypericin, isophypericin, and protohypericin [3]. The species are also rich in other phenolic compounds: qunic acid, chlorogenic acid, Catechin, (epi)catechin, rutin, quercetin, kaemperol, amentoflavone [4].

Georgia is an important part of the Caucasus ecoregion, which is one of the world's 36 biodiversity hotspots [5]. Up to 4,100 vascular plants are described in the flora of Georgia, It is characterized by a high level of endemism. Approximately 21% of Georgia's flora, around 900 species, is endemic. Of these, about 600 species are endemic to the Caucasus, while around 300 species are endemic specifically to Georgia [6]. The floristic region of Adjara belongs to the Eastern Euxine Province of the ancient Mediterranean world's Sub-Mediterranean zone (also known as the Colchic Province). The Eastern Euxine Province encompasses the coastal and mountainous floristic regions of western Georgia. The flora of Adjara is a vital part of the unique Colchic flora, characterized by remarkable diversity [7].

The flora of Georgia is rich in species of the genus *Hypericum* L represented by a total of 18 species: *H. mutilum* L; *H. calycinum*; *H. androseamum* L; *H. xylosteifolium* (spach) N. Robson; *H. numularoides* Trautv.; *H. bupleroides* Griseb.; *H. ptarmicaefolium* Spach; *H. tetrapterum* Fries; *H. nordmannii* Boiss; *H. caucasicum* (Woronow) Gorschkova; *H. perforatum* L; *H. origanifolium* Willd.; *H. hyristum* L.; *H. montanum* L. ; *H. venustum* Fenzl.; *H. linarioides* Boiss.; *H. hyssopifolium* Chaix.; *H. Grosssheimii* Kem.-Nath [8]. Of these, 12 species are found in the floristic region of Adjara [9].

## MATERIALS AND METHODS

Literary sources were reviewed on the diversity, distribution ranges, and morphological-structural composition of Hypericum L. species . Species identification was conducted using plant field guides [9; 10;11; 12; 13; 14].

The description of species habitats was conducted using the *Relevé* method. The term *relevé* (pronounced rel-ə-vā), derived from French, can be translated as "list" or "summary." In this context, a relevé refers to a detailed record of plant species within a defined area, including data on their coverage, as well as information about the substrate and other environmental factors present in the plot. The *relevé* is any kind of plot that includes a catalog of plant species, their coverage or frequency, along with an outline of the vegetation's structure based on height categories and life forms. Habitat is characterized by the biotic and abiotic factors of the environment that directly affect species populations. Abiotic factors include: climate (temperature, humidity), soil type, landscape slope and exposure, and elevation. Biotic factors involve the relationships between living organisms. Plant grouping – phytocenosis – is a complex community of organisms. The anthropogenic impact on plant communities and individual species populations is significant [14].

## RESULTS

Some *Hypericum L.* species are widely distributed throughout the entire Adjara region, while others have a narrow, local distribution. The vertical distribution of species populations above sea level is diverse. By processing literary sources and describing species habitats through relevé, the table presents the distribution areas, life forms, and habitat characteristics of Hypericum L. species found in the Adjara region.

**Table 1**: *Hypericum* L Species in Adjara Region: Distribution, life forms, and Habitats.

| Hypericum species | Distribution area | Life form | Habitat |
|---|---|---|---|
| ***H. mutilum* L.** | Native to: North America<br>Introduced into: Europe: Mediterranean area; Georgia: Adjara | Annual herb | Coastal wetland habitats |
| ***H.androsaemum L.*** | Europe, Turkey, North Iran, Transcaucasia. | subshrub | Shaded, moist forests, From sea level up to 100-1200 meters. |
| ***H. nordmanii Boiss.*** | Transcaucasus<br>Endemic species | subshrub | the upper forest and subalpine zones, on dry slopes, from sea level up to 2000 meters. |
| ***H. bupleuroides Griseb*** | North Caucasus, Transcaucasus, Turkey region. | perennial herb | Shaded forests, from the lower to upper mountain zones in moist areas, at elevations from 200 to 2000 meters above sea leve<br>Endemic and relict species |
| ***H.caucasicum (Woronow) Gorschk*** | North Caucasus, Transcaucasus, Turkey region.<br>Endemic species | perennial herb | Meadows and forest edges in the subalpine and alpine zones, from sea level up to 2000 meters zones, |

https://doi.org/10.5593/sgem2024v/3.2/s13.32

| | | | |
|---|---|---|---|
| ***H.grossheimii Kem.-Nath*** | Transcaucasus.<br><br>Endemic species | shrub | the upper forest and subalpine zones, on dry slopes, from sea level up to 2000 meters |
| ***H. linarioides*** | Balkans, North Caucasus, Transcaucasus, Turkey, Iran | subshrub | Sunny and dry slopes in the alpine and subalpine zones. |
| ***H.montanum*** | Europe, Transcaucasus, Turkey, NW. Africa | perennial herb | Forests, forest edges, shrublands, moist slopes, from the middle forest zone to the subalpine zone. |
| ***H. perforatum L.*** | Native to: Europe, Transcaucasus, Central Asia.<br>Introduced into: North America and South America | perennial herb | Meadows, forests, and shrublands from sea level to the subalpine zone |
| ***H.venustum Fenzl*** | North Caucasus, Transcaucasus, Turkey, Syria | Perennial herb | From the middle mountain zone to the alpine zone, along river and stream banks, in moist areas. |
| ***H. xylosteifolium Spach*** | North Caucasus, Transcaucasus, Turkey.<br>Endemic species | shurb | Forests, forest edges, shrublands, moist slopes, from the middle forest zone to the subalpine zone. |
| ***H. tetrapterum Fries.*** | Europe, Transcaucasus, Turkey, NW. Africa. | Perennial herb | Moist areas up to the middle forest zone, at elevations up to 300 meters above sea level |

In Adjara, certain areas, particularly the coastal zone and roadside locations, experience strong anthropogenic impact. Species that are endemic and have limited, localized distributions are especially vulnerable. Such a species is *H. xylosteifolium*, which is found in the transboundary zone between Georgia and Turkey. It is an endemic species of the Caucasus

ecoregion. The rapid increase in the level of urbanization, followed by construction and infrastructure works, has damaged the natural habitat ranges of *H. xylosteifolium* populations in the Sarpi area (Adjara, The Georgia-Turkey transboundary zone).

## DISCUSSION

The discussion emphasizes the delicate balance between human development and the conservation of biodiversity, particularly for endemic species like *H. xylosteifolium*. Understanding the distribution and habitat requirements of these species is key to implementing effective conservation measures. The anthropogenic impact on these species and their habitats calls for more targeted and sustainable approaches to land management, ensuring that biodiversity is preserved for future generations.

## CONCLUSION

Adjara is an important floristic area in the Caucasus ecoregion. The unique flora here is a shelter of endemic and relict species, which is distinguished by diversity. Out of 12 species of Hypericum L common in Adjara, 4 are endemic to the Caucasus: *H. xylosteifolium* Spach*., H.caucasicum (Woronow)* Gorschk., *H. nordmanii* Boiss*., H.grossheimii* Kem.-Nath. Species with medicinal properties are also represented. The most famous of them are: *H. perforatum L. and H.androsaemum L. H. xylosteifolium* is used as a decorative plant and is cultivated for ornamental purposes. However, the natural habitats of these species are under threat and are experiencing significant anthropogenic pressure. This species is not well-studied in Georgia, especially regarding its biological activity. The findings emphasize the importance of preserving the unique flora of the Adjara region, particularly the endemic species that are highly susceptible to environmental changes. The anthropogenic pressures, such as urbanization and construction, need to be carefully managed to protect these delicate ecosystems. Further research should focus on the long-term monitoring of these populations, habitat restoration efforts, and the impact of human activities on biodiversity. Additionally, more in-depth studies on the ecological requirements of H. xylosteifolium and other endemic species could provide crucial data for effective conservation strategies.

## REFERENCES

[1] Crockett, S.L., Robson, N.K., Taxonomy and chemotaxonomy of the genus Hypericum, Medicinal and Aromatic Plant Science and Biotechnology, 2011.

[2] Davis PH, Mill RR, Tan K Flora of Turkey and the East Aegean Islands, Edinburgh University Press, p. 590, 1988

[3] Barnes J, Anderson L. A, Phillipson J. D. St. John's wort (Hypericum perforatum L.): A review of its chemistry, pharmacology, and clinical properties, *Journal of Pharmacy and Pharmacology*, Volume 53, Issue 5, pp. 583–600, 2001.

[4] Tusevski, O. , Krstikj M., Phenolic Compounds Composition of Hypericum perforatum L. Wild-Growing Plants from the Republic of Macedonia, Agriculturae Conspectus Scientificus, pp 67-74 , 2019.

[5] Williams L. (redactor) Critical ecosystem Partnership fund, Caucausus Biodiversity Hotspot, pp 4-6, 2003.

https://doi.org/10.5593/sgem2024v/3.2/s13.32

[6] Gagnidze R., Biologycal and Landscape Diversity of Georgia, Tbilisi,Gergia, pp: 21-22, 2000.

[7] Gagnidze R., Davitadze M., *"Local Flora"*, (Adjara Floristic Region), Batumi, Georgia, pp. 80-90, 2000.

[8] Ketzchoveli N. (redactor), Flora Georgia, VIII, Tbilisi, Georgia, pp 312 -335, 1983.

[9] Dimitrieva A.A. , Adjara Plant Survey, II, Tbilisi, Georgia, pp 75-79, 1990.

[10] Fisher E., Groger A. , Illustrated Field Guide to the Flora of Georgia, Koblenz, Germany, pp 566-570, 2018.

[11] Sukhitashvili K., Field survey of flowering plants of Georgia, Tbilisi, Georgia, pp 364-368, 2018.

[12] Eminağaoğlu Ö., the natural plants of Artvin, Turkey, Instanbul, Turkey, pp 283-285, 2015.

[13] Eminağaoğlu Ö., Aromatic and medicinal plant of Artvin, Turkey, pp 206-214, 2023.

[14] Minnesota Department of Natural Resources, *Releve* Method, State of Minnesota, USA, pp 1-2, pp 5-8, 2013.

# DYNAMICS ASSESSMENT OF CHANGES IN FOREST COVER AREA ON THE UKRAINE TERRITORY IN THE 21TH CENTURY BASED ON SATELLITE DATA

**PhD. Alexander Apostolov**[1,2]
**PhD. Lesya Yelistratova**[1,2]
**Dmytro Todchuk**[3]
**Igor Onopchuk**[3]
[1] State Institution "Scientific Centre for Aerospace Research of the Earth of the Institute of Geological Sciences of the National Academy of Sciences of Ukraine", **Ukraine**
[2] State Institution "Center for evaluation of activity of research institutions and scientific support of regional development of Ukraine NAS of Ukraine", **Ukraine**
[3] Budget Institution "National Center for GHG Emission Inventory", **Ukraine**

## ABSTRACT

In Ukraine, as well as all regions of the world, deforestation processes are taking place. Monitoring forests in real-time is one of the key ways to solve the problem of deforestation. Satellite technologies make it possible to do this promptly and in time and space.

In this research, the online platform Google Earth Engine was used, which provides access to remote sensing data and geospatial data sets with analysis capabilities. The research was conducted for the period 2001-2023 at the regional level and each administrative oblast. Noting that the war started on the territory of Ukraine in 2022, the research was also conducted separately for the years 2022-2023. Comparison of the obtained data with the pre-war period made it possible to assess the impact of hostilities on the forest cover within each administrative oblast, and they were ranked by the total area of forest cover loss.

The analysis of the obtained data shows that a significant increase in deforestation, compared to 2001-2021, occurs in those areas where hostilities are taking place: Luhansk, Kharkiv, Kherson, Donetsk oblasts, or occurred in 2022 and where the strengthening of the northern border is currently taking place, by creating defensive structures in forest areas (Kyiv and Zhytomyr oblasts).

**Keywords:** Deforestation, remote sensing data, Ukraine

## INTRODUCTION

Deforestation is the process of turning forested land into treeless land. Deforestation is one of the most urgent problems today. Forests occupy almost a third of the entire land surface of our planet, but at the current rate of deforestation, humanity may lose most of its forest cover in the near future.

Deforestation processes disrupt natural ecosystems, change the habitats of living organisms, as well as the extinction of various species of animals, plants, microorganisms, fungi, etc. These processes change landscapes, turning them into territories unsuitable for life for those species of biodiversity whose habitat was located in this territory [1].

https://doi.org/10.5593/sgem2024v/3.2/s13.33

The species richness of forests made the ecosystem sustainable by providing ecosystem services. In many countries, deforestation and forest degradation have led to a decrease in the level of forest cover in their territories. These processes had a negative effect on the ecosystem as a whole, as an example of the disappearance of endemic biodiversity. Forests are one of the main natural factors that determine and regulate the climate. A significant increase in deforestation is observed as a result of a rapid increase in the level of urbanization, industrialization, and military conflicts [2-3]. As a result, there is an increase in the global average temperature of the earth's surface, which directly or indirectly affects climate change. Deforestation is a consequence of human activity that partially removes carbon reserves in forests. This process is done without recovery for a reasonable time period. The rate of biomass carbon removal is faster than the duration of the recovery process. This process leads to a gradual decrease in carbon stocks in biomass. The result of the deforestation process is the release of carbon dioxide oxidation occurs during the removal of forests. Scientists estimate that 25 percent of the world's greenhouse gas production comes from deforestation [4]. The consequences of deforestation vary from local, regional, national, and transboundary areas of landscapes. Deforestation can also occur naturally as a result of forest fires and various cataclysms, which cause climate change on our planet [5].

One of the methods of measuring the level of deforestation is the use of remote sensing methods [6]. Wang et al. conducted a study of long-term forest dynamics in protected areas of northeastern China based on Landsat data [7]. Braun, based on Landsat satellite data, conducted a study related to land use change in the coastal part of Chile with the main topic of forest destruction through deforestation [8]. Matosak et al., using a time series of Sentinel and Landsat images based on medium spatial resolution time series and hybrid deep learning architecture, mapped deforestation in the Cerrado [9]. Torres et al., using Landsat-8 and Sentinel-2 images in the Amazon forest using convolutional networks, detected deforestation [10]. Naing Tun et al., using the program for deciphering space images ArcGIS, developed models, provided certain recommendations, and characterized the factors of deforestation and forest degradation in Myanmar [11]. Mitchell et al. characterized modern remote sensing approaches to forest degradation monitoring in support of country reporting, measurement, and verification (MRV) systems for REDD+ [12]. Lee et al., using the SegNet and U-Net algorithms for remote sensing data, conducted landscape classification. The authors noted that they suffered from deforestation. Deep learning methods and high-resolution remote sensing data were used in the paper [13]. González-González et al. characterized the spatio-temporal dynamics of deforestation and its driving forces. These forces point to the need for ecological management adapted to local conditions in Colombia [14].

The problem of deforestation has been relevant for the territory of Ukraine for many years. Ukraine began to lose its forests in the 1830s. During the 19th and 20th centuries, the area of forests decreased by 30.5%. The Russian-Ukrainian war caused and continues to cause great damage to forest plantations. Therefore, the problem of forest loss in the territory of our country is urgent.

Monitoring forests in real-time is one of the key ways to solve the problem of deforestation. Taking into account the significant size of the territory and the need to quickly solve the task remote sensing data was used for the research. These are the only data that allow solving this task most economically and efficiently.

*The purpose of the research* is to assess the dynamics of changes in the area of forest cover on the territory of Ukraine in the 21st century using remote sensing data and to determine its impact under conditions of climate change.

## MATERIALS AND METHODS

The research was carried out in general on the territory of Ukraine and all administrative oblasts. To obtain the result, we used in the research the online platform Google Earth Engine, which provides access to remote sensing data and sets of geospatial data with analysis capabilities. The results of work on the Google Earth Engine platform can be presented in raster form with a coordinate system (*tif* format) in tabular form (*CSV* format), and it is also possible to visualize the received data in graphic form.

To study the deforestation issue, we use the results of the time-series analysis of Landsat images to characterize the global area and change of forests - the Hansen Global Forest Change v1.11 product [15]. This product was developed by scientists of the University of Maryland Department of Geographical Sciences and allows us to determine for each year the gross loss of forest cover for the period from 2001 to 2023.

The research methodology consisted of the following stages: 1) in the online environment of Google Earth Engine (https://earthengine.google.com/) shapefiles with geometry were selected; 2) the collection "HansenGlobalForestChange v1.11 (2000-2023)" was opened in the form var gfc2023 = ee.Image ("UMD/hansen/global_forest_change_2023_v1_11"); 3) Javascript was typed to obtain an image of forest loss with bandloss, which shows forest loss during the studied period, which was defined as a disturbance of the tree stand (transition from a forest state to a treeless one); 4) the function ee.Image.pixelArea was applied to BandLoss, which generates an image in which the value of each pixel is the area of that pixel in square meters. This image is rotated and has one band called "area". (https://developers.google.com/earth-engine/apidocs/ee-image-pixelarea); 5) the next stage was the selection of Bandlossyear, which shows the year of the gross loss of forest cover. Forest loss during the studied period is defined as a disturbance of plantation or change of forest to a non-forest state. Coded as 0 (no losses) or as a value in the range 1-23, representing losses detected in 2001-2023, respectively; 6) the next stage is the summation of the area of forest cover loss; 7) the next stage is to write a dictionary for generating data in a graphic format; 8) the generated graph was downloaded as CSV format data; 9) editing the file, converting it to Excel format, building tables and graphs of research results; 10) GIS programs: ArcGIS and MapInfo Professional were used to visualize the received information by constructing maps of the distribution of deforestation values both throughout the territory of Ukraine and for ranking the administrative regions of Ukraine.

## RESULTS

The results of the analysis of a time series of Landsat images for the characterization of the global area and forest change (deforestation) of the Hansen Global Forest Change v1.11 product for the period from 2001 to 2023 for the territory of Ukraine are presented in Fig. 1.

https://doi.org/10.5593/sgem2024v/3.2/s13.33

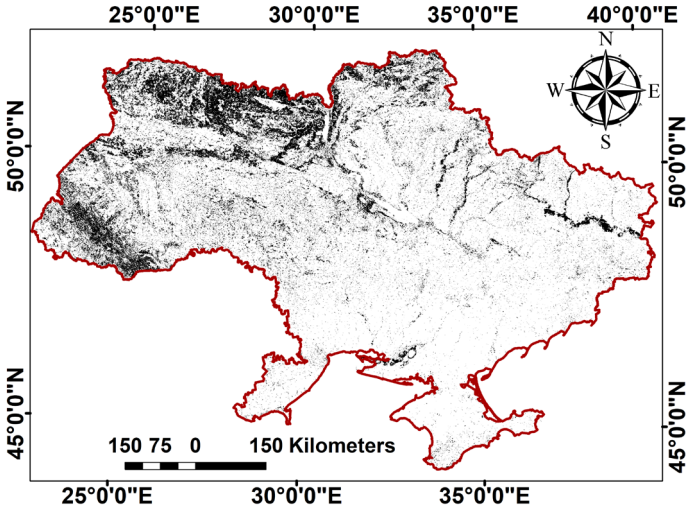



Figure 1 – Distribution of the gross loss of forest cover (deforestation) for the period from 2001 to 2023 for the territory of Ukraine according to data [15] (shown in *black*). The borders of Ukraine are shown in *red*.

The processing of the Hansen Global Forest Change v1.11 product made it possible to obtain data on deforestation for the entire territory of Ukraine, to present them in the form of a graph, and to establish the trend of changes in the loss of forest cover (Fig. 2).

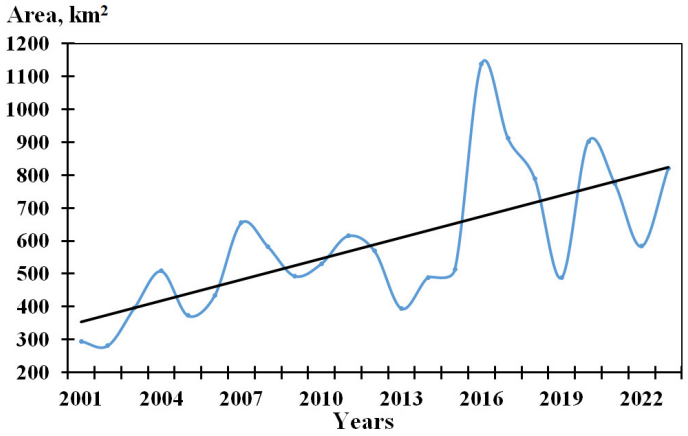



Figure 2 – Graph of forest cover loss (deforestation) in Ukraine by year for 23 years based on the processing of the Hansen Global Forest Change product

For each administrative oblast of Ukraine, a ranking of administrative oblasts was carried out in relation to the total area of forest cover losses (deforestation) for the entire observation period of 2001-2023 (Fig. 3).

To determine the impact of military operations on forest plantations, a comparison of the average data of deforestation areas for two periods, 2001-2021 and 2022-2023, was carried out, and the administrative oblasts of Ukraine were ranked according to the area of changes (Fig. 4) and the value of the ratio (Fig. 5) between 2022-2023 and 2001-2021.




Figure 3 –Ranking of administrative regions of Ukraine by the total area of forest cover loss (deforestation) for the entire study period 2001 – 2023 years.

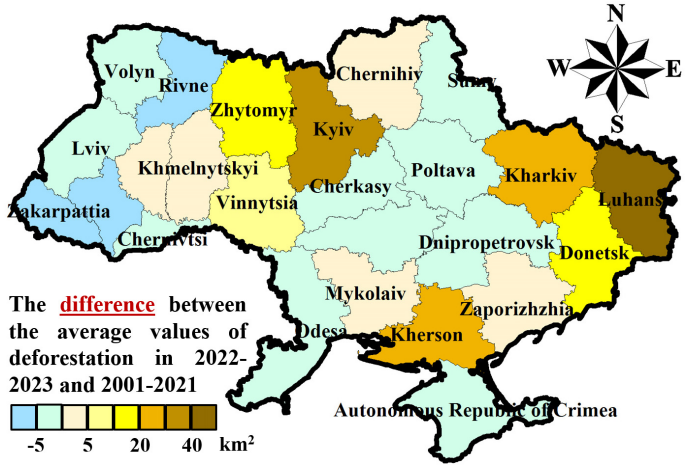



Figure 4 – Determination of the impact of military operations in 2022-2023 on deforestation in the administrative oblasts of Ukraine with the comparison period 2001-2021 by ***area***.

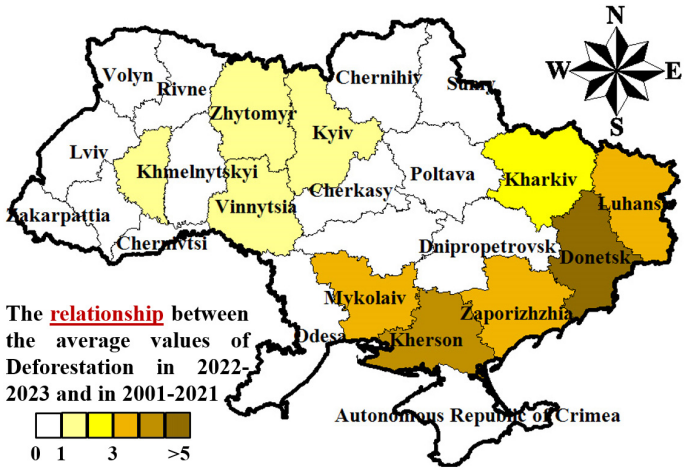



Figure 5 – Determination of the impact of military operations in 2022-2023 on deforestation in the administrative oblasts of Ukraine with the comparison period 2001-2021 by ***ratio***.

https://doi.org/10.5593/sgem2024v/3.2/s13.33

## DISCUSSION

During the entire observation period, the process of increasing forest cover loss (deforestation) is observed for the territory of Ukraine, which is convincingly indicated by the trend line (Fig. 2). The average value of deforestation for the period 2001-2023 is 588 $km^2$ per year. On the graph of forest cover loss (Fig. 2), it is possible to establish two periods: 2001-2014 and 2015-2023. For the first period, the average value of Deforestation is 472.6 km2 per year, for the second - 768.8 $km^2$ per year that is, for the period from 2015 to 2023, the area of deforestation increased by 1.6267 times or by 62.67%.

Analysis of the map of the distribution of forest losses throughout Ukraine (Fig. 3) showed that the highest losses were found in the west (within the Zakarpattia and Lviv oblasts) and the north (within the Volyn, Rivne, Zhytomyr, and Kyiv oblasts) of Ukraine. This territory belongs to the zone of mixed forests, broad-leaved, and Ukrainian Carpathians, where the highest areas of forests in Ukraine are concentrated, and their loss is proportional to the spread of forests in this territory. In addition, the forests in this area are also being lost due to human activity, namely the barbaric destruction of forests during amber hunting. Further, south approximately 48°30'N, areas with significantly less forest loss are located, and the forest cover is much less developed in this area. To the south, there are territories with insignificant areas occupied by forests, where the area of deforestation is also proportional to the area of forests.

An attempt was made to identify areas where, during the war, the amount of deforestation increased significantly compared to the pre-war years (Fig. 4-5). During the war, the loss of forest cover occurs in those oblasts where hostilities are taking place: Luhansk, Kharkiv, Kherson, and Donetsk oblasts. And also in the oblasts (Kyiv and Zhytomyr), where the strengthening of the northern border is taking place through the formation of defensive structures (Fig. 4). If we look at the changes between the two periods not in absolute terms, as shown in Fig. 4, and in times (Fig. 5), then the oblast with the largest increase in deforestation in 2022-23 compared to 2001-2021 is the Donetsk oblast (by 6.28 times), the second Kherson oblast by 4.68 times, then Mykolaiv oblast (by 3 .87 times), Luhansk oblast (3.76 times), Zaporizhia oblast (3.42 times) and Kharkiv oblast (2.8 times). That is, the increase in deforestation is caused by the brutal hostilities that have taken place and are taking place now, and all this can be recorded with the help of satellite surveying. Destruction of forests in war zones occurs both due to direct war and during their use for defense structures.

## CONCLUSION

The use of the online platform Google Earth Engine for the initial processing of remote sensing data, namely the Hansen Global Forest Change product, which was created by processing data from Landsat satellites, made it possible to determine that the dynamics of deforestation in Ukraine is increasing over the period 2001-2023.

Also, the use of remote sensing data made it possible to establish the areas where deforestation occurs the most. These are areas located in the zone of mixed forests, the zone of broad-leaved forests, and the Ukrainian Carpathians, that is, in the areas covered with coniferous trees, which are the main object of deforestation.

The impact of military actions on deforestation has been established, so in the administrative oblasts of the east and south of Ukraine, where hostilities are directly taking place, the value of Deforestation increased on average from 2.8 to 6.3 times compared to the peaceful period of 2001-2021.

In this way, using objective remote sensing data makes it possible to quickly identify places of change in the state of forest cover (deforestation). The received information on Deforestation can significantly help planning, executive, control, and other state structures in the measures taken to maintain and restore forest ecosystems.

## ACKNOWLEDGEMENTS

The paper was carried out within the scope of the scientific project RC№ 0122U000552, "Comprehensive analysis of robust preventive and adaptive measures of management of food, energy, water, and the social sphere in conditions of systemic risks and consequences of COVID-19".

## REFERENCES

[1] Bodo, T., Gimah, B.G., & Seomoni, K.J. (2021). Deforestation and Habitat Loss: Human Causes, Consequences and Possible Solutions. Journal of Geographical Research. 4(2), 22–30. DOI: https://doi.org/10.30564/jgr.v4i2.3059

[2] Ievsiukov T. O., Martyn A., Elistratova L., Apostolov A., Kostyuchenko Yu. V. and Yuschenko M. (2018) An Investigation of the Impact of the Military Crisis in Ukraine on Agricultural Production and Land Resources in Crisis Territories: Approaches, Algorithms, and Methods. in: Agricultural Production: Management, Opportunities and Challenges, ed. by Sarah Waechter, Nova Science Publishers, USA, pp. 21-86, ISBN: 978-1-53613-719-4

[3] Lesia Yelistratova, Alexander Apostolov, Vadim Lyalko, Olha Tomchenko, Anna Khyzhniak, Artur Hodorovsky (2022). The results of socio-ecological monitoring during military operations in Ukraine using satellite information. Rev. Roum. Géogr./Rom. Journ. Geogr., 66, (2), p. 117–1361

[4] Oral, H.V. (2020). Deforestation. In: Romaniuk, S., Thapa, M., Marton, P. (eds) The Palgrave Encyclopedia of Global Security Studies. Palgrave Macmillan, Cham. DOI: https://doi.org/10.1007/978-3-319-74336-3_390-1

[5] Berenguer, Erika., Armenteras, Dolors., Lees, Alexander., Smith, Charlotte., Fearnside, Philip., Nascimento, Nathália., G, Ane., Almeida, Cláudio., Aragão, Luiz., Barlow, Jos., Bilbao, Bibiana., Brando, Paulo., Bynoe, Paulette., Finer, Matt., Flo-Res, Bernardo., Jenkins, Clinton., Silva-Junior, Celso., Souza Jr, Carlos., Garcia-Villacorta, Roosevelt. (2021). Chapter 19: Drivers and ecological impacts of deforestation and forest degradation. Amazon Assessment Report 2021. DOI: http://dx.doi.org/10.55161/AIZJ1133

[6] Blanc, Lilian, Gond, Valery, Ho Tong Minh, Dinh. (2016). Remote Sensing and Measuring Deforestation. Land Surface Remote Sensing. Environment and Risks. 27-53. DOI: https://doi.org/10.1016/B978-1-78548-105-5.50002-5

[7] Wang, J.; He, Z.; Wang, C.; Feng, M.; Pang, Y.; Yu, T.; Li, X. Investigation of Long-Term Forest Dynamics in Protected Areas of Northeast China Using Landsat

Data. Remote Sens. 2022. V. 14. 2988. [Electronic resource]. - Mode access: https://doi.org/10.3390/rs14132988

[8] Braun, A.C. (2022). Deforestation by Afforestation: Land Use Change in the Coastal Range of Chile. Remote Sens. 14, 1686. DOI: https://doi.org/10.3390/rs14071686

[9] Matosak, B.M.; Fonseca, L.M.G.; Taquary, E.C.; Maretto, R.V.; Bendini, H.d.N.; Adami, M. (2022). Mapping Deforestation in Cerrado Based on Hybrid Deep Learning Architecture and Medium Spatial Resolution Satellite Time Series. Remote Sens. 14, 209. DOI: https://doi.org/10.3390/rs14010209

[10] Torres, D.L.; Turnes, J.N.; Soto Vega, P.J.; Feitosa, R.Q.; Silva, D.E.; Marcato Junior, J.; Almeida, C. (2021). Deforestation Detection with Fully Convolutional Networks in the Amazon Forest from Landsat-8 and Sentinel-2 Images. Remote Sens. 13(24), 5084. DOI: https://doi.org/10.3390/rs13245084

[11] Naing Tun, Z., Dargusch, P., McMoran, D., McAlpine, C., Hill, G. (2021). Patterns and Drivers of Deforestation and Forest Degradation in Myanmar. Sustainability. 13(14), 7539. DOI: https://doi.org/10.3390/su13147539

[12] Mitchell, A.L., Rosenqvist, A. & Mora, B. (2017). Current remote sensing approaches to monitoring forest degradation in support of countries measurement, reporting and verification (MRV) systems for REDD+. Carbon Balance Manage 12, 9. DOI: https://doi.org/10.1186/s13021-017-0078-9

[13] Lee, S.-H.; Han, K.-J.; Lee, K.; Lee, K.-J.; Oh, K.-Y.; Lee, M.-J. (2020). Classification of Landscape Affected by Deforestation Using High-Resolution Remote Sensing Data and Deep-Learning Techniques. Remote Sens. 12(20), 3372. DOI: https://doi.org/10.3390/rs12203372

[14] González-González, A., Villegas, J. C., Clerici, N., & Salazar, J. F. (2021). Spatial-temporal dynamics of deforestation and its drivers indicate need for locally-adapted environmental governance in Colombia. Ecological Indicators, 126, 107695. DOI: https://doi.org/10.1016/j.ecolind.2021.107695

[15] Hansen, M. C., P. V. Potapov, R. Moore, M. Hancher, S. A. Turubanova, A. Tyukavina, D. Thau, S. V. Stehman, S. J. Goetz, T. R. Loveland, A. Kommareddy, A. Egorov, L. Chini, C. O. Justice, and J. R. G. Townshend (2013). High-ResolutionGlobalMapsof 21st-Century ForestCoverChange. Science 342 (15 November), 850-853. DOI: https://doi.org/10.1126/science.1244693

# EFFECTIVE PROTECTION AGAINST PINE WEEVIL (*HYLOBIUS ABIETIS*) DAMAGES IN CONIFEROUS PLANTATIONS

**Uldis Grīnfelds**[1]
**Liene Zēberga**[1]
**Kristaps Ozoliņš**[1]
**Raitis Rieksts – Riekstiņš**[2]
**Linda Robalte**[1]
[1]Latvian State Forest Research Institute Silava, Rigas street 111, Salaspils, **Latvia**
[2]Lithuanian Research Centre for Agriculture and Forestry, Instituto al. 1, Akademija, **Lithuania**

## ABSTRACT

Climate change manifest itself as increased natural disturbances. These effects can be reduced by planting adapted forest reproductive material. Such plantation ensure the source of raw material for bioeconomy, but are affected by dendrophagous insects, including pine weevil (*Hylobius abietis*). This species is estimated to cause 120 million EUR financial losses annually. Untreated coniferous seedlings have very high mortality, therefore pesticides are applied in nurseries, before delivering the plants to forest. Use of pesticides is have a negative impact on the environment. Therefore several European countries are working on the development of protective agents based on biological components. The purpose of this study is to assess the performance of a new plant oil-based protective agent, developed in Latvia.

Study is based on six experimental sites – fresh clearcuts, where soil was prepared in furrows and coniferous seedling planted at spring. One of the sites was regenerated by pine and five by spruce. Three types of treatments were ensured: by protection agent (woodcoat), repellent, produced in Latvia – Jifte (weak concentration, standard concentration and strong concentration) and control (untreated trees). Inventory was performed by visually assessing the trunk of young trees after the vegetation period and reporting the level of damages.

The repellent Jifte ensured satisfactory level of protection – in all of the assessed sites the proportion of damaged seedling was below 20%: it ranged from 5% to 11%. The developed new repellent in low and standard concentrations endured the level of protection comparable to that of the established (commercially available) alternative, in high concentration – even better protection. Thus, further analysis and development work should focus on economic feasibility of the new solution, to ensure, that it can be taken up and used at a large scale in potential areas of need – northern Europe and northern America.

**Keywords:** coniferous seedlings, biotic risks, damages, forest regeneration

## INTRODUCTION

In recent years, forest ecosystems are being affected on a global scale, driven by rapid climate change. Trees are being subjected to physiological disturbances, making them more susceptible to various diseases and insect pests (Dvořáková et al., 2024; Heber et al., 2024). Europe has seen widespread outbreaks of bark beetles, which have led to accelerated deforestation, as the most effective way to combat bark beetles is to cut

https://doi.org/10.5593/sgem2024v/3.2/s13.34

down and remove infested trees from the forest (Dvořáková et al., 2024 ). The large amount of clearing provides favourable conditions for the spread and reproduction of the most dangerous conifer pest, the pine weevil *(Hylobius abietis)* (Dvořáková et al., 2024; Heber et al., 2024; Willoughby et al., 2021). The pine weevil is considered a major pest of young stands throughout Europe (Doležal et al., 2021), damaging around 3.4 million hectares of forest stands each year (Tudoran et al., 2019). It causes significant damage to pine, spruce and other conifer species (Skrzecz et al., 2021). Adults feed on planted conifer seedlings, which in most cases contributes to tree mortality (Björklund et al., 2003) and may require replanting or replanting of regenerating areas, resulting in large economic losses (Galko et al., 2022). The pine weevil causes financial losses of €120 million per year in Europe (Dvořáková et al., 2024; Galko et al., 2022). If untreated seedlings are planted against this pest or other preventive measures are not taken, the amount of dead trees in a stand can be as high as 60-80% (Doležal et al., 2021; Lalík et al., 2021; Luoranen & Viiri, 2012; Örlander & Nordlander, 2003).

Lalík et al., 2021 in their study, point out that the intensity of weevil damage is influenced by various factors: the year of planting after harvesting, the planting period, the vegetation, the type of soil preparation, the presence of older stands, the type and size of seedlings and their condition. In order to protect young stands from this pest, it is necessary to carry out control measures in areas where forests have been felled and subsequently regenerated, as large numbers of beetles are attracted to freshly felled areas each year (Björklund et al., 2003; Tudoran et al., 2019). The beetle can be reduced by leaving areas untreated for at least three years (Domevscik et al., 2024), but this practice imposes significant additional costs in terms of vegetation removal (Heber et al., 2024) and maintenance, as well as hindering reforestation and undermining the positive impact of forestry on climate change mitigation. Soil tillage can also significantly reduce the spread of weevils and the risk of damage, compared to planting in untreated soil (Örlander & Nordlander, 2003). The removal of logging residues, stumps (Rahman et al., 2018), from the stand, which is one of the main sources of attraction and feeding of weevils, can also be used to reduce damage, but such activities are in most cases not cost-effective as they generate additional costs for the logging company, thus increasing the cost price of the tree assortment to be harvested.

Dendrophagous insect control - a long-standing issue in northern Europe (Doležal et al., 2021). So far it has been solved by the use of pesticides in nurseries and forests, formulated from oil-based products, which have a negative impact on the environment (Galko et al., 2022; Moore et al., 2021) by affecting aquatic organisms and can have long-term negative effects on the aquatic environment (Lalík et al., 2021). Several European countries are working on alternative solutions (Barta et al., 2019), but the results so far do not show an equivalent level of protection. However, the development of such protective measures is of great relevance at a time when society is moving towards environmentally friendly solutions. For example, Norsk Wax has developed a wax as a protection against the pine weevil, where a thin layer of wax applied to trees lasts for at least two growing seasons. A white pigment is added to the wax during development to act as a weevil repellent and protect the trees from sunlight. At the beginning of the study, the wax was found to have various imperfections, such as cracking, but further research added environmentally friendly additives to make it more flexible and at the same time more durable (Lalík et al., 2021). Conniflex - an

environmentally friendly protection method developed in Sweden and in practice since 2003. This protection product is described as a sand barrier on tree seedlings (framework plants), a protection method recognised as effective because it provides protection for at least two years and is adaptable to the growing tree (Lalík et al., 2021). However, the alternative means of protection developed so far are relatively more expensive and not always effective, so it is important to continue research in this area. The aim of this study is to test the performance of a new plant oil-based product developed in Latvia.

## MATERIALS AND METHODS

The experimental plantations will be established in spring 2024. A pine protection experiment was set up in one stand and spruce trials in five stands. The spruce stands have an average tree length of 43 cm and a diameter of 0.8 cm, the pine stands 35 cm and 0.5 cm. The stands are located in central and northern Latvia, one in the Zemgale planning region in Ozolnieki and five in the Ainaži district of the western Vidzeme region (Fig. 1).

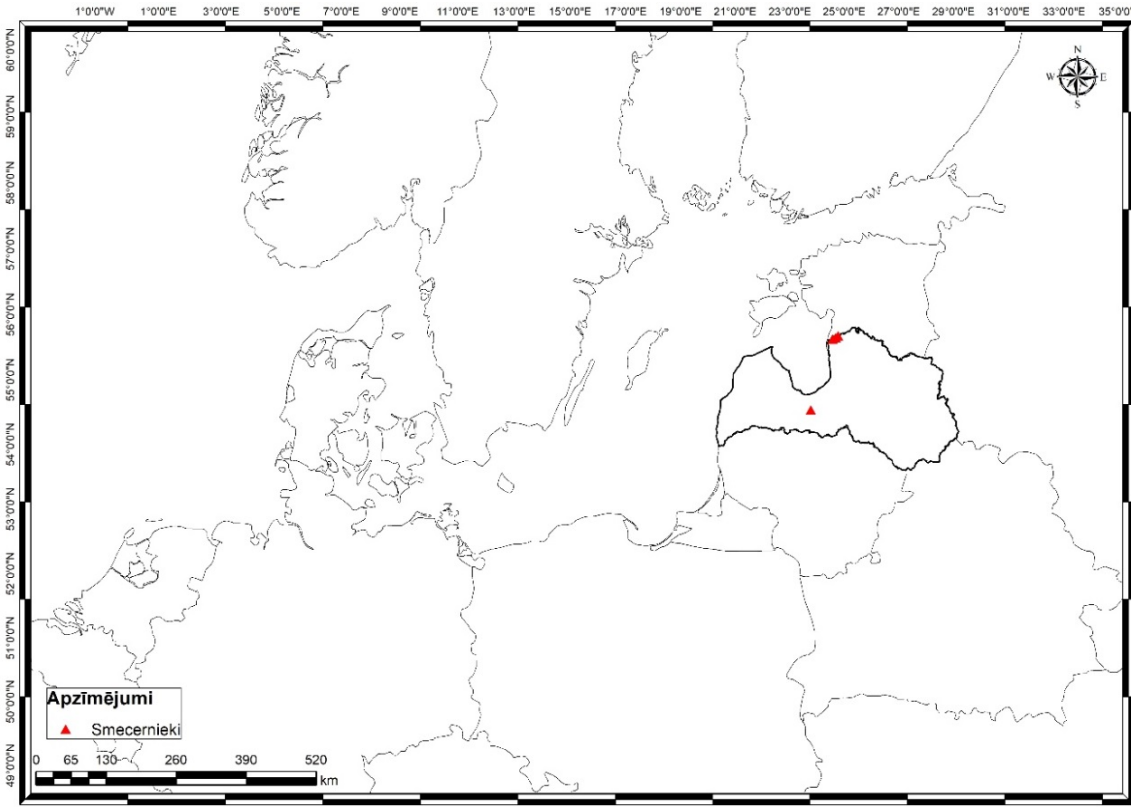



**Figure 1. Location of experimental plantations**

The study compares three options for seedling treatment:

1. untreated seedlings - control;
2. a treatment (control) widely used in practice - woodcoat;
3. a repellent produced in Latvia - Jifte (weak concentration, standard concentration and strong concentration).

https://doi.org/10.5593/sgem2024v/3.2/s13.34

One spruce stand was treated with a strong concentration of Jifte, four with a weak concentration and all stands were treated with woodcoat (control). In the pine stand, trees were treated with the weakest concentration of Jifte and a control with untreated trees was installed.
In summer 2024, all stands were monitored for pine weevil (*Hylobius abietis)* from 28 August to 2 September. In each stand 200 trees treated with Jifte and 200 control trees were surveyed, for a total of 400 trees assessed in each stand. Damage inventories were carried out by visual assessment of the tree trunks along their entire length, paying particular attention to the neck of the roots. A six-grade system was used to assess damage: undamaged trees - 0, slightly damaged (no significant damage to the viability of the seedling) - 1, slightly damaged (damage does not affect the survival of the seedling) - 2, severely damaged (damage affects the survival of the seedling) - 3, killed by damage - 4, killed by other causes (moisture, drought, etc.) - 5.

## RESULTS

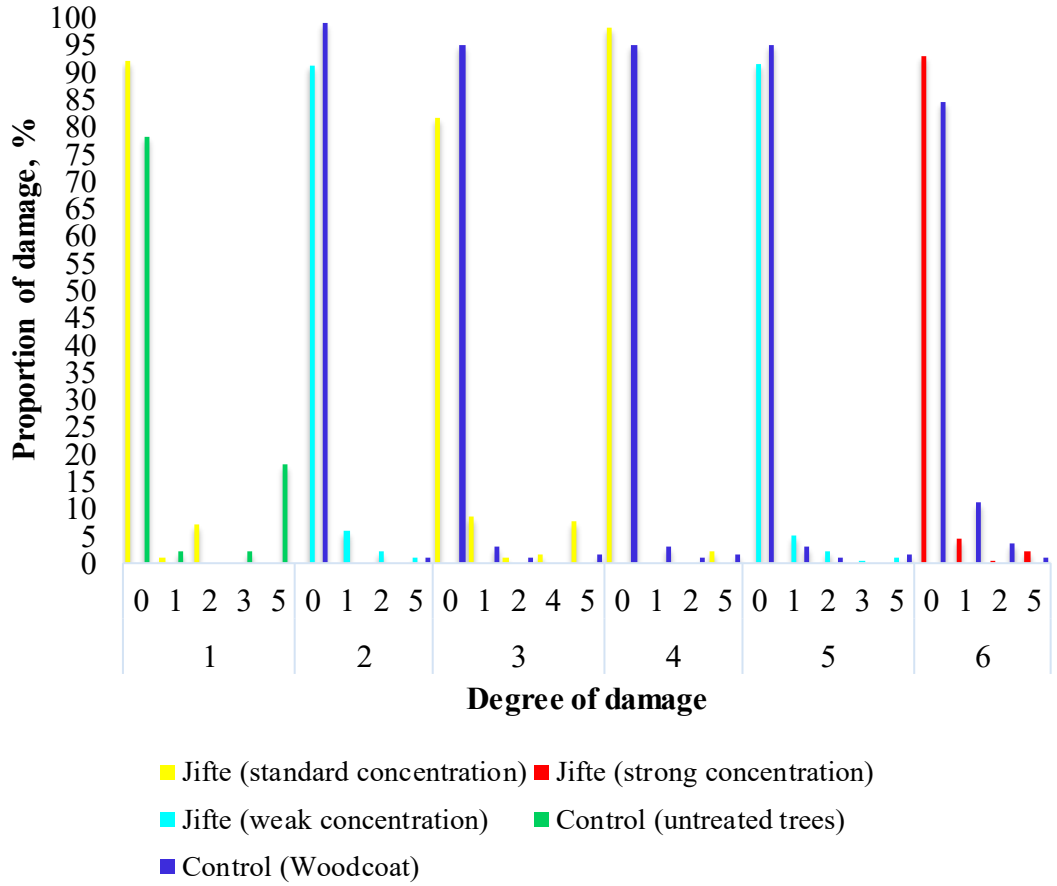



**Figure 2. Proportion of trees damaged by weevils (%) by forest plot**

In all forest plots, Jifte showed a good level of protection, with less than 20% of trees damaged by weevils, ranging from 1 to 11% in all stands. The proportion of damaged trees treated with Jifte ranged from 1 to 9 % in the first damage class, from 1 to 7 % in the second, 1 % in the third and 2 % in the fourth. For the control trees in the first damage class, the proportion of damaged trees ranged from 2 to 11 %. In the second

class, between 1 and 2 %, in the third between 1 and 3 %, and in the fourth class no damage was observed in any stand. The extent of damage observed is moderate compared with other studies, since, for example (Galko et al., 2022), in the present study the proportion of damaged trees ranged from 17 to 31 %.

Comparing the Jifti-treated trees with the control trees, it can be observed that in the first stand, on average, 4% of the Jifti-treated trees are damaged, compared with 2% of the control trees (untreated). In the second stand, the Jifti-treated trees were damaged on average 4 %, while no weevil damage was observed in the control trees. In the third stand, 4% (Jifte) and 2% control trees, in the fourth stand no weevil damage was found in Jifte-treated trees, but it caused an average of 2% damage in control trees, in the fifth stand 4% Jifte-treated but 2% control trees and in the fifth stand 3% (Jifte) but 7.5% control trees.

In the first stand (pine), 18 % of the control trees showed grade 5 damage, which the author concluded could be due to lack of moisture. The results obtained on tree mortality due to drought are in line Domevscik et al., 2024 with the results obtained in the study, which indicated that drought has a significant impact on seedling survival, where additional stress on the trees may create conditions conducive to tree mortality caused by other damage factors. This is an important aspect to take into account as more frequent droughts are predicted in the future, which may have a significant impact on the viability of young trees (Domevscik et al., 2024). Interestingly, the highest proportion of second-degree weevil damage, 7 %, was caused to trees treated with Jifti. Comparing the other stands (spruce), it can be seen that the second and fifth forest plots have the highest incidence of first-degree weevil damage, which may be an indication that the protection agent has contributed to preventing more extensive damage. The third, fourth and fifth stands were adjacent, all had high levels of leaf litter in mid-summer and were surrounded by deciduous forest plots, which may have contributed to the low incidence of weevil populations. Doležal et al., 2021 the study suggests that creating mixed broadleaf and conifer forests could reduce weevil damage.

Comparing the Jiftes concentrations, there are small differences in the results. The strongest concentration showed the best results, with a total damage of 7%. The weakest concentration treated both the second and the fifth stand, where the damaged trees reached 9 % and 8,5 %. In the first and third stands treated with the standard concentration, 8 % of the first stand and 11 % of the third stand were damaged.

## CONCLUSION

The new preperate developed provides protection as good as that currently available commercially, with even better protection at higher concentrations. It is useful to assess the economics of its production. It would also be worthwhile to continue the ongoing study covering the whole country to see whether the changing conditions in each location affect the effectiveness and persistence of the repellent.

## ACKNOWLEDGEMENTS

The material has been prepared in the European Fund for Agriculture and Rural Development project "Protection of conifer seedlings against damage caused by dendrophagous insects in a way that is safe for nature and humans" (No. 22-00-A01612-000019)

https://doi.org/10.5593/sgem2024v/3.2/s13.34

## REFERENCES

[1] Barta, M., Lalík, M., Rell, S., Kunca, A., Horáková, M. K., Mudrončeková, S., & Galko, J. (2019). Hypocrealean fungi associated with Hylobius abietis in Slovakia, Their virulence against weevil adults and effect on feeding damage in laboratory. *Forests*, *10*(8). https://doi.org/10.3390/f10080634

[2] Björklund, N., Nordlander, G., & Bylund, H. (2003). Host-plant acceptance on mineral soil and humus by the pine weevil Hylobius abietis (L.). *Agricultural and Forest Entomology*, *5*(1), 61–66. https://doi.org/10.1046/j.1461-9563.2003.00163.x

[3] Doležal, P., Kleinová, L., & Davídková, M. (2021). Adult feeding preference and fecundity in the large pine weevil, hylobius abietis (Coleoptera: Curculionidae). *Insects*, *12*(5). https://doi.org/10.3390/insects12050473

[4] Domevscik, M., Wallertz, K., & Hjelm, K. (2024). Effect of drought and pine weevil damage on mechanically protected Norway spruce seedlings. *Forest Ecology and Management*, *566*. https://doi.org/10.1016/j.foreco.2024.122053

[5] Dvořáková, B., Holuša, J., Horák, J., Hradecký, J., Bledý, M., & Zelenka, M. (2024). Pine weevil (Hylobius abietis) preferences among species of conifer seedlings planted on clear-cuts in central Europe. *Frontiers in Forests and Global Change*, *7*. https://doi.org/10.3389/ffgc.2024.1399405

[6] Galko, J., Lalík, M., Rell, S., Nikolov, C., Barta, M., Pittner, J., Hyblerová, S., Zúbrik, M., Kunca, A., Vakula, J., Gubka, A., & Holuša, J. (2022). Comprehensive comparison of treatments for controlling the large pine weevil (Hylobius abietis) in Central Europe. *Scientific Reports*, *12*(1). https://doi.org/10.1038/s41598-022-13729-6

[7] Heber, T., Helbig, C. E., Osmers, S., Larquette, M., & Müller, M. G. (2024). Evaluation of trap type and attractant composition for potential mass trapping of Hylobius abietis. *Agricultural and Forest Entomology*, *26*(1), 1–17. https://doi.org/10.1111/afe.12593

[8] Lalík, M., Galko, J., Kunca, A., Nikolov, C., Rell, S., Zúbrik, M., Dubec, M., Vakula, J., Gubka, A., Leontovyč, R., Longauerová, V., Konôpka, B., & Holuša, J. (2021). Ecology, management and damage by the large pine weevil (Hylobius abietis) (Coleoptera: Curculionidae) in coniferous forests within Europe. In *Central European Forestry Journal* (Vol. 67, Issue 2, pp. 91–107). Sciendo. https://doi.org/10.2478/forj-2021-0005

[9] Luoranen, J., & Viiri, H. (2012). Soil preparation reduces pine weevil (Hylobius abietis (L.)) damage on both peatland and mineral soil sites one year after planting. *Silva Fennica*, *46*(1), 151–161. https://doi.org/10.14214/sf.71

[10] Moore, R., Willoughby, I. H., Moffat, A. J., & Forster, J. (2021). Acetamiprid, chlorantraniliprole, and in some situations the physical barriers MultiPro® or Kvaae® wax, can be alternatives to traditional synthetic pyrethroid insecticides for the protection of young conifers from damage by the large pine weevil Hylobius abietis L. *Scandinavian Journal of Forest Research*, *36*(4), 230–248. https://doi.org/10.1080/02827581.2021.1906313

[11] Örlander, G., & Nordlander, G. (2003). Effects of field vegetation control on pine weevil (Hylobius abietis) damage to newly planted Norway spruce seedlings. *Annals of Forest Science*, *60*(7), 667–671. https://doi.org/10.1051/forest:2003059ï

[12] Rahman, A., Viiri, H., & Tikkanen Olli-Pekka. (2018). Is stump removal for bioenergy production effective in reducing pine weevil (Hylobius abietis) and Hylastes spp. breeding and feeding activities at regeneration sites? *Forest Ecology and Management*, *424*, 184–190.

[13] Skrzecz, I., Sukovata, L., Jabłoński, T., Sowińska, A., & Szmidla, H. (2021). Spatio-temporal distribution of Hylobius abietis in Scots pine stands – implications for pest monitoring. *Journal of Pest Science*, *94*(4), 1393–1404. https://doi.org/10.1007/s10340-021-01339-6

[14] Tudoran, A., Oltean, I., & Varga, M. (2019). Control and Management of the Pine Weevil Hylobius abietis L. *Bulletin of University of Agricultural Sciences and Veterinary Medicine Cluj-Napoca. Horticulture*, *76*(1), 11–18. https://doi.org/10.15835/buasvmcn-hort:2018.0049

[15] Willoughby, I. H., Moore, R., Moffat, A. J., Forster, J., Sayyed, I., & Leslie, K. (2021). Are there viable chemical and non-chemical alternatives to the use of conventional insecticides for the protection of young trees from damage by the large pine weevil Hylobius abietis L. In UK forestry? *Forestry*, *93*(5), 694–712. https://doi.org/10.1093/FORESTRY/CPAA013

# GROUND VEGETATION BIOMASS AND CARBON POOL IN HEMIBOREAL OLD-GROWTH CONIFEROUS STANDS ON ORGANIC SOILS

**Mg.silv. Valters Samariks**
**Mg.silv. Ieva Jaunslaviete**
**Mg.silv. Andis Adamovičs**
**Mg.silv. Sabīne Dubašinska**
**Dr.silv. Āris Jansons**

Latvian State Forest Research Institute "Silava", Rigas street 111, LV2169, Salaspils, **Latvia**

## ABSTRACT

Forest ground vegetation biomass plays a significant role in carbon (C) storage and contributes to the overall carbon pool of forest ecosystems. Ground vegetation, including understory plants, shrubs, and grasses, not only affects carbon sequestration through photosynthesis but also contributes to the carbon cycle as it decomposes and release carbon into atmosphere and soil. This process adds to soil organic matter and affects it carbon dynamics. Understanding the above and below-ground biomass of forest ground vegetation and its associated carbon pool is essential for improving local and global estimates of carbon storage and cycling, especially in forests on organic soils where the information is scarce.

A total of 12 study sites were selected, with six stands dominated by Norway spruce (*Picea abies* (L.) H. Karst.) and six stands dominated by Scots pine (*Pinus sylvestris* L.). Of the selected stands, six were on drained organic soils and six on undrained organic soils. In each study site, four samples of ground vegetation biomass (both above- and below-ground) were collected in tree replicates. Each sample (above- and below-ground) was sorted into three groups (herbs, shrubs, trees), air-dried until reaching a constant weight, and then weighed to determine dry weight and carbon content.

Our study provides novel information on ground vegetation biomass and C pool estimates in old-growth stands dominated by different coniferous tree species in the hemiboreal region. Ground vegetation biomass and carbon pools were similar between drained and undrained stands.

**Keywords:** climate change mitigation, overmature stands, peat soil, forest amelioration

## INTRODUCTION

Forests play a crucial role in carbon storage and sequestration, making them increasingly important in climate change mitigation strategies and research. As a result, there is a pressing need to assess biomass and carbon stocks at regional and national levels to guide forest-related policies and strategies for climate change mitigation and adaptation. However, the research and policy initiatives has traditionally focused on tree aboveground biomass, while the role of ground vegetation has often been overlooked.

Ground vegetation—comprising grasses, dwarf shrubs, mosses, ferns, and other understory plants—plays an important role in forest ecosystems carbon (C) cycling. Ground vegetation biomass, though smaller in quantity compared to trees, is vital for

https://doi.org/10.5593/sgem2024v/3.2/s13.36

nutrient and carbon cycling, and biodiversity [1]. Carbon stock in this layer consists of live plant material above-ground, plant roots below-ground, and decomposing organic matter, making it an essential part of the forest carbon pool each playing distinct roles in carbon storage and ecosystem function. The ground vegetation is relatively small compared to trees and it contributes to short-term carbon storage by capturing carbon dioxide through photosynthesis. As ground vegetation dies and decomposes, it releases carbon into the atmosphere or transfers it to the soil, contributing to the nutrient cycle [2]. Below-ground carbon pool consists of roots, soil organic matter, and decomposed material that has been incorporated into the soil. The carbon stored below ground is typically more stable and longer-lasting than above-ground biomass, as it is less vulnerable to disturbances. Together, the above- and below-ground carbon pools form a dynamic system that not only influences the carbon cycle but also plays a key role in mitigating climate change by acting as a carbon sink.

The carbon sequestration potential of ground vegetation has not been extensively quantified, particularly at regional and national levels. This gap in knowledge presents a challenge for climate change mitigation, which are increasingly reliant on accurate estimates of forest carbon pools. Commonly used method for ground vegetation biomass estimation is destructive sampling, and is time consuming, compared to non destructive methods such as remote-sensing [3]. Moreover, accurate empirical estimates of ground vegetation biomass are necessary and can help in further remote sensing research to simplify biomass and C stock estimation at larger scale [4]. It is crucial to understand both the above- and below-ground biomass of forest ground vegetation and this is particularly important in forests with organic soils, where such data is limited, and especially in old-growth stands. The aim of the study is to assess ground vegetation biomass and carbon stock in old-growth stands on drained and undrained organic soils. We hypothesize that ground vegetation carbon stock will be similar between drained and undrained sites.

## MATERIALS AND METHODS

The study was carried out in the hemiboreal vegetation zone [5]. The climate in this region is temperate, significantly influenced by the Baltic Sea and the North Atlantic. The average annual precipitation sum is 692 mm, and the mean annual air temperature is +6.4°C. According to data from the Latvian Environment, Geology, and Meteorology Centre, February is the coldest month with an average temperature of -3.7°C, but July is the warmest, with an average temperature of +17.4°C.

Study object is Norway spruce (*Picea abies* (L.) H. Karst.) and Scots pine (*Pinus sylvestris* L.) old-growth stands on organic soils. In total 12 study sites were selected, of which 6 were drained and 6 undrained. Drained sites are representing fertile drained organic soils - the *Myrtillosa turf. mel* forest type, but undrained sites - *Caricoso-phragmitosa* forest type according to the Latvian forest type classification [6]. Following forest drainage, the *Caricoso-phragmitosa* forest type is transformed into the *Myrtillosa turf. mel* forest type.

**Table 1.** Description of study sites

| Site type | Dominant species | Mean age | DBH, cm | H, m | Basal area, $m^2$ $ha^{-1}$ | M, $m^3$ $ha^{-1}$ |
|---|---|---|---|---|---|---|
| Drained | Scots pine | 150 | 34.9±1.5 | 27.5±5.0 | 32.0±6.0 | 404.7±82.4 |
| Undrained | Scots pine | 179 | 27.9±2.2 | 19.2±1.0 | 18.7±2.9 | 168.1±26.5 |
| Drained | Norway spruce | 162 | 34.1±2.7 | 28.9±2.0 | 32.6±4.4 | 443.0±81.9 |
| Undrained | Norway spruce | 153 | 26.9±1.6 | 24.6±0.7 | 35.6±2.7 | 428.7±35.3 |

The soil in drained forest type contains tree (70%), sedge (30%), and small amount of *Spghagnum* peat. The ground vegetation in drained forest type was characterized by a diverse dwarf shrub layer, dominated by European blueberry (*Vaccinium myrtillus* L.) and lingonberry (*Vaccinium vitis-idaea* L.), a herb layer (up to 87 species recorded in this forest type) dominated by purple moor-grass (*Molinia caerulea* [L.] Moench.), and a moss layer (up to 60 species recorded in this forest type) dominated by *Pleurozium schreberi*, *Hylocomium splendens*, and *Dicranum* spp. [6].

The soil in undrained forest type contains moderately decomposed acidic *Carex* and tree peat, and might be mixed with *Spagnum* peat. The ground vegetation in undrained forest type was characterized by a dense herb and moss layer (up to 150 species recorded in this forest type), dominated by sedges (*Carex* spp.), reedgrass (*Calamagrostis* spp.), and common reed (*Phragmites australis*). The moss layer was dominated by *Sphagnum*, *P. schreberi*, *H. splendens*, and *Dicranum* spp. [6].

In each stand three 1x1 m large sampling plots were selected, and in each plot four 25x25x25cm large ground vegetation biomass samples were collected. In field, samples were divided in two parts: above-ground and below-ground part. Samples were delivered to Latvian State Forest Research Institute "Silava" laboratory, where all samples were sorted into smaller fractions and air-dried at 70°C until reaching constant weight, weighted to determine dry mass. Above-ground samples were sorted in three fractions: herbaceous plants, dwarf shrubs and mosses, but below-ground samples were sorted in herbaceous plant roots, dwarf shrub roots, and tree root fractions. Below-ground root group classification was based on root diameter, where we analysed only small roots (diameter 2–20 mm) based on ICP Forest classification [7] [Cools et al., 2010]. All sorted roots were larger than 2mm in dimeter, to exclude fine-roots from the study, but smaller than 20mm in diameter to exclude coarse tree roots.

*Statistical analysis*

From each analysed sample plot average ground vegetation values were calculated as tons per hectare. Obtained biomass dry weight was expressed as C tons per hectare. Mean C content of ground vegetation above-ground, below-ground parts and moss was used from local study conducted in Latvia [8]. Normal distribution of data was checked with the Shapiro–Wilk normality test. Mann–Whitney U test was used to assess significant differences between the non-parametric variables. All tests were performed with the statistical software R 4.1.2. [9].

https://doi.org/10.5593/sgem2024v/3.2/s13.36

## RESULTS

Ground vegetation biomass is similar between study sites in all cases ($p>0.05$). Ground vegetation above-ground biomass dry weight in drained and undrained pine stands was 0.85±0.64 t ha$^{-1}$ and 0.93±0.97 t ha$^{-1}$, respectively, but in spruce stands it was 2.14±1.50 t ha$^{-1}$ and 1.95±1.57 t ha$^{-1}$, respectively. Ground vegetation above-ground biomass carbon stock in drained and undrained pine stands was 0.42±0.32 t ha$^{-1}$ and 0.41±0.43 t ha$^{-1}$, respectively, but in spruce stands it was 1.06±0.74 t ha$^{-1}$ and 0.96±0.78 t ha$^{-1}$, respectively (Fig. 1A).

Ground vegetation below-ground biomass dry weight in drained and undrained pine stands was 5.66±3.0 t ha$^{-1}$ and 2.85±1.73 t ha$^{-1}$, respectively, but in spruce stands it was 5.98±4.09 t ha$^{-1}$ and 7.06±2.88 t ha$^{-1}$, respectively. Ground vegetation below-ground biomass carbon stock in drained and undrained pine stands was 2.88±1.52 t ha$^{-1}$ and 1.45±0.88 t ha$^{-1}$, respectively, but in spruce stands it was 3.05±2.09 t ha$^{-1}$ and 3.60±1.47 t ha$^{-1}$, respectively (Fig. 1B). Significant differences have been observed only between drained pine and spruce stand below-ground biomass dry weight and carbon stock ($p<0.05$).

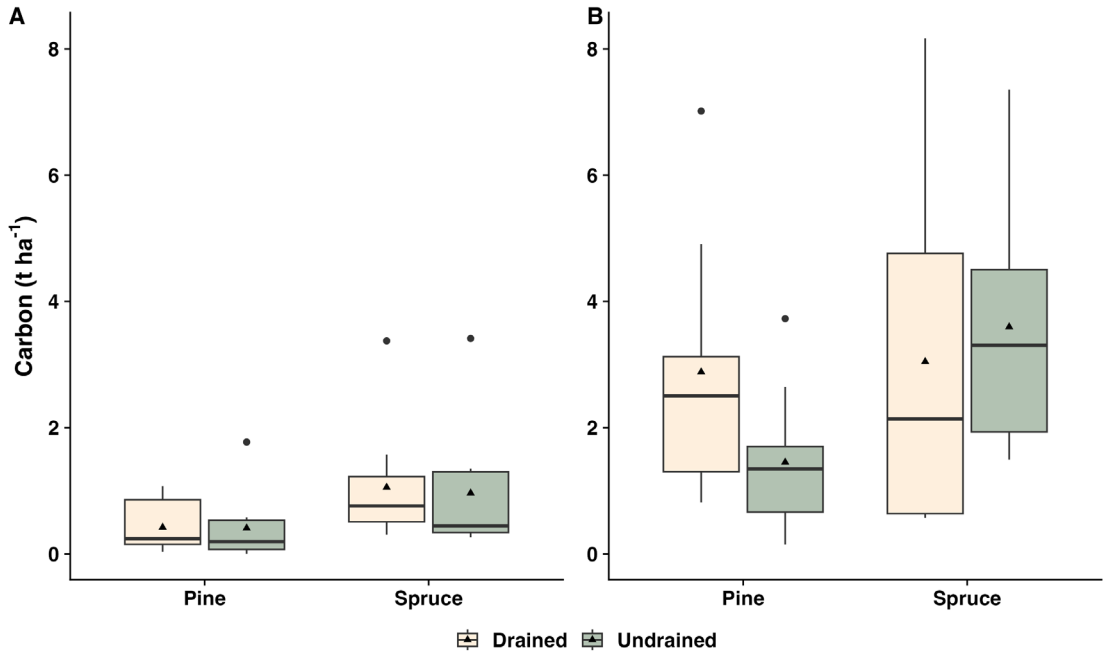



**Figure 1.** Ground vegetation above-ground (A) and below-ground (B) biomass carbon stock per forest type and dominant tree species. The box plots represent median values and the 25% and 75% percentiles; the whiskers indicate the maximum and minimum values; and the black dots represent outliers. Black triangles indicate mean values.

Above-ground part of ground vegetation biomass was sorted in three fractions: moss, herbaceous plants and dwarf shrubs (Fig. 2A). The largest fraction in all sites was moss biomass. In pine dominated stands the biomass distribution was similar between drained and undrained sites. In drained sites carbon stock of moss, herbaceous plant and dwarf shrub biomass was 0.34±0.25 C t ha$^{-1}$, 0.03±0.03 C t ha$^{-1}$, and 0.09±0.11 C t ha$^{-1}$, respectively. In undrained sites carbon stock of moss, herbaceous plant and dwarf shrub

biomass was 0.38±0.42 C t ha$^{-1}$, 0.04±0.04 C t ha$^{-1}$, and 0.06±0.07 C t ha$^{-1}$, respectively. In spruce dominated stands the herbaceous plant and dwarf shrub biomass distribution differed between drained and undrained sites. In drained sites carbon stock of moss, herbaceous plant and dwarf shrub biomass was 0.73±0.67 C t ha$^{-1}$, 0.06±0.06 C t ha$^{-1}$, and 0.26±0.25 C t ha$^{-1}$, respectively. In undrained sites carbon stock of moss, herbaceous plant and dwarf shrub biomass was 0.61±0.57 C t ha$^{-1}$, 0.22±0.25 C t ha$^{-1}$, and 0.14±0.08 C t ha$^{-1}$, respectively.

Below-ground part of ground vegetation biomass was sorted in three fractions: tree roots, herbaceous plant roots and dwarf shrub roots (Fig. 2B). The largest fraction in all sites was tree root biomass. In pine dominated drained sites carbon stock of tree root, dwarf shrub root, and herbaceous plant root biomass was 2.81±1.56 C t ha$^{-1}$, 0.18±0.11 C t ha$^{-1}$, and 0.20±0.53 C t ha$^{-1}$, respectively. In pine dominated undrained sites carbon stock of tree root, dwarf shrub root, and herbaceous plant root biomass was 0.91±0.53 C t ha$^{-1}$, 0.54±0.58 C t ha$^{-1}$, and 0.07±0.10 C t ha$^{-1}$, respectively. In spruce dominated drained sites carbon stock of tree root, dwarf shrub root, and herbaceous plant root biomass was 2.99±2.15 C t ha$^{-1}$, 0.18±0.12 C t ha$^{-1}$, and 0.10±0.10 C t ha$^{-1}$, respectively. In spruce dominated undrained sites carbon stock of tree root, dwarf shrub root, and herbaceous plant root biomass was 3.20±1.65 C t ha$^{-1}$, 0.83±1.64 C t ha$^{-1}$, and 0.01±0.10 C t ha$^{-1}$, respectively.

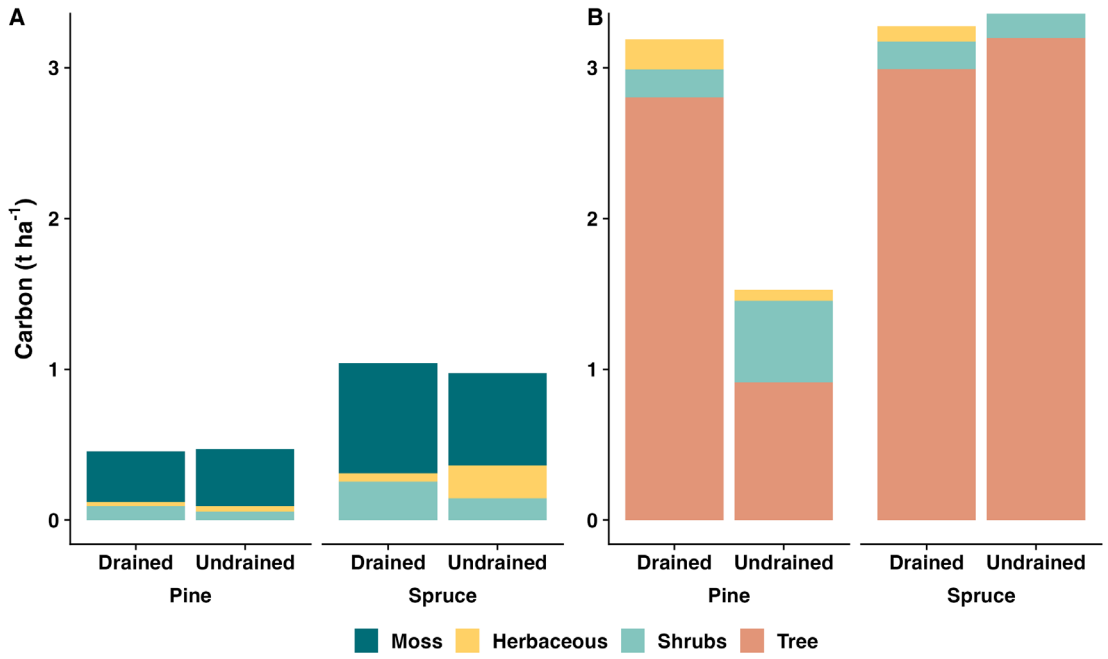



**Figure 2.** Ground vegetation above-ground (A) and below-ground (B) biomass carbon stock per forest type, dominant tree species and functional group

Correlation matrix shows tree height as the single variable correlating with above-ground vegetation biomass, however the correlation is weak r=0.34. Below-ground vegetation biomass positively correlates with stand growing stock, tree height and basal area, r=0.48, r=0.49, and r=0.39, respectively, but negatively (r=-0.39) with stand age.

https://doi.org/10.5593/sgem2024v/3.2/s13.36

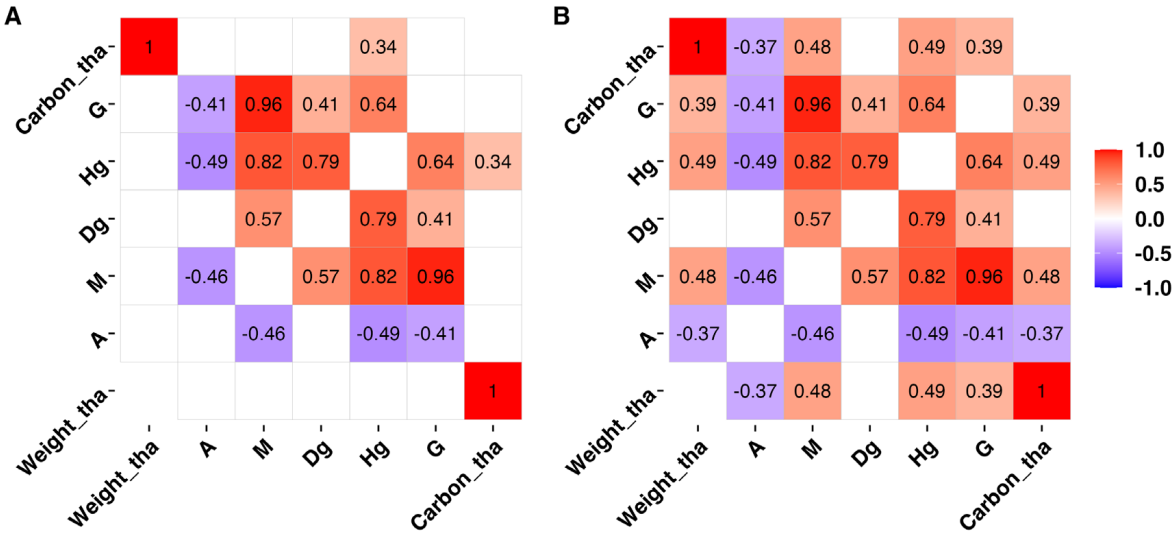



**Figure 3.** Correlation matrix of significant variables of ground vegetation above ground (A) and below-ground (B) root biomass weight (t $ha^{-1}$), carbon stock (t $ha^{-1}$) and stand parameters. A – mean stand age, years; M – mean stand growing stock, $m^3$ $ha^{-1}$; Dg – mean diameter at breast height, cm; Hg – mean stand tree height, m; G – stand basal area, $m^2$.

## DISCUSSION

Ground vegetation biomass carbon stock is small, but significant carbon pool in forest ecosystems. Study results indicate that ground vegetation biomass is similar between drained and undrained stands, however biomass might differ between different functional groups making up this carbon pool. The proportion of above-ground biomass C stock from total ground vegetation C stock is 13%, 26%, 22%, and 21% in drained pine, spruce, and undrained pine and spruce stands, respectively. However, the proportion of below-ground biomass C stock from total ground vegetation C stock is 87%, 74%, 78%, and 79% in drained pine, spruce, and undrained pine and spruce stands, respectively. Obtained biomass values have high confidence intervals, indicating large variability within sites.

Above-ground biomass C stock differed between functional groups, but moss biomass was the largest part in all forest types. Moss as the largest part could be explained with soil and growing conditions of forests on peat soils, as some part of peat is formed from *Sphagnum*. Overall, proportion of moss biomass C stock from total above-ground C stock ranged from 63% to 81%, but herbaceous plant biomass C stock ranged from 5% to 22%, and dwarf shrub biomass C stock ranged from 12% to 25%. All functional group biomass of above-ground part was similar between forest types and tree species ($p>0.05$). The above-ground vegetation biomass C stock in our study is slightly larger than those reported in young to mature pine stands on mineral soil of boreal region of Canada, and it has been reported not to be age-dependent after first two decades [10]. However, compared to study in Sweden our study results of above-ground biomass are

in line with their findings [11]. Moreover, ground vegetation biomass has been reported to be dependent on light availability in lower levels to promote vegetation growth and diversity [12], thus affected by genetically determined differences in adaptation of genotypes [13-14].

Blow-ground biomass C stock differed between functional groups, and tree small root biomass was the largest part in all forest types. Typically, tree roots could be expected as the largest C stock of below-ground biomass in forest ecosystems. Overall, proportion of tree root biomass C stock from total above-ground C stock ranged from 58% to 91%, but herbaceous plant biomass C stock ranged from 0% to 7%, and dwarf shrub biomass C stock ranged from 6% to 37%. All functional group biomass of below-ground part was similar between forest types and tree species ($p>0.05$), except for tree root biomass C stock of undrained pine dominated stands which was noticeably lower compared to other analysed stands. Lower values for below-ground tree root C stock can be explained with notably lower stand parameter values (tree height, diameter at breast height, basal area and growing stock).

## CONCLUSION

The study provides novel information on ground vegetation biomass and C pool estimates in old-growth stands on drained and undrained organic soils dominated by different coniferous tree species in the hemiboreal region. Overall, the above- and below-ground biomass C stock does not differ between drained and undrained stands, however are linked to stand parameters (especially tree height), and indicates light availability as important factor. Dominant tree species alone does not affect vegetation biomass C stock; however, tree size plays a role in below-ground biomass amount of small tree roots. The largest part of ground vegetation biomass C pool is below-ground part and tree root biomass which makes up 87%, 74%, 78%, and 79% of total ground vegetation biomass samples in drained pine, spruce, and undrained pine and spruce stands, respectively

Further studies should focus on assessing ground vegetation biomass of different aged forest, forest types and ground vegetation biomass influencing factors to develop accurate models for this C pool, because ground vegetation biomass is often omitted from ecosystem C models. Moreover, accurate empirical estimates of ground vegetation biomass can help in further remote sensing research to simplify biomass and C stock estimation at larger scales.

## ACKNOWLEDGEMENTS

The study was funded by the European Regional Development Fund Project "Development of a decision support tool integrating information from old-growth semi-natural forest for more comprehensive estimates of carbon balance" (No. 1.1.1.1/16/A/130) and Rural Support Service project "The role of old-growth forests in climate change mitigating: information for forest sector policy makers in Latvia and the European Union" (No. 10.9.1-11/24/1841-e).

https://doi.org/10.5593/sgem2024v/3.2/s13.36

## REFERENCES

[1] Gilliam F.S., The Ecological Significance of the Herbaceous Layer in Temperate Forest Ecosystems, BioScience, 2007, vol. 57, Issue 10, pp 845–858, DOI: 10.1641/B571007

[2] Heinrichs, S.; Bernhardt-Römermann, M.; Schmidt, W. The estimation of aboveground biomass and nutrient pools of understorey plants in closed Norway spruce forests and on clearcuts. Eur. J. For. Res. 2010, 129, 613–624.

[3] Catchpole, W.R.; Wheeler, C.J. Estimating plant biomass: A review of techniques. Austral Ecol. 1992, 17, 121–131.

[4] Somogyi, Z.; Cienciala, E.; Mäkipää, R.; Muukkonen, P.; Lehtonen, A.; Weiss, P. Indirect methods of large-scale forest biomass estimation. Eur. J. For. Res. 2006, 126, 197–207.

[5] Ahti T., Hämet-Ahti L., Jalas J., Vegetation zones and their sections in northwestern Europe, Ann. Bot. Fenn. 1968, 5, 169-211.

[6] Bušs K., Forest ecosystem classification in Latvia. In Proceedings of the Latvian Academy of Sciences, Rīga, Latvia, 1997, 15:204–218

[7] Cools, N.; De Vos, B. 2010: Sampling and Analysis of Soil. Manual Part X, 208 pp. In Manual on Methods and Criteria for Harmonized Sampling, Assessment, Monitoring and Analysis of the Effects of Air Pollution on Forests; UNECE, ICP Forests: Hamburg, Germany, 2010; ISBN 978-3-926301-03-1. Available online: http://www.icp-forests.org/Manual.htm (accessed on 10 November 2024).

[8] Butlers, A., Laiho, R., Soosaar, K., Jauhiainen, J., Schindler, T., Bārdule, A., Kamil-Sardar, M., Haberl, A., Samariks, V., Vahter, H., Lazdiņš, A., Čiuldienė, D., Armolaitis, K., and Līcīte, I.: Soil and forest floor carbon balance in drained and undrained hemiboreal peatland forests, EGUsphere [preprint], DOI:10.5194/egusphere-2024-1397, 2024.

[9] R Core Team (2021) R: A language and environment for statistical computing. R Foundation for Statistical Computing, Vienna, Austria. URL https://www.R-project.org/

[10] Peichl M., and Arain, M.A., Above- and belowground ecosystem biomass and carbon pools in an age-sequence of temperate pine plantation forests, Agricultural and Forest Meteorology, 2006, 140,vol. 1-4, pp 51-63

[11] Ilvesniemi H., Levula J., Ojansuu R., Kolari P., Kulmala L., Pumpanen J., Launiainen S., Vesala T., Nikinmaa E., Long-term measurementsof the carbon balance of a boreal Scots pine dominated forest ecosystem, Boreal Environment Research 2009, 14, 731–753

[12] Sigurdsson BD., Magnusson B., Elmarsdottir A., Bjarnadottir B., Biomass and composition of understory vegetation and the forest floor carbon stock across Siberian larch and mountain birch chronosequences in Iceland, 2005, Ann. For. Sci. 62, pp 881-888. DOI: 10.1051/forest:2005079

[13] Jansone B., Neimane U., Šēnhofa S., Matisons R., Jansons Ā. Genetically determined differences in annual shoot elongation of young Norway spruce, Forests, 2020, 11, 1260; DOI:10.3390/f11121260

[14] Matisons, R., Zeltiņš, P., Danusevičius, D., Džeriņa, B., Desaine, I., Jansons, Ā. Genetic control of intra-annual height growth in 6-year-old Norway spruce progenies in Latvia, iForest, 2020, 12: 214–219. DOI: 10.3832/ifor2777-012

# MODELING LANDSCAPE PERMEABILITY USING FOREST PATCHES AND ENVIRONMENTAL VARIABLES

**Nicu Alexandru Gîlea [1,2]**
**Ileana Patru-Stupariu [2,3]**
**Mioara Clius [3]**

[1]PhD Ress, Faculty of Geography, Doctoral School Simion Mehedinti, University of Bucharest Bd. N. Bălcescu, 1, 010041 Bucharest, **Romania**

[2]Institute of Research of University of Bucharest, ICUB, Transdisciplinary Research Centre Landscape-Territory-Information Systems, CeLTIS, Splaiul Independţei no. 91 - 95, 050095 Bucharest, **Romania**

[3]Department of Regional Geography and Environment, Faculty of Geography, University of Bucharest, N. Bălcescu, 1, 010041 Bucharest, **Romania**

## ABSTRACT

This study examines the impact of the risk of illegal logging on landscape permeability in a region where 8,060 km² of the total area is covered by forests. According to official data, 29% of this forested area is located in zones at risk of illegal logging. Given that forests play a crucial role in maintaining landscape permeability and ecological connectivity, the study employs the CSI index, which integrates the risk of illegal logging, to assess how these activities affect the ecological integrity and functionality of the landscape. We modelled landscape permeability in two scenarios. In the first scenario, we considered the current situation on the ground. In the second scenario, we took into account the risk of illegal logging presented by the forests in the study area. The results indicate that the risk associated with illegal logging in forested areas generates a negative impact on landscape permeability, reflected in an 11.74% reduction in areas classified as SACA 1. These findings will provide insight into the influence of the risk of illegal logging on landscape permeability and will support the development of more effective conservation strategies.

**Keywords:** landscape permeability, illegal logging, forest, environmental variables.

## INTRODUCTION

The forests of Romania, renowned for their exceptional biodiversity and ecological resilience, constitute one of the most important natural ecosystems in Europe [1]. They play a crucial role in providing vital ecosystem services, such as provisioning, regulating, supporting, and cultural functions, while also sustaining a complete trophic pyramid. However, forests are under considerable pressure due to illegal logging, a major issue in Romania [2], [3], which threatens both forest resources and the ecological integrity of the landscape.[4].

The exploitation of forests has multiple negative effects on the environment, including biodiversity loss, soil erosion, alteration of hydrological regimes, and climate change [5]. These activities reduce the ecosystems' capacity to function optimally and affect habitat quality. A less discussed yet critically important aspect is the impact of forest exploitation on landscape permeability. Ecological connectivity and species mobility often depend on landscape permeability, as highlighted in studies recommending the enhancement of connectivity through habitat restoration and the reduction of fragmentation [6]. Forests

play an essential role in maintaining structural connectivity and supporting crucial ecological flows, a fact evidenced by landscape permeability assessment models, which consistently identify them as having the highest permeability values [6], [7], [8].

Landscape permeability is a fundamental concept in landscape ecology, used to assess and prioritise conservation and ecological restoration measures at the macro-regional level. The Continuous Suitability Index (CSI), a recognised methodology for assessing landscape permeability, serves as a tool for determining ecological connectivity and identifying Strategic Connectivity Areas (SACA) [9], [10]. The strategic connectivity areas approach originates from the Interreg Alpine ALPBIONET2030 programme and provides a way to visually display via GIS the most significant sites for the global ecological network at the macro-regional level (SACA1), areas with potential for ecological improvement interventions (SACA2), and ecological barriers (SACA3) [11].

Given the critical importance of forests for maintaining a high level of landscape permeability, this research aims to investigate the extent to which the risk of illegal logging influences landscape permeability and Strategic Connectivity Areas in the Transylvanian Continental Biogeographic Region (TCBR). The research hypothesis is that the risk of illegal logging decreases landscape permeability and influences the area of SACA in the TCBR. The main objectives include modelling landscape permeability incorporating the risk of illegal logging, determining the areas of SACA, and investigating the impact of illegal logging on landscape permeability.

We used the CSI to model landscape permeability in two scenarios. In the first scenario, we considered the existing situation on the ground at the present time. In the second scenario, we included in the landscape permeability modelling the risk of illegal logging that the forests in the TCBR present. Since there was no national database on illegal logging, we instead used a database that reflects the risk of illegal logging. This database is an official one, compiled by the Romanian Ministry of Environment, Waters, and Forests based on its own methodology [12].

This scenario-based approach aims to highlight how the risk of illegal logging affects the structure and functionality of the landscape. The research has the potential to contribute to the development of effective landscape conservation strategies and provide valuable insights for the sustainable management of forests in Romania, in a context where anthropogenic pressures continue to increase.

## DATA AND METHODS

### Study Area

The study was conducted in the TCBR, located in central Romania (fig. 1). The landscape, which spans an area of 34,289 km², is delineated between the coordinates 303,444.23E and 602,323.09E longitude, and 439,400.01N and 693,648.78N latitude. The boundaries of this landscape have been established based on the extent of the Continental Biogeographical Region in the Transylvania Region. The TCBR partially overlaps with 13 counties and includes 8,683.50 km² of protected natural areas. The landscape is dominated by unirrigated arable land, broadleaf forests, predominantly agricultural land, pastures, and fragmented urban areas. In the past, a large portion of this area was covered by broadleaf forests, which have gradually been replaced by agricultural land. Currently,

extensive forest areas in the TCBR face the risk of illegal logging [12], raising concerns about the impact of this activity on the permeability of the landscape.

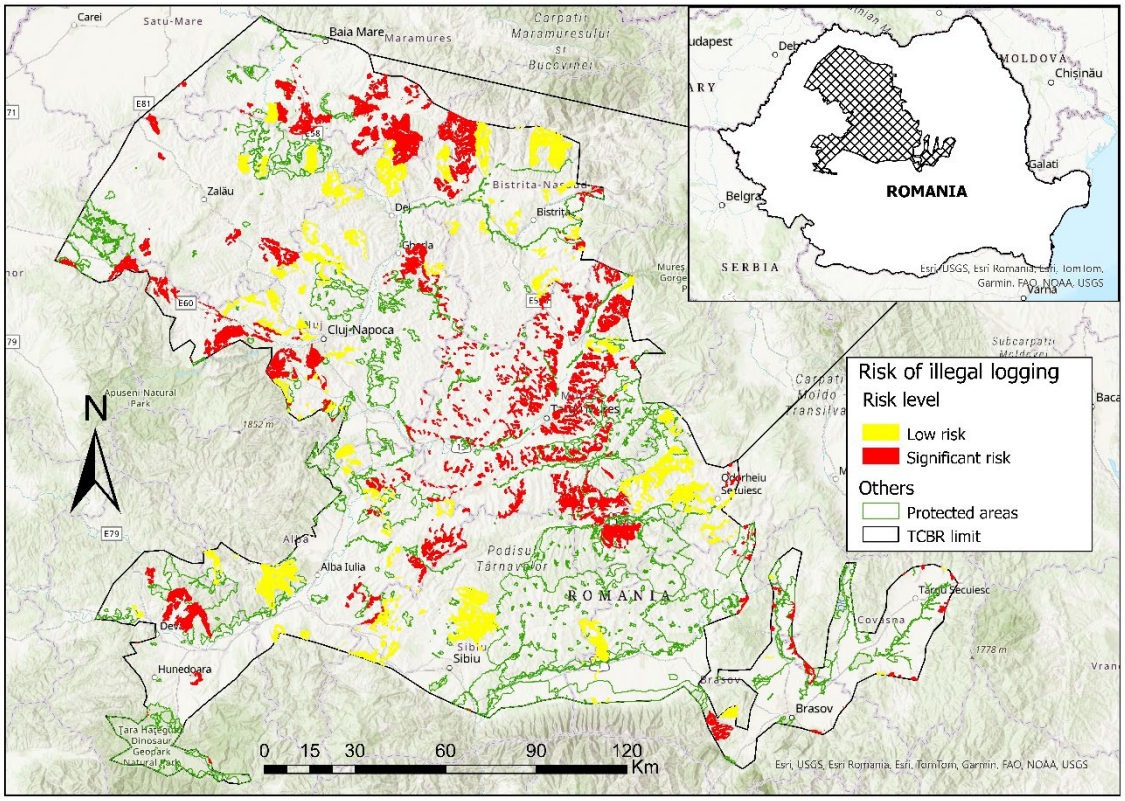



**Figure 1: Location map of TCBR with illegal logging risks and protected sites.**

## Data

For this analysis, various datasets obtained from official sources were used, covering several dimensions relevant to modelling. The land cover data (LAN) were sourced from the Corine Land Cover service for the year 2018, with a raster resolution of 100x100 m. Population density data (POP) were obtained from Geostat for the year 2021, disaggregated at the locality level and represented on a 1x1 km grid. Protected natural areas (ENV) and risk zones associated with illegal logging (LOG) were provided by the Ministry of Environment, Waters and Forests in vector format. These data were subsequently converted to raster with a resolution of 100 x 100 m. For the topographical variable (TOP), the European Digital Elevation Model (EU-DEM), version 1.1 (2020), was used, with a raster resolution of 25x25 m, from which information on terrain slope was derived. Regarding landscape fragmentation (FRA), the Landscape Fragmentation Effective Mesh Density dataset for the year 2015 was employed, which includes major anthropogenic elements and medium fragmentation (FGA2-S), version 1.0 (2019), with a raster resolution of 1x1 km. For areas with missing values (NoData) in the fragmentation raster, interpolation was applied based on the mean values of neighbouring pixels, using the "Focal Statistics" and "Con" functions in ArcGIS Pro 3.3.1. Finally, all datasets were standardised by converting them to raster format, aligning them, and projecting them into the same coordinate system at a uniform spatial resolution of 100x100 m.

**Assessment of the risk of illegal logging (LOG) on permeability**

The data on the risk of illegal logging from the TCBR were obtained from the Ministry of the Environment website and extracted for the following land cover classes in the study area: 311 – broad-leaved forest; 312 – coniferous forest; 313 – mixed forest; 324 – transitional woodland-shrub. The specialised literature was consulted to assign permeability values to areas at risk of illegal logging. The proposed values (Table 1) were deduced by comparing the permeability differences from the analysed studies [8], [13] and adapting them on a scale from 1 to 10, taking into account the relative impact observed in the specialised literature. It was found that for deforested areas, the permeability values were, on average, 2 units lower than the original forest. Considering that the areas are divided into 2 risk types (Table 1), a value 2 units lower was assigned for forested areas with significant risk levels and a value 1 unit lower for forested areas with low risk levels. The remaining areas remained unchanged.

**Table 1. Risk Assessment Scheme for Illegal Logging**

| Risk level | Permeability value |
|---|---|
| Wooded areas with significant risk level | Initial LAN perm value - 2 |
| Wooded areas with low risk level | Initial LAN perm value - 1 |
| Wooded areas with no risk | Initial LAN perm value - 0 |

Based on the land cover classes (CLC), we subsequently calculated the forested area in TCBR. We also calculated the area of forest exposed to the risk of illegal logging in the investigated region as well as in protected natural areas.

**Landscape permeability modelling**

To model landscape permeability, the CSI index was applied, which includes five indicators: land use/cover, population, topography, protected areas, and fragmentation. The methodology used was that described in the AlpBioNet and DianalpConnect projects [9], [10]. Permeability values were assigned from 0 to 10 according to the specialist literature (the AlpBioNet and DianalpConnect projects). Landscape permeability was assessed in two distinct scenarios:

1. **Scenario 1 (CSI S1):**Assessment of landscape permeability without considering the risk of illegal logging. The formula used is:

$$\text{CSI S1} = \frac{(2 * \text{LAN} + 2 * \text{POP} + \text{TOP} + \text{ENV} + \text{FRA})}{7}$$

2. **Scenario 2 (CSI S2):** Assessment of landscape permeability, taking into account the risk of illegal logging associated with the forests in the study area. In this scenario, the LAN indicator was combined with the raster data concerning the risk of illegal logging. To integrate the impact of illegal logging into the permeability model, we subtracted from the land cover raster the raster that contains the risk of illegal logging (LAN-LOG). We did this because LAN is the only indicator that changes as a result of illegal logging, through the partial alteration of land cover. The formula used is:

$$\text{CSI S2} = \frac{(2 * (\text{LAN} - \text{LOG}) + 2 * \text{POP} + \text{TOP} + \text{ENV} + \text{FRA})}{7}$$

The analyses were conducted at a spatial resolution of 100x100 m using ArcGIS Pro 3.3.1, with the Stereo 70 coordinate system.

**Identification of SACA surfaces**

The SACA surfaces for CSI S1 and CSI S2 have been calculated similarly to Favilli et al. [9]. SACA is based on the CSI index and is classified into three categories [11]:

- SACA1 (Ecological Conservation Areas): CSI≥8 and Area≥100 ha;
- SACA2 (Ecological Intervention Areas): 4<CSI<8;
- SACA3 (Ecological Restoration Areas/Barriers): CSI≤4.

After identifying the SACA areas within the TCBR, the characteristics of the SACA1 area were calculated, including its total extent, average area, the proportion covered by protected natural areas, as well as that situated outside of them. Additionally, the land cover in these areas was assessed.

**Statistical analysis of CSI values**

In the analysis, numerical values were obtained from the two rasters (CSI S1 and CSI S2) by applying the raster to point conversion in ArcGIS Pro, a process that allowed for the extraction of the corresponding CSI values for each pixel. To characterise the datasets and understand the distribution of CSI values in each scenario, descriptive statistics were applied to the permeability values (CSI S1 and CSI S2), calculating indicators such as minimum, maximum, mean, and standard deviation. These statistics summarised the essential characteristics of the data and facilitated comparisons between the two scenarios, providing an initial assessment of the variations.

To investigate the statistical relevance of the differences between the two permeability scenarios, the following hypotheses were formulated: the null hypothesis (H0) states that there is no difference between the values of CSI S1 and CSI S2, while the alternative hypothesis (H1) suggests that a difference exists between the values of CSI S1 and CSI S2. The distribution of the values was checked using the Shapiro-Wilk test, and the results indicated deviations from normality, which necessitated the use of non-parametric statistical tests. To assess the statistical significance of the differences between CSI S1 and CSI S2, the Wilcoxon paired test was applied, a non-parametric test suitable for related datasets without normal distribution [14]. Analyses were performed using Datatab and the R software package, version 4.4.1.

## RESULTS

**Assessment of the risk of illegal logging in TCBR**

The total forested area in TCBR is approximately 8,060 km², of which 2,372 km² (29%) is at risk of illegal logging. Of the exposed areas, 1,364 km² (58%) are under significant risk, while 1,008 km² (42%) present a low risk. An area of 499.73 km² (21%) of the at-risk surface is found within Natura 2000 sites, with 267.7 km² (54%) exposed to significant risk and 232.04 km² (46%) to low risk.

**Comparative analysis of CSI in TCBR for scenarios S1 and S2.**

In TCBR, the CSI index yielded a minimum value of 1.71 and a maximum value of 9.29 for both analysed scenarios (CSI S1 and CSI S2). The results indicate minor differences between CSI S1 and CSI S2 regarding the mean and standard deviation (Table 2).

**Table 2. Descriptive statistics of CSI S1 and CSI S2**

| | n | Mean | Median | Standard deviation |
|---|---|---|---|---|
| CSI S1 | 3391603 | 6.69 | 6.71 | 0.92 |
| CSI S2 | 3391603 | 6.66 | 6.71 | 0.90 |

The Shapiro-Wilk test indicated that the data do not follow a normal distribution (CSI S1: $W = 0.95778$, $p < 2.2e\text{-}16$; CSI S2: $W = 0.95739$, $p < 2.2e\text{-}16$), necessitating the use of non-parametric tests. Following the application of the Wilcoxon test, the alternative hypothesis was confirmed, highlighting a statistically significant difference between the values of CSI S1 and CSI S2 ($p < 0.001$). The rank analysis (Table 3) revealed that 233,367 cases were classified as negative (CSI S2 < CSI S1), while 172 cases showed positive values (CSI S2 > CSI S1), and 3,158,064 cases were equal. Table 4 presents the results of the Wilcoxon test, with a W statistic of 30,440,057, $z = -420.05$, and $r = 0.23$.

**Table 3. Distribution of ranks for the differences between CSI S2 and CSI S1.**

| | | n | Mean Rank | Sum of Ranks |
|---|---|---|---|---|
| CSI S2 - CSI S1 | Negative Ranks | 233367 | 116725.63 | 27239908973 |
| | Positive Ranks | 172 | 176977.08 | 30440057 |
| | Ties | 3158064 | | |
| | Total | 3391603 | | |

- Negative Ranks: CSI S2 < CSI S1
- Positive Ranks: CSI S2 > CSI S1
- Ties: CSI S2 = CSI S1

**Tabelul 4. Rezultatele testului Wilcoxon pentru diferențele dintre CSI S2 și CSI S1**

| | W | z | p | r |
|---|---|---|---|---|
| CSI S2 - CSI S1 | 30440057 | -420.05 | <.001 | 0.23 |

**SACA surfaces in TCBR under CSI S1 reference scenario.**

The findings indicate that 5.24% of the total area of the TCBR is classified as SACA1 zones. The majority of the area, namely 93.38%, falls within SACA2 zones. The remaining 1.38% of the total area is classified as SACA3 zones.

Within the TCBR, 98.71% of the SACA1 area is located in protected sites (Natura 2000). The land cover in SACA1 primarily consists of forests (83.57%), natural meadows (8.7%), pastures (3.11%), land primarily occupied by agriculture, with significant areas of natural vegetation (2.45%), and other classes (2.17%). The largest SACA1 area identified measures 145.29 km², while the average size of these zones is 8.50 km².

**Impact of illegal logging on SACA areas in the CIS S2**

The analysis revealed that 4.62% of the total area of TCBR is classified as SACA1 zones. The majority of the area, specifically 93.98%, falls within SACA2 zones. The remaining 1.39% of the total area is classified as SACA3 zones. In comparison to the baseline scenario (CSI S1), the area designated as SACA1 in the CSI S2 scenario decreases by 11.74% (fig. 2). This reduction results in an increase of 0.65% in the area of SACA2 and a 0.04% increase in the area of SACA3.

## DISCUSSIONS

Our findings confirm the hypothesis that the risk of illegal logging reduces the permeability of the landscape, while also influencing the distribution and extent of SACA areas in TCBR. We further discuss the implications of these findings.

**Permeability of the landscape and SACA surface in TCBR**

In the TCBR, the lowest values of the CSI index are recorded at 1.71. Such values occur in heavily anthropised landscapes, such as the cities of Cluj Napoca, Sibiu, and Brașov (fig. 2), which exhibit a high density of human population, elevated levels of fragmentation, and extensive impermeable surfaces. In contrast, the maximum value of the CSI index reaches a peak of 9.29. These higher values are characteristic of areas with a high degree of naturalness and have been observed in the protected sites RONPA0233 Lacul Zagra and ROSCI0320 Mociar, where the influence of human activities is considerably reduced. The average value of the CSI in the TCBR (6.69) aligns with values obtained in previous studies, suggesting an ecological status similar to landscapes in the Balkan region, in countries such as Croatia (6.67) and Greece (6.71) [9].

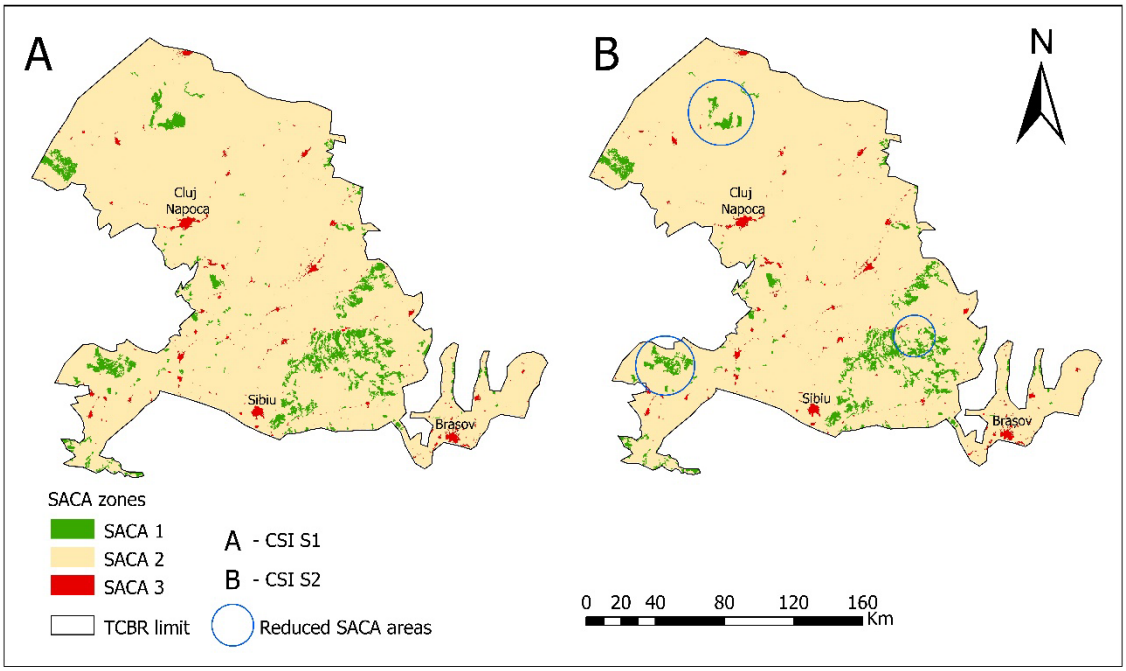



**Figure 2. Map of SACA areas within TCBR. A) shows the SACA areas for S1; B) shows the SACA areas for S2**

In the TCBR, the range of values generated by the CSI indicator allowed for the identification and delineation of the three SACA zones. This range of variation facilitated a clear distinction between zones, contributing to their classification (fig. 3). Of major importance for conservation are SACA1 zones. These represent the backbone of biodiversity conservation, and the primary management objective should be the maintenance and promotion of connectivity between them [9]. At the TCBR level, the percentage of these zones is below that identified in the DinalpConnect project. Furthermore, the average area of SACA1 (8.50 km²) ranks among the lowest of the analysed regions, being similar to that of Bosnia and Herzegovina (8.7 km²) [9].

Unlike other regions, in the TCBR, high landscape permeability cannot be achieved without the protection of natural protected areas. This is evidenced by the high percentage of SACA1 areas within protected natural areas (98.71%), compared to that outside (1.29%). The area of SACA1 in the TCBR is found 98.71% within protected sites, similar to that in Croatia (98.7%) and close to those in Slovenia (99.5%) and Greece (96.7%) [9]. The largest SACA1 area is located in the Natura 2000 site ROSCI0322 Muntele Șes, designated for the protection of priority forest habitats, such as alluvial forests and beech forests of the *Asperulo-Fagetum* type. Significant areas of SACA1 are also present in the sites ROSCI0227 Sighișoara - Târnava Mare and ROSPA0099 Podișul Hârtibaciului, which protect important forest habitats.

An important aspect identified in the current study is the potential of the TCBR as a SACA2 area (over 93%) for implementing concrete on-ground actions to create stepping stones and ecological corridors connecting larger SACA1 areas. This aspect is essential for ensuring species mobility and maintaining genetic flows, which are vital for the resilience of ecosystems in the face of climate change and anthropogenic pressures.

### Impact of risk of illegal logging on landscape permeability and SACA surfaces

The results of the research highlight that the forests in TCBR constitute a key element for landscape permeability, supporting the SACA1 areas. Forests account for over 83% of land cover in SACA1. However, 29% of the forested area in TCBR is at risk of illegal logging, with more than half (58%) of this area being under significant risk. Furthermore, the presence of substantial areas exposed to risk in the Natura 2000 sites (499.73 km²) raises concerns regarding the effectiveness of protection measures in these zones. These findings underline a high vulnerability of the forests in TCBR, which should lead to the strengthening of protection and monitoring policies for forested areas, and even the development of more effective conservation strategies.

Statistical analysis confirmed that there is a difference between CSI S1 and CSI S2, with the result being statistically significant due to the low p-value (<.001). According to Cohen [15], the r = 0.23 value associated with the Wilcoxon test indicates a small effect size. This suggests that the difference between scenarios may not be significant from an immediate practical perspective. However, contextual interpretation shows that within the specific framework of this study, even a small effect size has important implications. In this case, the decrease in CSI index values in the CSI S2 scenario impacts landscape permeability by reducing SACA1. The 11.74% reduction in the area of SACA1 in CSI S2 is attributed to the risk of illegal logging, which has led to decreased permeability values of the LAN indicator. This positioned CSI below the classification threshold of SACA1 (CSI≥8), thereby increasing the areas of SACA2 (4<CSI<8) (fig. 3). Therefore, at the level of TCBR, relatively small differences in CSI values can accumulate to produce major effects at a larger spatial scale.

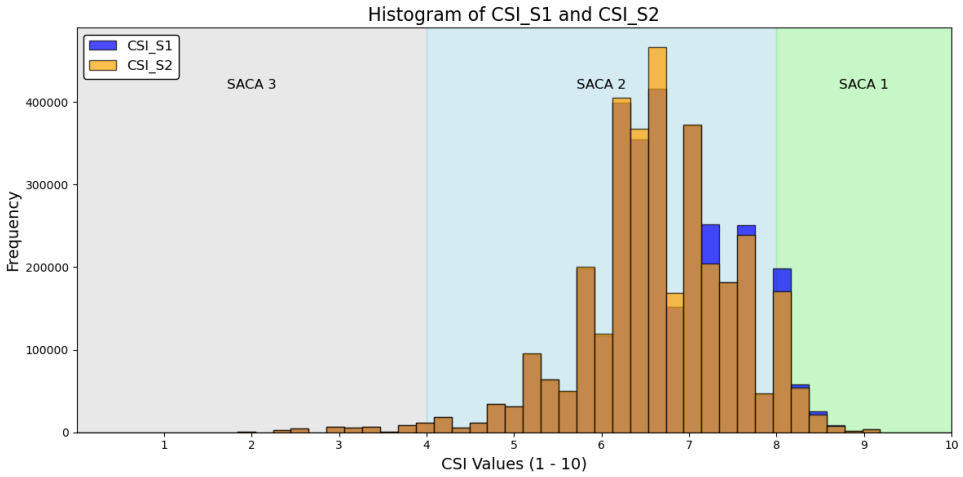



**Figure 3. Histogram of CSI values for S1 and S2 segmented according to SACA zones**

### Study limitations and directions for future research

Although this study provides useful insights, certain limitations remain. The use of a database concerning illegal logging risk, rather than concrete data on actual illegal logging incidents, introduces a degree of uncertainty in assessing the real impact. Additionally, the modelling of landscape permeability has been influenced by the resolution and quality of the available data. Future research should focus on enhancing the database regarding illegal logging and explore alternative methods of impact

assessment, including field studies and continuous forest monitoring. Furthermore, replicating the model at a broader scale (across the Carpathian Mountains or nationally) will yield a better understanding of the actual impact that the risk of illegal logging has on landscape permeability.

## CONCLUSION

Our study on the modelling of landscape permeability, based on environmental variables and forest patches, highlights the subtle yet significant impact of the risk of illegal logging on the ongoing suitability of the landscape and the distribution of SACA areas in TCBR. The results suggest a degradation of high ecological value areas (SACA1), which are transitioning to lower conservation categories (SACA2). These findings underscore the imperative for implementing more stringent conservation and forest resource management measures, given that the forests in TCBR represent the dominant land cover class for the identified SACA1 areas. Furthermore, our research results indicate that TCBR has the potential to function as a focal point for conservation interventions (SACA2), with a particular emphasis on developing ecological corridors and functional links, thereby facilitating the connection of high ecological value areas (SACA1). These interventions are vital for maintaining biodiversity and the integrity of ecosystems in the face of anthropogenic pressures and climate change.

## ACKNOWLEDGEMENTS

Thank you for the support provided for this study, which was partially funded by a doctoral grant from the Romanian Ministry of Education and a grant from the Research Institute of the University of Bucharest (ICUB) for the project "Design of Landscape Networks with Machine Learning," grant no. 7420.

## REFERENCES

[1] J. Oszlányi, K. Grodzińska, O. Badea, and Y. Shparyk, “Nature conservation in Central and Eastern Europe with a special emphasis on the Carpathian Mountains,” *Environmental Pollution*, vol. 130, no. 1, pp. 127–134, Jul. 2004, doi: 10.1016/j.envpol.2003.10.028.

[2] A. Pokorná and M. Matejova, “Forest Defenders: Explaining the Violent Politics of Illegal Logging in Romania,” *Environment: Science and Policy for Sustainable Development*, vol. 66, no. 1, pp. 19–31, Jan. 2024, doi: 10.1080/00139157.2023.2269042.

[3] I. Vorovencii, I. Ienciu, L. Oprea, and C. Popescu, “Identification Of Illegal Loggings In Harghita Mountains, Romania, Using Landsat Satellite Images,” Bulgaria: International Multidisciplinary Scientific GeoConference-SGEM, 2013.

[4] J. Aubad, P. Aragón, M. Á. Olalla-Tárraga, and M. Á. Rodríguez, “Illegal logging, landscape structure and the variation of tree species richness across North Andean forest remnants,” *For Ecol Manage*, vol. 255, no. 5–6, pp. 1892–1899, Apr. 2008, doi: 10.1016/j.foreco.2007.12.011.

[5] E. A. Kukavskaya *et al.*, “Influence of logging on the effects of wildfire in Siberia,” *Environmental Research Letters*, vol. 8, no. 4, p. 045034, Dec. 2013, doi: 10.1088/1748-9326/8/4/045034.

[6] R. G. Rodrigues, A. Srivathsa, and D. Vasudev, “Dog in the matrix: Envisioning countrywide connectivity conservation for an endangered carnivore,” *Journal of Applied Ecology*, vol. 59, no. 1, pp. 223–237, Jan. 2022, doi: 10.1111/1365-2664.14048.

[7] M. Makwana, V. Vasudeva, S. A. Cushman, and R. Krishnamurthy, "Modelling landscape permeability for dispersal and colonization of tigers (Panthera tigris) in the Greater Panna Landscape, Central India," *Landsc Ecol*, vol. 38, no. 3, pp. 797–819, Mar. 2023, doi: 10.1007/s10980-022-01590-x.

[8] G. Schmitt, M. Franchomme, and C. Hinnewinkel, "Towards an index of biodiversity potential: example in an anthropised and fragmented landscape matrix," 2022, doi: 10.4000/cybergeo.39205ï.

[9] F. Favilli, P. Laner, and I. Bertoncelj, "Application of the continuum suitability index (csi) model to display the permeability of the alpine-dinaric landscape and to define intervention priorities for ecological linkages," *Biodivers Conserv*, vol. 32, no. 10, pp. 3237–3254, Aug. 2023, doi: 10.1007/s10531-023-02651-6.

[10] P. Laner *et al.*, "Landscape permeability for ecological connectivity at the macro-regional level: The Continuum Suitability Index and its practical implications," *Ecol Indic*, vol. 164, Jul. 2024, doi: 10.1016/j.ecolind.2024.112145.

[11] P. Laner and F. Favilli, "Report on ecological connectivity assessment Evaluations for the project area and transboundary pilot regions Deliverable T1.3.1," 2022. [Online]. Available: https://dinalpconnect.adrioninterreg.eu

[12] " Ministry of Environment, Waters and Forests." Accessed: Sep. 15, 2024. [Online]. Available: https://www.mmediu.ro/categorie/paduri/25

[13] R. C. Freeman and K. P. Bell, "Conservation versus cluster subdivisions and implications for habitat connectivity," *Landsc Urban Plan*, vol. 101, no. 1, pp. 30–42, 2011, doi:
10.1016/j.landurbplan.2010.12.019.

[14] H. K. T. Ng and N. Balakrishnan, "WILCOXON-TYPE RANK-SUM PRECEDENCE TESTS," *Aust N Z J Stat*, vol. 46, no. 4, pp. 631–648, Dec. 2004, doi: 10.1111/j.1467-
842X.2004.00358.x.

[15] J. Cohen, *Statistical Power Analysis for the Behavioral Sciences*. Routledge, 2013. doi: 10.4324/9780203771587.

# SIZE AND VITALITY CHARACTERISTICS OF STELLARIA HOLOSTEA L. PLANTS AND POPULATIONS IN DESNIANSKO-STAROHUTSKYI NATIONAL NATURE PARK

**Prof. Dr. Viktoriia Skliar**[1]
**PhD Nataliia Yaroshenko**[1]
**PhD Maryna Sherstiuk**[2]
**Assoc. Prof. Yurii Skliar**[1]

[1] Sumy National Agrarian University, **Ukraine**
[2] Czech University of Life Science Prague, **Czech Republic**

## ABSTRACT

The study of coenotic species in forest herb layers enables detection of ecosystem-level changes, with research in protected areas providing a foundation for long-term monitoring. This study assessed *Stellaria holostea* L. populations in forest phytocoenoses of Desniansko-Starohutskyi National Nature Park, typical of the Sumy Polissia region. Populations were surveyed in various forest types: *Pinetum (sylvestris) convallarioso (majalis) – hylocomiosum, Pinetum (sylvestris) vaccinioso (myrtilli) – moliniosum (caeruleae), Pinetum (sylvestris) vaccinioso (myrtilli) – sphagnosum, Betuletum (pendulae) caricosum (pilosae), and Quercetum (roboris) convallariosum (majalis).* Morphometric analysis of plant size traits and vitality assessments, following Yu. A. Zlobin's method, enabled classification of populations as depressive, balanced, or thriving. Ecological indicators from Y. P. Didukh's scales provided insight into edaphotope and climatotope influences. Statistical analysis revealed significant morphometric variability across phytocoenoses, and model plants were developed for each type. Vitality levels were categorized into three classes (a, b, and c), with quality index (Q) values ranging from 0.10 to 0.48. Depressive populations were found in *Pinetum (sylvestris) convallarioso (majalis) – hylocomiosum* and *Betuletum (pendulae) caricosum (pilosae)*, balanced in *Pinetum (sylvestris) vaccinioso (myrtilli) – sphagnosum*, and thriving in *Pinetum (sylvestris) vaccinioso (myrtilli) – moliniosum (caeruleae)* and *Quercetum (roboris) convallariosum (majalis).* Findings indicate a strong response to soil moisture and fertility, with inter-factor interactions significantly impacting plant characteristics. These results underscore the effectiveness of using size and vitality traits in long-term monitoring of *Stellaria holostea* populations.

**Keywords:** population analysis, *Stellaria holostea*, vitality, phytocoenose, morphometry.

## INTRODUCTION

The herbaceous layer is not only an important component of forest systems but also a structure that is highly sensitive to changes in the ecological and coenotic conditions of habitats, driven by both natural and anthropogenic factors. Given this, studying the processes occurring at the herbaceous layer level holds significant theoretical and practical importance. Priority should be given to research focusing on dominant coenosis-forming species, such as *Stellaria holostea*. Conducting studies within protected areas facilitates the implementation of long-term monitoring.

https://doi.org/10.5593/sgem2024v/3.2/s13.38

## MATERIALS AND METHODS

The research was conducted using a combination of diverse methods. To establish the species composition and leading characteristics of the phytocoenoses mentioned, geobotanical descriptions were based on generally accepted approaches. The materials from the geobotanical descriptions allowed for the eco-indication of environmental conditions in the habitats of *Stellaria holostea* populations. [7] For this, ecological scales developed under the guidance of Ya.P. Didukh were used.[5] The processing and summarizing of geobotanical description data were conducted using specialized computer software adapted by the M.G. Kholodny Institute of Botany of the National Academy of Sciences of Ukraine to the Turboveg software interface. As a result, score values for ten ecological factors were determined for each habitat: soil moisture regime (Hd), soil moisture variability (Fh), soil acidity (Rc), carbonate content in soil (Ca), nitrogen content in soil (Nt), soil salinity (Tr), light availability (Lc), temperature regime of the area (Tm), climate continentality (Cn), and cryoregime (Cr) (Table 2).

The assessment of *Stellaria holostea* populations was comprehensive. Using morphometric analysis, the size parameters of plants (ramets) from each of the six populations were evaluated (Table 3).

Based on the results of morphometric analysis and the subsequent application of vitality analysis following the algorithm developed by Yu.A. Zlobin, *Stellaria holostea* plants were classified into three vitality classes: high ("a"), intermediate ("b"), and low ("c"). [9]The populations, depending on the representation of plants from these three classes, were categorized into three qualitative types: depressive, balanced, and thriving.

The results of the morphometric and vitality analyses, along with phytindication, were processed using correlation, variance, and regression analyses, as well as mathematical modeling. [6, 7] These methods allowed for the identification of ecological relationships within *Stellaria holostea* populations and the analysis of the influence of 10 ecological factors on them.

## TABLES, GRAPHS & FIGURES

Table 1

Forest vegetation associations in which the studied populations of Stellaria holostea grow

| № of population | Association |
|---|---|
| 1 | *Betuletum (pendulae) caricosum (pilosae)* |
| 2 | *Betuletum (pendulae) vacciniosum (myrtilli)* |
| 3 | *Pinetum (sylvestris) convallarioso (majalis) – hylocomiosum* |
| 4 | *Pinetum (sylvestris) vaccinioso (myrtilli) – moliniosum (caeruleae)* |
| 5 | *Pinetum (sylvestris) vaccinioso (myrtilli) – sphagnosum* |
| 6 | *Quercetum (roboris) convallariosum (majalis)* |

Table 2

Generalized information on the ecological conditions of the studied populations of *Stellaria holostea*

| Ecological factors | The range of values (from Min to Max) of the ecofactor score indicators registered by the growing sites of Stellaria holostea populations and their characteristics according to the Y.P. Didukh's ecoscales | |
|---|---|---|
| | Min | Max |
| Hd | 12,4 | 12,6 |
| | Transitional from dry forest meadow to wet forest meadow | |
| Fh | 5,2 | 5,6 |
| | Weakly variable humidification | Transitional from weakly variable to moderately variable humidification |
| Rc | 6,5 | 7,5 |
| | Transitional from acidic (pH = 4.5–5.5) to slightly acidic soils | Slightly acidic soils (pH = 5,5–6,5) |
| Ca | 5,3 | 6,2 |
| | Carbonate content 0, 5% | Carbonate content 0,5–1,0% |
| Nt | 5,4 | 6,5 |
| | Transitional soils from poor in mineral nitrogen (0.2–0.3%) to sufficiently supplied with nitrogen | Soils sufficiently supplied with nitrogen (0,3–0,4 %) |
| Tr | 5,8 | 6,5 |
| | Salt-poor podzolic soils | Transitional from salt-poor podzolic soils to fairly salt-rich leached chernozems |
| Lc | 5,2 | 6,3 |
| | Partial shade plants that grow in relative light of less than 10%, occasionally in full light | Transitional conditions for plants from partial shade to partial light |
| Tm | 8,3 | 8,6 |
| | Transitional thermal zone from subboreal to nemoral, RB = 40 kcal/cm$^2$/year | |
| Cn | 8,4 | 8,7 |
| | Conditions transitional from hemioceanic to hemicontinental climate (Kn = 121–130%) | |
| Cr | 7,9 | 8,3 |
| | Winters are moderately severe. (Cr = –14 – –10 $^0$C) | Transitional winters from moderately severe to mild (Cr= –10 – –6$^0$C) |

https://doi.org/10.5593/sgem2024v/3.2/s13.38

Table 3
Morphoparameters which have been measured for *Stellaria holostea* plants

| Morphoparameters | Symbol and calculation formula | Units of measurement |
|---|---|---|
| Static metric morphoparameters | | |
| The length of the shoot | H | cm |
| Total number of leaves | NL | pcs. |
| The total mass of the aerial part of the plant | W | g |
| Total surface area of the leaves | A | $cm^2$ |
| Static allometric morphoparameters | | |
| Leaf surface per plant mass | LAR = A/W | $cm^2/g$ |
| Photosynthetic effort | LWR = WL/W | g/g |

Table 4
The significance of morphological parameters of *Stellaria holostea* plants in different forest vegetation associations

| Morphoparameters[1] | Populations[2] and average values of morphoparameters | | | | | | P-level |
|---|---|---|---|---|---|---|---|
| | 1 | 2 | 3 | 4 | 5 | 6 | |
| | $\overline{X} \pm S_{\bar{x}}$ | $\overline{X} \pm S_{\bar{x}}$ | $\overline{X} \pm S_{\bar{x}}$ | $\overline{X} \pm S_{\bar{x}}$ | $\overline{X} \pm S_{\bar{x}}$ | $\overline{X} \pm S_{\bar{x}}$ | |
| W | 0,65±0,064 | 0,82±0,078 | 0,67±0,069 | 1,70±0,14 | 0,57±0,058 | 1,43±0,109 | 0,00000 |
| H | 15,0±0,57 | 14,8±0,73 | 17,1±0,86 | 28,1±1,43 | 18,5±0,98 | 25,7±0,88 | 0,00000 |
| NL | 12,9±0,68 | 14,7±0,60 | 16,2±1,47 | 18,5±0,90 | 25,5±1,42 | 16,9±0,62 | 0,00000 |
| A | 90,5±4,76 | 68,9±2,82 | 69,8±6,33 | 157,3±7,66 | 76,5±4,25 | 80,4±2,96 | 0,00000 |
| LAR | 152,1±10,00 | 91,0±5,81 | 114,3±8,83 | 100,7±6,99 | 144,6±11,50 | 69,8±9,85 | 0,00000 |
| HWR | 25,8±1,99 | 19,6±1,40 | 29,0±2,13 | 18,2±1,57 | 34,4±2,08 | 21,7±2,37 | 0,00000 |

Notes:
[1]The symbols of morphoparameters here and further in the text correspond to Table 3;
[2]Here and further in the text the numbering of populations corresponds to Table1

Table 5
Vitality structure of *Stellaria holostea* populations in different forest vegetation associations

| № of population | Populations of associations | The share of plants of different classes of vitality | | | The value of the quality index Q | Qualitative type of population |
|---|---|---|---|---|---|---|
| | | a | b | c | | |
| 1 | *Betuletum (pendulae) caricosum (pilosae)* | 0 | 0.20 | 0.80 | 0.100 | depressed |
| 2 | *Betuletum (pendulae) vacciniosum (myrtilli)* | 0.07 | 0 | 0.93 | 0.035 | depressed |
| 3 | *Pinetum (sylvestris) convallarioso (majalis) – hylocomiosum* | 0.18 | 0.09 | 0.73 | 0.135 | depressed |
| 4 | *Pinetum (sylvestris) vaccinioso (myrtilli) – moliniosum (caeruleae)* | 0.9 | 0.05 | 0.05 | 0.475 | prosperous |
| 5 | *Pinetum (sylvestris) vaccinioso (myrtilli) – sphagnosum* | 0.07 | 0.27 | 0.66 | 0.170 | balanced |
| 6 | *Quercetum (roboris) convallariosum (majalis)* | 0.78 | 0.13 | 0.09 | 0.455 | prosperous |

## RESULTS

It was established that the *Stellaria holostea* plants from the studied populations statistically significantly differed (p=0.00000) in all six dimensional characteristics (Table 4). Moreover, in different habitats, they exhibited specific features of habitus and morphostructure.

For instance, a distinctive feature of Stellaria holostea plants from population No. 4 (associated with *Pinetum (sylvestris) vaccinioso (myrtilli) – moliniosum (caeruleae)*) is their substantial size. These plants demonstrated the highest values for total phytomass (1.70±0.14 g), leaf area (157.3±7.66 cm²), and shoot length (28.1±1.43 cm).

https://doi.org/10.5593/sgem2024v/3.2/s13.38

A characteristic feature of plants in population No. 1 (associated with *Betuletum (pendulae) caricosum (pilosae)*) is the smallest number of leaves (12.9±0.68) and the highest leaf area ratio (LAR=152.1±10.00 $cm^2/g$).

In contrast, plants from population No. 6 (associated with *Quercetum (roboris) convallariosum (majalis)*) were notable for the lowest LAR values (69.8±9.85 $cm^2/g$).

According to the results of the correlation analysis, the most significant and statistically reliable relationships in *Stellaria holostea* were found between plant mass (r=0.96540), shoot length (r=0.94779), and nitrogen content in the soil. A strong and statistically significant correlation was also observed between leaf surface area and soil salinity (r=0.90061), as well as soil calcium content (r=0.85975) and soil acidity (r=0.82806).

It has been determined that *Stellaria holostea* plants are clearly differentiated into three vitality classes based on their vitality levels: the lowest (class "c"), intermediate (class "b"), and highest (class "a") (Table 5). Depending on the representation of plants in these classes, the quality index (Q) values of the studied populations range from 0.035 to 0.475, with the populations belonging to all three quality types: from depressive to thriving.

The study of the impact of ecological factors on the vitality characteristics of populations revealed a significant and strong correlation between the quality index (Q) values and soil nitrogen content (r=0.90668). The influence of thermal regime conditions is also significant and reliable (r=0.795208). Regular changes in the vitality characteristics of Stellaria holostea populations occur under the interaction of these factors: as their scores increase, the vitality levels of the populations, and consequently the quality index (Q), also rise.

## DISCUSSION

The study of *Stellaria holostea* populations in the Desniansko-Starohutskyi National Nature Park highlights how environmental factors shape plant vitality and morphological characteristics. Populations exhibited statistically significant differences in morphometric parameters such as shoot length, leaf area, and plant mass, reflecting the influence of soil nitrogen levels, salinity, and acidity. These results align with similar studies conducted in diverse forest ecosystems across Europe and emphasize the utility of morphometric and vitality analyses in ecological monitoring.

Our findings regarding the strong correlation between soil nitrogen content and plant vitality (r = 0.90668) echo results reported by Dubuis et al., who identified nitrogen availability as a key determinant of plant species distribution and fitness in temperate forests. [1] In particular, populations in nitrogen-rich habitats (e.g., Population 4) exhibited higher vitality indices and morphological robustness. This relationship underscores the critical role of nutrient availability in supporting forest understory species.

Studies by Ellenberg on the ecological requirements of central European flora also provide a comparative basis. [2] Like *Stellaria holostea*, many shade-tolerant species demonstrated a preference for mildly acidic to slightly basic soils. Our observation of significant vitality differences between populations in pine-dominated versus oak-dominated associations aligns with Ellenberg's findings that soil pH and calcium content influence understory community composition and vigour.

Additionally, research conducted by Hédl et al. in mixed forests of the Czech Republic supports the observed influence of light availability and thermal conditions on plant morphology. [4] The balanced and prosperous populations in our study, such as Population 6 (*Quercetum roboris convallariosum*), reflected similar adaptations to intermediate light conditions and moderate temperature variability, consistent with Hédl et al.'s conclusions.

Our results contrast with findings from Mediterranean forest ecosystems, where nutrient-poor soils and higher temperatures constrain the growth and vitality of understory species. For instance, García-Camacho et al. reported limited morphometric variation in species subjected to more extreme climatic conditions, underscoring the influence of macroclimatic factors. [3] In this context, the moderate climate of northeastern Ukraine provides a more favorable environment for morphological plasticity in *Stellaria holostea* populations.

The strong statistical relationships between ecological factors and plant vitality indices underscore the importance of monitoring edaphic and climatic conditions in protected areas. Integrating methodologies like those employed by Didukh and Zlobin et al., which combine ecological scaling and mathematical modelling, enhances our ability to predict population responses to environmental change. [5, 9] Our study adds to the growing body of evidence supporting long-term ecological monitoring programs, which are increasingly critical in the face of anthropogenic pressures and climate change.

Our studies also confirmed statistically significant changes in the morphometric parameters and vitality levels of *Stellaria holostea* plants and populations under different forest site conditions, as well as the dependence of these characteristics on soil acidity and organic matter content. [8]

Future studies could benefit from incorporating genetic and phenotypic analyses to investigate adaptive mechanisms within *Stellaria holostea* populations. Moreover, comparisons with species occupying similar niches in other climatic zones could provide insights into broader ecological strategies and resilience mechanisms.

## CONCLUSION

The study of ecological relationships in *Stellaria holostea* populations has revealed statistically significant responses of their size-vitality characteristics to a range of ecological factors. These factors primarily include those characterizing the edaphotope, such as soil nitrogen and calcium content, soil acidity levels, and soil salinity.

The observed responses of *Stellaria holostea* populations to changes in ecological conditions and their distribution within various forest vegetation associations in the Desniansko-Starohutskyi National Nature Park are consistent with findings from parallel studies conducted in the Göttingen Forest in southern Lower Saxony, Germany. In both study regions, the size-vitality traits of *Stellaria holostea* populations have proven to be highly informative for assessing the impact of environmental factors. This reinforces their utility in ecological monitoring and research. The consistent findings from Ukraine and Germany also emphasize the significance of employing standardized methodologies for population studies across different biogeographical regions.

In conclusion, the results of these investigations, conducted in distinct and geographically distant parts of the *Stellaria holostea* range, objectively confirm the high informativeness of size-vitality traits. This makes a compelling case for incorporating

https://doi.org/10.5593/sgem2024v/3.2/s13.38

these characteristics into comprehensive population analysis of *Stellaria holostea* systems and long-term population monitoring programs.

**ACKNOWLEDGEMENTS**
The reported results are based on a project funded by DBU (www.dbu.de).

**REFERENCES**

[1] Dubuis, A., Giovanettina, S., Pellissier, L., et al. Improving the prediction of plant species distributions by integrating edaphic and climatic factors. Journal of Biogeography, United Kingdom, vol. 40/issue 11, pp. 2108–2119, 2013.

[2] Ellenberg, H. Vegetation Ecology of Central Europe. Cambridge University Press, United Kingdom, vol. 1, 1-731, 1988.

[3] García-Camacho, R., Iriondo, J. M., Escudero, A. Seedling dynamics in a Mediterranean forest: Recruitment patterns and spatial distribution. Acta Oecologica, France, vol. 39, pp. 31–39, 2012.

[4] Hédl, R., Kopecký, M., Komárek, J. Half a century of succession in a temperate oakwood: From species-rich community to mesic forest. Diversity and Distributions, United Kingdom, vol. 16/issue 2, pp. 267–276, 2010.

[5] Didukh Ya. P. The ecological scales for the species of Ukrainian flora and their use in synphytoindication. Phytosociocentre, Ukraine, vol. 1, pp. 1-176, 2011.

[6] Phytodiversity of reserves and national nature parks of Ukraine, National natural parks, Phytosociocenter, Ukraine, vol. 2, 2012.

[7] Yakubenko B., Popovych S., Ustymenko P., Dubyna D., Churilov A. Geobotany: Methodological Aspects of Research. Kyiv National University, Ukraine, 2020.

[8] Yaroshenko N., Skliar V., Rosenthal G. Evaluation of ontogenetic and vital structures of *Stellaria holostea* L. in beech forests in the South of Low Saxony, Germany. International Multidisciplinary Scientific GeoConference: SGEM, Bulgaria, vol. 23/issue 3.2, pp. 325-332, 2023. DOI: 10.5593/sgem2023V/3.2/s14.40.

[9] Zlobin Y., Kovalenko I., Klymenko H., Kyrylchuk K., Bondarieva L., Tykhonova O., Zubtsova I. Vitality Analysis Algorithm in the Study of Plant Individuals and Populations. The Open Agriculture Journal, United Arab Emirates, vol. 15, pp. 119-129, 2021.

# SPECIES DIVERSITY OF HARMFUL BARK BEETLES IN SPRUCE FORESTS OF ADJARA REGION (GEORGIA)

**PhD Ress Nino Manvelidze[1]**
**Prof. Dr. Medea Burjanadze[2]**
**Assoc. Prof. Dr. Lali Jgenti[1]**
**Assoc. Prof. Dr. Natela Varshanidze[1]**

[1] Batumi Shota Rustaveli State University, **Batumi, Georgia**
[2] Georgian Technical University, **Tbilisi, Georgia**

## ABSTRACT

Several species of Bark beetles (Coleoptera: Scolytinae) are capable of causing significant amounts of tree mortality in conifer forests throughout much of the world and in the South Caucasian Mountain as well.

In the paper, is discussed about species diversity of harmful bark beetles, which are damage and cause the decline of the *Picea orientalis*, in the conifer forest of Shuakhevi and Khulo municipalities of Adjara (Western Georgia), at an altitude of 700-1500 m a.s.l. This is one of the current problems in spruce forests of mentioned region.

Field studies were carried out in Shuakhevi municipality at 700-900 m a.s.l. and in Khulo municipality 1200-1500 m a.s.l.

The route expedition, planning of the research area, insect identification, bioecology-phenology, using pheromon traps were used for the accepted methods. The statistical processing of the data was carried out mathematically modeling through the IMB-SPSS23 program.

As a result of the research, it was revealed that in the coniferous forest of Shuakhevi and Khulo, where represented *Picea orientalis* , damage to the bark and the drying of the plant are caused by the most important three species of bark beetle: *Ips typographus* L., *Ips sexdentatus* Boern. and *Dendroctonus micans* Kugelann. Also, were found that all three species live together under the bark. The optimal limit of their distribution was established. It should be noted that all three species gives only one generation in a year in spruce forests of Adjara. Compared to spruce forests damages by bark beetles of Khulo municipality, to Shuakhevi municipality is 30% higher. The optimal limit of their distribution is 700-1000 m. a.s.l.

**Keywords:** Bark beetles, Spruce forest, South Caucasian, Adjara, Pheromones

## INTRODUCTION

The Autonomous Republic of Adjara is located in the southwestern part of Georgia on the Black Sea coast. Its southern border coincides with the Turkey-Georgia state border and follows the Shavsheti ridge. It is bordered by the Meskheti range from the north, the Arsian range from the east, and the Black Sea from the west.

The floristic region of Adjara is distinguished by the variety of relict Colchian mountain and foothill forests, among which a large place is occupied by conifer forests with the species of *Picea orientalis* (L.) and *Abies nordmanniana* (Stev.). It should be

https://doi.org/10.5593/sgem2024v/3.2/s13.39

noted that in the initiative of the World Wildlife Fund (WWF) "about 100 hotspots of European forests, i.e. about 100 sections of protected forests that definitely need protection, one of the first priorities was given to the unique forest ecosystems of Adjara [1].

In recent years, the situation became alarming regarding *Picea orientalis* (L.), that decline has become in the mountainous of coniferous forests of Adjara, which is caused by various species of bark beetles (Coleoptera: Scolytidae IN: CABI 2024), some species were particularly harmful and threatened the existence and reproduction of spruce groves.

Bark beetles are known worldwide as important pests of woody species, as they develop and feed under the bark of the plant. Different parts of the tree (roots, root neck, lower part of the trunk, middle part of the trunk, trunk, branches, twigs) and different layers of wood in the same part are chosen for settlement. This circumstance is typical for the species [2]. They mainly cause physiological damage to the plant, some species cause technical damage as well.

In the presented paper, is discussed about bark beetles, spreading in the territory of Shuakhevi and Khulo municipalities of Adjara, 700-1500 m. a.s.l.

Species diversity of harmful bark beetles, which damage the bark of *Picea orientalis* and cause the plant decline, is one of the current problems for the region. In the paper, it is discussed about species diversity of harmful bark beetles, which are damage and cause the decline of the *Picea orientalis*, in the conifer forest of Shuakhevi and Khulo municipalities of Adjara (Western Georgia), at an altitude of 700-1500 m a.s.l. This is one of the current problems in spruce forests of the mentioned region.

## MATERIALS AND METHODS

In order to assess the species composition and intensity of distribution of harmful bark beetles, research were conducted in Shuakhevi Municipality within 700-900 m. and in the municipality of Khulo, Within the height of 1200-1500 m. a.s.l. in 2021-2023. Only one species of spruce, *Picea orientalis* L., is common in the mentioned areas.

The detection of beetles' composition, their damage and determination of their intensity were used existing method for studying harmful insects [3]. Studies were conducted using squaring and routing methods to assess the entomological condition of the gardens [4].

The square method involves identifying specific areas (squares) in the study area where observations and data collection on insects and plant conditions are conducted. This allows for more accurate and representative data to be obtained. The route method involves surveying the area along a predetermined route, which allows for identifying the spread of pests in different zones. This method can be useful for assessing the dynamics of the phytosanitary condition during the season. The combined use of these methods provide a complete picture of the ecosystem condition and will help in developing plant protection measures.

Insects in all stages of development (eggs, larvae, adults) were collected. The percentage of collected material were determined in laboratory. The number of insects were determined on a 4-point scale using existing methods [3, 4].

The material collected in the field were placed in a special container, in line with the common methodology; it was appropriately labeled and placed in a special ice bag. The biomaterial were delivered to the laboratory for further research [5]. Entomological books were used for insect identification and taxonomic study [6, 7].

In order to monitoring the bio-ecological characteristics of bark beetles, permanent sample areas (Shuakhevi, Khulo) in the spruce forests of Adjara, 700-1500 m.a.s.l., were placed signaling pheromone traps. From each trap, were inspected daily before the mass flight, and then once a week, based on which determined of adults flight seasonal dynamics and distribution areas.

Biologically active substances, pheromones, were used in order to track the nests and flight dynamics of the beetles. For the purpose of making sign, 1 trap per 10 ha will be hung in the conifer forest. Seasonal dynamics of beetle flight and pest stock were determined by pheromone traps [8].

The obtained data were reliably processed and calculated using the formula of Abbott, 1925 [9] and mathematical modeling program IMB-SPSS23 [10].

## RESULTS

In order to identify the species composition and new foci of distribution of bark beetles common in spruce forests, studies were conducted in natural spruce groves of Shuakhevi and Khulo (24305.1 ha) municipalities, where it was revealed that in the spruce groves of Shuakhevi and Khulo, damage to the bark of oriental spruce - *Picea orientalis* L. and spruce stands decline are caused by three species of bark beetles: *Ips typographus* L., *Ips sexdentatus* Boern. and *Dendroctonus micans* Kugelann among which *Ips typographus* L. dominates in terms of distribution intensity and population size (Table 1).

Table 1. Collected bark beetles in the administrative unit of Shuakhevi Spruce forest (600-1000 a.s.l λ = 41°62′09″ - ά =42°19′17″). H* – tree height, D* – tree diameter, P* – tree age

| # | Data collection | meter a.s.l. | name of bark beetle | Species of host plant | H* (m) | D* (cm) | P* (age) | Number of insects | % |
|---|---|---|---|---|---|---|---|---|---|
| 1 | 10.07.23 | 700 | *Ips typographus* | *Picea orientalis* | 20-25 | 40-55 | 75-100 | 197 | 42 |
| 2 | 18.09.23 | 800 | *Dendroctanus micans* | *Picea orientalis* | 15-25 | 35-50 | 80-100 | 42 | 9 |
| 3 | 02.06.23 | 1000 | *Ips typographus*<br>*Ips sexdentatus* | *Picea orientalis*<br>*Picea orientalis* | 20-25 | 35-55 | 75-100 | 132<br>98 | 28.1<br>20.9 |
| | | | | | | | | Total ∑=469 | 100 |
| *Ips typographus* – 70.2%; *Ips sexdentatus* - 20.9%; *Dendroctanus micans* – 0.9% | | | | | | | | | |

https://doi.org/10.5593/sgem2024v/3.2/s13.39

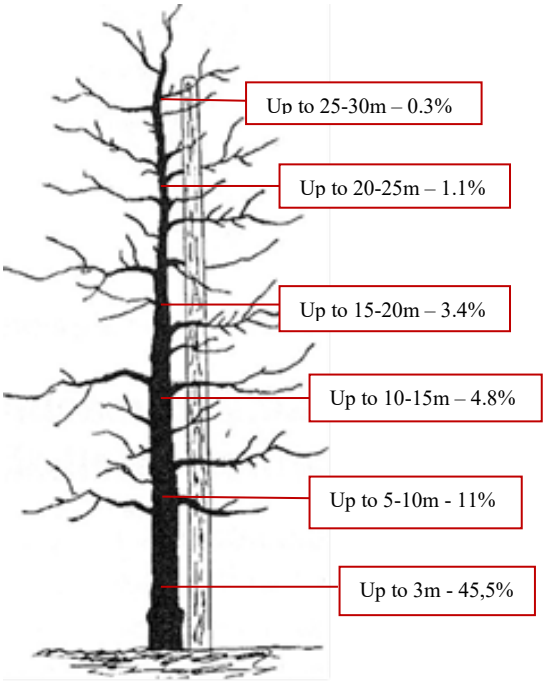
By examining and studying bark samples damages, we determined that all three species of bark beetles live together under the bark with different rates of settlement frequency.

The flight dynamics of bark beetles using pheromone traps placed at different altitudes and temperatures above sea level were studied. In particular, bark beetles flew at temperatures of 5-16$^0$C, while constant flight and strong activity occurred at temperatures of 20-25$^0$C.

Observations of pheromone traps showed that bark beetles are found with varying intensity of settlement everywhere where eastern spruce is widespread, but they are mainly found between 700 and 1000 m above sea level, which indicates the optimal limit of their distribution.

The intensity of settlement of individual species of identified bark beetles on different parts of the host plant were studied. *Ips typographus* was found as a along the entire length of the stem and on the branches as well, but it is not found on the roots. *Ips sexdentatus* and *Dendroctonus micans* were examinate on the roots and stem mainly up to a height of 3 m from the ground surface, but above they settlement rate gradually decreases (Figure 1). Settlement of *Dendroctonus micans* on the branches of the trees do not observed.

Figure 1. Frequency of *Dendroctonus micans* settlement on different sections of *Picea orientalis* stem.




## DISCUSSION

Nowadays, the most dangerous of the bark beetles harmful to conifers is the spruce bark beetle *Ips typographus*. Since 2001, massive reproduction has begun in the spruce forests of the Borjomi Valley and spread in territory of Georgia. The harmful effects of

the pest have been noted in recent years not only in Georgia, but also in the coniferous forests of neighboring countries, in particular, the border region of Turkey [11, 12].

*I. thypographus* in European country attack to Norway spruce - *Picea abies* Karst. [13], however its attract *Picea orientalis,* which is dominant species in conifer forest of South Caucasian region [14]. It is widely recognised and poses a serious threat to forestry in the Adjaria coniferous forest in Khulo and Khelvachauri municipality [15].

These results show that the attack of trees by bark beetles, study they composition can be used in management of endangered spruce forests.

## CONCLUSION

Three primary species *Ips typographus*, *Ips sexdentatus* and *Dendroctonus micans* have been identified as major contributors to tree mortality and forest decline within the altitudinal range of 700-1500 m a.s.l. Notably, *Ips typographus* has emerged as the dominant species in terms of both distribution intensity and population size.

The optimal distribution of these pests was determined to be between 700-1000 m a.s.l., with a marked increase in damage severity observed in the Shuakhevi municipality compared to Khulo.

The study underscores the urgent need for monitoring and management strategies to mitigate the effects of bark beetles on spruce forests in the region. Given the ecological importance of *Picea orientalis* and the unique forest ecosystems of Adjara, further research is necessary to develop effective pest management practices and to safeguard these vital habitats from further decline. The findings contribute valuable insights into the dynamics of bark beetle populations and their interactions with coniferous forest ecosystems, emphasizing the necessity for ongoing surveillance and conservation efforts in the face of these growing threats.

## ACKNOWLEDGEMENTS

We would like to express our gratitude to Mr. Rezo Vasadze, Head of the Pest and Disease Control Service of the Ajara Forestry Agency and Doctor of Agricultural Sciences, for his assistance and sharing of expertise during the fieldwork.

## REFERENCES

[1] Manvelidze Z., Memiadze N., IN: The map-"100 European Forests We Should Protect Now", 1997, Georgia, 2022.

[2] Burjanadze M., Supatashvili A., Harmful Bark beetles common in coniferous forests of Georgia, Georgia, 2020.

[3] Zehnder G., Overview of Monitoring and Identification Techniques for Insect Pests, 2020. https://eorganic.org/node/2721

[4] Dobrovolsky B. B. Phenology of insects: Ucheb. пособие для ун-тов, ped. и с.-х. узов. - M.: Vysshaya Shkola, 1969, p 232. (in Russia).

[5] LSAM. How to Make an Insect Collection. lsuinsects. Org / DIY Insect Collection. pdf. DIY Insect Collection. http://lsuinsects.org

[6] Busarova N.V., Negrobov O.P. Entomology. Key to insect families 2nd ed., Per. and additional Textbook for universities, 2020, p 182. (in Russia).

https://doi.org/10.5593/sgem2024v/3.2/s13.39

[7] Jacobson G.G., Beetle determinant Eur. parts of the USSR. Leningrad, 1931, p 454. (in Russia).

[8] Santín C., Doerr SH., Preston C., González-Rodríguez G., Pyrogenic organic matter production from wildfires: a missing sink in the global carbon cycle. Global Change Biology, 1633, 2015.

[9] Abbott W.S., A method of computing the effectiveness of an insecticides, Journal of Economic Entomology 18, 1925, pp 265-267.

[10] Marcus R., Eaves D.M., Statistical and Computational Analysis of Bioassay Data. In: Bioassays of Entomopathogenic Microbes and Nematodes. Navon, Amos, Ascher, K. R. S. (Editor), CAB Intl, p 324, 2000.

[11] Burjanadze M. Entomopathogenic fungi of Ips Typographus in Georgia. IOBC wprs Bulletin, Bulletin OILB srop, "Insect Pathogens and Insect Parasitic Nematodes", Vol. 30(1) pp 151-156, 2005.

[12] Gokturk T., Burjanadze M., Aksu Y., Supatashvili A. Nature Enemies, Predator, Pathogens and Parasitic Nematodes of Bark Beetles in Hatila Valley National Park in Turkey. Proceedings of Georgian Academy of Sciences. Biological Series B, 8:47-58. ISSN 1412-2123, 2010.

[13] Blomqvist M,. Kosunen M., Starr M., Kantola T, Modelling the predisposition of Norway spruce to Ips typographus L. infestation by means of environmental factors in southern Finland - European Journal of Forest research , V.137, pp 675–691, 2018.

[14] Tvaradze M., Supatashvili A., Kobakhidze L., Kraveishvili I., Perspectives of integrated control against the Ips typographus L in Georgia. Journal of the Georgian Academy of Agriculture, Tbilisi, vol. 17, pp. 70-77, 2006.

[15] Vasadze R., Mamuladze M. and Vasadze Z., SOME BIOLOGICAL FEATURES OF THE CRUSTACEAN TYPOGRAPHER, International journal of advanced research (IJAR), pp255-267, 2023.

# STRUCTURAL CONNECTIVITY ANALYSIS IN THE CARPATHIAN ECOREGION: PRELIMINARY STEPS FOR DEVELOPING LANDSCAPE NETWORKS

**Radu Tudor** [1]
**Ileana Patru-Stupariu** [2]
**Ancuța Fedorca** [3]
**Mirea Marian** [1]

[1]PhD Ress, Faculty of Geography, Doctoral School Simion Mehedinti, University of Bucharest Bd. N. Bălcescu, 1, 010041 Bucharest, **Romania**;

[2]Institute of Research of University of Bucharest, ICUB, Transdisciplinary Research Centre Landscape-Territory-Information Systems, CeLTIS, Splaiul Independței no. 91 - 95, 050095 Bucharest, **Romania**;

[3]CSI Senior Researcher at National Research and Development Institute in Forestry "Marin Dracea" Bulevardul Eroilor 128, Voluntari 077190 | ICAS · Department of Wildlife Biology, **Romania**

## ABSTRACT

Landscape and ecosystem preservation represents an integrated approach for conserving healthy and interconnected ecosystems. In order to maintain high-quality habitats and maximising the ecosystem services is crucial to have a good bond between connected areas. On both the Romanian and European levels, the backbone of these interconnected areas is formed by Natura 2000 networks [1]

The objectives of our study aim to address the Biodiversity 2030 Directive, which mandates the establishment of a coherent network of protected areas and the legal protection of at least 30% of the terrestrial surface of each EU country [2]. Currently, Romania has 23% of its terrestrial surface under protection.

To summarise, our goal is to create a landscape network at the level of the Romanian Carpathian ecoregion using structural connectivity analyses, of course, we will accomplish several secondary objectives before reaching this final goal, such as: identifying and classifying connectors, identifying forest patches favourable to the connectivity of protected areas, and classifying protected areas based on connectivity. To ensure high-quality habitats and maximize ecosystem services, such a network requires strong connections between different areas.

**Keywords:** landscape network, structural connectivity, forest habitat, Natura 2000, connectors

## INTRODUCTION

### Study area

The Carpathian Ecoregion is one of Europe's most ecologically valuable areas, crucial for biodiversity conservation at national and European levels. Centrally located in Romania, it stretches over a vast area that includes extensive depression zones, hills, and

plateaus, along with three Carpathian subgroups. These regions are characterised by diverse landscapes, ranging from dense forests and alpine meadows to rivers and glacial lakes. This region hosts Romania's highest density of protected areas, including national and natural parks as well as Natura 2000 sites, forming an essential network dedicated to safeguarding valuable ecosystems and rare species [3].

According to WWF, the Carpathians are key to maintaining ecological connectivity between Western and Eastern Europe. Preserving this region's ecological integrity is vital for biodiversity and the ecosystem services supporting the local economy and human well-being [3]. Romania's forests, rich in biodiversity and ecological value, form an ecosystem of major importance at the European level [4].

**Study motivation**

This study aims to support the EU Biodiversity Strategy for 2030, part of the European Green Deal, which seeks to restore biodiversity and halt ecosystem degradation in Europe, establishing a framework for nature protection and sustainability [5]. A central goal of the strategy is to increase protected areas so that at least 30% of each EU state's land and marine territories are legally protected by 2030. Romania currently protects about 23.4% of its land, showing progress but still below the directive's target [6]. Another focus of the directive is enhancing protected areas through a cohesive network, primarily based on Natura 2000, to create interconnected ecological landscapes ensuring ecosystem continuity [5].

According to the report *Building a Coherent Trans-European Nature Network*, published by the European Environment Agency, establishing a trans-European nature network is a crucial step toward ensuring ecological continuity across the continent [1]. This insight helped shape our research question: *"Can we model a structural landscape network using spatial data from forest plots and protected areas through GIS techniques?"* Our study represents an initial step in this direction, aiming to identify ecological structures that could facilitate connectivity at both national and cross-border levels.

**Objectives**

Aligned with the 2030 Biodiversity Strategy, this study contributes to its goals by examining structural connectivity in Romania's Carpathian ecoregion, a precursor to functional connectivity. Structural connectivity addresses physical links between habitats, while functional connectivity considers species' use of these links for migration, dispersal, and other ecological functions [7]. Our analyses will focus on structural connectivity, utilizing GIS data and techniques to meet specific objectives:
**O1.** Identify Natura 2000 protected areas containing significant forest habitats that are suitable for inclusion in the study.
**O2.** Identify forest plots (OECM ≥ 3500 ha) directly connected to the Natura 2000 Protected Area Network and classify them based on their importance to structural connectivity; assess protected areas directly linked to the network.
**O3.** Evaluate the connectivity cost within the Carpathian ecoregion.
**O4.** Identify ecological connectors, calculate their density within each Carpathian subgroup, and prioritize them accordingly.
**O5.** Finalize the structural network for the Carpathian ecoregion and conduct an in-depth analysis of this network.

## DATA AND METHODS

### Data

The geographic analysis was conducted using ArcGIS Pro. The initial step involved acquiring vector data for different types of landcover from the Corine Land Cover (CLC) dataset. Corine Land cover 2018 (vector) - the land cover data (LAN) were sourced from the Corine Land Cover service for the year 2018, with a raster resolution of 100x100 m. (https://land.copernicus.eu/en/products/corine-land-cover/clc2018).

Data for Sites of Community Importance (SCI) and Special Protection Areas (SPA) were imported into the project. Natura 2000 End 2021 – Shapefile (https://www.eea.europa.eu/data-and-maps/data/natura-14/natura-2000-spatial-data)

The study area boundary was derived from the ConnectGREEN project.

### Selection of Protected Areas Included in the Study

Landscape network modeling, based on connectivity analyses, prioritises forests, as these areas are crucial for landscape connectivity, which supports ecosystem functioning and biodiversity dispersal. Protected forests, under strict regulations, show the highest cover and connectivity, while forest expansion further strengthens structural connectivity [8]. We selected Natura 2000 sites with at least 100 hectares, the minimum area needed to support biodiversity and ecosystem functionality in forest habitats [9]. Additionally, we included areas with at least 65% forest cover, the lowest percentage for small protected sites designated for critical forest habitats, to ensure the inclusion of smaller Natura 2000 areas (<100 ha) with high conservation value. To identify relevant areas, we followed a structured approach: we extracted CLC data for different forest types and merged them into a single polygon layer in ArcGIS Pro. Using the Identity function, SCI/SPA data was integrated with forest polygons, linking each forest area to its corresponding protected zone. We then applied the Dissolve tool to merge polygons with shared SCI/SPA identifiers, simplifying the dataset so each polygon represented forest cover within protected areas. After calculating forest cover percentages within each SCI/SPA, we refined the selection to sites in the Carpathian ecoregion, excluding overlapping zones and small sites within larger areas to maintain connectivity analysis accuracy.

### Identification and Prioritization of OECM ≥ 3500 ha; Identification of Directly Connected Areas/Disconnected Areas

We selected all forest plots of 3,500 hectares or more, a benchmark in forest habitat connectivity studies [1], [10]. These plots qualify as Other Effective Area-based Conservation Measures (OECMs) due to their significant role in habitat connectivity, biodiversity conservation, and ecosystem health, even outside traditional protected areas, fulfilling long-term conservation goals [11]. To maintain connectivity, we included smaller plots directly connected to these main plots, analysed using the *Spatial Join* function in ArcGIS Pro. We then used the same function to identify and prioritize forest plots directly connected to protected areas based on the number of protected areas each intersects. Finally, we reversed this *Spatial Join* (from protected areas to forest plots) to confirm connected and disconnected protected areas within the preliminary network.

### Connectivity Cost Assessment in the Carpathian Ecoregion

To gain a comprehensive view of connectivity across the study area, we applied the "cost-distance" method in ArcGIS Pro, allowing us to model a raster that represents favourable

and unfavourable zones for connectivity in a gradient. This method was applied to a land-use raster derived from Corine Land Cover (CLC) 2018 data, where each land-cover class was reclassified based on its suitability for connectivity. The reclassification process involved assigning a score to each land-cover class, prioritizing forests, and following a scale adapted from a previous study aimed at facilitating forest connectivity. The scores assigned were as follows: Forests - 1, Bushes - 5, Agroforestry mosaics - 15, Pastures - 30, Meadows - 40, Rocks - 40, Crops - 60, Water bodies - 100, and Urban areas and highways – 1000 [12].

### Connector Identification

To identify connections between forest plots and protected areas, we used the least-cost path method in ArcGIS Pro. This method is commonly applied in landscape cost analysis and habitat connectivity studies, forming part of raster-based cost modeling techniques. It evaluates accessibility between different "patches" of land, such as habitat fragments, by calculating the movement cost across a surface between specified locations [13]. The method involves designating start and endpoint locations to determine the least-cost paths. Here, we used the centroids of protected areas not directly connected to the previously established network as starting points, while centroids of forest plots and directly connected protected areas within the network served as endpoints. After generating all connectors, we calculated their density within each Carpathian subgroup using the formula: $\frac{\text{connector length } (Km)}{\text{carpathian group area } (Km^2)}$. To retain only those connectors with substantial network value, we prioritised them based on two criteria: connectors linking protected areas that were previously unconnected to the network, and connectors that link at least two unconnected elements within the network.

### Finalization of the Structural Network at the Carpathian Ecoregion Level

The final step involves consolidating all previously derived elements to model the landscape network. We mapped both protected areas within the network and unprotected zones to obtain a percentage-based distribution between these two categories across the Carpathian ecoregion. This provides a clear overview of the proportion of protected versus unprotected areas, contributing to a more comprehensive assessment of connectivity and conservation coverage within the region.

## RESULTS

### Protected Areas Included in the Study

Initially, we compiled data on forested areas within protected sites and gathered specific information on forests within Sites of Community Importance (SCI) and Special Protection Areas (SPA). This included the number of protected areas within each category (SCI and SPA) and whether or not they contain forested regions (***Table.1)***

| Total forest area in km2 for Romania - 71345.8 km2 |
|---|
| *SCI* |
| Total forest area outside SCI - 48267.1 km2 |
| Total forest area inside SCI - 23078.6 km2 |
| Number of SCI with forest cover - 357 |
| Number of SCI without forest cover - 78 |
| *SPA* |
| Total forest area outside SPA - 55271.6 km2 |
| Total forest area inside SPA - 16074.1 km2 |
| Number of SPA with forest cover - 136 |
| Number of SPA without forest cover - 35 |

***Table.1 Total forest data***

Within the area of interest, we selected 195 protected areas suitable for structural analyses, following the selection criteria: areas with a minimum of 100 hectares of forest, or areas with at least 65% forest cover even if they do not meet the 100 - hectare threshold.

## OECMs ≥ 3500 ha; Identification of Directly Connected/Disconnected Areas

The results reveal significant differences between the eastern and western sections of the Carpathian ecoregion. In the eastern section, specifically within the Apuseni Mountains group, forest plots have increased importance, connecting between 10 and 15 protected areas. This is largely due to the high density of small protected areas within the Apuseni region. In contrast, in the southern and western parts of the ecoregion, specifically within the Meridional and Oriental Carpathian groups, forest plots connect fewer protected areas. Here, the mountain ranges are larger, leading to more extensive protected areas with lower density. Thus, terrain fragmentation is another factor that influences structural connectivity. This analysis showed that 158 Natura 2000 sites are directly connected to forest plots ≥ 3500 hectares, while 37 lack direct connections. Most of the unconnected sites are situated in depressions within the Carpathian arc, with a few exceptions located at the outer edges or in smaller isolated depressions (Fig. 1).

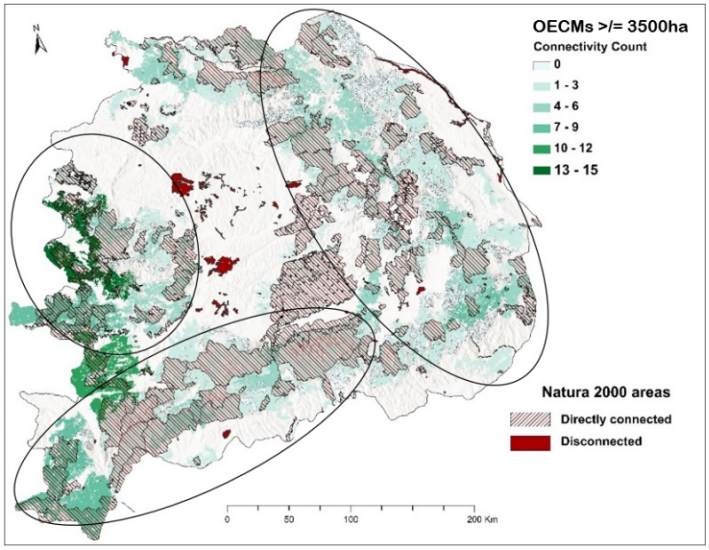



*Fig.1 OECMs >/= 3500ha – Connectivity Count*

## Cost-Distance Raster & Connectors

The "cost-distance" function, applied using the reclassified values from Gurrutxaga et al., 2011 [12], provided a broad view of connectivity cost distribution across the Carpathian ecoregion. Figure 2 highlights high-cost "islands" in the main mountainous depressions, with the most extensive unfavourable connectivity area found within the Transylvanian Depression. The elevated cost in these regions results from the scarcity of forests, as forests were assigned the highest score for facilitating connectivity. The Transylvanian Depression is characterized by a hilly landscape of gentle slopes and broad valleys [14], hosting the major urban centres of the Carpathian ecoregion. As seen in the cost-benefit map, these extensive urban areas significantly increase connectivity costs, further reducing connectivity potential across this section of the ecoregion.

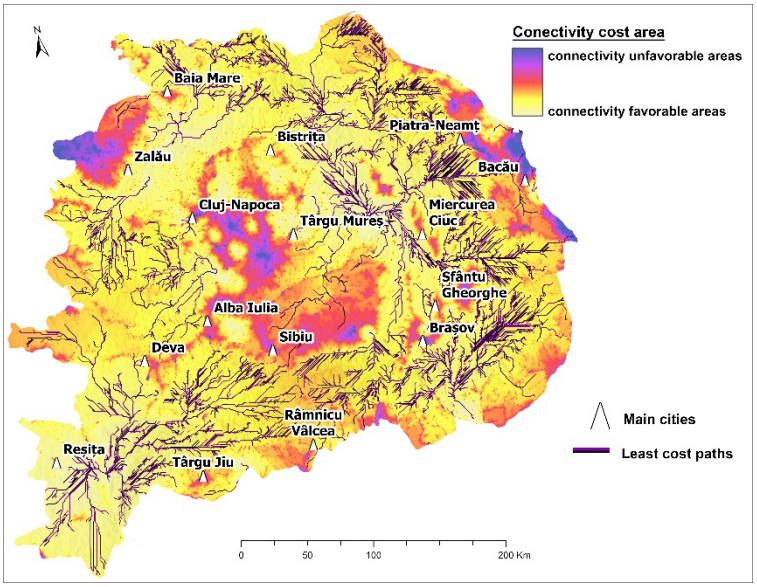



*Fig.2 Conectivity cost area*

The areas most favourable for connectivity are predominantly found in the western part of the ecoregion, especially in the Eastern Carpathians, though high connectivity favorability spans the entire Carpathian arc. By calculating connector density, we obtained values for each Carpathian subgroup, which help assess connectivity favorability relative to each subgroup. This density calculation can be considered a "connectivity indicator," with values providing insights into the density and fragmentation of forest habitats. The results indicate that this "indicator" is twice as high in the Eastern Carpathians (0.40) compared to the Western Carpathians (0.20), while values in the Southern Carpathians (0.36) are only slightly lower than those in the Eastern Carpathians (Fig. 3).

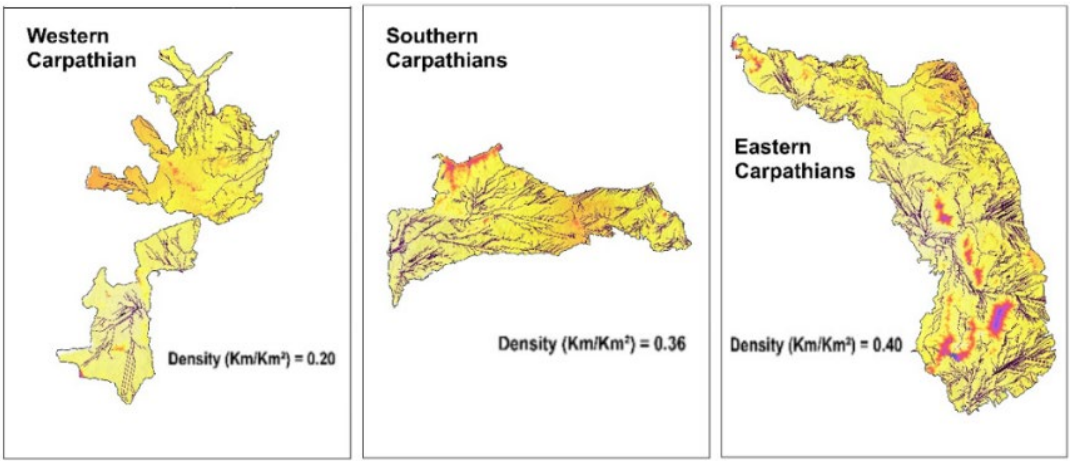



*Fig.3 Density indicator in Carpathian groups*

After removing connectors that linked already-connected elements of the network, we retained a total of 91 connectors that provide essential connections for the network's elements. Some of these connectors facilitate connectivity for 18 protected areas that are not directly linked to the primary network. Through these connectors, we gained a comprehensive view of the connectivity across the 195 sites included in the study, highlighting critical linkage points and areas needing enhanced connectivity.

| Protected areas | Directly connected | Connected by connectors | Disconnected |
|---|---|---|---|
| 195 | 158 | 18 | 19 |

*Table.2 Protected areas situation*

## Finalization of the Structural Network

In the final stage, after consolidating all elements, we achieved a clear representation of the Carpathian structural network. Over half of this network—56.7%, covering 3,274,712.91 hectares—is under protection through the Natura 2000 program, and in some cases, through stricter national protections (such as national parks, natural reserves, or conservation areas of national significance). Meanwhile, 43.3% of the network—2,496,937.73 hectares—consists of unprotected forest plots, areas with no formal protection despite their high structural importance and key role in network connectivity.

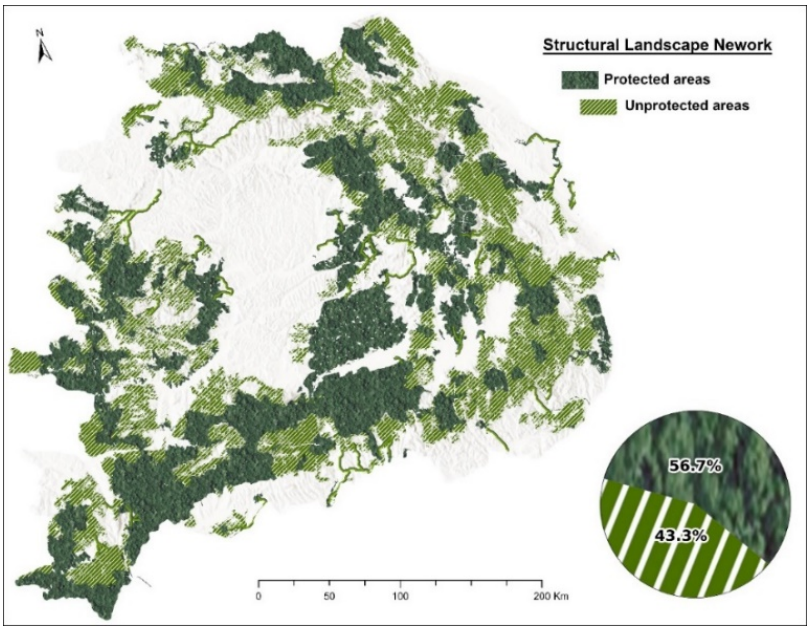



***Fig.4 Structural Landscape Networks in romanian carpathian ecoregion***

## DISCUSSION

The Natura 2000 network forms the foundation for developing the connectivity network identified in our analysis. Key elements within this network, particularly forest plots of 3,500 hectares or more with high structural importance, can be prioritised as future protected areas. This approach aligns with the EU Biodiversity Strategy for 2030, which highlights forest habitat conservation due to their ecosystem services: preventing genetic isolation, supporting species migration, stabilizing climate, storing carbon, and enhancing resilience to natural disasters, as stated in the directive. [5]

The connectivity potential data for the Romanian Carpathian ecoregion reveals vulnerable points, particularly in depression areas with unique landscapes and large urban centres, which are less favourable for connectivity. Initially, 37 protected areas were unconnected, but our methodology identified connectivity potential for 18 of these, linking nearly 50% and raising the overall connectivity rate to 90.25%. The indicator calculated for each Carpathian subgroup provides insight into forest density, primarily reflecting connectivity potential. The highest indicator value in the Eastern Carpathians aligns with other studies showing this subgroup's relatively high forest density within the Romanian Carpathians, underscoring its importance as a key area for maintaining structural connectivity in the ecoregion. [15]

Identifying structural connectors is essential for modeling ecological corridors across the study area. These initial structures, based on the resistance of different landscape types and land uses, help configure ecological corridors [16]. The EU Biodiversity Strategy encourages member states to incorporate ecological corridors into national conservation plans to support species migration and ecosystem adaptation, aiding the goal of protecting 30% of the EU's terrestrial and marine areas by 2030, aligning national efforts with European conservation targets [5]. Some identified connectors, classified as Small Woody Features (SWFs), are small-scale vegetative structures (such as hedgerows, bushes, and tree clusters) within agricultural and natural landscapes. These features enhance connectivity by serving as stepping stones for species movement and habitat

continuity in fragmented environments, playing a vital role in biodiversity and providing habitats for various plant and animal species [17].

## CONCLUSION

The framework provided by the Natura 2000 network, along with data on forest plots within the study area, allowed us to form a structural landscape network in the Romanian Carpathian ecoregion. In other words, this initial data can be used to model a broad ecological network that could be part of a cross-border network.
The results obtained, particularly concerning connectivity, hold significant relevance as they provide insights into the structural status of protected areas (with forest habitats) within the Carpathian ecoregion. The structural network modelling represents an important outcome, offering a detailed graphical representation of landscape structures in the Romanian Carpathians. This enables us to identify structurally vulnerable and prolific regions, enhancing our understanding of the area's landscape dynamics.
The method used addresses a gap in the structural phase as a preliminary step, serving as a foundation for future functional and ecological analyses. Advancing from this point toward a cohesive ecological network will require transdisciplinary collaboration among experts in various fields (e.g., biologists, spatial planning specialists) and the involvement of other key stakeholders.

## REFERENCES

[1] H. Carrao *et al.*, “Contributions to building a coherent Trans-European Nature Network,” 2020.

[2] European Commission, *EU Biodiversity Strategy for 2030*. 2020.

[3] WWF România, “ConnectGREEN - Drum cu prioritate pentru natură. Retrieved from.” Accessed: Sep. 29, 2024. [Online]. Available: https://wwf.ro/ce-facem/specii/coridoare-ecologice/connectgreen/

[4] J. Oszlányi, K. Grodzińska, O. Badea, and Y. Shparyk, “Nature conservation in Central and Eastern Europe with a special emphasis on the Carpathian Mountains,” *Environmental Pollution*, vol. 130, no. 1, pp. 127–134, Jul. 2004, doi: 10.1016/J.ENVPOL.2003.10.028.

[5] European Commission, “EU Biodiversity Strategy for 2030: Bringing nature back into our lives. Retrieved from,” 2021. doi: 10.2779/048.

[6] Biodiversity Information System for Europe, “Romania - Country Information on Biodiversity. Retrieved from.” Accessed: Oct. 23, 2024. [Online]. Available: https://biodiversity.europa.eu/countries/romania

[7] K. Meiklejohn, R. Ament, and G. Tabor, “Habitat Corridors & Landscape Connectivity: Clarifying the Terminology,” 2009. [Online]. Available: www.climateconservation.org

[8] H. Brumberg *et al.*, “Increasing Forest Cover and Connectivity Both Inside and Outside of Protected Areas in Southwestern Costa Rica,” *Remote Sens (Basel)*, vol. 16, no. 6, Mar. 2024, doi: 10.3390/rs16061088.

[9] P. Castro, J. P. Sousa, and J. Alves, “Toward Forests’ Sustainability and Multifunctionality: An Ecosystem Services-Based Project,” *Handbook of Sustainability Science in the Future*, pp. 1–22, 2023, doi: 10.1007/978-3-030-68074-9_115-1.

[10] B. de la Fuente *et al.*, "Natura 2000 sites, public forests and riparian corridors: The connectivity backbone of forest green infrastructure," *Land use policy*, vol. 75, pp. 429–441, Jun. 2018, doi: 10.1016/J.LANDUSEPOL.2018.04.002.

[11] IUCN-WCPA Task Force on OECMs, "Recognising and reporting other effective area-based conservation measures World Commission on Protected Areas Task Force on OECMs," Gland, 2019. doi: 10.2305/IUCN.CH.2019.PATRS.3.en.

[12] M. Gurrutxaga, L. Rubio, and S. Saura, "Key connectors in protected forest area networks and the impact of highways: A transnational case study from the Cantabrian Range to the Western Alps (SW Europe)," *Landsc Urban Plan*, vol. 101, no. 4, pp. 310–320, Jun. 2011, doi: 10.1016/J.LANDURBPLAN.2011.02.036.

[13] Esri, "Understanding Cost Distance Analysis - ArcGIS Pro Documentation. Retrieved from." Accessed: Sep. 30, 2024. [Online]. Available: https://pro.arcgis.com/en/pro-app/latest/tool-reference/spatial-analyst/understanding-cost-distance-analysis.htm

[14] M. Ielenicz and I. Stupariu, *România. Geografie fizică. Vol. I*, vol. Vol. I. Bucharest: Editura Universitara, 2005.

[15] D. Kholiavchuk, W. Gurgiser, and S. Mayr, "Carpathian Forests: Past and Recent Developments," Jan. 01, 2024, *Multidisciplinary Digital Publishing Institute (MDPI)*. doi: 10.3390/f15010065.

[16] H. Ye, Z. Yang, and X. Xu, "Ecological corridors analysis based on MSPA and MCR model-a case study of the tomur world natural heritage region," *Sustainability (Switzerland)*, vol. 12, no. 3, Feb. 2020, doi: 10.3390/su12030959.

[17] European Environment Agency, "Small Woody Features 2015 (raster 100 m), Europe, 3-yearly - Nov. 2019. Retrieved from." Accessed: Oct. 27, 2024. [Online]. Available: https://sdi.eea.europa.eu/catalogue/srv/api/records/2adfe942-186d-4ee0-af41-b8b864dfb6b6

# TAXONOMIC STRUCTURE OF THE NEMATODE COMMUNITIES IN AGROECOSYSTEMS OF SHUAKHEVI (AJARA, GEORGIA)

**Prof. Dr. Eka Tskitishvili**[1,3]
**Assoc. Prof. Dr. Lali Jgenti**[2]
**Prof. Dr. Nino Lomidze** [3]
**Tengiz Vadachkoria**[2]
[1] Ilia State University, Institute of Zoology, **Georgia**
[2] Batumi Shota Rustaveli State University **Georgia**
[3] Georgian Technical University, **Georgia**

## ABSTRACT

Potatoes is the fourth important food crop worldwide after maize, wheat, and rice and are grown in more than 100 countries worldwide under temperate, subtropical and tropical conditions, however, they are considered as cool temperature crop. Potato is one of the most important food crops in Georgia and potato growing has always been the subject of great importance for settlement of food supply problems in country. Potato crops are severely affected by approximately forty soil borne diseases worldwide including those caused by soil inhabiting fungi, bacteria and nematodes. Plant-parasitic nematodes are among the important pests of potato production, they can cause serious yield losses but remain unnoticed, in most cases. Above ground symptoms of nematode damage are rarely observed since most nematodes cause damage on roots and tubers. The aim of this study is to determine the prevalence of plant parasitic nematodes in the main potatoe growing area in Ajara. Fauna of soil nematodes was studied in three villages of Shuakhevi municipality: Dgvani, Dabadzveli and Okhropilauri. Sampling was conducted in nine sites in early spring, in middle summer and in late fall. The 3 composite soil samples collected from each field (weighing 300-500g) consist of 50 individual sub-samples of soil and roots. Nematodes were extracted by a modified Baermann's method from a sample of 50 g. and exposition time was 48 h. From a total of 83 species of nematodes were found. The richest by the number of species was Dorylaimida order that was presented by 26 species (32 % of species composition). The registered nematodes belong to 2 subclasses, 7 orders, 63 genus and 27 families. The largest abundance of nematodes was observed in the Dgvani village with115 specimens/ 50g soil , and the smallest was in Okhropilauri, with - 37 specimens/50g. Plant-parasitic nematodes from 6 genera (Ditylenchus, Tylechus, Tylenchorhynchus, Helicotylenchus, Pratylenchus, Aphelenchus) were found in soil and (or) potato root samples. All these nematodes can be divided into five groups according to their feeding habits. The omnivore group with 23 species (45,9%) in Spring, 38 species (34,2%) in Summer and 41 species (40,2%) in Autumn, constitut the core of nematode community. Investigations reveal that nematode populations and communities vary seasonally. Plant parasitic nematodes does not exceed a certain limit, which causes measurable economic damage.

**Keywords:** Nematoda, species composition, agroecosystems, Ajara

https://doi.org/10.5593/sgem2024v/3.2/s13.41

## INTRODUCTION

Potato is an important crop which holds promise food to millions of people especially in developing countries. Thus, it is an important consumed commodity in Georgia, where the annual per capita consumption is 55 kg [1], while it is considered by consumers as "second bread". The crop cultivation area covers approximately 20,000 ha. Despite the potato's importance in Georgia the yields still remain rather low (11 t/ha) due to the fact that the production of potatoes is associated with big challenges [2]. Potato production plays a crucial role in ensuring food security and income for small peasant farms in the Autonomous Republic of Adjara. Five municipalities (Keda, Kobuleti, Khelvachauri, Shuakhevi, Khulo) cover three main agro ecological zones, namely mountains to the west, a coastal strip and mountain valleys. Shuakhevi region has lower overall rainfall and hotter, drier summers. Parts of the Acharistskali river valley have a sub-tropical climate and can grow many of the same fruit and vegetable crops as the coastal strip, together with field crops, such as maize and bean. In Shuakhevi region across an area of 1272 hectares, approximately 4402 small farms operate, with an average size of landholding not exceeding 0.06-0.5 hectares. According to the Ministry of Agriculture of Ajara, no nematologial studies have been carried out in the Shuakhevi region. Therefore, all the data obtained on the distribution of phytoparasitic and free-living nematodes in the studied agrocenoses will be a novelty for the fauna of Georgia.

## MATERIALS AND METHODS

The study was carried out in the agroecosystems of the shuakhevi municipality in the Autonomous Republic of Adjara. Three villages were selected: **Dgvani** (41°34′50.9″ N, 42° 12′ 38.5″ E), **Dabadzveli** (41°37′25″N, 42°9′47″E) and **Okhropilauri** (41°37′9″ N, 42°10′55″ E)**.** Within the villages, three potato fields with different ecological conditions were chosen for stationary research, focusing on edaphic factors, temperature regime and humidity. To determine the maximum total number and species composition of the nematode population, three composite samples were collected from each selected field using the zigzag method. Each composite sample weighed between 450-550 grams and comprised 50 primary samples. The research depth for each sample was 25-30 cm. Samples were collected to encompass the complete vegetation cycle: before planting the seed material (in March), during the vegetation period (in April and September), and after harvesting (at the end of November). Approximately 850 primary soil samples were collected throughout the entire research period. In addition to taking samples, we also made a record of the general situation of the land at the time. The average temperature and humidity, the area of land, crop varieties, were recorded. The information was gathered by discussing with the farmers in charge of the land surveyed. For the extraction of nematodes from soil, Baermann's funnel technique was used [3]. Exposition term was 5 days. TAF (triethanolamine 2 ml (40 %) formalin 7 ml and distilled water 91 ml) was used for fixation of the nematodes [4]. Temporary microscope slides preparation and nematodes staining were done by standard techniques [5]. Species identification was carried out with using the microscopes OMAX 14 Mp Digital USB3.0 Microscope Camera with Stage Micrometer A35140U3. We used the monographs by [6], [7], [8], [9], [10] [11], Frequency of detection and the average quantity of nematodes were counted for the 50 $cm^3$ of soil.

## RESULTS

Totally 83 forms of nematodes belonging to 7 orders, 32 families, and 63 genera were registered in the studied biotopes on the key sites. Among these, 65 forms have been identified down to the species level, 4 forms to the family level, and 14 forms to the genus level [12]. Some specimens could not be identified to the species level due to being in larval forms or being damaged. (Table 1.)

The largest abundance of nematodes was observed in the Dgvani village with115 specimens/ 50g soil , and the smallest was in Okhropilauri, with - 37 specimens/50g

Table 1. Distribution of nematodes identified in potato fields in Shuakhevi

| Genus of nematodes | Trophic groups | c-p | Key sites | | | | | |
|---|---|---|---|---|---|---|---|---|
| | | | Dgv/1 | Dgv/2 | Dab/1 | Dab/2 | Okh/1 | Okh/2 |
| Ditylenchus | Ph | 2 | - | - | + | - | + | - |
| Helicotylenchus | Ph | 3 | + | + | + | + | + | - |
| Longidorella | Ph | 4 | - | + | + | - | - | + |
| Neotylenchus | Ph | 2 | - | + | - | - | + | - |
| Psilenchus | Ph | 2 | + | - | - | + | - | + |
| Pratylenchus | **Ph** | 3 | - | - | - | - | - | + |
| Rhotylenchus | Ph | 3 | - | - | - | - | - | + |
| Tylenchorinchus | Ph | 3 | - | - | + | + | - | + |
| Xiphinema | Ph | 5 | + | + | - | + | - | - |
| Acrobeloides | B | 2 | + | + | - | + | + | + |
| Alaimus | B | 4 | - | + | - | - | + | + |
| Amphidelus | B | 4 | + | + | - | - | + | + |
| Anaplectus | B | 3 | + | + | + | + | + | + |
| Cephalobus | B | 2 | + | + | + | - | - | + |
| Cervidelus | B | 2 | - | + | - | + | - | - |
| Chiloplacus | B | 2 | + | + | + | - | - | - |
| Cylindrolaimus | B | 2 | - | - | + | + | + | - |
| Eucephalobus | B | 2 | + | + | + | + | - | + |

https://doi.org/10.5593/sgem2024v/3.2/s13.41

| | | | | | | | | |
|---|---|---|---|---|---|---|---|---|
| Heterocephalobus | B | 2 | - | + | - | - | + | + |
| Geomonhistera | B | 1 | - | - | + | + | - | + |
| Mesodipologaster | B | 1 | + | + | + | - | - | - |
| Mesorhabditis | B | 1 | - | - | + | - | - | + |
| Panagrolaimus | B | 1 | - | - | - | + | - | - |
| Pelodera | B | 1 | + | - | - | - | + | + |
| Plectus | B | 2 | + | + | + | + | + | + |
| Prismatolaimus | B | 3 | + | + | + | - | - | - |
| Rhabditis | B | 1 | - | - | + | - | + | + |
| Tripyla | B | 3 | + | + | + | + | + | + |
| Tripilina | B | 3 | + | - | - | + | + | - |
| Aporcelaimellus | O | 5 | + | + | + | + | + | + |
| Aporcelaimus | O | 5 | - | + | - | + | - | - |
| Allodorylaimus | O | 4 | - | + | + | - | - | - |
| Axonchium | O | 5 | + | + | - | + | - | - |
| Belondira | O | 5 | + | - | + | - | - | + |
| Discolaimus | O | 5 | + | - | - | - | - | - |
| Dorylaimus | O | 4 | - | + | - | - | - | + |
| Drepanodorylaimus | O | 4 | + | - | - | + | - | - |
| Ecumenicus | O | 4 | - | - | + | + | + | + |
| Epidorylaimus | O | 4 | + | + | - | - | + | - |
| Eudorylaimus | O | 4 | + | + | + | + | + | + |
| Labronema | O | 4 | - | + | - | - | + | + |
| Mesodorylaimus | O | 5 | + | + | + | + | + | + |
| Paraxonchium | O | 4 | + | - | - | + | - | - |
| Prodorylaimus | O | 5 | - | + | + | - | - | - |
| Pungentus | O | 4 | + | + | - | - | + | + |
| Sicaguttur | O | 5 | + | - | + | - | - | - |

| | | | | | | | | |
|---|---|---|---|---|---|---|---|---|
| Thornenema | O | 5 | - | + | - | + | - | - |
| Tylencholaimus | O | 4 | + | + | + | + | - | - |
| Aphelenchus | M | 2 | + | - | - | + | - | - |
| Aglenchus | M | 2 | - | - | + | + | + | + |
| Aphelenchoides | M | 2 | - | - | + | - | - | + |
| Tylenchus | M | 2 | + | + | - | - | + | - |
| Actinolaimus | Pr | 5 | - | + | - | - | - | - |
| Anatonchus | Pr | 4 | + | + | + | - | - | + |
| Clarcus | Pr | 4 | - | - | - | + | - | - |
| Comansus | Pr | 4 | + | + | - | - | - | + |
| Mylonchulus | Pr | 4 | - | - | - | + | + | - |
| Mononchus | Pr | 4 | + | - | - | - | - | - |
| Nygolaimus | Pr | 5 | - | - | + | + | - | - |
| Paravulvus | Pr | 5 | - | - | + | - | - | - |
| Prionchulus | Pr | 4 | + | + | + | + | + | - |
| Seinura | Pr | 2 | - | - | - | + | - | - |

Note. (B)bacterivorous, (F)fungivorous, (O) omnivorous, (P) predators (Ph) phytotrophes**.** (c-p)-Colonizer-Persister Classes [13]. **(**Dgv)-village Dvani; (Dab)-village Dabadzveli; (Okh)-village Okhropilauri. «+» species presented; «–» species absent.

## DISCUSSION

The order Dorylaimida (37,3%) leads the count, with the family Qutsianematidae being the most prominent within it. The diversity of species within this order is attributed to a wide range of adaptations. Following closely, the second and third places are occupied by representatives of the *Rhabditida; Chitwood, 1933* (21.4%) and *Tylenchida* (19.25%) groups, respectively. The order Enoplida, Mononchida, Aphelenchida and Areolaimida were the smallest by the number of species. (Fig 1).

https://doi.org/10.5593/sgem2024v/3.2/s13.41

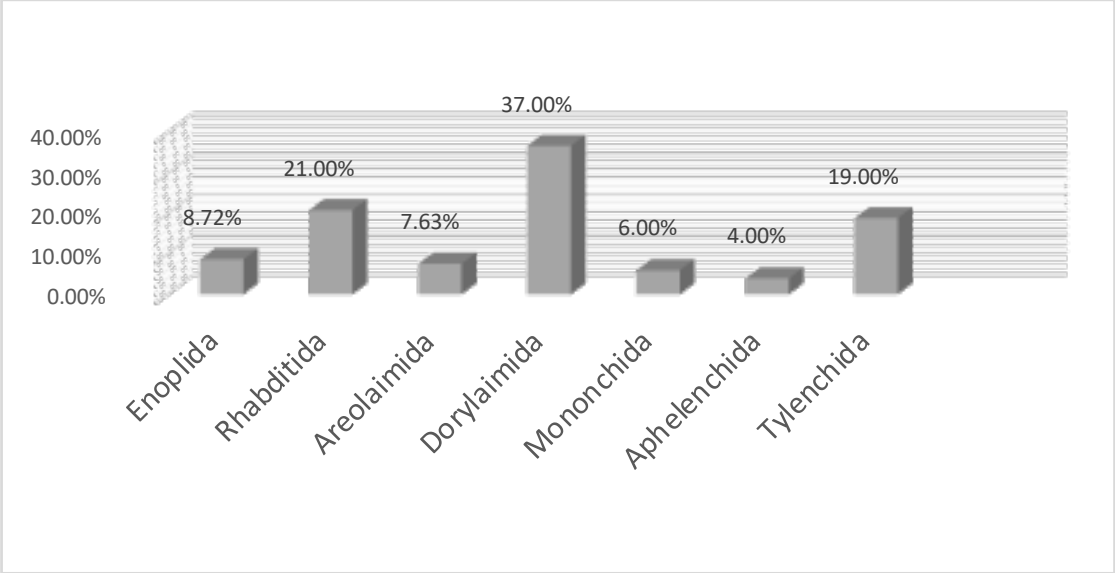



Fig. 1. Percentage of species in orders

22 eudominant and dominant soil-nematode genera constituting the basis of the community structure were identified. They constitute 51.4–62.1% of the total number of the registered genera in spring, 43.2–56,8% in summer, 54.7–70.1% in fall, and 34.7–41.3% in winter.

As the ecological characteristics of nematode populations are determined by the nature of their adaptation within the biocenosis, all found nematodes can be divided into five ecological groups according to their feeding habits: bacterivorous, fungivorous, omnivorous, predators and plant parasitic nematodes. [14] The group of omnivorous nematodes represented by 30 species (37,14 % of species composition) appeared to be the richest by the number of species. The most wide spread among them were *Eudorylaimus carteri (Bastian, 1865) Andrassy, 1959; E. obtusicaudatus (Bastian, 1865) Andrassy, 1959*; *Aporcelaimellus obtusicaudatu*s (Bastian, 1865) Altherr, 1968; *Mesodorylaimus bastiani* (Bütschli, 1873) Andrássy, 1959. Group of bacteriovorous took the second place from a trophic standpoint (27 species- 32,53% of species composition). True plant parasites are represented by 12 species (15,4% % of species composition). . *Helicotylenchus digonicus Perry, 1959, Longidorus elongatus (de Man, 1976) Thorne et Swanger, 1936* and *Xiphinema brevicolle Lordello & Da Costa, 1961* were the most coomon species Slightly behind them were true predators and fungivorous (10 species-12,04%) and 4 species-4.8% respectively). Among fungivorous nematodes (which accounted for 4.8% of species composition- 4 species) the most common species was *Aglenchus agricola (Andrassy, 1954) Meyl, 1960* (Fig2.) [15].

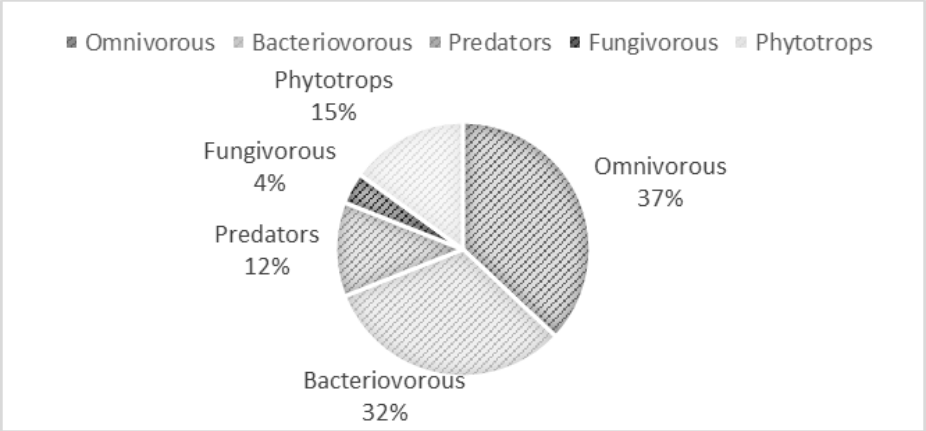



Fig2. Shares of the environmental–trophic groups of soil nematodes on the key sites.

## CONCLUSION

By this study, a survey conducted in three main potato growing areas in Shuakhevi, (Dgvani, Dabadzveli and Okhropilauri). Nematodes were found in all agroecosystems. The plant parasitic nematodes associated with this crop have a low diversity, since only 9 genera (*Helicotylenchus,Ditylenchus, Longidorella, Tylenchus, Psilenchus, Pratilenchus, Rotylenchus, Tylenchorinchus and Xiphinema*) of plant parasitic nematodes were found in the rhizosphere of the plants. 12 species of phytonematodes were identified, although the number did not exceed 5-6 individuals per 50 grams of soil. The highest abundance of nematodes was observed in the Dgvani village with 115 specimens/ 50g soil, while the lowest was recorded in the in Okhropilauri, with - 37 specimens/50g. 22 eudominant and dominant soil-nematode genera constituting the basis of the community structure were identified. They constitute 51.4–62.1% of the total number of the registered genera in spring, 43.2–56,8% in summer, 54.7–70.1% in fall, and 34.7– 41.3% in winter.

## ACKNOWLEDGEMENTS

This work was carried out within the framework of the Project "**Fauna of Georgia – current trends and conservation**", funded by the Ministry of Science and Education of Georgia. Authors gratefully acknowledge support of all members of Department of Nematology at Institute of Zoology of Ilia State University.

## REFERENCES

[1] Geostat (2019) Food balance sheets. Balance sheet for potato. National Statistical Office for Georgia, T'bilisi, Georgia.

[2] CIP (2019). Plan for improving seed potato in Georgia. RTB Working Paper. CIP, Lima, Peru

[3] Baermann, G. Eine einfache Methode zur Affi ndung von Ankylostomum (Nematoden) larven in Erdprobem // Geneesk. Tijdschr. Ned. (1917) Ind. 57. — S. 131–137.

[4] Courtney WD, Polley D, Miller VL. TAF: An improved fixative in nematode technique. Plant Disease Reporter. 1955; 39:570–571

https://doi.org/10.5593/sgem2024v/3.2/s13.41

[5] Decker, H. Plant nematodes and their control. (Phytonematology). — Moscow : Kolos, 1972. 444 p. Russian

[6] Siddiqi, M. R.. Tylenchida: parasites of plants and insects. Norfolk: CABI,. 2000 834 p

[7] Stirling, G., Nicol, J., Reay, F. Services for Nematode Pests : Operational Guidelines // Rural Industries Research and Development Corporation. — Canberra, 2002. —120 p

[8] Mai, W. F., Mullin, P. G. Plant-parasitic nematodes. A pictorial key to genera. — New-York : Cornell University Press, 1996. — 278 p

[9] Ryss, A. Yu. Parasitic root nematodes of the family Pratylenchidae (Tylenchida) of the world fauna. Leningrad : Nauka, 1988. 368 p. Russian

[10] Goodey, T. Soil freshwater nematodes. London: Methuen. 1963. 544 p.

[11] Eliava, I. J. Free-living nematodes of the family Dorylaimidae.. Nauka Leningrad, 1988. 264 p. (In Russ)

[12] Ferris Howard (1999). University of California.
http://nemaplex.ucdavis.edu/index.htm

[13] Ferris, H. and Bongers, T. 2009. Indices for analysis of nematode assemblages. *Chapter* 5 *in:* "Nematodes as Environmental Bioindicators". *Editors:* M.J. Wilson and T. Kakouli-Duarte. CAB International, Wallingford, UK, pp 124-145.

[14] Yeates G.W., Bongers T., De Goede R.G.M. [et al.]. Feeding habits in soil nematode families and genera. An outline for soil ecologists. Journal of Nematology.;25.1993. 315–331

[15] Yeates, G.W., Bongers, T., Nematode diversity in agroecosystems. Agriculture, Ecosystems and Environment 74, 1999. pp.113–135

# VEGETATION OF SMALL-LEAVED LIME *TILIA CORDATA* MILL. FOREST STANDS IN LATVIA

**Prof. Dr. Inga Straupe**
**B.sc. Patriks Kikusts**
**M.sc. Diana Jansone**
**Prof. Dr. Aris Jansons**
University of Life Sciences and Technologies, **Latvia**

## ABSTRACT

Broadleaved forest distribution in Europe and in Latvia is relatively small. Small-leaved lime *Tilia cordata* Mill. stands are even rarer, so it is important to study and protect them, as well as to assess their biodiversity and future potential. The aim of research is to investigate and assess the vegetation in lime forest stands. In total, 12 plots have been established for long-term monitoring of lime stands. In the sample plots, the survey of growing trees, dead wood, the inventory of vegetation species and the determination of the projective cover were carried out. The natural regeneration of lime was also investigated.

During the research it was found out that stock of growing trees does not differ significantly by research objects. It varies from 169 to 446 $m^3$ $ha^{-1}$. The amount of dead wood in the objects is 0.06 to 56.6 $m^3$ $ha^{-1}$. The objects mainly contain debris of the II and III degrees of decomposition.

The number of vegetation species found in the research objects varies from 21 to 35 species. A total of 26 species characteristic of European broad-leaved forests can be found in the objects. The projective cover of the tree, shrub and herb layers does not differ significantly from measurements in 2018. Small-leaved lime stands are stable and have continuous regeneration of lime trees under forest canopy.

**Keywords:** *Tilia cordata* Mill., broadleaved forests, vegetation, dead wood

## INTRODUCTION

The territory of Latvia is located in the transition zone between boreal (coniferous) and nemoral (broad-leaved) forest zone, which is also called hemiboreal intermediate zone. The broad-leaved forests occur in river valleys, on the banks of water bodies, lake islands and plains. As a result of intensive economic activities, they are rarely found. These forests are characterized by stand layering and uneven age structure with groups of younger trees. Broad-leaved forests are characterized by formation of openings, which is one of their main natural disturbances. Openings can form due to windfalls, snowbreaks or the death of a tree when it reaches its biological age [1].

Broad-leaved forests reached their distribution peak in the Atlantic period about 7,000 years ago. As the average air temperature increased, the growth conditions for heat-demanding broad-leaved tree species, such as *Tilia cordata* Mill. improved. Under the influence of climate change, the climate in Latvia will become warmer in the near future, which will improve the growth conditions of broad-leaved tree species in Northern Europe [2].

Small-leaved lime is a widespread broad-leaved tree species in Europe. Low summer temperatures and frosts are major factors limiting the distribution of small-leaved lime in the north [3]. Latvia is located in the north of *Tilia cordata* distribution range. It grows throughout Latvia, mostly in admixture with other broad-leaved species. *Tilia cordata* stands occupy only 0.07% of the total territory of the country [2]. Small-leaved lime is not an economically important species due to its poor wood properties, but it has a high ecological value. It is mainly used in the manufacturing of musical instruments and furniture [3].

Despite its rapid initial growth in height, small-leaved lime is eventually overtaken by other broad-leaved species. That is why in forestry it is mainly grown in mixed stands with more valuable broad-leaved species in order to shade them from the sides and prevent trunk forking [3]. Vegetative regeneration of *Tilia cordata* with stump shoots, root shoots occurs more frequently and more intensively than regeneration with seeds [4]. This type of regeneration allows it to grow at the limits of its range and successfully compete with other broad-leaved species [3]. For successful regeneration with small-leaved lime the optimal stand area should be at least two hectares [5].

The aim of the study is to evaluate the vegetation in *Tilia cordata* Mill. forest stands. To achieve the aim, the following research tasks were defined: to assess the dendrometric indicators of the tree stand (growing trees and deadwood), to analyze the vegetation - plant species and their projective cover (%) for each species and by the layers, as well as to evaluate the natural regeneration of *Tilia cordata* Mill. under canopy cover.

## MATERIALS AND METHODS

*Tilia cordata* Mill. stands were measured for the first time in 2018 to determine the condition and vegetation of stands, and in 2023 it was done repeatedly. Data were collected in the permanent sample plots in 12 research sites all over Latvia. The study plots are located in 6 geobotanical districts. The geobotanical district of Kurzeme includes the sample plots of Dunalka and Ciecere. Zemgale district includes Ziedkalne sample plot. The other sample plots are located in the geobotanical districts of Northern Vidzeme, Central Latvia, Eastern Latvia and Southeast Latvia (Fig.1).

The shape of the sample plots is circular, with a radius of 15.0 m, an area of 706.5 m2 (Fig.2). In the sample plot, all growing trees (over 5 m in height) were measured, as well as deadwood: standing dead trees, snags and fallen deadwood. For all growing trees the following parameters were determined: diameter of the trunk at a height of 1.3 m from the root collar; tree height was measured during the vegetation period, including the crown with leaves (Vertex IV). For standing dead trees - the species, trunk diameter and height were determined. For fallen deadwood - the species, diameter, length, as well as the stage of decay according to the five class categories were determined.

The vegetation was recorded in three smaller plots (radius 5 m) whose distance from the center is 7 m. All species growing in the tree layer (E3), shrub layer (E2), herbaceous plant layer (E1) and moss layer (E0) have been listed in the plot. The projective cover of each species in percentage was estimated by sight.




Fig.1. Geographical location of research sites (source: balticmaps.eu)

The data obtained in the plots were processed using MS Excel. For all the forest stands, the growing stock and the number of trees per hectare, basal area, average height and diameter of the stand were calculated according to generally accepted formulas in forest inventory. The volume of deadwood was calculated according to its stage.

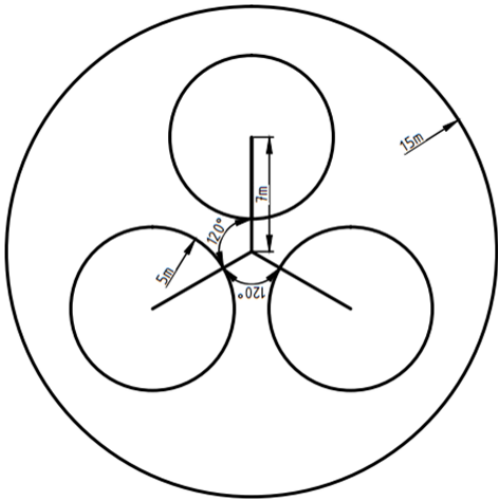



Fig.2. Scheme of the sample plot

Using the Raunkiaer's formula, the occurrence coefficient was calculated for all vegetation species, which shows the frequency of occurrence of each species in the sample plots (Markov, 1965). The occurrence coefficients correspond to 5 (percentage frequency) constancy classes: class I (1-20%), class II (21-40%), class III (41-60%), class IV (61-80%) and class V (81-100%) [6].

In order to compare the sample plots, a statistical analysis of the data was performed. The Shannon - Wiener diversity index (Shannon - Wiener index) characterizes species diversity by projective cover. Ellenberg ecological indicators were determined for the species of herbaceous plant layer. They were determined for four environmental factors – moisture and light [7].

## RESULTS

*Characteristics of growing trees*. The growing stock has been calculated in all the research sites, including the stock of *Tilia cordata* (Fig.3). The total volume of small-leaved lime growing stock in the research sites is 2277.83 $m^3$ $ha^{-1}$. The average growing stock is 189.8 $m^3$ $ha^{-1}$. The largest volume of growing stock is in the 40 - 60 cm diameter degree. It varies between 77.9 – 257.9 $m^3$ $ha^{-1}$. The stock of these diameter grades accounts for almost a half of the total growing stock of *Tilia cordata* - 1114.85 $m^3$ $ha^{-1}$.

The lowest stock is in the 4 - 20 cm and 64 cm diameter grades. The low stock of the 4-20 cm diameter grades can be explained by the higher proportion of young and middle-aged trees in the stands. The smaller volume of the growing stock in the 64 cm diameter grade may be influenced by the large amount of deadwood in the lower diameter grades. A one-factor analysis of variance showed that the growing stock of small-leaved lime in the research sites did not differ significantly from the average growing stock of small-leaved lime $F = 1.1899 < Fcrit = 4.3512$ (p-value $0.2883 > 0.05$).

*Deadwood.* The volume of deadwood by its type was calculated in all the research sites. The largest volume of deadwood is in Skriveri research site - 56.5 $m^3$ $ha^{-1}$. *Tilia cordata* and *Quercus robur* L. account for the largest proportion of deadwood. In order to promote the ecosystem biodiversity, the optimal volume of deadwood should be within the limits of 20 - 50 $m^3$ $ha^{-1}$ [8].

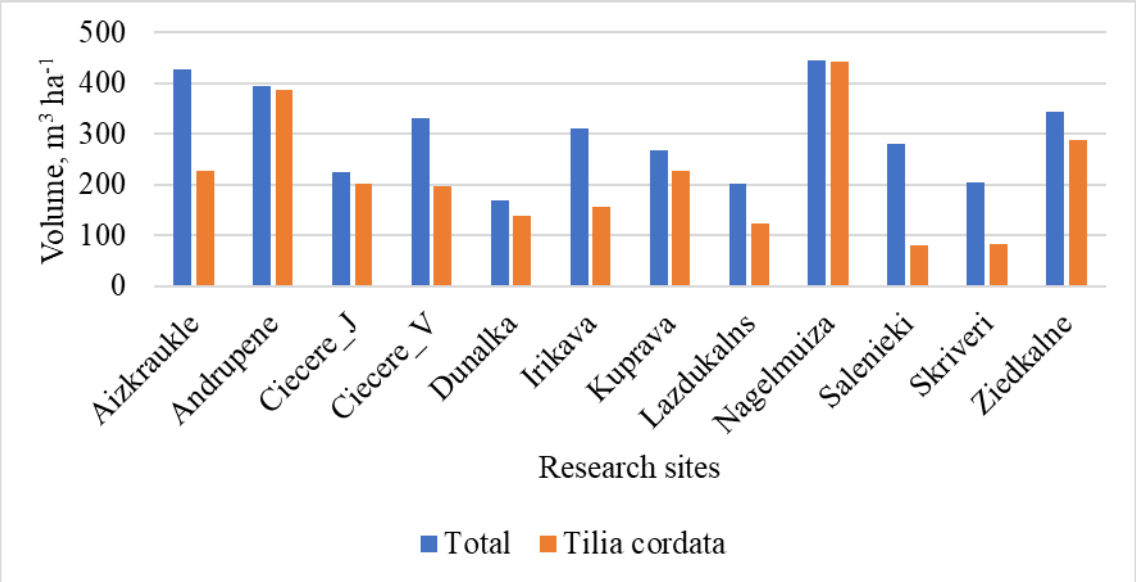



Fig.3. Growing stock in research sites

The only research sites where the deadwood stock is sufficient are those of Irikava, Lazdukalns and Skriveri. The proportion of snag stock in the research sites is low. The highest volume of snags is found in Salenieki research site, where snags of 32 and 40 cm diameter grade are predominant, with a total volume of 3.1 $m^3$ $ha^{-1}$. The lowest stock of snags is found in Dunalka research site – 0.002 1 $m^3$ $ha^{-1}$. The volume of dead standing trees is also low in the research sites. The total stock of standing dead trees in the research sites is 77.1 $m^3$ $ha^{-1}$. The stock of standing dead trees ranges from 0 – 44.4 $m^3$ $ha^{-1}$. The largest volumes of standing dead trees are registered in the 20 - 36 cm diameter degree. The amount of fallen deadwood by research site is also small. The total

fallen deadwood stock by site is 66.1 $m^3$ $ha^{-1}$. The fallen deadwood stock by research sites is within the limits of 0 – 15.8 $m^3$ $ha^{-1}$. The largest volume of fallen deadwood by sites is in the 16-32 cm diameter degree. No fallen deadwood was observed in four research sites (Ciecere_J, Dunalka, Nagelmuiza, Salenieki). In some research sites there is a high anthropogenic impact, since all types of deadwood are removed from the stand. In all the research forest stands, the deadwood in the II and III decay classes dominates.

*Number of vegetation species*. The total number of vegetation species was calculated for all the research sites (Fig.4). The greatest diversity of species is found in Aizkraukle research site - 35 species, of which 7 are tree species and 25 are herbaceous plant species. The poorest stands in terms of the number of species are those of Nagelmuiza and Salenieki, with 24 and 21 species respectively. In Nagelmuiza research site no shrubs at all are found, and it also has the lowest number of tree species - 2 species.

Small-leaved lime is present in the tree and shrub layer in all research sites. The highest diversity index was calculated in Aizkraukle site H' = 1.3. This can be explained by the fact that this research site has the highest number of occurring species. The second highest index is in Irikava research site H' = 1.15. This site has the second highest number of species. The other research sites have a diversity index ranging from 0.52 to 1.1, due to the fact that the number of species varies between the research sites. One of the most abundant European broad-leaved forest indicator species is *Tilia cordata* (92 %), *Corylus avellana* L. in the shrub layer (E2), *Galeobdolon luteum* Huds. in the herbaceous layer (E3) and *Eurhynchium angustirete* (Broth.) T.J.Kop. (67 %) in the moss layer (E0).

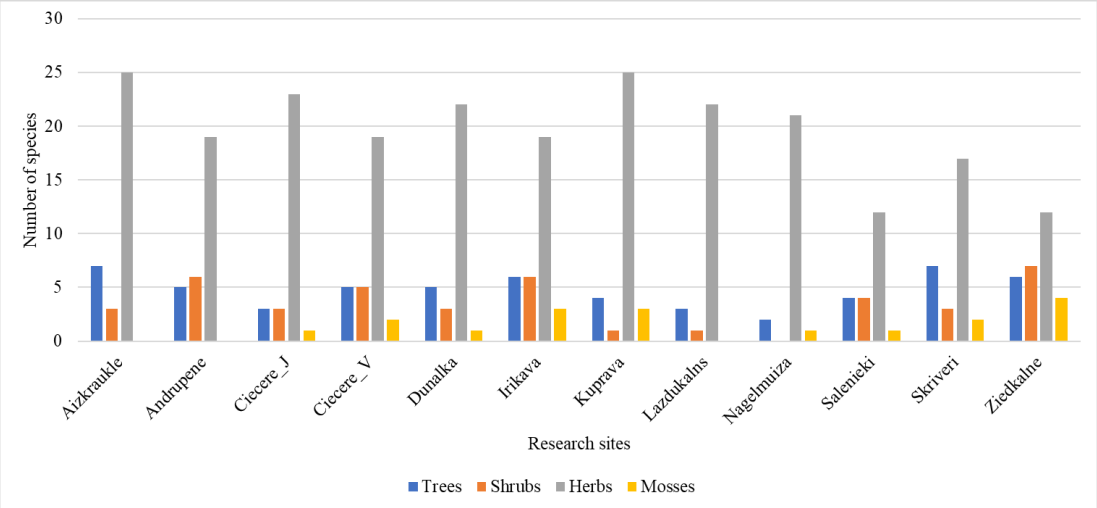



Fig.4. Number of plant species in vegetation layers

*The projective cover of vegetation*. The projective cover of the tree layer (E3) ranges from 45% to 95%. The largest projective cover in the tree layer is in the research sites of Ciecere_V and Lazdukalns - 95%, where small-leaved lime makes up 75% and 45% respectively. A two-factor analysis of variance showed that the projective cover of the tree layer in 2023 does not differ significantly from the measurements carried out in 2018 - F = 0.3739 < Fcrit = 3.1058 (p-value 0.8570 > 0.05). The projective cover of the shrub layer (E2) is in the range of 0 - 70 %. The projective cover of the shrub layer is also not significantly different from the measurements carried out in 2018 - F = 1.4189 < Fcrit = 3.1085 (p – value 0.2859 > 0.05). The projective cover of the herbaceous plant layer (E1) is in the range of 15 - 90 %. The largest E1 projective cover was found

in Aizkraukle research site - 90%. The largest projective covers are created by *Galeobdolon luteum* and *Aegopodium podagraria* L. By performing a two-factor analysis of variance, it was found that the projective cover of the herbaceous plant layer does not differ significantly from the measurements carried out in 2018 - $F = 0.2049 < Fcrit = 3.1085$ (p – value 0.9540 >0.05).

*Analysis of ecological indicators*. In all the research sites, Ellenberg ecological indicators - for moisture and light have been calculated for the species of herbaceous plant layer [7]. In most research sites, the soil is characterized as dry, but in some research sites more moisture-demanding species are found (*Aegopodium podagraria* L., *Poa nemoralis* L., *Allium ursinum* L., *Padus avium* Mill., *Lonicera xylosteum* L.). However, when performing a one-factor variance analysis, it was found that the values of humidity conditions in the research sites are not significantly different- $F = 0.1587 < Fcrit = 1.8618$ (p – value 0.999 > 0.05).

The research sites mainly contain light-demanding species - *Tilia cordata*, *Fraxinus excelsior* L., *Padus avium*, *Populus tremula* L., *Sambucus nigra* L. and *Viburnum opulus* L. The research sites of Dunalka, Nagelmuiza, Lazdukalns, Ciecere_V and Ciecere_J contain semi-shade species - *Carex digitata* L., *Galeobdolon luteum*, *Hepatica nobilis* Mill. and *Corylus avellana*. By performing a one-factor variance analysis, it was found that the values of light conditions in the research sites do not differ significantly - $F = 0.7817 < Fcrit = 1.8518$ (p – value 0.657 > 0.05).

## DISCUSSION

When assessing the natural regeneration of small-leaved lime, Ellenberg's light ecological indicator value was used and analyzed, as well as the correlation of the projective cover of the shrub layer with the projective cover of the tree layer. The light indicator of small-leaved lime is rated 8 on the Ellenberg's scale [7] - light-demanding tree species that cannot grow in heavy shade. However, at a young stand age, it is able to tolerate a deep shading and grow under the canopy of the forest stand [4]. Although some research sites have good light conditions, the projective cover of small-leaved lime in the shrub layer is small (2-12% respectively), because there is either a large projective cover of the tree layer, or the cover of the shrub layer and competition (*Padus avium*, *Corylus avellana*), which limits the regeneration of small-leaved lime in the advanced growth. Correlation analysis was performed for the projective cover of tree and shrub layer with the projective cover of small-leaved lime shrub layer. It was found that there is a weak negative correlation between the projective cover of small-leaved lime and the projective covers of the tree and shrub layer. Consequently, as one value increases, the other decreases or vice versa. There are no significant differences between the projective covers of small-leaved lime shrub layer in 2018 and 2023 (p – value 0.7628 > 0.05). This indicates continuous regeneration of small-leaved lime and future tree stand, since *Tilia cordata* is found in almost all age classes and vegetation layers [5].

## CONCLUSION

The growing stock of *Tilia cordata* Mill. forest stands does not differ significantly by the research sites. It is within the range of 169 – 446 $m^3$ $ha^{-1}$. The growing stock of small-leaved lime constitutes 63% (2277.83 $m^3$ $ha^{-1}$) of the total growing stock in the research sites. The growing stock of small-leaved lime in the research sites does not differ significantly from the average growing stock of small-leaved lime.

The volume of deadwood in the research sites is 0.06 - 56.5 $m^3$ $ha^{-1}$. The largest volume of deadwood is for two tree species - *Tilia cordata* and *Quercus robur* L., 31.7 % and 21.7%, respectively. In the research sites there is fallen deadwood of the II - V decay classes. The largest volume of fallen deadwood is in the II decay class - 60.8% of the total volume of fallen deadwood. The fallen deadwood in the III decay class makes up 25.9% of their volume. The fallen deadwood in the IV and V decay classes in total makes up 13.2% of the volume of fallen deadwood. The large volume of fallen deadwood in the II and III decay classes indicates a relatively recent wood dying process.

The number of vegetation species found in the research sites varies from 21 to 35 species. Overall, the species characteristic of broad-leaved forests are present in all the research sites. The most common indicator species are *Corylus avellana* L., *Quercus robur*, *Galeobdolon luteum* Huds. and small-leaved lime. The projective cover of the tree layer in the research sites varies from 45 to 95%. It is smaller in the areas with a large anthropogenic influence (Nagelmuiza) and a large volume of deadwood (Skriveri). The projective cover of the shrub layer ranges from 0 - 70%. In all the research sites, except Nagelmuiza, *Corylus avellana* is found in the shrub layer. The projective cover of the herbaceous plant layer is 15 - 90 %. The projective cover of the tree, shrub and herb layers in 2023 did not differ significantly from the measurements carried out in 2018.

Stable and continuous natural regeneration of *Tilia cordata* occurs in the research sites, which is indicated by the presence of small-leaved lime in the advanced growth.

## ACKNOWLEDGEMENTS

This study was funded by LBTU Z72 project 'Influence of meteorological factors on radial increment of introduced tree species in Latvia'.

## REFERENCES

[1] Priedītis N., Latvijas mežs: daba un daudzveidība (Latvian forest: nature and diversity), Latvia, 1999, 209 p. (in Latvian)

[2] Snepsts G., Donis J., Kaupe D., Laivins M., Deciduous broad-leaved species (*Quercus robur*, *Tilia cordata*, *Acer platanoides* and *Ulmus laevis*) forest stand productivity in Latvia, Latvia, vol.75, pp 239-247, 2021.

[3] De Jaegere T., Hein S., Claessens H., A Review of the characteristics of small-leaved lime (*Tilia cordata* Mill.) and their implications for silviculture in a changing climate, Forests 7(3), 56, 2016. https://doi.org/10.3390/f7030056

[4] Radoglou K., Dobrowolska D., Spyroglou G., Nicolescu V. N., A review on the ecology and silviculture of limes: (*Tilia cordata* Mill., *Tilia platyphyllos* Scop and *Tilia tomentosa* Moench.) in Europe, vol. 60 (3), pp 10 – 17, 2009.

[5] Laivins M., Platlapju mežaudžu stabilizējošā loma ilgspējīgā mežsaimniecībā Latvijā (The stabilizing role of broadleaf stands in sustainable forestry in Latvia), Latvia, LVMI Silava, 131 p., 2018. (in Latvian)

[6] Mueller-Dombois D., Ellenberg H., Aims and methods of vegetation ecology, USA, New York, Wiley, 547 pp., 1974. DOI: 10.2307/213332

[7] Ellenberg H., Weber H. E., Dull R., Wirth V., Werner W., Paulbent D., Zeigerwerte von Pflanzen in Mitteleuropa, Germany, Göttingen, Verlag Erich Goltze, 248 pp., 1992.

[8] Muller J., Butler R., A review of habitat thresholds for dead wood: a baseline for management recommendations in European forests, European Journal of Forest Research, vol. 129, pp 980 – 992, 2010. DOI: 10.1007/s10342-010-0400-5

# SECTION

# SUSTAINABLE OIL, GAS, AND ENERGY TRANSITION

# EXPLORATION

# BEST AVAILABLE TECHNIQUES IN OIL AND GAS EXPLORATION: OPPORTUNITIES FOR POLLUTION PREVENTION AND CLIMATE CHANGE MITIGATION

**Dr. Sci. Dmitry Skobelev**[1]

**PhD Maria Dobrokhotova**[1]

**PhD Natalia Popadko**[1,2]

**Mrs. Yuliya Ukhina**[1]

**PhD Rauf Ismayilov**[3]

[1] Research Institute 'Environmental Industrial Policy Centre', **Russian Federation**
[2] Gubkin Russian State University of Oil and Gas, **Russian Federation**
[3] Independent Consultant, **Azerbaijan**

## ABSTRACT

The concept of Best Available Techniques (BAT) encompasses a set of technological, technical, and organizational solutions for preventing and controlling negative environmental impacts while improving resource efficiency. Within key technological processes, built-in solutions play a crucial role in pollution prevention, while end-of-pipe measures are applied to control emissions that cannot be prevented by primary solutions.

In most countries, BAT applies to key resource-intensive sectors, including hydrocarbon exploration and production in the oil and gas industry. The scope of BAT implementation is estimated via assessing (1) the share of industries obtaining Integrated Environmental Permits (IEPs) and (2) the gradual enhancement of sectoral environmental performance and resource efficiency.

In contrast to BAT Reference Documents developed by other countries applying BAT approaches to regulate the oil and gas industry, Russia has established compulsory BAT-associated emission levels (BAT-AELs) and target BAT-associated resource efficiency parameters.

The main challenge lies in the need to phase out outdated and inefficient production techniques and ensure a transition to modern, cost-effective, and environmentally sound solutions. This research analyzes the current status of BAT implementation based on existing and prospective techniques in the oil and gas industry and synthesizes data on IEPs.

An assessment of sectoral BAT compliance helps to evaluate the effectiveness of BAT-based policies in terms of (1) the modern techniques implemented and (2) improvements in environmental performance and resource efficiency.

BAT-based assessments of the oil and gas industry are relevant to Azerbaijan, Kazakhstan, and BRICS countries that have either adopted or are planning to develop Reference Documents and BAT-AELs for this sector.

**Keywords:** Best Available Techniques, oil and gas, pollution prevention, environmental performance, climate change mitigation.

## INTRODUCTION

Despite the ongoing global energy transition – a key strategy for reducing greenhouse gas (GHG) emissions and combating climate change – revenues from the energy sector, including the oil and gas industry, continue to make significant contributions to the GDP of many countries.

As of 2023, according to the World Energy & Climate Statistics – Yearbook 2024 (https://yearbook.enerdata.net), the leading producers of oil and natural gas are the United States, Saudi Arabia, Russia, Canada, Iraq, Iran, and China. In these countries, the share of oil and gas in their GDP reaches as high as two-thirds of the total GDP.

Given that 74% of global GHG emissions originate from the energy sector, it is not surprising that major energy-importing countries are also the world's largest GHG emitters.

The UN Climate Change Conference (COP 28), held in the United Arab Emirates from November 30 to December 12, 2023, reaffirmed the right of UN Framework Convention on Climate Change member states to pursue a fair, orderly, and equitable energy transition. This transition provides significant opportunities for achieving climate neutrality in national economies by 2050 (https://unfccc.int/sites/default/files/resource/cma2023_L17E.pdf).

According to the official statistics, in Russia, the share of oil and gas in the total GDP amounts to 16.5% (https://rosstat.gov.ru/statistics/accounts). The oil and gas industry is responsible for approximately 160.3 million tons of $CO_2$-equivalent GHG emissions annually [1].

The intensive scenario outlined in Russia's Strategy for Low Greenhouse Gas Emissions Development until 2050 (hereafter – the Strategy) identifies key tools for decarbonizing the economy. These include a complete transition to Best Available Techniques with low GHG emissions and the implementation of technological solutions providing for high resource and energy efficiency within industrial production processes.

Achieving a fair energy transition within the energy sector, as envisioned in the Strategy, requires the gradual phase-out of outdated and inefficient technologies, the implementation of BAT, and the development of innovative low-carbon and resource-saving technologies in oil and natural gas production.

The aim of this study is to assess the effectiveness of BAT implementation in the hydrocarbon exploration and production sector. This includes evaluating the share of products manufactured by BAT implementing industries (hereafter – BAT products) in total production, as well as exploring the potential for implementing the BAT concept in BRICS+ countries, which are either currently using or planning to adopt BAT for their oil and gas industries.

## MATERIALS AND METHODS

The methodological basis of the study is the systematic approach developed by the authors, which is a constructive toolkit for studying complex industrial ecology problems.

An analysis of the BAT implementation pattern was carried out using statistical data from national regulatory agencies and specialized organizations such as: the Federal State Statistics Service (National accounts, available at https://rosstat.gov.ru/statistics/

accounts); the Federal Service for Supervision in the Field of Natural Resources (Register of the installations – sources of negative environmental impacts available at https://uonvos.rpn.gov.ru); the Innovation Center Skolkovo (Decarbonization of Oil and Gas Sector, available at https://energy.skolkovo.ru).

Information on sectoral BAT requirements was from the database of the Russian BAT Bureau (available at: https://burondt.ru/itc).

The analysis focused on the number of Integrated Environmental Permits (IEPs) issued across relevant industrial sectors, with particular attention given to oil and natural gas production industries. Data on the total number of IEPs granted to oil and gas producers were synthesized, and the trends in the number of IEPs obtained by the focus industries were tracked over the period from 2019 to 2024.

## RESULTS

### The Concept of Best Available Techniques

The Concept of Best Available Techniques is widely used in many countries and regions both to prevent and control industrial emissions and to stimulate the technological development of key industrial sectors [2]. Integrated Pollution Prevention and Control (IPPC) became an internationally recognized term (and abbreviation) along with BAT. In Russia, the BAT implementation is the requirement faced by more than 30 economic sectors characterized by high resource intensity and significant negative environmental impacts [3].

The EIP campaign started in 2019, and it is expected that by end 2024 all Russian IPPC installations categorized as those obliged to implement BAT and obtain IEPs (5,655 installations in total), will have demonstrate their compliance with BAT requirements.

In Russia, over 45% of IPPC installations are part of the energy sector. Among these, more than 70% are involved in oil and natural gas production.

### Integrated Environmental Permits: Statistics in Russia

From February 2019 to October 2024, 1,449 out of the 5,655 installations received IEPs (Figure 1).

The share of IEPs granted to the industries in the oil and gas sector exceeds 60% of the total number of IEPs granted during this period (Figure 2).

### Products manufactured by industries implementing Best Available Techniques

Based on the analysis of the number of installations required to implement BAT and the number of IEPs granted, we can introduce a universal coefficient for assessing the rate of BAT implementation at (1) the industrial enterprise, and (2) the industrial sector. This coefficient reflects the share of products manufactured by implementing BAT relative to the total production.

$$Share_{BAT\ products} = Products_{BAT} / Products_{TOTAL} \quad (1)$$

where $Share_{BAT\ products}$ represents the percentage of total production implementing BAT in the industry (%); $Products_{BAT}$ is the quantity of products manufacture by means of

implementing BAT (e.g., t/year, $m^3$/year), as stated in the IEP; *Products* $_{TOTAL}$ is the total production (e.g., t/year, $m^3$/year).

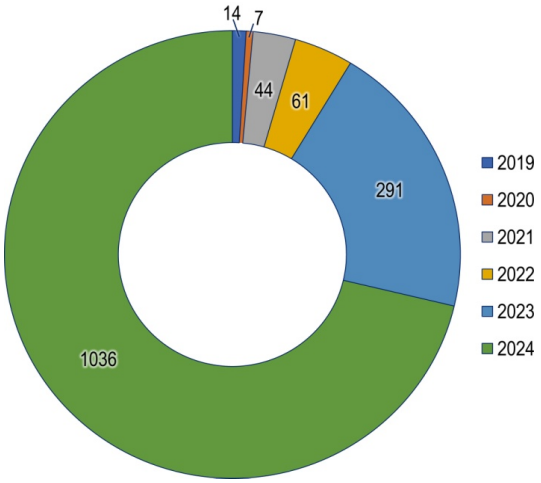



**Figure 1.** The number of Integrated Environmental Permits granted in 2019-2024
Source: Prepared by the authors

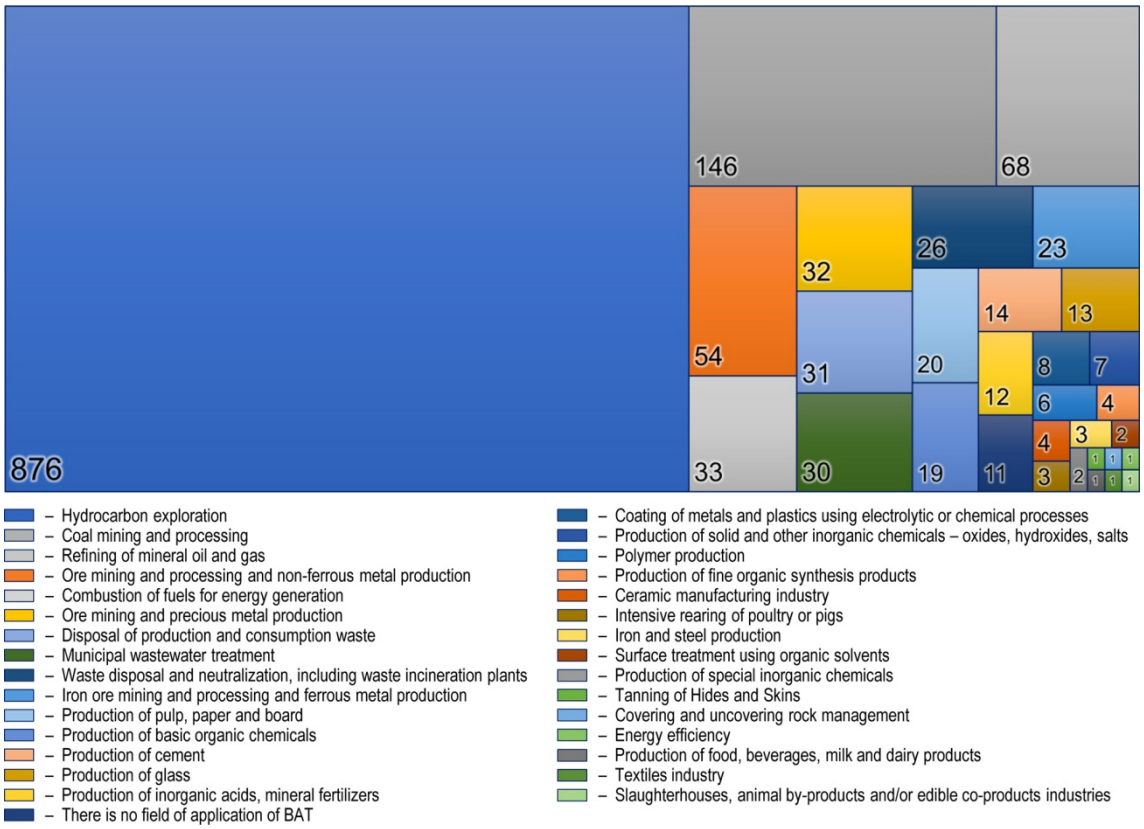



**Figure 2.** Distribution of granted Integrated Environmental Permits by the Economic Sectors, 2019-2024
Source: Prepared by the authors

We analyzed the National IEP statistics from 2019 to 2022 using data from the Federal Service for Supervision in the Field of Natural Resources.

In 2019, the share of BAT-products amounted to 0.88 % of all natural gas and oil produced in the Russian Federation. The following 2020 showed 0.96 % for natural gas and 1.11 % for oil production; 2021 – 3.97 % and 1.5 % and 2022 – 6.29 % and 6.32 % for respective sectors.

Thus, the share of BAT products shows gradual increase but it remains rather low – just 20.15 % of all natural gas and oil produced in Russia.

## DISCUSSION

The BAT concept, first developed in the 1960s and recognized internationally, is evolving in the Russian Federation along a unique trajectory:
1) 53 industry-specific reference documents (BREFs) were first developed for just three years (2015-2017);
2) for several sectors (such as Upstream Hydrocarbon Exploration and Production, Iron Ore, and Coal Mining, etc.) sector-specific BAT-Associated Emission Levels were established (unlike in other countries and regions [4, 5]);
3) since 2022, drawing up BREFs involves also the carbon intensity analysis and establishment of so-called indicative BAT-Associated GHG emission levels [6, 7].

BAT-AELs, outlined in sectoral reference documents (BREFs), serve as criteria for obtaining Integrated Environmental Permits. Along with BAT-associated resource efficiency parameters, BAT-AELs help determine the need for specific environmental performance enhancement programs (EPEPs) aimed at improving the production environmental performance. This set of indicators can also be used as compliance criteria for obtaining government support and in the implementation of sustainable (including green) development projects.

As part of the ongoing development of the BAT concept, BREFs are periodically reviewed. For instance, the evolution of reference documents in the oil and natural gas production industry, from 2017 to the present, highlights the transition from first-generation to third-generation BREFs.

Generally, the process of reviewing a BREF follows the same steps as its initial drawing up process. These stages include collecting data on the environmental performance and resource efficiency of industrial companies, defining BAT, identifying environmental marker parameters, establishing BAT-AELs and BAT-AEPLs, and finally, approving the updated reference document by the sectoral Technical Working Group.

The Oil Production BREF, originally developed in 2017 as the first-generation document, was reviewed in 2021. The main changes involve expanding the scope to include offshore oil production processes, in addition to land-based operations; both national and international best practices are considered (such as [8, 9]).

The list of BATs is divided into two main groups. The first group includes generally applicable BATs, which address environmental and energy management systems. The second group covers industry-specific BAT, the list if which have been significantly expanded. Notably, the use of associated petroleum gas (APG) for internal needs was added, which has greatly reduced APG losses – previously vented or flared – and, consequently, minimized emissions of air pollutants and GHGs.

https://doi.org/10.5593/sgem2024v/3.2/s06.45

The list of environmental marker parameters (also called key environmental issues) for each BAT, along with the corresponding BAT-AELs, has undergone a substantial revision. Resource efficiency parameters, such as fuel gas and electricity consumption during the extraction and processing of gas-oil-water mixtures, have been established. The focus on the resource efficiency is the characteristic feature of the second-generation BTRFs.

The next BREF review is scheduled for 2026, during which BAT-AELs are expected to be tightened, and indicative GHG emission levels for oil production will be introduced.

The Natural Gas Production BREF is currently the first-generation reference document, drawn up in 2017; it is being reviewed in 2023. Data from industrial producers have been collected, and the scope of the BREF has been refined in two key areas:
1) Due to the global increase in liquefied natural gas (LNG) consumption, the Technical Working Group has decided to include LNG production technologies in a separate chapter of the Processing of Natural and Associated Gas BREF, which is also being updated;
2) Processes for natural gas production on the continental shelf have been incorporated.
As part of the update, the Technical Working Group will revise the list of BATs for natural gas production, update the corresponding BAT-AELs, and develop BAT-associated resource efficiency parameters. Additionally, industry benchmarking of specific GHG emissions will be conducted to establish indicative GHG emission levels. Thus, BREF reviewed in 2024 will reflect the requirements of environmental, industrial, and climate policies [10].

BAT-AELs established in the two BREFs discussed are used to assess the BAT compliance of IPPC installations, which have been applying for IEPs since 2019. As it is emphasized, the number of installations demonstrated their compliance and the share BAT products has been growing to achieve 20.15 % in October 2024. At the same time, since the hydrocarbon exploration and production sector is characterized by the lowest number of EPEPs (nearly all installations meet the sectoral BAT requirements), it is possible to assume that in the reality, the share of BAT products is much higher, and we expect to receive the necessary confirmation of this assumption as soon as all IEPs are granted to the sectoral installations.

The Russian methodological approach to assessing the hydrocarbon exploration sector using BAT can be applied in other countries that apply similar technologies and equipment for oil and gas extraction, both on land and offshore. This approach is especially relevant for international cooperation projects in border oil and gas regions, such as the Caspian region [11, 12].

The observed shrinking of the Caspian Sea necessitates the implementation of unified or internationally harmonized approaches to mitigate negative impacts from oil and gas production in its coastal and offshore zones. Oil and gas producers in this region include not only Russia but also Kazakhstan and Azerbaijan – members of the Commonwealth of Independent States (CIS) – which facilitates cooperation in this area. Notably, Kazakhstan has already developed a national BAT implementation system, approving its Oil and Gas Production BREF in 2023. In September 2024, a bilateral working group consisting of representatives from the Russian government and federal executive bodies of Russia and Azerbaijan was formed to address the Caspian Sea problems.

In June 2024, China proposed to form a BRICS registry of green technologies. Since BRICS was founded in 2006, 10 countries have joined the association (nowadays –

BRICS+), including major oil and gas producers like Brazil, Iran, Saudi Arabia, and China.

Within the BRICS framework, the discussion has expanded to include trade relations and the reorientation of Russian exports. A unified approach to assessing the production and tracking the domestic consumption and external supply of BAT products across various industries is under consideration. For this purpose, a system is being proposed to assess such products (using formula (1)) and develop national statistical reporting on the share of products manufactured implementing BAT. This toolkit will help evaluate the effectiveness of BAT implementation and its contribution to national GDP.

## CONCLUSION

The BAT concept has been implemented in Russia since 2014, with Reference Documents for oil and gas production being regularly reviewed. These reviews focus on industry benchmarking to establish BAT-AELs and BAT-associated resource efficiency parameters for different hydrocarbon production techniques. Compliance with BAT enables industrial companies to improve the resource efficiency and reduce negative environmental impacts by preventing emissions of pollutants and lowering GHG emissions.

To assess the share of products manufactured by implementing BAT, a special coefficient is proposed, which can be used to analyze the share of installations in various sectors that comply with the sectoral BAT requirements.

The Russian approach to establishing BAT-AELs and BAT-associated resource efficiency parameters for upstream hydrocarbon exploration and production could serve as a methodological framework for the implementation of the BAT concept in other countries. This could help fulfill the provisions of international environmental protection agreements [13] and aid in the development of technological standardization systems in the world's largest oil and gas-producing countries.

## AUTHOR CONTRIBUTIONS

Methodology, Yu.U., D.S., and M.D.; Validation, N.P., R.I., and M.D.; Resources, Tu.U.; Data curation, Yu.U., N.P., and M.D.; Writing original draft, M.D., Yu.U., and N.P.; Writing review & editing, D.S., and R.I. All authors have read and agreed to the published version of the manuscript.

## CONFLICTS OF INTEREST

We have no conflicts of interest to disclose. We confirm that this work is original and has not been published elsewhere, nor is it currently under consideration for publication elsewhere. We declare no conflicts of interest.

## REFERENCES

[1] National Inventory Report of Anthropogenic Emissions by Sources and Removals by Sinks of Greenhouse Gases not Controlled by the Montreal Protocol for the Period from 1990 to 2021, Part 1, Moscow 2023 (in Russian), URL: http://downloads.igce.ru/kadastr/RUS_NIR_2023.rar.

[2] Directive 2010/75/EU of the European Parliament and of the Council of 24 November 2010 on industrial emissions (integrated pollution prevention and control) (recast) (Text with EEA relevance), URL: https://eur-lex.europa.eu/eli/dir/2010/75/oj.

[3] Hjort M., Skobelev D., Almgren R., Guseva T., Koh T., Best Available Techniques and Sustainable Development Goals, The 19th International Multidisciplinary Scientific GeoConference SGEM 2019, vol. 19, is. 4.2, pp 185-192, 2019, DOI: 10.5593/sgem2019V/4.2/S06.025.

[4] Best Available Techniques Guidance Document on Upstream Hydrocarbon Exploration and Production, European Commission, URL: https://eippcb.jrc.ec.europa.eu/sites/default/files/inline-files/hydrocarbons_guidance_doc.pdf.

[5] Best Available Techniques Reference Document for the Management of Waste from Extractive Industries, European Commission, URL: https://eippcb.jrc.ec.europa.eu/sites/default/files/inline-files/jrc109657_mwei_bref_-_for_pubsy_online.pdf.

[6] Bashmakov I., Myshak A., Bashmakov V. A., Bashmakov V. I., Borisov K., Dzedzichek M., Lunin A., Lebedev O., Shishkina T., Russian Energy Balance, Energy Efficiency, and Energy-Related GHG Emission Accounting System, Energy Efficiency, vol. 16. no. 6, p. 67, 2023, DOI: 10.1007/s12053-023-10132-6.

[7] Mazlova E., Smirnova T., Kulikova O., Blinovskaya Y., Implementation of the Climate Agreement in the Russian Oil and Gas Sector, IKsibi M., et al, Recent Advances in Environmental Science from the Euro-Mediterranean and Surrounding Regions (2nd Edition), EMCEI 2019, Environmental Science and Engineering, Springer, Cham, DOI: 10.1007/978-3-030-51210-1_166.

[8] Yang S., Xing K., Yang Y., Offshore Oil Pollution and Prevention Measures, E3S Web of Conferences 271, 02010, 2021, DOI: 10.1051/e3sconf/202127102010.

[9] Adebayo A. R., Tawabini B., Hydrocarbon Exploration and Production- A Balance between Benefits to the Society and Impact on the Environment, Journal of Petroleum & Environmental Biotechnology, vol. 3, is. 3, 2012, DOI: 10.4172/2157-7463.1000122.

[10] Titova N., Cherepovitsyna A., Guseva T., Meeting the UT's Sustainable Development Goals in the Decarbonization Agenda: A Case of Russian Oil and Gas Companies, Resources, vol. 12, is. 10, p. 121, 2023, DOI: 10.3390/resources12100121.

[11] Efendiyeva I. M. Ecological Problems of Oil Exploitation in the Caspian Sea Area, Journal of Petroleum Science and Engineering, vol. 28, is. 4. pp 227-231, 2000, DOI: 10.1016/S0920-4105(00)00081-4.

[12] Huseynov A., Environmental and Economic Indicators of Sustainable Development of Enterprises of Oil and Gas Complexes, SHS Web of Conferences, Globalization, and its Socio-Economic Consequence, is. 92, p. 08009, 2021, DOI: 10.1051/shsconf/20219208009.

[13] Mikaelsson Å., Guseva T., Tikhonova I., Shchelchkov K., Best Available Techniques as Criteria for Excluding Russian Industrial Installation from the Environmental Hot Spot List of the Barents Region. The 20th International Multidisciplinary Scientific GeoConference SGEM 2020, vol. 20, is. 5.1, pp 91-98, 2020, DOI: 10.5593/sgem2020/5.1/s20.012.

# NATIONAL GREENHOUSE GAS EMISSION FACTORS AT OIL AND GAS CONDENSATE PRODUCTION AND TREATMENT FACILITIES IN RUSSIAN FEDERATION

**PhD. Nakhutin Alexander**[1]
**Popov Nikita**[1]
**Berdin Vladimir**[2]
**Mironov Andrey**[2]
**Uledova Anastasia**[2]
**Kozlova Daria**[3]
**Karimova Kamila**[3]
**Simonyan Elen**[3]

[1] Yu. A. Izrael Institute of Global Climate and Ecology, **Russian Federation**
[2] International Sustainable Energy Development Center (ISDEC), **Russian Federation**
[3] Center for energy research, **Russian Federation**

## ABSTRACT

Accurate estimation of greenhouse gases in national inventory reports, submitted by countries every year under the UNFCCC and the Paris Agreement is an important task. Fugitive greenhouse gas emissions from oil production, gathering and treatment is a key category in the Russian national inventory report. Total emissions from this category accounted to more than 30 million tons of $CO_2$ equivalent in 2021. Since in Russian inventory the default IPCC emission factors from these operations are used, in the framework of government project "Russian climate monitoring system" new country-specific $CH_4$ and $CO_2$ emission factors has been developed. Three main tasks were completed. First, representative sample of 18 oil-producing field which relevantly represents type of production, gathering and treatment technologies and oil mode of occurrence in each of 3 major petroleum provinces, or macro-regions of Russia were selected. Second, data on oil and associated petroleum gas production, technical losses and gas composition, $CH_4$ as pollutant emissions, gas to oil ratio, and other characteristics we collected for each field. Third, actual and retrospective values of $CH_4$ and $CO_2$ emission factors were calculated on the base of collected data and approved methodology and emissions were estimated as well. Comparison of the results of our study with the estimates included in the Russian national inventory report submitted in 2023 shows that average estimate of annual emissions for the whole period from 1990 to 2021 is 23 million tons lower than the estimate currently included in the national inventory.

**Keywords:** Greenhouse gas inventarisation, IPCC, oil recovery, emission factors, emissions, $CO_2$, $CH_4$.

## INTRODUCTION

The importance of development, including improving the accuracy of emission estimates of The National Report of the Russian Federation on the Inventory of the Anthropogenic Emissions and Sinks of Greenhouse Gases Not Controlled by the Montreal Protocol (hereinafter – NIR) couldn't be underestimated. Fugitive greenhouse gas (hereinafter –

https://doi.org/10.5593/sgem2024v/3.2/s06.46

GHG) emissions from oil production, gathering and treatment (subcategory 1.B.2.a.2 in Russian NIR) appears from leakages and venting of associated petroleum gas (hereinafter – APG) during above mentioned operations and oil field infrastructure maintaining works. Also, these emissions are occurring during evaporations from oil reservoirs. All described operations are estimated in Russian NIR under category 1.B.2.a. "Fugitive emissions from oil operations" which is a key category: in 2021 total GHG emissions amounted to 38,9 million tons of $CO_2$ equivalent, or 82 %[1].

For all Russian NIR's submitted before 2024 the emission factor from The Intergovernmental Panel on Climate Change (hereinafter – IPCC) 2006 guidelines was implemented[2]. This type of estimation corresponds to tier 1 – the first level of national GHG estimation for which high uncertainty values are inherent.. Given that this is a key category, the objective was to develop the most accurate emission factor possible for this category. In 2024, under government project "Russian climate monitoring system" the country-specific $CH_4$ and $CO_2$ emission factors were developed. New emission factors correspond to tier 2 – second level of GHG estimation which includes national oil production circumstances and gas composition and, therefore, has less uncertainty.

To achieve this goal the following tasks were set:

- Definition of a representative sample set of oil production fields for national oil industry;
- Main operations and sources of $CH_4$ and $CO_2$ emissions on oil-producing fields analysis;
- Collecting data, to develop country specific emission factor;
- Country specific GHG emission factors (hereinafter – CS EF) calculation;
- GHG emission estimates with new CS EF and its comparison with past values.

## MATERIALS AND METHODS

Russian oil and gas onshore production industry covers 4 petroleum provinces: North Caucasus, Volga-Ural, West Siberia, East Siberia with Far-Eastern Russia. Major onshore oil production occurs at Volga-Ural, West Siberia, East Siberia with Far-Eastern Russia [3]. Statistics from oil production is provided on the base of administrative subjects of Russia, that are within borders of this provinces and potentially few major oil fields from different subjects could represent oil production-specific emission characteristics of all province. Therefore, it was decided to identify samples of few oil production fields in each province based on the following criteria:

- Sample should contain oil fields of different types: oil, gas and oil (oil is major component), oil and gas (gas is major component), oil and gas condensate field;

- Fields with different amounts of reserves should be included: “unique” (deposits on categories ABC1+C2[1] are more than 300 million tons) and “large” (deposits on categories ABC1+C2 are from 30 to 300 million tons);
- Fields with different depletion rate should be presented;
- Different types of oil reservoirs should be presented: uncomplicated and hard to recover;
- Fields with different gas – to oil ratios should be included: low and middle (less than 200 $m^3$/tonne) and high (more than 200 $m^3$/tonne).

Above mentioned criteria directly affect on the type of emission source and operations, that occur at oil field. For example: “unique” oil production fields with big amount of APG production have compressor stations to pump it on long gas gathering system, when relatively small oil fields don’t need them. Analysis of emission sources was performed on the base of typical oil and APG production, gathering and treatment scheme that is representative for the most fields, included in sample.

In the last work on CS EF development methodology (Popov et. al. 2024) it was emphasized, that most comprehensive estimation of GHG emissions from oil production, gathering and treatment could be performed with confidential data on $CH_4$ as pollutant emission estimates, calculated by field operators on the base of methodologies, approved by the Ministry of Natural Resources and Environment of the Russian Federation (hereinafter – MNRE) and data on technical losses of APG, oil production, gas to oil ratio factor, oil density and APG composition. For this reason, mentioned data was collected for each of 18 oil production fields within the representative sample for each year from 2019 to 2021[4].

Emission factors – oil production-specific parameters, that are recalculated on the unit of oil production (kt/ths. $m^3$) for each type of greenhouse gas on formula:

$$EF_{j,i,y} = E_{j,i,y} \div V_{j,i,y} \quad (1)$$

Where:

$EF_{j,i,y}$ – emission factor of j-th greenhouse gas on the field “i” in year y,kt./ths. $m^3$;

$E_{j,i,y}$ – emissions of j-th greenhouse gas from oil production, gathering and treatment on the field “i” in year y, kt;

$V_{i,y}$ – oil production at year y, ths $m^3$

Since data on $CH_4$ emissions were already collected from field operators it was necessary to develop $CH_4$ CS EF, and calculate $CO_2$ emissions and CS EF.

$CH_4$ CS EF were calculated from the formula 2:

$$CSEF_{CH4,y} = \frac{\sum_i E_{CH4,i,y}}{\sum_i V_{i,y}} ; \quad (2)$$

[1] 1The Russian designation ABC1 corresponds to proved reserves (proved developed producing, proved developed nonproducing, and proved undeveloped), while C2 corresponds to probable and possible reserves.

https://doi.org/10.5593/sgem2024v/3.2/s06.46

Where:

$CSEF_{CH4,y}$ – is country-averaged $CH_4$ emission factor, kt. $CH_4$/ths. $m^3$ oil production;

$E_{CH4,i,y}$ – emissions of $CH_4$ from oil production, gathering and treatment on field "i", in year y, kt.;

$V_{i,y}$ – oil production at year y, ths $m^3$

$CSEF_{CO2}$ were calculated from formula 3:

$$CSEF_{CO2,y} = \frac{\sum_i ((E_{CH4,i,y}/\rho_{CH4})/w_{CH4,i,y}) \times w_{CO2,i,y} \times \rho_{CO2})}{\sum_i V_{i,y}} \quad (3)$$

Where:

$CSEF_{CO2,y}$– is country-averaged $CO_2$ emission factor, kt. $CO_2$/ths. $m^3$ oil production;

$\rho_{CH4}$, $\rho_{CO2}$– density of $CH_4$ and $CO_2$ respectively, kg/$m^3$ according to MNRE guidelines on anthropogenic GHG estimation[];

$w_{CH4,i,y}$, $w_{CO2,i,y}$– molar fraction of $CH_4$ and $CO_2$ in APG of field "i" on a year $y$, respectively, %.

New CS EF's are representative for period from 2019 to 2021 year. To estimate GHG emissions for the whole timeline from 1990, it has to be other CS EF relevant to older time period. It was assumed, that ratio of APG technical losses to oil production best reflects level of production, gathering and treatment technologies, because APG technical losses appear during: emptying pipelines and process equipment of oil and APG gathering and treatment before maintaining and recovery works, degassing of process liquids, liquid entrainment, and sampling and maintenance of safety valves[5]. Thus, on the basis of above-mentioned ratio $CH_4$ CS EF and $CO_2$ CS EF timeline were restored. The ratio of APG technical losses to oil production in Russia is presented on Figure 1.

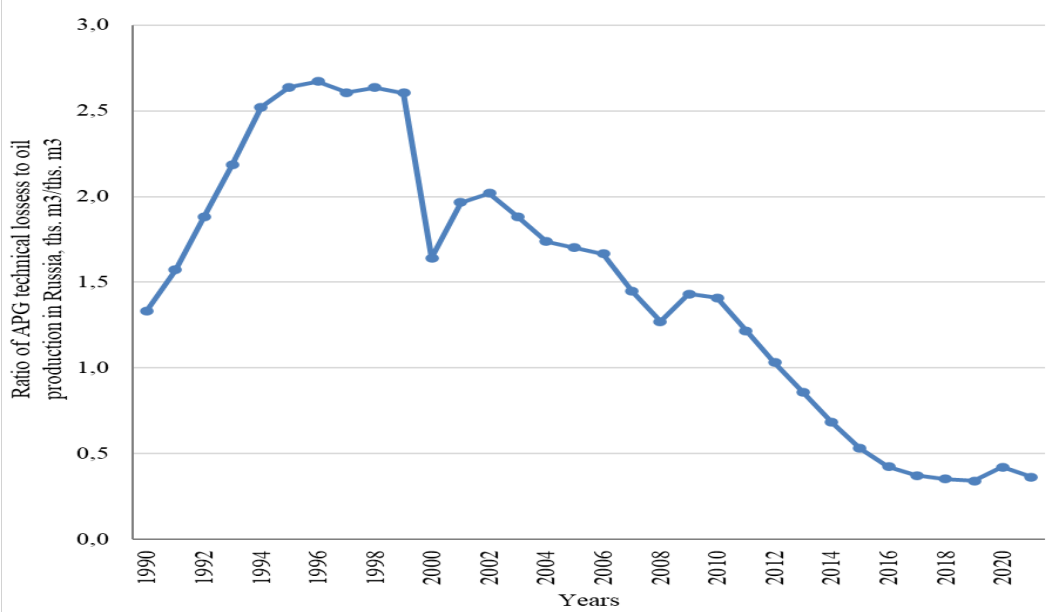



Figure 1. The ratio of APG technical losses to oil production in Russia from 1990 to 2021

**Results**

The final sample contained 18 oil production fields: 5 from Volgo-Ural, 9 from West Siberia, and 4 from East Siberia with Far East oil production macro regions/provinces.

Result of analysis of typical oil production, gathering and treatment scheme showed that main sources of GHG emission were:

- on oil production stage – operations on well pad sites, reservoirs, pig startup valves, automated group metering station;
- on gathering stage – inf-field product transport;
- on oil treatment stage – operations on central gathering plant, complex gas treatment unit, and on oil delivery and acceptance point.

For each of 18 fields and each year from 2019 to 2021 above-mentioned data was collected and, in addition to it – information on production of oil, APG, and other hydrocarbons and oil density.

Results for $CH_4$ and $CO_2$ CS EF's calculation and its comparison to IPCC 2006 guidelines emission factors, and recovered $CH_4$ and $CO_2$ CS EF's for timeline are demonstrated in the tables 1 and 2 respectively. GHG emission estimates with new CS EF's and their comparison with past values are demonstrated on Figure 2

https://doi.org/10.5593/sgem2024v/3.2/s06.46

Table 1. Results of $CH_4$ and $CO_2$ CS EF's calculation and its comparison to IPCC 2006 guidelines emission factors[2].

| Reference | $CH_4$ CSEF kt.·$10^{-3}m^{-3}$ | | Uncertainty | $CO_2$ CSEF kt.·$10^{-3}m^{-3}$ | | Uncertainty |
|---|---|---|---|---|---|---|
| IPCC 2006 guidelines | $1,5*10^{-6(1)}$ | $1,8*10^{-3(3)}$ | ±100% | $1,1*10^{-7(1)}$ | $1,3*10^{-4(3)}$ | ±100% |
| | $3,6*10^{-3(2)}$ | | | $2,6*10^{-4(2)}$ | | |
| | $7,2*10^{-4(4)}$ | | ±50% | $9,5*10^{-5(5)}$ | | ±50% |
| Work results | $2,74*10^{-4(5)}$ | | ±47% | $7,6*10^{-6(4)}$ | | ±45% |

*(1)(2)(3) – minimum (1), maximum (2) and mean value (3) from range of emission factors from fugitives during conventional oil production, listed in IPCC 2006 guidelines;*

*(4) – emission factors from venting during conventional oil production, listed in IPCC 2006 guidelines;*

*(5) Developed CS EF are relevant to period from 2017 .*

Table 2. Recovered $CH_4$ and $CO_2$ CS EF's for the 1990-2021 timeline

| CS EF | unit | 1990 | 1995 | 2000 | 2005 | 2010 | 2015 | 2017-present |
|---|---|---|---|---|---|---|---|---|
| $CH_4$ CS EF | kt./ths. $m^3$ | $9,6*10^{-4}$ | $1,9*10^{-3}$ | $1,2*10^{-3}$ | $1,2*10^{-3}$ | $1,0*10^{-3}$ | $3,8*10^{-4}$ | $2,7*10^{-4}$ |
| $CO_2$ CS EF | | $2,7*10^{-5}$ | $5,4*10^{-5}$ | $3,3*10^{-5}$ | $3,5*10^{-5}$ | $2,9*10^{-5}$ | $1,1*10^{-5}$ | $7,6*10^{-6}$ |

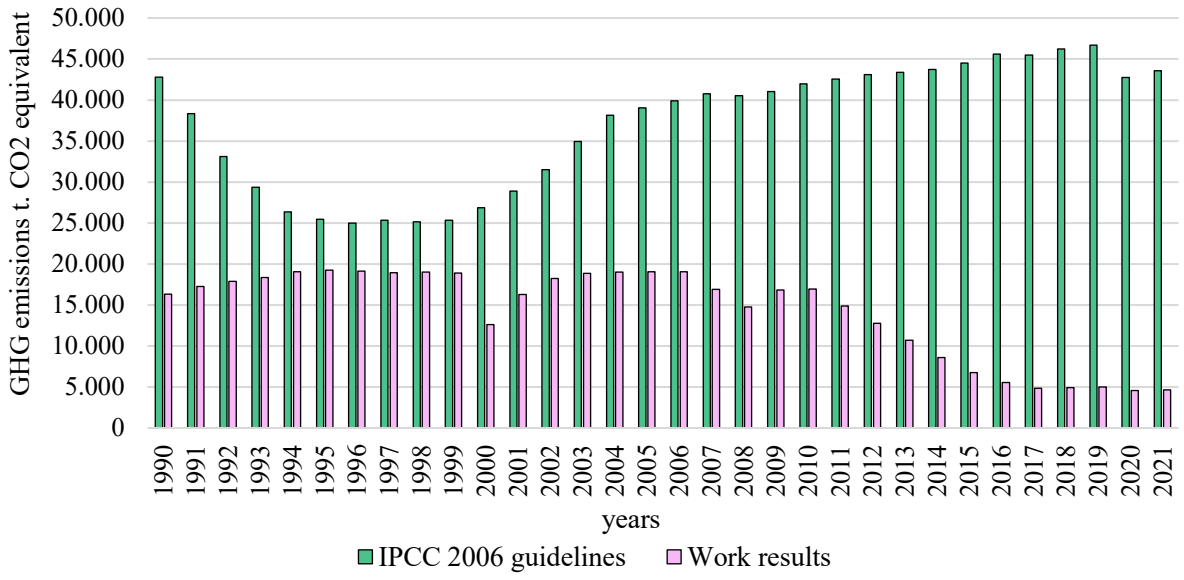



Figure 2. GHG emission estimates with new CS EF's and its comparison with past values

**DISCUSSION**

As a result of the analysis of the country-specific emission factors implied in NIR of other oil-producing countries it was found that developed $CH_4$ and $CO_2$ CS EF's are in line of their range. Analysis was performed on the base of data on EF in common reporting format tables, results are showed on Figure 3.

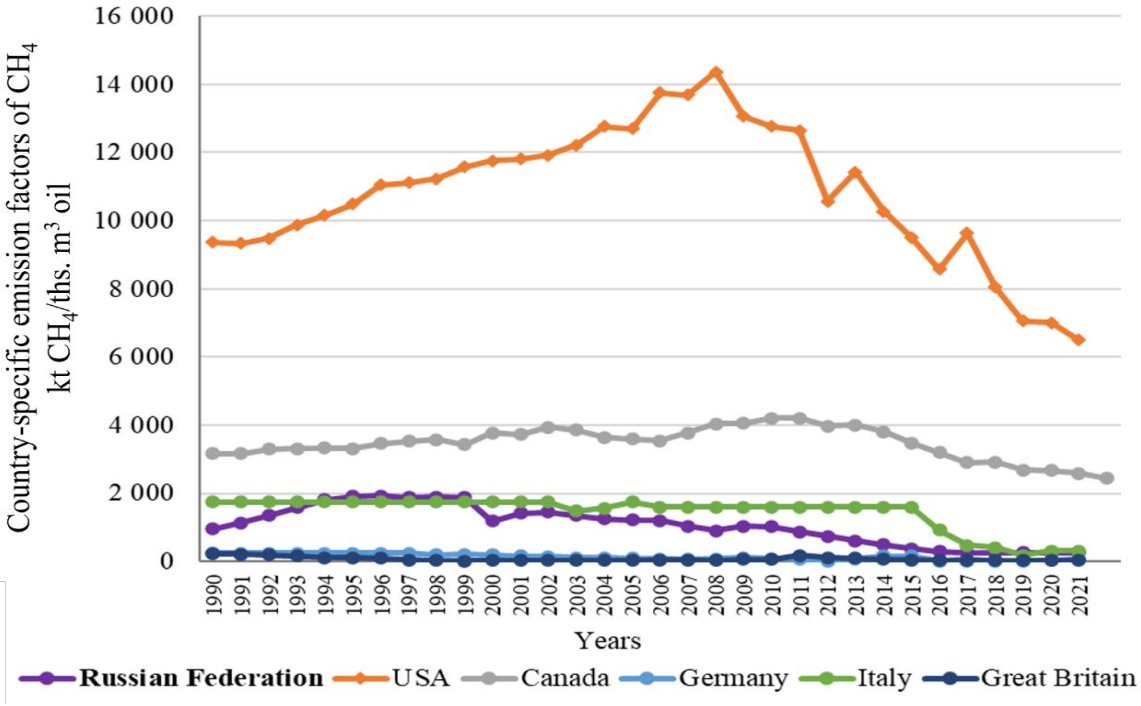



Figure 3. $CH_4$ CS EF from oil production between different countries [6].

It was found that Italy country-specific emission factors have the most similar with developed $CH_4$ and $CO_2$ CS EF's dynamic which is explained by the influence of regulatory measures, that are applied to oil field operators [1,7]. It has to be mentioned, that correct comparison of emission factors between different countries is a non-trivial task due to: use of different methodologies of emission factors calculation, and use an original data on $CH_4$ emission measures, provided by different operators [6]. Therefore, the information, provided on picture 3 is for reference only, and emphasizes a problem of high variability in GHG estimation methodologies.

But it should be mentioned, that many countries, including Australia, Norway and others include their production GHG emissions together with oil exploration emissions. Hence, future improvement of GHG estimations from oil upstream segment in Russia and refinement of their level relative to other countries could lie in the development of country-specific GHG emission factors for oil and gas exploration stage [6].

https://doi.org/10.5593/sgem2024v/3.2/s06.46

## CONCLUSION

New country-specific $CH_4$ and $CO_2$ emission factors from oil production, gathering and treatment for Russian Federation were developed. Their values are provided in table 1 and 2. Summarized fugitive and venting emissions factor used in Russian NIR, submitted in 2023 (table 1, summed emission factors multiplied on global warming potential) is $7{,}08*10^{-2}$ kt. of $CO_2$ equivalent. New summarized country-specific emission factor is $7{,}6*10^{-3}$ kt. of $CO_2$ equivalent which is more than 9 times lower. Selected sample of data on 18 oil production fields provide complete picture of methane and carbon dioxide oil-specific emission factors and, by taking into account the gas to oil ratio and type of deposits in sample selection, describes well the variability of oil mode of occurrence in Russia.

From table 1 it follows, that $CH_4$ and $CO_2$ CS EF's and their uncertainty value are much lower than average emission factors listed in IPCC 2006 guidelines and used in Russian NIR, but they are in line with range of emission factors, listed for fugitives in IPCC 2006 guidelines. Venting and fugitive emissions are together included in new $CH_4$ and $CO_2$ CS EF's, however emission factors from venting from IPCC 2006 is higher – this may be due to scheme of maintaining work procedures on oil production fields in Russia, where all venting gas is directed to flaring facility.

Figure 1 shows that analyzed ratio of APG technical losses to oil production relevantly describes all main stages of Russian oil production industry development: economic crisis from 1990 to 1998; economic restructuring and oil production recovery from 2000 to 2010, implementation of regulatory measures for APG rational utilization from 2012 and oil production fields modernization since 2015[1]. Hence, all described characteristics are inherent for recovered timeline of $CH_4$ and $CO_2$ CS EF's listed in table 2.

Figure 2 shows that average reduction of GHG emissions from implementation of new CS EF's for whole timeline is 23 million tons of $CO_2$ equivalent: maximum reduction is in 2019 – 41,7 million tons, and minimum is in 1996 – 5,8 million tons of $CO_2$ equivalent.

Developed $CH_4$ and $CO_2$ CS EF's are in range of the same country-specific GHG emission factors provided for European oil-producing countries. For rough comparison of Russian GHG emissions from upstream segment in oil industry, there should be developed country-specific GHG emission factors from oil and gas exploration.

## ACKNOWLEDGEMENTS

Country-specific $CH_4$ and $CO_2$ emission factors were developed within the governmental project "Russian climate monitoring system". Authors of the work are grateful for assistance and cooperation to the Ministry of Economic Development of the Russian Federation and to the Ministry of Energy of the Russian Federation.

## REFERENCES

[1] National inventory report of anthropogenic emissions by sources and removals by sinks of greenhouse gases not controlled by the Montreal Protocol for 1990 – 2021. Mode of access – https://unfccc.int/documents/631719

[2] IPCC 2006, 2006 IPCC Guidelines for National Greenhouse Gas Inventories, Prepared by the National Greenhouse Gas Inventories Programme, Eggleston H.S., Buendia L., Miwa K., Ngara T. and Tanabe K. (eds). Published: IGES, Japan.

[3] Russian fuel and energy complex 2019 – Analytical Center for the Government of the Russian Federation. Mode of access – https://ac.gov.ru/uploads/2-Publications/TEK_annual/TEK.2019.pdf

[4] Popov N.V., Tret'yak O.S. Analysis of approaches to develop greenhouse gas emission factors from oil and gas condensate production and upgrading // Environmental Monitoring and Ecosystem Modelling, vol. XXXV, no. 1-2, 2024, p. 70-72 DOI: 10.21513/0207-2564-2024-1-2-62- 72

[5] Methodological Recommendations for Determination and Justification of Technological Losses of Natural Gas, Gas Condensate and Associated Gas during Production Technologically Related to the Adopted Field Development Scheme and Technology (approved by the Ministry of Energy of the Russian Federation on April 12, 2018).

[6] National Inventory Submissions 2023 | UNFCCC. Mode of access – https://unfccc.int/ghg-inventories-annex-i-parties/2023

[7] Italian Greenhouse Gas Inventory 1990-2021 National Inventory Report 2023. Mode of access – https://unfccc.int/documents/627845

https://doi.org/10.5593/sgem2024v/3.2/s06.46

# PHASE BOUNDARY EQUILIBRIUM CONDITIONS FOR $CH_4$, $C_2H_6$ AND $C_3H_8$ IN MARINE QUARTZ-BASED POROUS SAND: THERMODYNAMIC EVOLUTION OF THE SYSTEM AND DEVIATION FROM THE IDEAL TREND

**Dr. Alberto Maria Gambelli**
**Dr. Jessica Di Mario**
**Full Prof. Enrico Gigliotti**
University of Perugia, Civil and Environmental Engineering Department, Via G. Duranti 93, 06125, Perugia, **Italy**

## ABSTRACT

Natural gas hydrate reservoirs often consist of a mixture of various gaseous species: small-chain hydrocarbons, as methane, ethane, propane and butane, and other species, as carbon dioxide, nitrogen, oxygen, hydrogen sulfide and others. Every species shows different forming conditions. Moreover, those conditions may change as a function of the mixture composition and the properties of the surrounding environment. The present study deals the production of hydrates with small-chain hydrocarbons, within a silica-based porous marine sediment. Hydrates were formed and melted, the experimental phase boundary equilibrium conditions were then compared with the ideal ones, obtained from literature. Such a comparison allowed to characterize how the sediment acted during the process. In presence of methane and ethane, It was found capable to promote the process, while It acted as inhibitor for propane hydrates. The difference observed between the various species, were finally explained in terms of typology of hydrate structure formed and molecular diameter of the guest species.

**Keywords:** natural gas hydrates; phase boundary equilibrium conditions; marine porous sediments; cage occupancy; small-chain hydrocarbons.

## INTRODUCTION

Natural gas hydrates are solid and crystalline compounds, where the solid lattice is constituted by hydrogen bonded water molecules, which form polyhedral cavities around specific gaseous molecules, referred as “hosts” [1]. Among the various species capable to form hydrates, the most widespread are methane, ethane, propane, carbon dioxide, nitrogen, noble gases, oxygen, hydrogen sulfide, and others [2, 3]. Those species have physical and chemical properties often different among each other; the main common property is their hydrophobicity, even if some exceptions exist, as carbon dioxide and hydrogen [4]. Natural gas hydrates are widely diffused in nature, divided between deep oceans and continental margins (97%) and permafrost regions (3%). The most abundant offshore reservoirs were discovered in the South China Sea, Japan Sea, Indian Ocean, Gul3f of Mexico, Seas of Korea and Bearing Strait, while the main permafrost findings are sited in Siberia, Alaska and Tibet Plateau [5, 6]. The growing interest on natural reservoirs is due to the huge quantities of methane stored in these sites, approximately equal to $10^{15} – 10^{17}$ $m^3$, enough to produce twice the energy which

https://doi.org/10.5593/sgem2024v/3.2/s06.47

can still be obtained from all the known and available conventional energy reservoirs (oil, gas and coal) [7].

The hydrate lattice is based on five different polyhedral cages, named pentagonal dodecahedron ($5^{12}$), tetrakaidecahedron ($5^{12}6^2$), hexakaidecahedron ($5^{12}6^4$), irregular dodecahedron ($4^3 5^6 6^3$) and icosahedron ($5^{12}6^8$). The numerical identification proposed between parenthesis describes the geometry of each cavity: such a nomenclature can be identified as "$ni^{mi}$", where "ni" is the number of edges of a specific face, while "mi" is the number of faces having "ni" edges. The type of cage formed depends on the specific guest molecule involved in the process. Moreover, those cages rearrange themselves by forming three different possible hydrate structures: the cubic sI, the cubic sII and the hexagonal sH. Molecules as methane, ethane and carbon dioxide naturally form sI hydrates, whose unit cell contains the small $5^{12}$ and the (relatively) large $5^{12}6^2$ [8, 9]. Conversely, molecules having smaller diameters, as nitrogen, or larger diameters, as propane, than the species previously mentioned, usually lead to the production of sII hydrates, a structure including $5^{12}$ and $5^{12}6^4$ cavities [10]. Gaseous mixtures often show different behaviour than the pure species in them contained. For instance, in presence of suitable aid species, methane can easily form sII hydrates instead of sI. The reason can be explained in terms of cage occupancy: the guest molecules must obviously have size lower than that of the hosting cavity; however, in order to ensure the highest stability possible, their size must be as much as possible close to the one of hosting cavities. By itself, methane produces sI hydrates, since It can easily fit both the cavities and its diameter is only slightly smaller than the $5^{12}$ cavity diameter. Conversely, if methane is used in mixture with propane, it could lead to the production of sII hydrates. In this second configuration, methane molecules would fit the small cavities, while propane molecules the large cavities, thus reaching high cage filling ratios and ensure the stability of the whole hydrate lattice [11].

In addition, the type of structure formed, the cage filling ratio and, more in general, the forming conditions of the system, strongly depend on the hosting sediment [12, 13]. In particular, permeability and porosity of sediments are the main factors affecting the overall gas saturation, thus acting as leading parameters during the hydrate production process [14, 15]. The present study aims to characterize the production and dissociation of hydrates with the most common short-chain hydrocarbon species present in natural gas mixtures: methane, ethane and propane. The experiments were carried out within a fine-grained porous sediment, with the aim of observing how a similar sediment may affect the hydrate-liquid-vapour (HLV) phase boundary conditions of the system. For the scope, the experimental results were compared with the theoretical equilibrium conditions, defined according to the recent scientific literature.

## MATERIALS AND METHODS

The experimental apparatus consists of a small-scale reactor, appositely designed to reproduce marine porous sediments and form hydrates within. The reactor is positioned within a cooling room, in order to regulate temperature from the external. Pressure and temperature and constantly monitored by using a digital manometer (MAN-SD, by Kobold) and three Type K thermocouples (by TC-Direct). Here only few details about the experimental apparatus are provided; further details can be found elsewhere in literature [16].

The reactor was filled with 744 $cm^3$ of porous sand and 236 $cm^3$ of demineralized water. Finally, It was closed and the gaseous species was injected, until reaching the target pressure. The porous sediment consists of pure quartz spherical grains, having diameter ranging from 0.09 to 0.15 mm. The mean porosity was measured with a porosimeter, model Thermo Scientific Pascal 140 and is equal to 34%.

Gas was injected at temperatures enough elevated to avoid the accidental production of hydrates during injection. The reactor was then definitively closed and the cooling room switched on. As soon as the thermodynamic conditions became feasible for the process, the growth of hydrates took place and continued until the system stabilized in correspondence of the lowest temperature fixed for the tests. The dissociation started immediately later: the cooling room was switched off and hydrates started melting. The tests continued until the hydrate phase was completely melted.

## RESULTS AND DISCUSSION

The pressure evolution, measured during hydrates dissociation, was described for each species in Figure 1.

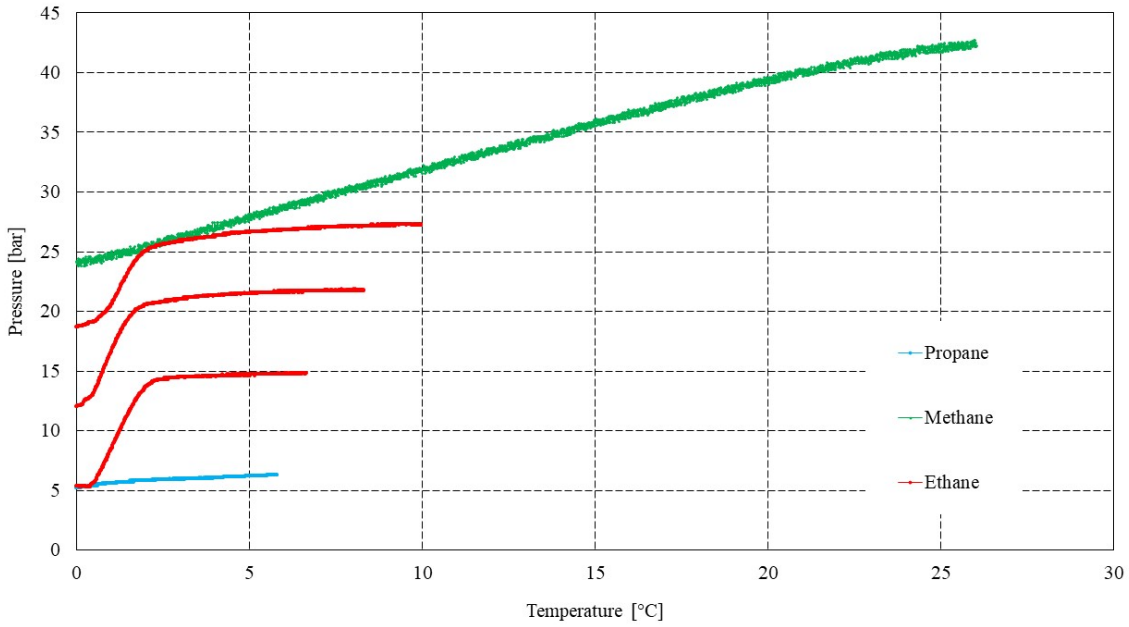



**Figure 1.** Pressure evolution over time, during hydrates dissociation, for the various guest species.

The curves shown in Figure 1 describe the sole dissociation of hydrates, which can be considered a deterministic process, mainly dominated by heat and mass transfer properties of the system. Conversely, the formation process is highly stochastic, mainly due to the initial nucleation step. As visible from the diagrams, the melting of methane and propane hydrates was gradual and occurred along the whole temperature range selected for the experiments. The corresponding curves (in green for methane and in blue for propane hydrates), show an approximately constant trend. Conversely, the dissociation of ethane hydrates occurred differently. The melting of hydrates took place immediately after the cooling room was switched off and the temperature started increasing. The dissociation was almost completed when the increase of temperature

https://doi.org/10.5593/sgem2024v/3.2/s06.47

was still lower than +2 °C. The different behaviour between ethane hydrates and the other species, can be explained in terms of hydrates stability. By itself, ethane forms sI hydrates. In this kind of crystalline structure, its molecules preferentially fit the large cavities, while the small-size cavities remain empty, with a consequent low stability of the whole hydrate lattice. Conversely, methane which, as ethane, form sI hydrates, due to its smaller size, can enter within both the cavities, thus ensuring high stability to the whole structure. Similarly to ethane, also propane can fit exclusively the large cages; however, pure propane leads to the production of sII hydrates, a structure showing higher stability than sI in correspondence of the phase boundary equilibrium conditions. This latter configuration was observed and measured for each species and the results were compared with the ideal equilibrium, defined according to the current literature (methane [17]; ethane [18]; propane [19]). The collected results are shown in Figure 2.

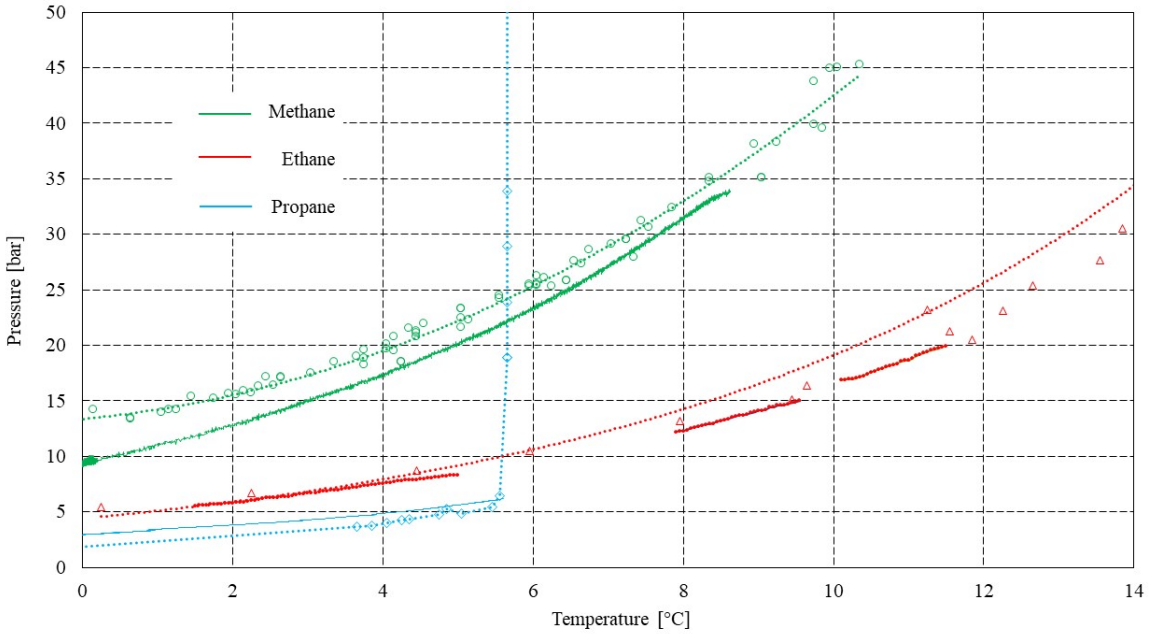



**Figure 2.** Phase boundary dissociation conditions, measured for methane, ethane and propane hydrates, compared with the ideal equilibrium conditions, collected from literature.

As visible in Figure 2, the phase boundary equilibrium values of methane hydrates always remained below the ideal values. The melting trend was completely comparable but, due to the porous sediment, the melting temperatures were shifted to milder values, proving that sand acted as promoter for the process, ensuring the stability of hydrates also at conditions outside from the theoretical hydrate stability zone.

The promoting action, observed for methane hydrates, can be attributed to the geometry of sand. In fact, geometrical, physical and chemical properties of sediments can significantly change the forming and melting conditions of the system, both promoting or inhibiting, also as a function of the guest species involved in the process. For instance, nano fossil-rich sediments shift the dissociation temperatures to lower values, approximately about 0.5 °C, therefore slightly inhibiting the process, differently from the porous sediment tested in this study. More in general, the production of hydrates is strongly dependent on the size of sand particles. In addition, sediments hosting natural gas hydrate reservoirs are often complex, containing numerous mineral particles,

organic debris, remnant of fossils, and so on. For that reason, the role of sediments cannot be defined in advance and requires direct experimentation.

The promoting effect of silica-based porous sand was previously asserted in literature and was associated to the tendency of water to produce a thin film over fine grains, thus favoring the production of clathrates on their surface and pores.

Similar results were also reached for ethane hydrates. Referring to Figure 2, at temperatures below 12-12.5 °C, the experimental phase boundary conditions always remained below the theoretical ones. The overall promoting action is clear; however, It is less pronounced than what observed for methane hydrates: difference in melting pressures up to 5.5 bar were observed for methane hydrates while, in tests carried out with ethane, such a difference remained below 1.5 – 2.0 bar.

Opposite results were reached for propane hydrates: the dissociation of hydrates occurred at slightly higher pressures than those belonging to the ideal equilibrium for this species. It should be noted that propane hydrates were tested only within a limited temperature range, if compared with the other species. At temperatures higher than 5.5 °C, the equilibrium pressure for propane hydrates immediately changes, growing about tens of bars even for very contained variations of temperatures [19]. For this latter species, the sediment acted as weak inhibitor.

Based on these results, it can be concluded that the same sediment, used for experiments carried out with the same procedure and the same equipment, played the role of promoter for methane and ethane hydrates, while inhibited the process in presence of propane.

Such a different behaviour can be mainly attributed to the different structures formed by the various species: while methane and ethane form sI hydrates, propane leads to the production of sII. The two unit cells have different mean size, approximately equal to 12Å for sI and 17.3 Å for sII. The pore size of the sediment resulted more appropriated for sI structures, while It made, the production of sII, more difficult.

Also the size of guest molecules had a role: the promoting effect for methane hydrates was higher than what observed for ethane hydrates, even if the structure formed is the same. It depends on the different size of guests: methane molecules easily fit both the small and large cavities of sI, while ethane molecules preferentially fit the large ones, thus producing a less stable hydrate lattice. For that reason, the promoting effect, related to the porous sediment, was less pronounced for this guest species.

## CONCLUSION

The present research explored the production of gas hydrates, having small-chain hydrocarbons as guest species, within a typical marine porous sediment. The guest species were selected since represent the main hydrocarbon component of natural gas mixtures commonly contained into natural hydrate reservoirs. The experiments were carried out in a small-scale experimental apparatus, appositely designed to simulate deep oceans and continental margins environments. The thermodynamic evolution of tests was measured and compared with the ideal phase boundary equilibrium conditions of the corresponding species, defined according to the existing scientific literature.
The result proved that the porous sediment promoted the production of methane and ethane hydrates, even if with different intensity. In detail, the sediment strongly

https://doi.org/10.5593/sgem2024v/3.2/s06.47

promoted the production of methane hydrates, while the same action was weaker for ethane hydrates.
Conversely, the sediment acted as weak inhibitor for propane hydrates, whose experimental phase boundary curve occurred at higher pressures than those describing the ideal phase boundary equilibrium.
The difference between promotion and inhibition depended on the different hydrate structure formed: methane and ethane lead to the production of sI, while propane forms sII. The unit cells of these two structures have different mean size, respectively 12 and 17.3Å; therefore, the production of these structures within sand porous clearly occurred differently and the latter one resulted disadvantaged.
Also the size of guest species played a role: within sI hydrates, methane is capable to fit both the small and large cavities, while ethane preferentially occupies the large cages. As a consequence of it, ethane hydrate assumed a less stable configuration and the promoting effect, related to the porous sediment, was consequently less pronounced.

## ACKNOWLEDGEMENTS

The authors would acknowledge the Department of Civil and Environmental Engineering of the University of Perugia.

## REFERENCES

[1] Sloan E.D., Koh C.A., Clathrate hydrates of natural gases, 3rd Ed, CRC Press, 2008.
[2] Ndlovu P., Babaee S., Naidoo P., Experimental study of $CH_4$-$CO_2$ replacement in gas hydrates in the presence of nitrogen and graphene nanoparticles. J. Mol. Liq. 371, 121109, 2023.
[3] Yan P., Luan H., Jiang Y., Liang W., Liu M., Chen H., Influence of depressurization mode on natural gas hydrate production characteristics: One-dimensional experimental study. Geoen. Sci. Eng. 234, 212671, 2024.

[4] Giovannetti R., Gambelli A.M., Castellani B., Rossi A., Minicucci M., Zannotti M., Li Y., Rossi F., May sediments affect the inhibiting properties of NaCl on $CH_4$ and $CO_2$ hydrates formation? An experimental report. J. Mol. Liq. 359 119300, 2022.
[5] Sun Y., Li B., Guo W., Lu X., Zhang Y., Li K., Wang P., Jin G., Ji R., Qu L., Comparative analysis of the production trial and numerical simulations of gas production from multiplayer hydrate deposits in the Qilian Mountain Permafrost. J. Nat. Gas Sci. Eng. 21, 456 – 466, 2014.
[6] Li X.S., Xu C.G., Zhang Y., Ruan X.K., Li G., Wang Y., Investigation into gas production from natural gas hydrate: a review. Appl. Energy 172, 286 – 322, 2016.
[7] Moridis G.J., Sloan E.D., Gas production potential of disperse low-saturation hydrate accumulation in oceanic sediments. Energy Convers. Manag. 48, 1834 – 1849, 2007.

[8] Ohmura R., Uchida T., Takeya S., Nagao J., Minagawa H., Ebinuma T., Narita H., Clathrate hydrate formation in (methane+water+methylcyclohexanone) systems: the first phase equilibrium data. J. Chem Thermodyn. 35, 2045 – 2054, 2003.

[9] Semenov A.P., Medvedev V.I., Guschin P.A., Yakushev V., Effect of heating rate on the accuracy of measuring equilibrium conditions for methane and argon hydrates. Chem. Eng. Sci. 137, 161 – 169, 2015.

[10] Sundramoorthy J.D., Hammonds P., Lal B., Philips G., Gas hydrate equilibrium measurement and observation of gas hydrate dissociation with/without a KHI. Procedia Eng. 148, 870 – 877, 2016.

[11] Li Y., Gambelli A.M., Chen J., Yin Z., Rossi F., Tronconi E., Mei S., Experimental study on the competition between carbon dioxide hydrate and ice below the freezing point. Chem. Eng. Sci. 268, 118426, 2023.

[12] Kaschiev D., Verdoes D., van Rosmalen G.M., Induction time and metastability limit in new phase formation. J. Cryst. Growth 110, 373 – 380, 1991.

[13] Englezos P., Kalogerakis N., Dholabai P.D., Bishnoi P.R., Kinetics of formation of methane and ethane gas hydrate. Chem. Eng. Sci. 42, 2647 – 2658, 1987.

[14] Winters J.W., Waite W.F., Mason D.H., Gilbert L.Y., Pecher I.A., Methane gas hydrate effect on sediments acoustic and strength properties. J. Pet. Sci. Eng. 56, 127 – 135, 2017.

[15] Oshima M., Suzuki K., Yoneda J., Kato A., Kida M., Konno Y., Muraoka M., Jin Y., Nagao J., Tenma N. Lithological properties of natural gas hydrate-bearing sediments in pressure-cores recovered from the Krishna-Godavari Basin. Mar. Pet. Geol. 108, 439 – 470, 2019.

[16] Gambelli A.M., Rossi F., Experimental characterization of the difference in induction period between CH4 and CO2 hydrates: Motivations and possible consequences on the replacement process. J. Nat. Gas Sci. Eng. 108, 104848, 2022.

[17] Bavoh C.B., Partoon B., Lal B., Keong L.K., Methane hydrate-liquid-vapor-equilibrium phase condition measurements in the presence of natural amino acids. J. Nat. Gas Sci. Eng. 37, 425 – 434, 2017.

[18] Subramanian S., Kini R.A., Dec S.F., Sloan E.D., Evidence of structure II hydrate formation from methane + ethane mixtures. Chem. Eng. Sci. 55, 1981 – 1999, 2000.

[19] Moojer-van der Heuvel M.M., Peters C.J., Aron J.S., Gas hydrate phase equilibria for propane in the presence of additive components. Fluid Phase Equilibr. 193, 245 – 249, 2002.

https://doi.org/10.5593/sgem2024v/3.2/s06.47

# PRODUCTION OF sI AND sII HYDRATES WITH BINARY MIXTURES CONTAINING $CH_4$ AND LOWER CONCENTRATIONS OF $C_2H_6/C_3H_8$: POSSIBLE CONSEQENCES ON REPLACEMENT IN MARINE NATURAL DEPOSITS

**Dr. Alberto Maria Gambelli**
**Dr. Jessica Di Mario**
**Prof. Dr. Giovanni Gigliotti**
University of Perugia, Department of Civil and Environmental Engineering, Via G. Duranti 93, 06125, Perugia, **Italy**

## ABSTRACT

The most attractive option to recover methane trapped within natural gas hydrate reservoirs, consists of the so-called "replacement process", mainly based on the contemporary injection of carbon dioxide during the mining process. If appropriately carried out, this process allows to improve the amount of methane recovered, preserve the crystalline hydrate cages and permanently store enough carbon dioxide to make this source definitively carbon neutral. For that reason, this process is widely studied worldwide. However, most of lab-scale experiments do not consider the presence of further small-chain hydrocarbons within the natural gas mixtures. These species may be crucial in determining key properties of the system, as type of crystalline structure, overall stability, phase boundary equilibrium conditions and others. Therefore, experimentally defining how methane behaves, in terms of hydrates formation, when mixed with ethane and/or propane, is crucial to correctly calculate the $CO_2/CH_4$ replacement efficiency.

**Keywords:** natural gas hydrates, carbon capture and storage, $CO_2/CH_4$ replacement, carbon neutral energy production, alternative energy sources.

## INTRODUCTION

Natural gas hydrates consist of non-stoichiometric and ice-like crystalline compounds, showing highly porous lattice, formed by hydrogen-bonded water molecules and filled with specific gas molecules, referred as "guests", as methane, ethane, propane, carbon dioxide and others [1]. The guest molecules are only physically trapped within the crystalline lattice [4], since the sole forces connecting them with water molecules are van der Waals forces and the energy required to breaks these bonds is equal to 0.3 kcal/mol [3]. Depending on the typology of guest species captured within the lattice, hydrates require different pressure and temperature conditions to form [5]; however, relatively high pressures and low temperatures are often required.

Gas hydrates started being studied mainly as a scientific curiosity. Then, the frequent accidental blockage of gas transport pipelines, due to their formation, incentivized the research, mainly aiming at preventing their formation. Finally, during the last decades, the huge potentialities behind the existing hydrate reservoirs and also related to their formation and dissociation processes, were discovered and gradually explored. Due to

https://doi.org/10.5593/sgem2024v/3.2/s06.48

the enormous amount of methane naturally existing in form of hydrates (approximately $2*10^{16}$ $m^3$ of methane at std conditions), the main cause of interest remain the production of energy from natural reservoirs [10-12]. In addition to this: carbon dioxide permanent storage in deep oceanic sediments [14, 15], temporary storage and transportation of energy gases [16, 17], waste water treatment, desalination and, more in general, treatment of electrolytes solutions [18, 22], cold energy storage [25], preservation of food [23, 24], and others.

In order to, at the same time, producing methane from natural reservoirs and storing carbon dioxide, during the first years of 1980, the so-called replacement process was theorized [31]. The injection of $CO_2$ enhances the release of $CH_4$ from hydrate cavities; moreover, the exchange ratio between these two molecules is theoretically equal to one, thus completely preventing the melting of the hydrate lattice during the process and making the process carbon neutral [33]. The replacement process is based on the capability of carbon dioxide molecules to form hydrates at milder thermodynamic conditions than those required for methane. It can be proved in terms of enthalpy of formation, which is equal to -57.98 kJ/mol for $CO_2$ hydrates and -54.49 kJ/mol for $CH_4$ hydrates [37]. Both the species form the same typology of hydrate structure, or the cubical sI. This structure contains two different cavities: the small pentagonal dodecahedron ($5^{12}$) and the large tetrakaidecahedron ($5^{12}6^2$). In the unit cell of sI, the ratio between these two cavities is equal to 1:3. The relatively small-size methane molecules can easily fit both the cavities, while carbon dioxide can easily occupy only the larger one. For that reason, the replacement process, when carried out with pure carbon dioxide, shows a maximum efficiency equal to 75% [40, 41]. The present upper limit can be overcome by adding other molecules to the replacing mixtures, having molecular diameter lower than carbon dioxide. The most common of these molecules is nitrogen. However, the addition of those species shifts the pressures required for the process to higher values, with consequent additional problems. Moreover, natural hydrate reservoirs often contain other hydrocarbon species, in addition to methane, even if present in smaller concentrations.

This study deepens the effect of ethane and propane on the forming conditions of methane hydrates. Hydrates were consequently formed with binary and premixed mixtures and the results were discussed along the text.

## MATERIALS AND METHODS

The equipment used for gas hydrates production has been previously adopted for several experimental researches; therefore, a detailed description of it is available elsewhere in literature [19]. In this section, a picture of whole apparatus and its main components is provided.



Figure 1. Picture of the apparatus used for gas hydrates production.

The reactor has cylindrical shape and internal volume equal to 1L. It is equipped with three Type K thermocouples (by TC-Direct) for the measure of temperature and one digital manometer (model MAN-SD, by Kobold) for pressure.

The reactor was filled with 744cm$^3$ of porous silica sand (porosity equal to 34%, measured with a porosimeter, model Thermo Scientific Pascal 140) and 236 cm$^3$ of demineralized water. The remained free space was used for the injection of gases.

The gaseous mixtures were prepared before being injected within the reactor and then inserted from the bottom, in order to ensure the highest diffusion possible within the porous sediment. The injection was carried out at temperatures enough elevated to completely avoid the production of hydrates during the process. Finally, the reactor was closed and the temperature gradually and slowly decreased (approximately 0.2 °C/h). The lowering of temperature made the conditions suitable for the production of hydrates and the process started, with the consequent drop in pressure, due to the capture of gas molecules into solid cages. The formation process continued until the pressure stabilized in correspondence of the lowest temperature fixed for the system. Then the temperature was increased again, with the same gradient previously mentioned, and the dissociation took place and continued until the complete melting of hydrates. The values measured during dissociation were used to define the phase boundary equilibrium conditions for the system.

## RESULTS AND DISCUSSION

As previously stated in Section 2, gas hydrates were formed with binary mixtures always containing methane, alternatively mixed with ethane and propane. Different concentrations were used for the respective species, due to the different crystalline structure they allow to form and the consequently different ratio between small and large cavities. When used in purity, methane leads to the production of sI hydrates. In this typology of structure, its molecules can easily fit both the cavities, even if they preferred the smaller ones, since the difference between cage diameter and molecular diameter is lower. Also ethane spontaneously forms sI hydrates; however, due to the

https://doi.org/10.5593/sgem2024v/3.2/s06.48

larger molecular diameter, its molecules tendentially fit the large cavities. Conversely, propane molecules can occupy only the larger cavities of sII hydrates. The ratio between large and small cavities is equal to 3 in sI and 2 in sII. It means that, when pure species are involved, the highest cage occupancy can be reached with methane, followed by ethane and propane. However, the usage of the proposed binary mixtures, allows to still reach theoretical cage occupancy equal to 100% but, at the same time, to increase the stability of the hydrate lattice. In fact, the molecule of methane is too tiny to stabilize the large cavities of sI. Therefore, methane/ethane mixtures lead to the production of sI hydrates, while methane/propane mixtures to the formation of sII hydrates.

In this study, the first mixture was tested at concentrations equal to (75/25) and (25/75) vol%, while the second mixture at concentrations equal to (90/10) and (85/15) vol%. Different concentrations were selected for the two mixtures because of the different typology of hydrate structure that can be form with them.

The production of hydrate with the methane/ethane mixture is described in Figure 2, while the same process for the methane/propane mixture is shown in Figure 3.

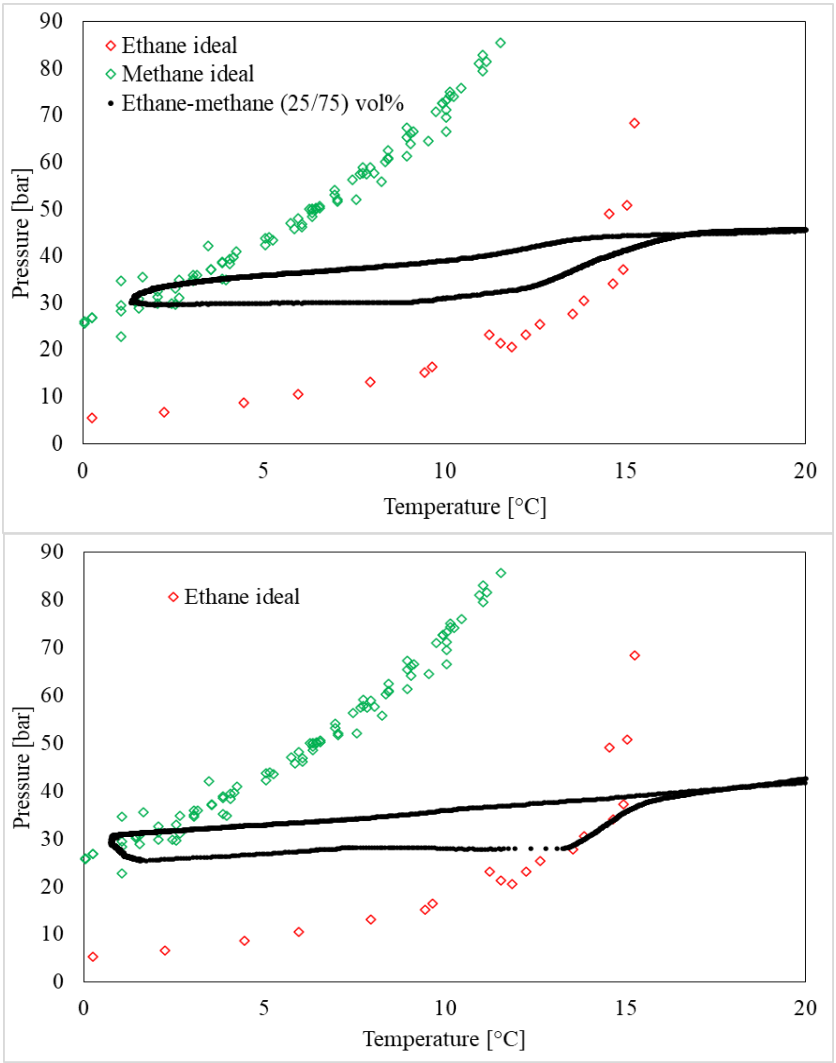



**Figure 2.** Formation and dissociation of methane/ethane hydrates, carried out at concentration equal to (75/25) vol% above and to (25/75) vol% below.

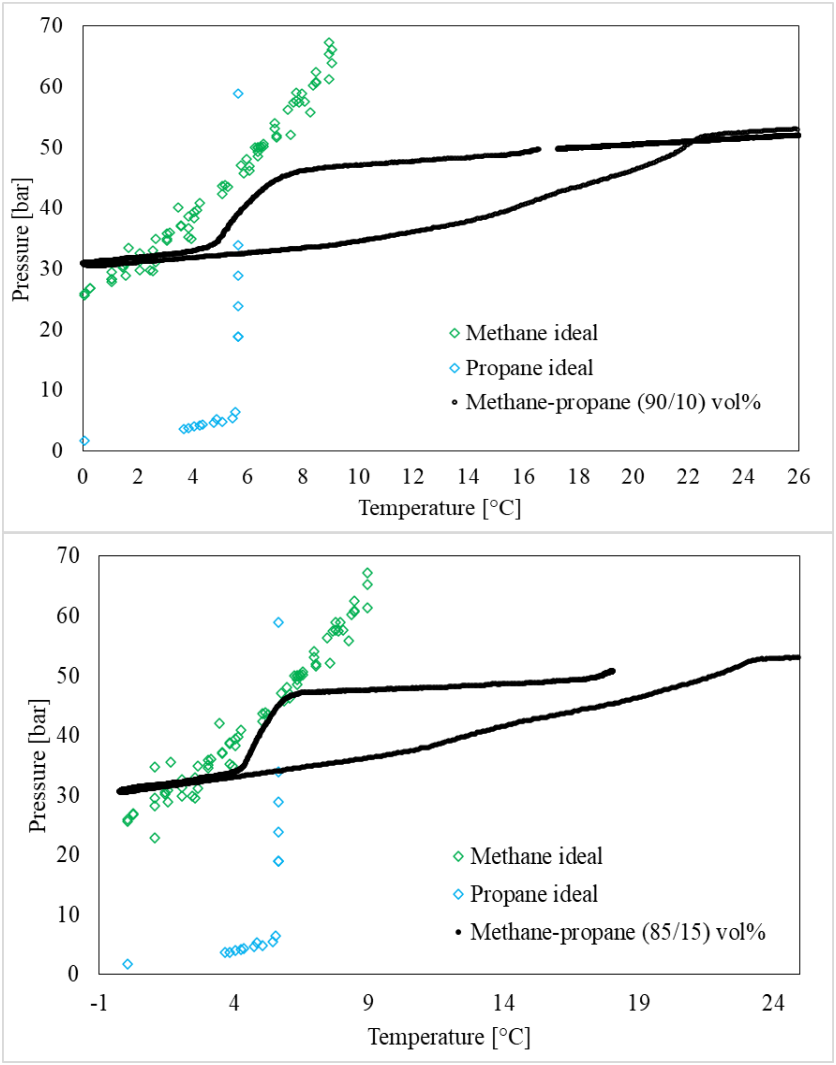



**Figure 3.** Formation and dissociation of methane/propane hydrates, carried out at concentration equal to (90/10) vol% above and to (85/15) vol% below.

The addition of both propane and ethane promotes the process, but the promotion occurred in extremely different ways, as a function of the supporting species selected. The diagrams of Figure 2 describe the production of hydrates with mixtures containing ethane. Independently from the concentration fixed for the mixture, the formation process occurred slowly, gradually and ended only after the system approached the phase boundary equilibrium conditions for pure methane hydrates (showed in the figures with a dotted and green curve). It means that the addition of propane did not enhance significantly the formation process. As previously asserted, methane molecules can easily fit both the cavities; therefore, the addition of propane did not particularly improve the cage occupancy of the system and the forming thermodynamic conditions remained mainly depending on methane. Conversely, the greater size of ethane molecules made, the sI structures formed with the mixture, more stable, thus highly preserving their melting during the dissociation phase. For that reason, hydrates melted at conditions far from the phase equilibrium of methane hydrates and shifted to higher temperatures. In detail, the melting conditions approached the phase equilibrium curve of pure ethane hydrates and, when the concentration of these latter species was

https://doi.org/10.5593/sgem2024v/3.2/s06.48

predominant in the gaseous mixture, the two curves resulted completely overlapped, proving that the dissociation process was mainly governed by ethane molecules. In conclusion, the addition of ethane generally promoted the capture of hydrate and also enhanced the stability of the crystalline lattice. However, the role of the two different species was markedly different: the forming conditions mainly depended on methane molecules, while ethane molecules drove and characterized the dissociation process.
The addition of propane led to a completely different configuration for the system: the capture of methane occurred at thermodynamic conditions slightly milder than those required in absence of propane, while the experimental formation trend was extremely similar (only slightly shifted to higher temperatures). Propane surely played a role during the process, allowing the formation also at conditions of instability for pure methane hydrates. However, the trend mainly depended on methane. Differently from the tests carried out with ethane, here high similarity was observed between the phase equilibrium of pure methane hydrates and the experimental curves related to the mixtures. It should be also noted that higher concentrations of methane were used within these second mixtures.

Also in these tests, the dissociation of hydrates occurred slowly and at conditions widely outside from the stability region of methane hydrates. Differently from the previous experiments, the melting trend cannot be attributed to any of the species involved and ended at conditions of instability for both pure ethane and pure propane hydrates, as clearly visible in Figure 3. Propane molecules can form exclusively sII hydrates; methane molecules can fit the small cavities of this structure and, due to their higher concentration, also form sI hydrates. For that reason, the thermodynamic conditions are only slightly shifted to milder pressure-temperature conditions, since the formation below the phase equilibrium line of pure methane hydrates only refers to the production of sII hydrates. Conversely, since in sII hydrate at least 50% of guest molecules consists of propane, the dissociation conditions were strongly modified from the addition of this heavier hydrocarbon. However, the reason why the dissociation process ended at conditions out from the region of stability of both the species, is still unclear and needs of further experimentation to be determined.

## CONCLUSION

This study deepened the role of small-chain hydrocarbons, as ethane and propane, during the formation and dissociation of natural gas hydrates. Most of lab-scale experiments are carried out with pure methane, while the remaining hydrocarbons are often neglected, even if always present in natural reservoirs. In this study, hydrates were formed with $CH_4/C_2H_6$ and $CH_4/C_3H_8$ mixtures. Two different concentrations were selected for each mixture. While ethane spontaneously forms sI hydrates, as methane, the molecules of propane, due to their greater size, lead to the production of sII hydrates.

Both the species generated a promoting effect on the capture of methane and delayed the melting process. However, the thermodynamic evolution was completely different between the two groups of tests. In presence of ethane, the formation occurred at conditions close to those of pure methane, while the dissociation at conditions similar to those of pure ethane hydrates. However, the forming conditions evolved differently from the methane hydrates phase equilibrium boundary, while the experimental dissociation had trend completely comparable with that of pure ethane hydrates.

Conversely, when the mixtures containing propane were used, the forming trend of hydrates was almost equal to the phase equilibrium of pure methane (even if slightly shifted to milder thermodynamic conditions), while the dissociation trend was far from the ideal and markedly deviated to higher temperatures.

## ACKNOWLEDGEMENTS

The authors would acknowledge the Department of Civil and Environmental Engineering of the University of Perugia.

## REFERENCES

[1] Siazik J., Malcho M., Lehnard R., Proposal of experimental device for the continuous accumulation of primary energy in natural gas hydrates, EPJ Web Conf., vol. 143, pp. 02106, 2017.

[2] McGrail B.P., Schaef, H.T., White, M.D., Zhu, T., Kulkami, A.S., Hunter, R.B., Patil S.L., Owen A.T., Martin P.F., Using carbon dioxide to enhance recovery of methane from gas hydrate reservoirs: final summary report, U.S. Department of Energy, pp. 17035, 2007.

[3] Sloan E.D., Koh C.A., Clathrate hydrates of natural gases, 3rd Edition, Taylor&Francis Group, CRC Press, Boca Raton, FL, USA, 2008.

[4] Hassanpouryouzband J., Yang B., Tohidi B., Chuvilin E., Istomin V., Bukhanov B., et al., $CO_2$ capture by injection of flue-gas or $CO_2$-$N_2$ mixtures into hydrate reservoirs: dependence of $CO_2$ capture efficiency on gas hydrate reservoir conditions, Environ. Sci. Technol., vol. 52, pp. 4324-4330, 2018.

[5] Makogon Y.F., Hydrates of natural gas, PennWell, Tulsa (OK), USA, 1981.

[6] Li X.S., Xu C.G., Zhang Y., Ruan X.K., Li G., Wang Y. Investigation into gas production from natural gas hydrate: a review, Appl. Energy, vol. 172, pp. 286-322, 2016.

[7] Collet, T.S., Energy resource potential of natural gas hydrates, AAPG Bull., vol. 86, pp. 1971-1992, 2002.

[8] Cao X., Wang H., Yank K., Wu S., Chen Q., Bian J., Hydrate-based $CO_2$ sequestration technology: feasibilities, mechanisms, influencing factors, and applications, J. Pet. Sci. Eng., vol. 219, pp. 111121, 2022.

[9] Aminu M.D., Nabavi S., Rochelle C., Manovìc V., A review of developments in carbon dioxide storage, Appl. Energy, vol. 208, pp. 1389-1419, 2017.

[10] Dyadin Y.A., Larionov E.G., Manakov A.Y., Zhurko F.V., Aladko E.Y., Mikina T.V., Komarov V.Y., Clathrate hydrates of hydrogen and neon, Mendeleev Commun., vol. 9, pp. 209-210, 1999.

[11] Smirnov G.S., Stegailov V.V., Toward determination of the new hydrogen hydrate clathrate structures, J. Phys. Chem. Lett., vol. 4, pp. 3560-3564, 2013.

[12] Karamoddin M., Varaminian F., Water desalination using R141b gas hydrate formation, Desalin. Water Treat., vol. 52, pp. 2450-2456, 2014.

https://doi.org/10.5593/sgem2024v/3.2/s06.48

[13] Gaikward N., Nakka R., Khavala V., Bhadani A., Mamane H., Kumar R., Gas hydrate-based process for desalination of heavy metal ions from an aqueous solution: kinetics and rate of recovery, ACS Es&T Water, vol. 1, pp. 134-144, 2021.

[14] Zhang L., Dong H., Dai S., Kuang Y., Yang L., Wang J., Zhao J., Song Y. Effects of depressurization on gas production and water performance from excess-gas and excess-water methane hydrate accumulations, Chem. Eng. J., vol. 431, pp. 133223, 2021.

[15] Claben T., Seidl P., Loekman S., Gatternig B., Rauch C., Delgado A., Review on the food technological potentials for gas hydrate technology, Curr. Opin. Food Sci., vol. 29, pp. 48-55, 2019.

[16] Srivastava S., Hitzmann B., Zettel V., A future road map for carbon dioxide ($CO_2$) gas hydrate as an emerging technology in food research. Food Bioprocess. Technol., vol. 14, pp. 1758-1762, 2021.

[17] Li Y., Gambelli A.M., Chen J., Yin Z., Rossi F., Tronconi E., Mei S., Experimental study on the competition between carbon dioxide hydrate and ice below the freezing point. Chem. Eng. Sci., vol. 268, pp. 118426, 2023.

[18] Giovannetti R., Gambelli A.M., Castellani B., Rossi A., Minicucci M., Zannotti M., Li Y., Rossi F., May sediments affect the inhibiting properties of NaCl on $CH_4$ and $CO_2$ hydrates formation? An experimental report, J. Mol. Liq., vol. 359, pp. 119300, 2022.

[19] Giovannetti R., Gambelli A.M., Rossi A., Castellani B., Minicucci M., Zannotti M., Nicolini A., Rossi F., Thermodynamic assessment and microscale Raman spectroscopy of binary $CO_2/CH_4$ hydrates produced during replacement applications in natural reservoirs, J. Mol. Liq., vol. 368, pp. 120739, 2022.

[20] Yi L., Liang D., Zhou X., Li D., Molecular dynamics simulations for the growth of $CH_4$-$CO_2$ mixed hydrate, J. Energy Chem., vol. 23, pp. 747-754, 2014.

[21] Gambelli A.M., Filipponi M., Nicolini A., Rossi F., Natural gas hydrate: Effect of sodium chloride on the $CO_2$ replacement process, International Multidisciplinary Scientific GeoConference (SGEM), vol. 19, pp. 333-343, 2019.

# SMALL UAV SYSTEMS CAPABLE OF CARRYING OUT RECONNAISSANCE MISSIONS TO DETECT LEAKS IN OIL AND GAS PIPELINES, AIMING TO LIMIT ACCIDENTAL ENVIRONMENTAL POLLUTION

**Senior lecturer Eng. Ștefan-Mircea Mustață – PhD.**
**Third degree researcher Eng. Cristian Vidan – PhD.**
**Eng. Ionuț-Mihai Nacu – PhD Ress.**
Military Technical Academy "Ferdinand I", **Romania**

## ABSTRACT

The paper presents an alternative approach for detecting potential oil or gas leaks from transport and distribution pipelines. The detection of possible accidental pollution is carried out using small UAV systems with the help of photogrammetry. Currently, significant material and human resources are allocated to detect such events, and the use of UAVs can solve the problem of monitoring both small areas like oil platforms, gas extraction stations, or oil wells by implementing multirotor-type architectures, as well as long pipeline systems by using fixed-wing systems suitable for endurance flights. An essential aspect of these systems is the versatility shown in use depending on the payload. Thus, the paper considers the use of a wide range of sensors, such as optical sensors in the visible spectrum, gas sensors capable of detecting potential leaks in real time or allowing post-mission analysis of gas concentration levels in different areas of the responsibility zone, as well as LIDAR sensors, which allow mapping of the areas traversed by such transport and distribution systems. Widely studied, the presented technology represents a decisive factor in reducing environmental pollution globally, by limiting accidents involving oil and gas leaks, which are increasingly frequent in the vast existing networks. The paper begins with an overview of the system, continues with methods for mission planning and execution, simulation and actual realization of some scenarios, and concludes with the post-mission analysis of the data provided by the onboard sensors to determine the system's efficiency and the impact of its use, both economically by reducing losses and ecologically.

**Keywords:** oil and gas, environmental protection, UAV, photogrammetry, sensors.

## INTRODUCTION

The continuous development of fuel distribution networks, both at the European Union level and intercontinental level (Nord Stream, Blue Stream, Turk Stream, Yamal-Europe, etc.), requires a revision of monitoring and prevention methods to address potential leaks that could cause pollution accidents along the routes of the network's main pipelines.

Currently, most states and subcontractors responsible for maintenance and monitoring use specialized teams that conduct on-site, spot checks along the entire length of the pipelines. This method is slow, requires a large workforce, and can only guarantee proper functioning for the specific segment inspected at that given time.

As an alternative to this method, developed countries propose the use of satellite imagery to identify potential leaks. While this approach is efficient, it is limited by the

https://doi.org/10.5593/sgem2024v/3.2/s06.49

high operational costs of a satellite and the inability to detect gas leaks or other substances that are not visible to the naked eye.

Nowadays, the use of remotely operated systems is increasingly widespread due to the efficiency of various types of systems, low operational costs, and the relatively minimal training required for an operator to complete a mission successfully. UAV technology offers significant potential, encompassing the aerial vehicle, payload, and ground station that provides the user interface. The potential of these systems for surveillance missions and target identification across different areas of responsibility prompts studies to demonstrate the reliability of using drones over conventional systems (such as aircraft, satellites, etc.).

Given these considerations, the most accessible solution is the use of UAV systems, capable of conducting missions over large areas and providing the user with relevant information about the status of the monitored network. This is feasible both through computer vision functions that integrate and process data from onboard sensors and by simply supplying the user with images needed to identify potential pollution points. Major advantages of these systems include low operating costs, minimal personnel involvement, and the ability to scan vast areas in a short amount of time.

These systems utilize a complex, branched hardware architecture that can incorporate a wide range of sensors to detect various types of leaks: optical sensors in the visible spectrum, which can identify contrasting liquid leaks on surfaces; thermal optical sensors, capable of detecting both liquid and gas leaks with temperatures different from the ambient environment; LIDAR sensors, which can map the scanned area and provide information about terrain anomalies; and gas sensors, which can trigger alarms upon detecting leaks by identifying levels exceeding the permissible maximum in a given area.

The integration of various sensor types with avionics architectures is, in most cases, the key stage underpinning the development of these systems. Although this requires special attention during the development process and substantial resources to overcome challenges, correlating payload sensors with those used in the navigation algorithm provides a significant advantage. In some cases, it allows the user to overlay mission sensor data with location information from the navigation system. This is extremely helpful in such missions and is known as georeferencing.

Current emerging technologies have enabled photogrammetry-based georeferencing to achieve increasingly high precision, with modern systems incorporating RTK (Real-Time Kinematic) technology that allows target identification with centimeter-level accuracy.

Thus, by knowing the precise location of the leak, repairs can begin immediately, while the aerial units involved can continue their mission, providing the user with real-time images, alerts, and metadata. Using a system based on multiple aerial units allows for an overview of a large area of responsibility, offering extensive coverage.

## SYSTEM ARCHITECTURE AND IMPLEMENTATION METHOD

The proposed system is based on an aerial vector of the multirotor type (quadcopter). It integrates the autonomous navigation system, telemetry system, and the video data link transmission to the ground, along with the onboard payload, which includes an optical

sensor in the visible spectrum that communicates with a processing unit integrated into the autopilot.

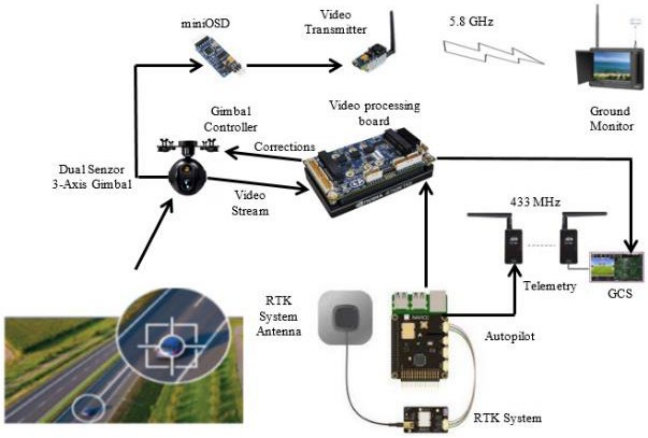



Fig. 1. Overall hardware structure schematics

**Figure 1** illustrates the developed and implemented hardware architecture. As shown, there are three distinct zones, each dedicated to a specific task. Given the mission's execution with a limited personnel number, the flight controller plays a particularly important role, as it can store mission data, perform navigation calculations, and control the motors accordingly. The integration of the control architecture with a ground control station (GCS) can also be observed, allowing real-time monitoring of flight parameters and the possibility of adjusting mission data. The section dedicated to mission execution is represented by the onboard payload, responsible for capturing video data from the video sensor, processing the obtained data using the video processing board, and transmitting relevant information to the user after processing.

**A** draft of the software module as an independent unit, unaffected by hardware architecture type. The video stream from the EO/IR sensors is processed as input to our software, starting with the pre-processing module. Here, a variety of data reduction, filtering, and feature extraction techniques are applied. As the selection of specific filters and extractors is part of our ongoing research, some sub-modules in the diagram are generically labeled. The features produced by the Pre-processing block are then sent to the Classification block, where a pre-trained and selected classifier predicts the class for each target of interest in the video stream.

This Classification block generates two outputs, described as follows. The first output provides information to the GUI (Graphical User Interface), allowing the input video to be replayed with predicted class annotations overlaid on targets. The second output flags a target of interest for the Tracking Algorithm. In turn, this Tracking block generates two outputs: (1) a confirmation signal sent back to the Classification block and (2) a video stream in the GUI, displaying the adjusted tracking of the selected target.

For the Machine Learning (ML) classification block, an adaptable database will be implemented to supply essential information on all potential targets, whether static or dynamic, within the area of responsibility. The objective of the software classification algorithm is to achieve a minimum classification accuracy of 85%. Accurate classification enables the user to make real-time decisions based on the information displayed on the GUI.

https://doi.org/10.5593/sgem2024v/3.2/s06.49

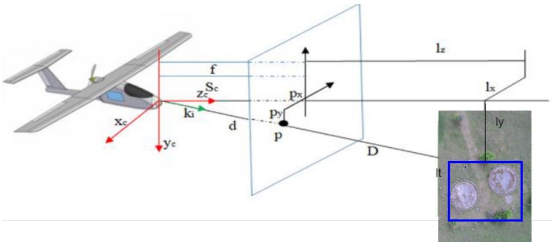



Fig. 2. Video source (EO/IR camera) coordinate system

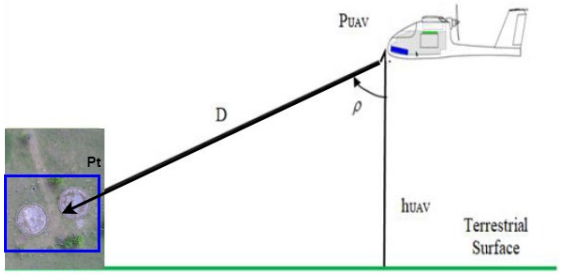



Fig. 3. Estimation of the distance to the target using the Flat Earth method

In fig. 2, knowing the coordinate system of the gimbal platform and the technical characteristics of the camera, the distance to the target can be determined by processing the received enhanced video stream. Such as, the Flat Earth Model method is used to determine the distance to the target. Fig. 3 shows this method of estimating the distance to the target assuming that the Earth is flat (the relief is uniform).

In fig. 4 is presented the process of determining the coordinates of the target (geo-location). To accomplish this task, data from different onboard sub-sistem will be integrated as follows: 1 – the inertial coordinates (PUAV) and the velocity of the UAV (VUAV), in addition, to reduce the error as much as possible (up to 50 cm) these coordinates will be taken from the RTK (Real Time Kinematics) module. Next, 2 - the distance to the target is used. This has been determined in the previously described process. Other data that are integrated into the math model of the target coordinates algorithm are acquired from the autopilot and are related to 3 - the attitude of the platform (roll and pitch angles). In the end, the last input parameters that will be introduced into the equations model are those related to 4 - the position of the gimbal (azimuth and elevation angles). Using all this data and relying on their high accuracy combined with the reduction of errors throughout the algorithm, we assume that we will reach an estimation of the coordinates with an accuracy of at least 90%.

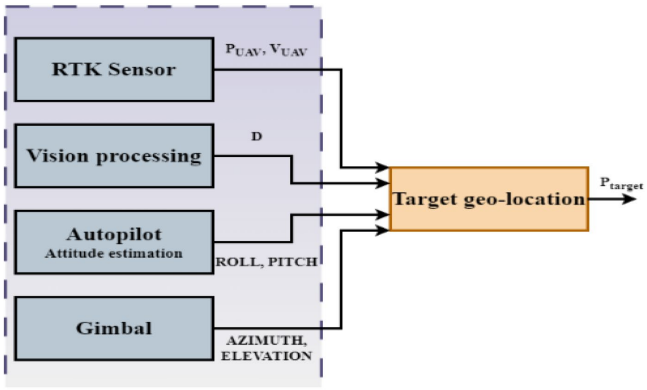



Fig. 4. Estimation of the target geo-location

## MISSION PLANNING

With the hardware and software architectures configured and stable, relevant testing will be conducted to demonstrate the functionality of the proposed system. This process is grounded in mission planning using dedicated software capable of interfacing information for the user. The implementation involves the following steps: defining the area of responsibility and determining the flight path by generating waypoints, identifying key points for capturing relevant images based on the characteristics of the onboard optical sensor, and analyzing the collected data, both through real-time image analysis and post-mission analysis using data stored in the onboard recorders.

Planning a flight mission for a quadcopter using waypoints (fig. 5) involves setting precise waypoints on a digital map, each defined by geographic coordinates, altitude, and travel speed. Depending on the mission objectives, the altitude at each waypoint is configured to ensure optimal coverage and the quadcopter's safety relative to the terrain and any obstacles. Known speed values allow precise control over the mission duration and energy consumption, essential for resource optimization. The planning software interprets this information and generates an automated path, enabling the quadcopter to navigate autonomously through the predefined waypoints, ensuring faithful mission execution and data collection at designated locations.




Fig. 5 Planning a flight mission for a quadcopter using waypoints

Figure 6 shows the possibility of reduction of the number of waypoints in flight mission planning can be influenced by the camera's characteristics and the set flight altitude. A camera with a wide field of view or high resolution enables a larger area to be covered with each capture, allowing for greater distances between waypoints without compromising the quality and detail of the collected information. Additionally, a higher flight altitude expands the camera's visual range, enabling the quadcopter to cover a broader area with fewer stops, which conserves energy resources and optimizes mission duration. Thus, adjusting the waypoints takes into account the optical equipment specifications and chosen altitude to ensure mission efficiency and accuracy.

https://doi.org/10.5593/sgem2024v/3.2/s06.49

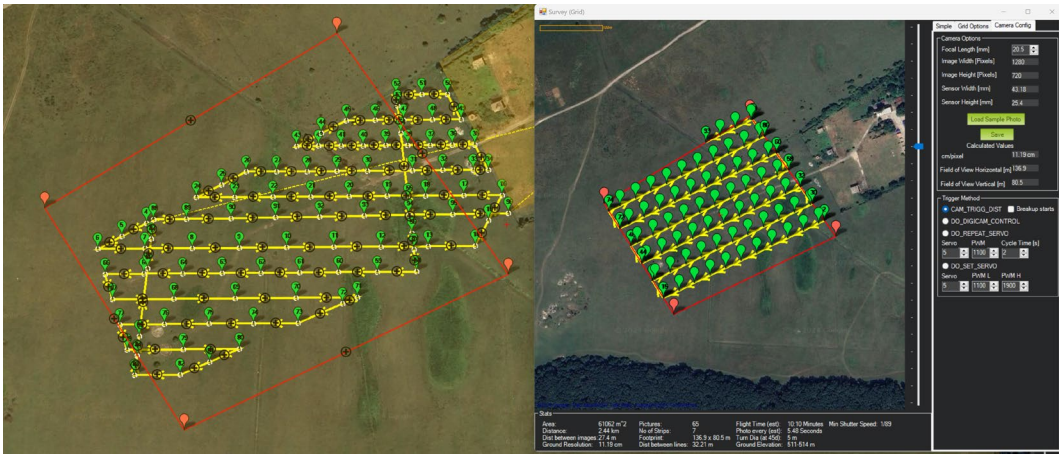


Fig. 6 Planning a flight mission for a quadcopter using waypoints according camera specification

The use of geolocation functionality for images is a valuable tool in various applications, from professional photography to environmental monitoring. This feature allows geographic coordinates to be associated with each captured image, facilitating the organization and search of photos based on location. For instance, in the case of field photography, geolocation provides precise information about where each capture was taken, thereby enhancing documentation and data analysis. Additionally, using geolocation in images enables their integration into GIS (Geographic Information Systems) applications, which increases the value of visual information by providing geographic context. This approach is extremely useful in fields such as wildlife conservation, tourism, and urban management, where knowing the exact location of images can influence strategic decision-making.

The following figure illustrates fuel tanks identified on the ground, located using the geolocation function of an image captured by an UAV (Unmanned Aerial Vehicle). By leveraging geolocation data, the exact coordinates of the fuel tanks were pinpointed, demonstrating the effectiveness of integrating geospatial information with aerial imagery. This capability not only enhances situational awareness but also facilitates rapid response in various scenarios, such as search and rescue operations or security assessments. The UAV's ability to provide real-time visual data, combined with precise geolocation, significantly improves the efficiency of locating and tracking objects of interest, ultimately contributing to more informed decision-making processes.



Fig. 7 Image from the payload

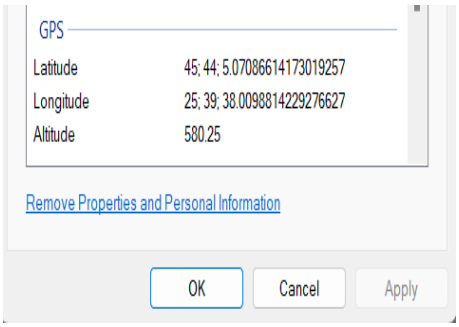



Fig. 8 Geolocation data of the image

Reforming a terrain map using geolocated images is an innovative process that combines image capture technology with geographic data. By utilizing geolocated images, the physical features of the terrain, such as fuel tanks and fuel pipeline, can be accurately identified. These images are integrated into GIS (Geographic Information Systems) software, where they are processed to create an updated and detailed representation of the targeted area. By overlaying the images onto the base map, changes in the landscape can be highlighted, current conditions can be analyzed, and more effective strategic planning can be conducted. Additionally, this method allows for continuous monitoring of terrain changes over time, providing essential information for natural resource management, urban development, or environmental conservation. This integrated approach contributes to the creation of more accurate and useful maps, tailored to the current needs of communities and local authorities.

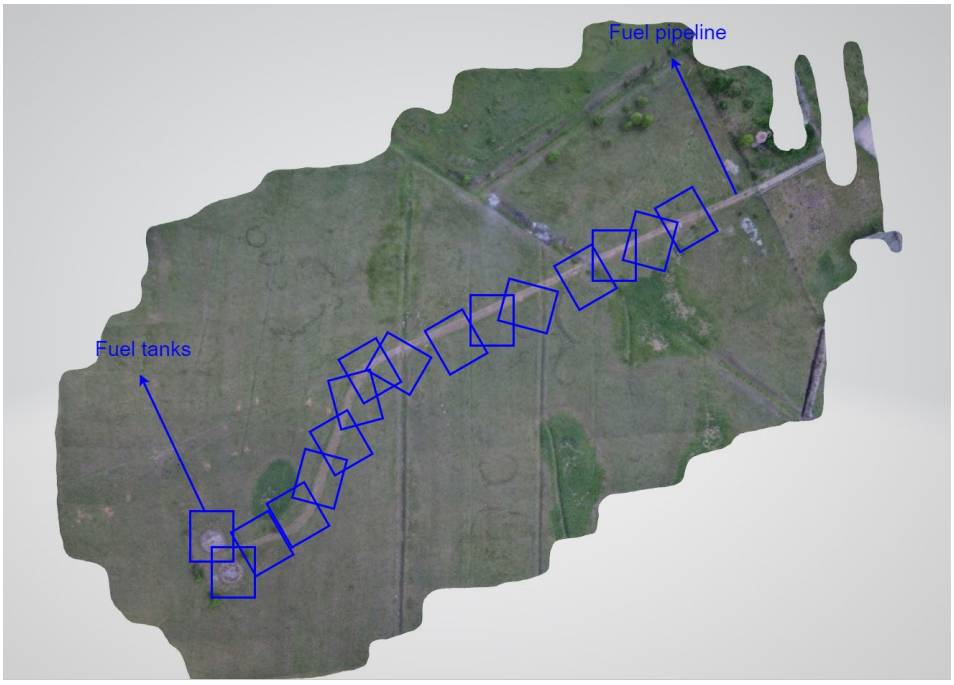



Fig. 9 Map of the monitored area reconstructed from geolocated images

## CONCLUSION

The use of UAVs (Unmanned Aerial Vehicles) to scan gas and oil distribution networks for potential leaks has proven to be an effective and innovative solution, revolutionizing the way critical infrastructure is monitored. Through georeferenced images, UAVs can conduct detailed inspections of pipelines, valves, and pumping stations, quickly identifying problematic areas and significantly reducing the time required to assess the state of the network. This ability to obtain precise, up-to-date data in real-time allows operators to respond promptly to emergency situations, minimizing the risks associated with gas or oil leaks, which can have devastating consequences for the environment and local communities.

Furthermore, analyzing georeferenced images not only facilitates the accurate localization of leaks but also helps evaluate their impact on surrounding ecosystems, providing essential information for informed decision-making. This innovative

https://doi.org/10.5593/sgem2024v/3.2/s06.49

approach replaces traditional inspection methods, which are often dangerous and time-consuming, with automated and safe solutions. Additionally, UAVs can access hard-to-reach areas, thereby reducing risks for personnel involved in inspections.

In conclusion, integrating UAVs into the inspection processes of distribution networks not only optimizes operational efficiency but also contributes to increased safety and sustainability in the energy industry. By enabling continuous and detailed monitoring, UAVs prove to be an indispensable tool in managing critical infrastructure, promoting a culture of responsibility and environmental protection.

## REFERENCES

[1] Yilmaz, A., Javed, O., & Shah, M. (2006). "Object tracking: A survey." ACM Computing Surveys, 38(4), Article 13.

[2] Smeulders, A. W. M., Chu, D. M., Cucchiara, R., Calderara, S., Dehghan, A., & Shah, M. (2014). "Visual tracking: An experimental survey." IEEE Transactions on Pattern Analysis and Machine Intelligence, 36(7), 1442-1468.

[3] Bewley, A., Ge, Z., Ott, L., Ramos, F., & Upcroft, B. (2016). "Simple online and real-time tracking." In 2016 IEEE International Conference on Image Processing (ICIP) (pp. 3464-3468).

[4] Bar-Shalom, Y., & Li, X. R. (1995). "Multitarget-Multisensor Tracking: Principles and Techniques." YBS Publishing.

[5] Gordon, N. J., Salmond, D. J., & Smith, A. F. M. (1993). "Novel approach to nonlinear/non-Gaussian Bayesian state estimation." IEE Proceedings F (Radar and Signal Processing), 140(2), 107-113.

[6] Danelljan, M., Bhat, G., Khan, F. S., & Felsberg, M. (2017). "Eco: Efficient convolution operators for tracking." In Proceedings of the IEEE Conference on Computer Vision and Pattern Recognition (pp. 6638-6646).

[7] Bertinetto, L., Valmadre, J., Henriques, J. F., Vedaldi, A., & Torr, P. H. S. (2016). "Fully-convolutional siamese networks for object tracking." In European Conference on Computer Vision (pp. 850-865).

[8] Zhu, Z., Wang, Q., Bo, L., Wu, Y., Yan, J., & Hu, W. (2018). "Distractor-aware Siamese Networks for visual object tracking." In Proceedings of the European Conference on Computer Vision (ECCV) (pp. 101-117).

# ADVANCES IN DROP-IN SUSTAINABLE AVIATION FUELS (SAF): PATHWAYS, CHALLENGES, AND FUTURE DIRECTIONS

**Scientist Dr. Odi Alrebei**[1]

[1] Qatar Environment and Energy Research Institute-Hanad Bin Khalifa University, **Qatar**

## ABSTRACT

Drop-in sustainable aviation fuels (SAFs) are critical for reducing the aviation sector's reliance on fossil fuels while utilizing existing infrastructure. This review paper explores various approaches to producing drop-in SAFs, focusing on their technical pathways, compatibility with current engines, and environmental performance. Key technologies include thermochemical processes like Fischer-Tropsch synthesis, hydroprocessed esters and fatty acids (HEFA), and alcohol-to-jet (ATJ), as well as emerging biological and electrochemical conversion methods. These pathways are assessed based on feedstock flexibility, fuel properties, and the ability to meet aviation fuel standards (ASTM D1655). The paper also evaluates the economic and policy challenges hindering large-scale SAF production, including feedstock availability, production costs, and regulatory incentives. Advances in catalyst design, process optimization, and carbon capture integration are highlighted as essential innovations for scaling SAF production. By examining the potential and limitations of each approach, the review aims to guide future research and policy development in sustainable aviation fuel technologies.

**Keywords:** Fuel diversity, Biological Feedstocks, SAF

## INTRODUCTION

The aviation industry is a significant contributor to global greenhouse gas emissions, accounting for approximately 2.5% of global CO2 emissions [1]. As the sector is projected to grow substantially in the coming decades, the challenge of reducing its reliance on fossil fuels while maintaining operational efficiency and safety is more pressing than ever [2]. Drop-in sustainable aviation fuels (SAFs) have emerged as a promising solution to address this challenge. These fuels are designed to be fully compatible with existing aviation infrastructure and engines, enabling their adoption without requiring significant modifications to aircraft or fuel distribution systems [3,4].

The development of SAFs has seen notable advancements in recent years, driven by an urgent need to meet international climate targets, including those set by the International Civil Aviation Organization (ICAO) under the Carbon Offsetting and Reduction Scheme for International Aviation (CORSIA) [5,6]. However, the large-scale implementation of SAFs faces significant technical, economic, and policy hurdles. Key challenges include securing sustainable and scalable feedstock supplies, reducing production costs, and ensuring compliance with stringent aviation fuel standards such as ASTM D1655 [7,8].

This paper provides a comprehensive review of the current state of SAF production technologies, including thermochemical pathways like Fischer-Tropsch synthesis, hydroprocessed esters and fatty acids (HEFA), and alcohol-to-jet (ATJ) processes. It also

explores emerging methods, such as biological and electrochemical conversions, highlighting their potential to enhance feedstock flexibility, improve fuel properties, and reduce environmental impact [9–13]. In addition, the paper examines critical innovations in catalyst design, process optimization, and carbon capture integration, which are vital for scaling SAF production [14,15].

By addressing the technical and policy barriers to SAF adoption, this study aims to contribute to the ongoing development of sustainable solutions for the aviation sector. The findings of this review seek to inform future research directions and guide policymakers in creating frameworks that facilitate the transition to a more sustainable aviation industry.

## MATERIALS AND METHODS

This review employs a systematic methodology to evaluate the state of sustainable aviation fuels (SAFs), focusing on their production pathways, technological advancements, and associated challenges. The approach integrates systematic data collection and a comprehensive evaluation framework to ensure replicability and rigor. All data used in this study were obtained from peer-reviewed journal articles, technical reports, and publicly available sources, adhering to ethical standards.

The data collection process involved an extensive search of major scientific databases such as *Scopus*, *Web of Science*, and *Google Scholar*. Keywords including "sustainable aviation fuels," "Fischer-Tropsch synthesis," "hydroprocessed esters and fatty acids," "alcohol-to-jet," and "biofuels for aviation" were used to identify relevant studies. Publications from the past decade were prioritized to capture recent advancements, while foundational studies were included to provide historical context. Studies were selected based on their focus on SAF production processes, feedstock analysis, and compliance with aviation fuel standards. Studies lacking detailed methodologies or those addressing non-aviation biofuels were excluded. Extracted data were systematically organized into a structured database, recording key parameters such as feedstock types, conversion efficiencies, catalyst performance, lifecycle emissions, and economic assessments. This organization facilitated the identification of research gaps and the refinement of the review scope. Data were validated by cross-referencing multiple sources, while emerging technologies were evaluated through comparisons between experimental results and theoretical projections.

The evaluation framework encompassed several criteria, summarized in **Table 1**, and included sustainability metrics, process performance, environmental impact, and economic feasibility.

**Table 1.** Evaluation criteria

| Criterion | Description | Metrics/Equations Used |
|---|---|---|
| Feedstock Sustainability | Assesses the availability, scalability, and environmental impact of feedstocks. | Feedstock availability, resource use efficiency, and land-use implications. |
| Energy Efficiency | Evaluates the efficiency of SAF conversion processes. | $\eta = \frac{Energy\ in\ feedstock\ input}{Energy\ in\ SAF\ produced} \times 100$ (Eq. 1) |

| | | |
|---|---|---|
| Lifecycle Emission Reduction | Quantifies the reduction in greenhouse gas emissions compared to conventional jet fuels. | $\Delta CO2 = \frac{Baseline\ CO_2 - SAF\ CO_2}{Baseline\ CO_2} \times 100$ (Eq. 2) |
| Feedstock-to-Fuel Conversion | Measures the mass efficiency of converting feedstock to SAF. | $Cf = \frac{Mass\ of\ feedstock\ used}{ass\ of\ SAF\ produced}$ (Eq. 3) |
| Fuel Properties | Ensures SAF meets ASTM D1655 standards for compatibility with aviation engines and infrastructure. | Comparison of energy density, freezing point, and combustion characteristics. |
| Economic Feasibility | Assesses the scalability and production costs of SAF technologies. | Cost analysis of production pathways and assessment of policy support (e.g., subsidies and tax incentives). |

Feedstock sustainability was assessed based on availability, scalability, and environmental impact, with a focus on feedstocks such as lignocellulosic biomass, municipal solid waste, algae, and electrochemically captured $CO_2$. Conversion

The assessment of SAF properties included comparisons of energy density, freezing point, and combustion characteristics against ASTM D1655 standards to ensure compatibility with aviation infrastructure. Reported lifecycle greenhouse gas emissions highlighted significant reductions for SAFs, particularly when carbon capture technologies were integrated into production processes, as evidenced by values derived using Equation (222) in prior studies [5, 14]. Economic feasibility was evaluated based on reported production costs, feedstock scalability, and infrastructure requirements, considering the role of government subsidies and policy incentives. Calculations of feedstock utilization efficiency using Equation (333) played a crucial role in assessing the economic scalability of production pathways [11].

## RESULTS

This section presents the outcomes of the systematic review and analysis of sustainable aviation fuel (SAF) production pathways. The key performance metrics, including energy efficiency, lifecycle $CO_2$ reduction, and feedstock-to-fuel conversion rates, are summarized in Table 2. Additionally, visual representations in Figures 1 and 2 provide insights into the comparative performance of different SAF production technologies. The data in Table 2 highlight significant variations across the examined pathways. HEFA (Hydroprocessed Esters and Fatty Acids) demonstrates the highest energy efficiency at 70%, followed by Alcohol-to-Jet (ATJ) and Fischer-Tropsch at 60% and 45%, respectively. Electrochemical pathways, though promising, lag slightly with an energy efficiency of 50%. This disparity is largely attributable to the maturity of HEFA processes compared to the emerging nature of electrochemical methods. In terms of lifecycle $CO_2$ reduction, Electrochemical pathways achieve a remarkable 95% reduction, outperforming all other technologies. HEFA and ATJ show substantial reductions at 85% and 75%,

respectively, while Fischer-Tropsch achieves 60%. These results underscore the potential of integrating renewable energy and carbon capture technologies, particularly in electrochemical methods. The feedstock-to-fuel conversion rates reveal HEFA as the most resource-efficient pathway, converting 0.8 kg of feedstock into 1 kg of fuel. ATJ and Fischer-Tropsch perform moderately, with conversion rates of 0.6 and 0.5, respectively, while Electrochemical methods show a rate of 0.4. This observation emphasizes the importance of feedstock optimization and process efficiency improvements for emerging pathways. Figures 1 and 2 illustrate the energy efficiency and lifecycle $CO_2$ reduction across the pathways, highlighting the superior efficiency of HEFA and the exceptional environmental benefits of electrochemical methods, respectively.

**Table 2**: Key Performance Metrics for SAF Production Pathways

| Production Pathway | Energy Efficiency (%) | Lifecycle $CO_2$ Reduction (%) | Feedstock Conversion Rate (kg/kg) |
|---|---|---|---|
| Fischer-Tropsch | 45 | 60 | 0.5 |
| HEFA | 70 | 85 | 0.8 |
| Alcohol-to-Jet | 60 | 75 | 0.6 |
| Electrochemical | 50 | 95 | 0.4 |

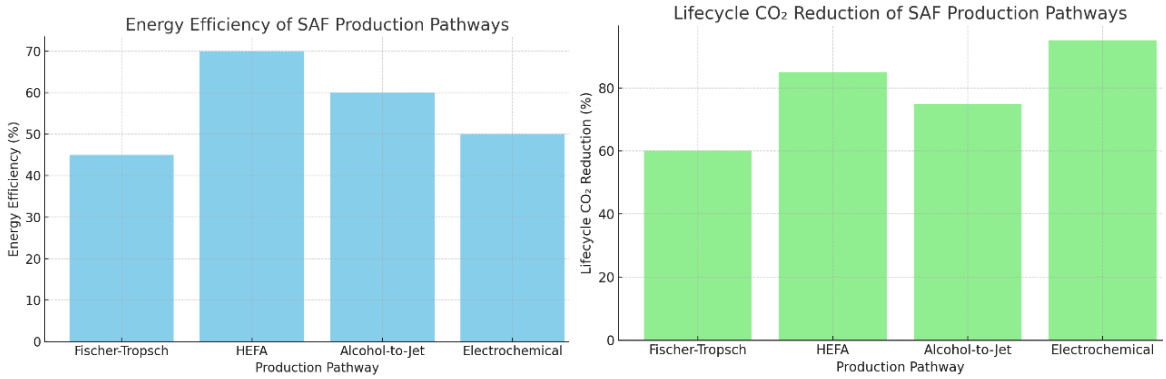



**Figure 1**: (A) Energy Efficiency of SAF Production Pathways. (B) Lifecycle $CO_2$ Reduction of SAF Production Pathways

## DISCUSSION

The results demonstrate that HEFA is the most energy-efficient SAF production pathway (70%), consistent with its technological maturity. Electrochemical methods, while less efficient (50%), achieve the highest lifecycle $CO_2$ reduction (95%), highlighting their long-term potential. These findings align with previous studies emphasizing the environmental benefits of advanced technologies. Unexpectedly, the feedstock-to-fuel conversion rate for electrochemical methods (0.4 kg/kg) was lower than predicted, reflecting their early-stage development. Fischer-Tropsch processes performed moderately, aligning with their known dependency on feedstock and process conditions. Overall, the data support the hypothesis that HEFA is ideal for near-term deployment, while electrochemical methods offer significant promise for long-term decarbonization efforts.

## CONCLUSION

This study highlights HEFA as the most efficient near-term SAF production pathway, achieving 70% energy efficiency and 85% $CO_2$ reduction. Electrochemical methods showed exceptional environmental potential with a 95% $CO_2$ reduction, though limited by lower feedstock efficiency. These results underscore the need to scale mature technologies like HEFA while advancing emerging pathways through further optimization and research. Future work should address feedstock utilization and energy demands to enhance scalability and sustainability in SAF production.

## REFERENCES

[1] Lee D. S., Fahey D. W., Skowron A., et al., The contribution of global aviation to anthropogenic climate forcing for 2000 to 2018, Atmospheric Environment, UK, 2021, pp. 117834.

[2] International Civil Aviation Organization (ICAO), Environmental Protection: Aviation Emissions, ICAO, Canada, 2022.

[3] Schafer A. W., Barrett S. R. H., Doyme K., et al., Technological, economic and environmental prospects of all-electric aircraft, Nature Energy, UK, 2016, pp. 16063.

[4] Hileman J. I., Stratton R. W., Alternative jet fuels, Environmental Science & Technology, USA, 2014, pp. 14043-14049.

[5] International Civil Aviation Organization (ICAO), CORSIA: The Carbon Offsetting and Reduction Scheme for International Aviation, ICAO, Canada, 2019.

[6] Zhang X., Myhre G., Kramer L. J., Aviation fuel and climate mitigation pathways: Long-term scenarios, Nature Sustainability, UK, 2022, pp. 125-133.

[7] ASTM International, ASTM D1655 - Standard Specification for Aviation Turbine Fuels, ASTM, USA, 2020.

[8] De Jong S., Antonissen K., Hoefnagels R., et al., Life-cycle analysis of greenhouse gas emissions from renewable jet fuel production, Biotechnology for Biofuels, Netherlands, 2017, pp. 64.

[9] Lobo P., Hagen D. E., Whitefield P. D., Comparison of PM emissions from a commercial jet engine burning conventional, biomass, and Fischer-Tropsch fuels, Environmental Science & Technology, USA, 2015, pp. 4087-4095.

[10] Liu X., Zhang Y., Wang J., Chen P., Advances in biofuel production technologies for aviation applications, Renewable Energy, USA, 2022, pp. 203-216.

[11] Yan Q., Wang J., Lin H., Hydroprocessed renewable jet fuels: Production pathways and catalytic challenges, Catalysis Today, China, 2022, pp. 65-79.

[12] Cames M., Graichen J., Siemons A., Aviation biofuels: Technology roadmap and policy recommendations, Transport Research Part D: Transport and Environment, Germany, 2021, pp. 103088.

[13] Dhar A., Kumar S., Bose P. K., Electrochemical pathways for sustainable jet fuel production: Advances and prospects, Energy & Environmental Science, India, 2022, pp. 1043-1057.

[14] Arora P., Deshmukh A. G., Catalyst developments in hydroprocessing for renewable aviation fuel production, Fuel Processing Technology, India, 2023, pp. 107170.

[15] Zhang Y., Jiang J., Yuan W., Integration of carbon capture and SAF production: Challenges and opportunities, Journal of Cleaner Production, China, 2022, pp. 134865.

# STRATEGIC SOCIO-ENVIRONMENTAL ASSESSMENT: KEY APPROACHES AND PROSPECTS IN THE PETROLEUM EXPLORATION SECTOR

**Assoc. Prof. Dr. Irina Tikhonova**[1,2]

[1] Research Institute 'Environmental Industrial Policy Centre', **Russian Federation**
[2] Dmitry Mendeleev University of Chemical Technology of Russia, **Russian Federation**

## ABSTRACT

The article considers the Strategic Socio-Environmental Assessment (SSEA), which aims to contribute to the integration of social and environmental considerations into the preparation, adoption and implementation of strategies, plans, and programmes, with a view of promoting sustainable development. The Environmental Impact Assessment of individual projects does not necessarily guarantee that at the regional level, the state of the environment as well as social and cultural characteristics do not deteriorate due to the economic development. At present, no official regulations govern SSEA procedures in Russia. Certain practices do exist, and the article considers such cases as the environmental assessment of rationales of new protected areas, territorial development plans and collaborative international programmes in the field of hydrocarbons exploration. Most researchers focus attention on the stakeholder involvement and the necessity to run special studies rather than use statistical data on the state of the environment. The article presents a new case study and recommends implementing SSEA for making decisions of the remediation of older petroleum exploration sites. The author emphasises that the primary goal of economic development should be to generate real value within socio-economic systems while accounting for the ecological limits of natural environments, and concludes that there is a necessity to work out a special SSEA-related legislative act and practical recommendations.

**Keywords:** sustainable development, environmental assessment, social aspects, hydrocarbon exploration, ecosystem restoration

## INTRODUCTION

Environmental assessment (EA) has been recognized as a preventive tool in environmental regulation since the 1980s, when various countries and regions began developing regulatory frameworks and guidelines, and, through pilot projects, initiated public consultations. However, the philosophy behind environmental assessment emerged earlier, during the 1960s, primarily in response to the growing tension between economic development and environmental protection [1].

Over time, both researchers and practitioners have recognised the need to distinguish two primary types of environmental assessment: (1) environmental impact assessment (EIA) of specific projects, such as the construction of industrial plants or energy facilities [2], and (2) strategic environmental assessment (SEA), or more specifically, strategic socio-environmental assessment (SSEA), which applies to various industrial or

https://doi.org/10.5593/sgem2024v/3.2/s06.50

regional development plans, policies, and justifications for establishing protected areas [3, 4].

Currently, the Ministry of Natural Resources and Environment of the Russian Federation regulates EIA requirements in the domain of business activities. It is important to emphasize that these regulations specifically apply to the documents (or materials) that are prepared as a result of the EIA process itself.

At present, no official regulations govern SEA or SSEA processes in Russia. However, certain practices do exist, as indicated by publications on the environmental assessment of materials justifying the establishment of protected areas [5], territorial development plans and collaborative international programmes in the field of hydrocarbons exploration [6, 7]. It is important to note that environmental expertise represents the final stage of the environmental assessment process. This stage involves evaluating the compliance of the materials with legislative provisions and environmental protection requirements, or as commonly referred to in international contexts, assessing the quality of the reports (materials) generated during the EIA process.

The goal of this study is to substantiate the necessity of developing and standardizing approaches to SSEA implementation in Russia. This would serve as a preventive instrument of environmental regulation for strategies, plans, and programmes concerning the development of territories, regions, and industrial centres. A special case study of the SSEA applicability for making decisions of the remediation of older petroleum exploration sites is presented to demonstrate the usefulness of this environmental regulation instrument.

## METHODS

This study employed a combination of analytical and synthetic methods typically used in environmental and economic research. This methodological approach enables a systematic and comprehensive examination of the evolving SSEA concept. In discussing environmental assessment approaches (both EIA and SEA), we drew on methods developed by experts from the Organisation for Economic Co-operation and Development (OECD) [8] and the World Bank [9], as well as a number of practical guides published in Russian. Additionally, publicly available information on EIA and SEA procedures and outcomes for various projects was utilised. This information includes materials made accessible through public discussions of EIA and SEA findings.

## RESULTS AND DISCUSSION

### STRATEGIC SOCIO-ENVIRONMENTAL ASSESSMENT: CLARIFICATION OF TERMINOLOGY AND GOAL SETTING

The proposal to refine and expand the SEA concept, which, as previously noted, is not explicitly defined in Russian legislation but appears in various publications, is driven by two key factors. First, an analysis of articles by Russian researchers reveals that most assessments not only include a social component but also focus on addressing the interests of the population. This approach aligns with the concept of environmental and social assessment. In the context of national development goals, this involves achieving environmental well-being and, to some extent, creating a comfortable and safe living

environment. Second, international documents also highlight that SEA incorporates social aspects. It is important to note that SEA is not mentioned in Russian legislation on strategic planning or in environmental protection regulations.

The Protocol on Strategic Environmental Assessment (a UN document) provides the following definition of SEA: "Strategic environmental assessment means the evaluation of the likely environmental, including health, effects, which comprises the determination of the scope of an environmental report and its preparation, the carrying out of public participation and consultations, and the taking into account of the environmental report and the results of the public participation and consultations in a plan or programme" [3].

Why is the EIA concept not enough? To answer this question, we can refer to the Clean Air Federal Project, which is "... aimed at improving the environmental situation and reducing pollutant emissions in twelve large industrial centres" [10]. These industrial centres suffer from excessive air pollution, largely because SSEA approaches were not applied when establishing facilities and making decisions about their spatial distribution. While individual industrial projects, such as the construction or reconstruction of facilities, may comply with the Best Available Techniques (BAT) [11], the cumulative effect of dense industrial activities – including chemical, metallurgical, coal-fired, and cement plants – exceeds the ecological capacity of these areas. As a result, natural processes, such as the dispersion and self-purification of atmospheric pollutants, cannot keep pace with the anthropogenic load [10, 11].

In practice, impact assessments of natural objects are typically conducted when justifying the establishment of protected areas. Both EIA and SSEA often evaluate the expected consequences of particular activities or development plans that may affect the status of objects classified as anthropogenic.

Based on the discussion above, the following definition of SSEA is proposed: "Strategic environmental and social assessment involves evaluating the state of natural-anthropogenic systems, identifying environmental and socio-cultural factors, and assessing the potential positive and negative consequences of proposed strategies, plans, and programmes for these systems. The findings are then integrated into the decision-making processes for these strategies, plans, and programs" (see Figure 1).

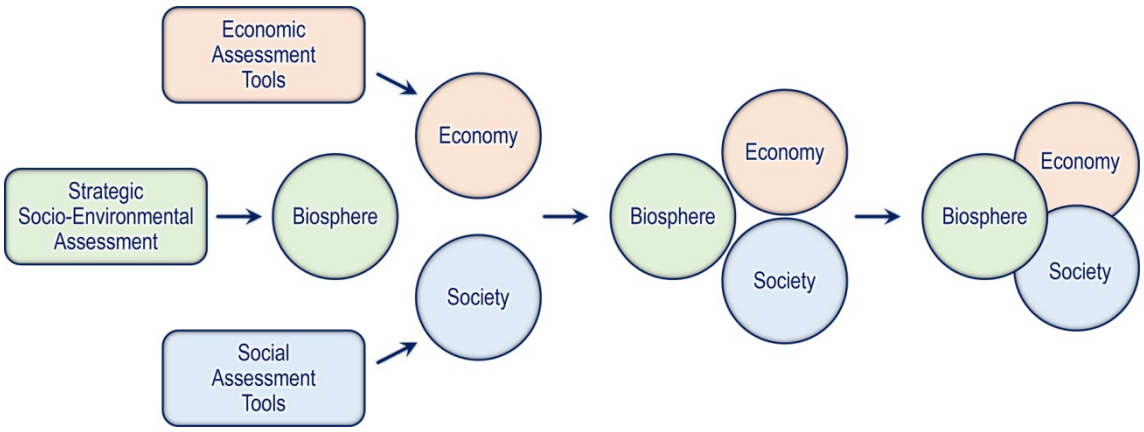



**Figure 1.** Strategic Socio-Environmental Assessment: Factoring in Environmental, Social, and Economic Aspects (based on [12], with changes)

https://doi.org/10.5593/sgem2024v/3.2/s06.50

It should be emphasized that the proposed definition builds upon approaches developed by both Russian and international researchers, as well as international organizations. However, it also highlights three key requirements: 1) to incorporate the three pillars of sustainable development; 2) to place greater emphasis on assessing the current status of natural and anthropogenic systems, identifying priority factors influencing these systems, and determining ways to both mitigate negative impacts and enhance positive effects; 3) to ensure collaboration with relevant organizations and stakeholders when improving plans, strategies, and programs for spatial, socio-economic, and territorial development.

## GOALS, OBJECTIVES, AND STAGES OF STRATEGIC SOCIO-ENVIRONMENTAL ASSESSMENT

The Strategy for Spatial Development of the Russian Federation is set for approval at the end of 2024. During discussions on preliminary versions of the document, experts and members of the Interdepartmental Working Group debated the feasibility of developing SSEA principles. It was noted also that SSEA is necessary at the decommissioning stage of certain facilities, such as hydrocarbons exploration sites or industrial plants nearing the end of their life cycle.

The primary purpose of SSEA, as reflected in its definition, is to identify the potential outcomes of strategies, programs, and plans in order to achieve desired results (intentional changes) while mitigating undesirable consequences (unintentional negative changes). For each specific situation, SSEA goals, objectives, and evaluation criteria should be tailored accordingly.

The analysis of SEA experiences in Russia, as published by domestic researchers, provides the following insights:

1) In practice, the focus during SEA has been primarily on strategic planning documents, despite the core purpose of the assessment being the analysis of social and environmental factors.
2) The assessment has often been conducted to make changes to existing documents, such as the strategy for the socio-economic development of Kamchatka Krai, or to explore opportunities for integrating different types of economic activities (e.g., iron ore and coal mining with tourism), as well as for justifying the creation or expansion of protected areas [5].
3) While assessment findings include recommendations advocating for regulatory and legal frameworks that mandate SSEA application and the development of domestic methodological approaches, the Federal Law “On Environment Impact Assessment” remains in effect without substantial changes.

As a result, the so-called ‘environmental expertise’ (the quality assessment of EIA Reports) continues to dominate environmental assessment regulation. This means that priority is given not to improving impact assessment methodologies, procedures, or recommendations for obtaining reliable results, but rather to the examination of EIA materials. It is worth noting that SSEA is still largely absent from the Russian framework.

## STRATEGIC SOCIO-ENVIRONMENTAL ASSESSMENT: PROSPECTS FOR THE IMPLEMENTATION IN THE PETROLEUM EXPLORATION SECTOR

The exploitation of oil resources poses serious challenges to sustainability of the regions encompassing petroleum provinces. This is why SSEA becomes as an important instrument to promote sustainability-driven decision-making [13]. While developing new petroleum exploration plans, it is necessary to cover emergency oil spills, decommission operations as well as the remediation of damaged territories. In general, oil spills typical by the petroleum exploration sector in many countries are characterised by a large ingresses of oil in a relatively short period of time and a shock load on the environment. This leads to a rapid negative response to the extent of total loss of the biota [13, 14].

The case study presents a comparative analysis of practices and techniques for the restoration of oil-contaminated ecosystems in the Khanty-Mansi Autonomous Okrug – Yugra (KhMAO-Yugra). KhMAO-Yugra is the fiat lowlands located in the boreal geobotanical zone (taiga) of the Ob-Irtysh geobotanical province, in the southern taiga subzone of the West Siberian taiga zone. Swamp formation is widespread due to the poor drainage conditions of the territory. The KhMAO-Yugra wetland ecosystems experience very strong impacts of oil pollution during accidental spills due to the high oil capacity of peat soils (in natural conditions, the oil content in sphagnum peat can reach 70-80%). This primarily applies to raised bogs confined to watershed areas. Semi-terrestrial spruce or pine-spruce forests are formed in periodically waterlogged conditions. Oil mainly permeates the peat ground litter and shallow peat horizons in these type of forests.

Automorphic forests occupy relatively elevated, well- and moderately drained areas that are not subject to long-term watering. The main amount of oil in automorphic forests during an accidental spill accumulates in the ground litter and the top mineral horizon of the soil. Oil contamination of these most biologically active layers of forest ecosystems is facilitated by their high oil capacity (up to 20% in the litter of automorphic forests and significantly higher values in the upper horizons of semi-terrestrial forests). This leads to the almost complete death of the soil microbial and animal population, loss of the moss-lichen layer, and destruction of the tree layer.

To restore the KhMAO-Yugra ecosystems disturbed by emergency oil spills, it is recommended to apply the following techniques.

Automorphic forests, semi-terrestrial forests dominated by forest-forming processes:

- Soil application of native **oil-oxidizing microorganisms**.
- Correction of the soil environment, structure, temperature, humidity, mineral nutrition.
- **Mechanical tillage** depending on the level, duration of contamination and soil texture.
- **Seed treatment** with fungicides and growth-stimulator to increase germination, survival rate and optimization of crop growth processes.
- **Sowing green manure crops** to ensure rapid growth of green mass intended to activate the work of the substratum microbial population.
- **Grasslanding of restored areas** by sowing specially selected mixtures of cereal and legume grasses.

https://doi.org/10.5593/sgem2024v/3.2/s06.50

Wetlands, semi-terrestrial forests dominated by swamp-forming processes:

- Oil spill containment, free oil gathering by manual or mechanized methods. Determination of residual oil content on the surface ($dm^3/m^2$) to decide on the ability of the biocenosis to recover naturally or the need to fill it with a layer of air-dry peat.
- Conducting flood control measures to retain residual oil within the boundaries of the emergency spill area.
- **Adding peat backfill** to contaminated wetland areas using machines and mechanisms.
- Organizing a monitoring system for reclaimed areas of peat deposits to obtain information on the content of residual oil in these areas and assessing the effectiveness of swamp restoration measures.

The nature and duration of restoration for forest phytocenoses exposed to accidental spills are determined by the presence of certain plant species, the level of residual soil contamination and the presence of bituminized crust. Restoration of the original phytocenoses occurs in the first decade for moderate soil contamination (up to 5 $dm^3/m^2$) and more than 20 years are required for medium and high contaminated soils (10-100 $dm^3/m^2$). Considering the large areas of oil-contaminated lands, it is necessary to conduct a strategic socio-environmental assessment for making decisions on the restoration of areas of the territory disturbed by oil production while developing various land reclamation projects. It should be taken into account that in Russia, requirements (such as national standards) to the permissible content of oil in soils have not been established, and current status leaves the possibility for certain subjectivity in land reclamation issues.

Agricultural and forestry reclamation of ecosystems disturbed by oil spills, practiced in Western Siberia, does not correspond to the restoration of natural ecosystems. The application of various agricultural techniques leads to the disruption of habitats which is good for agricultural or forestry use of land, but is not aimed at restoring the natural vegetation (see Figure 2).



**Figure 2.** Reclamation of Ecosystem Disturbed by Oil Spills

It is necessary to develop sound techniques for restoring ecosystems contaminated by oil spills. These techniques will make it possible to improve not only generalized automorphic and swamp habitats, but also contribute to the main habitats of automorphic and semi-terrestrial forests, as well as wetlands.

## CONCLUSION

The primary goal of economic development should be to create processes that generate real value within socio-economic systems while accounting for the ecological limits of natural environments. Current approaches to evaluating sectoral and regional development strategies, which are predominantly cantered on financial outcomes, often fail to consider the risks of long-term environmental degradation and social problems.

In Russia, there is both a need and an opportunity to establish a comprehensive system of environmental regulation. Such a system should ensure that when making management decisions regarding regional, territorial, or industrial development, national goals, stakeholder perspectives, scientific research, and data on the actual state of natural and anthropogenic ecosystems are taken into account. Additionally, it should incorporate assessment of the expected positive and negative outcomes of these decisions.

For the petroleum exploration sector, SSEA objectives include the following:
- to help reduce risks and ensure preparedness for the consequences of oil and gas development;
- to identify social, environmental, and social priorities and how these may be influenced by the petroleum sector development options and alternatives in the region of interest;
- to assess the related institutional and economic capacity to deal with the identified negative consequences of oil and gas development; and
- to recommend institutional and governance-strengthening measures.

A region-based case study implemented in Khanty-Mansi Autonomous Okrug – Yugra was focused on the issues dealing with the oil spills as typical negative impacts of the petroleum exploration activities. The necessity to consider these impacts is emphasised and practical recommendations on the remediation of damaged ecosystems are developed.

Taking into account the system of environmental legislation and standardisation in the Russian Federation, it would be reasonable working out a national standard that outlines the methodology for running SSEA with respect to the development of petroleum exploration plans and programmes. Later on depending on the results of the practical implementation of this standard (on the voluntary basis), SSEA-related legislative documents can be drafted, discussed with stakeholders, and officially passed in the Russian Federation.

## REFERENCES

[1] Burdge R. J., A Brief History and Major Trends in the Field of Impact Assessment, Impact Assessment, 9:4, 93-104, 1991, DOI: 10.1080/07349165.1991.9726070.

[2] Pope J., Squires G., Witt K., Williams G., Womersley J., Evolution or Revolution: Where Next for Impact Assessment? Impact Assess. Proj. Apprais., 36 (6), pp 506-515, 2018, DOI: 10.1080/14615517.2018.1516846.

[3] Protocol on Strategic Environmental Assessment to the Convention on Environmental Impact Assessment in a Transboundary Context, 2017, URL: https://unece.org/DAM/env/eia/documents/legaltexts/protocolenglish.pdf.

https://doi.org/10.5593/sgem2024v/3.2/s06.50

[4] Assessment of the Effects of Certain Plans and Programmes on the Environment, URL: https://eur-lex.europa.eu/legal-content/EN/TXT/?uri=CELEX%3A32001L0042.

[5] Masloboev V. A., Borovichev E. A., Nenasheva M. A., Kluchnikova E. M., Environmental Report. Strategic Environmental Assessment of the Russian Territory CBC Kolarctic 2021-2027, January 2022, DOI: 10.37614/978.5.91137.459.4.

[6] Zhichkina L., Zhichki K., Sharipov F., Takhumova O. V., Perfilyev A. A., Temnyshov I. A., Environmental Foundations of Oil and Gas Production in the Russian Federation, IOP Conf. Ser.: Earth Environ. Sci., vol. 1070, 012034, 2022, DOI: 10.1088/1755-1315/1070/1/012034.

[7] Vorobeva Yu. A., Drapalyuk N. A., Burak E., Zherlykina M. N., Isanova A. V., Assessment of the Importance of Environmental Aspects in the Construction of Oil and Gas Facilities, IOP Conference Series: Earth and Environmental Science, vol. 723, 052004, 2021, DOI: 10.1088/1755-1315/723/5/052004.

[8] Applying Strategic Environmental Assessment: Good Practice Guidance for Development Co-operation / DAC Guidelines and Reference Series. OECD Publishing, Paris, 2006, URL: https://doi.org/10.1787/9789264026582-en.

[9] Strategic Environmental Assessment in Policy and Sector Reform: Conceptual Model and Operational Guidance, The World Bank, Washington DC, 2011, DOI: 10.1596/978-0-8213-8559-3.

[10] Labzovskii L. D., Hey J. V., Romanov A. A., Golovatina-Mora P., Belikov D. A., Lashkari A., Kenea S. T., Hekman E., Who Should Measure Air Quality in Modern Cities? The Example of Decentralization of Urban Air Quality Monitoring in Krasnoyarsk (Siberia, Russia), Environmental Science & Policy, vol. 140, pp 93-103, 2023, DOI: 10.1016/j.envsci.2022.11.016.

[11] Tikhonova I., Guseva T., Nature-Based Solutions in Industrial Environmental Monitoring Programmes, Proceedings of the 21st Multidisciplinary GeoConference SGEM 2021, Bulgaria, vol. 21, is. 7.2, pp 335-342, 2021. DOI: 10.5593/sgem2021/5.1/s20.042.

[12] Gonçalves L. R., Oliveira M., Turra A., Assessing the Complexity of Social-Ecological Systems: Taking Stock of the Cross-Scale Dependence, Sustainability, vol. 12, is. 15, 6236, 2020. DOI: 10.3390/su12156236.

[13] Lamorgese L., Geneletti D., Partidario M. R., Reviewing Strategic Environmental Assessment Practice in the Oil and Gas Sector, Journal of Environmental Assessment Policy and Management, vol. 17, no. 02, 1550017, 2015. DOI: 10.1142/S1464333215500179.

[14] Fomenko N., Hamad Al., Main Aspects of the Oil Industry within the Sustainable Development Concept, IOP Conference Series: Materials Science and Engineering, vol. 952, 012019, 2020. DOI: 10.1088/1757-899X/952/1/012019.

# TECHNO-ECONOMIC ASPECTS OF LITHIUM RECOVERY FROM OILFIELD BRINES USING 3D PRINTED SORBENTS

**Przemysław Ziemba**
**Ewa Knapik**
AGH University of Krakow, Faculty of Drilling, Oil and Gas, Al. Mickiewicza 30, 30-059 Krakow, **Poland**

## ABSTRACT

With the continuous technological advancement the global demand for selected chemical elements in both emerging and established solutions is rising. This is particularly evident in energy storage applications, such as lithium-ion batteries for increasingly popular electric vehicles. The growing need for lithium carbonate drives the search for innovative extraction methods, including recovery from brine through chemical processes. This approach not only aids in lithium recovery but also positively impacts the environment by repurposing "waste" from oil exploitation. The lithium recovery process from brine is complex with selective lithium separation as a critical stage. Within the CompLithium project 3D-printed sorbents have been developed, enabling a tenfold increase in lithium concentration in the concentrate compared to the initial brine. The system operates with at least two columns: one column sorbs lithium while the other one undergoes regeneration. Lithium is extracted from the acidic concentrate by precipitation using sodium carbonate. This technological sequence encompasses preliminary brine preparation, lithium capture, acidic concentrate production, and lithium carbonate precipitation. Under the CompLithium project the efficiency and selectivity of whole process were evaluated, the final product's purity was tested, and the consumption of auxiliary chemicals was estimated. A total of 12 sorbents with varying compositions and sintering temperatures were analyzed. In this paper the results (kinetic studies and adsorption isotherm assessments) for the best-performing sorbents are presented. The adsorption capacities of the sorbents were tested under static conditions. Results indicate that the process effectively recovers at least 80% of the initial lithium content.

**Keywords:** CompLithium, sorbent, 3D printing, lithium recovery, brine

## INTRODUCTION

The demand for lithium is escalating year by year, which puts lithium among critical materials in the energy transition. Lithium is widely used in various industries, particularly in battery production, electronics, and energy storage. The rapidly growing electromobility market has a significant impact on the increasing demand for lithium, because the production of lithium-ion batteries expands to meet the needs of electric vehicles and renewable energy storage solutions. According to U.S Geological Survey report [1], worldwide lithium production increased from 146,000 in 2022 to approximately 180,00 metric tons in 2023. This represents a 23 % increase in production over the course of a year. Moreover, the report indicate the global lithium reserves were 28 million tons and the measured global resources have increased to 105 million metric tons. Nowadays, nearly 60% of global lithium production is used in the battery sector,

https://doi.org/10.5593/sgem2024v/3.2/s06.51

and this share is expected to increase to about 95% by 2030. This surge in demand will require a corresponding increase in lithium production, as the reserves, while substantial, are limited, and much of the supply comes from a few key countries like Australia, Chile, and Argentina [2]. The alternative (and more sustainable comparing the evaporation) lithium extraction techniques include membrane separation, solvent extraction, precipitation, and ion-sieve adsorption. The adsorption method is more sustainable for low grade brines, such as produced water from oilfields. Direct lithium extraction (DLE) from brines offers numerous advantages compared to the evaporation process, including greater efficiency, reduced time, and reduced land use [3]. Recovering concentrated lithium directly from brine using crystal sieve reduces significant water losses, enabling lithium recovery from geothermal waters and oilfield brines, that must be reinjected into the formation. Titanium-based lithium ion sieves (LIS-Ti) are promising materials for lithium recover from brines. LIS-Ti sorbents show strong potential for lithium extraction, particularly when compared to other materials like manganese oxides. Sun et al. [4] compared various ion-sieve adsorbents for lithium recovery in salt lake brines with different lithium concentrations, demonstrating a good adsorption capacity for Ti materials comparing to other sorbents. Titanium-based sorbents are especially effective under alkaline conditions (pH of about 9). Titanium oxide-based materials are noted highlighted for their stability, high selectivity, and strong performance in lithium extraction processes [5]. Li et al. [6] demonstrated high adsorption capacity and selectivity for lithium recovery using various $TiO_2$ precursors, with effectiveness dependent on factors such as temperature and pH. 3D printing is a promising solution for lithium adsorption by enabling the creation of highly customizable adsorbent structures. This technology allows for the design of complex geometries that can provide high surface areas, which are essential for maximizing lithium recovery. Xu et al. [7] developed durable monolithic adsorbents using 3D printing, showing great potential as catalyst supports. The literature suggests that 3D printing technologies can produce monolithic absorbents with high levels of active lithium-recovery components and substantial mechanical strength. The aim of this paper is to evaluate the Ti-based powder as a base material for lithium recovery. The promising results show that obtained powder can be further processed to obtain a 3D printed sorbent.

## MATERIALS AND METHODS

### Materials

Titanium(IV) oxide (anatase), hydrochloric acid, lithium hydroxide monohydrate and lithium carbonate were delivered by the Vitaya company, Poland. The real reservoir brine was sampled from one of Polish oilfields located in the Polish Lowlands.

### Methods

### Sorbents synthesis

20 g of $TiO_2$ was mixed with 18.6 g of $Li_2CO_3$ and calcinated at 700 ºC for 4 in a muffle furnace. After free cooling to room temperature, the mixture was ground and sieved to a size of 50 μm. The activation of obtained material relies on lithium removal from its structure using acid treatment. The powder was contacted with 0.1 M HCl (the ratio of powder to acid ratio was 1:100) for 1 h and left to settled down. Then the solution was decanted and new portion of 0.1 M HCl was added. Washing with HCl was repeated

3 times, then the sorbent was washed with distilled water to remove acid. The obtained material called LIS-Ti was dried at 40 °C to a constant mass and used in adsorption study.

**Analytical methods**

The concentration of Li in water solutions was measured by the atomic absorption spectrometry (AAS) using the AAnalyst 100 Atomic Absorption Spectrometer manufactured by PerkinElmer.

**Kinetics of adsorption**

75 ml of initial brine was alkalized with NaOH to a pH of 8 and contacted with 0.5 g of LIS-Ti sorbent in a 100 ml plastic container. The contact time ranged from 1 minute to 24 hours, with continuous pH monitoring throughout. Approximately 0.5 ml samples of the sorbent-brine suspension were centrifuged at 2500 rpm for 45 seconds, then diluted with distilled water to measure lithium content. Capacity of sorbent towards lithium at a given time was calculated using equation (1):

$$q_t = V_s \frac{C_i - C_t}{m_s} \quad (1),$$

where: $C_i$ – initial lithium concentration in brine (mg/L), $C_t$ – lithium concentration in brine at given time (mg/L), $V_s$ – volume of used brine, $m_s$ – mass of sorbent (g).

**Isotherm of adsorption**

0.2 g of sorbent was contacted with 50 ml of a pure LiOH solution in distilled water. Seven samples were prepared in 100 ml plastic containers with Li concentrations ranging from 80 to 1000 ppm. The samples were left 24 hours, then diluted to measure the lithium content using an atomic absorption spectrometer.

**Modelling approach**

The pseudo-first-order (PFO) and pseudo-second-order models (PSO) were used to describe kinetics of sorption. The PFO model can be described as follows [8]:

$$\frac{dq_t}{dt} = K_1(q_e - q_t) \quad (2),$$

where: $q_t$ – amount of lithium adsorbed at time (mg/g), $q_e$ - amount of lithium at equilibrium (mg/g), $K_1$ – rate constant (1/min).

The pseudo-first-order model effectively describes the initial phase of sorption prior to reaching equilibrium [9]. The PSO kinetic model can be represented as [8]:

$$\frac{dq_t}{dt} = K_2(q_e - q_t)^2 \quad (3),$$

where: $K_2$ – adsorption rate constant of the PSO kinetic model.

The distribution of metal ions between the liquid and solid phases can be modeled by various isotherm equations, including the Langmuir and Freundlich models, which are commonly used to describe adsorption processes. These models predict how metal ions interact with adsorbents under different conditions of concentration and temperature [10]. The Langmuir isotherm equation can be described as [10]:

$$q_e = \frac{q_{max} \cdot b \cdot C_e}{1 + b \cdot C_e} \quad (4),$$

where: $C_e$ – Li concentration in water at equilibrium (mg/L), $q_{max}$ – maximum of sorption capacity for lithium (mg/g), $q_e$ - amount of adsorbed lithium at equilibrium (mg/g), $b$ – Langmuir isotherm constant (L/mg).

https://doi.org/10.5593/sgem2024v/3.2/s06.51

The Freundlich isotherm is an empirical model that can be described as [10]:

$$q_e = K_f C_e^{1/n} \quad (5)$$

where: $K_f$ – Freundlich constant (-), $n$ – constant indicating the degree of nonlinearity between solution concentration and adsorption (-) progress.

The kinetic models and isotherms were fitted to experimental data using nonlinear regression. To evaluate the fit quality the RMSE (Root Mean Square Error) and chi$^2$ statistics were applied. These values were computed based on the following formulas:

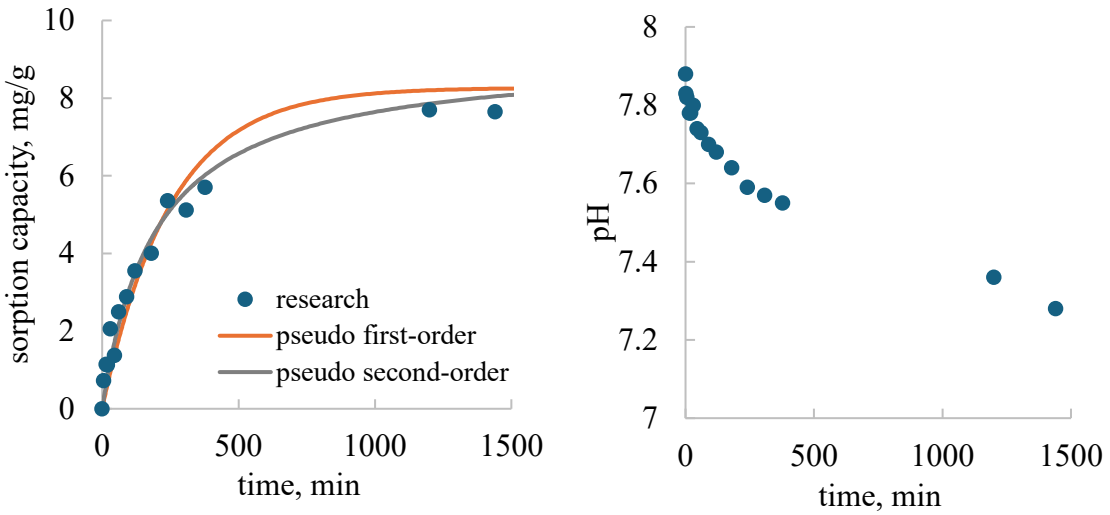
$$RMSE = \sqrt{\frac{1}{N}\sum_{i=1}^{N}\left(q_{e,exp} - q_{e,calc}\right)^2} \quad (6),$$

$$chi^2 = \sum_{i=1}^{N}\frac{\left(q_{e,exp} - q_{e,calc}\right)^2}{q_{e,calc}} \quad (7),$$

where: $N$ – numbers of experimental points, $q_{e,exp}$ and $q_{e,calc}$ – experimental and calculated sorption capacity, respectively.

## RESULTS

Figure 1a shows sorption kinetics for the LIS-Ti material in real oilfield brine. The values of fitted models are summarized in Table 1. The Figure 1b shows changes in pH as the sorption progressed.




(a) (b)

Figure 1 a) lithium sorption kinetics on LIS-Ti material in brine, b) pH change in time during kinetics research.

Table 1. Kinetic models parameters for Lithium recovery

| Model | Parameter | Unit | LIS-Ti |
|---|---|---|---|
| Pseudo-first order | $K_1$ | 1/min | 0.004 |
| | $q_e$ | mg/g | 8.268 |
| | $chi^2$ | [-] | 8.820 |
| | RSME | [-] | 0.592 |
| Pseudo-second order | $K_2$ | g/(mg·min) | 0.00056 |
| | $q_e$ | mg/g | 9.137 |
| | $chi^2$ | [-] | 5.150 |
| | RSME | [-] | 0.383 |
| Maximum sorption capacity determined experimentally, $q_{exp}$ | | mg/g | 9.19 |

The sorption isotherm in pure LiOH solution is shown in Figure 2 and summarized in Table 2.

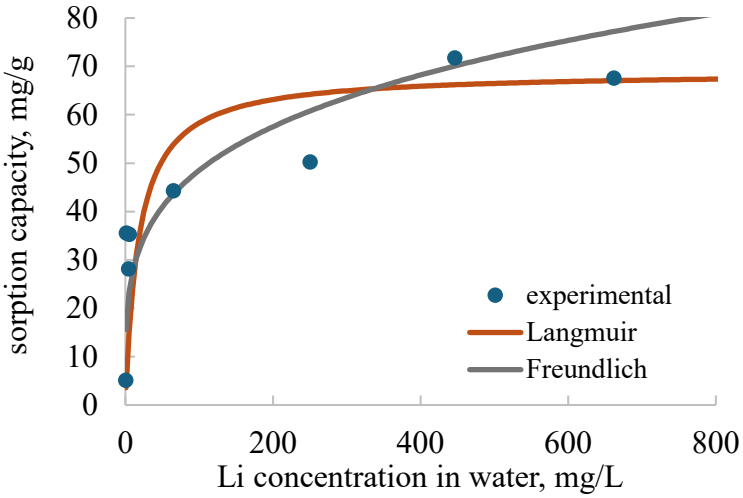



Figure 2. Lithium sorption isotherm from LiOH solution using the LIS-Ti adsorbent.

Table 2. Values of Langmuir and Freundlich parameters for adsorption isotherm.

| Langmuir | | | | Freundlich | | | |
|---|---|---|---|---|---|---|---|
| $Q_m$ (mg/g) | B (L/g) | $chi^2$ | RSME | n | $K_f$ | $chi^2$ | RSME |
| 68.894 | 0.055 | 204.358 | 15.036 | 4.066 | 15.629 | 34.094 | 9.849 |

## DISCUSSION

Figure 1 shows quick capacity rise in the initial period of sorption. More than 50 % of the total sorption capacity is achieved within first 2 hours. The equilibrium takes 24 hours to establish and is related to the migration of lithium cations deep into the crystalline structure of the sorbent. The experimental results were modeled using the PFO and PSO

https://doi.org/10.5593/sgem2024v/3.2/s06.51

models; the quality of the fit was assessed based on the RMSE and $chi^2$ coefficients. The second-order model better fits to the experimental data because the values of RSME and $chi^2$ for it are lower than for the PFO model. It may suggest that lithium recovery process is mainly controlled by the chemical interactions between adsorbate and adsorbent. Maximum sorption capacity reached in real brine was 9.19 mg of lithium per 1g of LIS-Ti sorbent. Table 3 summarizes lithium capacities of different Ti-based materials. It can be seen that the obtained value is promising and typical for Ti-based sorbents.

Table 3. Comparison of sorption capacity for selected titanium-based sorbents.

| Sorbent (name or structure) | Synthesis | Brine | Sorption capacity, mg/g | Reference |
|---|---|---|---|---|
| LIS-Ti | Solid-state reaction | Oilfield brine ($Li^+$: 220 mg/L) | 9.19 | this study |
| YS-$TIO_2$ | Hydrothermal synthesis | Model solution | 28.46 | [11] |
| P-HTO-NF | Calcination | Model solution | 7.58 | [12] |
| HFTO – 10% | Calcination | Salt lake brine ($L^+$: 1950 mg/L) | 34.27 | [13] |
| $TiO_3$ | Calcination | Model solution | 3.68 | [11] |

Experimental lithium sorption isotherm was compared to Langmuir and Freundlich theoretical models. Based on statistical coefficients the Freundlich equation better fits to the experiment data. This confirms the multi-step nature of Li recovery process.

## CONCLUSION

Lithium recovery from unconventional resources will play important role in green transformation towards more sustainable economy. Different methods may be applied for this purpose but adsorption is most often recommended. Among various sorbents the titanium-based materials are known for their chemical resistance and good sorption properties. These sorbents are resistant to hydrochloric acid so they are expected to operate for a long time, which will positively affect the economics of the recovery process. The results show that the sorbent obtained at a low calcination temperature (only 700 ºC) has a high sorption capacity. In LiOH solution under equilibrium conditions, it captures almost 70 $mg_{Li}/g$ and in a real brine up to 9.19 $mg_{Li}/g$. The brine is a challenging resource because it contains other ions at concentrations much higher than Li content. It explains the difference between lithium uptake from model Li solution and real brine. The kinetic measurements reveal that the sorption process needs at least 24 hours to achieve the equilibrium. After first few hours the sorbent reaches 50-60% of its maximal sorption capacity and it seems to be a reasonable efficiency. Further research should focus on technology upscaling and application of the obtained Ti-based powder in more practical form like shapes prepared via 3D printing technology.

## ACKNOWLEDGEMENTS

The research leading to these results has received funding from the National Centre for Research and Development (NCBR) in the frame of Project Contract No. LIDER/34/0174/L-12/20/NCBR/2021 under the LEADER Program

## REFERENCES

[1] U.S. Geological Survey, 2024, Mineral commodity summaries 2024: U.S. Geological Survey, 212 p. https://doi.org/10.3133/mcs2024

[2] Fleischmann, Jakob, et al. "Battery 2030: Resilient, sustainable, and circular." *McKinsey & Company* (2023): 2-18.[]US Geological Survey. *Mineral Commodities Summary 2020*; U.S. Geological Survey: Reston, VA, USA, 2020; p. 204

[3] Stringfellow, W.T.; Dobson, P.F. Technology for the Recovery of Lithium from Geothermal Brines. *Energies* **2021**, *14*, 6805. https://doi.org/10.3390/en14206805

[4] Sun, Ying, et al. "Recent advances in magnesium/lithium separation and lithium extraction technologies from salt lake brine." *Separation and Purification Technology* 256 (2021): 117807..

[5] Yu, Jiangtao, et al. "3D-printed titanium-based ionic sieve monolithic adsorbent for selective lithium recovery from salt lakes." *Desalination* 560 (2023): 116651

[6] Li, Xiaowei, et al. "Taming wettability of lithium ion sieve via different TiO2 precursors for effective Li recovery from aqueous lithium resources." *Chemical Engineering Journal* 392 (2020): 123731.

[7] Xu, Chenyang, et al. "3D printing of powder-based inks into functional hierarchical porous $TiO_2$ materials." *Advanced Engineering Materials* 22.3 (2020): 1901088.

[8] Płaziński, W., and Rudziński, W. (2011): "Kinetyka Adsorpcji Na Granicy Faz Roztwór/Ciało Stałe. Znaczenie Równań Pseudo-First Order Oraz Pseudo-Second Order." *Wiadomości Chemiczne* 65 (11–12): 1055–67 (in Polish).

[9] Tan, K.L., and Hameed, B.H. (2017): "Insight into the Adsorption Kinetics Models for the Removal of Contaminants from Aqueous Solutions." *Journal of the Taiwan Institute of Chemical Engineers* 74: 25–48. https://doi.org/10.1016/j.jtice.2017.01.024.

[10] C Desta, Mulu Berhe. "Batch sorption experiments: Langmuir and Freundlich isotherm studies for the adsorption of textile metal ions onto teff straw (Eragrostis tef) agricultural waste." *Journal of thermodynamics* 2013.1 (2013): 375830.

[11] Li, Na, et al. "Yolk-shell structured composite for fast and selective lithium-ion sieving." *Journal of Colloid and Interface Science* 520 (2018): 33-40.

[12] Wei, Shudan, et al. "Porous lithium-ion sieves nanofibers: General synthesis strategy and highly selective recovery of lithium from brine water." *Chemical Engineering Journal* 379 (2020): 122407.

[13] Wang, Qihui, et al. "Titanium-based lithium ion sieve adsorbent H2TiO3 with enhanced Li+ adsorption properties by magnetic Fe doping." *Separation and Purification Technology* 346 (2024): 127455.